

Documenting Bloodstain Patterns Concealed beneath
Architectural Paint Layers using Multi-Spectral
Forensic Photography Techniques

By

Natasha Arielle Dilkie

A Thesis Submitted to
Saint Mary's University, Halifax, Nova Scotia
In Partial Fulfilment of the Requirements for the Degree of
Masters of Science in Applied Science

December 2016, Halifax, Nova Scotia

Copyright Natasha Arielle Dilkie, 2016

Approved: _____
Dr. Christa L. Brosseau
Supervisor

Approved: _____
Heidi Nichols
Committee Member

Approved: _____
Dr. Michelle Patriquin
Committee Member

Approved: _____
Lisa Pessin
Committee Member

Approved: _____
Dr. Brian Yamashita
External Examiner

Date: December 7, 2016

ABSTRACT

Documenting Bloodstain Patterns Concealed beneath Architectural Paint Layers using Multi-Spectral Forensic Photography Techniques

By Natasha Arielle Dilkie

The development of forensic photography techniques can aid agencies in the documentation of information regarding crime scene cleanup. This study compared reflective infrared, reflective ultraviolet, and fluorescence photography in the documentation of bloodstain patterns that had been concealed beneath layers of architectural paint. High Dynamic Range (HDR) photography, as well as a chemical analysis of all four paint types using Raman, Fibre Optic Reflectance, and Attenuated Total Internal Reflectance-Fourier Transform Infrared Spectroscopy was performed. The photography results for reflective infrared were negative; reflective ultraviolet for two of the four paint types were positive. Fluorescence photography had the most definitive visual information for the two white paints but were concluded negative for black and maroon. HDR was concluded to be negative for reflective infrared and reflective ultraviolet; however, results for fluorescence were positive. Finally, spectroscopy results supported visual information as well as providing spectral data relevant for understanding specific chemical observations.

December 7, 2016

Dedication

I wish to dedicate this entire body of work to my dearest mother Judith. You have been a constant source of strength and support not only through this process but my through entire life. The road we walk is not always easy, and we will trip along the way, but there is no one more deserving of love and recognition than my mother. This is my dedication to you; I love you with all of my heart and soul.

To my little brother whom is always in my heart. This thesis is the accumulation of nearly three years of my own blood, sweat, and tears; all of which would not have been possible without you. When I was at my lowest I reached out to you for help and you guided me back on my path. I know that life is so very difficult little brother but just know that none of this would have been possible without your help.

That which guides me I shall follow, the light that surrounds me through love of kin, will comfort and support me until the end.

Acknowledgments

Firstly, I would like to thank Dr. Brosseau and the other chemistry students in her lab for taking me in and supporting my research. This thesis would not have been possible if not for the support of so many wonderful people. I would especially like to thank Osai, Reem, and Marwa for assisting me with my experiments and providing me with their expertise.

I offer my sincere gratitude to my committee members for offering their knowledge and wisdom during this arduous process: Heidi Nichols has been a constant spark of energy, absolutely over-flowing with ideas, and her drive has definitely kept me pushing forwards. I also wish to thank Lisa Pessin and Dr. Michelle Patriquin for your tutelage and patience in this process; the knowledge and refinement of ideas was only possible with the help of both of you. Additionally I wish to thank my external examiner Dr. Brian Yamashita for agreeing to take time to read my thesis.

To all of my dear friends I must thank you from the bottom of my heart. You have all had to deal with me at my best, and not so best, and I would not be here without each and every one of you. I would especially like to thank Meagan, Maddy, Kayla, Ciara, other Natasha, Natalie, Sam, Laura, Ally, Emily P., Emily W., Pey, and countless others. My friends and family whom I have not named just know that you are all important to me and your exclusion can be blamed on thesis brain.

I wish to give a special thank you to Constable Brian Veniot, Dr. Matt Bowes, and Investigator Eveline Gallant for their support and genuine friendship. The people from the NSMES are like a second family to me and I truly enjoyed working with them in all aspects. Whenever I felt like I would fall down I always found help and the strength to keep going through my colleagues. Additionally, I wish to give a special thank you to PSD Doc, your fuzzy warmth and overwhelming intelligence has made my research project absolutely enjoyable.

This thesis has taught me many things about myself; the need for patience and level-headedness, a keen sense of academic perseverance, and rigorous work ethic. It has also taught me to always fight for what I believe in, to stand back up no matter how many times I've been pushed down, and to never accept the negative inclinations from others as a truth about myself. Thank you to the people no longer in my life for shaping me into the strong, stubborn, successful woman that I am today.

Finally, I need to thank my dearest, wonderful mother Judith once more. I am so excited to start the next chapter of my life and I can't wait to share my adventures with those that are so very dear to me. Thank you everyone.

Table of Contents	Page
Abstract	II
Dedication	III
Acknowledgments	IV
Table of Contents	VI
List of Figures	X
List of Tables	XV
List of Abbreviations	XVII

Table of Contents	Page
Chapter 1: Introduction	1
1.1. Forensic Photography	1
1.1.1. Introduction	1
1.1.2. Case Study: Bloodstains under Paint	2
1.2. Objectives of Thesis	2
1.3. Outline of Thesis	4
Chapter 2: Literature Review	6
2.1. Camera Theory and Photography Practise	6
2.1.1. Documentation Photography	8
2.1.2. Forensic Photography	11
2.1.3 High Dynamic Range Photography	14
2.2. ‘Multi-Spectral’ Photography and Alternate Light Source Photography	16
2.2.1. Reflective Ultraviolet Photography	18
2.2.2. Fluorescence Photography	23
2.2.3. Reflective Infrared Photography	27
2.2.4. Image Editing Software for Photography Analysis	31
2.3. Bloodstain Patterns	33
2.3.1. Properties of Blood	35
2.3.1.1. Types of Bloodstain Patterns	37
2.3.1.2. Bloodstain Analysis Techniques	38
2.3.2. Viable Substitutes for Human Blood in Research	40
2.4. Chemiluminescence	42
2.4.1. Luminol	43
2.4.1.1. History of Luminol	43
2.4.1.2. The Reaction of Luminol to Substances	44
2.4.1.3. Effects of Luminol on Further Blood Testing	45
2.4.2. Comparison of Techniques: Advantages and Disadvantages	46

2.5. Chemical Analysis of Paint	48
2.5.1. Properties of Architectural Paint	49
2.5.2. Raman Spectroscopy	51
2.5.3. Fibre Optic Reflectance Spectroscopy	54
2.5.4. Attenuated Total Reflectance Fourier Transform Infrared Spectroscopy	55
2.6. Bloodstain Patterns beneath Paint: A Review	58
Chapter 3: Materials and Methods	60
3.1. Laboratory Set up and Equipment	60
3.2. Preparation of Materials	62
3.3. Stage Three: The Application of Bloodstain Patterns	63
3.3.1. Preparation and Application of Experiment and Equipment	65
3.4. Stages Four: The Application of the First Layer of Paint	67
3.5. Stages Five: The Application of the Second Layer of Paint	68
3.6. Stage Six: Luminol Treatment	68
3.6.1. Preparation of Experiment and Equipment	69
3.6.2. Application of Luminol Solution on Second Layer of Paint	70
3.7. Photography Set Up and Process	72
3.7.1. Standard Photography	72
3.7.2. Reflective Infrared Photography	77
3.7.3. Reflective Ultraviolet Photography	80
3.7.4. Fluorescence Photography	83
3.8. Photography Analysis	90
3.8.1. High Dynamic Range Enhancement in Photoshop CC	90
3.9. Chemical Analysis of Paint	91
3.9.1. Preparation of the Experimental Samples	92
3.9.2. Raman Spectroscopy	92
3.9.3. Fibre Optic Reflectance Spectroscopy	93
3.9.4. ATR FTIR Spectroscopy	95

Chapter 4: Results and Discussion	98
4.1. Stage Three: Application of Bloodstain Patterns	98
4.1.1. Standard Photography	98
4.1.2. Reflective Infrared Photography	99
4.1.3. Reflective Ultraviolet Photography	102
4.1.4. Fluorescence Photography	103
4.2. Stage Four: First Layer of Paint over Blood	106
4.2.1. Preparation and Application of First Layer of Paint	106
4.2.2. Standard Photography	107
4.2.3. Reflective Infrared Photography	109
4.2.4. Reflective Ultraviolet Photography	110
4.2.5. Fluorescence Photography	114
4.3. Stage Five: Second Layer of Paint over Blood	118
4.3.1. Preparation and Application of Second Layer of Paint	118
4.3.2. Standard Photography	119
4.3.3. Reflective Infrared Photography	121
4.3.4. Reflective Ultraviolet Photography	122
4.3.5. Fluorescence Photography	125
4.4. Stage Six: Application of Luminol	127
4.4.1. Standard Photography	128
4.5. Photography Analysis	131
4.5.1. High Dynamic Range Photography Analysis	131
4.5.1.1. Standard Photography	131
4.5.1.2. Reflective Infrared Photography	132
4.5.1.3. Reflective Ultraviolet Photography	135
4.5.1.4. Fluorescence Photography	138
4.6. Chemical Analysis of Paint	145
4.6.1. Raman Spectroscopy Results	147
4.6.2. Fibre Optic Reflectance Spectroscopy Results	153
4.6.3. ATR FTIR Spectroscopy Results	156

Chapter 5: Conclusion and Future Directions	166
5.1. Future Directions for Architectural Paint Analysis	171
5.2. Future Directions in Multi-Spectral Photography and High Dynamic Range Techniques	172
Chapter 6: References	174
Appendix	186
Appendix 2.2.3: Spectral Curves	187
Appendix 3.2: Stage One and Two: The Application of Primer and Paint Preparation of Experiment and Equipment	188
Appendix 3.4: First Layer of Paint Preparation of Experiment and Equipment	191
Appendix 3.5: Second Layer of Paint Preparation of Experiment and Equipment	192
Appendix 3.7: Camera Settings	194
Appendix: Photographs	215

List of Figures	Page
Figure 1: Copy-stand with tungsten light sources and mounted camera (example)	13
Figure 2: Example of High Dynamic Range photography (right) compared to one single photograph at normal exposure (left)	15
Figure 3: Electromagnetic spectrum depicting multi-spectral photography capabilities from the near-ultraviolet to near-infrared light spectrum (Adapted from Williams and Williams 1993).	16
Figure 4: Transmission spectra of the Baader-U (Baader Venus) Bandpass filter (Company Seven Astro-Optics Division).	21
Figure 5: Reflective ultraviolet photography set-up depicting the recording of a subject using a Wood's lamp UV light source, Baader-U filter and modified UV/IR DSLR camera with quartz lens (Adapted from Frey et al. 2011).	22
Figure 6: Spectral range of blood with a peak at approximately 415 nanometres (Stoilovic 1991).	23
Figure 7: Molecular excitation from a specialized light source and release of fluorescence (Adapted from West et al. 1992).	24
Figure 8: Spectral peaks of yellow, orange, red longpass filters (Schneider Kreuznach Company).	25
Figure 9: Fluorescence Photography using the SPEX Crimescope (Adapted from Frey et al. 2011).	27
Figure 10: Spectral output of a tungsten light source (Adapted from Williams and Williams 2002).	30
Figure 11: Reflective infrared photography with a tungsten light source and longpass filter (Adapted from Frey et al. 2011).	31
Figure 12: Average blood composition of a human adult per cubic millimetre (Adapted from Christman 1996).	34
Figure 13: Molecular reaction of Luminol to a catalyst. Luminol plus hydrogen peroxide come into contact with the catalyst (e.g. blood). The molecular reaction increases to an excited state before relaxing and releasing light as it returns to its ground state (James et al. 2005).	43

Figure 14: Copy stand table with tungsten light sources and mounted camera.	61
Figure 15: Example of Medium Velocity, Swipe, and Saturated Bloodstain Patterns	64
Figure 16: Bloodstain application set-up.	65
Figure 17: Baader-U (Baader Venus) 2-inch filter (Company Seven Astro-Optics Division).	81
Figure 18: SPEX Crimescope with coloured filters and goggles (SPEX Forensics).	84
Figure 19: DeltaNu benchtop Raman spectrometer (Intevac Photonics).	93
Figure 20: Fibre Optic Reflectance Spectroscopy system (Adapted from OceanOptics).	94
Figure 21: Attenuated Total Reflection Fourier Transform Infrared Spectrometer (Bruker Optics).	96
Figure 22. Basic process of IR light interacting with the sample of interest. A small fraction of the evanescent wave penetrates the sample and becomes attenuated (weakened) where the sample absorbs the energy (Adapted from Bruker Optics).	97
Figure 23: Example of Standard Photography for the Bloodstain Pattern Stage (HDR White Acrylic 1)	98
Figure 24: Example of Reflective Infrared Photography (Filter #87A) for the Bloodstain Pattern Stage (HDR White Acrylic 1).	100
Figure 25: Example of Reflective Ultraviolet Photography for the Bloodstain Pattern Stage (HDR White Acrylic 1)	102
Figure 26: Example of Fluorescence Photography (Yellow Filter 445 nm) for the Bloodstain Pattern Stage (HDR White Acrylic 1)	103
Figure 27: Example of Standard Photography for the First Layer of Paint Stage (HDR White Acrylic 1)	108
Figure 28: Example of Reflective Infrared Photography (Filter #87A) for the First Layer of Paint Stage (HDR White Acrylic 1)	109

Figure 29: Example of Reflective Ultraviolet Photography for the First Layer of Paint Stage (HDR White Acrylic 1)	111
Figure 30. Example of Reflective Ultraviolet Photography for the First Layer of Paint Stage (HDR White Latex 5).	112
Figure 31: Example of Fluorescence Photography (Yellow Filter 445nm) for the First Layer of Paint Stage (HDR White Acrylic 1)	114
Figure 32: Example of Standard Photography (Oblique Lighting Left) for the Second Layer of Paint Stage (HDR White Acrylic 1)	120
Figure 33: Example of Reflective Infrared Photography (Filter #87A Oblique Lighting Left) for the Second Layer of Paint Stage (HDR White Acrylic 1)	121
Figure 34: Example of Reflective Ultraviolet Photography for the Second Layer of Paint Stage (HDR White Acrylic 1)	123
Figure 35. Example of Reflective Ultraviolet Photography for the Second Layer of Paint Stage (HDR Black Latex 9).	124
Figure 36: Example of Fluorescence Photography (Yellow Filter 445 nm) for the Second Layer of Paint Stage (HDR White Acrylic 1)	125
Figure 37: Example of Standard Photography (Luminol testing) for the Second Layer of Paint Stage (White Acrylic 1)	128
Figure 38. Example of Standard Photography for the First Layer of Paint Stage (HDR White Acrylic 1 Left; Single White Acrylic 1 Right).	132
Figure 39: Example of Reflective Infrared Photography (Longpass Filter #87A) for the Bloodstain Pattern Stage (HDR White Acrylic 1 Left; Single White Acrylic 1 Right).	133
Figure 40: Example of Reflective Infrared Photography (Longpass Filter #87A) for the Bloodstain Pattern Stage (HDR Black Latex 9 Left; Single Black Latex 9 Right).	133
Figure 41: Example of Reflective Infrared Photography (Longpass Filter #87A) for the First Layer of Paint Stage (HDR White Acrylic 1 Left; Single White Acrylic 1 Right).	134

Figure 42: Example of Reflective Infrared Photography (Longpass Filter #87A Lighting Oblique Left) for the Second Layer of Paint Stage (HDR White Acrylic 1 Left; Single White Acrylic 1 Right).	135
Figure 43: Example of Reflective Ultraviolet Photography for the Bloodstain Pattern Stage (HDR White Acrylic 1 Left; Single White Acrylic 1 Right).	136
Figure 44: Example of Reflective Ultraviolet Photography for the First Layer of Paint Stage (HDR White Acrylic 1 Left; Single White Acrylic 1 Right).	136
Figure 45: Example of Reflective Ultraviolet Photography for the Second Layer of Paint Stage (HDR White Acrylic 1 Left; Single White Acrylic 1 Right).	137
Figure 46: Example of Fluorescence Photography (Yellow Filter 445 nm) for the Bloodstain Pattern Stage (HDR White Acrylic 1 Left; Single White Acrylic 1 Right).	139
Figure 47: Example of Fluorescence Photography (Yellow Filter 445nm) for the Bloodstain Pattern Stage (HDR Maroon Latex13 Left; Single Maroon Latex 13 Right).	139
Figure 48: Example of Fluorescence Photography (Yellow Filter 445 nm) for the First Layer of Paint Stage (HDR White Acrylic 1 Left; Single White Acrylic 1 Right).	140
Figure 49: Example of Fluorescence Photography (Red Filter 575 nm) for the Bloodstain Pattern Stage (HDR White Acrylic 1 Left; Single White Acrylic 1 Right).	141
Figure 50: Example of Fluorescence Photography (Yellow Filter 445 nm) for the Second Layer of Paint Stage (HDR Maroon Latex 13 Left; Single Maroon Latex 13 Right).	142
Figure 51: Example of Fluorescence Photography (Yellow Filter 445 nm) for the Second Layer of Paint Stage (HDR White Acrylic 1 Left; Single White Acrylic 1 Right).	143
Figure 52: Example of Fluorescence Photography (Red Filter 415 nm) for the Second Layer of Paint Stage (HDR White Acrylic 1 Left; Single White Acrylic 1 Right).	143

Figure 53: Normal Raman Spectra for White Acrylic Paint Analysis. Peaks are consistent with titanium dioxide (614 cm^{-1} , 453 cm^{-1}).	148
Figure 54: Norman Raman Spectra for White Latex Paint Analysis. Peaks are consistent with titanium dioxide (614 cm^{-1} , 453 cm^{-1}).	148
Figure 55: SERS Spectra for White Acrylic Paint Analysis	150
Figure 56: SERS Spectra for White Latex Paint Analysis	151
Figure 57: SERS Spectra for Black Latex Paint Analysis	151
Figure 58: SERS Spectra for Maroon Latex Paint Analysis	152
Figure 59: FORS results for white acrylic (red), white latex (blue), black latex (green), and maroon latex (pink) with the halogen light source.	154
Figure 60: ATR FTIR Spectra for White Acrylic Paint Analysis (C-H aliphatic stretching ~2958-2875; Carbonyl peak ~1732; Key peaks at ~1451, 1387) (Caddy 2001).	157
Figure 61: ATR FTIR Spectra for White Latex Paint Analysis (C-H aliphatic stretching in ~2900 region; Carbonyl peak ~1738; Key peaks at ~1435, 1371, 1240, 1021) (Caddy 2001).	158
Figure 62: ATR FTIR Spectra for Black Latex Paint Analysis (C-H aliphatic stretching in ~2900 region; Carbonyl peak ~1738; Key peaks at ~1435, 1371, 1240, 1021) (Caddy 2001).	159
Figure 63: ATR FTIR Spectra for Maroon Latex Paint Analysis (C-H aliphatic stretching in ~2900 region; Carbonyl peak ~1738; Key peaks at ~1435, 1371, 1240, 1021) (Caddy 2001).	160
Figure 64. ATR-FTIR Spectra and peaks of interest for Tributyl Phosphate (~1433, 1236, 1160, 1161, 1120, 1061, 1020, 992, 960, 867, 854, 810) (Spectral Database for Organic Compounds).	161

List of Tables	Page
Table 1: Ultraviolet range of electromagnetic spectrum (Adapted from Williams and Williams 1993; Mairinger 2000a).	18
Table 2: Examples of passive, transfer, and projected bloodstain patterns (Adapted from Wonder 2007).	38
Table 3: Photographic Equipment used for the Thesis Research	61
Table 4: Paint Materials	62
Table 5: Bloodstain Pattern Application and Subsequent Drywall Squares	67
Table 6: Standard photography equipment and parameters	73
Table 7: Infrared Longpass Filters (De Broux et al. 2007; Frey et al. 2011).	77
Table 8: Reflective infrared photography equipment and parameters for bloodstain pattern stage	78
Table 9: Reflective infrared photography equipment and parameters for first layer of paint stage	79
Table 10: Reflective infrared photography equipment and parameters for second layer of paint stage	80
Table 11: Reflective ultraviolet photography equipment and parameters for bloodstain pattern, first layer of paint, and second layer of paint	82
Table 12: Fluorescence photography equipment and parameters for all stages	86
Table 13: Fluorescence photography equipment and parameters for bloodstain pattern stage	87
Table 14: Fluorescence photography equipment and parameters for first layer of paint stage	88
Table 15: Fluorescence photography equipment and parameters for second layer of paint stage	89
Table 16: Raman spectroscopy analysis for all paint types	93
Table 17: Paint components as provided in the manufacturer information.	146

Table 18: Relevant peaks for chemical components present in white acrylic, white latex, black latex, and maroon latex paints

153

List of Abbreviations

ABFO	American Board of Forensic Odontologists
ALS	Alternate Light Source
ATR-FTIR	Attenuated Total Reflectance Fourier Transform Infrared Spectroscopy
EV	Exposure Value
FLS	Forensic Light Source
FORS	Fibre Optic Reflectance Spectroscopy
HDR	High Dynamic Range
IR	Infrared
ISO	International Standards Organization
JPEG	Joint Photographic Experts Group
K	Kelvin
LED	Light Emitting Diode
SERS	Surface Enhanced Raman Spectroscopy
TIFF	Tagged Image File Format
UV	Ultraviolet

Chapter 1: Introduction

1.1 Forensic Photography

1.1.1 Introduction

Forensic photography is a specialized type of photography responsible for the documentation of crime scenes, autopsies, evidence collection and other situations that have the potential to appear in a court of law. Although there are many similarities between photography techniques in the field of art conservation and forensics, the latter has a standard of conduct which must be followed. Failure to follow forensic photography procedure can result in the dismissal of cases, loss of certification, and other severe repercussions for the photographer (Duncan 2010; Robinson 2007).

Procedures followed in forensic photography often revolve around rigorously avoiding instances where the photographer might be accused of photograph manipulation. Contrary to popular belief, it is very difficult to manipulate digital photographs; it is easier to fake or manipulate film photography (Marin and Buszka 2013; Weiss 2009). Digital photographs and associated programs contain embedded information. By referring to the properties of a particular photograph, any relevant information is available, including traces of enhancement. Standard forensic photography procedure for documenting crime scenes would follow a structure of photographing the scene overall, orienting a particular aspect or piece of evidence in the scene, and taking final close-up photographs (Duncan 2010; Milliet et al. 2014). This standard of practise can be applied to any type of scene or evidence including but not limited to: accidents, suicides, homicides, suspicious death scenes, physical evidence on the body including tattoos,

gunshot residue, ligature marks, and anything else of note such as weapons, empty pill bottles, and bloodstain patterns (Duncan 2010; Robinson 2007; Weiss 2009).

1.1.2 Case Study: Bloodstains under Paint

There are multiple instances in the news and police reports alike of bloodstains being painted over in criminal acts. News articles from the United States, Australia and Canada have reported that along with criminal acts of burglary, assault and homicide, perpetrators have resorted to obscuring bloodstain patterns by painting over them. When details of particular crimes are available for media release in regards to types of paint used, an assortment of paints has been utilized. Scenes can potentially range from quick acts of obstruction with obvious painted sections of a wall; to meticulous cover-up of entire rooms. Although instances of criminal obstruction of bloodstain patterns using paint are not common practise, it has been known to occur enough to be addressed as a research study.

1.2. Objectives of Thesis

Forensic photography can be utilized in multiple ways in order to document different types of evidence. In the field of multi-spectral photography the visible light spectrum, near-ultraviolet light spectrum and near-infrared light spectrum may be photographically documented with a Digital Single Lens Reflex (DSLR) camera. Current research in the field of multi-spectral forensic photography tends to focus on physical evidence such as latent fingerprints, bite-mark analysis, gunshot residue and forged

documentation. This field of photography has also been shown to be useful in terms of bloodstain documentation and analysis. A multitude of research studies analyze one aspect of multi-spectral photography but fail to incorporate all techniques into a multi-spectral analysis. Research that does analyze more than one spectrum of light tends to lack a detailed explanation of variables and how they might be potentially addressed in the field. For the purpose of determining the effectiveness of a multi-spectral analysis of bloodstains beneath paint, three photography methods will be employed in this thesis work. Reflective ultraviolet photography will be used to document in the near ultraviolet light spectrum; fluorescence photography will be used to document in the visible light spectrum; and reflective infrared photography will be used to document in the near infrared light spectrum. The objectives of this research are as follows.

1. To compare and analyze reflective ultraviolet photography, reflective infrared photography, and fluorescence photography techniques to see if these techniques have the ability to document bloodstain patterns that have been concealed beneath architectural paint.
2. To test the validity of using High Dynamic Range photography in a HDR post-referential program to enhance the visibility of bloodstain patterns underneath paint layers.

3. To test the paint chemistry of each different paint type in order to: (A) analyze the chemical components of each paint to help explain results obtained from UV, IR, fluorescence photography and Luminol testing (B) and characterize the reflectance and absorption behaviour of each different paint over the wavelength range of 200 - 800 nanometres.

1.3. Outline of Thesis

This thesis consists of 6 chapters. Chapter 1 is an introduction to the research project being conducted, and covers the objectives of this work. A detailed literature review is provided in chapter 2 and covers the topics of camera theory and photography practise, ‘multi-spectral’ photography and forensic light sources, properties and characteristics of blood, chemiluminescence, and the chemical analysis of paint. Chapter 3 provides a detailed description of the materials and methods used for data collection and includes, preparation of experimental samples and application of bloodstain patterns, paint layers, Luminol testing, photography set up and process, high dynamic range enhancement in Photoshop CC, and chemical analysis of the paint samples using Attenuated Total Reflectance Fourier Transform Infrared Spectroscopy (ATR FTIR), Raman Spectroscopy and Surface-Enhanced Raman Spectroscopy (SERS), and Fibre Optic Reflectance Spectroscopy (FORS).

The results and discussion of this research project are stated in chapter 4. Results of the experimental research design and data collection, application processes, and photography using standard, reflective infrared, reflective ultraviolet and fluorescence

photography techniques are all discussed. This chapter also evaluates high dynamic range enhancement versus non-enhancement through Photoshop CC, as well as the evaluation of the paint analysis using ATR-FTIR, Raman, SERS, and FORS. Chapter 5 summarizes the conclusions of this thesis and discusses the future directions of this research including recommendations for paint analysis and further study of high dynamic range photography in a crime scene context. References are located in Chapter 6.

Chapter 2: Literature Review

2.1. Camera Theory and Photography Practise

Photography can be applied in many different venues from artistic capture to documentation techniques. Having an understanding of camera theory and practise is important for determining how different aspects can affect a desired outcome, and determining the methods that need to be applied in different situations. In the simplest terms, a camera can be described as a box which allows a certain amount of light to enter. In traditional film photography, light-sensitive film would be located inside of the box and would allow an image to be captured on the surface of this film (Gestring 2007; Duncan 2010). Digital photography is similar to film photography except for the lack of traditional film. Instead, an image is recorded on the internal sensor and displayed on the back screen as soon as it has been captured (Weiss 2009; Duncan 2010). This internal sensor is either a CCD (charge-coupled device) or a CMOS (complementary metal-oxide semiconductor) which are both capable of producing high-resolution images with excellent light sensitivity (Thryft 2009; Weiss 2009; Frey et al. 2011; Marin and Buszka 2013). CCD technology tends to provide higher resolution images over the cheaper to produce CMOS sensor images; however, CMOS sensors are capable of capturing images more quickly (Thryft 2009; Zamora et al. 2011; Marin and Buszka 2013).

Digital Single-Lens Reflex (DSLR) cameras refer to a photography system that allows light to travel through the lens, bounce off an internal mirror and be either imprinted on the sensor, or sent to the viewfinder (Weiss 2009; Frey et al. 2011). DSLR

cameras with full-frame sensors allow for increased sensitivity, making them ideal for use in a professional setting (Robinson 2007; Gestring 2007; Frey et al. 2011).

There are many factors to take into consideration depending on the subject being photographed. However, understanding the exposure pyramid will provide a strong foundation for capturing the most appropriate image. The three components to be taken into consideration include; the shutter speed, the aperture or f-number, and the 'film' speed (ISO) (Robinson 2007; Frey et al. 2011). Each component has a unique role during the process of photography. The shutter speed specifically refers to how quickly or slowly the camera shutter opens and closes, which determines how much light enters the camera. The aperture of the lens is represented by an 'f-number' and is responsible for determining the amount of light that is let through the lens; when the 'f-number' is increased while the shutter speed remains the same the resulting photograph would be darker, whereas if the 'f-number' was decreased while the shutter speed remained the same the resulting photograph would appear brighter. Adjusting the size of the aperture can let more or less light into the camera for a variety of exposure rates; additionally, the aperture is also responsible for the depth of field of the subject in a photograph. Similar to the iris of an eye, a shallow depth of field (larger aperture diameter opening) is capable of focusing on a particular subject while other subjects at further distances will appear unfocused or blurry. Alternately, an increase in the depth of field (smaller aperture diameter opening) will allow subjects in the foreground and the background to appear clearly (Weiss 2009; Duncan 2010).

Finally, the ISO (International Standard Organization) is a rating of the ‘film’ speed. Slower film speeds (100/200 ISO) require more light to capture the image and have a higher resolution; whereas faster film speeds (400/800/1000 ISO) have lower resolution but require less light in order to capture an image (Gestring 2007; Robinson 2007). Slower ISO speeds can display better colour rendition and finer pixel detail but are not recommended for low-light situations (Weiss 2009). Faster ISO speeds are capable of capturing information in low-light scenarios with contrast enhancement to compensate for less available light; however, there is an increased risk of camera ‘noise’. Noise can be described as the excessive information being picked up by the sensitive camera sensor and can appear in a photograph as ‘light’ or ‘dust’ particles which were not present at the time of photographing. This is simply a degradation of the image by the sensor’s inability to discern certain details or the longer signal processing of an image (Weiss 2009).

2.1.1. Documentation Photography

Documentation photography can be described as recording an accurate representation of a subject. Two components need to be taken into consideration in documentation photography; vision and perception (Weiss 2009). Vision is a mechanism that allows information from the world to be processed and subsequently analyzed; perception is an awareness of a subject through past-experiences (Weiss 2009). Specific visual elements such as perspective, lighting, contrast, and colour all need to be taken into consideration for an accurate representation. Understanding the importance of potential influences can aid in producing the most unbiased and accurate images. There needs to be

a connection between images and reality that takes different environments and conditions into consideration (Milliet et al. 2014). There are multiple variables which need to be addressed in terms of proper documentation photography.

One of the variables that needs to be addressed in documentation photography are file formats. There are several different types of file formats in which photographs can be saved either in the camera or stored externally. The most common type of file format is the JPEG (Joint Photographic Experts Group) and is considered a form of 'lossy compression' (Robinson 2007; Weiss 2009). In order to make files smaller, higher compression ratios are used which actively discard data. Externally, any enhancements made to a JPEG image which are saved discard even more information which cannot be recovered (Robinson 2007; Weiss 2009). For purposes of documentation photography, TIFF (Tagged Image File Format) or RAW file formats are recommended as they are uncompressed image files and therefore lossless (Weiss 2009; Frey et al. 2011; Rai and Kaur 2013). TIFF images are used for capturing and storing images in Adobe Photoshop, where editing and saving can occur without compression loss (Robinson 2007; Weiss 2009; Frey et al. 2011).

Another variable for an accurate representation of a subject being photographed would be the focal length. The focal length refers to the angle of view and magnification of the subject being photographed. A longer focal length will depict a narrower angle of viewing and a higher/greater magnification. Also known as telephoto images, subjects in the distance appear closer than they actually are. As well, 'pin cushion' distortion can occur and would not be considered an accurate representation of the subject (Gestring

2007; Frey et al. 2011; Rai and Kaur 2013). Shorter focal lengths have a wide angle of view and a lower rate of magnification. Wide angle images, or 'fish-eye', exhibit a form of barrel distortion which usually affects the edges of the frame and are not an accurate representation of the subject (Gestring 2007; Frey et al. 2011). The typical focal length of 50mm would result in an image without distortion, however, the angle of view should be calculated for the sensor being used as it compares to a standard full-frame 35mm sensor. For example, the physical dimensions of certain Nikon sensors are approximately 23.7mm x 15.6mm (Weiss 2009) whereas the dimensions of a 35mm full-frame sensor would be 36mm x 24mm. This would mean that the angle of view for the 35mm full-frame sensor is approximately 1.5 times larger than the smaller Nikon sensor (Weiss 2009). In order to capture the same subject area, this would be the difference between using a 50mm lens for the 35mm full-frame sensor, and an 80mm lens for the smaller Nikon sensor (Weiss 2009). These adjustments should be taken into consideration for an accurate representation of a subject.

Colour temperature can affect the accuracy of images if the incorrect white balance has been used during the photographing process. The white balance is an internal reference which will inform the camera of what is truly white under specific lighting (colour temperature) conditions (Weiss 2009). The colour temperature refers to the standard colour of light emitted at a specific temperature measured in kelvin (K) (Frey et al. 2011). Lower temperatures with less energy and longer wavelength ranges appear 'warm' and 'reddish'; such as a tungsten light source (3200 K) (Frey et al. 2011). Colour temperatures with greater energy levels and shorter wavelengths tend to appear 'cool' and

'bluish' such as daylight (~6000 K) (Frey et al. 2011). The temperature of white light (or an electronic flash) is approximately 5500K for comparison (Weiss 2009). Setting the incorrect white balance for specific light sources can result in a bluish or reddish image and an inaccurate representation. Awareness of all the aforementioned issues is needed in the field of documentation photography in order to produce an accurate representation of a subject.

2.1.2. Forensic Photography

Forensic photography is a specialized field of documentation photography that can be applied to any situation which might appear in a court of law. There are several fields of forensic photography including; crime/death scene photography, autopsy photography, and evidence photography (Weiss 2009; Marin and Buszka 2013). Evidence photography can be used in both a field and lab setting. For example, evidence would first need to be photographed at the scene before being moved, while additional photography techniques could be applied in the lab after scene removal. Images obtained in the field of forensics can be classified as referential, post-referential and non-referential (Shapter 2014). Non-referential tends to be limited to computer-generated images and are not often associated with forensics, whereas referential and post-referential are more common in this field. Referential photography simply refers to the accurate representation of an object as it has been photographed; additional enhancement to images using photography specific computer software can be classified as post-referential (post-processing) (Shapter 2014).

Specific forensic photography techniques and proper procedural conduct for post-referential photography will be discussed next.

The procedures of forensic photography follow documentation photography techniques with several added components. The use of references, case numbers, scales and rulers are standard in the field of forensic photography. Scene photography tends to use references (telling a story as photographs are taken through a scene) in order to view a set of images as if they could be compiled into a video. Autopsy and evidence photography utilize case numbers (scales/rulers when needed) in order to accurately document evidence, and attribute specific photographs to specific cases. ABFO rulers (American Board of Forensic Odontologists) are specially designed to provide an accurate system of measurement when photographing trace evidence and injuries (Dyer et al. 2004; Weiss 2009; Wright and Golden 2010; Rai and Kaur 2013). Rulers can show whether the camera is perpendicular to the subject being photographed and should be placed on the same plane of height as the detail being focused on.

There are specific types of evidence which are often photographed using a ‘copy-stand light table’ that requires a stationary set-up. The copy stand (Figure 1) consists of a flat surface, made of grey board or glass, with an adjustable metal arm which would allow the camera to be mounted with the lens facing perpendicular to the table top. On either side of the table are adjustable light sources (usually tungsten bulbs) that can be manually switched on/off for potential oblique (side) lighting (Frey et al. 2011). This table allows the camera to be perpendicular and stationary to the subject, while also being able to adjust camera height to the subject. In addition, oblique lighting can potentially be used in

order to enhance the definition of specific details when the light is coming from one direction (Adair 2006; Weiss 2009; Frey et al. 2011; Marin and Buszka 2013). The angle of the light source can affect the amount of shadow being cast off detail on the subject, and should be taken into consideration so as not to obscure potential information.



Figure 1. Copy-stand with tungsten light sources and mounted camera (example).

Finally, photographs themselves can be considered to be a form of secondary evidence which can be submitted to a court of law and it is important that both referential and post-referential images contain supporting information. Metadata consists of the electronic information that can be found when a specific image is created. This information is available for all file format types and includes date/time, camera settings, camera model/make, aperture settings, shutter speed, focal length, metering mode, ISO, and additional descriptions and copyright information (Weiss 2009; Frey et al. 2011). For post-referential image processing, metadata can be found in photography computer software such as Photoshop, which can be accessed and submitted along with the images.

There are several rules that should be followed in order to avoid complications in a court of law. All original photographs should be retained and unaltered, with no photograph deletions in order to keep the photographs sequential numbers. Post-referential enhancements should be saved as a separate file, and all metadata settings should be enabled in order to record all enhancements along with the proper date and time signatures.

2.1.3. High Dynamic Range Photography

There are a variety of techniques used by photographers working in the art conservation world, as well as artistic photographers, which can be applied in certain instances to the field of forensic photography. One of these techniques is known as High Dynamic Range (HDR) photography. HDR refers to the range of photographs taken at different exposure values of the same subject and the resulting merged image obtained using a post-referential program (Daly et al. 2013). This technique is often referred to as exposure bracketing; however, for the purpose of consistency, the term HDR will be used for this research. Exposure refers to the total amount of light which is allowed to enter the camera and be exposed to the internal sensor. The exposure value (EV) function on a camera is a simple to use substitute for manually adjusting the shutter speed/aperture combination to reduce/increase light entering the camera (Wagner and Miskelly 2003a; Weiss 2009). Exposure value is a measurement of the amount of change that has occurred in terms of light compensation. For example, if an image appears too bright the exposure value can be adjusted to reduce the amount of light entering the camera. The result is

displayed as a negative number (eg. -1 EV). The same process can be accomplished with an image that appears too dark by adjusting the exposure value to increase the amount of light entering the camera. The resulting photograph will appear brighter with a positive exposure value number (eg. +1 EV). High Dynamic Range photography uses the mechanics of adjusting only exposure values, while maintaining constant camera settings. The result would be five photographs identical in positioning and focus, but with each image representing a different exposure value (Sedgewick 2008; Albanese and Montes 2011). Two of the underexposed photographs would be displayed as -1 EV and -2 EV while two of the overexposed photographs displayed as +1 EV and +2 EV. One photograph would remain unaffected by the adjusted exposure values and is displayed as 0 EV (Miskelly and Wagner 2005; Daly et al. 2013). Any number of exposure values can be photographed but typically three or five photographs are taken using HDR (exposure bracketing). The next step for these photographs would be to overlay the five images in a post-referential program (Figure 2).



Figure 2. Example of High Dynamic Range photography (right) compared to one single photograph at normal exposure (left).

The resulting image would emphasize details that might not have been visible from a standard photograph (Wen and Chen 2004; Miskelly and Wagner 2005; Banterle et al. 2009; Albanese and Montes 2011). HDR photography has become very popular in the photography world as it is user friendly for both professional and amateur photographers. Scientific research into the applications and specific experimentations using HDR photography are limited but have increased recently with advances in both camera and post-referential technology (Park et al. 2005; Sedgewick 2008; Frey et al. 2011; Albanese and Montes 2011).

2.2. 'Multi-Spectral' Photography and Alternate Light Source Photography

Multi-spectral photography has many different meanings depending on the discipline being discussed. In the world of art conservation and restoration the term 'multi-spectral imaging' generally refers to the multiple light spectra (Figure 3) that can be utilized to document pieces of art work (Cosentino 2014).

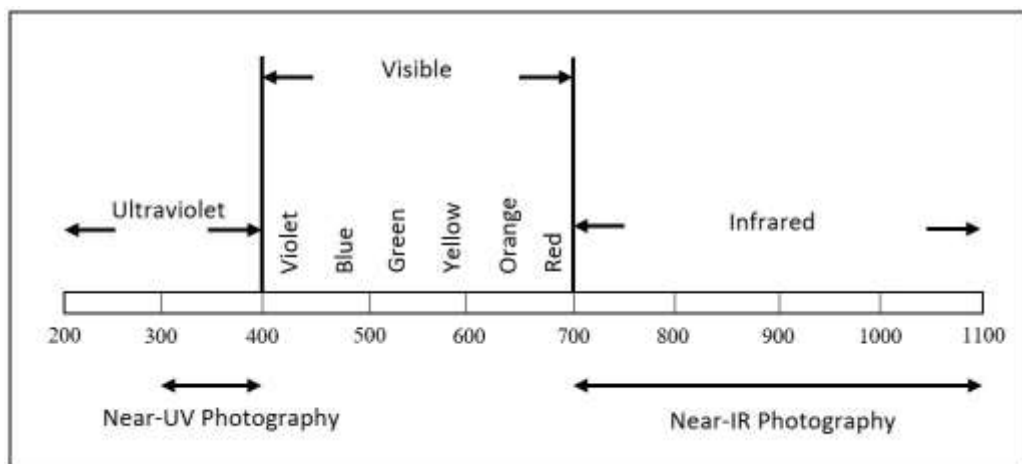


Figure 3. Electromagnetic spectrum depicting multi-spectral photography capabilities from the near-ultraviolet to near-infrared light spectrum (Adapted from Williams and Williams 1993).

Art conservators will state that documentation can occur in both the ‘Multi-Spectral’ or ‘Hyper-Spectral’ region of the light spectrum (Frey et al. 2011; Cosentino and Stout 2014), but the terminology varies between this discipline and the field of forensics. In the context of forensics and specifically forensic photography, multi-spectral photography consists of photographing in the near-ultraviolet light spectrum, the visible light spectrum and the near-infrared light spectrum (Miskelly and Wagner 2005; Wright and Golden 2010). Art conservators use both photography and other forms of specialized imaging equipment to document subjects; any imaging going beyond the capabilities of standard photography is defined as hyper-spectral imaging (Cosentino 2014). Infrared reflectography, a form of hyper-spectral imaging, occurs in the range of the short-wave infrared region from 1100 to 1700 nanometres and requires the use of a specialised camera known as the InGaAs Imager (Frey et al. 2011; Cosentino 2014). This form of hyper-spectral imaging could be further researched in other field of evidence analysis.

In the field of forensics the term ALS is widely used and often incorrectly applied as the same meaning as multi-spectral photography. ALS or Alternate Light Source photography technically refers to instances when forensic light sources are being used. However, not all photography techniques for specific light spectrums will necessarily use forensic light sources and/or modified cameras or additional filters (Golden 1996; Wright and Golden 2010). Although the term ALS is prevalent in the field of forensic photography, it would be more accurate to adopt a generic term for describing the sub-field of photography techniques that covers multiple light spectrums. Multi-spectral photography techniques could include reflective infrared photography, reflective

ultraviolet photography and fluorescence photography for the documentation of evidence. These techniques have the potential to be able to capture information that would not be available through standard photography.

2.2.1. Reflective Ultraviolet Photography

Ultraviolet (UV) photography is a useful technique that can be used in the field of forensics. The term ultraviolet photography can be broken down into two different techniques; fluorescence when illuminated with ultraviolet light and reflective (reflected) UV photography. A simple definition of reflective UV would be to record the nonvisible UV wavelength that has been reflected by an object photographically, while fluorescence is photographed as the excitation of molecules, and subsequent relaxation, resulting in light emission in the visible light spectrum (Mairinger 2000a; Richards 2010). The ultraviolet range of the electromagnetic spectrum is described in Table 1 but the range of interest for photography is the near (long wave) ultraviolet (UVA). The definition of spectral ranges differ in the research between physics and biology, but for consistency the spectral ranges used in the field of physics will be referenced in this research (Williams and Williams 1993; Mairinger 2000a; Sanfilippo et al. 2010; Verhoeven and Schmitt 2010).

Table 1. Ultraviolet range of electromagnetic spectrum. (Adapted from Williams and Williams 1993; Mairinger 2000a).

Ultraviolet Band (Physics)	Spectral Range (nm) ~Approximately	Ultraviolet Band (Biology)	Spectral Range (nm) ~Approximately
Near (long wave)	~320 – 400	UVA	~310 – 400
Middle	~280 – 320	UVB	~280 – 310
Far (short wave)	~200 – 280	UVC	~185 – 280
Vacuum	~10 – 200	UVD	~10 – 185

Reflective ultraviolet DSLR photography can be considered more difficult than film photography due to the fact that unlike specific types of film, the electronic sensor used to capture the image in digital photography is sensitive to both ultraviolet radiation and near infrared radiation. If both types of radiation are present during photography the infrared radiation will overwhelm the ultraviolet response (Williams and Williams 1993; Sanfilippo et al. 2010; Garcia et al. 2014). When photographing strictly in the ultraviolet spectrum, eliminating any potential infrared radiation light source is one of the first steps in reflective ultraviolet photography with a DSLR camera.

Unlike fluorescence photography, reflective ultraviolet photography requires a modified DSLR camera in order to properly record the UV image. Modern DSLR cameras contain a built-in UV/IR blocking filter mounted onto the camera sensor. This filter can either be professionally removed from the sensor, or a specific UV/IR manufactured DSLR camera can be purchased (Sanfilippo et al. 2010; Garcia et al. 2014). Another variable to take into consideration is the material used for the lens and how the transmission rate might affect capturing the image. Typically, lenses are made of glass and have a cut-off transmission of ~ 340 nm (Krauss 1993; Mairinger 2000a). Additionally, modern lenses have anti-reflection coatings which may exhibit fluorescence when in contact with ultraviolet light (Mairinger 2000a) and cause degradation in imaging ability. Finally, UV light transmission through a glass lens creates a focal shift due to the refraction of light from a wave-length shorter than visible light (Frey et al. 2011). The resulting image will not appear as sharp (in focus), but can be compensated for by

decreasing the aperture and creating a greater depth of field for a sharper image (Williams and Williams 1993; Mairinger 2000a; Sanfilippo et al. 2010).

Other types of lenses used in reflective ultraviolet photography are quartz-silica or fluorite lenses capable of transmitting further into the ultraviolet region (~200 nm) and also into the near infrared region (~1000 nm) (Krauss 1993; Mairinger 2000b; Sanfilippo et al. 2010). A quartz lens specifically manufactured for UV/IR photography is capable of transmitting more ultraviolet radiation than a glass lens, and the transmission of UV light through a quartz lens does not require adjustment for focal shift (Mairinger 2000a). Although glass lenses can be used in reflective ultraviolet photography, quartz manufactured lenses have greater transmission capabilities.

The sensitive nature of the DSLR camera sensor will allow any available infrared radiation to be recorded in the image and potentially overwhelm the ultraviolet light. Since many ultraviolet light sources also emit some infrared radiation, a filter needs to be positioned over the lens. In reflective ultraviolet photography a barrier, commonly called a bandpass filter, is used to allow ultraviolet light transmission, while blocking light in the visible and infrared regions (Miskelly and Wagner 2005; Sanfilippo et al. 2010; Richards 2010). Bandpass filters have a `red-leak` in the near infrared region (Sanfilippo et al. 2010) however, specific filters have significantly reduced infrared transmission percentages. One of these filters is the Baader-U (Baader Venus) bandpass filter originally designed to be mounted on a telescope for reflective ultraviolet photography of the planet Venus (Williams and Williams 1993; Sanfilippo et al. 2010). The transmission range of this filter is between 300/320 – 400 nanometres with a peak of approximately

~75% at 360 nm, as well as a weak red-leak between 700 – 900 nm (Company Seven Astro-Optics Division 2016) (Figure 4).

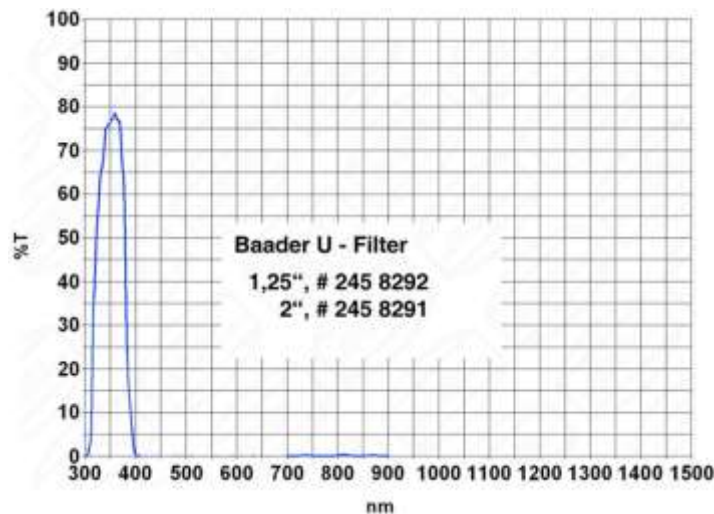


Figure 4. Transmission spectra of the Baader-U (Baader Venus) Bandpass filter (Company Seven Astro-Optics Division).

The final component needed for reflective ultraviolet photography is a light source capable of emitting ultraviolet radiation, and preferably having low or no infrared radiation emission. Sunlight, fluorescent tubes, mercury vapour lamps, electronic flash units, UV LED lights and Wood`s lamps are all sources of ultraviolet radiation (Mairinger 2000a; Nelson and Santucci 2002; Rai and Kaur 2013). Sunlight is a strong source of UV radiation however; it is not practical due to changing spectral intensities and additional emission of infrared radiation (Mairinger 2000b). Preferable sources of ultraviolet radiation would be gas discharge lamps, with stable radiation emission and constant intensity, which would include mercury lamps, fluorescent tubes, metal halide lamps, and the Wood`s lamp (Rai and Kaur 2013; Mairinger 2000a; Williams and Williams 1993). The Wood`s lamp has a broadband spectral emission between 325-400 nm with a peak at approximately 360 nm (Nelson and Santucci 2002; Wawryk and Odell 2005) and is a

popular light source used in dermatology. The combination of all of these components allow for an image to be taken in the ultraviolet region of the electromagnetic spectrum (Figure 5).

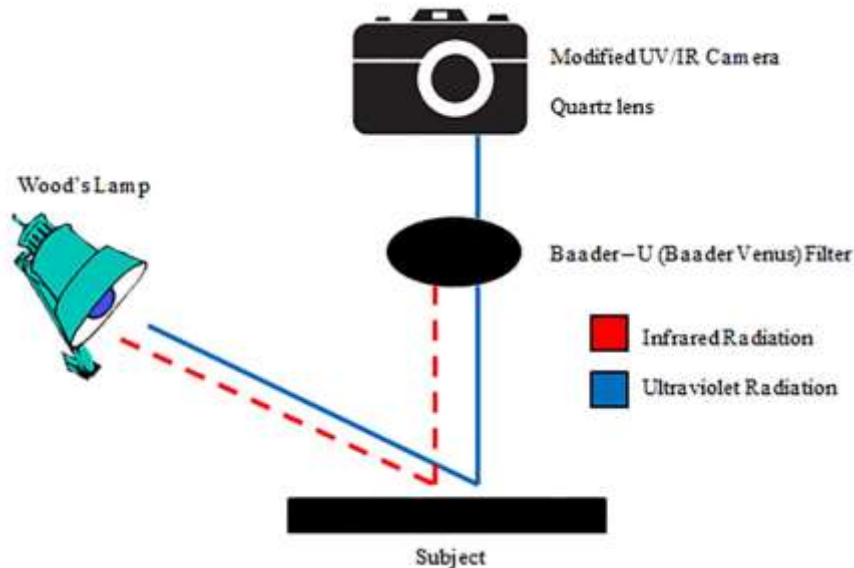


Figure 5. Reflective ultraviolet photography set-up depicting the recording of a subject using a Wood's lamp UV light source, Baader-U filter and modified UV/IR DSLR camera with quartz lens (Adapted from Frey et al. 2011).

Images captured using reflective ultraviolet photography will show several potential responses to the ultraviolet radiation. In particular, bloodstains have a wide spectral range of absorption (~300 – 900 nm) with a peak around 415 nm. This spectral range extends into the ultraviolet light spectrum and results in bloodstain patterns absorbing the ultraviolet radiation and appearing dark in contrast with a potential reflecting background (Stoilovic 1991; Lee et al. 2013) (Figure 6).

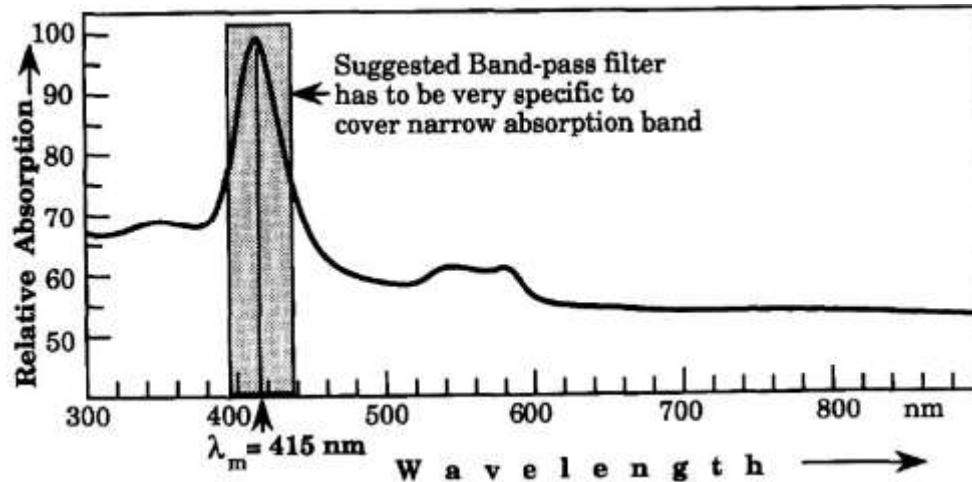


Figure 6. Spectral range of blood with a peak at approximately 415 nanometres (Stoilovic 1991).

2.2.2. Fluorescence Photography

Fluorescence photography occurs in the visible light spectrum and does not require a modified digital camera to document evidence. Therefore, an unmodified DSLR camera and glass lens can be used to photograph the subject. Fluorescence is the process of light emission after molecular excitation upon exposure to high energy incident light, such as ultraviolet light. The light source causes certain molecules to become excited which in turn causes some of their electrons to rise from the ground state to a higher electronic state. As these electrons return to the ground state, energy is released in the form of light. The light that is emitted has a longer wavelength and lower energy than the incident (excitation) light source, and can be seen and photographed as a different colour/intensity (Hooker et al. 1991; Golden 1996; Robinson 2007; Richards 2010). This wavelength shift between excitation and emission is known as the Stokes Shift (Figure 7) and is the result of some energy loss due to non-radiative processes.

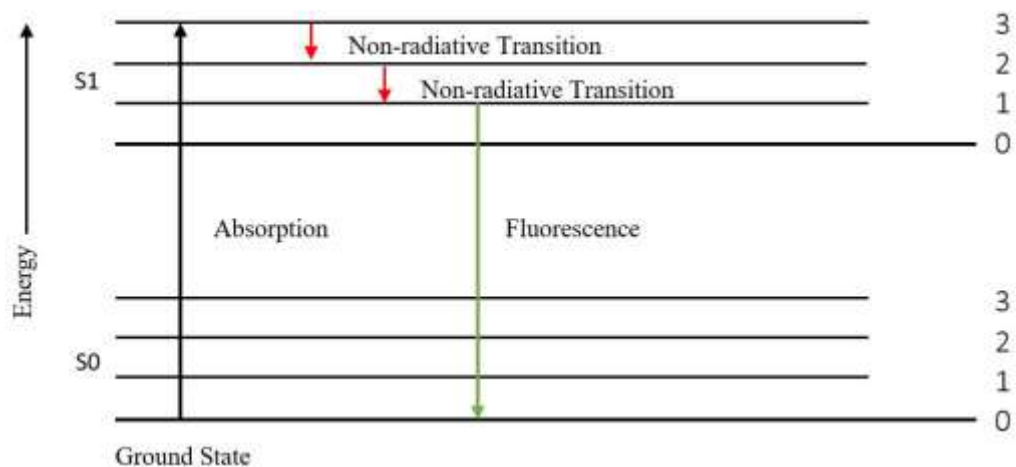


Figure 7. Molecular excitation from a specialized light source and release of fluorescence (Adapted from West et al. 1992).

Fluorescence emission is weaker in intensity than the incident light source. Therefore, a filter needs to be placed over the camera lens in order to block out the stronger wavelength of the light source, but allow the weaker fluorescence to pass through (Robinson 2007; Rai and Kaur 2013). Some of the filters used in fluorescence photography include yellow, orange, and red longpass filters (Schulz et al. 2007; Castro and Pelosi 2008). A longpass filter will allow light of wavelengths above the cut-off value to be transmitted at a specific nanometre and above to be transmitted and subsequently recorded on the camera sensor. In the visible light spectrum, the wavelengths of light in the yellow band are slightly shorter than those in the orange band, and the wavelengths of light in the orange band are slightly shorter than those in the red band. The spectral cut-off wavelengths for the yellow, orange and red filters can be seen in (Figure 8) and show peaks at approximately 490 nm, 565 nm, and 600 nm respectively (Stoilovic 1991; Schulz et al. 2007; Limmen et al. 2013).

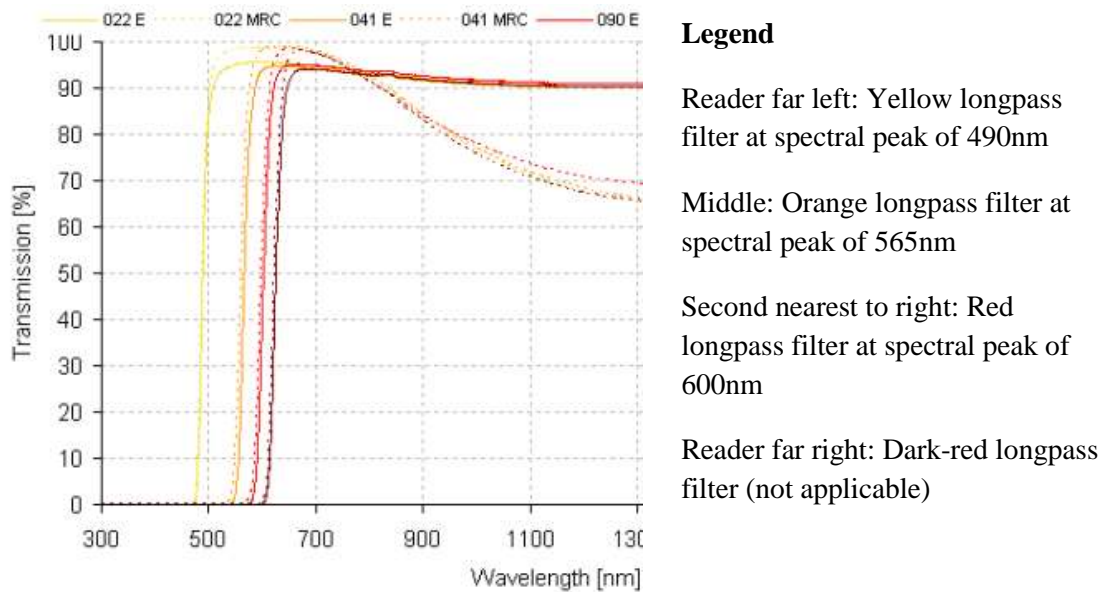


Figure 8. Spectral profiles of yellow, orange, red longpass filters (Schneider Kreuznach Company).

The light sources used in fluorescence photography vary in spectral range and intensity depending on certain variables such as the subjects being photographed, and high-quality/high-cost equipment being used. The term Alternate Light Source (ALS) and Forensic Light Source (FLS) should only be applied when describing the light source being used. Some types of light sources include; argon ion lasers, mercury arc lamps, xenon arc lamps, and UV light emitting diodes (LED) (Hooker et al. 1991; Castro and Pelosi 2008; Lee et al. 2013). Specific light sources are classified through these categories and might include; ‘crime-lites’, Lumatec super-lite, Polilight[®], and SPEX Crimescope (Schulz et al. 2007; Seidl et al. 2008; Limmen et al. 2013). Many LED light sources are only capable of emitting a narrow bandwidth of light (e.g. ~410 nm) and have weak intensity; therefore, these are usually used during initial crime scene searches (Limmen et al. 2013). Other light sources are considered tunable, where specific nanometre

wavelengths can be chosen (Seidl et al. 2008). The SPEX Crimescope is a xenon arc lamp with a 500 Watt bulb and a spectral range of 300 – 670 nm, with specific bandpass filters at; UV 300 – 400 nm, 415 nm, 445 nm, 455 nm, 475 nm, 495 nm, 515 nm, 535 nm, 555 nm, SP575 nm, 600 nm, 630 nm, and 670 nm (SPEX Forensics). SP575 nm is a short-pass and not a single bandwidth setting. Whereas longpass refers to light from a specific wavelength and up being allowed to pass through the filter, short-pass is the transmission of light up to a specific cut-off wavelength (e.g. all bandpass before 575 nm are transmitted).

If a particular source does not fluoresce it is possible that it absorbs the light source and any potential documentation can be accomplished by determining the parameters that best showcase the contrast between an absorbing source and fluorescing background. Some bodily fluids, household or industrial chemicals, and certain fruit and vegetable juices can fluoresce under specific light sources (Hooker et al. 1991). Blood does not fluoresce when illuminated by the radiation from an alternate light source, instead, a contrast between the absorbing blood, and fluorescing background must be determined. Specific research has stated that the best wavelength for photographing bloodstains is between 410 – 455 nm, with a peak around 415 nm, as these produce the best contrast with a fluorescing background (Stoilovic 1991; Seidl et al. 2008; Wagner and Miskelly 2003b; Lee et al. 2013). The alternate light source, with a specific bandpass wavelength and longpass coloured filter are used in fluorescence photography for the documentation of fingerprints, false documents, bruising, bite-marks, and bloodstains (Figure 9).

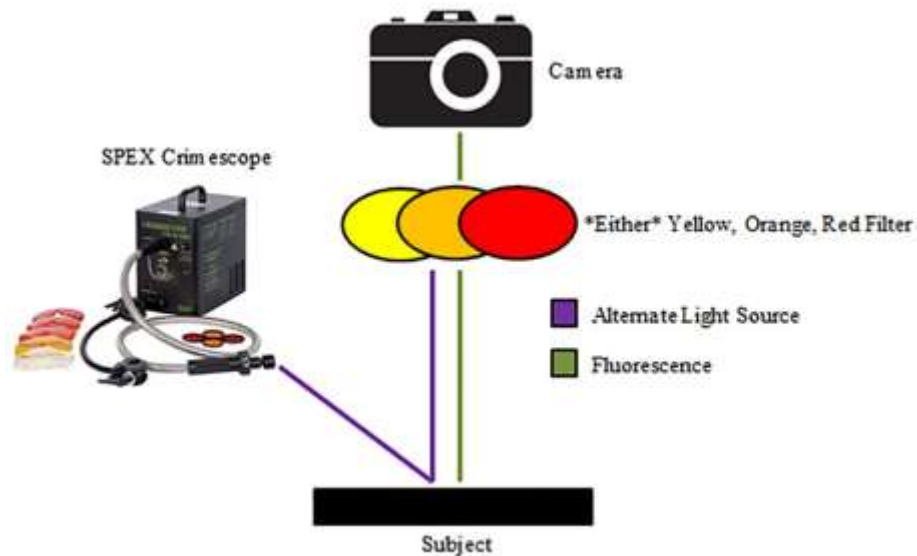


Figure 9. Fluorescence Photography using the SPEX Crimescope (Adapted from Frey et al. 2011).

2.2.3. Reflective Infrared Photography

Reflective infrared (IR) photography works on the same principles as reflective ultraviolet photography except the range of reflective infrared photography is in the near-infrared region (700 – 1100 nanometres) (Robinson 2007; Mangold et al. 2013). Wavelengths beyond 1100 nm are associated with thermal infrared radiation and extend into the radio wave region spectrum (De Broux et al. 2007). There are several different ways that a substance could react to infrared radiation from a light source. If the substance absorbs the IR light it will darken or remains dark in the image. In contrast, a substance might reflect IR light and appear to lighten in colour or tone often appearing to turn light grey (Mairinger 2000b; Robinson 2007). If the substance is capable of transmitting IR light then it may disappear from the image allowing other substances not capable of transmitting infrared radiation to be recorded (Robinson 2007; De Broux et al.

2007). Blood will absorb infrared light and appear darker in colour/tone if the surface it is located on reflects or transmits infrared radiation (De Broux et al. 2007; Howard and Nesson 2010; Farrar et al. 2012; Schotman et al. 2015). However, if blood is located on a surface which also absorbs infrared radiation, the contrast between the two is more difficult to observe (Li, Beveridge et al. 2014).

Reflective infrared photography requires the use of a modified DSLR camera that has either been manufactured without the UV/IR blocking filter over the internal sensor, or has had the filter removed. Over the past decade, infrared photography has gained in popularity in the professional and amateur photography world and various companies offer to modify DSLR cameras for use in infrared photography (Mairinger 2000b; De Broux et al. 2007). This modified camera is capable of photographing in both the ultraviolet light spectrum, as well as the infrared light spectrum, as long as an IR filter had not been placed over the internal sensor of the camera (Mangold et al. 2013; Schotman et al. 2015). Similar to reflective ultraviolet photography, the same issue arises when photographing with a glass lens in the infrared light spectrum. The longer infrared wavelengths are refracted by the glass lens at a different index than visible light wavelengths, resulting in an unfocused image (Frey et al. 2011; Mangold et al. 2013). Older lens models often had a 'red-dot' located on the lens to mark the appropriate infrared focal shift, but newer lens do not usually have this aid (De Broux et al. 2007; Frey et al. 2011). The issue with focal shift can be overcome in the same way as with reflective ultraviolet photography by using a quartz-silica based lens capable of

transmitting into the infrared region to approximately 1000 nm (Krauss 1993; De Broux et al. 2007).

Reflective infrared photography requires a light source that emits infrared radiation, and filters that will allow the radiation through the lens to be imprinted onto the sensor, but block out the visible light also being emitted from the light source. Unlike reflective ultraviolet photography, there are multiple different reflective infrared filters that can be used. These filters are typically referred to by their Wratten rating as the standard (Perkins 2005; De Broux et al. 2007) and are responsible for transmitting a different range of wavelengths in the infrared spectrum at specific transmission percentages. Peca brand filters have a complete set commercially available and are often used in forensic photography and the spectral output and transmission percentages can be found in Appendix 2.2.3.

The Wratten 70 filter does allow some visible red light into the camera but only a small portion of the longer red wavelength of the visible light spectrum (Perkins 2005; De Broux et al. 2007; Schotman et al. 2015). The introduction of visible light will overpower the infrared radiation being recorded on the DSLR sensor so the correct IR filter is important for accurate reflective infrared photography.

The light source used in reflective infrared photography needs to contain a high amount of IR radiation which is readily available from a multitude of sources. Sunlight and electronic flash units produce radiation at around 760 nanometres (Raymond et al. 1986) whereas tungsten light sources and halogen light sources produce radiation at a peak of 900 nanometres (Raymond et al. 1986; Mairinger 2000b). Sunlight is a natural

source of light but can be irregular in emission depending on time of day and weather conditions. Electronic flash units with a xenon tube are a good source of infrared radiation and are often used in biomedical analysis (De Broux et al. 2007; Mangold et al. 2013). Tungsten lights, incandescent bulbs, and halogen light sources all generate a certain amount of heat which needs to be taken into consideration if the light source is required to stay on for a longer amount of time (De Broux et al. 2007; Rai and Kaur 2013). The spectral output of a tungsten light source is shown in Figure 10 and can be considered a commercially available source of infrared radiation.

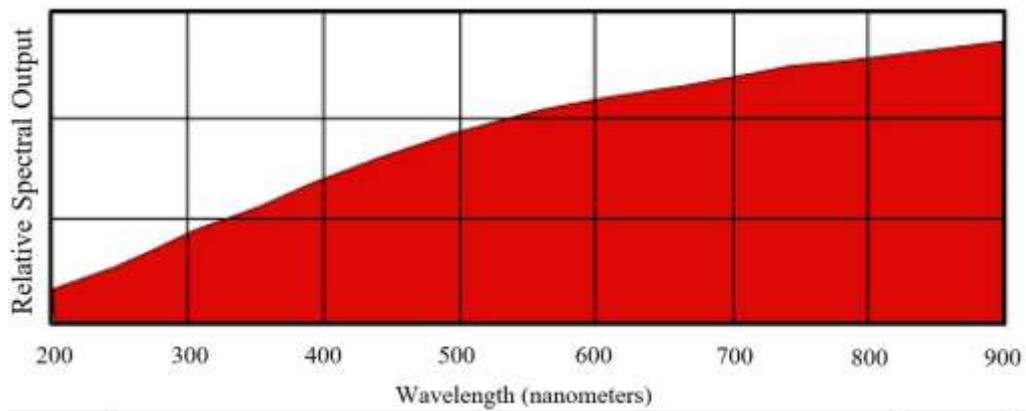


Figure 10. Spectral output of a tungsten light source (Adapted from Williams and Williams 2002).

The method for documentation of images in reflective infrared photography is identical to reflective ultraviolet photography except for the light source and filters. The infrared light source emits a small amount of ultraviolet radiation, but mostly visible light and infrared light. Unlike reflective ultraviolet photography, there is no need to attempt to block the ultraviolet radiation as the infrared radiation being emitted will over-power it. However, any visible light being emitted from the light source needs to be blocked by an infrared filter (Figure 11).

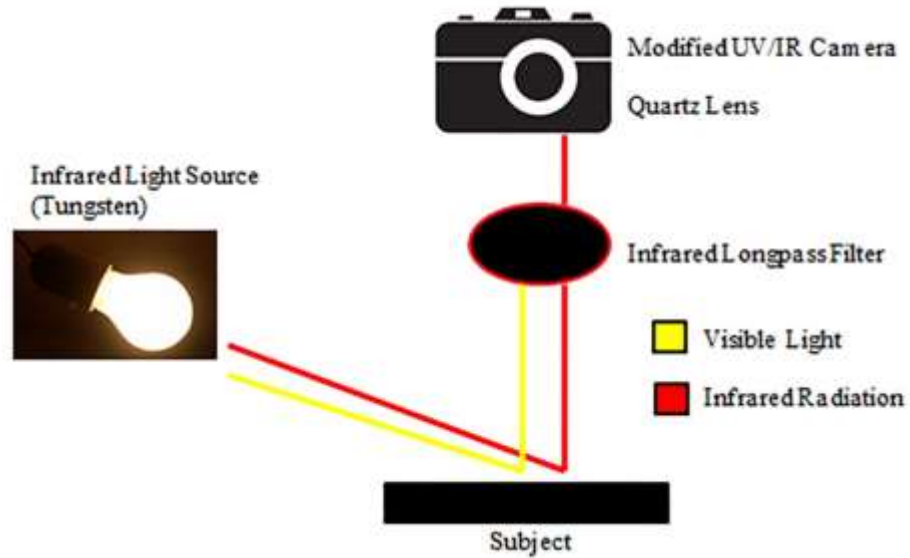


Figure 11. Reflective infrared photography with a tungsten light source and longpass filter (Adapted from Frey et al. 2011).

2.2.4. Image Editing Software for Photography Analysis

In the field of forensic photography it is ideal if a subject being photographed remains at the referential stage (Shapter 2014) for an accurate representation. However, there are several instances where post-referential (Shapter 2014) photography analysis and editing can be applied as image enhancement or processing. Image enhancement is most often used to emphasize a latent characteristic of importance from a piece of evidence (eg. fingerprints, written notes, obstructed labels) but it can be applied in a multitude of situations (Banterle et al. 2009; Frey et al. 2011; Consentino 2014).

There are many different types of image editing software commercially available, as well as no-cost alternatives. However, the most widely used and accepted software package in the field of forensic photography is Adobe Photoshop (Adobe Systems Incorporated). Adobe Photoshop is capable of supporting metadata, colour management

and RAW file processing (Sedgewick 2008; Frey et al. 2011) as the bare requirements needed in a software program for forensic photography. Using a program known and accepted in the industry is ideal when particular images are presented in a court of law (Garcia et al. 2014).

Research has been expanding into using scientific techniques for a quantitative analysis of image data using Photoshop, and other imaging systems such as ImageJ (Farrar et al. 2012; Consentino 2014; Garcia et al. 2014). It is possible to perform an analysis by measuring the pixel values of a specific area of interest using ImageJ (Garcia et al. 2014; Miranda et al. 2014), and this quantitative method of analysis might be useful when applied to complex coloured subjects such as paintings (Consentino 2014). Segmentation of relevant features from their background is another tool used to recognize changes in the image data (Park et al. 2005; Sedgewick 2008). Once these relevant features are identified and separated they can be measured in Photoshop or ImageJ (Sedgewick 2008; Miranda et al. 2014). Standardized technical procedures for this technique have not been prevalent in the literature but the potential ability to quantify image data for analysis and interpretation is important to take into consideration (Park et al. 2005; Sedgewick 2008). Quantitative analysis of image data is most often used for identifying important features in medical imaging (Wen and Chen 2003; Park et al. 2005).

Qualitative analysis of image data is common in the field of forensic photography and the procedures for post-referential enhancement are often more standardized than quantitative analysis (Sedgewick 2008; Banterle et al. 2009). As with any scientific field of study, it is important to keep a record of procedural steps so that the research can be

replicated. With the metadata option in Photoshop turned on, every action is recorded with a time/date stamp for a transparent working methodology, as well as keeping a record of any changes to the image (Sedgewick 2008; Frey et al. 2011). Both qualitative and quantitative analyses are important in the field of forensics, however, a lack of standardization in image data analysis can result in difficulty when it comes to defending a specific methodology in a court of law.

2.3. Bloodstain Patterns

Blood is referred to as a circulating tissue which passes through the heart, arteries, capillaries and veins (Christman 1996). It is responsible for transporting oxygen and nutrients to tissues, as well as carrying away waste products and carbon dioxide to be excreted (James et al. 2005). The physical properties of blood can aid the bloodstain pattern analyst in understanding how and why patterns are formed in specific ways. The composition of blood, response to breaching (an act of blood leaving the body through a traumatic event), and fluid dynamics are all important factors to take into consideration (Bevel and Gardner 2000).

Blood is a complex fluid that is comprised of several different components (Bevel and Gardner 2000). A representative sample of healthy humans shows that blood comprises approximately 8% of the total body weight, with the other 92% belonging to fluids and tissues. On average, there is approximately 5 to 6 litres of blood for male adults and 4 to 5 litres of blood for female adults based on body weight calculations (Bevel and Gardner 2000). The specific components of blood and their accompanying percentages

can be seen in Figure 12. The amounts of each component are relatively similar for healthy adult humans; however, those suffering from a severe medical condition might have compromised blood viscosity, resulting in altered bloodstain patterns (Bevel and Gardner 2000).

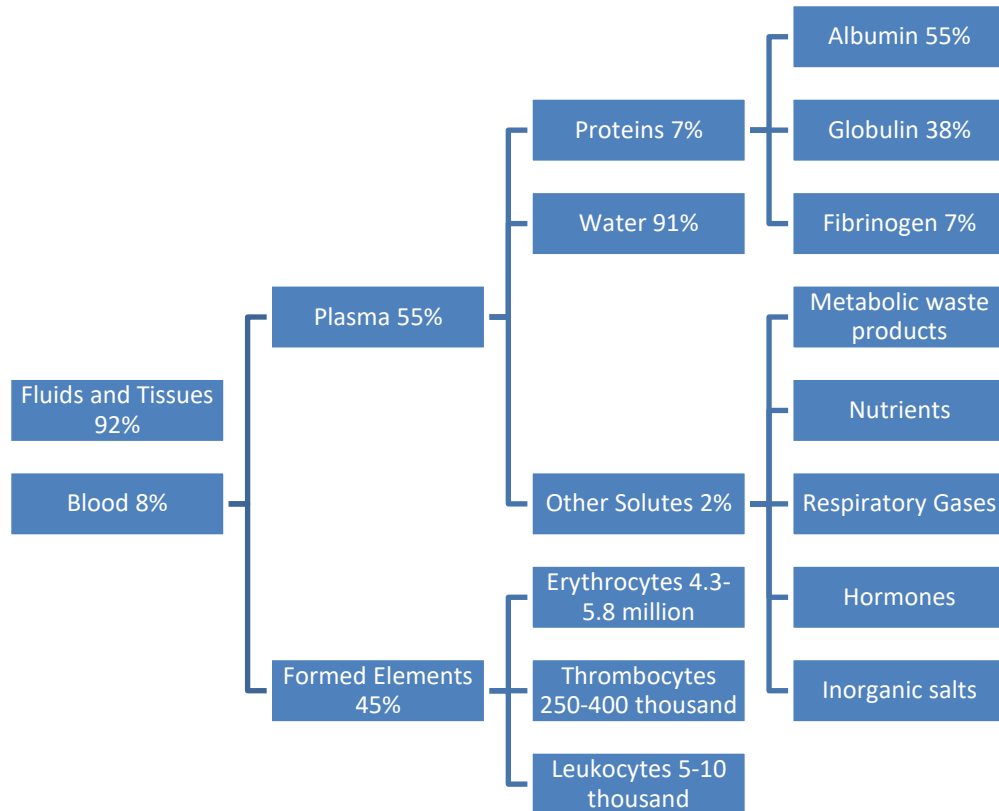


Figure 12. Average blood composition of a human adult per cubic millimetre (Adapted from Christman 1996).

Blood is comprised of two main components; plasma which makes up approximately 55% of blood, and formed elements which makes up approximately 45% of blood (Christman 1996; Bevel and Gardner 2000). Plasma is the fluid component of the blood and consists of mainly water, as well as proteins, organic acids, and inorganic salts (Bevel and Gardner 2000). Additionally, fibrinogen is located in the blood plasma

and is an important protein in the clotting process. Plasma is effectively responsible for transportation of cellular elements throughout the body (James et al. 2005) in a suspended medium.

Hemocytoblasts are manufactured in the bone marrow of the body and separate into the three formed elements: erythrocytes (red blood cells), leucocytes (white blood cells), and thrombocytes (platelets). Arterial red blood cells have been oxygenated and appear as a brighter red colour, whereas venous red blood cells appear darker in colour after depositing the oxygen molecules and picking up carbon dioxide (James et al. 2005). White blood cells are responsible for defending the body against pathogens, foreign organisms, and chemicals, and are additionally responsible for dead cell removal (Christman 1996). Finally, platelets are responsible for reacting to damaged blood vessels through clotting and are capable of forming blood clots both inside and outside of the body (James et al. 2005).

2.3.1 Properties of Blood

Understanding bloodstain characteristics and how they can be affected by the environment is an important factor for bloodstain pattern analysts. Blood is considered to be a non-Newtonian fluid where each blood drop separates and remains stable in droplet form through internal cohesion. A Newtonian fluid on the other hand forms through surface tension and tends to oscillate during flight (Wonder 2007). Blood does have the ability to act as a Newtonian fluid under specific circumstances, and potential oscillations in the droplet can be affected by size, viscosity and time. These factors must be taken into

consideration by the bloodstain pattern analyst during impact angle observations (Bevel and Gardner 2000; Wonder 2007).

There are three main physical properties of blood which are directly related to flight dynamics and the resulting bloodstain patterns; viscosity, surface tension and the relative density (gravity) of the blood (James et al. 2005). Viscosity can be described as the 'thickness' or 'thinness' of the liquid and can be categorized by the amount of resistance to shear as the fluid is in motion (Christman 1996; James et al. 2005). Pressure changes do not adversely affect the viscosity of the fluid; however, increased temperature can cause a decrease in fluid viscosity, while decreased temperature causes an increase in viscosity.

Surface tension is typically used to describe the levels of stress in the surface layer of a fluid (Chrisman 1996). Whereas the molecules in a liquid are freely moving, the spacing between them is spatially fixed by cohesive forces (James et al. 2005). This surface, which is created by the molecules, acts as a 'membrane' allowing for a pressure difference across an air-to-liquid surface such as an open container (i.e. a test tube) (Chrisman 1996). The differences in the relationship between surface tension and cohesion can be observed in the concave meniscus behaviour of the water surface, and the convex meniscus of the surface of blood (Wonder 2007). The relationship between surface tension and cohesion helps maintain the spherical shape of the blood droplet in flight.









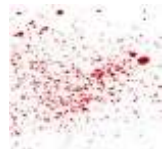
Relative density refers to the ratio of the density of a substance in comparison to water. If the substance has a relative density lower than water it will float in the water; or

if it has a relative density greater than the water it will sink (James et al. 2005). The term relative density has generally replaced the description of gravity forces on a liquid, however, the movement of external bloodstains as flow patterns and internal body pooling should be taken into consideration during analysis (Christman 1996). These three physical properties of blood are important to take into consideration when analyzing bloodstain patterns and the potential effects of the environment as a changing variable.

2.3.1.1. Types of Bloodstain Patterns

Bloodstain patterns can be classified into three general categories: passive stains, transfer stains, and projected (impact) stains (Bevel and Gardner 2000; Wonder 2007). However, terminology in the field of bloodstain pattern analysis is continually being changed and adapted and newer terminology (defined through the organization SWGSTAIN) needs to be taken into consideration. Passive stains can be described as pool, droplet, clot, saturation and blood flow patterns. Transfer stains refer to any method by which blood can be transferred from one substance to another. This could include swipes, wiping, and pattern stains (Bevel and Gardner 2000). Projected or impact bloodstains include spatter, cast-off (i.e. from a weapon) and arterial spurts/gushes (i.e. directly from the body). Blood spatter from projected (impact) events can be further subcategorized into three main types based on their relationship between the force used and size of blood drop diameter. These bloodstain patterns include low-velocity impact blood spatter, medium-velocity impact blood spatter, and high-velocity impact blood spatter (Table 2) (James et al. 2005).

Table 2. Examples of passive, transfer, and projected bloodstain patterns (Adapted from Wonder 2007).

Passive Stains		Transfer Stains		Projected Stains	
	Pool/ Saturation		Swipes		Low- velocity
	Droplet		Wiping		Medium- velocity
	Blood flow		Pattern stain		High- velocity

In addition to the general categories of bloodstain patterns, there are several miscellaneous stains that should be taken into consideration. Void stains, capillary stains, and fly spots can occur at a scene (Bevel and Gardner 2000) and should be taken into consideration by the bloodstain analyst during death scene reconstruction.

2.3.1.2. Bloodstain Analysis Techniques

The classification of bloodstain patterns is an important step in understanding the context of a death scene. Unfavourable environmental conditions and/or the presence of multiple bloodstain patterns have the potential to cause difficulty in analysis. The bloodstain pattern analyst should approach the complexity of the scene with overall observations before narrowing down analysis to single bloodstain pattern events (De Wael et al. 2008).

One of the challenges of bloodstain pattern analysis is the lack of standardized methodologies associated with pattern analysis (Arthur et al. 2015) between different countries and agencies. It is the responsibility of the analyst to recognize and classify the bloodstain patterns and their grouping characteristics, rather than the potential mechanisms used in their formation (Bevel and Gardner 2000; Arthur et al. 2015). After the bloodstain pattern groupings are identified, the formation of these patterns can be investigated. Using geometric principles of analysis a sequence of actions can be determined including the discovery of the point of origin (Kettner et al. 2014). Directional analysis of bloodstain patterns is a field of continuing methodological development. Mathematical theories are often based on the 'string method' and combine an understanding of the laws of motion, resolution of velocity and trigonometry instead of relying on qualitative analysis of droplet size and speed (Kettner et al. 2014). The 'string method' analyzes the width to length ratio of a blood droplet as it can be approximately related to its impact angle. By using this calculated angle of impact, a 'string' is drawn back from the resulting stain along this impact angle. This is done for multiple droplets and where the strings intersect is assumed to be the original source position for the blood event (Knock and Davison 2007). This technique does not take gravity into consideration which suggests that a combination of several methods can significantly increase the likelihood of positively identifying the point of origin belonging to the bloodstain pattern (Knock and Davison 2007).

2.3.2. Viable Substitutes for Human Blood in Research

Practical experimentation and research is an important aspect of any scientific field, including bloodstain pattern analysis. However, with increased knowledge pertaining to blood-borne diseases such as HIV, Hepatitis B and C viruses, and other pathogens, an alternative to human blood needed to be implemented (Raymond 1995). There are several important questions that need to be considered when determining the viability of a human blood substitute including: how do characteristics differ in composition; are there differences in flight trajectories; and are the resulting bloodstains different depending on the blood being used (Christman 1996).

Extensive research has been conducted in this particular field and generally includes studies of alternate mammalian subjects. There are additional studies in blood characteristics of amphibians (Palenske and Saunders 2002) in comparison to mammals which have concluded a lack of differentiation in blood viscosity between these two classifications. However, certain animals including llamas, birds and reptiles have nucleated red blood cells (these cells contain a nucleus whereas human blood cells do not) and as a result lack the volume needed for experimentation (Christman 1996). Most studies focus on the characteristics of mammalian blood as a substitute for human blood in experimental research. Specific bloodstain pattern parameters including surface tension, viscosity, density, diameter of resulting bloodstains, number of spines and other characteristics are all taken into consideration when comparing the results to human bloodstain patterns (Larkin and Banks 2014).

The most popular substitutes for human blood include bovine, equine, porcine, and ovine. In terms of potential biological hazards, according to a study by Christman (1996), there were no records of mammalian blood-borne pathogen incidents occurring in slaughterhouses in the United States, and that the greatest chance of risk would potentially occur from 'misted blood' (small droplets that can potentially be inhaled) (Christman 1996). Equine (horse) blood is a common substitute and has been determined to be a viable alternative to human blood for research purposes. However, there is evidence that particular anti-clotting methods could affect the size and shape of stains (Larkin and Banks 2014). In order to be able to keep the experimental blood for any length of time without using anti-clotting agents, the blood should be defibrinated. The process involves removing the fibrinogen from the blood, rendering it incapable of clotting. A study by Larkin and Banks (2014) has shown that defibrinated equine blood is comparable in all characteristics to human blood when used in experiments involving passive, transfer and impact bloodstain patterns (Larkin and Banks 2014).

Considerations should be made when accounting for physical properties of viable human blood substitutes. One of these considerations involves the age of the animal blood being used for experimental purposes. Impact characteristics, stain patterns and other parameters of porcine and equine blood have shown to be comparable to human blood up to a 14 day period after collection from the animal (Raymond 1996; Larkin and Banks 2014). Diameters of bloodstain droplets were shown to significantly decrease over time after the initial 14 day period. The cause of this degradation is not exactly known, however, it is believed to be affected by the aging of red blood cells rather than plasma

viscosity (Carallo et al. 2011). It has been observed that blood (plasma) viscosity increases with age but is due to the presence and production of fibrinogen. In experiments where equine blood has the fibrinogen removed to prevent clotting, this cannot be a factor in aging effects on bloodstain diameter.

The physical properties of blood as well as potential reactions in specific environments are important to take into consideration when attempting to replicate a study involving bloodstain pattern analysis. Understanding current techniques used for bloodstain classification can aid in determining what tests are potentially feasible in both field and lab settings, therefore determining what could realistically be used in a crime scene investigation. It is difficult to acquire human blood for research studies so an understanding of viable substitutes removes any factor of unrealistic results from the bloodstain pattern analysis.

2.4. Chemiluminescence

Chemiluminescence is a term used to describe the process whereby a molecule is promoted to an excited state through a chemical reaction and emission of light is observed when the molecule subsequently relaxes back down to the ground state (Laux 1999; James et al. 2005; Bily and Maldonado 2006). An example of chemiluminescence as applied in the field of bloodstain analysis is the catalytic oxidation of Luminol by iron in hemoglobin. The chemical structure of Luminol is shown in Figure 13 (Quickenden and Creamer 2001; James et al. 2005; Webb et al. 2006; Barni et al. 2007).

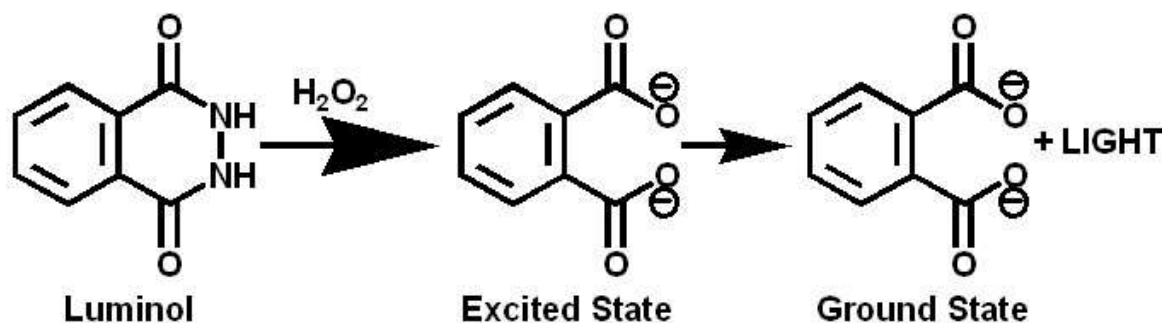


Figure 13. Molecular reaction of Luminol to a catalyst. Luminol plus (an alkaline agent) hydrogen peroxide come into contact with the catalyst (e.g. blood). The molecular reaction increases to an excited state before relaxing and releasing light as it returns to its ground state (James et al. 2005).

2.4.1. Luminol

2.4.1.1. History of Luminol

The history of Luminol and its usage in presumptive testing can be traced back to German origins and discovery as early as 1853 (James et al. 2005). Studies conducted in 1928, known as the Albrecht investigations, demonstrated that a compound (Luminol) produced enhanced light emission when in contact with hypochlorites (e.g. bleach), plant peroxidases, and blood, in conjunction with an alkaline agent (such as hydrogen peroxide) (James et al. 2005; Creamer et al. 2005). A detailed study by Specht (Specht 1937) tested a mixture of Luminol, calcium carbonate and hydrogen peroxide on a vast array of different substances to determine positive or negative chemical reactions (Quickenden and Creamer 2001; James et al. 2005). Tested substances included soil, leaves, wood, metals, milk, coffee, fabrics, wallpaper, and leather. Apart from blood, other bodily human fluids such as sperm, saliva, and urine did not show a chemical reaction (James et al. 2005; Li, Beveridge et al. 2014). Following the discovery of the capabilities of

Luminol, multiple studies emerged with different preparation techniques in order to improve the sensitivity of the chemical reactions, including the use of sodium carbonate and sodium perborate as the alkaline agent (James et al. 2005; Barni et al. 2007).

2.4.1.2. The Reaction of Luminol to Substances

The reaction between Luminol and blood is complex, and an understanding of how bloodstains change over time is an important factor in the chemical reaction. When blood is in the body the hemoglobin functions normally as the iron in the heme maintains stability through constant gain and loss of oxygen molecules (James et al. 2005; Barni et al. 2007). When blood exits the body it can no longer maintain this stability. As the hemoglobin ages it oxidizes; the heme changes to hemin (or hematin), producing the reddish brown colour of an old blood stain (Lytle and Hedgecock 1977; James et al. 2005).

When the Luminol solution is sprayed on the bloodstains, the intermediate form is irreversibly oxidized and elevated into an excited state (James et al. 2005; Bily and Maldonado 2006; Barni et al. 2007; Howard and Nessian 2010). As the Luminol molecule relaxes back to its ground state, an emission of blue-green light can be observed (Bily and Maldonado 2006; Barni et al. 2007). Luminol does react with the iron present in fresh blood stains; however, older blood stains react better or brighter than fresh blood (Lytle and Hedgecock 1977).

Luminol is a widely useful technique for detecting pattern evidence such as pooled blood, swipe marks, footwear impressions, drag marks, weapon marks, and other

bloodstain patterns even with the presence of superficial cleaning (Bily and Maldonado 2006). However, Luminol has been known to react with other substances. It has been observed to react with certain metals and cleaning agents and produce a rippling or twinkling effect and not the long, constant luminescence that can be seen with blood contact (Quickenden and Creamer 2001; King and Miskelly 2004; James et al. 2005; Bily and Maldonado 2006). Luminol has also been known to react to different plant peroxidases since they are also capable of producing the oxidation reaction with the Luminol solution even in the absence of blood (heme) (Creamer et al. 2003; Barni et al. 2007; Kobilinsky 2012). There have been studies attempting to improve the Luminol reagent in order to reduce false positive reactions. A study by King and Miskelly (2004) tested the addition of glycine to the Luminol solution in order to show discrimination in luminescence intensity between blood and bleach (King and Miskelly 2004; Barni et al. 2007). Luminol requires a completely darkened environment to be photographed and the effects of the luminescence are short-lasting from seconds to a few minutes. The capabilities of Luminol as a presumptive and enhancement tool in forensics are widely known; however, the limitations should always be taken into consideration.

2.4.1.3. Effects of Luminol on Further Blood Testing

Luminol testing can be considered a destructive procedure due to the fact that spraying the reagent onto a suspected bloodstain can lead to dilution of the stain as well as an alteration of its shape (Barni et al. 2007; Li, Beveridge et al. 2014). This can cause issues with further bloodstain pattern analysis. The other field that warrants discussion are

the effects of Luminol reagent on additional presumptive chemical tests. These tests include confirmatory blood tests, species determination by immunoelectrophoresis, ABO typing by absorption elution, and genetic marker analysis by multienzyme system electrophoresis (Laux 1991; Barni et al. 2007; Santos et al. 2009). Results indicate that Luminol does not have an effect on confirmation testing, species determination, serological testing and DNA recovery; however, certain genetic markers (E.g. erythrocyte acid phosphatase and peptidase A) can be effected by the chemical reaction of Luminol (Lytle and Hedgecock 1977; Laux 1991; James et al. 2005).

2.4.2. Comparison of Techniques: Advantages and Disadvantages

There are several tests that can be applied to suspected bloodstains. These tests can be separated into two different categories: presumptive tests and enhancement tests. Presumptive tests refer to situations where the bloodstain pattern analyst is trying to determine if a stain might be blood. Hemastix, Phenolphthalein (Kastle-Meyer) solution, Leucomalachite green, and Hematrace are all presumptive tests that aim to determine if a specific substance reacts chemically similar to blood (Bevel and Gardner 2000; James et al. 2005; Li, Beveridge et al. 2014). Many of the presumptive tests have the possibility of resulting in false positives, so the bloodstain pattern analyst should be aware of the risks and investigate without making assumptions (Bevel and Gardner 2000).

The second category of testing is enhancement. Once an area is suspected of containing a bloodstain, enhancement techniques can be applied to the scene. Fluorescein, Leuco crystal violet, and Bluestar Forensic Latent Bloodstain Reagent can be utilized in

enhancement testing. Luminol and Phenolphthalein can be categorized as both presumptive and enhancement testing techniques when trying to determine the extent of bloodstain patterns (Bevel and Gardner 2000; Webb et al. 2006; Barni et al. 2007; Li, Beveridge et al. 2014). However, reagents like Bluestar and Luminol which are water-based are not ideal when used on fine details. The three most popular enhancement techniques include; Fluorescein, Bluestar, and Luminol testing. Fluorescein testing does not require complete darkness for observation and photography, as it has a long-lasting fluorescence. However, an ultraviolet light source is required in order to observe the fluorescence (Cheeseman 1999; Young 2006). Fluorescein will fluoresce when illuminated with ultraviolet light, as the heme group in blood reacts with the reagent. Nanometre wavelengths to produce this reaction are typically set at 450nm (James et al. 2005; Young 2006). In comparison to Luminol testing, Fluorescein does not fluoresce when in contact with bleach while Luminol has been known to do so (James et al. 2005) however, the requirement of a forensic light source makes this enhancement technique more cumbersome.

While Luminol and Fluorescein testing have been available for several decades, Bluestar forensic testing is a fairly new endeavor. Bluestar Forensic Latent Bloodstain Reagent contains the Luminol molecule, but consists of a different reagent formula. The sensitivity ratio for Bluestar is 1:10,000 parts, while Luminol has a sensitivity of 1:5,000,000 parts (James et al. 2005; Duncan 2010; Grafit et al. 2014). Bluestar Reagent reacts with blood in the same chemical manner as Luminol; however, Bluestar is known to have a stronger, longer lasting luminescence and does not require complete darkness

for observation (Barni et al. 2007; Howard and Nesson 2010; Grafit et al. 2014). Several studies have stated that when comparing Bluestar and Luminol reactions, Bluestar tends to luminesce brighter and lasts longer with fewer re-applications of the reagent (Young 2006; Barni et al. 2007; Howard and Nesson 2010; Grafit et al. 2014). One negative aspect of using Bluestar would be the potential for false positive reactions to chemicals containing strong oxidants; as well as plant peroxidases (e.g. horseradish/ potato juice) (James et al. 2005; Kobilinsky 2012), in addition to the lower sensitivity ratio. These potential negative aspects should be taken into consideration in a similar manner to Luminol.

2.5. Chemical Analysis of Paint

Paint chemistry is considered an important aspect of forensic examination especially in terms of trace evidence. Fragmented, multi-layered paint samples are one of the most complex types of materials examined by forensic scientists (Caddy 2001). A multitude of techniques can be applied to paint samples in order to determine chemical composition, compare samples for matching analysis, and determine the properties of paint which might affect other forensic techniques (e.g. chemiluminescence, multi-spectral photography). Among the techniques for paint analysis, several can be considered destructive; however, specific techniques have been modified in the art conservation world in order to reduce or eliminate destructive procedures. Forensic analysis of paint evidence usually requires samples to be taken from the scene and brought to the lab. Research in the field of art conservation shows the potential for

transporting equipment into the field where paint samples could be analyzed in situ. An application of art conservation techniques in the field of forensic analysis might prove useful.

2.5.1. Properties of Architectural Paint

There are many terms used to describe paint. Due to the mechanism of application, paint is referred to technically as a surface coating (Caddy 2001; Saferstein 2002; Kobilinsky 2012). Surface coatings that are applied to automobiles can be referred to as product coatings; whereas household applications are architectural surface coatings/paint (Saferstein 2002). Architectural paint will be used in reference to household paint for consistency.

Paint is defined as a heterogeneous solution containing suspended organic and inorganic components with the dual purpose of surface protection and decoration (Caddy 2001; Saferstein 2002; Kobilinsky 2012). The three main components of paint consist of a binder, pigment, and additives; where the combination of binder and additives allows for the classification of either an oil-solvent based paint or water-based latex paint (Weber 1960; Williams 2006). Oil-solvent based paint binders polymerize as they dry, whereas water-based latex binders already consist of polymers or copolymers (Schuerman and Bruzan 1989). The polymers and copolymers, also referred to as resins, can help further classify the paint types. There are many different types of resins including alkyl, polyester, urethane, epoxy, silicon, and amino; however, acrylic and vinyl resins are predominant in the field of architectural paint manufacturing (Saferstein 2002). Due to

the continual development of architectural paint, the definitions of these paints should also be modified. Most architectural paint are water-based latex with a modified or unmodified acrylic/vinyl resin.

The binder provides adhesion and cohesion to an intended surface, while simultaneously supporting pigment for an even distribution across the surface (Caddy 2001; Saferstein 2002). The pigment is a powdered solid which is insoluble (does not dissolve) in the binder solution. It is responsible for providing colour and opacity, as well as potentially modifying the physical properties of the paint (Caddy 2001; Saferstein 2002). The optical properties of pigments depend on particle size and structure and can absorb or scatter light based on the inorganic or organic compounds present (Kobilinsky 2012). Pigments that have the same index of refraction as the binder are considered extender pigments. These provide bulk to the paint as well as modify the physical and chemical characteristics such as texture, strength, viscosity, and gloss value (Caddy 2001; Kobilinsky 2012). The extender pigments do not interfere with other pigments, which may consist of a higher index of refraction. Some extender pigments in architectural paint include talc, kaolin (clay), calcium carbonate, quartz, mica, and barium sulfate (Weber 1960; Kobilinsky 2012).

The purest white pigment readily available in commercial architectural paint is titanium dioxide (TiO_2). Titanium dioxide in paint is referred to as either rutile or anatase, and has the ability to make paint opaque (white) as well as absorb UV light (Caddy 2001; Kobilinsky 2012; Li, Yin et al. 2014). Titanium dioxide has replaced lead and zinc pigments in paint as a non-toxic, environmentally friendly alternative (Saferstein 2002).

Research into titanium dioxide induced chemiluminescence suggests that pure rutile or anatase demonstrates a chemiluminescent response when in contact with Luminol (Hedenborg 1988). Although the industry usage of titanium dioxide in white paint has overtaken lead and zinc based paints in popularity, these pigments should still be taken into consideration especially in the examination of older forms of architecture.

The third component of paint refers to the additives. This category includes materials that accelerate drying and hardening, components that increase workability and storing agents, and the solvents (thinners) that aid in dissolving the binder for consistency in surface coating (Weber 1960; Saferstein 2002; Williams 2006). Some of the storing and workability agents are classified as defoaming and coalescing components. They act as ‘wetting’ additives responsible for joining new paint onto dried existing paint, to permit a fusion of particles upon drying (Schuerman and Bruzan 1989). The majority of additives are only present in small concentrations.

2.5.2. Raman Spectroscopy

Raman spectroscopy refers to the non-enhancement technique of analyzing and recording the vibrational transitions of the molecules of a sample (Das and Agrawal 2011; Kobilinsky 2012). Both Raman and Infrared spectroscopic techniques analyze molecular vibrational transitions of a sample; however, Raman spectra are generated by inelastic scattering of the incident light source while infrared spectroscopy is based on absorption of incident light (Kudelski 2008; Das and Agrawal 2011; Kobilinsky 2012). When some of the energy from the incident light source is transferred to the vibrational modes of the

molecules, the resulting scattered radiation has less energy being recorded as intensity versus frequency by a spectrometer (Kobilinsky 2012). The recording of the changes in molecular vibrational states results in the quantifiable Raman spectrum and a 'structural fingerprint' of a particular molecule (Kneipp et al. 2002; Kudelski 2008). However, this inelastic (Raman) scattering of radiation usually produces weak signals which can be easily over-whelmed by fluorescence of the sample. In order to reduce or 'quench' the intense fluorescence, and allow the weaker Raman peaks to emerge, metal nanoparticles can be placed on the sample (Kobilinsky 2012; Schlücker 2014). In a technique known as Surface-Enhanced Raman Spectroscopy or SERS, the application of a layer of specific nanoparticles onto the surface of the sample reduces fluorescence and allows weaker signals to emerge (Schlücker 2014).

SERS is a sensitive tool for the detection of adsorbed organic molecules on rough metal surfaces which allow for both a boost in Raman signal intensity, and fluorescence quenching (Kudelski 2008; Casadio et al. 2010; Das and Agrawal 2011). Metal substances used as surface-enhancing nanoparticles must be chemically inert or stable, and plasmonically active to produce enhancement (Schlücker 2014). Many experiments utilize silver nanoparticles for SERS due to their stability and large enhancement factors; however, gold and copper are also readily used (Kneipp et al. 2002; Kudelski 2008; Das and Agrawal 2011).

Raman spectroscopy and SERS can be applied in a variety of different tests in the field of forensic science. These analytical methods can be applied to the analysis of inks, paint, and blood for the identification of specific chemical characteristics (Buzzini and

Suzuki 2016). Raman spectroscopy has been used as a non-destructive method for the identification of blood stains, with evidence of being able to differentiate between human and animal blood, and between blood and paint stains (De Wael et al. 2008; Boyd et al. 2011). The identification of bloodstain patterns via scattering peaks of the hemoglobin and fibrin available in the dried stains are possible using Raman spectroscopy, up to a dilution ratio of 1:250 (Boyd et al. 2011). With the portability of certain Raman spectrometers, the in situ identification of potential bloodstains, as well as paint analysis is possible (Kogou et al. 2015). In terms of paint analysis, Raman spectroscopy is useful for the identification of inorganic pigments, but can be limited in the identification of synthetic organic pigments due to the generation of fluorescence from particular compounds (Harroun et al. 2011; Buzzini and Suzuki 2016). Some binders and other additives are also known to cause fluorescence and subsequently over-power weaker Raman signals; therefore, the application of a metallic substrate in surface-enhanced Raman spectroscopy can boost weak signals, as well as quench organic pigments/binder/additive fluorescence (Harroun et al. 2011).

Paint is a complex matrix of organic and inorganic components with a wide range of different concentrations, and the application of different analytical techniques greatly increases the probability of chemical signature identification (Kobilinsky 2012). The use of SERS aids the Raman scattering in order to enhance the signal output when attempting to classify organic molecules adsorbed with metal nanoparticles (Casadio et al. 2010). This enhancement technique quenches the fluorescence of the paint sample while attempting to identify organic and inorganic pigment components (Harroun et al. 2011;

Kobilinsky 2012). The application of a small layer of nanoparticles can be considered a destructive technique, and should be used with caution in the field of forensics.

2.5.3. Fibre Optic Reflectance Spectroscopy

The term reflectance spectroscopy broadly covers an array of sub-terminology utilized in different disciplines. UV-VIS; UV/VIS/NIR diffuse reflectance spectroscopy and fibre optic reflectance spectroscopy refer to similar techniques with only certain differences in equipment and extent of spectral region analysis (Aceto et al. 2012; Baraldi et al. 2016; Fermo et al. 2016). Fibre optics reflectance spectroscopy (FORS) is a non-invasive, portable technique with an operating range from the ultraviolet (~200 nm), through the visible light spectrum and up into the near-infrared (~800 nm) (Bacci et al. 2007; Fermo et al. 2016). The exact spectral range analyzed depends on the spectral range of the light source used in FORS. The optical range of the tungsten halogen light source falls into the near-UV light spectrum (~380 nm), through the visible light spectrum, as well as providing a sufficient amount of infrared light onto a sample so that the near-infrared spectrum can be analyzed (Bracci et al. 2015; Kogou et al. 2015; Baraldi et al. 2016; Fermo et al. 2016). For further analysis into the ultraviolet spectrum, a deuterium light source can be applied to the samples. The spectral range of the deuterium light source begins in the UV spectrum (~200 nm) and continues into the visible light and near-infrared spectrums (Aceto et al. 2012). The application of analyses using both light sources can expand the overall spectral range of the fibre optic reflectance spectroscopy

analysis; however, depending on applications of comparison it might not necessarily be warranted.

FORS analysis is non-invasive in nature and readily available for in situ measurements. This technique is often used for the identification of pigments, dyes and alterations in historical artwork (Bacci et al. 2007; Kogou et al. 2015), however, the identification of reflectance and absorption properties of multiple substances is also possible. FORS is typically used to provide information on the pigments present in the outer-most layer of an object and spectra are often analyzed in conjunction with a suitable spectral database (Bacci et al. 2007; Aceto et al. 2012). The pigments are identified based on their spectral reflectance; specifically, the amount of light that has been reflected off of the sample surface at different wavelengths (Marušić et al. 2016). The FORS spectra of white pigments (titanium dioxide, lead white, zinc white etc.) are characterized with a higher overall spectral reflectance (Bacci et al. 2007). In an attempt to categorize specific pigments, interpretation of absorption bands within a spectral database reference has the potential of identifying multiple pigments from a single sample (Bacci et al. 2007; Kogou et al. 2015). Additionally, this non-destructive technique can simply be used to determine the spectral reflectance or absorption levels of a painted surface in the near-ultraviolet, visible, and near-infrared light spectrums.

2.5.4. ATR-FTIR Spectroscopy

Attenuated Total Reflectance Fourier-Transform Infrared spectroscopy (ATR-FTIR) is a reflectance infrared spectroscopy technique for measuring the absorption

levels of a sample in the infrared spectral region (Kobilinsky 2012). This technique is readily used by forensic scientists analyzing paint chemistry of known and unknown samples. ATR-FTIR is a useful tool for the characterization of paint samples, especially for determining binders, pigments, and other additives (Ziçba-Palus 1999; Caddy 2001; Saferstein 2002; Stuart 2004; Kobilinsky 2012). These reflectance techniques allow for an analysis of opaque samples, as well as in situ examination (Caddy 2001; Szafarska et al. 2009). Due to the lower IR absorption wavenumbers of extender pigments, these components might not be entirely accessible through ATR-FTIR analysis (Saferstein 2002). In conjunction with other analyses such as Raman, SERS, and FORS; ATR-FTIR spectroscopy can provide a detailed analysis of the chemical components present in a specific paint sample.

Reflectance techniques can be categorized as either internal reflectance measurements, or external reflectance measurements. Whereas external reflectance measurements involve analyzing a sample using a reflected infrared beam, internal reflectance measurements use an optical element in direct contact with the sample of interest (Stuart 2004). ATR is an example of the internal reflectance measurement technique which utilizes an optical element with refractive infrared-transparent properties to be pressed into the sample (Kobilinsky 2012). Materials used for this element must have low solubility in water, as well as a high refractive index and includes materials such as; zinc selenide, germanium, thallium-iodide, and diamond (Stuart 2004). The beam of infrared radiation enters the element and penetrates slightly beyond the reflecting surface. When the sample (capable of absorbing radiation) is in direct contact with the element,

the beam loses energy at the specific wavelength where the material absorbs the infrared radiation (Stuart 2004). This resulting attenuated radiation is measured by the FTIR spectrometer as a wavelength, depicting the absorption characteristics of the sample's spectral profile (Stuart 2004). The penetration depth is very shallow, allowing spectra of lower-frequency components to be intensified. Dried paint samples need to be taken, or prepared, in order to conduct this analysis, and slight indentation might occur where the ATR element was pushed down into the sample.

Infrared spectroscopy is quite sensitive to the common binders present in a paint sample. The peak absorption wavenumbers can be analyzed and attributed to specific components (Kobilinsky 2012). ATR-FTIR is also capable of identifying paint pigments, particularly those comprised of inorganic materials. The inorganic pigments are generally weak at absorbing visible light, and tend to possess strong capabilities of infrared radiation absorption (Stuart 2004; Kobilinsky 2012). Organic pigments, extenders, solvents and some other additives typically have weaker infrared absorption properties and therefore are more difficult to characterize from the ATR-FTIR spectral output (Saferstein 2002). In comparison to other techniques, major components present in the paint samples tend to over-shadow lower frequency or weak IR absorption components. A combination of techniques allows a full analysis of the paint samples in order to determine the chemical and physical properties.

2.6. Bloodstain Patterns beneath Paint: A Review

There have been several published articles specifically pertaining to the documentation of bloodstain patterns beneath layers of paint using different forensic photography techniques (Adair 2006; Bily and Maldonado 2006; Howard and Nesson 2010; Farrar et al. 2012). These articles range from only using one type of technique to using a multitude of multi-spectral analyses. Whereas the research is not new, it is not entirely consistent. Descriptions of techniques, methods used, and the results for identical techniques show a lack of standardization in the field of multi-spectral forensic photography. Whereas one technique (i.e. reflective infrared) was concluded to work for one study; for a different study with similar or identical methodology the same technique might have been concluded as negative. The variables encountered such as paint types, blood being used, photography settings, light sources, and qualitative analysis are just some of the variables that should be addressed. In broader terms, there is a lack of standardization in the definition of multi-spectral photography. In an article by Sanfilippo et al. (2010) the authors address the lack of definitive terms being used in this field. There are multiple different ways to photograph in 'infrared' and 'ultraviolet' and failure to define the types of methods being used easily creates confusion when replication studies are attempted.

The use of high dynamic range photography to enhance visual observations, and the collaboration of chemical analyses of paint specimens are novel attempts that have not been published to the knowledge of this author. High dynamic range photography has been studied by other authors (Park et al. 2005; Sedgewick 2008; Frey et al. 2011; Daly et

al. 2013) as well as tested in conjunction with ‘near-infrared photography’ (Albanese and Montes 2011); however, the specific use for bloodstain pattern enhancement under paint layers has not been attempted. A collaboration between forensic photography techniques and chemical analysis through Raman, SERS, Fibre Optic Reflectance, and ATR-FTIR spectroscopy is a new approach to supporting results obtained from the visual analysis of images. Past research might have concluded with positive or negative results but failed to elaborate on the significance of studying all aspects of the experiment; however, by addressing the chemical analysis of paint specimens, a well-rounded understanding of these variables may be reached.

Chapter 3: Materials and Methods

3.1. Laboratory Set up and Equipment

Photographic data collection was conducted at the Miami-Dade County Medical Examiner's Department in Miami-Dade County, Florida, between the dates of April 13th 2015 and May 7th 2015 during weekday working hours. All photography equipment and workspace was provided by the Forensic Photography Department. The equipment and workspace was only available at the Medical Examiner's Department in Miami for data collection; further photographic analysis was conducted once data collection had been completed.

The laboratory consisted of two main rooms: a larger room containing windows with blinds, and a smaller back room with a solid door and no windows. All samples, equipment and materials were kept in the larger room where photographs were taken with the blinds closed. The dark back room was only used for Luminol testing to take advantage of the pitch black environment. The laboratory door was kept closed to avoid ambient light from the hallway from entering the room.

All photographs were taken using a photography copy stand (Figure 14). The copy stand consisted of a flat, grey table, a sliding camera mount attached to a vertical column, and two light sources attached to adjustable arms on either side of the vertical column. The entire apparatus was positioned on a low table with wheels, 43 centimetres from the floor.



Figure 14. Copy stand table with tungsten light sources and mounted camera.

During the data collection period, photography equipment was only available at the Miami-Dade County Medical Examiner’s Department. All photography equipment used for this thesis experiment is included in Table 3. Non-photographic equipment used for this thesis work included an ABFO forensic 30 centimeter ruler, paper labels to identify which sample was being photographed, and a small piece of card to allow the label to be at uniform height with the drywall square and the ruler.

Table 3. Photographic Equipment used for the Thesis Research

Photography	Camera Used	Filters Used	Light Source Used	Lenses Used (millimetres)
Standard	Nikon D7000	N/A	Tungsten (3200 K)	16-85 mm
Infrared	Fujifilm Finepix S3 Pro	70, 87, 87A, 87B, 88A, 89B Longpass	Tungsten (3200 K)	60 mm quartz
Ultraviolet	Fujifilm Finepix S3 Pro	Baader U- Bandpass	Woods Lamp (315-400nm)	60 mm quartz
Fluorescence	Nikon D7000	Yellow, Orange, Red Longpass	SPEX Crimescope (500W Xenon) Bandpass	28-105 mm

3.2. Preparation of Materials

Paint materials are described in Table 4 along with their location of purchase and date of purchase and/or retrieval. From the building materials department of Home Depot, one sheet of Sheetrock Ultralight (½ inch x 4 foot x 8 foot) Gypsum Board (drywall) was purchased and cut in-store into 16 sections measuring 15 cm x 15 cm for the experiment. In addition, sixteen 3-inch sponge brushes were purchased for the painting component of the experiment as well as one pouring spout for the one gallon can of white primer.

Table 4. Paint Materials

Paint Type	Paint Name	Location of Purchase	Date of Purchase
White Acrylic Primer	Glidden Professional Interior PVA Drywall Primer and Sealer	Home Depot Miami, USA	April 13 2015
White Acrylic	Colorhouse Bisque .01 Flat Interior Paint	Home Depot Online	April 16 2015
White Latex	Glidden Premium White Flat Latex Interior Paint with Primer	Home Depot Miami, USA	April 13 2015
Black Latex	Glidden Premium black flat latex interior paint with primer	Home Depot Miami, USA	April 13 2015
Maroon Latex	Glidden deep burgundy flat latex paint with primer	Home Depot Miami, USA	April 13 2015

The research design for material usage was adapted from several other reports (Adair 2006; Farrar et al. 2012; Howard and Nesson 2010; Bily and Maldonado 2006) with several differences. An attempt was made to replicate a standard architectural wall (interior) and use the types of paint which would be consistent in this context. In order to remain consistent, ‘flat’ paint was used for this experiment. Flat or matte paint refers to the low-lustre or lack of sheen of the paint; other types of sheen include eggshell, satin, semi-gloss, and hi-gloss. The use of more than one type of paint sheen would have gone beyond the scope of this research project. The application of the primer and paint layers

including information regarding experiment preparation and equipment used can be found in the Appendix (Appendix 3.2).

3.3. Stage Three: The Application of Bloodstain Patterns

There were three main components that needed to be addressed for this stage of the experiment. The first variable was finding an appropriate substitute for human blood, without negating the effects of the bloodstain patterns themselves. Based on the research of several studies (Christman 1996; Larkin and Banks 2014; Raymond 1996) the use of mammalian blood is a suitable alternative to human blood. For this research, 100 mL of defibrinated horse blood procured from HemoStat Laboratories (Dixon, CA, USA) was used.

The second variable that needed to be considered was the anti-clotting mechanism. Anti-clotting agents are often added to human blood in instances of reuse (i.e. blood donation, lab tests) to prevent clotting. While the blood is outside of the body, clotting would result in an unusable blood source; however, there are other techniques besides anti-clotting agents that can eliminate blood clots. If the fibrinogen is removed from the blood, it is rendered incapable of clot formation. This is a viable alternative to adding anti-clotting agents to the blood, and is readily used and available for research purposes.

The final variable for this experiment was the types of bloodstain patterns assessed. Due to the scope of this research, only three bloodstain patterns were chosen for each paint type with one control of no blood. There were two questions that needed to be

answered. Firstly, would it be possible to identify specific details from a particular bloodstain pattern that would aid a bloodstain pattern analyst in their analysis and interpretation (e.g. type of bloodstain, velocity, droplet diameter, potential trajectory). The second question referred to which bloodstains might be considered more obvious and could be used as a standard for developing forensic photography techniques. To answer these two questions three bloodstain types were chosen. The medium-velocity bloodstain pattern and the swipe bloodstain patterns were both realistic potential bloodstain patterns which might be found on a wall, and could be further analyzed for specific information. The third stain was a saturated bloodstain which would not be typically found on a wall. This larger and more evident stain was included in an attempt to analyze and develop the forensic photography techniques that were being applied.

The three types of bloodstain patterns consisted of; a medium velocity spatter pattern resembling small to medium sized drops sprayed across the drywall square (James et al. 2005), a swipe pattern in the form of a dragged handprint, and a saturated stain pattern depicting pooling blood (Figure 15).



Figure 15. Example of Medium Velocity, Swipe, and Saturated Bloodstain Patterns

The application of bloodstains was first tested on scrap pieces of black matte board in order to determine the amount of blood to be used in the experiment. Matte board was

roughly cut into 15 cm by 15 cm squares to emulate the drywall pieces, and blood was applied several times before the optimal amount was determined.

3.3.1. Preparation and Application of Experiment and Equipment

Application of bloodstain patterns was conducted in the dark room section of the forensic photography lab. This room also worked as a wet lab consisting of a large counter space and sink area. Multiple newspapers were laid down along the counter and taped up the wall and under the cabinets protecting the counter, walls, and sink from blood spatter (Figure 16).



Figure 16. Bloodstain application set-up.

The researcher retrieved the defibrinated horse blood from the forensic photography fridge where it was being kept when not in use. Once in the lab, the researcher put on latex gloves to handle the blood. The first section to receive blood application was white acrylic number 1 which received the medium velocity stain (James et al. 2005) (Table 5). The square was placed vertically against the wall while the researcher deposited 1 mL of blood using a numbered syringe onto the fingers of the right hand. The researcher moved

the blood around the fingers before turning the gloved hand towards the drywall square. At a distance of 5 cm from the vertically placed drywall square, the researcher made a quick flicking motion to spray the blood onto the square. Once completed, the square was moved to another work bench and left in the vertical position to dry.

The second square for blood application was white acrylic number 2 for a swipe stain (James et al. 2005) (Table 5). The researcher changed gloves in between applications to avoid cross-contamination. The researcher transferred 4 mL of horse blood via syringe onto the right hand and spread the blood over the fingers and palm. In a fluid and even motion the researcher dragged the blood-covered right hand across the drywall square from the right side to the left side. The square was placed on another work bench to dry while lying horizontally.

The third section to receive a bloodstain was white acrylic number 3 for the saturated stain (James et al. 2005) (Table 5). The researcher measured out 6 mL of the defibrinated horse blood into the syringe and transferred the blood onto the middle of the drywall square. The blood was formed into a rough circle shape located in the middle of the square. The square was then carefully placed in the drying area. The final drywall section of white acrylic (number 4) was a control containing no blood so it remained in the main part of the photography lab during this stage of the research.

Application of bloodstain patterns for the remaining three paint types repeated the procedure that was used on white acrylic. White latex, black latex and maroon latex all received bloodstain patterns beginning with the medium velocity spatter pattern and were placed on the work bench to dry in the same manner (Table 5). All drywall squares

received blood application between 4pm and 5pm on a Friday and were allowed to dry over the weekend for a total of 64 hours.

Table 5. Bloodstain Pattern Application and Subsequent Drywall Squares

Square #	Paint type	Blood pattern	Blood amount (mL)	Drying position	Drying Time (Hours)
1	White Acrylic	Med. Velocity	1	Vertical	64
2	White Acrylic	Swipe	4	Horizontal	64
3	White Acrylic	Saturated	6	Horizontal	64
4	White Acrylic	No blood	0	n/a	n/a
5	White Latex	Med. Velocity	1	Vertical	64
6	White Latex	Swipe	4	Horizontal	64
7	White Latex	Saturated	6	Horizontal	64
8	White Latex	No blood	0	n/a	n/a
9	Black Latex	Med. Velocity	1	Vertical	64
10	Black Latex	Swipe	4	Horizontal	64
11	Black Latex	Saturated	6	Horizontal	64
12	Black Latex	No blood	0	n/a	n/a
13	Maroon Latex	Med. Velocity	1	Vertical	64
14	Maroon Latex	Swipe	4	Horizontal	64
15	Maroon Latex	Saturated	6	Horizontal	64
16	Maroon Latex	No blood	0	n/a	n/a

n/a = Not Applicable

3.4. Stage Four: The Application of the First Layer of Paint over Bloodstain Patterns

The bloodstains were allowed to dry for all 16 drywall squares before the application of the first layer of paint. Both the first and second paint layers were applied over the bloodstains to simulate a crime scene situation where the perpetrator would attempt to conceal the bloodstain patterns. The first layer of paint represents a scenario where a perpetrator attempted to hastily conceal the bloodstain patterns, or rely on the paint layer to obstruct forensic analysis.

The application of the first layer of paint over the dried bloodstains was completed for all 16 drywall pieces on the same day. The drywall squares were painted in ascending order and details of the application process can be found in the appendix (Appendix 3.4.).

3.5. Stage Five: The Application of the Second Layer of Paint

The second and final layer of paint was applied to all 16 drywall squares following the drying and photographing of the first paint layer. The application of the second layer of paint might represent a potential crime scene where the perpetrator would apply the paint more meticulously in an attempt to completely conceal the bloodstains from view. The amount of paint applied for the second layer covered a larger quantity in an attempt to completely obscure the bloodstain patterns.

The application of the second layer of paint over the dried bloodstains was completed for all 16 drywall pieces on the same day. For the sake of consistency, the paint was allowed to dry for the same amount of time. The pieces were painted on a Friday and inspected before photographing on Monday morning. The drywall squares were painted in ascending order from number 1 through drywall square number 16. Details of the application process can be found in the appendix (Appendix 3.5.).

3.6. Stage Six: Luminol Treatment

The final experiment for all 16 squares involved chemiluminescence testing. This process consisted of Luminol application and photography of the squares in a completely dark room. The amount of Luminol reagent to be applied, as well as camera exposure

times were first tested using defibrinated horse blood on scrap pieces of card, which were allowed to dry before being tested. Camera settings, Luminol application techniques and exposure times were all determined during this initial testing phase. The results were then applied to the experiment by testing the chemiluminescent capabilities of Luminol on all 16 drywall squares containing painted over bloodstain patterns as well as the no blood control. The Luminol testing experiment was considered a destructive technique and could only be applied at the end, following the addition of the second paint layer and subsequent photography.

3.6.1. Preparation of Experiment and Equipment

The Luminol chemical reagent was purchased from the online forensic supply store Evident (Union Hall, VA, USA) prior to the beginning of the Miami data collection phase. One 8-ounce spray bottle was purchased along with six 4-ounce vials of Luminol reagent. The Luminol reagent consisted of powdered mixture (5-Amino-2, 3-Dihydro-1, 4-Phthalazinedione; Sodium Carbonate; Sodium Perborate) contained within the vials which needed to be mixed with 4-ounces of water and used immediately after mixing.

Each paint type was moved into the dark room as they were being tested in the experiment, for a total of 4 drywall squares placed on the counter near the sink at one time. The photography copy stand and table were moved into the dark room of the photography lab to take advantage of both the sink and the ability to provide a completely black-out environment. The door was closed to prevent any ambient light from entering the dark room. One vial of Luminol reagent was prepared for each paint type. It was

recommended that the reagent be used within 20 minutes once prepared, so it was prepared after set up was completed and the squares were ready to be photographed.

4-ounces of water were added to the 8-ounce spray bottle and one vial of Luminol was added to the water. The spray unit was replaced on the bottle and tightly closed. The reagent was gently agitated by hand to mix the Luminol and water together for approximately 1 minute per the instructions. The resulting reagent was blue in colour and was ready to apply to the painted drywall squares.

3.6.2. Application of Luminol Solution on Second Layer of Paint

The Luminol reagent was first prepared at the beginning of this stage of the experiment. Each drywall square received the application of the Luminol reagent and then subsequently photographed in sequence beginning with white acrylic number 1. The researcher held the drywall square in the gloved, left hand in a vertical position, to simulate a wall, over the sink. The square was held along the backside in order to avoid any contact between the fingers and the testing surface containing the paint layers and bloodstain patterns.

In the right hand the researcher held the 8-ounce spray bottle containing the Luminol reagent. Held approximately 10 centimetres from the drywall square, the researcher slowly pumped the spray nozzle 4 times in a clockwise motion so as to cover the entirety of the square. The Luminol spray bottle was placed in the cupboard under the sink and the square was immediately positioned on the copy stand to be photographed.

Once the square was positioned on the copy stand the researcher turned off the overhead lights producing a completely pitch black environment.

Upon completion of the chemiluminescence photography the overhead lights were turned on and the drywall square was removed from the copy stand and placed on the counter. The Luminol reagent was retrieved from the cupboard under the sink and the process was replicated for all four white acrylic drywall squares. After the white acrylic drywall squares had been completed, they were moved into the main photography lab. The Luminol reagent was disposed of and the 8 ounce spray bottle was thoroughly washed out in the sink.

The white latex squares were retrieved from the main photography lab and placed on the counter in the dark room. The entire experiment was repeated at the beginning of each new paint type starting with preparing a new mixture of Luminol reagent. A total of four vials of Luminol were used for white acrylic, white latex, black latex, and maroon latex respectively.

The visual reaction of the Luminol coming into contact with the bloodstain patterns caused blue-green streaks of light as it ran down the drywall squares. The drywall squares were placed on the copy stand to be photographed immediately following the complete application of the Luminol reagent. As an additional note, during copy stand set-up the levelness of the table was adjusted in one direction but not the other due to researcher error. The resulting images depicted Luminol pooling towards one end of the drywall squares; however this pooling did not affect the Luminol testing results.

3.7. Photography set up and Process

The aim of this research project was to observe the effectiveness of a variety of different forensic photography techniques for the documentation of obstructed bloodstain patterns. Following the completion of every stage of the experiment, photographs were taken with four different types of photography. Every stage of the experiment had standard photography images taken and these images would represent what the researcher would be viewing without the aid of any other techniques. Reflective infrared photography, reflective ultraviolet photography and fluorescence photography were taken for the bloodstain pattern stage, the first layer of paint stage and the second layer of paint stage. Lastly, only standard photography was used during the Luminol treatment stage for standard forensic photography procedure and due to the fact that since the Luminol solution could only be applied once, only one type of photography technique could be used. Specific camera settings can be found in Appendix 3.7.

3.7.1. Standard Photography

Standard photography, also known as conventional photography, was the closest photographic representation of how the subject was viewed through the human eye. The equipment used for standard photography included the DSLR camera, lens and light source positioned on the copy stand and ready for use (Table 6).

Table 6. Standard photography equipment and parameters

Paint Type	Camera	Lens (mm)	Light Source (kelvin)	Stand Height (cm)	Focal Length (mm)
White Acrylic	Nikon D7000	16-85	Tungsten 3200	63.5	50
White Latex	Nikon D7000	16-85	Tungsten 3200	63.5	50
Black Latex	Nikon D7000	16-85	Tungsten 3200	63.5	50
Maroon Latex	Nikon D7000	16-85	Tungsten 3200	63.5	50

The camera was attached to the adjustable arm of the copy stand and moved into the marked position of 63.5 centimeters from the target table surface. The camera lens was adjusted by ‘zooming in’ until the focal length of 50 millimeters was indicated on the top of the lens. The automatic stabilizer was turned off to reduce vibrations.

Located on the left and right side of the copy stand were tungsten light sources consisting of two lights on each side. The lights were adjusted to a 45 degree angle, 61 centimetres from the target table surface and secured in place after all adjustments were made. Once all adjustments had been made, each drywall square was placed on the copy stand table. The ABFO ruler was positioned on the right hand side (photograph left) of the square while the information label was placed on the left hand side (photograph right). Photographs were all taken with the overhead lights turned off and the blinds drawn. The four tungsten lights attached to the copy stand were kept off when not in use.

A total of five photographs were taken for each drywall square. These five photographs covered different light exposure parameters resulting in two under-exposed darker photos, two over-exposed lighter photos, and one photo at the exposure value of zero. The photograph at zero exposure was determined by the camera focusing on the

drywall square and producing a number to inform the researcher if the amount of light for the photograph was too much, too little or already at zero exposure. Test exposures were taken and analyzed prior to continuing with the experiments. The camera settings were adjusted to automatically bracket (take the series of consecutive images at zero, two underexposed images and two over exposed images) without the shutter button needing to be depressed each time. The shutter button was pressed once while on the timer setting to avoid vibrations. After approximately two seconds the camera would take five sequential photographs at different exposures.

Bloodstain Pattern Stage

Standard photography for the bloodstain pattern stage was identical for all four paint types in terms of equipment, light source and lens focal length. Drywall squares were photographed in sequence beginning with square number 1 for white acrylic. The drywall square was placed on the copy stand table while the camera automatically focused on the square. The overhead lights in the lab were turned off and the tungsten copy stand lights were turned on. One set of five photographs were taken for each square.

First Layer of Paint Stage

After the drying period for the first layer of paint over blood, standard photographs were taken of all 16 drywall squares in sequence. Set-up was identical to the bloodstain pattern stage using the Nikon D7000 camera and 16-85 millimetre lens. The height of the copy stand was set at 63.5 centimetres while the focal length of the lens was positioned at the 50 millimetre point. Photographs were taken in the same manner using

the four tungsten lights attached to the copy stand while the overhead lights were turned off and the blinds were drawn. A total of five photographs were taken for each drywall square.

Second Layer of Paint Stage

For the second layer of paint stage standard photography had an added element. The procedure for photographing the second layer of paint was identical to both the bloodstain patterns stage and the first layer of paint stage. However, an additional technique was applied to the second layer of paint stage. Oblique photographs were taken for this stage due to the lack of visible evidence observed through the previous photography techniques. It is common practise to apply oblique lighting techniques in order to illuminate the subject in a different manner. The angles of the tungsten lights were reduced from a 45 degree angle to a 25 degree angle from the table surface and 66 centimetres from the centre of the light source to the centre of the subject. Photographs were first taken with both the left and right side tungsten lights turned on; all other setup parameters remained the same as the previous stages. Following the five photographs with both sides of the tungsten lights on, the right side (left side of the photograph) was turned off. Light was only emitted from the two tungsten lights on the left hand side for the five oblique photographs. The process was repeated with the left side lights turned off and the right hand side lights turned on. For the right hand side five oblique photographs were taken. This process was applied to all 16 drywall squares in sequence.

Luminol Test Stage

The Luminol testing stage required two different photographs to be taken for each drywall square. The first standard photograph followed the same set-up which was used during the bloodstain pattern stage and the first layer of paint stage. The Nikon D7000 camera and 16-85 millimetre lens was attached to the adjustable arm of the copy stand and positioned 63.5 centimetres from the target copy stand table. The focal point was set at 50 millimetres while the tungsten lights on either side of the copy stand were positioned at a 45 degree angle, 61 centimetres from the target. The overhead lights were turned off while the tungsten lights were switched on. One standard photograph was taken at this stage prior to the application of the Luminol reagent.

Following each standard photograph with the tungsten lights was the Luminol reaction photographs. Before Luminol was applied to the drywall square, the camera settings were adjusted. The camera aperture was opened up to F5.6 allowing the maximum amount of light through the lens, and the shutter speed was changed to Bulb. Attached to the camera was a shutter release button giving the photographer control over how long the shutter was kept open. When the drywall square had received the Luminol application and was positioned on the copy stand, the overhead lights were turned off to ensure a pitch black room. The shutter release button was depressed and locked at this time with the shutter kept open for the length of the luminescence. Once the luminescence response was over the shutter button was released to complete the photograph. Only one Luminol photograph could be taken due to the limited amount of time to fully photograph the chemiluminescence.

3.7.2. Reflective Infrared Photography

Reflective infrared (IR) photography was used for the bloodstain pattern stage, first layer of paint stage and second layer of paint stage. Equipment set up was similar to the standard photography stage but with a few additions. Mounted on the copy stand was the UV/IR Fujifilm Finepix S3 Pro, a DSLR camera specifically manufactured to be used for photographing in the ultraviolet and infrared regions of the spectrum. The UV/IR camera used the 60 mm quartz lens (Jenoptik CoastalOpt, USA) at the fixed focal point of 60 mm. Connected to the camera was an external portable monitor for real-time viewing of the drywall squares being photographed. PECA brand UV/IR longpass filters (Table 7) were used during the infrared photography stage.

Table 7. Infrared Longpass Filters (De Broux et al. 2007; Frey et al. 2011)

Transmittance wavelength (nanometres)	Kodak Wratten Brand Filter Numbers	PECA Brand Filter Numbers
675-700	70	902
795	87	904
1000	87A	906
930	87B	908
750	88A	912
720	89B	914

Bloodstain Pattern Stage

All drywall squares were set up and photographed sequentially starting with white acrylic number 1. Specific information on camera type, lens, light source used, stand height, focal length and filters that were utilized are included (Table 8). The target square was positioned on the copy stand table along with the ABFO ruler and information card. The quartz lens was adjusted to only allow manual fine focus as opposed to automatic

fine focus. The target drywall square was focused prior to proceeding with photographing.

Table 8. Reflective infrared photography equipment and parameters for bloodstain pattern stage

Paint Type	Camera	Lens (mm)	Light Source (kelvin)	Stand Height (cm)	Focal Length (mm)	Filters Used (UV/IR Longpass)
White Acrylic	Fujifilm Finepix S3 Pro	60 quartz	Tungsten 3200	85.5	60	70, 87, 87A, 87B, 88A, 89B
White Latex	Fujifilm Finepix S3 Pro	60 quartz	Tungsten 3200	85.5	60	70, 87, 87A, 87B, 88A, 89B
Black Latex	Fujifilm Finepix S3 Pro	60 quartz	Tungsten 3200	85.5	60	70, 87, 87A, 87B, 88A, 89B
Maroon Latex	Fujifilm Finepix S3 Pro	60 quartz	Tungsten 3200	85.5	60	70, 87, 87A, 87B, 88A, 89B

Located on the left and right side of the copy stand were tungsten light sources consisting of two lights on each side. The lights were adjusted to a 45 degree angle, 61 centimetres from the centre of the light to the target table surface. The lights were only kept on when photographs were being taken to avoid over-heating. For the bloodstain pattern stage, six different filters were used. The order in which each filter was used was consistent throughout the photographing of each stage and included; one photograph with no filter on the lens, PECA 902 (#70), PECA 904 (#87), PECA 906 (#87A), PECA 908 (#87B), PECA 912 (#88A), PECA 914 (#89B). Photographs taken with each filter consisted of two underexposed, two over exposed, and one normally exposed image at exposure value zero. Prior to attaching the filter, the fine focus was manually adjusted to focus the target square and each filter was carefully screwed onto the end of the lens to avoid any changes. The photographs were taken and automatically displayed on the externally connected monitor where they could be viewed before proceeding. Once all

photographs for each filter were completed, the next drywall square was positioned to be photographed with the entire process being repeated.

First Layer of Paint Stage

Following the application and drying of the first layer of paint, reflective infrared photographs were taken of the drywall squares in the same manner as the bloodstain pattern stage. Each drywall square was set up for photography with the UV/IR specific camera and 60 mm quartz lens. Stand height, focal length and light source used did not change from the bloodstain pattern stage (Table 9). The same six longpass filters were used for the infrared photography first layer of paint stage and a total of five photographs were taken with each filter, one at zero exposure, two underexposed and two overexposed. The order in which the filters were photographed was consistent for all 16 drywall squares and included; one photograph with no filter, #70, #87, #87A, #87B, #88A, and #89B. The process was repeated for all drywall squares in the same manner.

Table 9. Reflective infrared photography equipment and parameters for first layer of paint stage

Paint Type	Camera	Lens (mm)	Light Source (kelvin)	Stand Height (cm)	Focal Length (mm)	Filters Used (UV/IR Longpass)
White Acrylic	Fujifilm Finepix S3 Pro	60 quartz	Tungsten 3200	85.5	60	70, 87, 87A, 87B, 88A, 89B
White Latex	Fujifilm Finepix S3 Pro	60 quartz	Tungsten 3200	85.5	60	70, 87, 87A, 87B, 88A, 89B
Black Latex	Fujifilm Finepix S3 Pro	60 quartz	Tungsten 3200	85.5	60	70, 87, 87A, 87B, 88A, 89B
Maroon Latex	Fujifilm Finepix S3 Pro	60 quartz	Tungsten 3200	85.5	60	70, 87, 87A, 87B, 88A, 89B

Second Layer of Paint Stage

Set-up and photography of all drywall squares after the second layer of paint followed the same process as the bloodstain pattern stage and the first layer of paint stage (Table 10) with the addition of oblique photographs also being taken. Identical to the process used for standard photography of the second layer of paint stage, photographs were taken with the left tungsten lights only, right lights only, and both lights combined. Drywall squares 1, 2, and 3 for white acrylic were photographed using no filter, #87A, #87B, #88A, and #89B. For each filter, five photographs were taken, two underexposed, one at normal exposure and two over exposed. Due to time constraints, filtered photographs were not recorded for white latex, black latex, and maroon latex drywall squares.

Table 10. Reflective infrared photography equipment and parameters for second layer of paint stage

Paint Type	Camera	Lens (mm)	Light Source (kelvin)	Stand Height (cm)	Focal Length (mm)	Filters Used (UV/IR Longpass)
White Acrylic	Fujifilm Finepix S3 Pro	60 quartz	Tungsten 3200	85.5	60	No filter, 87A, 87B, 88A, 89B
White Latex	Fujifilm Finepix S3 Pro	60 quartz	Tungsten 3200	85.5	60	n/a
Black Latex	Fujifilm Finepix S3 Pro	60 quartz	Tungsten 3200	85.5	60	n/a
Maroon Latex	Fujifilm Finepix S3 Pro	60 quartz	Tungsten 3200	85.5	60	n/a

n/a = Not Applicable

3.7.3. Reflective Ultraviolet Photography

Reflective ultraviolet (UV) photography was used to photograph the bloodstain pattern stage, first layer of paint stage, and second layer of paint over bloodstain patterns

stage. Camera set-up was identical to the process used during IR photography using the Fujifilm Finepix S3 Pro UV/IR camera mounted on the copy stand at a height of 85.5 cm from the target. The 60 mm quartz lens was used for photographing all stages and was fixed at a 60 mm focal length to the target being photographed. Only one filter was used during this photography stage, the Baader-U filter (Baader Venus) (Figure 17).



Figure 17. Baader-U (Baader Venus) 2 inch filter (Company Seven Astro-Optics Division).

The light source used during reflective ultraviolet photography was a Wood's Lamp (black light) which was clamped to a stand separate from the photography apparatus. The Wood's Lamp emitted light between 325 – 400 nm with a peak at ~360 nm (Nelson and Santucci 2002) and required between three and five minutes to warm up after being turned on in order to be at one hundred percent emission capacity (Table 11).

Table 11. Reflective ultraviolet photography equipment and parameters for bloodstain pattern, first layer of paint, and second layer of paint stages

Paint Type	Camera	Lens (mm)	Light Source (315-400 nm)	Stand Height (cm)	Focal Length (mm)	Filters Used (Bandpass)
White Acrylic	Fujifilm Finepix S3 Pro	60 quartz	Wood's Lamp	85.5	60	Baader U
White Latex	Fujifilm Finepix S3 Pro	60 quartz	Wood's Lamp	85.5	60	Baader U
Black Latex	Fujifilm Finepix S3 Pro	60 quartz	Wood's Lamp	85.5	60	Baader U
Maroon Latex	Fujifilm Finepix S3 Pro	60 quartz	Wood's Lamp	85.5	60	Baader U

Bloodstain Pattern Stage

Drywall squares were photographed in sequence beginning with number 1 white acrylic. The square was placed on the photography copy stand table while the 60 mm quartz lens was fine focused before the Baader-U filter was screwed onto the end of the lens. The Wood's Lamp was positioned at an 80 degree angle to the surface of the target drywall square, 56 centimetres from the middle of the square to the centre of the Wood's Lamp light bulb. A total of five photographs were taken for each drywall square with two underexposed, one normal, and two over exposed photographs.

The Wood's Lamp needed a warm up time of approximately three to five minutes prior to photographing the drywall squares. The overhead lights were turned off during the photographing process and any ambient light entering the room was quenched as much as possible by closing the blinds and lab door. Once all four drywall squares for white acrylic were completely photographed, the Wood's Lamp was turned off to avoid over-heating. The entire process was replicated for the remaining drywall squares for white latex, black latex, and maroon latex.

First Layer of Paint Stage

The set-up and process for reflective ultraviolet photography of the drywall squares after the application of the first layer of paint was identical to the steps for the bloodstain pattern stage. For each drywall square, the 60 mm quartz lens was first fine focused before attaching the Baader-U filter to the lens. The position of the Wood's Lamp, as well as the process of allowing for a warm-up period, was also identical to the bloodstain pattern stage.

Second Layer of Paint Stage

Photography for the second layer of paint stage was identical to the bloodstain pattern stage and the first layer of paint stage except for the position of the Wood's Lamp. For the second layer of paint stage, the Wood's Lamp was positioned at a 45 degree oblique angle, 67 centimetres from the centre of the bulb to the middle of the target surface. This process removed the hot spot concentration of light made by the light source that could be seen in the photographs from the first layer of paint stage. The oblique angle also allowed the target drywall square to be fully illuminated while being photographed. The rest of reflective ultraviolet procedure was identical to the first layer of paint stage, and was replicated for all 16 drywall squares.

3.7.4. Fluorescence Photography

Fluorescence photography required the use of several pieces of equipment to be set-up prior to taking photographs. This stage in the photography process used the Nikon

D7000 DSLR camera which was also used during the standard photography stage. The 28-105 mm lens was mounted on the camera, and adjusted to a focal length of 50 mm. The height of the photography copy stand was adjusted to 63.5cm for all fluorescence photographs (Table 12).

The light source used during the fluorescence photography stage was a 500 Watt tunable Xenon lamp machine known as the SPEX Crimescope (Figure 18).



Figure 18. SPEX Crimescope with coloured filters and goggles (SPEX Forensics)

The SPEX Crimescope housing unit and connecting liquid light guide allowed light emission at specific nanometre bandwidths. Specific bandwidths were emitted through filters contained in the internal housing unit which displayed the nanometre being emitted on the front of the unit. The filters were all bandpass which allowed specific nanometres through, except for 575 (a shortpass, cut-on filter which allowed all light nanometres before 575 to be emitted). The liquid light guide that extended from the housing unit was clamped onto a stand on the right (photograph left) and at the same height as the mounted

camera on the copy stand; it was positioned 64 centimetres from the target drywall square.

Three longpass filters were used for the fluorescence stage of photography. One set of coloured goggles were worn with the accompanying coloured filter being used on the camera as each bandpass nanometre was being tested on the subject being photographed. With the yellow filter placed on the camera lens, and the yellow goggles worn, the specific bandpass nanometre settings with potential positive results were photographed. This process was repeated using the orange filter along with the orange goggles, and the red filter with the red goggles. The goggles provided both a protective barrier to view the light source, as well as 'real-time' interaction of specific light emission nanometres and the subject being photographed with a specific coloured filter.

Table 12. Fluorescence photography equipment and parameters for all stages

Paint Type	Camera	Lens (mm)	Light Source (500 W Xenon lamp)	Light Source (Bandpass nm)	Stand Height (cm)	Focal Length (mm)	Filters Used (Longpass)
White Acrylic	Nikon D7000	28-105	SPEX Crime Scope	415, 445, 455, 475, 495, 515, 535, 555, SP575, 600, 630, 670	63.5	50	Yellow, Orange, Red
White Latex	Nikon D7000	28-105	SPEX Crime Scope	415, 445, 455, 475, 495, 515, 535, 555, SP575, 600, 630, 670	63.5	50	Yellow, Orange, Red
Black Latex	Nikon D7000	28-105	SPEX Crime Scope	415, 445, 455, 475, 495, 515, 535, 555, SP575, 600, 630, 670	63.5	50	Yellow, Orange, Red
Maroon Latex	Nikon D7000	28-105	SPEX Crime Scope	415, 445, 455, 475, 495, 515, 535, 555, SP575, 600, 630, 670	63.5	50	Yellow, Orange, Red

Bloodstain Pattern Stage

For the bloodstain pattern stage, photographs were taken of the medium velocity spatter patterns for white acrylic 1, white latex 5, black latex 9, and maroon latex 13. Three photographs were taken for each of these drywall squares. One photograph was underexposed, one photograph was at normal exposure, and one photograph was overexposed. Specific details are stated in Table 13.

The SPEX Crimescope was set up with the liquid light guide positioned to the immediate right of the camera lens (photograph left). The drywall squares were fine focused prior to attaching the yellow longpass filter to the end of the lens. For the bloodstain pattern stage, only the yellow longpass filter was used in conjunction with the SPEX Crimescope bandpass of 445 nm.

Table 13. Fluorescence photography equipment and parameters for the bloodstain pattern stage

Paint Type	Camera	Lens (mm)	Light Source (500 W Xenon lamp)	Light Source (Bandpass nm)	Stand Height (cm)	Focal Length (mm)	Filters Used (Longpass)
White Acrylic	Nikon D7000	28-105	SPEX Crime Scope	445	63.5	50	Yellow
White Latex	Nikon D7000	28-105	SPEX Crime Scope	445	63.5	50	Yellow
Black Latex	Nikon D7000	28-105	SPEX Crime Scope	445	63.5	50	Yellow
Maroon Latex	Nikon D7000	28-105	SPEX Crime Scope	445	63.5	50	Yellow

First Layer of Paint Stage

The fluorescence photography process and set-up was repeated for the first layer of paint stage for all 16 drywall squares. The drywall squares were photographed in numerical order beginning with white acrylic 1. For the first layer of paint stage, a total of five photographs were taken. Two photographs were under exposed, one photograph was at normal exposure, and two photographs were over exposed.

The combination of coloured longpass filters with specific bandpass nanometres were consistent within each specific paint type for each drywall square (Table 14). White acrylic and white latex were photographed with the same longpass and bandpass combinations. The yellow longpass filter was photographed at 415 nm, 445 nm, and 455

nm. The orange longpass filter was photographed at 445 nm, 455 nm, 475 nm, 495 nm, and 515 nm and the red longpass filter was photographed at SP575 nm.

The drywall squares for black latex were all photographed using the same longpass and bandpass combinations. The yellow filter was photographed at 475 nm, 495 nm, and 670 nm. The orange longpass filter was photographed at 555 nm, and 630 nm and the red longpass filter was photographed at 600 nm.

The process was repeated for all maroon latex drywall squares with the yellow longpass filter being photographed at 415 nm, 445 nm, and 455 nm. The orange longpass filter was photographed at 415 nm, and 445 nm and the red longpass filter was photographed at 415 nm, 445 nm, 455 nm, and SP575 nm.

Table 14. Fluorescence photography equipment and parameters for first layer of paint

Paint Type	Camera	Lens (mm)	Light Source (500 W Xenon lamp)	Light Source (Bandpass nm)	Stand Height (cm)	Focal Length (mm)	Filters Used (Longpass)
White Acrylic	Nikon D7000	28-105	SPEX Crime Scope	415, 445, 455, 475, 495, 515, SP575	63.5	50	Yellow, Orange, Red
White Latex	Nikon D7000	28-105	SPEX Crime Scope	415, 445, 455, 475, 495, 515, SP575	63.5	50	Yellow, Orange, Red
Black Latex	Nikon D7000	28-105	SPEX Crime Scope	475, 495, 515, 555, 600, 630, 670	63.5	50	Yellow, Orange, Red
Maroon Latex	Nikon D7000	28-105	SPEX Crime Scope	415, 445, 455, 475, SP575	63.5	50	Yellow, Orange, Red

Second Layer of Paint Stage

Fluorescence photographs for the second layer of paint stage followed the same process used during the bloodstain pattern stage and the first layer of paint stage. A total of five photographs were taken for each drywall square consisting of two under exposed photographs, one normal exposed photograph, and two over exposed photographs.

Photographs for white acrylic and white latex used identical longpass and bandpass combinations for each. The yellow longpass filter was photographed at 415 nm, 445 nm, and 455 nm. The orange longpass filter was photographed at 415 nm, 445 nm, 455 nm, 475 nm, and 495 nm and the red longpass filter was photographed at 415 nm, 445 nm, 455 nm, 475 nm, and SP575 nm (Table 15).

Photography for black latex and maroon latex consisted of one longpass and bandpass combination. For black latex, the yellow longpass filter was photographed at 475 nm. For the maroon latex drywall squares, the yellow longpass filter was photographed at 455 nm.

Table 15. Fluorescence photography equipment and parameters for second layer of paint

Paint Type	Camera	Lens (mm)	Light Source (500 W Xenon lamp)	Light Source (Bandpass nm)	Stand Height (cm)	Focal Length (mm)	Filters Used (Longpass)
White Acrylic	Nikon D7000	28-105	SPEX Crime Scope	415, 445, 455, 475, 495, SP575	63.5	50	Yellow, Orange, Red
White Latex	Nikon D7000	28-105	SPEX Crime Scope	415, 445, 455, 475, 495, SP575	63.5	50	Yellow, Orange, Red
Black Latex	Nikon D7000	28-105	SPEX Crime Scope	475	63.5	50	Yellow
Maroon Latex	Nikon D7000	28-105	SPEX Crime Scope	455	63.5	50	Yellow

3.8. Photography Analysis

Following the data collection phase at the Miami-Dade County Medical Examiner's Department, all photographs needed to be merged into High Dynamic Range (HDR) images in Photoshop CC. All files were saved on an external hard drive in separate folders with labelled information including the photo card number, paint layer information, and the photography technique used. All of the original photographs were saved separately from the HDR merged images.

3.8.1. High Dynamic Range Enhancement in Photoshop CC

Prior to any photo enhancements in Photoshop CC, specific folders were created and designated for each different photographic technique. These folders were further divided into specific stages for each different paint colour. Enhanced photographs were saved as a separate, final image, from the originals.

The first step in the HDR enhancement phase was to open Photoshop CC and turn on history, in order to record all steps undertaken during this stage. Under the 'edit' tab – 'preferences', and then 'general'; 'history' was turned on and included the information for the 'metadata' and a 'textfile'. Once 'history' was turned on it remained on for the duration of this stage.

Only one set of photographs was merged into a HDR image at a time. This one set of photographs consisted of one photograph at normal exposure (0.0), one photograph at (-1.0), one photograph at (-2.0), one photograph at (+1.0), and one photograph at (+2.0) exposures. First, under the drop down 'file' tab in Photoshop CC the 'automate' option

was highlighted and the 'merge to HDR Pro' was selected. The pop-up window for 'merge to HDR Pro' asked for the photograph files to be uploaded. Once the upload was complete the 'merge to HDR Pro Preview' window opened. The check boxes for '32-bit imaging' and 'complete toning in Adobe Camera Raw' were selected and the OK button was clicked for the images to begin the merging process.

After several minutes of merging the five photographs, the 'Adobe Camera Raw' window opened revealing the final merged photograph. At this stage information was recorded in an excel spreadsheet and included; the ISO, focal length, shutter speed, and default enhancements (zero). No adjustments were undertaken and the OK button was clicked to complete the final merging of the photographs.

The resulting photograph was a compilation of five photographs at different exposure levels. This image was then saved as a separate TIFF file in one of the pre-existing folders for HDR enhanced images.

3.9. Chemical Analysis of Paint

After data collection in Miami was completed, all four paint types, and the one white primer, were stored in sterile, air tight sample containers to be transported back to Halifax for further laboratory analysis. Chemical analysis of the white acrylic, white latex, black latex, and maroon latex samples were conducted. Three tests were used during the chemical analysis and included; Raman Spectroscopy and Surface-Enhanced Raman Spectroscopy (SERS), Fibre Optic Reflectance Spectroscopy (FORS), and Attenuated Total Reflectance Fourier Transform Infrared spectroscopy (ATR FTIR).

3.9.1. Preparation of the Experimental Samples

One piece of white Bristol board and five sponge brushes were purchased for the preparation of the four paint samples, and one white primer sample, for this experiment. The white Bristol board was cut into 8 cm by 8 cm squares with three squares for each paint type, resulting in 15 squares. The back of each square was labelled with the corresponding paint type. The paint samples were liberally agitated for complete mixing before application. One unused sponge brush was used for each different paint application on the white Bristol board squares. Approximately three layers of paint were applied to each square, paying attention to maintaining a thick, uniform surface. Once all experimental squares received paint application they were allowed to dry over a two day period. Three squares of each paint type were viable for experimentation for the white primer, white acrylic, white latex, black latex, and maroon latex.

3.9.2. Raman Spectroscopy

Raman spectroscopy for all four paint types and one white primer used the DeltaNu benchtop dispersive Raman spectrometer with air-cooled CCD (Figure 19), a 785 nanometre diode laser, and a right angle optics attachment (Intevac Photonics, Santa Clara, USA).



Figure 19. DeltaNu benchtop Raman spectrometer (Intevac Photonics).

Each sample was individually placed 1.6 centimeters from the right angle optics attachment and analyzed. The laser powers, acquisition times, spectrometer resolution and spectral range are documented in Table 16.

Table 16. Raman spectroscopy analysis for all paint types

Paint Type	Laser Power (Peak 120mW)	Acquisition Time (Secs)	Spectrometer Resolution (cm⁻¹)	Spectral Range (cm⁻¹)
White Primer	Medium-High	30	3-5	100-2500
White Acrylic	Medium-High	30	3-5	100-2500
White Latex	Medium-High	30	3-5	100-2500
Black Latex	Medium	30	3-5	100-2500
Maroon Latex	Medium	30	3-5	100-2500

For data analysis, Origin 8.1 (OriginLab Corporation, Northampton, MA, USA) was used for all five experimental samples. Origin 8.1 was used for spectral processing and data analysis; corrections for time and power were completed during data analysis.

3.9.3. Fibre Optic Reflectance Spectroscopy

Reflectance measurements were recorded using a spectroscopy system in the ultraviolet – visible light – near infrared spectrums (~200 – 1100nm). The OceanOptics system (Florida, USA) consisted of a DH 2000 deuterium and tungsten halogen light

source, UBS 2000+ (custom) spectrometer, 600 micron fibre optics reflectance probe and reflectance holder (Figure 20).



Figure 20. Fibre Optic Reflectance Spectroscopy system (Adapted from OceanOptics).

The WS-1 diffuse standard was used as a baseline and consisted of a spectral range of 250 – 2000 nanometres and a reflectivity of >98% (250-1500nm) and >95% (250-2200nm). Tests were conducted with both the deuterium light source (25W deuterium light bulb) and the tungsten halogen light source (20W tungsten halogen light bulb) for the spectral coverage of 215 – 2500 nanometres. Information was sent to the spectrometer which had a detector range of 200 – 1000 nanometres. The results of the testing were then sent to the laptop attached to the spectrometer and were opened in the OceanView program for analysis (OceanOptics 2016).

Following the set-up of the equipment, the deuterium light source was turned on and left to warm up for approximately 10 minutes. The 600 micron fibre optics cable and probe, attached to the light source, was inserted in the reflectance holder at a 45 degree

angle for diffuse (angled) reflection. The probe was secured in the holder and then placed on the WS-1 diffuse standard light reference for determining the baseline before beginning analysis on the different paint samples. The baseline for the standard was saved in the OceanView program and sample measurements could then be collected. A total of five paint samples were analyzed in the order of; white primer, white acrylic, white latex, black latex, and maroon latex. All of the measurements were saved in the OceanView program and represented the level of reflectance versus wavelength from 200 – 800 nm.

The entire procedure was replicated for the halogen light source following the deuterium light source measurement collection. First, the halogen light source was turned on and allowed to warm up for approximately 10 minutes. A baseline was collected from the WS-1 diffuse standard and saved in the OceanView program. Measurements for all five paint types were taken in the order of; white primer, white acrylic, white latex, black latex, and maroon latex. The measurements from the OceanView program were saved and depicted the level of reflectance versus wavelength from 400 – 800nm. All five paint types were combined into spectral charts for comparison.

3.9.4. ATR-FTIR Spectroscopy

The last experiment performed on all paint samples was Attenuated Total Reflection Fourier Transform Infrared spectroscopy (ATR-FTIR) using a bench top spectrometer (Bruker Optics) (Figure 21).



Figure 21. Attenuated Total Reflection Fourier Transform Infrared Spectrometer (Bruker Optics).

The spectrometer is designed to have a sample placed between the horizontal crystal surface and secured in place with a clamping unit. The ATR crystal surface used consisted of an IR transparent diamond with a spectral region of approximately 45000 - 10 (cm^{-1}) and a penetration depth of approximately 1.66 (μm). An infrared diode laser entered the diamond crystal surface at a 45 degree angle and penetrated the subject material before reflecting back towards the crystal and to the detector. A small amount of infrared light, termed the evanescent wave, can penetrate the crystal surface at this critical angle where total internal reflection takes place. If a sample is present directly on the crystal surface (i.e. a paint sample), components in the sample can absorb this small amount of light, causing it to be attenuated (weakened). By measuring which energies of the light are absorbed, a vibrational spectrum can be provided (Figure 22).

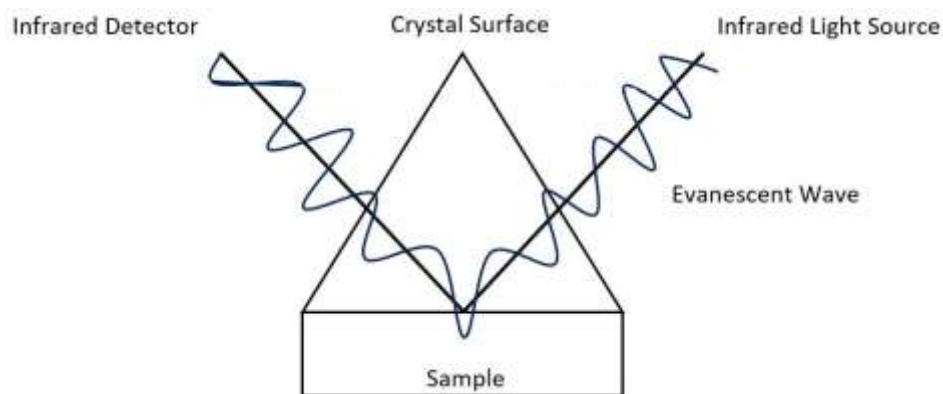


Figure 22. Basic process of IR light interacting with the sample of interest. A small fraction of the evanescent wave penetrates the sample and becomes attenuated (weakened) where the sample absorbs the energy (Adapted from Bruker Optics).

The process for ATR-FTIR measurement began with the cleaning of the crystal with isopropanol (rubbing alcohol) with cellulose based tissue. A background standard measurement was taken with the ATR unit prior to measuring the samples. Following this, one paint sample was placed on the diamond crystal surface with the painted side facing down. The clamping unit was closed and locked into place, ensuring a secure contact between the sample and diamond crystal surface. A measurement was taken and sent to the OPUS software (Bruker Optics) to display the spectral results. After the spectral results were displayed in the OPUS software and saved, the clamping unit was released and the sample removed. The diamond crystal surface was cleaned before each new measurement test and the procedure was replicated for all paint samples in the order of white primer, white acrylic, white latex, black latex, and maroon latex.

Chapter 4: Results and Discussion

4.1. Stage Three: Application of Bloodstain Patterns

4.1.1. Standard Photography

Standard photography was taken of each drywall square at the beginning of every stage in order to stay consistent, and to create a baseline of reference images (Figure 23).

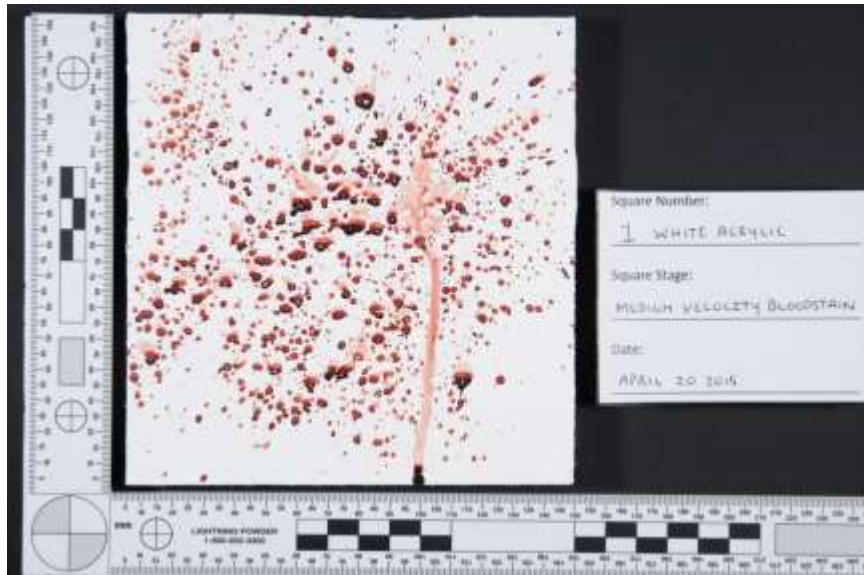


Figure 23. Example of Standard Photography for the Bloodstain Pattern Stage (HDR White Acrylic 1)

Photographs were combined in Photoshop to create a final HDR image for each drywall square and are included in the appendix (Appendix 4.1.1.). Photography camera settings were adjusted to accompany the tungsten light source as the only source of light illuminating the subject. The resulting images were well illuminated and showed a distinct contrast between the bloodstain patterns and the background paint layer.

Photography of the bloodstain pattern stage using standard photography was important in order to obtain reference images. Once paint layers had been applied over the bloodstain patterns, the original bloodstains would be obscured to some extent. A

reference was needed in order to compare how effective each multi-spectral photography technique was at capturing the subject. The collection of 5 images at different exposure levels allowed for one single photograph to be compared to the HDR combined image in order to determine whether the HDR image offered an advantage over one single photograph. For standard photography, both one single photograph and the HDR image for all 16 drywall squares were not significantly different; both containing the same amount of bloodstain pattern information. An example of HDR versus one single photograph for standard photography is available in the section on High Dynamic Range results.

4.1.2. Reflective Infrared Photography

Photography with reflective infrared for the bloodstain pattern stage yielded some interesting results. Firstly, the amount of time needed to photograph each drywall square with six filters and in-camera processing between photographs was much longer than for standard photography. Secondly, reflective infrared photography in the bloodstain pattern stage (prior to the application of the first layer of paint over bloodstain patterns) did not display as much information for the bloodstain patterns as was available for the standard photography (Figure 24).

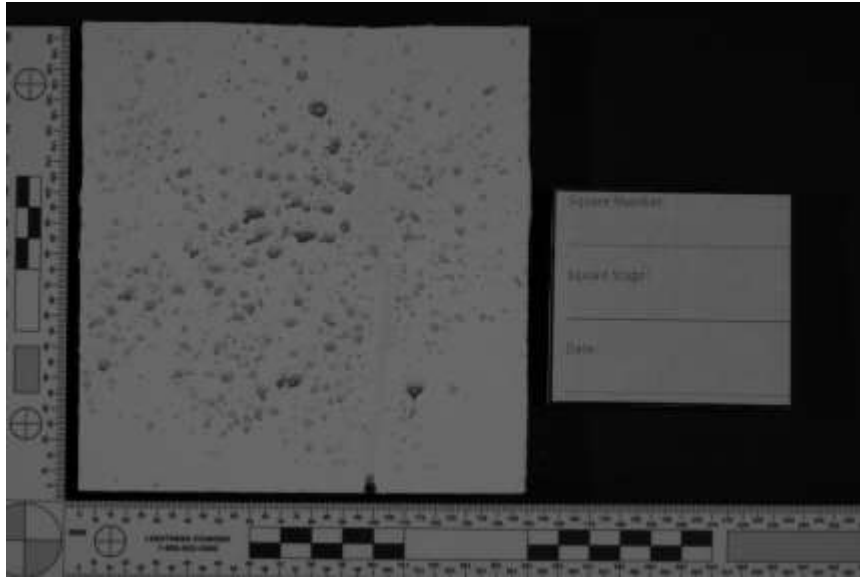


Figure 24. Example of Reflective Infrared Photography (Filter #87A) for the Bloodstain Pattern Stage (HDR White Acrylic 1).

There were several observations during this stage. The first observation was that both the white acrylic and white latex drywall squares showed more contrast between the painted background and the bloodstain patterns in comparison to the black latex and maroon latex squares. Blood is known to absorb infrared light (Li and Beveridge et al. 2014) but the contrast between an absorbing subject and a reflecting background is where reflective infrared photography becomes useful. Observations of the different paint types suggests that the white acrylic and white latex paints were capable of reflecting infrared light whereas the maroon latex and more so the black latex were capable of absorbing the infrared light. These observations will be discussed further in the section on Fibre Optic Reflectance Spectroscopy (FORS).

The results for white acrylic (Appendix 4.1.2.1) and white latex (Appendix 4.1.2.2) were similar for all longpass filters. Photographs displayed bloodstains absorbing the IR incident light source while reflecting the background paint layer; the result being a

visible contrast between the white acrylic and white latex paint types and the bloodstain patterns. The transmittance wavelengths for #87A and #87B were slightly further into the near-infrared spectrum; therefore having a longer cut-off wavelength transmission resulting in more visual information. The transmittance wavelengths of the other longpass filters (#70, #87, #88A, #89B) were closer to the visible light spectrum than the IR spectrum and were not considered useful for the documentation of blood beneath paint layers for this study..

Visual results for black latex (Appendix 4.1.2.3) and maroon latex (Appendix 4.1.2.4) were quite similar. Both black latex and maroon latex appeared to be paint types that enabled a level of absorption that affected the visibility of the bloodstain patterns. All longpass filters showed visual information, however, the level of contrast was significantly less when compared to the white acrylic and white latex paint types. The results for all filters were visible for white acrylic, white latex, black latex, and maroon latex.

There were several things that could be noted after this stage of the experiment and before the application of paint layers. Due to the high absorption for the black latex and maroon latex paints, successful photography of bloodstain patterns under these particular paint layers using reflective infrared photography would be unlikely. At this stage it was still unknown if these two paint types would also allow for transmittance of the infrared radiation through the paint and onto the bloodstain patterns located underneath.

4.1.3. Reflective Ultraviolet Photography

The photographs taken during the reflective ultraviolet stage required the use of only one filter (Baader-U) and the Wood's lamp (325-400 nm peak at ~360 nm) as a light source (Figure 25).



Figure 25. Example of Reflective Ultraviolet Photography for the Bloodstain Pattern Stage (HDR White Acrylic 1)

All four paint types, white acrylic (Appendix 4.1.3.1), white latex (Appendix 4.1.3.2), black latex (Appendix 4.1.3.3), and maroon latex (Appendix 4.1.3.4), seemed to react in a similar manner, depicting a contrast between the absorbing bloodstain patterns and reflecting paint background and were considered visible for the bloodstain pattern stage.

Due to the positioning of the incident light source, some of the light was scattering off the subject causing certain areas of the bloodstain patterns to appear lighter; although no visual information was lost during this effect, the scattering of the incident light source resulted in a difficult analysis of the bloodstain patterns. Both white acrylic and white

latex appeared to be absorbing some the incident light source, appearing darker compared to standard photography. On the other hand, both black latex and maroon latex reflected UV radiation and were noticeably brighter compared to standard photography results. These results were most likely due to one of the chemical components present in the white acrylic and white latex paints and will be discussed further in the chemistry section.

4.1.4. Fluorescence Photography

One square for each paint type was photographed using fluorescence at 445 nanometres with a yellow filter during the bloodstain pattern (Figure 26).

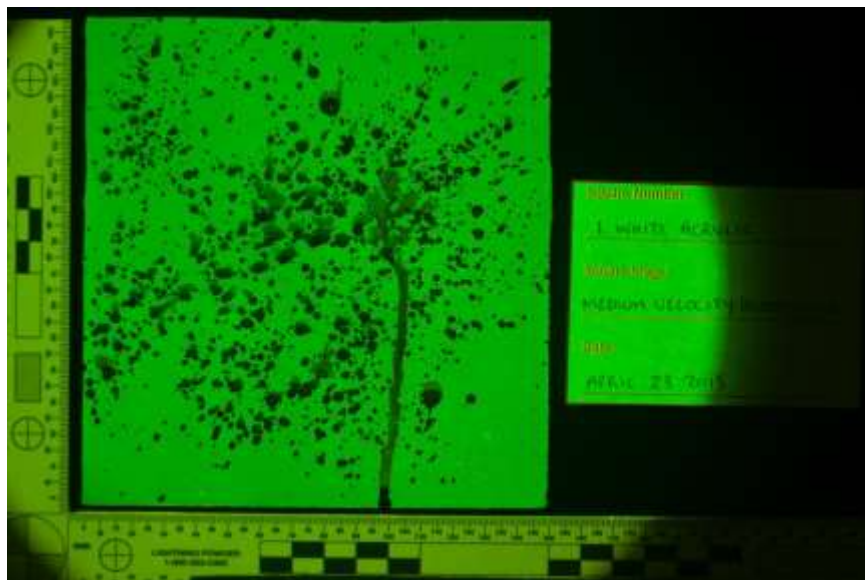


Figure 26. Example of Fluorescence Photography (Yellow Filter 445 nm) for the Bloodstain Pattern Stage (HDR White Acrylic 1)

The main reason was to observe the reaction of the bloodstain patterns using fluorescence photography in an attempt to determine whether the background paint absorbed or fluoresced at particular wavelengths when illuminated by the forensic light source, as well as observing the properties of the bloodstain patterns themselves. Both white acrylic

(Appendix 4.1.4.1) and white latex (Appendix 4.1.4.2) resulted in bloodstain patterns that contrasted with a fluorescing background. The black latex paint (Appendix 4.1.4.3) and maroon latex paint (Appendix 4.1.4.4) both depicted visual bloodstain pattern results, but not to the same intensity as white acrylic and white latex.

It was clear that both the white acrylic and white latex paints were capable of fluorescing at 445 nm with the yellow filter, allowing for a contrast with the darker bloodstain patterns. Black latex paint appeared to have no fluorescing capabilities resulting in lack of contrast between the bloodstain patterns and the background however, visual results were considered positive when compared to the amount of visual information available from standard photography. Maroon latex paint did appear to have minimal fluorescing properties and did allow for a definitive contrast between the bloodstain patterns and the background, but not to the same degree as with white acrylic and white latex. The chemical properties of the four paint types in terms of reflectance and absorption properties will be discussed further in the chemistry section.

Summary of Multi-Spectral Forensic Photography Techniques

For the bloodstain pattern stage a few preliminary photography observations could be seen. It was evident that white acrylic and white latex were reflecting the incident light source for reflective IR while absorbing the light source for reflective UV. Additionally it appeared that both white acrylic and white latex were capable of fluorescing and creating a contrast with the absorbing bloodstain patterns.

Black latex appeared to actively absorb the incident light for reflective IR and the results for reflective UV seemed similar to white acrylic and white latex in that black latex also absorbed the UV light. It was evident at this stage that black latex was incapable of fluorescing and creating a contrast with the absorbing bloodstain patterns.

The results for maroon latex for reflective IR appears to reflect a certain amount of the incident light however, whether or not this paint type would allow for transmission was still unknown. Similar results to black latex in the reflective UV stage could be seen; maroon latex appeared to be absorbing the UV light to a certain extent but allowed for a contrast with the absorbing bloodstain patterns to be seen. Finally, it appeared that maroon latex was capable of fluorescence but not to the same intensity as white acrylic and white latex.

These preliminary results for white acrylic, white latex and maroon latex appeared to be supported by past research conducted in IR photography, specifically of bloodstain patterns beneath paint (Howard and Nessian 2010; Farrar et al. 2012). However, the IR results for black latex did not show reflective capabilities and were not supported by past research in the field. Results for white acrylic and white latex appearing to fluoresce when illuminated by the incident light source can also be seen from the research by Adair (2006). The fluorescence capabilities of the two white paints as well as the maroon latex are also supported in the results from Howard and Nessian (2010). Results for the reflective UV photography were consistent with the appearance of blood absorption in the UV region resulting in a contrast with all four paint types. Blood absorption analyses are consistent with research by Stoilovic (1991) and Lee et al. (2013) for a higher percentage

of absorption in the UV region as opposed to the IR region; this would suggest that reflective UV and fluorescence photography would be recommended at this stage.

4.2. Stage Four: First Layer of Paint over Blood

The bloodstain patterns were allowed to dry completely before attempting to paint over them. This was to stay consistent with the literature, as well as refining the broad scope of this research. Blood dilution and blood cleanup research has been studied in the literature and was beyond the scope of this research.

The first layer of paint represented a scenario where a perpetrator attempted to hastily conceal the bloodstain patterns, or rely on the paint layer to obstruct forensic analysis. The paint layer was applied carefully in order to allow for uniform coverage in an attempt to keep all drywall squares equal or alike for interpretation and analysis. Different paint application techniques (e.g. hastily painting, non-uniform coverage) were not attempted since these variables fell outside the scope of this research project. However, attempting to closely replicate a scenario similar to crime scenes should be taken into consideration in future research.

4.2.1. Preparation and Application of First Layer of Paint

The application process of the first layer of paint over the bloodstain patterns was identical to the application process of the primer and paint layers stage. The setup and painting process was ideal when dealing with small squares and specific paint measurements. There was one major observation during the application of the first layer

of paint over the bloodstain patterns; the dried blood appeared to become 'wet' and was smeared along with the painting brush strokes. This occurred for all four paint types during this stage.

The 're-wetting' of the bloodstains created some interesting observations that should be taken into account. Especially noticeable on the medium velocity bloodstain patterns, information regarding trajectory, droplet size, and direction would all have been lost due to smearing. However, potentially being able to analyze bloodstain information available through reflective infrared, reflective ultraviolet or fluorescence photography was still a viable possibility. The bloodstain patterns were allowed to dry completely for a total of 64 hours prior to paint application; therefore, based on literature evidence (James et al. 2005), the cause of the re-wetting was not due to the bloodstains.

4.2.2. Standard Photography

Standard photography of the first layer of paint was identical in procedure to the previous stage of documenting the bloodstain patterns. These photographs were a reference to the available visual information and could be used as a comparison to photographs taken with reflective infrared, reflective ultraviolet and fluorescence photography. The photographs were combined in Photoshop to create one final HDR image for each drywall square (Figure 27) (Appendix 4.2.2).



Figure 27. Example of Standard Photography for the First Layer of Paint Stage (HDR White Acrylic 1)

Several things could be observed during this photography stage. The most obvious observation was the smearing of the bloodstain patterns during the painting process. The result of this occurrence is interesting considering that nowhere in the literature (Adair 2006; Bily and Maldonado 2006; Howard and Nesson 2010; Farrar et al. 2012) is this reaction alluded to, and due to the bloodstain patterns smearing, important information had been lost for analysis and interpretation by a bloodstain pattern analyst. Similar application methods were adapted from the literature including blood used, amount of paint used, and drying times. The amount of drying time both the bloodstain stage and first layer of paint stage were allotted exceeded drying times found in the literature. At this stage of analysis and interpretation it was hypothesized that the paint was responsible for the blood smearing. The paint used in this research was the only variable different from the literature due to the extensive amount of paint types available on the market and changing paint trends and formulas by manufacturers.

Although it would be difficult for a definitive analysis and interpretation of these results, the application of reflective IR, reflective UV, and fluorescence photography might be able to add information to this narrative. Chemical analyses were applied to the paint samples in an attempt to address this phenomenon and will be discussed further on.

4.2.3. Reflective Infrared Photography

Reflective infrared photography for the first layer of paint over the bloodstains was identical in procedure to reflective IR photography during the bloodstain pattern stage. The resulting photographs from this stage were also similar to the previous bloodstain pattern stage (Figure 28).

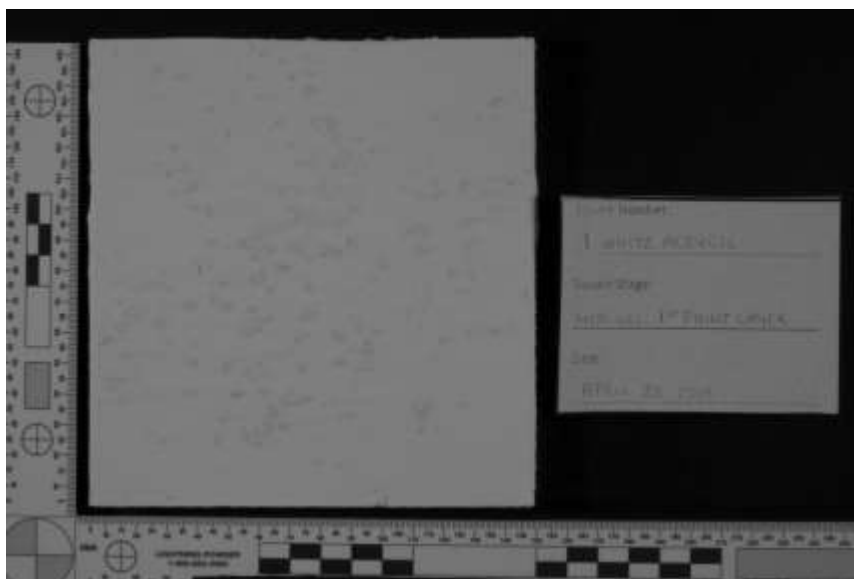


Figure 28. Example of Reflective Infrared Photography (Filter #87A) for the First Layer of Paint Stage (HDR White Acrylic 1)

Both white acrylic (Appendix 4.2.3.1) and white latex (Appendix 4.2.3.2) resulted in similar HDR images when combined in Photoshop, with minimal visual evidence observed with all filter types. Two of the filter types showed slightly more prominent

results (#87A, #87B) compared to the other filter types, but nothing of significance. Analyzing the reflective IR photographs as stand-alone results could potentially be interpreted as positive documentation of bloodstain patterns under the first layer of paint for white acrylic and white latex. However, when reflective IR photographs are compared to standard photographs, the latter depicts more detail than reflective IR. When determining which photography technique to use in this context, standard photography would result in more detailed images. Therefore, reflective IR photography can be considered impractical for use in this specific context.

Both the black latex (Appendix 4.2.3.3) and maroon latex (Appendix 4.2.3.4) paints seemed to absorb the infrared radiation and appeared darker in the resulting photographs. There was very minimal contrast between the bloodstain patterns and the black latex paint, and indistinguishable contrast for the maroon latex paint. A comparison of the reflective IR images and standard photography showed that the black latex paint did appear slightly lighter in reflective IR. However, for maroon latex, standard photography depicted some bloodstain pattern evidence whereas the reflective IR photography showed minimal or no evidence at all. At this stage it was apparent that reflective infrared photography for black latex and maroon latex could be considered negative.

4.2.4. Reflective Ultraviolet Photography

The results for reflective ultraviolet photography were quite different in comparison to reflective IR. Overall, a comparison between standard photography and

reflective UV photography showed that more information was present in standard photography. However, the results of the reflective UV photography added a different type of analysis to the narrative (Figure 29).



Figure 29. Example of Reflective Ultraviolet Photography for the First Layer of Paint Stage (HDR White Acrylic 1)

There was an observable difference between white acrylic (Appendix 4.2.4.1) and white latex (Appendix 4.2.4.2) in the reflective ultraviolet photography stage. Standard photography for both white acrylic and white latex showed evidence of the bloodstain patterns smearing and the resulting images depicted both the red smear lines and larger droplet sizes. A comparison between the white acrylic standard photography and reflective UV photography showed that this smearing was not evident in the reflective UV images. The scattering of the incident light source can also be seen with only the larger blood droplets being present for white acrylic.

The results for white latex were the most promising out of all four paint types. In comparison between the standard photography and reflective UV photography the

categorize which droplet patterns were located in the sub-surface, and which smearing patterns were located nearer to the surface during the painting process.

Black latex depicted similar results to white acrylic, absorbing the incident light source but still being able to reflect enough to show a contrast between the paint and bloodstain patterns (Appendix 4.2.4.3). In comparison between the standard photography and reflective UV photography, the reflective UV showed more prominent characteristics. As was noted with the white acrylic and white latex, prominent droplet information was also present for black latex with reflective UV photography, and could be used to aid bloodstain pattern analysts. The results of the black latex paint were not as dramatic as white latex; however, in comparison to available data between black latex standard photography and reflective UV photography, versus white acrylic standard photography and reflective UV photography, the black latex reflective UV photography depicted more observable information than standard photography.

Maroon latex behaved in a similar manner to black latex for the reflective UV photography stage (Appendix 4.2.4.4). The maroon latex paint appeared to absorb some of the incident light source resulting in a darker surface and less contrast with the absorbing bloodstain patterns. However, comparing the reflective UV photography to the standard photography for maroon latex did result in more visible information for the reflective UV. Comparing available reflective ultraviolet information to standard photography, white latex, black latex, and maroon latex can be concluded to have visual information present. White acrylic depicted less observable information for reflective

ultraviolet compared to standard photography and therefore could be considered a negative result.

4.2.5. Fluorescence Photography

The results of the bloodstain patterns under the first layer of paint for the fluorescence photography stage were drastically different from the reflective IR and reflective UV photographs (Figure 31).

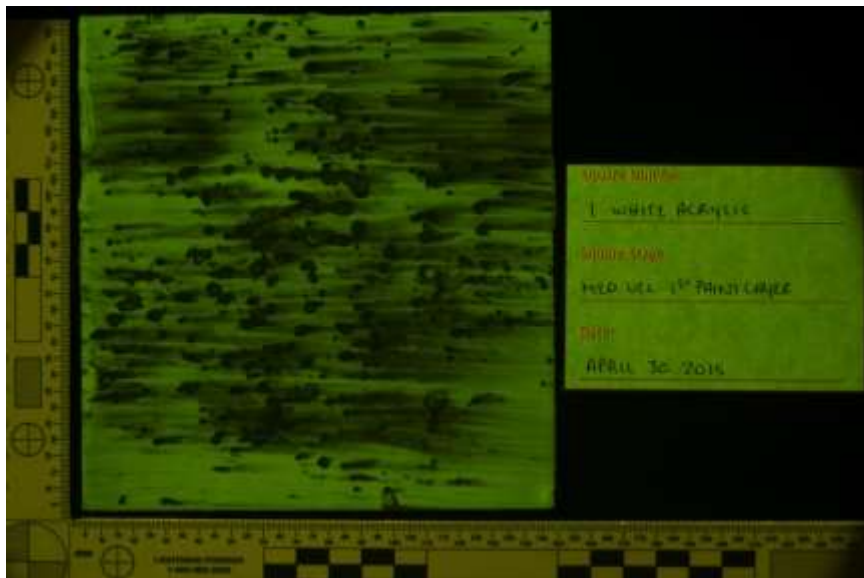


Figure 31. Example of Fluorescence Photography (Yellow Filter 445nm) for the First Layer of Paint Stage (HDR White Acrylic 1)

White acrylic and white latex were more prominent than black latex and maroon latex. Both the white acrylic and white latex allowed for a contrast between the bloodstain patterns and the paint; whereas this contrast was not as observable for maroon latex and even less so for black latex paint.

Photographs were taken with three different longpass filters (yellow, orange and red) with differing cut-off wavelengths. Each bandpass filter on the light source was

responsible for the emission of light over specific wavelength ranges except for SP575. This bandpass consisted of a shortpass cut-on filter that allowed all wavelengths up to 575 nm through. For white acrylic and white latex, the yellow longpass filter and orange longpass filter resulted in a definitive contrast between the absorbing bloodstain patterns and the fluorescing paint types. The best results for white acrylic occurred between 415 nm and 455 nm with the yellow and orange filters (Appendix 4.2.5.1). This result was consistent with the range of peak absorption of blood which would cause the highly visible contrast between the blood and paint. Similar results could be seen for white latex (Appendix 4.2.5.2) in the range of 415 nm to 455 nm with the yellow and orange filters. When comparing fluorescence images to standard photography images for white acrylic and white latex it is apparent that the subsequent blood smearing during the painting process was significantly more visible in the fluorescence images with the yellow and orange filters. When observing the results with the red filter, the smearing is less apparent, allowing for easier analysis of droplet size and distribution for white acrylic and white latex. This result was due to the longer spectral wavelength of the red filter compared to the yellow and orange filters. All three filters provided extensive visual information for white acrylic and white latex.

The black latex paint was not capable of fluorescing when in contact with the incident light source and any of the filters (Appendix 4.2.5.3). The results for black latex were similar in visual information to the images collected from the standard photography stage. This paint type was not capable of fluorescing and therefore the contrast with absorbing bloodstain patterns was not observed.

The maroon latex paint exhibited slightly more information than black latex, however not to the extent of the white acrylic and white latex. Unlike the white acrylic and white latex paint types, the results from all three filters were similar in nature (Appendix 4.2.5.4). The maroon paint appeared to contain some fluorescing properties when compared to the amount of visible information available between the fluorescence photography stage and standard photography stage. In this instance, fluorescence photography does provide more information for maroon latex than standard photography alone.

Summary of Multi-Spectral Forensic Photography Techniques

Several observations could be seen from the first layer of paint stage. It appeared that white acrylic and white latex were capable of reflecting the incident light source for reflective IR photography; however, there did not appear to be transmission through the paint. It was hypothesized that the chemical and physical properties of the paint types were not allowing for IR transmission. The light source being used as well as the sample blood being tested were both found to have worked in the literature suggesting that the paint variable would need to be further addressed. Both Farrar et al. (2012) and Howard and Nesson (2010) concluded that blood could be observed beneath several paint layers with reflective IR photography, which did not match the results of this study. Additionally, both a black and maroon/red paint were tested by Farrar et al. (2012) and Howard and Nesson (2012) that actively appeared to allow transmission of the incident light and

created a contrast between the bloodstain patterns and paint which could not be observed in this study.

Reflective UV photography was not conducted on bloodstain patterns beneath paint in the research to the knowledge of this author. However, based on research by Cosentino (2014) on the analysis of historic paintings, the results for all four paint types can be better understood. White acrylic appeared to absorb the incident light and failed to produce a contrast between the paint and bloodstain patterns. It was noted in the research (Cosentino 2014) that both titanium white and lead white absorbed during reflective UV photography, whereas zinc white reflected the incident light source. White latex appeared to allow for a certain amount of contrast between the paint and bloodstain patterns, potentially due to less titanium dioxide being present in the paint. The reflective UV results for black latex and maroon latex also appeared to actively absorb the incident light (Cosentino and Stout 2014) however, in comparison to the standard photography results this technique was concluded as positive for reflective UV for these two paint types.

The results for fluorescence photography appeared to be the most inconsistent with the literature, but the most conclusive photography technique for the first layer of paint stage. There was a visible contrast between the fluorescing paint and absorbing bloodstain patterns for both white acrylic and white latex that was not seen in past research (Adair 2006; Howard and Nessian 2010) and was most likely due to chemical properties in these two paint types. However, results for maroon latex were similar to those seen from Howard and Nessian (2010), where the paint was capable of some fluorescence and created a contrast with the bloodstain patterns. Black latex was not

capable of fluorescing which is consistent with the literature findings for different types of black paints by Cosentino (2014).

4.3. Stage Five: Second Layer of Paint over Blood

The second layer of paint over the bloodstain patterns was applied in the same manner as the first layer of paint; however, the parameters were different from the first layer. The application of the first layer of paint over the bloodstain patterns was an attempt to replicate a scene where bloodstain patterns were hastily painted over or obscured. The second layer of paint would result in a thicker layer and could be seen as an attempt to replicate a meticulous cover-up. If the clean-up of a crime scene was not rushed and any evidence could be meticulously hidden, full wall painting may result in an attempt to conceal bloodstain patterns. The amount of paint used in this stage was the highest quantity of paint that could be applied to completely obscure the bloodstain patterns.

4.3.1. Preparation and Application of Second Layer of Paint

The application and painting process of the second layer of paint over the bloodstain patterns was identical to the previous stages. As well, it was also observed that the blood 're-wetting' that occurred during the first layer of paint stage also occurred to some extent during this stage. Additional smearing was observed for all paint types, but not to the same extent as the previous stage. All drywall squares received the application of the second layer of paint except for the four control squares of no blood. This was due

to both time constraints and the redundancy of applying a second layer of paint to the control.

The second layer of paint applied over the bloodstain patterns was thick enough so as to cover any visible bloodstains in an attempt to completely obscure this visual component. However, once the paint dried, bloodstain patterns could still be seen, especially for the white acrylic and white latex squares. The reasons for this are a result of low-cost paint (versus premium paint brands) and the ratio of pigment particles to other paint components present in the two white paint types. The bases used for black latex and maroon latex, along with the addition of pigment, resulted in a visibly thicker layer. A third layer of paint could not be applied and analyzed due to time constraints.

4.3.2. Standard Photography

The standard photography for the second layer of paint stage was identical in procedure to the first two stages but with an added component. Photographs were also taken with oblique lighting from both the left and right side for all drywall squares (Figure 32).

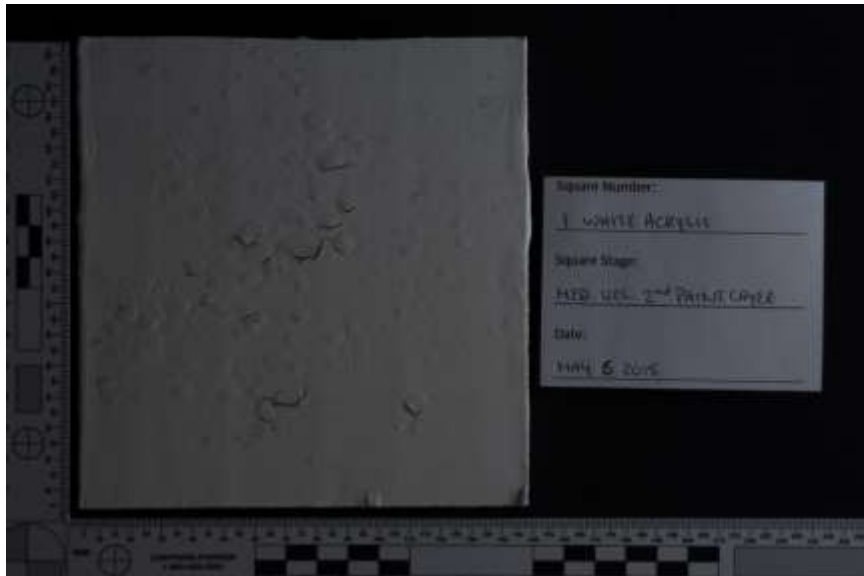


Figure 32. Example of Standard Photography (Oblique Lighting Left) for the Second Layer of Paint Stage (HDR White Acrylic 1)

The visual results for the bloodstain patterns of the drywall squares after the second layer of paint were more difficult to observe and analyze than the previous stage. For this reason oblique lighting was used to enhance any potential visual information by adjusting the angle of the light source until the optimum results could be seen. Oblique lighting is often used in forensic photography (Weiss 2009) in order to document information available through visual inspection.

A comparison of standard photography from both the left and right light sources, the left light source only, and the right light source only for white acrylic can be found in Appendix 4.3.2.1. For both white acrylic and white latex (Appendix 4.3.2.2) the oblique lighting images depicted more observable information than what could be seen for black latex (Appendix 4.3.2.3) and maroon latex (Appendix 4.3.2.4). For both black latex and maroon latex the oblique lighting images showed more visual information in comparison

with the standard photography using both light sources. The resulting images for all four paint types could be used as a baseline for comparison to the other techniques.

4.3.3. Reflective Infrared Photography

The reflective infrared photography procedure was identical to the previous two stages; however, the addition of photography using oblique lighting was implemented in the same manner as the standard photography stage for the second layer of paint over bloodstain patterns (Figure 33).

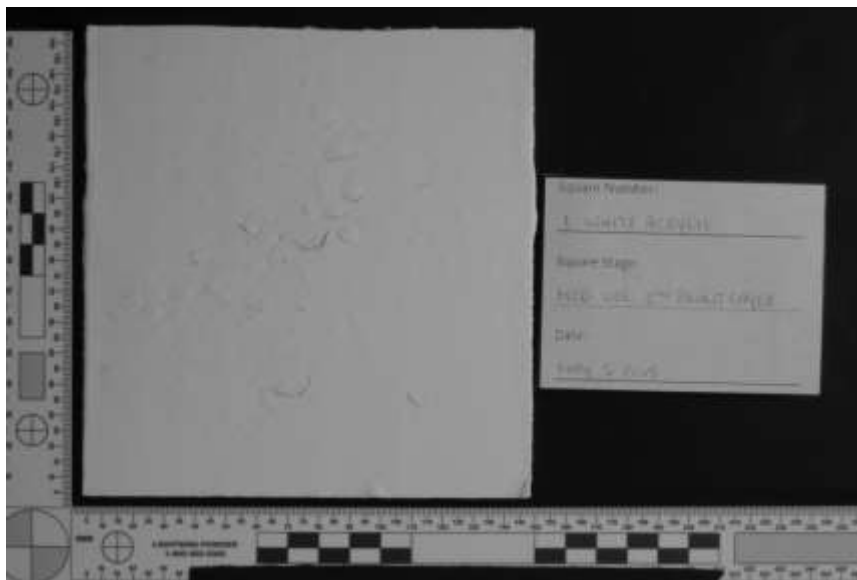


Figure 33. Example of Reflective Infrared Photography (Filter #87A Oblique Lighting Left) for the Second Layer of Paint Stage (HDR White Acrylic 1)

It was apparent during infrared photography of the white acrylic squares that visual information of bloodstain patterns was not viable using this technique. Due to time constraints, only the white acrylic medium velocity, swipe, and saturated bloodstain patterns were photographed (Appendix 4.3.3.1). All longpass filters were tested for white

latex, black latex, and maroon latex but not photographed due to the extensive in-camera processing time. Therefore, the results for white latex, black latex, and maroon latex were not applicable. A comparison between standard photographs and infrared photographs for white acrylic showed that more information was visually present in the standard images. For this reason, the reflective infrared photographs could be interpreted as a negative result.

These results were apparent during the first layer of paint stage but become more noticeable after the application of the second layer of paint over bloodstain patterns. The modified UV/IR camera was unable to penetrate all four paint types to document the contrast between the absorbing bloodstain patterns and the paint types. Photographing using oblique lighting did allow slightly more visual information; however, compared to oblique lighting with standard photography, the reflective infrared images were concluded as negative.

4.3.4. Reflective Ultraviolet Photography

The results for reflective ultraviolet photography for the second layer of paint stage were similar to what could be observed from the first layer of paint stage but with a few differences (Figure 34).

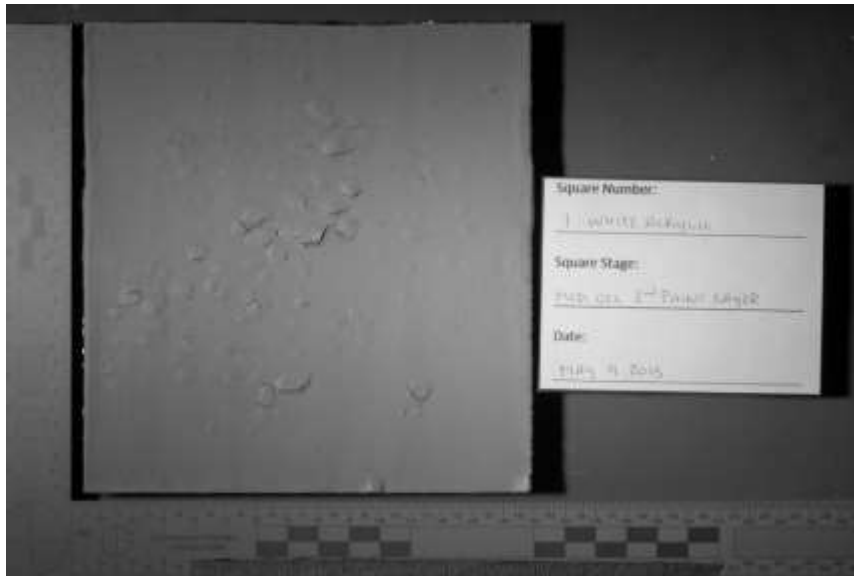


Figure 34. Example of Reflective Ultraviolet Photography for the Second Layer of Paint Stage (HDR White Acrylic 1)

Firstly, following a similar set-up procedure to the standard photography stage and reflective infrared photography stage, the light source for reflective ultraviolet was adjusted to an oblique angle. By adjusting the angle of the light source, the light was more evenly distributed to support the application of HDR photography and interpretation of the results.

The results for white acrylic and white latex were similar in that the two paint types appeared to absorb some of the UV radiation being emitted by the incident light source. The contrast between the absorption of the paint (as opposed to reflection) and absorption of the bloodstain patterns could not be better discerned with reflective ultraviolet compared to standard photography. White acrylic (Appendix 4.3.4.1) and white latex (Appendix 4.3.4.2) could be interpreted as negative when compared to standard photography of these paint types for the second layer of paint stage.

In contrast to the results for white acrylic and white latex, the results for black latex (Appendix 4.3.4.3) and maroon latex (Appendix 4.3.4.4) were more conclusive (Figure 35).

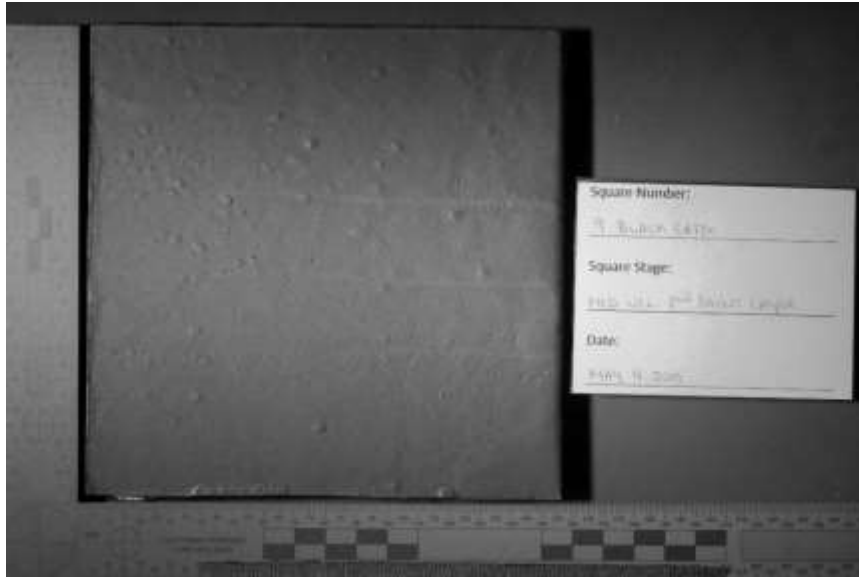


Figure 35. Example of Reflective Ultraviolet Photography for the Second Layer of Paint Stage (HDR Black Latex 9).

Both the black latex and maroon latex paint types were capable of reflecting UV radiation resulting in more visible contrast when compared to standard photography. Although the reflective ultraviolet images for black latex and maroon latex appeared similar to white acrylic and white latex, more visible information could be seen from the reflective ultraviolet images in comparison to the standard photography stage. These results suggest that the use of reflective ultraviolet photography could prove useful when photographing darker painted surfaces.

4.3.5. Fluorescence Photography

Fluorescence photography using the SPEX Crimescope was fairly easy to use in order to quickly test which combinations of longpass coloured filters to bandpass light wavelengths would produce the best results (Figure 36).

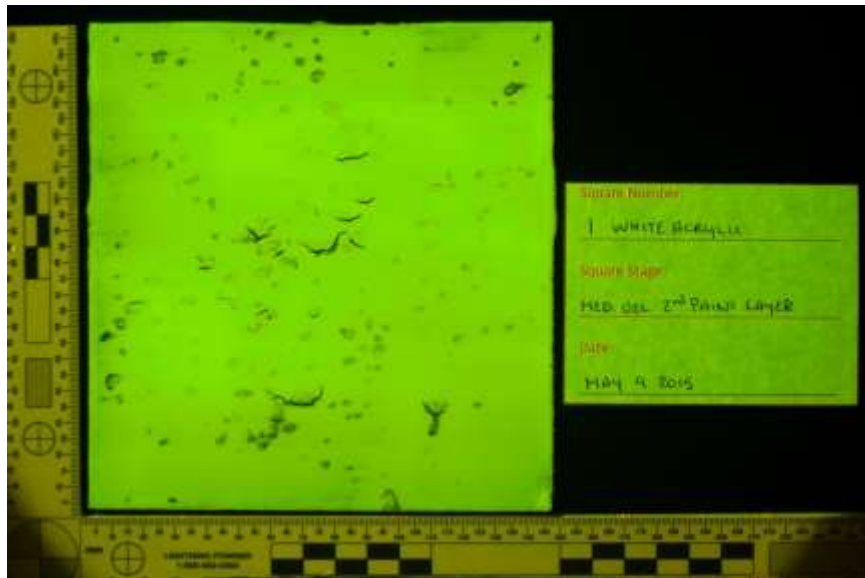


Figure 36. Example of Fluorescence Photography (Yellow Filter 445 nm) for the Second Layer of Paint Stage (HDR White Acrylic 1)

All combinations were first tested using the coloured goggles to determine which filter and light source wavelength range would be photographed. Both white acrylic and white latex received the same test combinations of yellow, orange, and red longpass viewing to light source wavelength range. Yellow and orange filters for white acrylic (Appendix 4.3.5.1) and white latex (Appendix 4.3.5.2) were the most visually positive in identifying the bloodstain patterns under the second layer of paint. The red filter for white acrylic and white latex did not depict the same level of distinctive contrast between a fluorescing background and absorbing bloodstain patterns; however, the visual information was more conclusive when compared to standard photography.

The results for black latex (Appendix 4.3.5.3) and maroon latex (4.3.5.4) were negative for all longpass filter and bandpass nanometre combinations when compared to standard photography. Black latex was incapable of fluorescing and could not produce a contrast between the bloodstain patterns and the background; however, maroon latex was capable of minimal fluorescence but could not produce a contrast between the paint and bloodstain patterns. For white acrylic and white latex the yellow and orange filters produced more successful results when compared to standard photography; however, the red filter was still able to produce results.

Summary of Multi-Spectral Forensic Photography Techniques

The results for reflective IR photography were concluded as negative for all four paint types. These results were different from the research by Farrar et al. (2012); however, the high amount of IR absorption and lack of transmission was most likely due to the specific paints being used. Further analysis in terms of paint chemistry are described in the section on chemistry analysis.

The second layer of paint stage for reflective UV resulted in more information being seen with standard photography rather than UV photography for both white acrylic and white latex. These results were supported by the multi-spectral photography results conducted by Cosentino and Stout (2014) on historical works of art. Similar results of absorption, and minimal reflectance, can be seen for black latex and maroon latex which is also supported through the literature that absorption appeared to occur (Cosentino and

Stout 2014). However, in comparison to standard photography, more visual information of the bloodstain patterns could be seen with reflective UV photography.

The results for the second layer of paint for white acrylic and white latex were positive for the fluorescence photography stage. These results were not seen in the literature (Adair 2006; Howard and Nessian 2010) and might suggest different paint chemistry from the products used in other research. Black latex was concluded as negative since it was incapable of fluorescing, and maroon latex was also concluded as negative for the second layer of paint. Similar results for maroon latex paint were concluded in a study by Howard and Nessian (2010) for the second layer of paint and these results appear consistent with the literature.

4.4. Stage Six: Application of Luminol

Following the completion of all photography techniques during the second layer of paint over bloodstain patterns stage, the chemiluminescence testing was undertaken. The application of the Luminol reagent could be considered a destructive process and was therefore only applied at the completion of the experiment. Due to this reasoning, the application of Luminol was only possible for the second layer of paint stage. There were two main components being observed during this stage; whether the bloodstain patterns under the painted layers chemiluminesced or not, and if there were any false positive results from the four controls of no bloodstain patterns for each paint type.

4.4.1. Standard Photography

Standard photography for the Luminol testing stage was identical in set-up and procedure as the previous standard photography stages. Prior to the application of the Luminol reagent, each drywall square was photographed with the tungsten light source in order to provide a comparison before image to the Luminol after image (Figure 37).



Figure 37. Example of Standard Photography (Luminol testing) for the Second Layer of Paint Stage (White Acrylic 1)

The drywall squares were sprayed with the Luminol reagent and then placed on the copy stand to be photographed. The room lighting was turned off resulting in a pitch black environment with the only light produced from the Luminol reaction. Due to the dark environment, the shutter of the camera needed to be left open for the duration of the chemiluminescent event. This provided sufficient light to enter the camera for recording of images. Due to weak or absent emission of light for specific drywall squares, a flash unit was set off once producing an instant flash of light while the camera shutter was kept open. The flash unit was held facing away from the copy stand and camera set-up, allowing for the quick flash of light to bounce off the walls. This was done for

consistency for all four controls of no blood drywall squares. By setting off the flash unit once, weak light emission, or the absence of chemiluminescence, could be viewed easier.

The results for white acrylic (Appendix 4.4.1.1) and white latex (Appendix 4.4.1.2) were nearly identical. Where the Luminol reagent was able to come into direct contact with blood through small cracks in the paint, chemiluminescence occurred. Additionally, the overall chemiluminescence was significantly brighter in comparison to the black latex and maroon latex paints. This was a result of a slight luminescence of the white acrylic and white latex paint themselves which could be seen from the controls of no blood. The chemical properties of these results will be discussed further on; however these same results were not observed for the black latex or maroon latex paints and therefore suggest the presence of a chemical component in the white paints which was effecting the Luminol reaction.

For black latex (Appendix 4.4.1.3) and maroon latex (4.4.1.4) the results were difficult to visibly see for the medium velocity bloodstain patterns and the swipe patterns, but more easily visible for the saturated stains. Small cracks in the paint allowed the Luminol reagent to enter and interact with the bloodstain patterns, resulting in the chemiluminescence and pooling around the stains. Without direct access to the blood, areas did not luminesce when simply in contact with the second layer of paint over the bloodstain patterns. Both the black latex and maroon latex controls of no blood did not depict any reaction to the Luminol reagent, further suggesting that a specific chemical component present in the white acrylic and white latex paints was responsible for the reaction.

Summary of Luminol Forensic Photography Results

The Luminol reagent was capable of detecting and luminescing when in direct contact with the bloodstain patterns, however, the areas solidly obstructed by the second layer of paint did not allow direct contact between the Luminol and bloodstain patterns and was unresponsive. This was consistent with a similar study by Bily and Maldonado (2006) that described spraying the Luminol reagent on bloodstain patterns beneath paint layers. The amount of Luminol sprayed on each drywall square was adapted from the study by Bily and Maldonado (2006); however, the amount of Luminol used for this study resulted in visible pooling for all four paint types but especially white acrylic and white latex. It was apparent that less Luminol reagent needed to be used and should be taken into consideration in future research.

The controls of no blood for both white acrylic and white latex created a false positive reaction when in contact with the Luminol reagent. There has been extensive research in the field of Luminol reactions (Quickenden and Creamer 2001; Creamer et al. 2003; King and Miskelly 2004; James et al. 2005; Bily and Maldonado 2006) in the absence of heme. A study by Bily and Maldonado (2006) looked at the Luminol reactions of bloodstains beneath paint and noted chemiluminescent reactions in the presence of superficial cleaning. The false positives created from both controls of no blood for white acrylic and white latex suggests the presence of a substance capable of chemiluminescence.

4.5. Photography Analysis

Bloodstain patterns on different surfaces and under paint layers have been studied in the literature using multi-spectral photography techniques. However, the application of High Dynamic Range photography in an attempt to produce more visual information has not yet been attempted in this context. The HDR photography was defined as the merging of photographs at different exposures into one compiled image in Photoshop CC. A visual analysis of the HDR results for reflective infrared photography, reflective ultraviolet photography, and fluorescence photography was performed in comparison with one single photograph at normal exposure (0.0) in the same set of photographs.

4.5.1. High Dynamic Range Photography Analysis

4.5.1.1 Standard Photography

Collecting HDR photographs for the standard photography stage was fairly quick and straightforward in comparison to the other stages. All three stages (bloodstain pattern, first layer of paint, and second layer of paint) did not depict any visually significant differences between the HDR image and one single photograph (Figure 38).

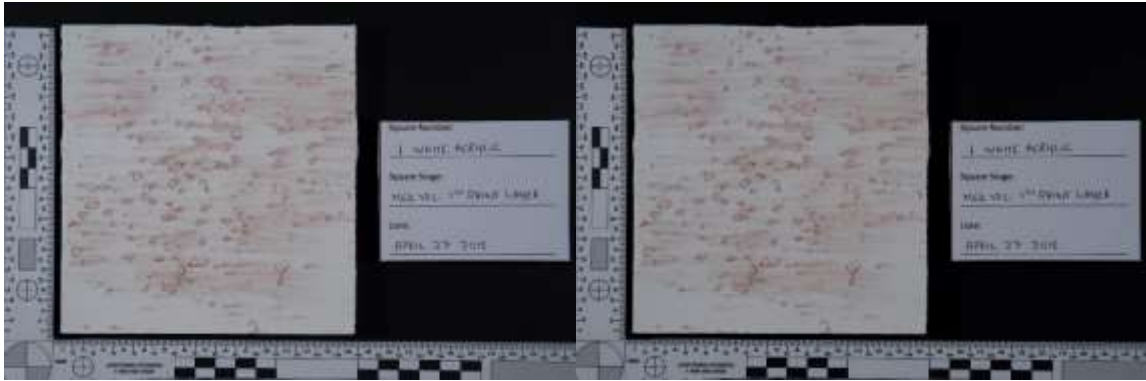


Figure 38. Example of Standard Photography for the First Layer of Paint Stage (HDR White Acrylic 1 Left; Single White Acrylic 1 Right).

The only observable differences would be the overall level of brightness in the combined HDR image which does not affect the visual information; another slight difference was that the oblique lighting images depicted more uniform distribution of light in the HDR image as opposed to one single image; however these results did not affect any visual information. Only one photograph was taken for each drywall square during the Luminol testing stage due to the length of time needed to capture the chemiluminescence event.

4.5.1.2 Reflective Infrared Photography

For the bloodstain pattern stage, a comparison of white acrylic between one single photograph and an HDR combined image did reveal some differences in the strength of the dark tones on a light background (Figure 39) (Appendix 4.1.2.1).

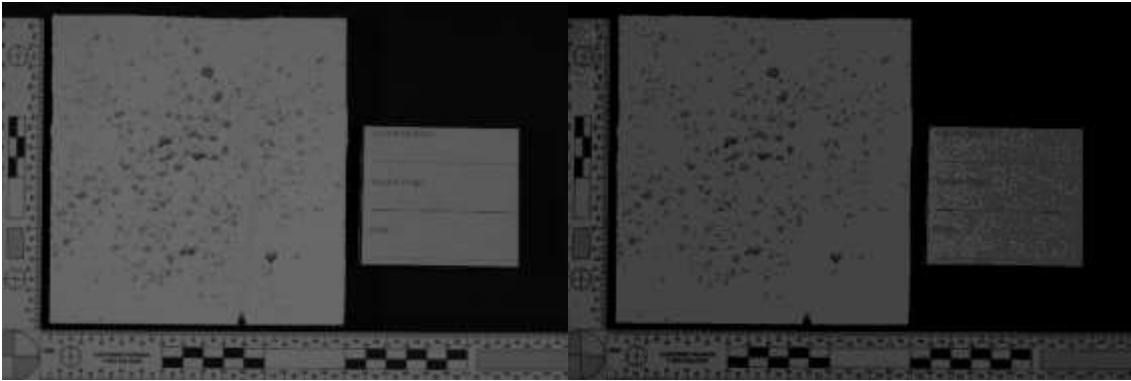


Figure 39. Example of Reflective Infrared Photography (Longpass Filter #87A) for the Bloodstain Pattern Stage (HDR White Acrylic 1 Left; Single White Acrylic 1 Right).

These differences could also be observed for the white latex drywall squares (Appendix 4.1.2.2). The opposite effect was observed for black latex and maroon latex. There was no significant difference between one single photograph and a HDR combined image for black latex (Appendix 4.1.2.3) and maroon latex (Figure 40) (Appendix 4.1.2.4).



Figure 40. Example of Reflective Infrared Photography (Longpass Filter #87A) for the Bloodstain Pattern Stage (HDR Black Latex 9 Left; Single Black Latex 9 Right).

This result is consistent with the negative visual results that could be observed for both black latex and maroon latex reflective infrared photography.

The results for the first layer of paint stage were similar to the bloodstain pattern stage. There were minute visual differences between one single photograph and the HDR

image for both white acrylic (Appendix 4.2.3.1) and white latex (Appendix 4.2.3.2). (Figure 41).



Figure 41. Example of Reflective Infrared Photography (Longpass Filter #87A) for the First Layer of Paint Stage (HDR White Acrylic 1 Left; Single White Acrylic 1 Right).

An over-exposed photograph would obscure hard to see darker features and could potentially overwhelm these features when combined in an HDR image. For both white acrylic and white latex, it would be recommended that bracketed photographs at different exposures be taken for individual analysis, but not combined as a HDR image post-referential. Black latex (Appendix 4.2.3.3) and maroon latex (Appendix 4.2.3.4) showed no significant difference between one single photograph and a combined HDR image. The reflective infrared results for black latex and maroon latex were concluded as negative for analysis of both single photographs and HDR images.

Only white acrylic (Appendix 4.3.3.1) was photographed for the second layer of paint over bloodstain patterns using reflective infrared photography (Figure 42).

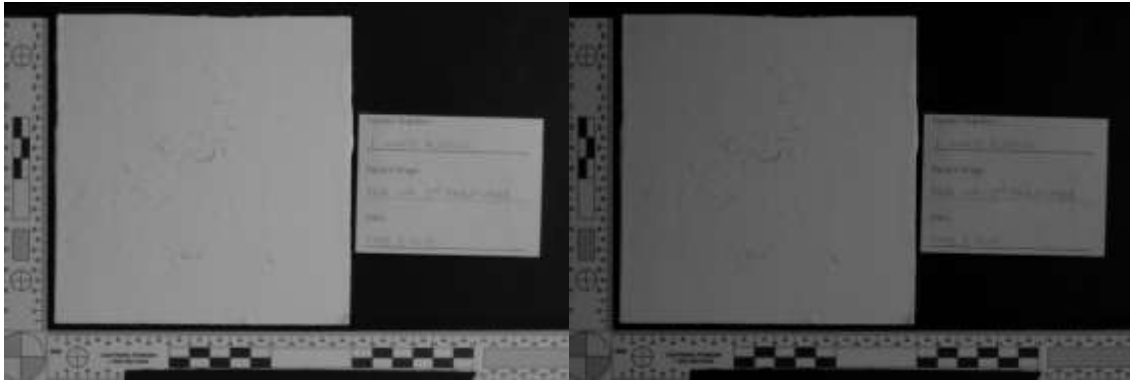


Figure 42. Example of Reflective Infrared Photography (Longpass Filter #87A Lighting Oblique Left) for the Second Layer of Paint Stage (HDR White Acrylic 1 Left; Single White Acrylic 1 Right).

The results were concluded as being negative, and similarly to the oblique standard photographs; there were no significant differences except for a slightly more uniform distribution of light across the surface of the square.

4.5.1.3 Reflective Ultraviolet Photography

Reflective ultraviolet photography for the bloodstain pattern stage would not be recommended for combined HDR image analysis due to the concentration of the incident light source in the middle of the subject. Information was not lost during HDR image combining in Photoshop CC; however, in comparison to one single photograph the illumination in the centre of the subject appears brighter in the HDR image (Figure 43).



Figure 43. Example of Reflective Ultraviolet Photography for the Bloodstain Pattern Stage (HDR White Acrylic 1 Left; Single White Acrylic 1 Right).

A comparison between a HDR image and one single photograph for white acrylic (Appendix 4.1.3.1), white latex (Appendix 4.1.3.2), black latex (Appendix 4.1.3.3), and maroon latex (Appendix 4.1.3.4) suggests that analysis would be better performed on one single photograph as opposed to the HDR image.

Similar results could be seen for the first layer of paint stage when comparing one single image to the HDR image for white acrylic (Appendix 4.2.4.1), white latex (Appendix 4.2.4.2), black latex (Appendix 4.2.4.3), and maroon latex (Appendix 4.2.4.4) (Figure 44).



Figure 44. Example of Reflective Ultraviolet Photography for the First Layer of Paint Stage (HDR White Acrylic 1 Left; Single White Acrylic 1 Right).

Overall the HDR images are more uniformly illuminated which does allow for a thorough analysis of the entire surface of each drywall square. However, the incident light source appears more concentrated in the centre of HDR image in comparison to one single image. Although no information is lost in the HDR analysis for reflective ultraviolet, visual information appears more detailed for one single photograph compared to the HDR image.

High dynamic range images for the second layer of paint stage produced viable results for the slightly altered procedure. The incident light source was adjusted in an attempt to remove the concentration of light from the centre of the subject (Figure 45).



Figure 45. Example of Reflective Ultraviolet Photography for the Second Layer of Paint Stage (HDR White Acrylic 1 Left; Single White Acrylic 1 Right).

A comparison between one single photograph and the HDR image for white acrylic (Appendix 4.3.4.1), white latex (Appendix 4.3.4.2), black latex (Appendix 4.3.4.3), and maroon latex (Appendix 4.3.4.4) depict only slight differences compared to observations during the first layer of paint stage. For the second layer of paint stage either the HDR image or one single photograph could be used for appropriate analysis, whereas the previous two stages it was suggested that the single photograph be used. This is due to the

removal of the concentration of light on the centre of the subject. For the second layer of paint stage, the HDR images depict a more uniform illumination of the subject compared to one single photograph; whereas an analysis of one single photograph shows slightly darker edges which could potentially obscure details.

For reflective ultraviolet photography, a set of bracketed images at different exposures can be taken and either merged into one HDR image or remain as single photographs for analysis. Both techniques provided a useful analysis, however, more information can be gleaned from a set of photographs at different exposures and taking advantage of this technique could prove useful in evidence collection.

4.5.1.4 Fluorescence Photography

Fluorescence photography for the bloodstain pattern stage consisted of an example set of one drywall square for each paint type. For white acrylic, an analysis of one single photograph with the yellow longpass filter at bandpass 445 nm and the merged HDR image showed that bloodstain pattern information in the HDR image contained more definable boundaries in terms of droplet visibility and placement (Figure 46) (Appendix 4.1.4.1).

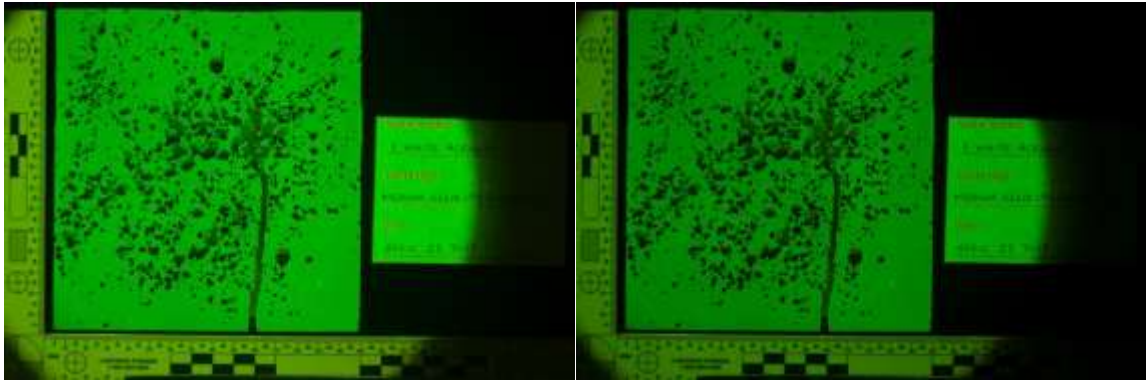


Figure 46. Example of Fluorescence Photography (Yellow Filter 445 nm) for the Bloodstain Pattern Stage (HDR White Acrylic 1 Left; Single White Acrylic 1 Right).

Similar results could be observed for white latex (Appendix 4.1.4.2) where the fluorescing background and dark bloodstain patterns appeared more uniform and consistent between the single photograph and the HDR image. Black latex on the other hand did not show any differences between one single photograph and the HDR image for the bloodstain pattern stage (Appendix 4.1.4.3). The absence of a fluorescing background paint for black latex resulted in a lack of contrast in the image. Finally, maroon latex did show some evidence of fluorescing during this stage, but not to the extent of white acrylic and white latex (Figure 47).

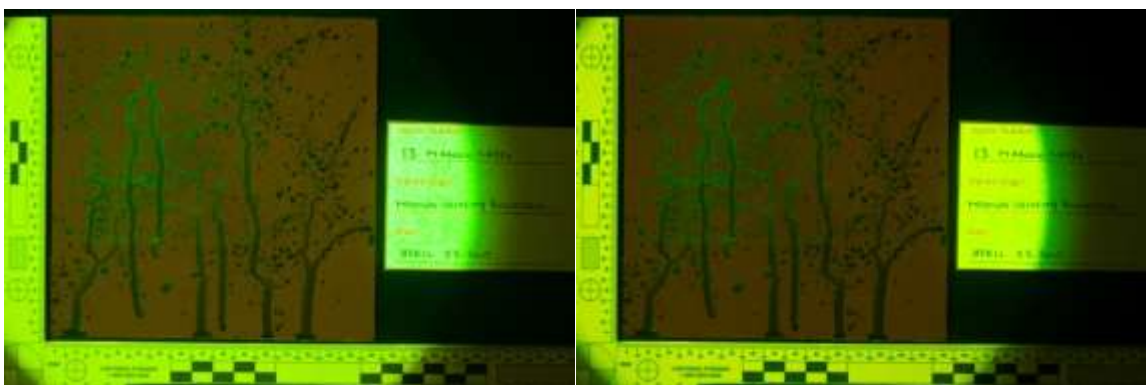


Figure 47. Example of Fluorescence Photography (Yellow Filter 445nm) for the Bloodstain Pattern Stage (HDR Maroon Latex13 Left; Single Maroon Latex 13 Right).

A comparison of one single photograph and the HDR image did not show significant differences, however, the HDR image appeared more uniform in light distribution across the surface with a clear distinction between the fluorescing paint and bloodstain patterns (Appendix 4.1.4.4).

The results for the first layer of paint stage were the most positive out of all multi-spectral photography techniques. An added bonus for the fluorescence photography was the effects of HDR images in comparison to one single photograph for three of the four paint types. The HDR results for white acrylic and white latex were quite similar in that both paint types fluoresced and provided significant contrast with the dark bloodstain patterns (Figure 48).

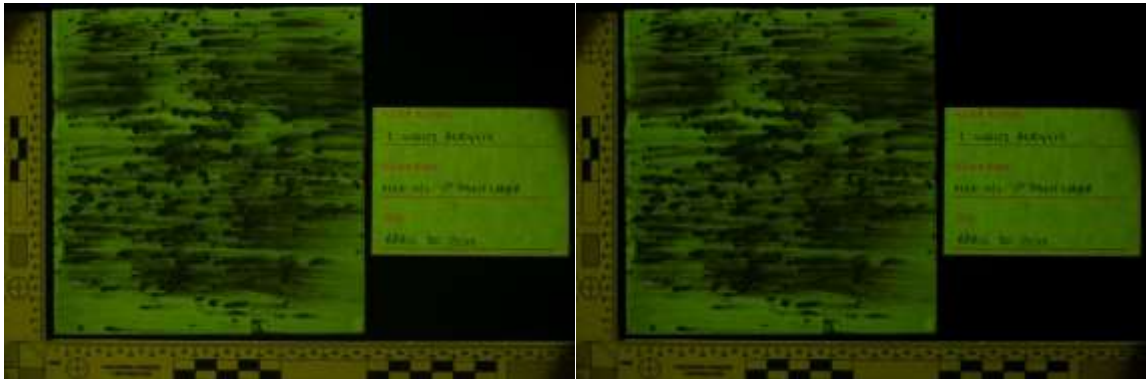


Figure 48. Example of Fluorescence Photography (Yellow Filter 445 nm) for the First Layer of Paint Stage (HDR White Acrylic 1 Left; Single White Acrylic 1 Right).

HDR images for the yellow and orange longpass filters for white acrylic (Appendix 4.2.5.1) and white latex (Appendix 4.2.5.2) were the best examples of uniform illumination and defined bloodstain parameters. There was no loss of information in a comparison to one single photograph; however, the HDR images contained useful light tone and dark tone contrasts which could make analysis easier. Similar results could be

stated for the red longpass filter however, due to the longer wavelength being used, it would be better for one single photograph to be visually analyzed compared to HDR images for white acrylic and white latex. The red filter would benefit from having less light exposure rather than more and although the resulting images were as detailed as with the yellow and orange filters; it would be recommended that for the red filter only one single photograph be analyzed as opposed to a HDR image (Figure 49).



Figure 49. Example of Fluorescence Photography (Red Filter 575 nm) for the Bloodstain Pattern Stage (HDR White Acrylic 1 Left; Single White Acrylic 1 Right).

Black latex results for the first layer of paint stage were similar to the bloodstain pattern stage in that not much could be seen. A comparison between one single photograph and a HDR image did not show any significant differences for any of the coloured longpass filters (Appendix 4.2.5.3). The results for bloodstain analysis under black latex paint for the first layer of paint stage could be concluded as negative. The final paint type consisting of maroon latex depicted minimal but apparent bloodstain results (Figure 50).

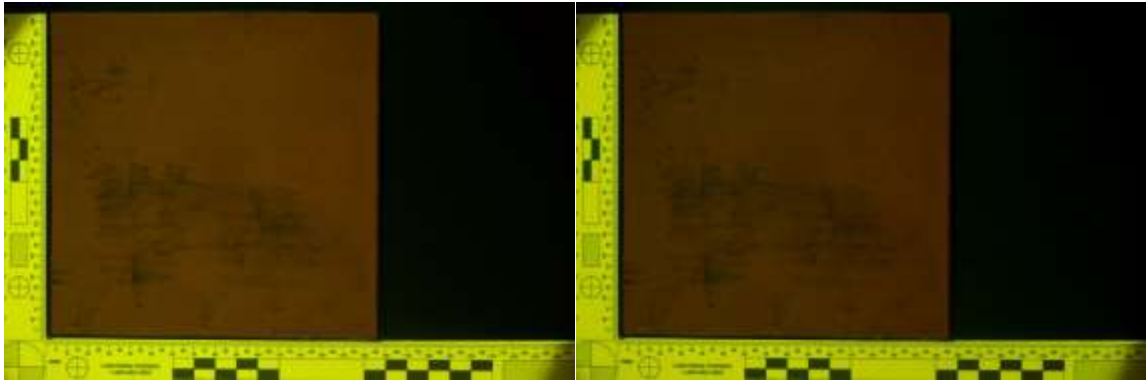


Figure 50. Example of Fluorescence Photography (Yellow Filter 445 nm) for the Second Layer of Paint Stage (HDR Maroon Latex 13 Left; Single Maroon Latex 13 Right).

Although not as conclusive as the results from white acrylic and white latex, a comparison between one single photograph and a HDR image for maroon latex provided distinctive information in the HDR image with the yellow and orange longpass filters (Appendix 4.2.5.4). Also similar to the white acrylic and white latex paint types, the HDR image with the red longpass filter appeared to somewhat overwhelm the contrasting bloodstain patterns. No information was lost with the red filter; however, for analysis only one single photograph would be needed.

The second layer of paint over the bloodstain patterns depicted similar observations to the previous first layer of paint for all paint types. An analysis of one single photograph compared to a HDR image for white acrylic (Appendix 4.3.5.1) and white latex (Appendix 4.3.5.2) presented more definable bloodstain characteristics against the fluorescing paint using both the yellow and orange longpass filters (Figure 51).



Figure 51. Example of Fluorescence Photography (Yellow Filter 445 nm) for the Second Layer of Paint Stage (HDR White Acrylic 1 Left; Single White Acrylic 1 Right).

On the other hand, the red longpass filter single photograph for white acrylic and white latex appeared to depict more visual information than the HDR image. It would not be recommended to analyze a HDR image with the red longpass filter (Figure 52).

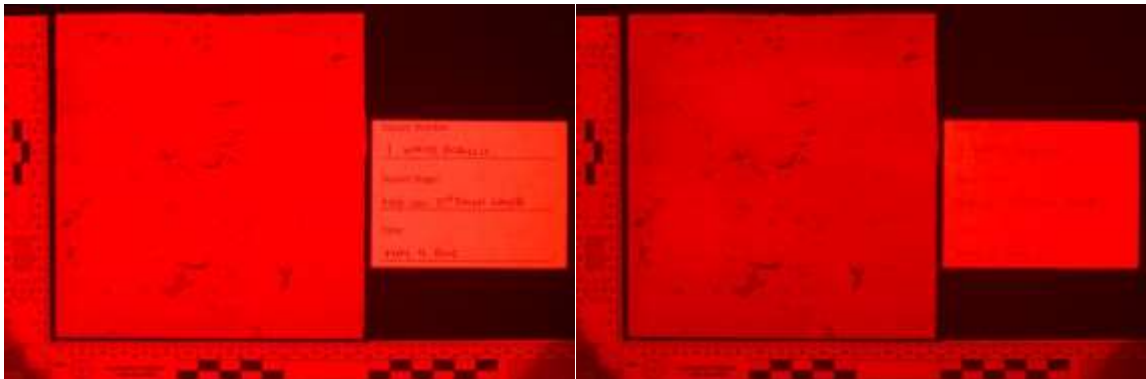


Figure 52. Example of Fluorescence Photography (Red Filter 415 nm) for the Second Layer of Paint Stage (HDR White Acrylic 1 Left; Single White Acrylic 1 Right).

Black latex results were negative during this stage and analysis of both a single photograph and HDR image provided no significant differences (Appendix 4.3.5.3). Finally, only a yellow longpass filter was used to document maroon latex for this stage. The bloodstain information was minimal, but what could be observed was more defined in the HDR image compared to one single photograph (Appendix 4.3.5.4). It could be

recommended that when photographing with a yellow or orange longpass filter, HDR images be used for analysis and interpretation purposes.

Summary of High Dynamic Range versus Single Photograph Analysis

An analysis of high dynamic range for standard photography depicted more visually observable information for HDR when in comparison with one single photograph. The results for HDR for all stages of reflective infrared photography were concluded as negative; however, research by Albanese and Montes (2011) described the use of reflective IR and HDR photography as positive in comparison to 'visible' spectrum photography for bloodstains on fabric. However, an analysis of the research conducted by Albanese and Montes (2011) shows extremely dark images for the visible light spectrum and subsequent brighter images for the reflective IR and HDR results. Black or dark fabric substances have been known to reflect infrared light (Robinson 2007) so the results found by Albanese and Montes (2011) are consistent. However for this research, the lack of contrast in an HDR image in comparison to one single photograph did not result in any additional visual information being seen. The results for reflective UV for all stages of photography analysis were similar to reflective IR photography. A lack of contrast between the bloodstain patterns and the paint did not provide an environment for HDR images to depict additional visual information.

The results for fluorescence photography in a comparison between HDR images and one single image were positive for white acrylic and white latex for the bloodstain pattern stage, first layer of paint stage, and second layer of paint stage with the yellow and

orange filters. Additionally, HDR images for maroon latex for the bloodstain pattern stage and first layer of paint stage also depicted more visual information than one single image with the yellow and orange filters. The results for black latex were negative for fluorescence photography and therefore were negative for the use of a HDR technique. For the white acrylic, white latex, and maroon latex photographed with the red filter, the merged HDR images appeared to overwhelm the contrasting bloodstain patterns due to inclusion of bright, over-exposed photographs and would not be recommended.

4.6. Chemical Analysis of Paint

Chemical analysis of the paint types was undertaken in an attempt to explain observations during the photography stage. The general chemical composition of the paint types was readily available through their respective companies; however, additional chemical analysis was conducted in an attempt to pinpoint the chemical properties of the paint types that led to the observed spectral properties.

Results of the chemical components, available through the manufacturing information, for white acrylic, white latex, black latex, and maroon latex can be found in Table 17. All four paint types contained water as the primary form of solvent, classifying them as water-based paints. Based on the binder types, white acrylic, black latex, and maroon latex all contained acrylic resins whereas white latex contained a vinyl acetate / acrylic copolymer resin; all of which were considered to be water-based latex paint types. White acrylic, black latex, and maroon latex consisted of similar chemical components; whereas white latex appeared to be the most chemically different in comparison.

Table 17. Paint components as provided in the manufacturer information.

Paint	Solvent	Binder	Extender	Filler	Pigment
White Acrylic	Water	Acrylic resin, Styrene/ acrylic copolymer	Barium Sulfate, Talc	Nepheline Syenite, Calcined Kaolin	Not Provided
White Latex	Water	Vinyl acetate/ acrylic copolymer resin	Pumice	Nepheline Syenite	Titanium Dioxide
Black Latex	Water	Acrylic resin	Limestone, Quartz	Uncalcined diatomaceous earth	Not Provided
Maroon Latex	Water	Acrylic resin	Limestone, Quartz	Uncalcined diatomaceous earth	Not Provided

Both the extenders and fillers for all four paint types consisted of mainly inorganic materials responsible for hardening, storing, and the workability of the paint types. These were all clearly stated in the manufacturers' information and were not the focus of this analysis. The final component was pigment, which was only stated for white latex. This was due to the fact that the paint base for white latex was different from the paint base for black latex and maroon latex. The white latex paint base could only be used for white, off-white, or pastel colour mixing; whereas the paint base for black latex and maroon latex was for mixing darker colours. Due to this differentiation, the white latex paint type already contained titanium dioxide, a brightening agent.

Chemical analysis of the four paint types was undertaken in order to answer several questions. Firstly, an analysis of the paint chemistry would aid in an understanding of the results obtained through reflective IR, reflective UV, and fluorescence photography: Secondly, the cause of the false positive Luminol reaction on the two controls of no blood for white acrylic and white latex could be ascertained; and

thirdly, the reason behind the bloodstain pattern ‘re-wetting’ and smearing during the painting process could be determined.

4.6.1. Raman Spectroscopy Results

Raman spectroscopy is a technique that can detect the signals belonging to both inorganic and organic molecules within a sample. However, due to certain organic molecules producing weak signals, and exhibiting intrinsic fluorescence, Raman spectra for organic molecules are often overwhelmed by the fluorescence of the sample. Fluorescence is often depicted as a broad peak covering the spectrum, usually accompanied by a large background. This broad peak obstructs weaker peaks but is still capable of letting stronger peaks emerge. Inorganic molecules can be stronger than sample fluorescence, which can be seen for both the white acrylic (Figure 53) and white latex (Figure 54) Raman spectrum. The two peaks at approximately 614 cm^{-1} and 453 cm^{-1} were consistent with spectral results for the rutile form of titanium dioxide (Kobilinsky 2012). Based on manufacturer information, the white latex paint contained titanium dioxide while this information was not stated by the manufacturer for white acrylic. Based on the peaks, titanium dioxide (rutile) is indeed present for both white acrylic and white latex. Rutile is a mineral comprised of titanium dioxide and is commonly used in architectural paint. Ground into a fine powder rutile appears as a white pigment and is used as a brightening agent. Anatase is another optical brightener used in architectural paint; however it is less common than rutile and consists of different spectral peaks (Kobilinsky 2012).

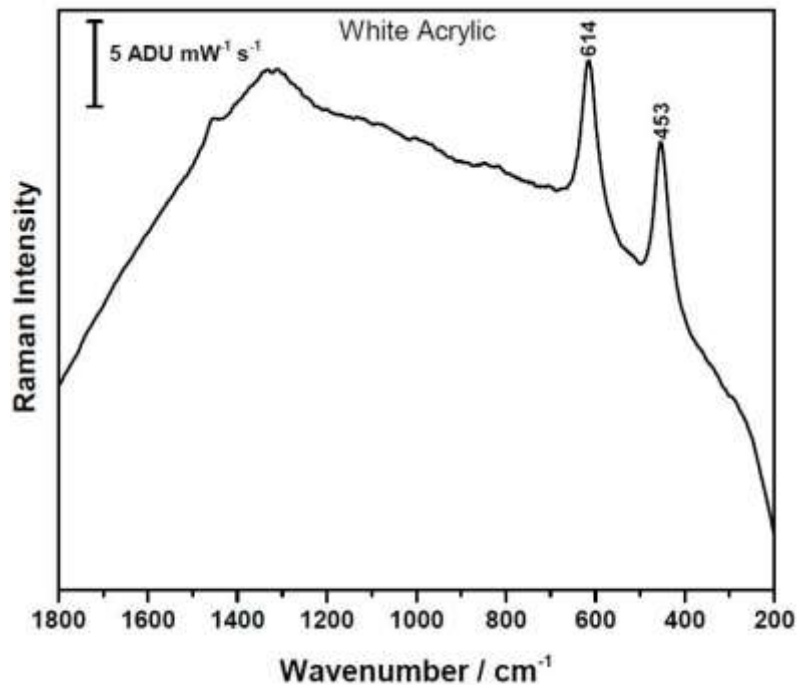


Figure 53. Normal Raman Spectrum for White Acrylic Paint Analysis. Peaks are consistent with titanium dioxide (614 cm^{-1} , 453 cm^{-1}).

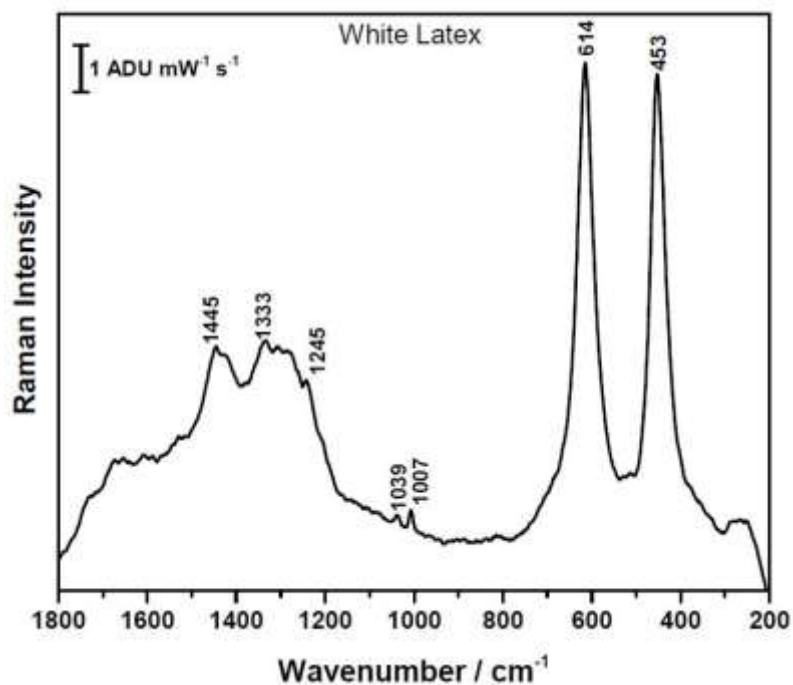


Figure 54. Normal Raman Spectrum for White Latex Paint Analysis. Peaks are consistent with titanium dioxide (614 cm^{-1} , 453 cm^{-1}).

The identification of titanium dioxide in both white acrylic and white latex supports two observations during the photography stage. First, titanium dioxide is capable of absorbing ultraviolet radiation (Kobilinsky 2012) and is an active component in many sunblock products. The presence of titanium dioxide supports observations during the reflective ultraviolet photography stage where both white acrylic and white latex appeared to absorb some of the ultraviolet light source appearing visually similar to black latex and maroon latex. The exact quantities of titanium dioxide in white acrylic and white latex could not be determined, but a higher quantity of this component in white acrylic versus white latex may account for the discrepancy between the two paint types in the reflective ultraviolet photography stage.

The presence of titanium dioxide also supports the observations that the controls of no blood for white acrylic and white latex exhibited chemiluminescence in contact with the Luminol reagent. Luminol has been known to produce a chemiluminescent response when in contact with rutile (Hedenborg 1988) and should be taken into consideration during scene analysis.

Surface-Enhanced Raman Spectroscopy (SERS) involves the application of a layer of metal nanoparticles onto the surface of the sample which reduces fluorescence and allows weaker signals to emerge through an enhancement of the Raman signal. Silver nanoparticles were used due to their stability and signal enhancing capability and were applied to the white acrylic (Figure 55), white latex (Figure 56), black latex (Figure 57), and maroon latex (Figure 58) paint types. The nanoparticles quenched the fluorescence

that was produced by the light scattering from the incident light source and allowed the weaker signals to be recorded.

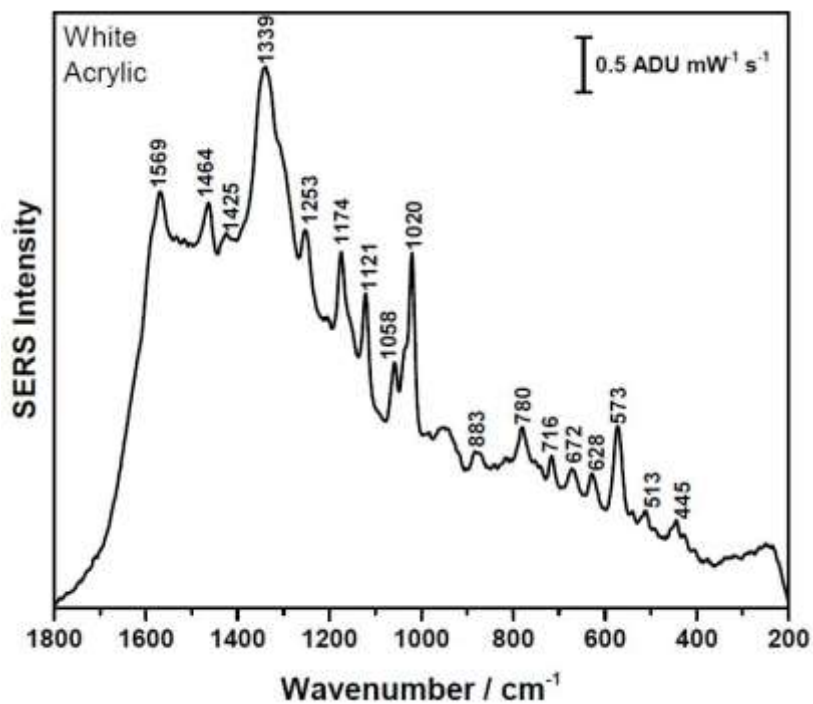


Figure 55. SERS Spectrum for White Acrylic Paint Analysis.

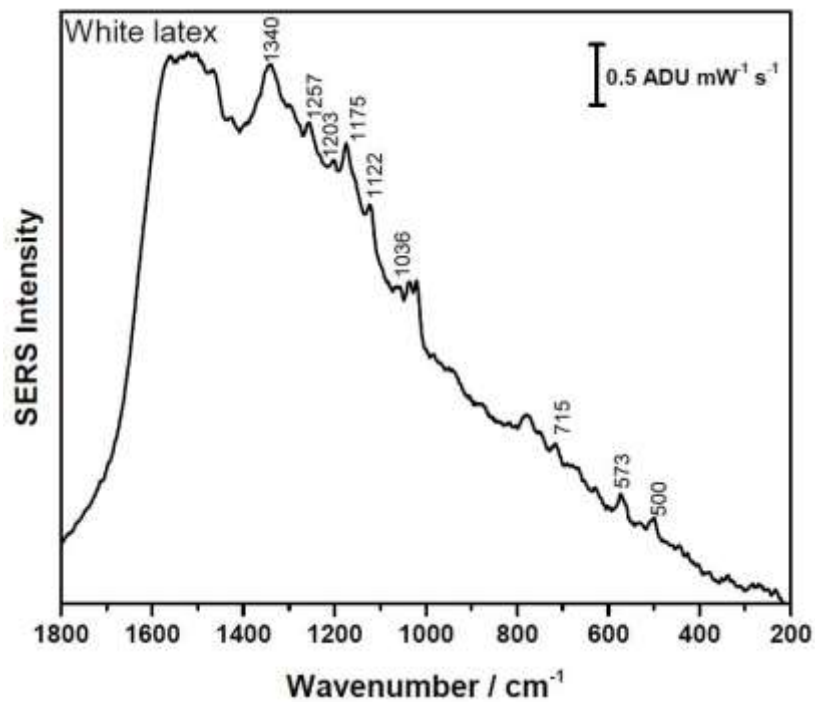


Figure 56. SERS Spectrum for White Latex Paint Analysis.

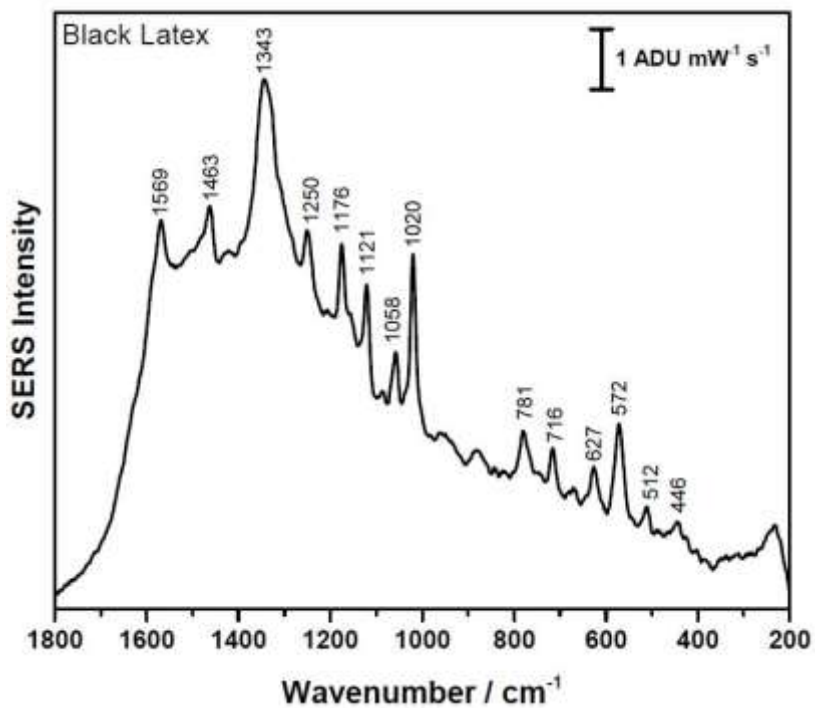


Figure 57. SERS Spectrum for Black Latex Paint Analysis.

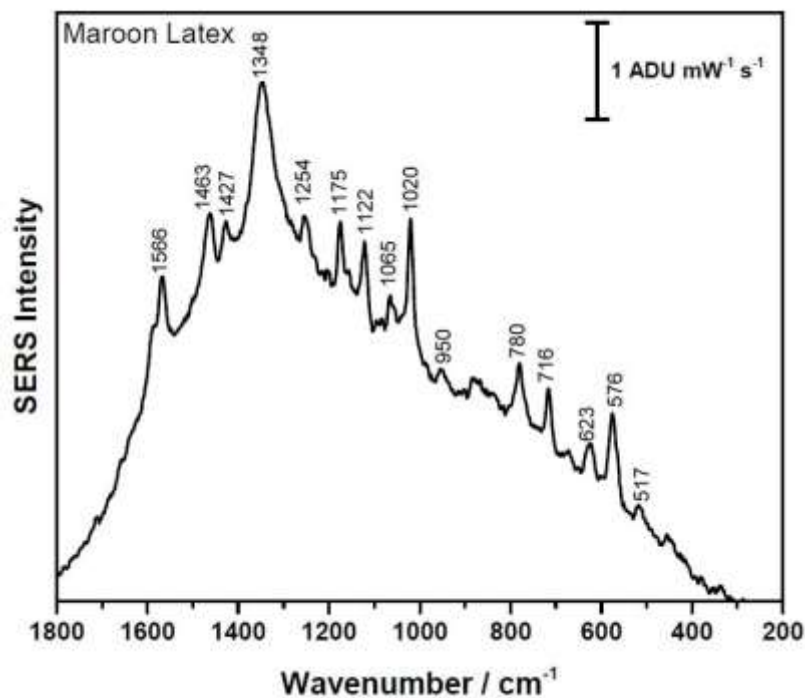


Figure 58. SERS Spectrum for Maroon Latex Paint Analysis.

Analysis of the SERS Spectrum for white acrylic, white latex, black latex and maroon latex support the manufacturers information for the presence of specific components mostly used as extenders and fillers in the paint. These components included Silicate (Quartz) and Calcium Carbonate (Limestone) as extenders in the black latex and maroon latex; Silicon Dioxide (Silica), Barium Sulfate, Nepheline Syenite (Feldspar minerals), and Magnesium Silicate (Talc) for both white acrylic and white latex (Table 18).

Table 18. Relevant peaks for chemical components present in white acrylic, white latex, black latex, and maroon latex paints

Paint	Extender	Peaks/ cm⁻¹	Filler	Peaks/ cm⁻¹
White Acrylic	Barium Sulfate Talc	~990 ~670	Nepheline Syenite Calcined Kaolin	~470 ~1000 ~550
White Latex	Pumice	~500	Nepheline Syenite	~470 ~1000
Black Latex	Limestone Quartz	~1050 ~520	Uncalcined diatomaceous earth	~570
Maroon Latex	Limestone Quartz	~1050 ~520	Uncalcined diatomaceous earth	~570

SERS results supported information obtained from the paint manufacturing companies and further analysis of specific chemical compounds and subsequent amounts available would be outside the scope of this research project. Raman Spectroscopy and Surface-Enhanced Raman Spectroscopy are useful techniques for determining extender and filler components in paint samples, but lacks sensitivity for pigment and binder analysis.

4.6.2. Fibre Optic Reflectance Spectroscopy Results

Fibre Optic Reflectance Spectroscopy (FORS) analysis is a non-invasive technique that is readily available for in situ measurements. This technique is often used for the identification of pigments, dyes and alterations in historical artwork; however, the identification of reflectance and absorption properties of specimens is possible. FORS analysis was applied in an attempt to determine the reflectance versus absorbance of all four paint types (Figure 59). Only the spectral analysis using the tungsten halogen light source is included due to the overlapping spectral results with the deuterium light source. Between 200 nm and 350 nm seen with the deuterium light source, all four paint types

were consistent with the tungsten halogen light source results showing low reflection, high absorption properties.

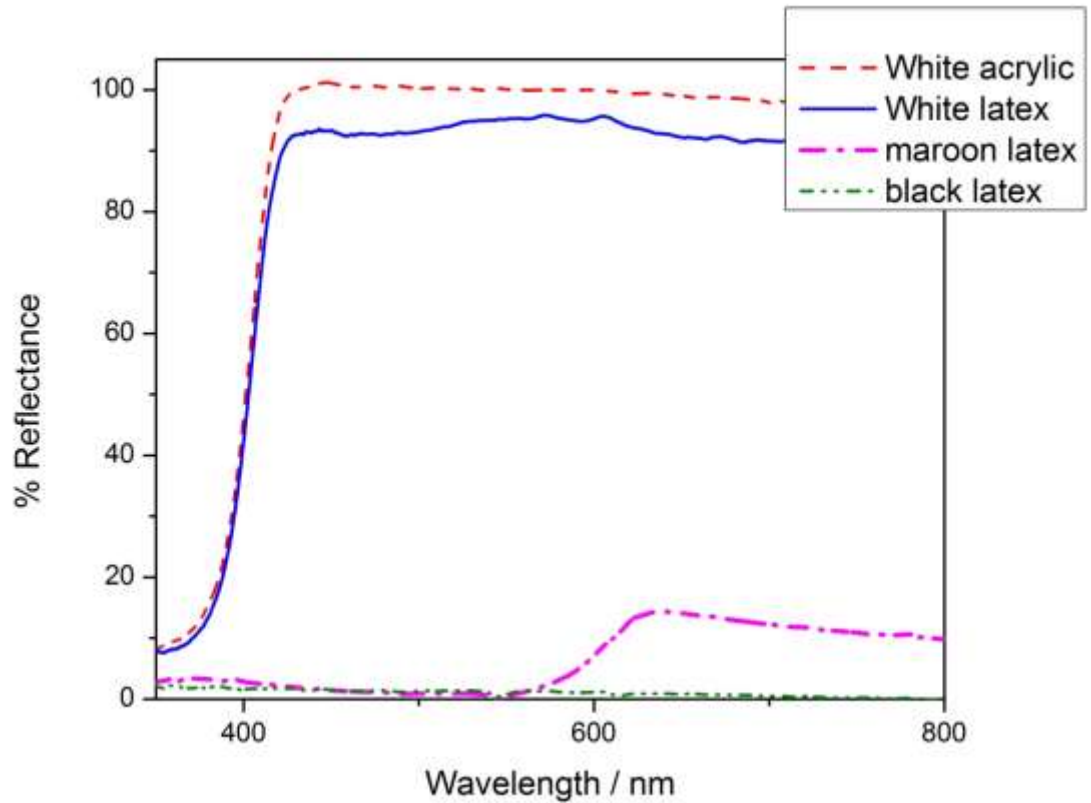


Figure 59. FORS results for white acrylic (red), white latex (blue), black latex (green), and maroon latex (pink) with the halogen light source.

The results for white acrylic and white latex with the halogen light source were very similar. At approximately 350 nanometres white acrylic and white latex began to show an increase in reflectance percentage and peak at approximately 400 nanometres before leveling off. Results for black latex show that between approximately 350 nm and 400 nm there is a slightly elevated reflectance percentage; however, from 400 nm to 800 nm there is essentially zero reflectance; and instead essentially one hundred percent

absorption. Maroon latex also appears similar to black latex between approximately 350 nm and 400 nm, with slightly more reflectance than black latex. Between approximately 400 nm and 560 nm the absorption percentage is approximately one hundred percent. However, starting at approximately 560 nanometres there is a gradual rise in reflectance where it peaks and levels off from 630 to 800 nanometres.

The results of the FORS analysis in conjunction with observations from the multi-spectral photography analysis show that white acrylic and white latex have a high percentage of reflectance that could be observed in the near infrared region. The lower percentage of reflectance at approximately 350 nm supports the observable results for the reflective ultraviolet stage; there was absorption during this stage for both white acrylic and white latex. Black latex shows a high level of absorption, which supports the lack of observable information for reflective infrared, and fluorescence photography due to incident light source absorption. There was a slight rise in reflectance between approximately 350 nm and 400 nm which could account for bloodstain information being more visible in a comparison between reflective ultraviolet and standard photography. Maroon latex depicted similar minimal reflectance percentages between 350 nm and 400 nm also supporting reflective ultraviolet observations; additionally, the increase of reflectance at approximately 560 nm to 800 nm suggests maroon latex was capable of reflecting some infrared light, but was incapable of transmission, as well as supporting visual observations for fluorescence photography.

FORS is a useful technique that is already widely used in the art conservation industry and could prove useful in the field of forensics. A quick analysis of the

reflectance versus absorption capabilities of unknown paint types may aid in determining what forensic photography multi-spectral techniques should be applied for a given circumstance.

4.6.3. ATR-FTIR Spectroscopy Results

ATR-FTIR spectroscopy results were complementary to the results obtained from the Raman and SERS spectra. Where SERS was useful for determining/confirming the extender and filler components of the paint types, ATR-FTIR analysis was capable of determining/confirming binders, modifiers, and other agents. The results for white acrylic support information available from the manufacturer that an acrylic resin was most likely used as the binder (Figure 60). Additionally, the broad peaks around $\sim 500\text{ cm}^{-1}$ supports the presence of the rutile form of titanium dioxide (Caddy 2001).

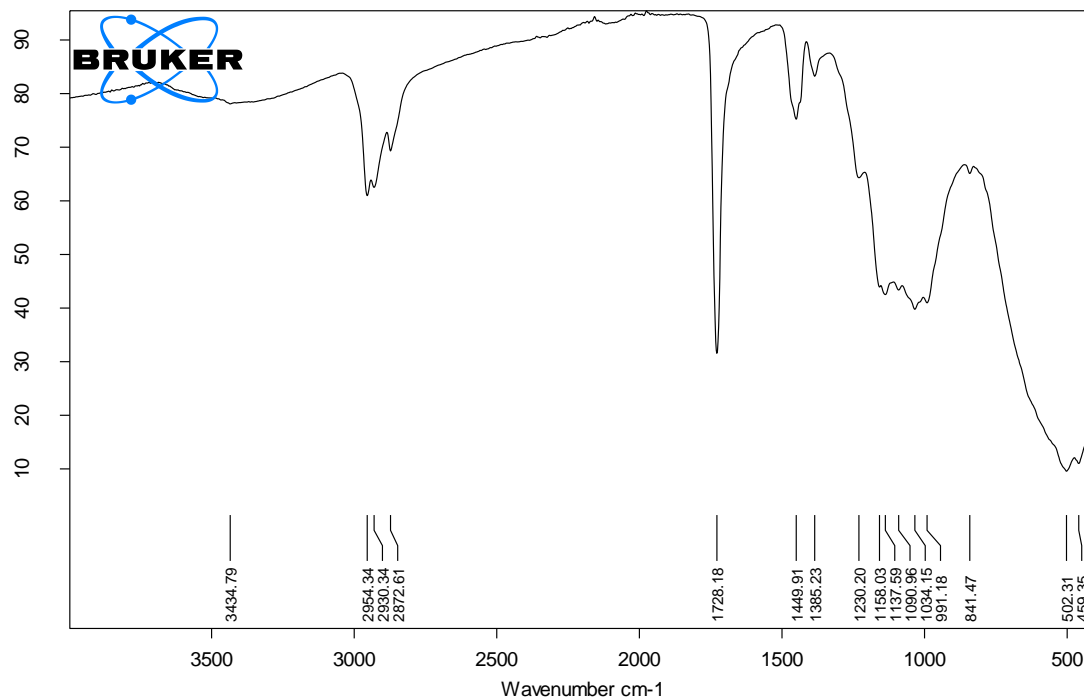


Figure 60. ATR FTIR Spectrum for White Acrylic Paint Analysis (C-H aliphatic stretching $\sim 2958\text{ cm}^{-1}$ - 2875 cm^{-1} ; Carbonyl peak $\sim 1732\text{ cm}^{-1}$; Key peaks at $\sim 1451\text{ cm}^{-1}$, 1387 cm^{-1}) (Caddy 2001).

The result for white latex was also supported by the manufacturer's information suggesting that a poly (vinyl acetate) binder was used (Figure 61). Similar to the results of white acrylic, the peak around $\sim 500\text{ cm}^{-1}$ supports the presence of the rutile form of titanium dioxide (Caddy 2001).

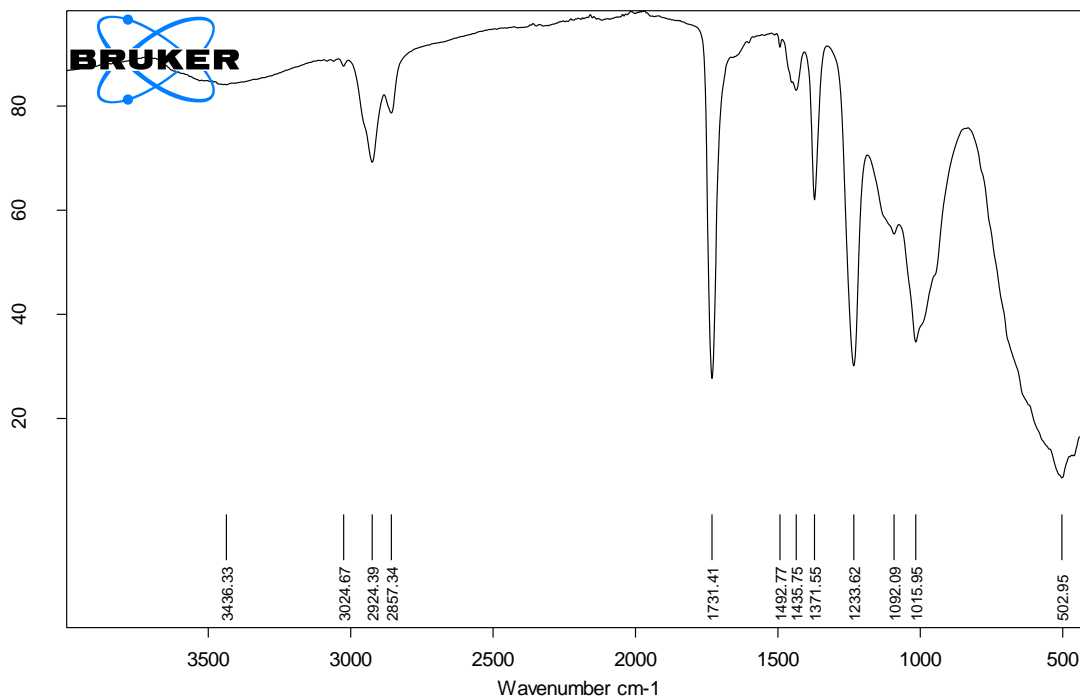


Figure 61. ATR FTIR Spectrum for White Latex Paint Analysis (C-H aliphatic stretching in $\sim 2900\text{ cm}^{-1}$ region; Carbonyl peak $\sim 1738\text{ cm}^{-1}$; Key peaks at $\sim 1435\text{ cm}^{-1}$, 1371 cm^{-1} , 1240 cm^{-1} , 1021 cm^{-1}) (Caddy 2001).

The results for black latex (Figure 62) and maroon latex (Figure 63) depict results similar to white latex, which do not match the manufacturer's information available. The spectrum suggests the presence of a poly (vinyl acetate) binder and not an acrylic resin that was stated in the manufacturer's information. The similarities in spectrum characteristics are more compatible between white latex than white acrylic. The absence of the peak around $\sim 500\text{ cm}^{-1}$ suggests the lack of rutile titanium dioxide, which supports results from both the multi-spectral photography, as well as the Raman and SERS chemical analyses. The additional peaks around 1000 cm^{-1} to 450 cm^{-1} are characteristic of the 'fingerprint' region and depict inorganic pigments (Caddy 2001). These results could have been due to the use of a base 2 instead of a base 3 during the paint mixing

stage, or potential contamination at the manufacturing facilities. However, additional results of binder analysis are beyond the scope of this research.

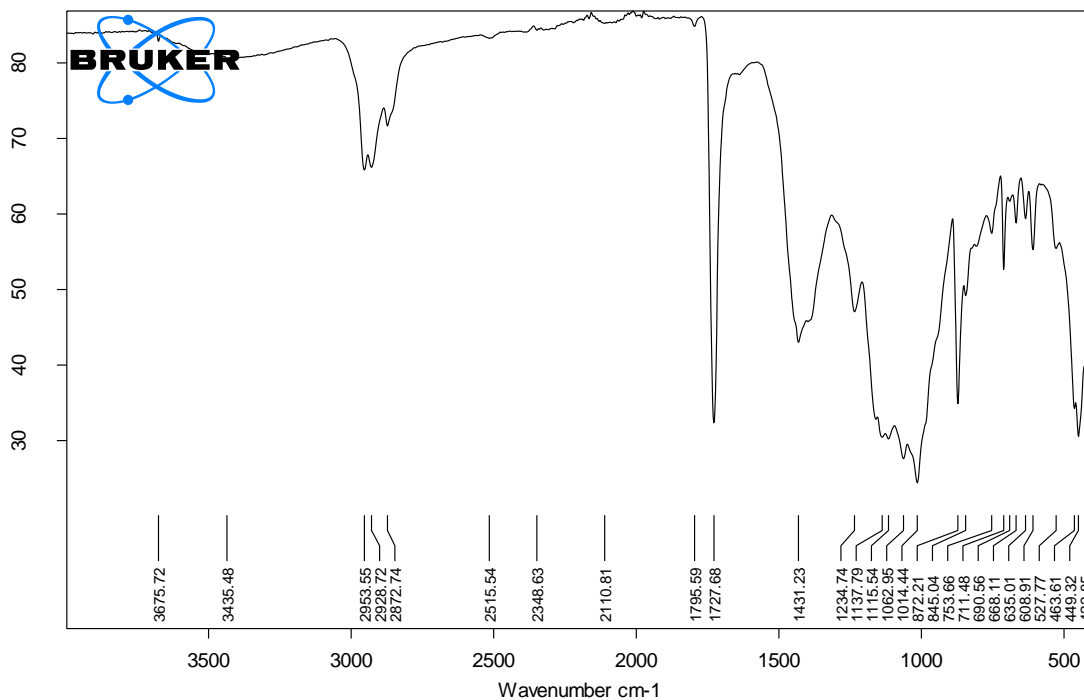


Figure 62. ATR FTIR Spectrum for Black Latex Paint Analysis (C-H aliphatic stretching in $\sim 2900\text{ cm}^{-1}$ region; Carbonyl peak $\sim 1738\text{ cm}^{-1}$; Key peaks at $\sim 1435\text{ cm}^{-1}$, 1371 cm^{-1} , 1240 cm^{-1} , 1021 cm^{-1}) (Caddy 2001).

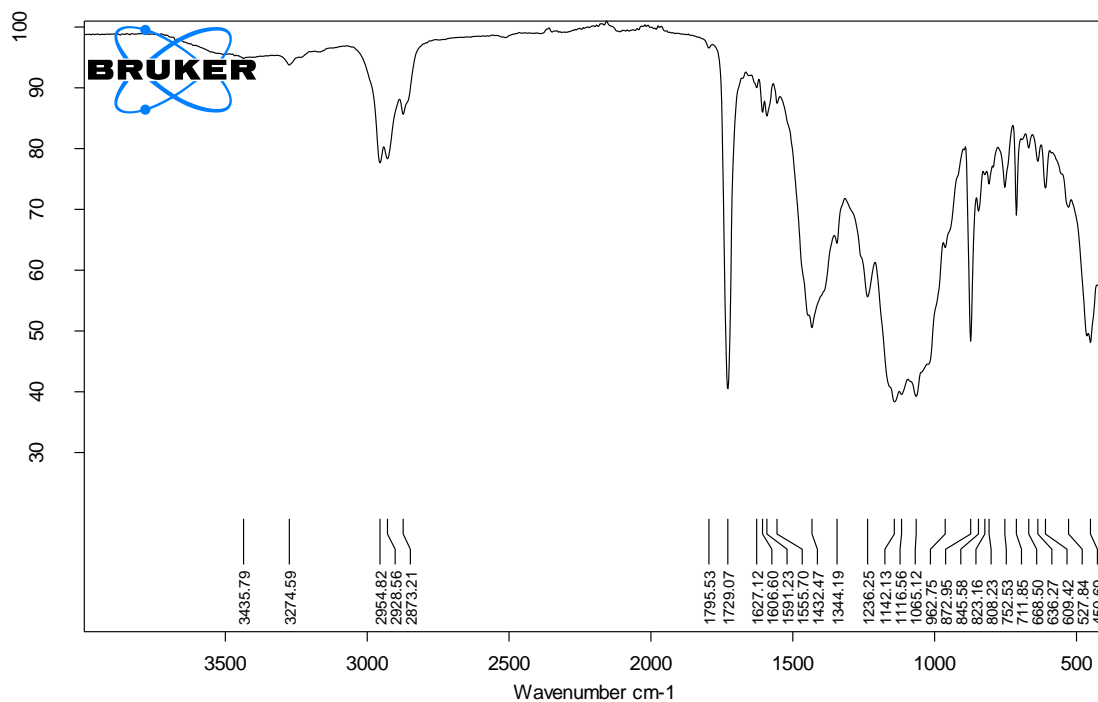


Figure 63. ATR FTIR Spectrum for Maroon Latex Paint Analysis (C-H aliphatic stretching in $\sim 2900\text{ cm}^{-1}$ region; Carbonyl peak $\sim 1738\text{ cm}^{-1}$; Key peaks at $\sim 1435\text{ cm}^{-1}$, 1371 cm^{-1} , 1240 cm^{-1} , 1021 cm^{-1}) (Caddy 2001).

Due to the sensitivity of ATR-FTIR spectroscopy, an analysis of potential paint additives could be undertaken. Only a fraction of the total volume of paint is made up of additives which might include preservatives, modifiers, de-foamers, and wetting agents. These components are responsible for paint viscosity, even distribution of pigment in the paint solution, reduction in the amount of trapped air in the paint, and inhibition of paint spoilage.

Tributyl phosphate is a de-foaming agent that can be used in paints and is capable of aiding other wetting agents; it appears to be present in all four paint types (Figure 64) (Brezinski 1991).

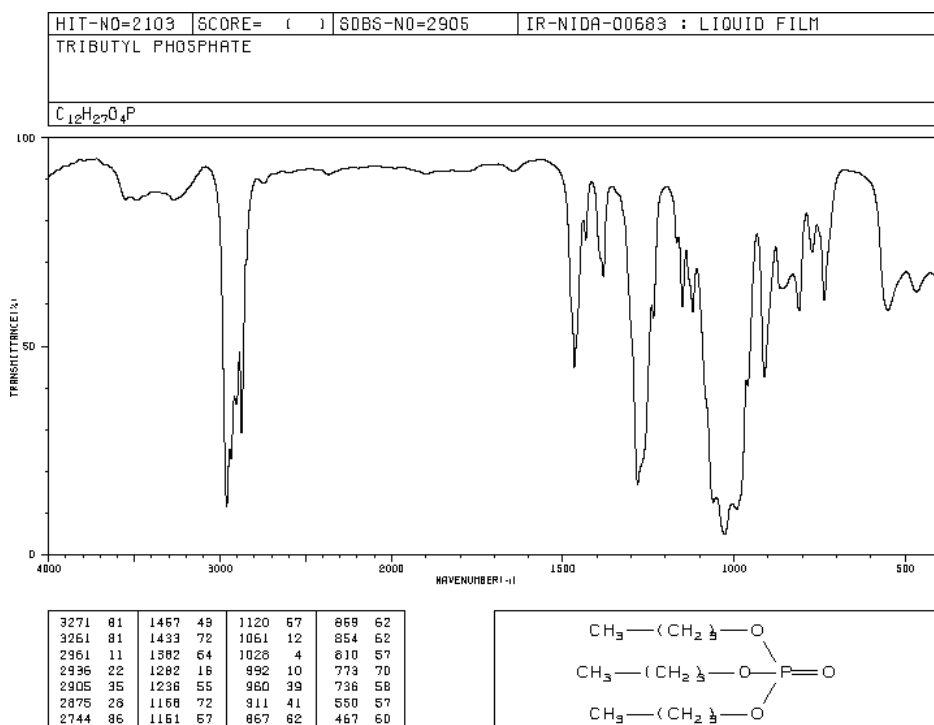


Figure 64. ATR-FTIR Spectrum and peaks of interest for Tributyl Phosphate ($\sim 1433 \text{ cm}^{-1}$, 1236 cm^{-1} , 1160 cm^{-1} , 1161 cm^{-1} , 1120 cm^{-1} , 1061 cm^{-1} , 1020 cm^{-1} , 992 cm^{-1} , 960 cm^{-1} , 867 cm^{-1} , 854 cm^{-1} , 810 cm^{-1}) (Spectral Database for Organic Compounds).

Paint manufacturing is an ongoing technical endeavor to create simple to use and effective commercial paints. The presence of certain de-foaming and wetting agents can be responsible for surface adhesion of the paint layer. This adhesion may be the cause of the ‘re-wetting’ and smearing of the bloodstain patterns during the painting process. Although unknown, it would be interesting to observe if this ‘re-wetting’ and smearing occurred if the type of paint applied over the bloodstain patterns was chemically different from the paint type under the bloodstain patterns. Based on the information available from infrared spectroscopy for the coatings industry (Brezinski 1991) the presence of this specific additive could account for visual observations during the painting process. The

presence of a water solvent might also attribute to the blood 're-wetting' and smearing, however further analysis is beyond the scope of this research.

A collaborative analysis of High Dynamic Range photography and paint chemistry has both uses and limitations in the field of multi-spectral photography. By applying both HDR and paint chemistry techniques, more information could be gathered from the research as opposed to using one technique alone. HDR photography did not prove to be particularly useful for reflective infrared and reflective ultraviolet for the bloodstain pattern, first layer of paint and second layer of paint stages; however, there was merit in using this technique for fluorescence photography for all stages. The chemical analysis of all paint types supported manufacturer information that was readily available for white acrylic and white latex; however, the chemical results for the binder classification for black latex and maroon latex were different from the information provided. Spectral analyses of architectural paints are not as prevalent in spectral data bases as automotive paint types and the lack of comparative spectra in conjunction with analyzing an unknown architectural paint proves to be difficult.

Fibre Optic Reflectance Spectroscopy in conjunction with multi-spectral photography has the most potential for future use. Analyzing the reflectance or absorption capabilities of a painted surface could aid in determining which photography technique would have the highest chance of success. FORS is capable of rapid analysis while also being fairly portable and non-destructive and could potentially be a deciding factor in determining the type of multi-spectral photography technique to utilize.

Summary of Chemical Analysis

There were several results obtained from the chemical analysis of the paint samples that could potentially be responsible for the visual results seen during the photography data collection. Raman spectroscopy identified the presence of the rutile form of titanium dioxide which is often used as an optical brightener to make white items appear whiter. Multiple research studies (Caddy 2001; Kobilinsky 2012; Li, Yin et al. 2014) conclude that the rutile form of titanium dioxide is capable of absorbing UV light, which could be seen during the reflective UV photography for white acrylic and white latex. Additionally, research by Hedenborg (1988) states that titanium dioxide induced chemiluminescence is possible which would account for the false positive results observed for the controls of no blood for white acrylic and white latex. Photographic results by Howard and Nesson (2010) for the white paints used appeared to depict similar chemiluminescent results as a 'rippling' or 'twinkling' effect where there appeared to be no bloodstain patterns. However, any observations in regards to false positives were not discussed (Howard and Nesson 2010).

The SERS results for all four paint types were capable of determining the extender and filler properties of each paint type. Flat paint brands of architectural paints usually consist of an extensive amount of extenders and fillers as inorganic pigments to modify gloss, texture, and viscosity (Weber 1960; Caddy 2001; Kobilinsky 2012). The amount of extenders and fillers for all four paint types may be the cause of lack of transmission seen during reflective IR photography. Additionally, with a low refractive index and therefore low hiding power of the extenders and fillers, the visual results seen for white acrylic and

white latex during fluorescence photography could potentially be due to the extensive inorganic pigments.

The FORS analysis depicts low reflectance, high absorption capabilities for white acrylic, white latex, black latex, and maroon latex in the ultraviolet region. This analysis supports the visual information seen during the reflective UV photography stage, where white acrylic and white latex appeared to absorb the incident light source; black latex and maroon latex were capable of a small amount of reflection in the UV region depicting similar UV results to the two white paints, but more visual information in comparison to the black and maroon standard photographs. Additionally, the FORS results showed a high amount of reflectance into the IR region for white acrylic and white latex, as well as some reflectance into the IR region for maroon latex. However, these three paint types were not capable of allowing transmission through the paint to the underlying bloodstain patterns. The black latex analysis showed complete absorption in the IR region which supported reflective IR photography results.

The final chemical analysis ATR-FTIR showed binder spectra for white acrylic and white latex that supported the manufacturer's information of an acrylic resin, and a poly (vinyl acetate) resin for white acrylic and white latex respectively. The results for black latex and maroon latex also depicted a poly (vinyl acetate) resin that did not match manufacturer's information; however, further analysis would be beyond the scope of this research. Finally, the potential presence of a defoaming agent such as tributyl phosphate might account for the blood 're-wetting' and smearing that was encountered in the photography data collection process. Due to the drying process of paint, additives and

solvents are only available in miniscule amounts for analysis. All four chemical analyses aided in understanding questions encountered during the photography process and the inclusion of these analyses helped produce some answers.

Chapter 5: Conclusions and Future Directions

Forensic photography is an important subfield of the forensic sciences that requires rigorous testing of scientific methodology and standardized procedure. Due to the nature of variables encountered during the photography process, an understanding of the mechanics associated with photographic techniques, as well as the subjects being photographed, are important factors for positive results. The field of multi-spectral forensic photography can be considered a multi-disciplinary approach to the documentation of clandestine evidence. Four multi-spectral photography techniques were employed in this thesis work in order to test their reliability in terms of documenting bloodstain patterns that had been concealed by paint layers.

Chemical analysis was applied to the different paint types in an attempt to support visual evidence encountered from the multi-spectral photography process. The second phase of this research involved analyzing the chemical and physical properties of all four paint types using Raman Spectroscopy, and Surface-Enhanced Raman Spectroscopy (SERS), Fibre Optic Reflectance Spectroscopy (FORS), and Attenuated Total Reflectance Fourier Transform Infrared Spectroscopy (ATR-FTIR). The resulting analysis consisted of both the visual examination of each forensic photography technique, as well as the chemical/ physical data associated with each paint type. This multi-disciplinary approach to analysis resulted in tangible evidence that could scientifically support the qualitative visual analysis of the multi-spectral forensic photography results.

Four different paint types were analyzed for this research; white acrylic, white latex, black latex, and maroon latex. Each paint type was applied over four different

bloodstain patterns and included; medium velocity, swipe, saturated, and a control of no blood. A total of three stages were photographed; the bloodstain pattern stage, the first layer of paint stage, and the second layer of paint stage. Four types of multi-spectral photography techniques were employed and included standard photography, reflective infrared photography, reflective ultraviolet photography and fluorescence photography. Multiple photographs were captured for each subject with different exposure values and merged into one final High Dynamic Range image in Photoshop CC. Qualitative analysis of the multi-spectral images yielded interesting results. Standard photography for each stage was used as a control for which the other three techniques could then be compared to.

Reflective infrared photography for all three stages did not reveal visually significant bloodstain pattern evidence when directly compared to the visual evidence available with standard photography. Based on the FORS and SERS chemical analyses, the presence of inorganic extender and filler paint properties could account for the lack of transmission through the paint for the documentation of the bloodstain patterns. The FORS analysis could potentially be used as an in-field technique to determine the absorption properties of the paint; if the paint absorbs in the infrared region, reflective IR photography should not be attempted.

Reflective ultraviolet photography for both white acrylic and white latex appeared to absorb some of the UV light source and both paint types were considered non-visible for the second layer of paint stage when compared to the standard photographs. Black latex and maroon latex showed more visual evidence of the bloodstain patterns for all

reflective ultraviolet stages, resulting in more available information than standard photography. Raman spectroscopy analysis determined the presence of titanium dioxide in the white acrylic and white latex paints; often used as an optical brightener, titanium dioxide is known to absorb UV radiation as well as cause a false positive reaction when in contact with Luminol reagent. The FORS analysis showed a low percentage of reflectance, high absorption for all four paint types which support the visual results for reflective UV photography. Out of all chemical analyses, FORS would be a useful pre-emptive technique to determine the absorption and reflectance properties of the paint before deciding which photography technique to use.

Fluorescence photography depicted the most striking contrast between the paint types and bloodstain patterns for white acrylic, white latex, and maroon latex for the bloodstain pattern stage and first layer of paint stage. Black latex was incapable of fluorescing and did not show any contrast between the paint and bloodstain patterns and was considered negative for all stages. Both white acrylic and white latex fluoresced in the presence of the incident light source for both the first layer of paint stage and the second layer of paint stage; whereas maroon latex, with a significantly reduced fluorescence capability, did not depict significant visual evidence for the second layer of paint stage compared to the available information from standard photography. The appearance of blood smearing under the painted layers was more definitive during fluorescence photography. The application of ATR-FTIR analysis aided in determining the binder type, as well as suggesting the presence of a defoaming agent which might have been responsible for the blood smearing. ATR-FTIR was a useful technique that can

be used for binder and pigment analysis, but not for paint extender and filler analysis. If paint samples are taken from a scene and tested, the application of SERS and ATR-FTIR chemical analyses could be useful for both determining which forensic multi-spectral photography technique to use, and understanding the chemical properties of the paint itself.

The final stage of Luminol testing resulted in positive reactions to the presence of the bloodstain patterns but only when the Luminol was capable of coming into contact with the blood through cracks in the paint and did not appear to react to the bloodstain patterns through the paint which could be seen with the black latex and maroon latex paints. Additionally, both the white acrylic and white latex controls of no blood visually luminesced when in contact with the Luminol reagent. This result was due to the presence of titanium dioxide, an optical brightener often used to enhance white paints that could be seen from both the Raman spectroscopy and ATR-FTIR spectroscopy analyses. Luminol is considered a destructive technique and should be used with caution, and further caution should be used in Luminol application in the presence of scenes involving white paint.

Testing the effectiveness of using High Dynamic Range photography for the documentation of bloodstains beneath paint layers in a forensic context has not been attempted to the best of the researcher's knowledge. HDR images from reflective infrared and reflective ultraviolet were not significantly different in terms of available visual evidence when compared to one single photograph. Fluorescence HDR images in comparison to one single photograph for white acrylic and white latex (also maroon latex but less apparent) appeared to create a significant uniform illumination and contrast

between the fluorescing paint and absorbing bloodstain patterns; however, results were negative for black latex. Overall, High Dynamic Range photography would not be an effective tool for use in the forensic context when photographing in reflective infrared or reflective ultraviolet; there are some areas for application in fluorescence photography under specific circumstances that produce visual contrast between fluorescing and absorbing characteristics. It would be recommended that multiple photographs at different exposures be taken for analysis, but merging in a post-referential program is not warranted.

For this research study the results for Fluorescence photography, in conjunction with HDR with a yellow or orange filter, were the most positively conclusive and would be recommended for future use. Additionally, FORS analysis had the potential to be used for chemical analysis of paint types without the need for samples to be taken back to a lab. Although results for reflective UV photography were also promising, the need for all non-UV light to be removed from the scene proposes a difficult realistic set-up for in-field photography. If evidence or samples can be brought back to a controlled lab setting, reflective UV photography can be applied without the use of HDR photography.

The application methodology, analysis and interpretation conducted for this research was multi-disciplinary in nature. Factors that had arisen during analysis and interpretation of the multi-spectral photography techniques could be supported through a chemical analysis of the different paint types. By combining different fields of study, this research resulted in a more robust, scientific analysis than if the research had been restricted to one single discipline. There are valid techniques available in the field of

multi-spectral forensic photography, but an added chemical analysis has the potential to significantly aid this field of research.

5.1. Future Directions in Architectural Paint Analysis

There are several observations that came out following the conclusion of this research project. An important variable to take into consideration was the paint being used to cover the bloodstain patterns. The chemical analysis of the architectural paint studied supported the suggestion that paint classifications have remained the same (e.g. latex, acrylic) however; the chemical composition did not necessarily support this classification. A majority of architectural paints are water based latex paint; oil based paints are no longer a popular alternative. The type of paint and potential classifications need to be taken into consideration when attempting to document bloodstain patterns that have been obstructed, as well as during future research studies.

Another paint variable that needs to be taken into consideration is market trends. Paint manufacturers are continually searching for new paint formulas for easier, cheaper, and faster application. The paint market is constantly changing and any architectural paint studied at one period of time might be out-of-date within a year. This is not to say that studying off market paint types would be redundant; multiple types of paint should be studied and compiled into a database in order to determine which photography techniques might work best. By combining a chemical analysis of specific paint samples with the results from multi-spectral photography techniques, a more complete understanding of the paint samples could potentially be achieved.

5.2. Future Directions in Multi-Spectral Photography and High Dynamic Range Techniques

The variables for different types of paint can be addressed through chemical analysis, whereas specific documentation variables should be understood from a forensic photography point of view. Forensic photography documentation relies on variables such as camera and lens equipment, light source, copy stand height, subject being photographed and more. An understanding of the physics behind photographing in different regions of the light spectrum is important in order to understand the types of photography settings that should be used. To address specific camera settings a larger study needs to be undertaken in a multitude of different environments with a variety of conditions. The hopeful conclusion of future research would be viable field applications for forensic photographers where it would be common to encounter a plethora of variables.

Application of HDR analysis for this research project resulted in the understanding that it works best when used to enhance contrast in colour photographs such as in fluorescence photography. Although the technique can be used for reflective infrared and reflective ultraviolet, it did not add any additional information to the narrative. However, collecting bracketed photographs at different exposures did prove useful during analysis in order to visually compare specific information between lighter and darker images. For future research and analysis, multiple bracketed photographs could be collected at different exposure values but not merged into one HDR image; the researcher should make observations based on information available in photographs taken

at different light exposures. Fluorescence photography did benefit from the HDR technique and future studies might wish to attempt to expand on this topic in other fields of analysis including bloodstain patterns on different substrates, bodily fluids that fluoresce, fingerprint analysis and any other situations that provide a contrasting fluorescence environment.

Chapter 6: References

Aceto, Maurizio, Angelo Agostino, Gaia Fenoglio, Monica Gulmini, Valentina Bianco, and Eleonora Pellizzi

2012 Non Invasive Analysis of Miniature Paintings: Proposal for an Analytical Protocol. *Spectrochimica Acta Part A: Molecular and Biomolecular Spectroscopy* 91:352-359.

Adair, Thomas W.

2006 Experimental Detection of Blood Under Painted Surfaces. *I.A.B.P.A. News*: 12-19.

Albanese, John, and Ronald Montes

2011 Latent Evidence Detection using a Combination of Near Infrared and High Dynamic Range Photography: An Example using Bloodstains. *Journal of Forensic Sciences* 56(6): 1601-1603.

Arthur, Ravishka M., Sarah L. Cockerton, and de Bruin, Karla G.: Taylor, Michael C.

2015 A Novel, Element-Based Approach for the Objective Classification of Bloodstain Patterns. *Forensic Science International* 257:220-228.

Bacci, M., M. Picollo, G. Trumpy, M. Tsukada, and D. Kunzelman

2007 Non-Invasive Identification of White Pigments on 20th-Century Oil Paintings using Fiber Optic Reflectance Spectroscopy. *Journal of the American Institute for Conservation* 46(1):27-37.

Banterle, Francesco, Patrick Ledda, Kurt Debattista, Marina Bloj, Alessandro Artusi, and Alan Chalmers

2009 A Psychophysical Evaluation of Inverse Tone Mapping Techniques. *Computer Graphics Forum* 28(1):13-25.

Baraldi, Pietro, Susanna Bracci, Elena Cristoferi, and Sara Fiorentino

2016 Pigment Characterization of Drawings and Painted Layers Under 5th-7th Centuries Wall Mosaics from Ravenna (Italy). *Journal of Cultural Heritage* In Press.

Barni F, Lewis S, Berti A, Miskelly G, Lago G

2007 Forensic Application of the Luminol Reaction as a Presumptive Test for Latent Blood Detection. *Talanta* 72(3):896-913.

- Bevel, Tom, and Ross M. Gardner
2002 Bloodstain Pattern Analysis: With an Introduction to Crime Scene Reconstruction. Second ed. Boca Raton, Florida, USA: CRC Press.
- Bily, Christopher, and Helene Maldonado
2006 The Application of Luminol to Bloodstains Concealed by Multiple Layers of Paint. *Journal of Forensic Identification* 56(6): 896-905.
- Boyd, Samantha, Massino F. Bertino, and Sarah J. Seashols
2011 Raman Spectroscopy of Blood Samples for Forensic Applications. *Forensic Science International* 208:124-128.
- Bracci, S., O. Caruso, M. Galeotti, R. Iannaccone, D. Magrini, D. Picchi, D. Pinna, and S. Porcinai
2015 Multidisciplinary Approach for the Study of an Egyptian Coffin (Late 22nd/early 25th Dynasty): Combining Imaging and Spectroscopic Techniques. *Spectrochimica Acta Part A: Molecular and Biomolecular Spectroscopy* 145:511-522.
- Brezinski, D. R., ed.
1991 An Infrared Spectroscopy Atlas for the Coatings Industry. Fourth ed. Vol. 1. Blue Bell, Pennsylvania: Federation of Societies for Coating Technology.
- Bruker Optics
2016 FTIR Spectrometers. Electronic document, <https://www.bruker.com/products/infrared-near-infrared-and-raman-spectroscopy/ft-ir-routine-spectrometers.html>, accessed October, 2016.
- Buzzini, Patrick, and Edward Suzuki
2016 Forensic Applications of Raman Spectroscopy for the in Situ Analyses of Pigments and Dyes in Ink and Paint Evidence. *Journal of Raman Spectroscopy* 47:16-27.
- Carallo, C., C. Irace, M. S. De Franceschi, F. Coppoletta, R. Tiriolo, and C. Scicchitano
2011 The Effect of Aging on Blood and Plasma Viscosity. An 11.6 Years Follow-Up Study. *Clinical Hemorheology and Microcirculation* 47:67-74.

- Casadio, Francesca, Marco Leona, John R. Lombardi, and Richard Van Duyne
2010 Identification of Organic Colorants in Fibers, Paints, and Glazes by Surface Enhanced Raman Spectroscopy. *Accounts of Chemical Research* 43(6):782-791.
- Castro, Fabio, and Claudia Pelosi
2008 Study of Wall Paintings and Mosaics by means of Ultraviolet Fluorescence and False Colour Infrared Photography. Electronic document, <http://hdl.handle.net/2067/1623>, accessed November 6, 2014.
- Cheeseman, Rob
1999 Direct Sensitivity Comparison of the Fluorescein and Luminol Bloodstain Enhancement Techniques. *Journal of Forensic Identification* 49(3):261-268.
- Christman, Daniel V.
1996 A Study to Compare and Contrast Animal Blood to Human Blood Product. *I.A.B.P.A. News* 12(2):10-25.
- Company Seven
2016 Baader Planetarium U-Filter BPU2 (UV or Venus Filter). Electronic document, http://www.company7.com/baader/options/u-filter_bpu2.html, accessed May 9, 2016.
- Cosentino, Antonio
2014 Identification of Pigments by Multispectral Imaging; a Flowchart Method. *Heritage Science* 2(8): 1-12.
- Cosentino, Antonio, and Samantha Stout
2014 Photoshop and Multispectral Imaging for Art Documentation. Electronic Document, *e-PRESERVATIONScience* 11: 90-98.
- Creamer, Jonathan I., Terence I. Quickenden, Leah B. Crichton, Patrick Robertson, and Rasha A. Ruhayel
2005 Attempted Cleaning of Bloodstains and its Effect on the Forensic Luminol Test. *Luminescence* 20(6):411-413.
- Daly, Scott, Timo Kunkel, Xing Sun, Suzanne Farrell, and Poppy Crum
2013 Viewer Preferences for Shadow, Diffuse, Specular, and Emissive Luminance Limits of High Dynamic Range Displays. *SID Symposium Digest of Technical Papers* 44(1):563-566.

- Das, Ruchita S., and Y. K. Agrawal
2011 Raman Spectroscopy: Recent Advancements, Techniques and Applications. *Vibrational Spectroscopy* 57:163-176.
- Davidhazy, Andrew
2006 Ultraviolet and Infrared Photography Summarized. Electronic document, <http://scholarworks.rit.edu/article/211>, accessed November 2, 2014.
- De Broux, Scott T., Katherine Kay McCaul, Sheri Shimamoto, and Michael J. Brooks
2007 Infrared Photography. *Forensic Photography III*: 1-21.
- De Wael, K., L. Lepot, F. Gason, and B. Gilbert
2008 In Search of Blood - Detection of Minute Particles using Spectroscopic Methods. *Forensic Science International* 180:37-42.
- Duncan, Christopher D.
2010 *Advanced Crime Scene Photography*. Boca Raton, FL: CRC Press Taylor & Francis Group.
- Dyer, A. G., L. L. Muir, and W. R. A. Muntz
2004 A Calibrated Gray Scale for Forensic Ultraviolet Photography. *Journal of Forensic Sciences* 49(5): 1-3.
- Farrar, Andrew, Glenn Porter, and Adrian Renshaw
2012 Detection of Latent Bloodstains Beneath Painted Surfaces using Reflected Infrared Photography. *Journal of Forensic Sciences* 57(5): 1190-1198.
- Fermo, P., M. Andreoli, L. Bonizzoni, M. Fantauzzi, G. Giubertoni, N. Ludwig, and A. Rossi
2016 Characterisation of Roman and Byzantine Glasses from the Surroundings of Thugga (Tunisia): Raw Materials and Colours. *Microchemical Journal* 129:5-15.
- Forensic Chemistry Handbook*
2012 Lawrence Kobilinsky, ed. Hoboken, New Jersey: John Wiley & Sons, Inc.
- Forensic Examination of Glass and Paint*
2001 Brian Caddy, ed. London: Taylor & Francis.
- Forensic Science Handbook: Volume 1*
2002 Richard Saferstein, ed. Second ed. New Jersey: Pearson Education Inc.

- Frey, Franziska, Dawn Heller, Dan Kushel, Timothy Vitale, and Gawain Weaver
2011 *The AIC Guide to Digital Photography and Conservation Documentation*.
Jeffrey Warda, ed. Second ed. Washington, DC: American Institute of Conservation
of Historic and Artistic Works.
- Garcia, Jair E., Philip A. Wilksch, Gale Spring, Peta Philp, and Adrian Dyer
2014 Characterization of Digital Cameras for Reflected Ultraviolet Photography;
Implications for Qualitative and Quantitative Image Analysis during Forensic
Examination. *Journal of Forensic Sciences* 59(1): 117-122.
- Gestring, Brian J.
2007 *A Forensic Scientist's Guide to Photography*. Bridgewater, NJ, USA: American
Board of Criminalistics.
- Golden, Gregory S.
1996 Forensic Photography: An Expanding Technology. *CDA Journal* 24(5): 50-56.
- Grafit, Arnon, Andrea Gronspan, Tzvi Rosenberg, and Zahit Hazan Eitan
2014 Influence of BlueStar Reagent on Blood Spatter Stains on Different Fabrics.
Journal of Forensic Identification 64(5): 475-488.
- Harroun, S. G., J. Bergman, E. Jablonski, and C. L. Brosseau
2011 Surface-Enhanced Raman Spectroscopy Analysis of House Paint and
Wallpaper Samples from an 18th Century Historic Property. *Analyst* 136:3453-3460.
- Hedenborg, M.
1988 Titanium Dioxide Induced Chemiluminescence of Human Polymorphonuclear
Leukocytes. *International Archives of Occupational and Environmental Health* 61:1-
6.
- Hooker, R. H., K. E. Creer, and J. S. Brennan
1991 Microspectrophotometry in the Development and Photography of Fluorescing
Marks. *Forensic Science International* 51:297-304.
- Howard, Maria C., and Mitch Nesson
2010 Detecting Bloodstains under Multiple Layers of Paint. *Journal of Forensic
Identification* 60(6): 682-717.
- James, Stuart H., Paul E. Kish, and T. Paulette Sutton
2005 *Principles of Bloodstain Pattern Analysis: Theory and Practice*. Boca Raton,
FL: CRC Press Taylor & Francis Group.

- Kettner, M., A. Schmidt, and M. Windgassen
2015 Impact Height and Wall Distance in Bloodstain Pattern Analysis - What Patterns of Round Bloodstains can tell us. *International Journal of Legal Medicine* 129(1):133-140.
- King, Richard, and Gordon M. Miskelly
2005 The Inhibition by Amines and Amino Acids of Bleach-Induced Luminol Chemiluminescence during Forensic Screening for Blood. *Talanta* 67:345-353.
- Kneipp, Katrin, Harald Kneipp, Irving Itzkan, Ramachandra R. Dasari, and Michael S. Feld
2002 Surface-Enhanced Raman Scattering and Biophysics. *Journal of Physics Condensed Matter* 14:597-624.
- Knock, Clare, and Marie Davison
2007 Predicting the Position of the Source of Blood Stains for Angled Impacts. *Journal of Forensic Sciences* 52(5):1044-1049.
- Kogou, Sotiria, Andrei Lucian, Sonia Bellesia, Lucia Burgio, Kate Bailey, Charlotte Brooks, and Haida Liang
2015 A Holistic Multimodal Approach to the Non-Invasive Analyses of Watercolour Paintings. *Applied Physics A* 121:999-1014.
- Krauss, Thomas C.
1993 Forensic Evidence Documentation using Reflective Ultraviolet Photography. *Photo Electronic Imaging*: 18-23.
- Kudelski, Andrzej
2008 Analytical Applications of Raman Spectroscopy. *Talanta* 76:1-8.
- Larkin, Bethany A. J., and Craig E. Banks
2014 Exploring the Applicability of Equine Blood to Bloodstain Pattern Analysis.
- Laux, Dale L.
1991 Effects of Luminol on the Subsequent Analysis of Bloodstains. *Journal of Forensic Sciences* 36(5):1512-1520.
- Lee, Wee Chuen, Bee Ee Khoo, Abdullah, Ahmad Fahmi Lim Bin, and Zalina Binti Abdul Aziz

- 2013 Statistical Evaluation of Alternative Light Sources for Bloodstain Photography. *Journal of Forensic Sciences* 58(3): 658-663.
- Li, Bo, Peter Beveridge, William T. O'Hare, and Meez Islam
2014 The Application of Visible Wavelength Reflectance Hyperspectral Imaging for the Detection and Identification of Blood Stains. *Science and Justice* 54:432-438.
- Li, Meng, Jun-Jie Yin, Wiayne G. Wamer, and Y. Martin Lo
2014 Mechanistic Characterization of Titanium Dioxide Nanoparticle-Induced Toxicity using Electron Spin Resonance. *Journal of Food and Drug Analysis* 22:76-85.
- Limmen, Roxane M., Manon Ceelen, Udo J. L. Reijnders, S. Joris Stomp, Koos C. de Keijzer, and Kees Das
2013 Enhancing the Visibility of Injuries with Narrow-Banded Beams of Light within the Visible Light Spectrum. *Journal of Forensic Sciences* 58(2): 518-522.
- Lytle, L. T., and D. G. Hedgecock
1978 Chemiluminescence in the Visualization of Forensic Bloodstains. *Journal of Forensic Sciences* 23(3):550-562.
- Mangold, Klaus, Joseph A. Shaw, and Michael Vollmer
2013 The Physics of Near-Infrared Photography. *European Journal of Physics* 34(6):52-71.
- Marin, Norman, and Jeffrey Buszka
2013 Alternate Light Source Imaging - Forensic Photography Techniques. Larry S. Miller, ed. New York, NY: Anderson Publishing Taylor & Francis Group.
- Mairinger, Franz
2000a The Infrared Examination of Paintings. *In Radiation in Art and Archaeometry*. D. C. Creagh and D. A. Bradley, eds. Pp. 40-55. New York, NY: Elsevier Science.
- Mairinger, Franz
2000b The Ultraviolet and Fluorescence Study of Paintings and Manuscripts. *In Radiation in Art and Archeometry*. D. C. Creagh and D. A. Bradley, eds. Pp. 56-75. New York, NY: Elsevier Science.
- Marušić, Katarina, Irina Pucic, and Vladan Desnica
2016 Ornaments in Radiation Treatment of Cultural Heritage: Color Ad UV-Vis Spectral Changes in Irrated Nacres. *Radiation Physics and Chemistry* 124:62-67.

- Milliet, Quentin, Olivier Delemont, and Pierre Margot
2014 A Forensic Perspective on the Role of Images in Crime Investigation and Reconstruction. *Science and Justice* 54:470-480.
- Miranda, Geraldo Elias, Felipe Bevilacqua Prado, Fabio Delwing, and Eduardo Daruge Junior
2014 Analysis of the fluorescence of body fluids on different surfaces and times. *Science and Justice* 54: 427-431.
- Miskelly, Gordon M., and John H. Wagner
2005 Using Spectral Information in Forensic Imaging. *Forensic Science International* 155:112-118.
- Nelson, David G., and Karen A. Santucci
2002 An Alternate Light Source to Detect Semen. *Academic Emergency Medicine* 9(10): 1045-1048.
- Palenske, Nicole M., and David K. Saunders
2002 Comparisons of Blood Viscosity between Amphibians and Mammals at 3°C and 38°C. *Journal of Thermal Biology* 27(6):479-484.
- Park, Jin Seo, Min Suk Chung, Sung Bae Hwang, Yong Sook Lee, and Dong-Hwan Har
2005 Technical Report on Semiautomatic Segmentation using the Adobe Photoshop. *Journal of Digital Imaging* 18(4):333-343.
- Peca Products
2015 IR - UV Filters. Electronic document, www.ir-uv.com/iruv.html, accessed September, 2016.
- Perkins, Michael
2005 The Application of Infrared Photography in Bloodstain Pattern Documentation of Clothing. *Journal of Forensic Identification* 55(1): 1-9.
- Quickenden, T. I., and J. I. Creamer
2001 A Study of Common Interferences with the Forensic Luminol Test for Blood. *Luminescence* 16: 295-298.
- Rai, B., and J. Kaur
2013 Different Types of Light in Forensic Photography. *Evidence-Based Forensic Dentistry*: 131-139.

- Raymond, MA
1996 The Physical Properties of Blood - Forensic Considerations. *Science & Justice* 36(3):153-160.
- Raymond, Michael Anthony, and Robert Lyndsay Hall
1986 An Interesting Application of Infra-Red Reflection Photography to Blood Splash Pattern Interpretation. *Forensic Science International* 31: 189-194.
- Richards, Austin
2010 Reflected Ultraviolet Imaging for Forensic Applications. Electronic document, [http://www.company7.com/library/nikon/Reflected UV Imaging for Forensics V2.pdf](http://www.company7.com/library/nikon/Reflected_UV_Imaging_for_Forensics_V2.pdf), accessed November 3, 2014.
- Robinson, Edward M.
2007 *Crime Scene Photography*. San Diego, California: Academic Press Elsevier.
- Sanfilippo, Philip, Austin Richards, and Heidi Nichols
2010 Reflected Ultraviolet Digital Photography: The Part Someone Forgot to Mention. *Journal of Forensic Identification* 60(2): 181-198.
- Santos, V. R. D., W. X. Paula, and E. Kalapothakis
2009 Influence of the Luminol Chemiluminescence Reaction on the Confirmatory Tests for the Detection and Characterization of Bloodstains in Forensic Analysis. *Forensic Science International: Genetics Supplement Series* 2:196-197.
- Schlücker, Sebastian
2014 *Surface-Enhanced Raman Spectroscopy: Concepts and Chemical Applications*. *Angewante Chemie International Edition* 53:4756-4795.
- Schneider Kreuznach Company
2016 Color Filters. Electronic document, www.schneiderkreuznach.com, accessed September, 2016.
- Schotman, Tom G., Antoinette A. Westen, Jaap van der Weerd, and Karla G. de Bruin
2015 Understanding the Visibility of Blood on Dark Surfaces: A Practical Evaluation of Visible Light, NIR, and SWIR Imaging. *Forensic Science International* 257:214-219.
- Schuerman, George, and Raymond Bruzan
1989 Chemistry of Paint. *Journal of Chemical Education* 66(4): 327-328.

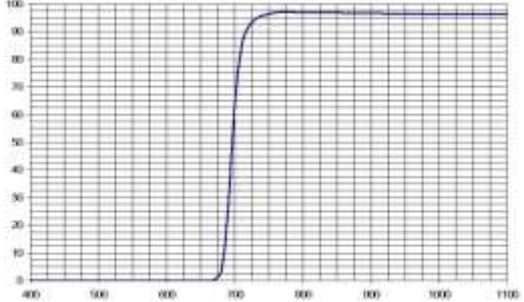
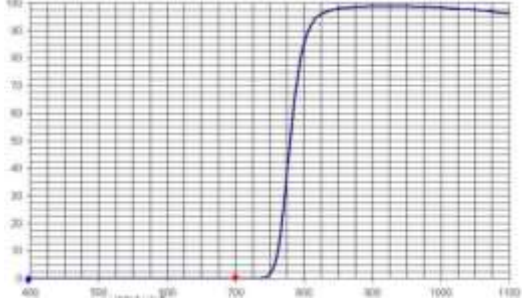
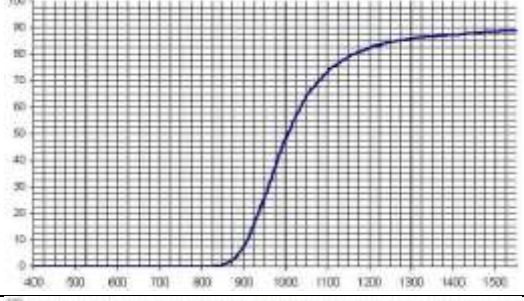
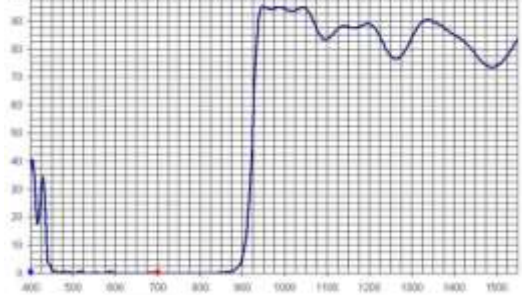
- Schulz, Martin, M., Frank Wehner, and Heinz-D Wehner
2007 The use of a Tunable Light Source (Mini-Crimescope MCS-400, SPEX Forensics) in Dissecting Microscopic Detection of Cryptic Epithelial Particles. *Journal of Forensic Sciences* 52(4): 879-883.
- Sedgewick, Jerry
2008 *Scientific Imaging with Photoshop: Methods, Measurements, and Output*. Victor Gavenda, ed. Berkeley, CA: New riders.
- Seidl, S., R. Hausmann, and P. Betz
2008 Comparison of Laser and Mercury-Arc Lamp for the Detection of Body Fluids on Different Substrates. *International Journal of Legal Medicine* 122:241-244.
- Shapter, Michael
2014 Applying a Verification Classification System to Medical and Forensic Digital Images. *Journal of Visual Communication in Medicine* 37(1-2):24-27.
- Slemko, J.
Forensic Consulting Inc. Bloodstain Tutorial. Electronic document, www.bloodspatter.com/, accessed September, 2016.
- Specht, W.
1937 The Chemiluminescence of Hemin: An Aid for Finding and Recognizing Blood Stains Important for Forensic Purposes. *Angewante Chemie* 50:155-157.
- SPEX Forensics
2016 Crimescope Forensic Light Source. Electronic document, www.spexforensics.com/applications/crimescope, accessed September, 2016.
- Stoilovic, Milutin
1991 Detection of Semen and Blood Stains using Polilight as a Light Source. *Forensic Science International* 51: 289-296.
- Stuart, Barbara
2004 *Infrared Spectroscopy: Fundamentals and Applications*. Chichester, West Sussex, England; Hoboken, NJ: John Wiley & Sons, Ltd.
- Szafarska, Malgorzata, Michal Wozniakiewicz, Mariusz Pilch, Janina Zieba-Palus, and Pawel Koscielniak

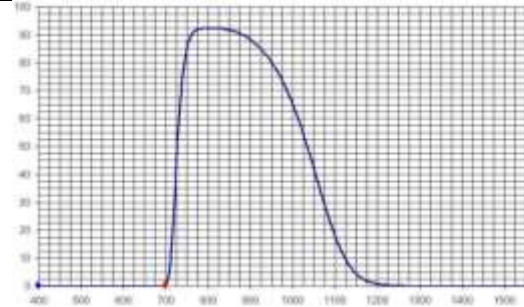

- 2009 Computer Analysis of ATR-FTIR Spectra of Paint Samples for Forensic Purposes. *Journal of Molecular Structure* 924-926:504-513.
- Thryft, Ann R.
2009 CCD and CMOS Sensors Become More Finely Tuned. *Test & Measurement World* 29(11): 65-67.
- Verhoeven, Geert J., and Klaus D. Schmitt
2010 An Attempt to Push Back Frontiers - Digital Near-Ultraviolet Aerial Archaeology. *Journal of Archaeological Science* 37:833-845.
- Wagner, John H., and Gordon M. Miskelly
2003a Background Correction in Forensic Photography I. Photography of Blood Under Conditions of Non-Uniform Illumination Or Variable Substrate Color - Theoretical Aspects and Proof of Concept. *Journal of Forensic Sciences* 48(3):593-603.
- Wagner, John H., and Gordon M. Miskelly
2003b Background Correction in Forensic Photography II. Photography of Blood Under Conditions of Non-Uniform Illumination Or Variable Substrate Color - Practical Aspects and Limitations. *Journal of Forensic Sciences* 48(3):604-613.
- Wawryk, Jacob, and Morris Odell
2005 Fluorescent Identification of Biological and Other Stains on Skin by the use of Alternative Light Sources. *Journal of Clinical Forensic Medicine* 12:296-301.
- Webb, Joanne L., Jonathan I. Creamer, and Terence I. Quickenden
2006 A Comparison of Presumptive Luminol Test for Blood with Four Non-Chemiluminescent Forensic Techniques. *Luminescence* 21: 214-220.
- Weber, Walter C.
1960 Chemicals in the Manufacture of Paint. *Journal of Chemical Education* 37(6): 322-324.
- Weiss, Sanford L.
2009 *Forensic Photography the Importance of Accuracy*. United State of America: Pearson Prentice Hall.
- Wen, C. Y., and J. K. Chen
2004 Multi-Resolution Image Fusion Technique and its Application to Forensic Science. *Forensic Science International* 140:217-232.

- West, Michael H., Robert E. Barsley, John E. Hall , Steve Hayne, and Mary Cimrmancic
1992 The Detection and Documentation of Trace Wound Patterns by use of an
Alternative Light Source. *Journal of Forensic Sciences* 37(6):1480-1488.
- Williams, Kathryn, R.
2006 House Paint. *Journal of Chemical Education* 83(10): 1448-1449.
- Williams, Robin, and Gigi Williams
1993 The Invisible Image - A Tutorial on Photography with Invisible Radiation, Part
1: Introduction and Reflected Ultraviolet Techniques. *Journal of Biological
Photography* 61(4): 115-132.
- Williams, Robin, and Gigi Williams
2002 Infrared Photography. Electronic document,
http://medicalphotography.com.au/Article_03/index.html, accessed November 2,
2014.
- Wonder, Anita Y.
2007 *Bloodstain Pattern Evidence Objective Approaches and Case Applications*.
Amsterdam; Boston: Elsevier/Academic Press.
- Wright, Franklin, and Gregory S. Golden
2010 The Use of Full Spectrum Digital Photography for Evidence Collection and
Preservation in Cases Involving Forensic Odontology. *Forensic Science International*
201:59-67.
- Young, Tina
2006 A Photographic Comparison of Luminol, Fluorescein, and Bluestar. *Journal of
Forensic Identification* 56(6):906-912.
- Zamora, L. Lahuerta, A. M. Mellado Romero, and J. Martinez Calatayud
2011 Quantitative Colorimetric Analysis of some Inorganic Salts using Digital
Photography. *Analytical Letter* 44:1674-1682.
- Zięba-Palus, J.
1999 Application of Micro-Fourier Transform Infrared Spectroscopy to the
Examination of Paint Samples. *Journal of Molecular Structure* 511-512:327-335.

Appendix

Appendix 2.2.3. Wratten rating and Peca Filter equivalency; bandpass transmission and spectral curve of IR filters. (Table adapted from De Broux 2007; Frey 2011; Spectral charts from Peca Products Inc.).

Wratten Rating	Peca Brand	0% Transmission (nm)	50% Transmission (nm)	Spectral Curve (transmission % y axis; nanometre x axis)
70	902	675	700	
87	904	740	795	
87A	906	880	1000	
87B	908	820	930	

88A	912	700	720	
89B	914	680	720	

Appendix 3.2. Stages One and Two: The Application of Primer and Paint

Preparation of Experiment and Equipment

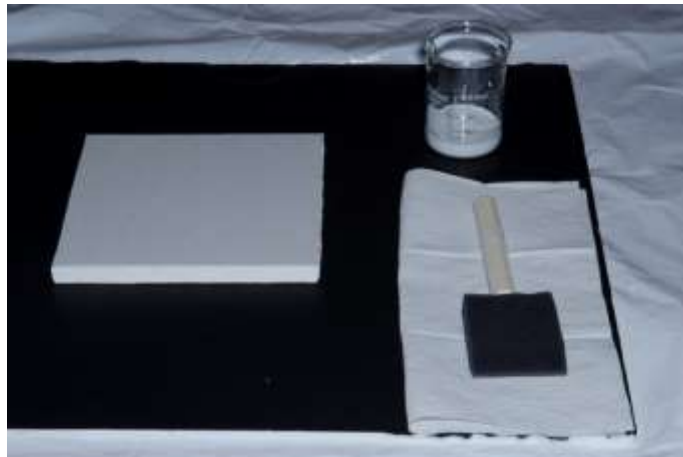
All painting was conducted outdoors in an area protected from both the sun and wind. The 16 sections were painted and moved indoors into the photography lab for drying. The materials used for painting the 16 sections are listed in the Table below. Each drywall square had a numbered sticker placed on the back for experiment identification. Due to time constraints, the application of the primer layer was separated into two days. Drywall squares 1, 2, 3, 4, 5, 6, and 16 were painted on the first day while squares 7, 8, 9, 10, 11, 12, 13, 14, and 15 were painted on the second day.

Materials for Drywall Painting

Material	Use	Amount
3-inch Sponge Brushes	To paint each drywall section	16
Scrap Matte Board	Used as a painting and transfer surface	2
Plastic Sheets	To protect the ground	1
Plastic Bucket	To clean the sponges and beakers	1
Pour Spout	To easily pour the 1 gallon primer	1
Paper towel	Clean up	multiple
10 mL beaker	To measure out exact amount of paint	1
30 mL beaker	To measure out exact amount of paint	1
Screw driver	To open cans of paint	1
Hammer	To close cans of paint	1

Stage One and Two: Application of the Primer Paint Layer and First Layer of Paint

The application of the primer paint layer consisted of nine steps. The primer was poured into the 30 mL glass beaker for a total of 20 mL of primer paint in the beaker (See below), paint amounts are provided in the Table below.



Example of paint set up for primer paint layer.

A drywall section was placed onto the centre of the scrap mat board to be painted. The researcher held one 3-inch sponge brush in the right hand and the beaker of paint in the left hand. The paint was poured onto the square and the sponge was used to remove all of the remaining paint from the beaker. The beaker was set aside and the researcher began to gently brush the primer paint from the left side of the square to the right side beginning in the top left corner. After a uniform coverage and thickness had been applied, excess paint remaining in the brush was returned into the beaker, measuring 5 mL. The paint was then disposed of and the beaker and sponge brush was placed in the plastic bucket of warm water for cleaning. Both the beaker and sponge were cleaned of all paint and dried with the paper towel. The sponge brush was set aside to dry while a new brush was used on each subsequent square. The entire process was repeated for each section of drywall.

The painted sections were placed on a mobile cart (See below) and left inside the photography lab to dry out of the elements and for security reasons.



Drying cart with painted drywall squares.

These steps were replicated on the following day for the remaining drywall squares which were also left to dry in the photography lab. All 16 primed drywall squares dried for at least 24 hours before the first paint layer was applied.

Amount of Primer Applied for the Primer Layer

Paint Type	Beaker Used (mL)	Allotted Paint Amount (mL)	Actual Paint Amount (mL)	Amount of Paint in Brush (mL)	Drying Time (Hours)
White Acrylic	30	20	15	5	24
White Latex	30	20	15	5	24
Black Latex	30	20	15	5	24
Maroon Latex	30	20	15	5	24

The application of the first paint layer was identical in set up and procedure for the application of the primer paint layer. A total of 25 mL of paint was evenly applied to each drywall square over the primer layer for this stage of the experiment (See below). Firstly, 30 mL of paint was measured out into the beaker and applied to the drywall square. Excess paint remaining in the sponge brush was replaced into the beaker and measured for a total of 5 mL. The paint was then disposed of and the beaker and sponge brush were placed in the plastic bucket of warm water for cleaning.

White latex squares 5, 6, 7, and 8 were the first to have the paint layer applied. Following the application of the white latex, the black latex squares 9, 10, 11, and 12 had the first layer of paint applied. Maroon latex squares 13, 14, 15, and 16; as well as white acrylic paint squares 1, 2, 3, and 4 as the final squares to be painted. All of the drywall

squares were left to dry in the photography lab over the weekend for a total drying time of approximately 64 hours.

Amount of Paint Applied for the Paint over Primer Layer.

Paint Type	Beaker Used (mL)	Allotted Paint Amount (mL)	Actual Paint Amount (mL)	Amount of Paint in Brush (mL)	Drying Time (Hours)
White Acrylic	30	30	25	5	64
White Latex	30	30	25	5	64
Black Latex	30	30	25	5	64
Maroon Latex	30	30	25	5	64

Appendix 3.4. Stage Four: First Layer of Paint Preparation of Experiment and Equipment

The materials and equipment used in the application of the first layer of paint are identical to those used in the application of the primer and paint layers (See below). The application of the first layer of paint over the dried bloodstains was conducted outdoors in a well-protected area out of the sun, wind and foot traffic. Each section was returned to the photography lab cart to be brought inside to dry following the painting process.

Materials for Painting First Layer over Bloodstain Patterns

Material	Use	Amount
3-inch Sponge Brushes	To paint each drywall section	16
Scrap Matte Board	Used as a painting and transfer surface	2
Plastic Sheets	To protect the ground	1
Plastic Bucket	To clean the sponges and beakers	1
Pour Spout	To easily pour the 1 gallon primer	1
Paper towel	Clean up	multiple
10 mL beaker	To measure out exact amount of paint	1
30 mL beaker	To measure out exact amount of paint	1
Screw driver	To open cans of paint	1
Hammer	To close cans of paint	1

Stage Four: Application of First Layer of Paint over Bloodstain patterns

The application of the first layer of paint over bloodstains followed the same steps as the application of primer and paint layers prior to adding the bloodstain patterns to

each drywall square. Beginning with drywall square number 1, the square was placed on the black matte board on the ground in front of the researcher. White acrylic paint was carefully measured out into the 30 mL beaker for a total of 20 mL to be applied to the square (See below). The paint was poured onto the square while the researcher used the 3-inch sponge brush to remove any excess paint from the beaker. The researcher gently brushed the paint starting from the top left side of the square in one continuous horizontal line to the top right side. The researcher continued on the next line from the left side to the right side until the entire square had been painted. After uniform coverage had been applied the excess paint from the sponge brush was placed in the beaker. A total of 5 mL of paint excess was observed to be in the beaker. The excess paint was then disposed of and both the beaker and the paint brush was placed in the water bucket for cleaning and then dried with paper towel. The sponge brush was placed off to the side to completely air dry. The entire process was repeated for each drywall section with complete clean-up and changing of the water bucket in between each paint type. Following the application of the first layer of paint over blood, all of the drywall sections were allowed to dry in the photography lab for a total of 64 hours over the weekend.

Amount of Paint Applied for the First Layer of Paint over Bloodstain Patterns

Paint Type	Beaker Used (mL)	Allotted Paint Amount (mL)	Actual Paint Amount (mL)	Amount of Paint in Brush (mL)	Drying Time (Hours)
White Acrylic	30	20	15	5	64
White Latex	30	20	15	5	64
Black Latex	30	20	15	5	64
Maroon Latex	30	20	15	5	64

Appendix 3.5. Stage Five: Second Layer of Paint Preparation of Experiment and Equipment

The painting of the second layer of paint over the dried bloodstains was conducted outdoors in a well-protected area out of the sun, wind and foot traffic. Each section was returned to the photography lab cart to be brought inside to dry following the painting process. The materials for painting the second layer of paint over bloodstains are the same used for the primer and paint layer stages and the first layer of paint over bloodstain patterns stage (See below).

Materials for Painting

Material	Use	Amount
3-inch Sponge Brushes	To paint each drywall section	16
Scrap Matte Board	Used as a painting and transfer surface	2
Plastic Sheets	To protect the ground	1
Plastic Bucket	To clean the sponges and beakers	1
Pour Spout	To easily pour the 1 gallon primer	1
Paper towel	Clean up	multiple
10 mL beaker	To measure out exact amount of paint	1
30 mL beaker	To measure out exact amount of paint	1
Screw driver	To open cans of paint	1
Hammer	To close cans of paint	1

Stage Five: Application of Second Layer of Paint over Bloodstain patterns

The application of the second layer of paint over bloodstain patterns followed the same steps as the application of primer and paint, and the first layer of paint over bloodstains. Beginning with drywall square number 1, the square was placed on the black matte board in front of the researcher. White acrylic paint was carefully measured out into the 30 mL beaker for a total of 30 mL to be applied to the square (See below). The paint was poured onto the square while the researcher used the 3-inch sponge brush to remove any excess paint from the beaker. The researcher gently brushed the paint starting from the top left side of the square in one continuous horizontal line to the top right side. The researcher continued for the next line from the left side to the right side until the entire square had been painted. After uniform coverage had been accomplished the excess paint from the sponge brush was placed in the beaker. A total of 5 mL of paint excess was observed to be in the beaker. The excess paint was then disposed of and both the beaker and the paint brush was placed in the water bucket for cleaning and then dried with paper towel. The sponge brush was placed off to the side to completely air dry. The entire process was repeated for each drywall square with complete cleaning up and changing of the water bucket in between each paint type. Following the application of the second layer of paint over bloodstain patterns, all of the drywall squares were allowed to dry in the photography lab for a total of 64 hours over the weekend.

Amount of Paint Applied for the Second Layer of Paint over Bloodstain Patterns

Paint Type	Beaker Used (mL)	Allotted Paint Amount (mL)	Actual Paint Amount (mL)	Amount of Paint in Brush (mL)	Drying Time (Hours)
White Acrylic	30	30	25	5	64
White Latex	30	30	25	5	64
Black Latex	30	30	25	5	64
Maroon Latex	30	30	25	5	64

Appendix 3.7. Camera Settings for Standard Photography, Reflective Infrared Photography, Reflective Ultraviolet Photography, Fluorescence Photography and Luminol Treatment Photography

Exp. Layer	Paint Layer	Square #	F #	ISO	Lens	Focal Length	Shutter Speed
Standard Blood	WA	1	F11	100	16-85	50mm	(1/10s)
Standard Blood	WA	2	F11	100	16-85	50mm	(1/10s)
Standard Blood	WA	3	F11	100	16-85	50mm	(1/10s)
Standard Blood	WA	4	F11	100	16-85	50mm	(1/10s)
Standard Blood	WL	5	F11	100	16-85	50mm	(1/15s)
Standard Blood	WL	6	F11	100	16-85	50mm	(1/15s)
Standard Blood	WL	7	F11	100	16-85	50mm	(1/15s)
Standard Blood	WL	8	F11	100	16-85	50mm	(1/15s)
Standard Blood	BL	9	F11	100	16-85	50mm	(1/15s)
Standard Blood	BL	10	F11	100	16-85	50mm	(1/15s)
Standard Blood	BL	11	F11	100	16-85	50mm	(1/15s)
Standard Blood	BL	12	F11	100	16-85	50mm	(1/15s)
Standard Blood	ML	13	F11	100	16-85	50mm	(1/15s)
Standard Blood	ML	14	F11	100	16-85	50mm	(1/15s)
Standard Blood	ML	15	F11	100	16-85	50mm	(1/15s)
Standard Blood	ML	16	F11	100	16-85	50mm	(1/15s)
Standard 1st Paint	WA	1	F11	200	16-85	50mm	(1/100s)
Standard 1st Paint	WA	2	F11	200	16-85	50mm	(1/100s)
Standard 1st Paint	WA	3	F11	200	16-85	50mm	(1/100s)
Standard 1st Paint	WA	4	F11	200	16-85	50mm	(1/100s)
Standard 1st Paint	WL	5	F11	200	16-85	50mm	(1/100s)
Standard 1st Paint	WL	6	F11	200	16-85	50mm	(1/100s)
Standard 1st Paint	WL	7	F11	200	16-85	50mm	(1/100s)
Standard 1st Paint	WL	8	F11	200	16-85	50mm	(1/100s)
Standard 1st Paint	BL	9	F11	200	16-85	50mm	(1/25s)

Standard 1st Paint	BL	10	F11	200	16-85	50mm	(1/25s)
Standard 1st Paint	BL	11	F11	200	16-85	50mm	(1/25s)
Standard 1st Paint	BL	12	F11	200	16-85	50mm	(1/25s)
Standard 1st Paint	ML	13	F11	200	16-85	50mm	(1/30s)
Standard 1st Paint	ML	14	F11	200	16-85	50mm	(1/30s)
Standard 1st Paint	ML	15	F11	200	16-85	50mm	(1/30s)
Standard 1st Paint	ML	16	F11	200	16-85	50mm	(1/30s)
Standard 2nd Paint	WA	1	F11	200	16-85	50mm	(1/100s)
Standard 2nd Paint	WA	2	F11	200	16-85	50mm	(1/100s)
Standard 2nd Paint	WA	3	F11	200	16-85	50mm	(1/100s)
Standard 2nd Paint	WA	4	F11	200	16-85	50mm	(1/100s)
Standard 2nd Paint	WL	5	F11	200	16-85	50mm	(1/100s)
Standard 2nd Paint	WL	6	F11	200	16-85	50mm	(1/100s)
Standard 2nd Paint	WL	7	F11	200	16-85	50mm	(1/100s)
Standard 2nd Paint	WL	8	F11	200	16-85	50mm	(1/100s)
Standard 2nd Paint	BL	9	F11	200	16-85	50mm	(1/20s)
Standard 2nd Paint	BL	10	F11	200	16-85	50mm	(1/20s)
Standard 2nd Paint	BL	11	F11	200	16-85	50mm	(1/20s)
Standard 2nd Paint	BL	12	F11	200	16-85	50mm	(1/20s)
Standard 2nd Paint	ML	13	F11	200	16-85	50mm	(1/25s)
Standard 2nd Paint	ML	14	F11	200	16-85	50mm	(1/25s)
Standard 2nd Paint	ML	15	F11	200	16-85	50mm	(1/25s)
Standard 2nd Paint	ML	16	F11	200	16-85	50mm	(1/25s)
Standard 2nd Paint Oblique	WA	1	F11	200	16-85	50mm	(1/100s)
Standard 2nd Paint Oblique	WA	1	F11	200	16-85	50mm	(1/60s)
Standard 2nd Paint Oblique	WA	1	F11	200	16-85	50mm	(1/80s)
Standard 2nd Paint Oblique	WA	2	F11	200	16-85	50mm	(1/100s)
Standard 2nd Paint Oblique	WA	2	F11	200	16-85	50mm	(1/60s)
Standard 2nd Paint Oblique	WA	2	F11	200	16-85	50mm	(1/80s)
Standard 2nd Paint Oblique	WA	3	F11	200	16-85	50mm	(1/100s)
Standard 2nd Paint Oblique	WA	3	F11	200	16-85	50mm	(1/60s)
Standard 2nd Paint Oblique	WA	3	F11	200	16-85	50mm	(1/80s)
Standard 2nd Paint Oblique	WL	5	F11	200	16-85	50mm	(1/100s)
Standard 2nd Paint Oblique	WL	5	F11	200	16-85	50mm	(1/60s)
Standard 2nd Paint Oblique	WL	5	F11	200	16-85	50mm	(1/80s)
Standard 2nd Paint Oblique	WL	6	F11	200	16-85	50mm	(1/100s)
Standard 2nd Paint Oblique	WL	6	F11	200	16-85	50mm	(1/60s)
Standard 2nd Paint Oblique	WL	6	F11	200	16-85	50mm	(1/80s)
Standard 2nd Paint Oblique	WL	7	F11	200	16-85	50mm	(1/100s)

Standard 2nd Paint Oblique	WL	7	F11	200	16-85	50mm	(1/60s)
Standard 2nd Paint Oblique	WL	7	F11	200	16-85	50mm	(1/80s)
Standard 2nd Paint Oblique	BL	9	F11	200	16-85	50mm	(1/10s)
Standard 2nd Paint Oblique	BL	9	F11	200	16-85	50mm	(1/6s)
Standard 2nd Paint Oblique	BL	9	F11	200	16-85	50mm	(1/8s)
Standard 2nd Paint Oblique	BL	10	F11	200	16-85	50mm	(1/10s)
Standard 2nd Paint Oblique	BL	10	F11	200	16-85	50mm	(1/6s)
Standard 2nd Paint Oblique	BL	10	F11	200	16-85	50mm	(1/8s)
Standard 2nd Paint Oblique	BL	11	F11	200	16-85	50mm	(1/10s)
Standard 2nd Paint Oblique	BL	11	F11	200	16-85	50mm	(1/6s)
Standard 2nd Paint Oblique	BL	11	F11	200	16-85	50mm	(1/8s)
Standard 2nd Paint Oblique	ML	13	F11	200	16-85	50mm	(1/15s)
Standard 2nd Paint Oblique	ML	13	F11	200	16-85	50mm	(1/10s)
Standard 2nd Paint Oblique	ML	13	F11	200	16-85	50mm	(1/13s)
Standard 2nd Paint Oblique	ML	14	F11	200	16-85	50mm	(1/15s)
Standard 2nd Paint Oblique	ML	14	F11	200	16-85	50mm	(1/10s)
Standard 2nd Paint Oblique	ML	14	F11	200	16-85	50mm	(1/13s)
Standard 2nd Paint Oblique	ML	15	F11	200	16-85	50mm	(1/15s)
Standard 2nd Paint Oblique	ML	15	F11	200	16-85	50mm	(1/10s)
Standard 2nd Paint Oblique	ML	15	F11	200	16-85	50mm	(1/13s)

Exp. Layer	Paint Layer	Square #	Filter	F #	ISO	Lens	Focal Length	Shutter Speed
Infrared Blood	WA	1	no fil.	F16	400	60mm	60mm	(1/90s)
Infrared Blood	WA	1	70	F16	400	60mm	60mm	(1/90s)
Infrared Blood	WA	1	87	F16	400	60mm	60mm	(1/90s)
Infrared Blood	WA	1	87A	F16	400	60mm	60mm	(1/90s)
Infrared Blood	WA	1	87B	F16	400	60mm	60mm	(1/90s)
Infrared Blood	WA	1	88A	F16	400	60mm	60mm	(1/90s)
Infrared Blood	WA	1	89B	F16	400	60mm	60mm	(1/90s)
Infrared Blood	WA	2	no fil.	F16	400	60mm	60mm	(1/90s)
Infrared Blood	WA	2	70	F16	400	60mm	60mm	(1/90s)
Infrared Blood	WA	2	87	F16	400	60mm	60mm	(1/90s)
Infrared Blood	WA	2	87A	F16	400	60mm	60mm	(1/90s)
Infrared Blood	WA	2	87B	F16	400	60mm	60mm	(1/90s)
Infrared Blood	WA	2	88A	F16	400	60mm	60mm	(1/90s)
Infrared Blood	WA	2	89B	F16	400	60mm	60mm	(1/90s)
Infrared Blood	WA	3	no fil.	F16	400	60mm	60mm	(1/90s)
Infrared Blood	WA	3	70	F16	400	60mm	60mm	(1/90s)
Infrared Blood	WA	3	87	F16	400	60mm	60mm	(1/90s)

Infrared Blood	WA	3	87A	F16	400	60mm	60mm	(1/90s)
Infrared Blood	WA	3	87B	F16	400	60mm	60mm	(1/90s)
Infrared Blood	WA	3	88A	F16	400	60mm	60mm	(1/90s)
Infrared Blood	WA	3	89B	F16	400	60mm	60mm	(1/90s)
Infrared Blood	WA	4	no fil.	F16	400	60mm	60mm	(1/90s)
Infrared Blood	WA	4	70	F16	400	60mm	60mm	(1/90s)
Infrared Blood	BL	9	no fil.	F16	400	60mm	60mm	(1/30s)
Infrared Blood	BL	9	70	F16	400	60mm	60mm	(1/30s)
Infrared Blood	BL	9	87	F16	400	60mm	60mm	(1/15s)
Infrared Blood	BL	9	87A	F16	400	60mm	60mm	(1/15s)
Infrared Blood	BL	9	87B	F16	400	60mm	60mm	(1/3s)
Infrared Blood	BL	9	88A	F16	400	60mm	60mm	(1/15s)
Infrared Blood	BL	9	89B	F16	400	60mm	60mm	(1/15s)
Infrared Blood	BL	10	no fil.	F16	400	60mm	60mm	(1/30s)
Infrared Blood	BL	10	70	F16	400	60mm	60mm	(1/30s)
Infrared Blood	BL	10	87	F16	400	60mm	60mm	(1/30s)
Infrared Blood	BL	10	87A	F16	400	60mm	60mm	(1/15s)
Infrared Blood	BL	10	87B	F16	400	60mm	60mm	(1/3s)
Infrared Blood	BL	10	88A	F16	400	60mm	60mm	(1/15s)
Infrared Blood	BL	10	89B	F16	400	60mm	60mm	(1/15s)
Infrared Blood	BL	11	no fil.	F16	400	60mm	60mm	(1/30s)
Infrared Blood	BL	11	70	F16	400	60mm	60mm	(1/30s)
Infrared Blood	BL	11	87	F16	400	60mm	60mm	(1/30s)
Infrared Blood	BL	11	87A	F16	400	60mm	60mm	(1/15s)
Infrared Blood	BL	11	87B	F16	400	60mm	60mm	(1/3s)
Infrared Blood	BL	11	88A	F16	400	60mm	60mm	(1/15s)
Infrared Blood	BL	11	89B	F16	400	60mm	60mm	(1/15s)
Infrared Blood	BL	12	no fil.	F16	400	60mm	60mm	(1/30s)
Infrared Blood	BL	12	70	F16	400	60mm	60mm	(1/30s)
Infrared Blood	ML	13	no fil.	F16	400	60mm	60mm	(1/30s)
Infrared Blood	ML	13	70	F16	400	60mm	60mm	(1/30s)
Infrared Blood	ML	13	87	F16	400	60mm	60mm	(1/30s)
Infrared Blood	ML	13	87A	F16	400	60mm	60mm	(1/15s)
Infrared Blood	ML	13	87B	F16	400	60mm	60mm	(1/3s)
Infrared Blood	ML	13	88A	F16	400	60mm	60mm	(1/15s)
Infrared Blood	ML	13	89B	F16	400	60mm	60mm	(1/15s)
Infrared Blood	ML	14	no fil.	F16	400	60mm	60mm	(1/30s)
Infrared Blood	ML	14	70	F16	400	60mm	60mm	(1/30s)
Infrared Blood	ML	14	87	F16	400	60mm	60mm	(1/30s)

Infrared Blood	ML	14	87A	F16	400	60mm	60mm	(1/15s)
Infrared Blood	ML	14	87B	F16	400	60mm	60mm	(1/3s)
Infrared Blood	ML	14	88A	F16	400	60mm	60mm	(1/15s)
Infrared Blood	ML	14	89B	F16	400	60mm	60mm	(1/15s)
Infrared Blood	ML	15	no fil.	F16	400	60mm	60mm	(1/60s)
Infrared Blood	ML	15	70	F16	400	60mm	60mm	(1/60s)
Infrared Blood	ML	15	87	F16	400	60mm	60mm	(1/60s)
Infrared Blood	ML	15	87A	F16	400	60mm	60mm	(1/30s)
Infrared Blood	ML	15	87B	F16	400	60mm	60mm	(1/6s)
Infrared Blood	ML	15	88A	F16	400	60mm	60mm	(1/30s)
Infrared Blood	ML	15	89B	F16	400	60mm	60mm	(1/30s)
Infrared Blood	ML	16	no fil.	F16	400	60mm	60mm	(1/60s)
Infrared Blood	ML	16	70	F16	400	60mm	60mm	(1/60s)
Infrared Blood	WL	5	no fil.	F16	400	60mm	60mm	(1/90s)
Infrared Blood	WL	5	70	F16	400	60mm	60mm	(1/90s)
Infrared Blood	WL	5	87	F16	400	60mm	60mm	(1/90s)
Infrared Blood	WL	5	87A	F16	400	60mm	60mm	(1/45s)
Infrared Blood	WL	5	87B	F16	400	60mm	60mm	(1/15s)
Infrared Blood	WL	5	88A	F16	400	60mm	60mm	(1/90s)
Infrared Blood	WL	5	89B	F16	400	60mm	60mm	(1/90s)
Infrared Blood	WL	6	no fil.	F16	400	60mm	60mm	(1/90s)
Infrared Blood	WL	6	70	F16	400	60mm	60mm	(1/90s)
Infrared Blood	WL	6	87	F16	400	60mm	60mm	(1/90s)
Infrared Blood	WL	6	87A	F16	400	60mm	60mm	(1/45s)
Infrared Blood	WL	6	87B	F16	400	60mm	60mm	(1/15s)
Infrared Blood	WL	6	88A	F16	400	60mm	60mm	(1/90s)
Infrared Blood	WL	6	89B	F16	400	60mm	60mm	(1/90s)
Infrared Blood	WL	7	no fil.	F16	400	60mm	60mm	(1/90s)
Infrared Blood	WL	7	70	F16	400	60mm	60mm	(1/90s)
Infrared Blood	WL	7	87	F16	400	60mm	60mm	(1/90s)
Infrared Blood	WL	7	87A	F16	400	60mm	60mm	(1/45s)
Infrared Blood	WL	7	87B	F16	400	60mm	60mm	(1/15s)
Infrared Blood	WL	7	88A	F16	400	60mm	60mm	(1/90s)
Infrared Blood	WL	7	89B	F16	400	60mm	60mm	(1/90s)
Infrared Blood	WL	8	no fil.	F16	400	60mm	60mm	(1/90s)
Infrared Blood	WL	8	70	F16	400	60mm	60mm	(1/90s)
Infrared 1st Paint	WA	1	no fil.	F22	400	60mm	60mm	(1/250s)
Infrared 1st Paint	WA	1	70	F22	400	60mm	60mm	(1/180s)
Infrared 1st Paint	WA	1	87	F22	400	60mm	60mm	(1/125s)

Infrared 1st Paint	WA	1	87A	F22	400	60mm	60mm	(1/60s)
Infrared 1st Paint	WA	1	87B	F22	400	60mm	60mm	(1/30s)
Infrared 1st Paint	WA	1	88A	F22	400	60mm	60mm	(1/180s)
Infrared 1st Paint	WA	1	89B	F22	400	60mm	60mm	(1/250s)
Infrared 1st Paint	WA	2	no fil.	F22	400	60mm	60mm	(1/250s)
Infrared 1st Paint	WA	2	70	F22	400	60mm	60mm	(1/180s)
Infrared 1st Paint	WA	2	87	F22	400	60mm	60mm	(1/125s)
Infrared 1st Paint	WA	2	87A	F22	400	60mm	60mm	(1/60s)
Infrared 1st Paint	WA	2	87B	F22	400	60mm	60mm	(1/30s)
Infrared 1st Paint	WA	2	88A	F22	400	60mm	60mm	(1/180s)
Infrared 1st Paint	WA	2	89B	F22	400	60mm	60mm	(1/250s)
Infrared 1st Paint	WA	3	no fil.	F22	400	60mm	60mm	(1/250s)
Infrared 1st Paint	WA	3	70	F22	400	60mm	60mm	(1/180s)
Infrared 1st Paint	WA	3	87	F22	400	60mm	60mm	(1/125s)
Infrared 1st Paint	WA	3	87A	F22	400	60mm	60mm	(1/60s)
Infrared 1st Paint	WA	3	87B	F22	400	60mm	60mm	(1/30s)
Infrared 1st Paint	WA	3	88A	F22	400	60mm	60mm	(1/180s)
Infrared 1st Paint	WA	3	89B	F22	400	60mm	60mm	(1/250s)
Infrared 1st Paint	WA	4	no fil.	F22	400	60mm	60mm	(1/250s)
Infrared 1st Paint	WA	4	70	F22	400	60mm	60mm	(1/180s)
Infrared 1st Paint	WL	5	no fil.	F22	400	60mm	60mm	(1/250s)
Infrared 1st Paint	WL	5	70	F22	400	60mm	60mm	(1/180s)
Infrared 1st Paint	WL	5	87	F22	400	60mm	60mm	(1/125s)
Infrared 1st Paint	WL	5	87A	F22	400	60mm	60mm	(1/60s)
Infrared 1st Paint	WL	5	87B	F22	400	60mm	60mm	(1/30s)
Infrared 1st Paint	WL	5	88A	F22	400	60mm	60mm	(1/180s)
Infrared 1st Paint	WL	5	89B	F22	400	60mm	60mm	(1/250s)
Infrared 1st Paint	WL	6	no fil.	F22	400	60mm	60mm	(1/250s)
Infrared 1st Paint	WL	6	70	F22	400	60mm	60mm	(1/180s)
Infrared 1st Paint	WL	6	87	F22	400	60mm	60mm	(1/125s)
Infrared 1st Paint	WL	6	87A	F22	400	60mm	60mm	(1/60s)
Infrared 1st Paint	WL	6	87B	F22	400	60mm	60mm	(1/30s)
Infrared 1st Paint	WL	6	88A	F22	400	60mm	60mm	(1/180s)
Infrared 1st Paint	WL	6	89B	F22	400	60mm	60mm	(1/250s)
Infrared 1st Paint	WL	7	no fil.	F22	400	60mm	60mm	(1/250s)
Infrared 1st Paint	WL	7	70	F22	400	60mm	60mm	(1/180s)
Infrared 1st Paint	WL	7	87	F22	400	60mm	60mm	(1/125s)
Infrared 1st Paint	WL	7	87A	F22	400	60mm	60mm	(1/60s)
Infrared 1st Paint	WL	7	87B	F22	400	60mm	60mm	(1/30s)

Infrared 1st Paint	WL	7	88A	F22	400	60mm	60mm	(1/180s)
Infrared 1st Paint	WL	7	89B	F22	400	60mm	60mm	(1/250s)
Infrared 1st Paint	WL	8	no fil.	F22	400	60mm	60mm	(1/250s)
Infrared 1st Paint	WL	8	70	F22	400	60mm	60mm	(1/180s)
Infrared 1st Paint	BL	9	no fil.	F22	400	60mm	60mm	(1/10s)
Infrared 1st Paint	BL	9	70	F22	400	60mm	60mm	(1/8s)
Infrared 1st Paint	BL	9	87	F22	400	60mm	60mm	(1/4s)
Infrared 1st Paint	BL	9	87A	F22	400	60mm	60mm	(0.50s)
Infrared 1st Paint	BL	9	87B	F8	400	60mm	60mm	(1/20s)
Infrared 1st Paint	BL	9	88A	F22	400	60mm	60mm	(1/8s)
Infrared 1st Paint	BL	9	89B	F22	400	60mm	60mm	(1/10s)
Infrared 1st Paint	BL	10	no fil.	F22	400	60mm	60mm	(1/10s)
Infrared 1st Paint	BL	10	70	F22	400	60mm	60mm	(1/8s)
Infrared 1st Paint	BL	10	87	F22	400	60mm	60mm	(1/4s)
Infrared 1st Paint	BL	10	87A	F22	400	60mm	60mm	(0.50s)
Infrared 1st Paint	BL	10	87B	F8	400	60mm	60mm	(1/20s)
Infrared 1st Paint	BL	10	88A	F22	400	60mm	60mm	(1/8s)
Infrared 1st Paint	BL	10	89B	F22	400	60mm	60mm	(1/10s)
Infrared 1st Paint	BL	11	no fil.	F22	400	60mm	60mm	(1/10s)
Infrared 1st Paint	BL	11	70	F22	400	60mm	60mm	(1/8s)
Infrared 1st Paint	BL	11	87	F22	400	60mm	60mm	(1/4s)
Infrared 1st Paint	BL	11	87A	F22	400	60mm	60mm	(0.50s)
Infrared 1st Paint	BL	11	87B	F8	400	60mm	60mm	(1/20s)
Infrared 1st Paint	BL	11	88A	F22	400	60mm	60mm	(1/8s)
Infrared 1st Paint	BL	11	89B	F22	400	60mm	60mm	(1/10s)
Infrared 1st Paint	BL	12	no fil.	F22	400	60mm	60mm	(1/10s)
Infrared 1st Paint	BL	12	70	F22	400	60mm	60mm	(1/8s)
Infrared 1st Paint	ML	13	no fil.	F22	400	60mm	60mm	(1/45s)
Infrared 1st Paint	ML	13	70	F22	400	60mm	60mm	(1/20s)
Infrared 1st Paint	ML	13	87	F22	400	60mm	60mm	(1/15s)
Infrared 1st Paint	ML	13	87A	F22	400	60mm	60mm	(1/6s)
Infrared 1st Paint	ML	13	87B	F11	400	60mm	60mm	(1/10s)
Infrared 1st Paint	ML	13	88A	F22	400	60mm	60mm	(1/20s)
Infrared 1st Paint	ML	13	89B	F22	400	60mm	60mm	(1/20s)
Infrared 1st Paint	ML	14	no fil.	F22	400	60mm	60mm	(1/45s)
Infrared 1st Paint	ML	14	70	F22	400	60mm	60mm	(1/20s)
Infrared 1st Paint	ML	14	87	F22	400	60mm	60mm	(1/15s)
Infrared 1st Paint	ML	14	87A	F22	400	60mm	60mm	(1/6s)
Infrared 1st Paint	ML	14	87B	F11	400	60mm	60mm	(1/10s)

Infrared 1st Paint	ML	14	88A	F22	400	60mm	60mm	(1/20s)
Infrared 1st Paint	ML	14	89B	F22	400	60mm	60mm	(1/20s)
Infrared 1st Paint	ML	15	no fil.	F22	400	60mm	60mm	(1/45s)
Infrared 1st Paint	ML	15	70	F22	400	60mm	60mm	(1/20s)
Infrared 1st Paint	ML	15	87	F22	400	60mm	60mm	(1/15s)
Infrared 1st Paint	ML	15	87A	F22	400	60mm	60mm	(1/6s)
Infrared 1st Paint	ML	15	87B	F11	400	60mm	60mm	(1/10s)
Infrared 1st Paint	ML	15	88A	F22	400	60mm	60mm	(1/20s)
Infrared 1st Paint	ML	15	89B	F22	400	60mm	60mm	(1/20s)
Infrared 1st Paint	ML	16	no fil.	F22	400	60mm	60mm	(1/45s)
Infrared 1st Paint	ML	16	70	F22	400	60mm	60mm	(1/20s)
Infrared 1st Paint Oblique	ML	13	no fil. L	F22	400	60mm	60mm	(1/30s)
Infrared 1st Paint Oblique	ML	13	no fil. R	F22	400	60mm	60mm	(1/45s)
Infrared 1st Paint Oblique	ML	13	87B L	F11	400	60mm	60mm	(1/15s)
Infrared 1st Paint Oblique	ML	13	87B R	F11	400	60mm	60mm	(1/20s)
Infrared 1st Paint Oblique	ML	13	89B L	F22	400	60mm	60mm	(1/20s)
Infrared 1st Paint Oblique	ML	13	89B R	F22	400	60mm	60mm	(1/30s)
Infrared 1st Paint Oblique	ML	14	no fil. L	F22	400	60mm	60mm	(1/30s)
Infrared 1st Paint Oblique	ML	14	no fil. R	F22	400	60mm	60mm	(1/45s)
Infrared 1st Paint Oblique	ML	14	87B L	F11	400	60mm	60mm	(1/15s)
Infrared 1st Paint Oblique	ML	14	87B R	F11	400	60mm	60mm	(1/20s)
Infrared 1st Paint Oblique	ML	14	89B L	F22	400	60mm	60mm	(1/20s)
Infrared 1st Paint Oblique	ML	14	89B R	F22	400	60mm	60mm	(1/30s)
Infrared 1st Paint Oblique	ML	15	no fil. L	F22	400	60mm	60mm	(1/30s)
Infrared 1st Paint Oblique	ML	15	no fil. R	F22	400	60mm	60mm	(1/45s)
Infrared 1st Paint Oblique	ML	15	87B L	F11	400	60mm	60mm	(1/15s)
Infrared 1st Paint Oblique	ML	15	87B R	F11	400	60mm	60mm	(1/20s)
Infrared 1st Paint Oblique	ML	15	89B L	F22	400	60mm	60mm	(1/20s)
Infrared 1st Paint	ML	15	89B R	F22	400	60mm	60mm	(1/30s)

Oblique								
Infrared 1st Paint Oblique	ML	16	87B L	F11	400	60mm	60mm	(1/15s)
Infrared 1st Paint Oblique	ML	16	87B R	F11	400	60mm	60mm	(1/20s)
IR 2nd Paint + Oblique	WA	1	no fil	F22	400	60mm	60mm	(1/180s)
IR 2nd Paint + Oblique	WA	1	no fil. L	F22	400	60mm	60mm	(1/90s)
IR 2nd Paint + Oblique	WA	1	no fil. R	F22	400	60mm	60mm	(1/125s)
IR 2nd Paint + Oblique	WA	1	87A	F22	400	60mm	60mm	(1/30s)
IR 2nd Paint + Oblique	WA	1	87A L	F22	400	60mm	60mm	(1/15s)
IR 2nd Paint + Oblique	WA	1	87A R	F22	400	60mm	60mm	(1/20s)
IR 2nd Paint + Oblique	WA	1	87B	F22	400	60mm	60mm	(1/15s)
IR 2nd Paint + Oblique	WA	1	87B L	F22	400	60mm	60mm	(1/8s)
IR 2nd Paint + Oblique	WA	1	87B R	F22	400	60mm	60mm	(1/10s)
IR 2nd Paint + Oblique	WA	1	88A	F22	400	60mm	60mm	(1/90s)
IR 2nd Paint + Oblique	WA	1	88A L	F22	400	60mm	60mm	(1/45s)
IR 2nd Paint + Oblique	WA	1	88A R	F22	400	60mm	60mm	(1/60s)
IR 2nd Paint + Oblique	WA	1	89B	F22	400	60mm	60mm	(1/90s)
IR 2nd Paint + Oblique	WA	1	89B L	F22	400	60mm	60mm	(1/45s)
IR 2nd Paint + Oblique	WA	1	89B R	F22	400	60mm	60mm	(1/60s)
IR 2nd Paint + Oblique	WA	2	no fil	F22	400	60mm	60mm	(1/180s)
IR 2nd Paint + Oblique	WA	2	no fil. L	F22	400	60mm	60mm	(1/90s)
IR 2nd Paint + Oblique	WA	2	no fil. R	F22	400	60mm	60mm	(1/125s)
IR 2nd Paint + Oblique	WA	2	87A	F22	400	60mm	60mm	(1/30s)
IR 2nd Paint + Oblique	WA	2	87A L	F22	400	60mm	60mm	(1/15s)
IR 2nd Paint + Oblique	WA	2	87A R	F22	400	60mm	60mm	(1/20s)
IR 2nd Paint + Oblique	WA	2	87B	F22	400	60mm	60mm	(1/15s)
IR 2nd Paint + Oblique	WA	2	87B L	F22	400	60mm	60mm	(1/8s)
IR 2nd Paint + Oblique	WA	2	87B R	F22	400	60mm	60mm	(1/10s)
IR 2nd Paint + Oblique	WA	2	88A	F22	400	60mm	60mm	(1/90s)
IR 2nd Paint + Oblique	WA	2	88A L	F22	400	60mm	60mm	(1/45s)
IR 2nd Paint + Oblique	WA	2	88A R	F22	400	60mm	60mm	(1/60s)
IR 2nd Paint + Oblique	WA	2	89B	F22	400	60mm	60mm	(1/90s)
IR 2nd Paint + Oblique	WA	2	89B L	F22	400	60mm	60mm	(1/45s)
IR 2nd Paint + Oblique	WA	2	89B R	F22	400	60mm	60mm	(1/60s)
IR 2nd Paint + Oblique	WA	3	no fil	F22	400	60mm	60mm	(1/180s)
IR 2nd Paint + Oblique	WA	3	no fil. L	F22	400	60mm	60mm	(1/90s)
IR 2nd Paint + Oblique	WA	3	no fil. R	F22	400	60mm	60mm	(1/125s)
IR 2nd Paint + Oblique	WA	3	87A	F22	400	60mm	60mm	(1/30s)
IR 2nd Paint + Oblique	WA	3	87A L	F22	400	60mm	60mm	(1/15s)

IR 2nd Paint + Oblique	WA	3	87A R	F22	400	60mm	60mm	(1/20s)
IR 2nd Paint + Oblique	WA	3	87B	F22	400	60mm	60mm	(1/15s)
IR 2nd Paint + Oblique	WA	3	87B L	F22	400	60mm	60mm	(1/8s)
IR 2nd Paint + Oblique	WA	3	87B R	F22	400	60mm	60mm	(1/10s)
IR 2nd Paint + Oblique	WA	3	88A	F22	400	60mm	60mm	(1/90s)
IR 2nd Paint + Oblique	WA	3	88A L	F22	400	60mm	60mm	(1/45s)
IR 2nd Paint + Oblique	WA	3	88A R	F22	400	60mm	60mm	(1/60s)
IR 2nd Paint + Oblique	WA	3	89B	F22	400	60mm	60mm	(1/90s)
IR 2nd Paint + Oblique	WA	3	89B L	F22	400	60mm	60mm	(1/45s)
IR 2nd Paint + Oblique	WA	3	89B R	F22	400	60mm	60mm	(1/60s)
IR 2nd Paint + Oblique	WL	5	no fil.	F22	400	60mm	60mm	(1/180s)
IR 2nd Paint + Oblique	WL	5	no fil. L	F22	400	60mm	60mm	(1/90s)
IR 2nd Paint + Oblique	WL	5	no fil. R	F22	400	60mm	60mm	(1/125s)
IR 2nd Paint + Oblique	WL	6	no fil.	F22	400	60mm	60mm	(1/180s)
IR 2nd Paint + Oblique	WL	6	no fil. L	F22	400	60mm	60mm	(1/90s)
IR 2nd Paint + Oblique	WL	6	no fil. R	F22	400	60mm	60mm	(1/125s)
IR 2nd Paint + Oblique	WL	7	no fil.	F22	400	60mm	60mm	(1/180s)
IR 2nd Paint + Oblique	WL	7	no fil. L	F22	400	60mm	60mm	(1/90s)
IR 2nd Paint + Oblique	WL	7	no fil. R	F22	400	60mm	60mm	(1/125s)
IR 2nd Paint + Oblique	BL	9	no fil.	F22	400	60mm	60mm	(1/30s)
IR 2nd Paint + Oblique	BL	9	no fil. L	F22	400	60mm	60mm	(1/15s)
IR 2nd Paint + Oblique	BL	9	no fil. R	F22	400	60mm	60mm	(1/20s)
IR 2nd Paint + Oblique	BL	10	no fil.	F22	400	60mm	60mm	(1/30s)
IR 2nd Paint + Oblique	BL	10	no fil. L	F22	400	60mm	60mm	(1/15s)
IR 2nd Paint + Oblique	BL	10	no fil. R	F22	400	60mm	60mm	(1/20s)
IR 2nd Paint + Oblique	BL	11	no fil.	F22	400	60mm	60mm	(1/30s)
IR 2nd Paint + Oblique	BL	11	no fil. L	F22	400	60mm	60mm	(1/15s)
IR 2nd Paint + Oblique	BL	11	no fil. R	F22	400	60mm	60mm	(1/20s)
IR 2nd Paint + Oblique	ML	13	no fil.	F22	400	60mm	60mm	(1/45s)
IR 2nd Paint + Oblique	ML	13	no fil. L	F22	400	60mm	60mm	(1/20s)
IR 2nd Paint + Oblique	ML	13	no fil. R	F22	400	60mm	60mm	(1/30s)
IR 2nd Paint + Oblique	ML	14	no fil.	F22	400	60mm	60mm	(1/45s)
IR 2nd Paint + Oblique	ML	14	no fil. L	F22	400	60mm	60mm	(1/20s)
IR 2nd Paint + Oblique	ML	14	no fil. R	F22	400	60mm	60mm	(1/30s)
IR 2nd Paint + Oblique	ML	15	no fil.	F22	400	60mm	60mm	(1/45s)
IR 2nd Paint + Oblique	ML	15	no fil. L	F22	400	60mm	60mm	(1/20s)
IR 2nd Paint + Oblique	ML	15	no fil. R	F22	400	60mm	60mm	(1/30s)

Exp. Layer	Paint Layer	Square #	F #	ISO	Lens	Focal Length	Shutter Speed
Ultraviolet Blood	WA	1	F4	400	60mm	60mm	(1/3s)
Ultraviolet Blood	WA	2	F4	400	60mm	60mm	(1/3s)
Ultraviolet Blood	WA	3	F4	400	60mm	60mm	(1/3s)
Ultraviolet Blood	WA	4	F4	400	60mm	60mm	(1/3s)
Ultraviolet Blood	WL	5	F4	400	60mm	60mm	(1/3s)
Ultraviolet Blood	WL	6	F4	400	60mm	60mm	(1/3s)
Ultraviolet Blood	WL	7	F4	400	60mm	60mm	(1/3s)
Ultraviolet Blood	WL	8	F4	400	60mm	60mm	(1/3s)
Ultraviolet Blood	BL	9	F4	400	60mm	60mm	(1/3s)
Ultraviolet Blood	BL	10	F4	400	60mm	60mm	(1/3s)
Ultraviolet Blood	BL	11	F4	400	60mm	60mm	(1/3s)
Ultraviolet Blood	BL	12	F4	400	60mm	60mm	(1/3s)
Ultraviolet Blood	ML	13	F4	400	60mm	60mm	(1/3s)
Ultraviolet Blood	ML	14	F4	400	60mm	60mm	(1/3s)
Ultraviolet Blood	ML	15	F4	400	60mm	60mm	(1/3s)
Ultraviolet Blood	ML	16	F4	400	60mm	60mm	(1/3s)
Ultraviolet 1st Paint	WA	1	F4	400	60mm	60mm	(1/3s)
Ultraviolet 1st Paint	WA	2	F4	400	60mm	60mm	(1/3s)
Ultraviolet 1st Paint	WA	3	F4	400	60mm	60mm	(1/3s)
Ultraviolet 1st Paint	WA	4	F4	400	60mm	60mm	(1/3s)
Ultraviolet 1st Paint	WL	5	F4	400	60mm	60mm	(1/3s)
Ultraviolet 1st Paint	WL	6	F4	400	60mm	60mm	(1/3s)
Ultraviolet 1st Paint	WL	7	F4	400	60mm	60mm	(1/3s)
Ultraviolet 1st Paint	WL	8	F4	400	60mm	60mm	(1/3s)
Ultraviolet 1st Paint	BL	9	F4	400	60mm	60mm	(1/3s)
Ultraviolet 1st Paint	BL	10	F4	400	60mm	60mm	(1/3s)
Ultraviolet 1st Paint	BL	11	F4	400	60mm	60mm	(1/3s)
Ultraviolet 1st Paint	BL	12	F4	400	60mm	60mm	(1/3s)
Ultraviolet 1st Paint	ML	13	F4	400	60mm	60mm	(1/3s)
Ultraviolet 1st Paint	ML	14	F4	400	60mm	60mm	(1/3s)
Ultraviolet 1st Paint	ML	15	F4	400	60mm	60mm	(1/3s)
Ultraviolet 1st Paint	ML	16	F4	400	60mm	60mm	(1/3s)
Ultraviolet 2nd Paint	WA	1	F4	400	60mm	60mm	(1/3s)
Ultraviolet 2nd Paint	WA	2	F4	400	60mm	60mm	(1/3s)
Ultraviolet 2nd Paint	WA	3	F4	400	60mm	60mm	(1/3s)
Ultraviolet 2nd Paint	WL	5	F4	400	60mm	60mm	(1/3s)
Ultraviolet 2nd Paint	WL	6	F4	400	60mm	60mm	(1/3s)
Ultraviolet 2nd Paint	WL	7	F4	400	60mm	60mm	(1/3s)

Ultraviolet 2nd Paint Oblique	BL	9	F4	400	60mm	60mm	(0.50s)
Ultraviolet 2nd Paint Oblique	BL	10	F4	400	60mm	60mm	(0.50s)
Ultraviolet 2nd Paint Oblique	BL	11	F4	400	60mm	60mm	(0.50s)
Ultraviolet 2nd Paint Oblique	ML	13	F4	400	60mm	60mm	(0.70s)
Ultraviolet 2nd Paint Oblique	ML	14	F4	400	60mm	60mm	(0.70s)
Ultraviolet 2nd Paint Oblique	ML	15	F4	400	60mm	60mm	(0.70s)
Ultraviolet 2nd Paint Oblique	WA	1	F4	400	60mm	60mm	(0.50s)
Ultraviolet 2nd Paint Oblique	WA	2	F4	400	60mm	60mm	(0.50s)
Ultraviolet 2nd Paint Oblique	WA	3	F4	400	60mm	60mm	(0.50s)
Ultraviolet 2nd Paint Oblique	WL	5	F4	400	60mm	60mm	(0.50s)
Ultraviolet 2nd Paint Oblique	WL	6	F4	400	60mm	60mm	(0.50s)
Ultraviolet 2nd Paint Oblique	WL	7	F4	400	60mm	60mm	(0.50s)

Exp. Layer	Paint Layer	Sq. #	Colour	Filter	F #	ISO	Lens	Focal Length	Shutter Speed
Fluorescence Blood	WA	1	Yellow	445	F8	400	28-105	50mm	(3.00s)
Fluorescence Blood	WL	5	Yellow	445	F8	400	28-105	50mm	(4.00s)
Fluorescence Blood	BL	9	Yellow	445	F8	400	28-105	50mm	(15.00s)
Fluorescence Blood	ML	13	Yellow	445	F8	400	28-105	50mm	(15.00s)
Fluorescence 1st Paint	WA	1	Yellow	415	F8	400	28-105	50mm	(4.00s)
Fluorescence 1st Paint	WA	1	Yellow	445	F8	400	28-105	50mm	(4.00s)
Fluorescence 1st Paint	WA	1	Yellow	455	F8	400	28-105	50mm	(4.00s)
Fluorescence 1st Paint	WA	1	Orange	445	F8	400	28-105	50mm	(6.00s)
Fluorescence 1st Paint	WA	1	Orange	455	F8	400	28-105	50mm	(6.00s)
Fluorescence 1st Paint	WA	1	Orange	475	F8	400	28-105	50mm	(5.00s)
Fluorescence 1st Paint	WA	1	Orange	495	F8	400	28-105	50mm	(4.00s)
Fluorescence 1st Paint	WA	1	Orange	515	F8	400	28-105	50mm	(1.00s)
Fluorescence 1st Paint	WA	1	Red	575	F8	400	28-105	50mm	(8.00s)
Fluorescence 1st Paint	WA	2	Yellow	415	F8	400	28-105	50mm	(4.00s)
Fluorescence 1st Paint	WA	2	Yellow	445	F8	400	28-105	50mm	(4.00s)

Fluorescence 1st Paint	WA	2	Yellow	455	F8	400	28-105	50mm	(4.00s)
Fluorescence 1st Paint	WA	2	Orange	445	F8	400	28-105	50mm	(6.00s)
Fluorescence 1st Paint	WA	2	Orange	455	F8	400	28-105	50mm	(6.00s)
Fluorescence 1st Paint	WA	2	Orange	475	F8	400	28-105	50mm	(5.00s)
Fluorescence 1st Paint	WA	2	Orange	495	F8	400	28-105	50mm	(4.00s)
Fluorescence 1st Paint	WA	2	Orange	515	F8	400	28-105	50mm	(1.00s)
Fluorescence 1st Paint	WA	2	Red	575	F8	400	28-105	50mm	(8.00s)
Fluorescence 1st Paint	WA	3	Yellow	415	F8	400	28-105	50mm	(4.00s)
Fluorescence 1st Paint	WA	3	Yellow	445	F8	400	28-105	50mm	(4.00s)
Fluorescence 1st Paint	WA	3	Yellow	455	F8	400	28-105	50mm	(4.00s)
Fluorescence 1st Paint	WA	3	Orange	445	F8	400	28-105	50mm	(6.00s)
Fluorescence 1st Paint	WA	3	Orange	455	F8	400	28-105	50mm	(6.00s)
Fluorescence 1st Paint	WA	3	Orange	475	F8	400	28-105	50mm	(5.00s)
Fluorescence 1st Paint	WA	3	Orange	495	F8	400	28-105	50mm	(4.00s)
Fluorescence 1st Paint	WA	3	Orange	515	F8	400	28-105	50mm	(1.00s)
Fluorescence 1st Paint	WA	3	Red	575	F8	400	28-105	50mm	(8.00s)
Fluorescence 1st Paint	WA	4	Yellow	415					
Fluorescence 1st Paint	WA	4	Yellow	445					
Fluorescence 1st Paint	WA	4	Yellow	455					
Fluorescence 1st Paint	WA	4	Orange	445					
Fluorescence 1st Paint	WA	4	Orange	455					
Fluorescence 1st Paint	WA	4	Orange	475					
Fluorescence 1st Paint	WA	4	Orange	495					
Fluorescence 1st Paint	WA	4	Orange	515					
Fluorescence 1st Paint	WA	4	Red	575					

Paint									
Fluorescence 1st Paint	WL	5	Yellow	415	F8	400	28-105	50mm	(4.00s)
Fluorescence 1st Paint	WL	5	Yellow	445	F8	400	28-105	50mm	(4.00s)
Fluorescence 1st Paint	WL	5	Yellow	455	F8	400	28-105	50mm	(4.00s)
Fluorescence 1st Paint	WL	5	Orange	445	F8	400	28-105	50mm	(6.00s)
Fluorescence 1st Paint	WL	5	Orange	455	F8	400	28-105	50mm	(6.00s)
Fluorescence 1st Paint	WL	5	Orange	475	F8	400	28-105	50mm	(5.00s)
Fluorescence 1st Paint	WL	5	Orange	495	F8	400	28-105	50mm	(4.00s)
Fluorescence 1st Paint	WL	5	Orange	515	F8	400	28-105	50mm	(1.00s)
Fluorescence 1st Paint	WL	5	Red	575	F8	400	28-105	50mm	(8.00s)
Fluorescence 1st Paint	WL	6	Yellow	415	F8	400	28-105	50mm	(4.00s)
Fluorescence 1st Paint	WL	6	Yellow	445	F8	400	28-105	50mm	(4.00s)
Fluorescence 1st Paint	WL	6	Yellow	455	F8	400	28-105	50mm	(4.00s)
Fluorescence 1st Paint	WL	6	Orange	445	F8	400	28-105	50mm	(6.00s)
Fluorescence 1st Paint	WL	6	Orange	455	F8	400	28-105	50mm	(6.00s)
Fluorescence 1st Paint	WL	6	Orange	475	F8	400	28-105	50mm	(5.00s)
Fluorescence 1st Paint	WL	6	Orange	495	F8	400	28-105	50mm	(4.00s)
Fluorescence 1st Paint	WL	6	Orange	515	F8	400	28-105	50mm	(1.00s)
Fluorescence 1st Paint	WL	6	Red	575	F8	400	28-105	50mm	(8.00s)
Fluorescence 1st Paint	WL	7	Yellow	415	F8	400	28-105	50mm	(4.00s)
Fluorescence 1st Paint	WL	7	Yellow	445	F8	400	28-105	50mm	(4.00s)
Fluorescence 1st Paint	WL	7	Yellow	455	F8	400	28-105	50mm	(4.00s)
Fluorescence 1st Paint	WL	7	Orange	445	F8	400	28-105	50mm	(6.00s)
Fluorescence 1st Paint	WL	7	Orange	455	F8	400	28-105	50mm	(6.00s)
Fluorescence 1st Paint	WL	7	Orange	475	F8	400	28-105	50mm	(5.00s)

Fluorescence 1st Paint	WL	7	Orange	495	F8	400	28-105	50mm	(4.00s)
Fluorescence 1st Paint	WL	7	Orange	515	F8	400	28-105	50mm	(1.00s)
Fluorescence 1st Paint	WL	7	Red	575	F8	400	28-105	50mm	(8.00s)
Fluorescence 1st Paint	WL	8	Yellow	415					
Fluorescence 1st Paint	WL	8	Yellow	445					
Fluorescence 1st Paint	WL	8	Yellow	455					
Fluorescence 1st Paint	WL	8	Orange	445					
Fluorescence 1st Paint	WL	8	Orange	455					
Fluorescence 1st Paint	WL	8	Orange	475					
Fluorescence 1st Paint	WL	8	Orange	495					
Fluorescence 1st Paint	WL	8	Orange	515					
Fluorescence 1st Paint	WL	8	Red	575					
Fluorescence 1st Paint	BL	9	Yellow	475	F8	400	28-105	50mm	(5.00s)
Fluorescence 1st Paint	BL	9	Yellow	495	F8	400	28-105	50mm	(1/6s)
Fluorescence 1st Paint	BL	9	Yellow	670	F8	400	28-105	50mm	(1/10s)
Fluorescence 1st Paint	BL	9	Orange	555	F8	400	28-105	50mm	(1/40s)
Fluorescence 1st Paint	BL	9	Orange	670	F8	400	28-105	50mm	(1/20s)
Fluorescence 1st Paint	BL	9	Red	600	F8	400	28-105	50mm	(1/25s)
Fluorescence 1st Paint	BL	10	Yellow	475	F8	400	28-105	50mm	(5.00s)
Fluorescence 1st Paint	BL	10	Yellow	495	F8	400	28-105	50mm	(1/6s)
Fluorescence 1st Paint	BL	10	Yellow	670	F8	400	28-105	50mm	(1/10s)
Fluorescence 1st Paint	BL	10	Orange	555	F8	400	28-105	50mm	(1/40s)
Fluorescence 1st Paint	BL	10	Orange	670	F8	400	28-105	50mm	(1/20s)
Fluorescence 1st Paint	BL	10	Red	600	F8	400	28-105	50mm	(1/25s)
Fluorescence 1st Paint	BL	11	Yellow	475	F8	400	28-105	50mm	(5.00s)

Paint									
Fluorescence 1st Paint	BL	11	Yellow	495	F8	400	28-105	50mm	(1/6s)
Fluorescence 1st Paint	BL	11	Yellow	670	F8	400	28-105	50mm	(1/10s)
Fluorescence 1st Paint	BL	11	Orange	555	F8	400	28-105	50mm	(1/40s)
Fluorescence 1st Paint	BL	11	Orange	670	F8	400	28-105	50mm	(1/20s)
Fluorescence 1st Paint	BL	11	Red	600	F8	400	28-105	50mm	(1/25s)
Fluorescence 1st Paint	BL	12	Yellow	475					
Fluorescence 1st Paint	BL	12	Yellow	495					
Fluorescence 1st Paint	BL	12	Yellow	670					
Fluorescence 1st Paint	BL	12	Orange	555					
Fluorescence 1st Paint	BL	12	Orange	670					
Fluorescence 1st Paint	BL	12	Red	600					
Fluorescence 1st Paint	ML	13	Yellow	415	F8	400	28-105	50mm	(30.00s)
Fluorescence 1st Paint	ML	13	Yellow	445	F8	400	28-105	50mm	(30.00s)
Fluorescence 1st Paint	ML	13	Yellow	455	F8	400	28-105	50mm	(30.00s)
Fluorescence 1st Paint	ML	13	Orange	415	F8	400	28-105	50mm	(25.00s)
Fluorescence 1st Paint	ML	13	Orange	445	F8	400	28-105	50mm	(25.00s)
Fluorescence 1st Paint	ML	13	Red	415	F8	400	28-105	50mm	(30.00s)
Fluorescence 1st Paint	ML	13	Red	445	F8	400	28-105	50mm	(30.00s)
Fluorescence 1st Paint	ML	13	Red	455	F8	400	28-105	50mm	(30.00s)
Fluorescence 1st Paint	ML	13	Red	575	F8	400	28-105	50mm	(4.00s)
Fluorescence 1st Paint	ML	14	Yellow	415	F8	400	28-105	50mm	(30.00s)
Fluorescence 1st Paint	ML	14	Yellow	445	F8	400	28-105	50mm	(30.00s)
Fluorescence 1st Paint	ML	14	Yellow	455	F8	400	28-105	50mm	(30.00s)
Fluorescence 1st Paint	ML	14	Orange	415	F8	400	28-105	50mm	(25.00s)

Fluorescence 1st Paint	ML	14	Orange	445	F8	400	28-105	50mm	(25.00s)
Fluorescence 1st Paint	ML	14	Red	415	F8	400	28-105	50mm	(30.00s)
Fluorescence 1st Paint	ML	14	Red	445	F8	400	28-105	50mm	(30.00s)
Fluorescence 1st Paint	ML	14	Red	455	F8	400	28-105	50mm	(30.00s)
Fluorescence 1st Paint	ML	14	Red	575	F8	400	28-105	50mm	(4.00s)
Fluorescence 1st Paint	ML	15	Yellow	415	F8	400	28-105	50mm	(30.00s)
Fluorescence 1st Paint	ML	15	Yellow	445	F8	400	28-105	50mm	(30.00s)
Fluorescence 1st Paint	ML	15	Yellow	455	F8	400	28-105	50mm	(30.00s)
Fluorescence 1st Paint	ML	15	Orange	415	F8	400	28-105	50mm	(25.00s)
Fluorescence 1st Paint	ML	15	Orange	445	F8	400	28-105	50mm	(25.00s)
Fluorescence 1st Paint	ML	15	Red	415	F8	400	28-105	50mm	(30.00s)
Fluorescence 1st Paint	ML	15	Red	445	F8	400	28-105	50mm	(30.00s)
Fluorescence 1st Paint	ML	15	Red	455	F8	400	28-105	50mm	(30.00s)
Fluorescence 1st Paint	ML	15	Red	575	F8	400	28-105	50mm	(4.00s)
Fluorescence 1st Paint	ML	16	Yellow	415					
Fluorescence 1st Paint	ML	16	Yellow	445					
Fluorescence 1st Paint	ML	16	Yellow	455					
Fluorescence 1st Paint	ML	16	Orange	415					
Fluorescence 1st Paint	ML	16	Orange	445					
Fluorescence 1st Paint	ML	16	Red	415					
Fluorescence 1st Paint	ML	16	Red	445					
Fluorescence 1st Paint	ML	16	Red	455					
Fluorescence 1st Paint	ML	16	Red	575					
Fluorescence 2nd Paint	WA	1	Yellow	415	F8	400	28-105	50mm	(13.00s)
Fluorescence 2nd	WA	1	Yellow	445	F8	400	28-105	50mm	(13.00s)

Paint									
Fluorescence 2nd Paint	WA	1	Yellow	455	F8	400	28-105	50mm	(8.00s)
Fluorescence 2nd Paint	WA	1	Orange	415	F8	400	28-105	50mm	(15.00s)
Fluorescence 2nd Paint	WA	1	Orange	445	F8	400	28-105	50mm	(15.00s)
Fluorescence 2nd Paint	WA	1	Orange	455	F8	400	28-105	50mm	(13.00s)
Fluorescence 2nd Paint	WA	1	Orange	475	F8	400	28-105	50mm	(13.00s)
Fluorescence 2nd Paint	WA	1	Orange	495	F8	400	28-105	50mm	(8.00s)
Fluorescence 2nd Paint	WA	1	Red	415	F8	400	28-105	50mm	(30.00s)
Fluorescence 2nd Paint	WA	1	Red	445	F8	400	28-105	50mm	(30.00s)
Fluorescence 2nd Paint	WA	1	Red	455	F8	400	28-105	50mm	(25.00s)
Fluorescence 2nd Paint	WA	1	Red	475	F8	400	28-105	50mm	(20.00s)
Fluorescence 2nd Paint	WA	1	Red	575	F8	400	28-105	50mm	(6.00s)
Fluorescence 2nd Paint	WA	2	Yellow	415	F8	400	28-105	50mm	(13.00s)
Fluorescence 2nd Paint	WA	2	Yellow	445	F8	400	28-105	50mm	(13.00s)
Fluorescence 2nd Paint	WA	2	Yellow	455	F8	400	28-105	50mm	(8.00s)
Fluorescence 2nd Paint	WA	2	Orange	415	F8	400	28-105	50mm	(15.00s)
Fluorescence 2nd Paint	WA	2	Orange	445	F8	400	28-105	50mm	(15.00s)
Fluorescence 2nd Paint	WA	2	Orange	455	F8	400	28-105	50mm	(13.00s)
Fluorescence 2nd Paint	WA	2	Orange	475	F8	400	28-105	50mm	(13.00s)
Fluorescence 2nd Paint	WA	2	Orange	495	F8	400	28-105	50mm	(8.00s)
Fluorescence 2nd Paint	WA	2	Red	415	F8	400	28-105	50mm	(30.00s)
Fluorescence 2nd Paint	WA	2	Red	445	F8	400	28-105	50mm	(30.00s)
Fluorescence 2nd Paint	WA	2	Red	455	F8	400	28-105	50mm	(25.00s)
Fluorescence 2nd Paint	WA	2	Red	475	F8	400	28-105	50mm	(20.00s)
Fluorescence 2nd Paint	WA	2	Red	575	F8	400	28-105	50mm	(6.00s)

Fluorescence 2nd Paint	WA	3	Yellow	415	F8	400	28-105	50mm	(13.00s)
Fluorescence 2nd Paint	WA	3	Yellow	445	F8	400	28-105	50mm	(13.00s)
Fluorescence 2nd Paint	WA	3	Yellow	455	F8	400	28-105	50mm	(8.00s)
Fluorescence 2nd Paint	WA	3	Orange	415	F8	400	28-105	50mm	(15.00s)
Fluorescence 2nd Paint	WA	3	Orange	445	F8	400	28-105	50mm	(15.00s)
Fluorescence 2nd Paint	WA	3	Orange	455	F8	400	28-105	50mm	(13.00s)
Fluorescence 2nd Paint	WA	3	Orange	475	F8	400	28-105	50mm	(13.00s)
Fluorescence 2nd Paint	WA	3	Orange	495	F8	400	28-105	50mm	(8.00s)
Fluorescence 2nd Paint	WA	3	Red	415	F8	400	28-105	50mm	(30.00s)
Fluorescence 2nd Paint	WA	3	Red	445	F8	400	28-105	50mm	(30.00s)
Fluorescence 2nd Paint	WA	3	Red	455	F8	400	28-105	50mm	(25.00s)
Fluorescence 2nd Paint	WA	3	Red	475	F8	400	28-105	50mm	(20.00s)
Fluorescence 2nd Paint	WA	3	Red	575	F8	400	28-105	50mm	(6.00s)
Fluorescence 2nd Paint	WL	5	Yellow	415	F8	400	28-105	50mm	(13.00s)
Fluorescence 2nd Paint	WL	5	Yellow	445	F8	400	28-105	50mm	(13.00s)
Fluorescence 2nd Paint	WL	5	Yellow	455	F8	400	28-105	50mm	(8.00s)
Fluorescence 2nd Paint	WL	5	Orange	415	F8	400	28-105	50mm	(15.00s)
Fluorescence 2nd Paint	WL	5	Orange	445	F8	400	28-105	50mm	(15.00s)
Fluorescence 2nd Paint	WL	5	Orange	455	F8	400	28-105	50mm	(13.00s)
Fluorescence 2nd Paint	WL	5	Orange	475	F8	400	28-105	50mm	(13.00s)
Fluorescence 2nd Paint	WL	5	Orange	495	F8	400	28-105	50mm	(8.00s)
Fluorescence 2nd Paint	WL	5	Red	415	F8	400	28-105	50mm	(30.00s)
Fluorescence 2nd Paint	WL	5	Red	445	F8	400	28-105	50mm	(30.00s)
Fluorescence 2nd Paint	WL	5	Red	455	F8	400	28-105	50mm	(25.00s)
Fluorescence 2nd Paint	WL	5	Red	475	F8	400	28-105	50mm	(20.00s)

Paint									
Fluorescence 2nd Paint	WL	5	Red	575	F8	400	28-105	50mm	(6.00s)
Fluorescence 2nd Paint	WL	6	Yellow	415	F8	400	28-105	50mm	(13.00s)
Fluorescence 2nd Paint	WL	6	Yellow	445	F8	400	28-105	50mm	(13.00s)
Fluorescence 2nd Paint	WL	6	Yellow	455	F8	400	28-105	50mm	(8.00s)
Fluorescence 2nd Paint	WL	6	Orange	415	F8	400	28-105	50mm	(15.00s)
Fluorescence 2nd Paint	WL	6	Orange	445	F8	400	28-105	50mm	(15.00s)
Fluorescence 2nd Paint	WL	6	Orange	455	F8	400	28-105	50mm	(13.00s)
Fluorescence 2nd Paint	WL	6	Orange	475	F8	400	28-105	50mm	(13.00s)
Fluorescence 2nd Paint	WL	6	Orange	495	F8	400	28-105	50mm	(8.00s)
Fluorescence 2nd Paint	WL	6	Red	415	F8	400	28-105	50mm	(30.00s)
Fluorescence 2nd Paint	WL	6	Red	445	F8	400	28-105	50mm	(30.00s)
Fluorescence 2nd Paint	WL	6	Red	455	F8	400	28-105	50mm	(25.00s)
Fluorescence 2nd Paint	WL	6	Red	475	F8	400	28-105	50mm	(20.00s)
Fluorescence 2nd Paint	WL	6	Red	575	F8	400	28-105	50mm	(6.00s)
Fluorescence 2nd Paint	WL	7	Yellow	415	F8	400	28-105	50mm	(13.00s)
Fluorescence 2nd Paint	WL	7	Yellow	445	F8	400	28-105	50mm	(13.00s)
Fluorescence 2nd Paint	WL	7	Yellow	455	F8	400	28-105	50mm	(8.00s)
Fluorescence 2nd Paint	WL	7	Orange	415	F8	400	28-105	50mm	(15.00s)
Fluorescence 2nd Paint	WL	7	Orange	445	F8	400	28-105	50mm	(15.00s)
Fluorescence 2nd Paint	WL	7	Orange	455	F8	400	28-105	50mm	(13.00s)
Fluorescence 2nd Paint	WL	7	Orange	475	F8	400	28-105	50mm	(13.00s)
Fluorescence 2nd Paint	WL	7	Orange	495	F8	400	28-105	50mm	(8.00s)
Fluorescence 2nd Paint	WL	7	Red	415	F8	400	28-105	50mm	(30.00s)
Fluorescence 2nd Paint	WL	7	Red	445	F8	400	28-105	50mm	(30.00s)

Fluorescence 2nd Paint	WL	7	Red	455	F8	400	28-105	50mm	(25.00s)
Fluorescence 2nd Paint	WL	7	Red	475	F8	400	28-105	50mm	(20.00s)
Fluorescence 2nd Paint	WL	7	Red	575	F8	400	28-105	50mm	(6.00s)
Fluorescence 2nd Paint	BL	9	Yellow	475	F8	400	28-105	50mm	(8.00s)
Fluorescence 2nd Paint	BL	10	Yellow	475	F8	400	28-105	50mm	(8.00s)
Fluorescence 2nd Paint	BL	11	Yellow	475	F8	400	28-105	50mm	(8.00s)
Fluorescence 2nd Paint	ML	13	Yellow	455	F8	400	28-105	50mm	(30.00s)
Fluorescence 2nd Paint	ML	14	Yellow	455	F8	400	28-105	50mm	(30.00s)
Fluorescence 2nd Paint	ML	15	Yellow	455	F8	400	28-105	50mm	(30.00s)

Exp. Layer	Paint Layer	Square #	F #	ISO	Lens	Focal Length	Shutter Speed
Luminol 2nd Paint	WA	1	5.6	1600	16-85	50mm	157.6s
Luminol 2nd Paint	WA	2	5.6	1600	16-85	50mm	148.7s
Luminol 2nd Paint	WA	3	5.6	1600	16-85	50mm	141.7s
Luminol 2nd Paint	WA	4	5.6	1600	16-85	50mm	261.9s
Luminol 2nd Paint	WL	5	5.6	1600	16-85	50mm	189.5s
Luminol 2nd Paint	WL	6	5.6	1600	16-85	50mm	146.4s
Luminol 2nd Paint	WL	7	5.6	1600	16-85	50mm	170.9s
Luminol 2nd Paint	WL	8	5.6	1600	16-85	50mm	358s
Luminol 2nd Paint	BL	9	5.6	1600	16-85	50mm	223s
Luminol 2nd Paint	BL	10	5.6	1600	16-85	50mm	318.8s
Luminol 2nd Paint	BL	11	5.6	1600	16-85	50mm	172.9s
Luminol 2nd Paint	BL	12	5.6	1600	16-85	50mm	267.1s
Luminol 2nd Paint	ML	13	5.6	1600	16-85	50mm	348.3s
Luminol 2nd Paint	ML	14	5.6	1600	16-85	50mm	278.5s
Luminol 2nd Paint	ML	15	5.6	1600	16-85	50mm	141.8s
Luminol 2nd Paint	ML	16	5.6	1600	16-85	50mm	285.7s

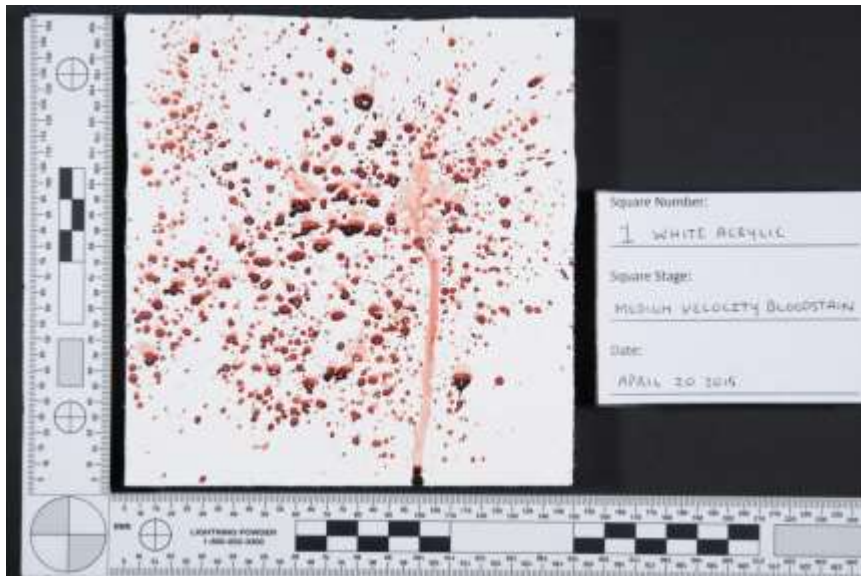
Appendix: Photographs

Bloodstain Pattern Stage

Appendix 4.1.1. Standard Photography

Appendix 4.1.1.1. White Acrylic Bloodstain Pattern Stage

White Acrylic 1 – Medium Velocity



White Acrylic 2 – Swipe



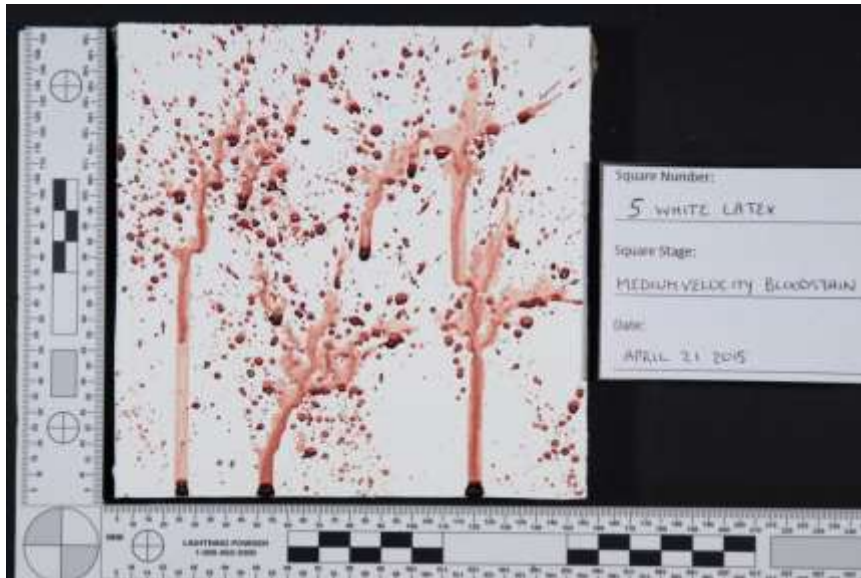
White Acrylic 3 – Saturated



White Acrylic 4 – Control No Bloodstain



Appendix 4.1.1.2. White Latex Bloodstain Pattern Stage
White Latex 5 – Medium Velocity



White Latex 6 - Swipe



White Latex 7 – Saturated



White Latex 8 – Control No Bloodstain



Appendix 4.1.1.3. Black Latex Bloodstain Pattern Stage
Black Latex 9 – Medium Velocity



Black Latex 10 - Swipe



Black Latex 11 – Saturated



Black Latex 12 – Control No Bloodstain



Appendix 4.1.1.4. Maroon Latex Bloodstain Pattern Stage
Maroon Latex 13 – Medium Velocity



Maroon Latex 14 – Swipe



Maroon Latex 15 – Saturated

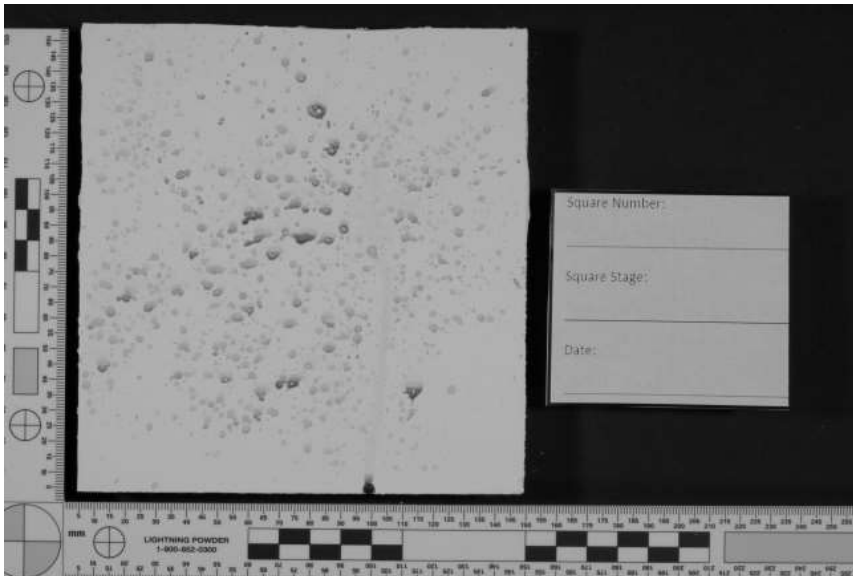


Maroon Latex 16 – Control No Bloodstain



Appendix 4.1.2. Reflective Infrared Photography

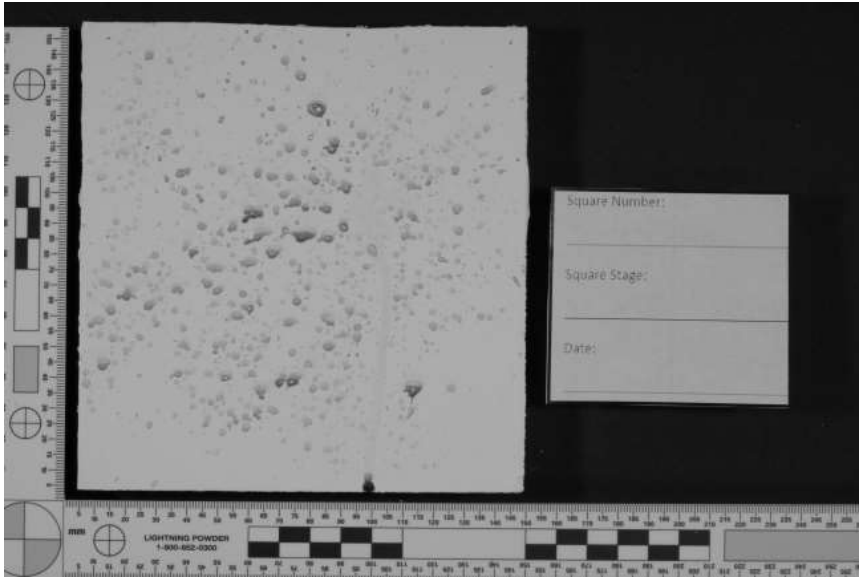
Appendix 4.1.2.1. White Acrylic Bloodstain Pattern Stage – 70, 87, 87A, 87B, 88A, 89B White Acrylic 1 – Medium Velocity



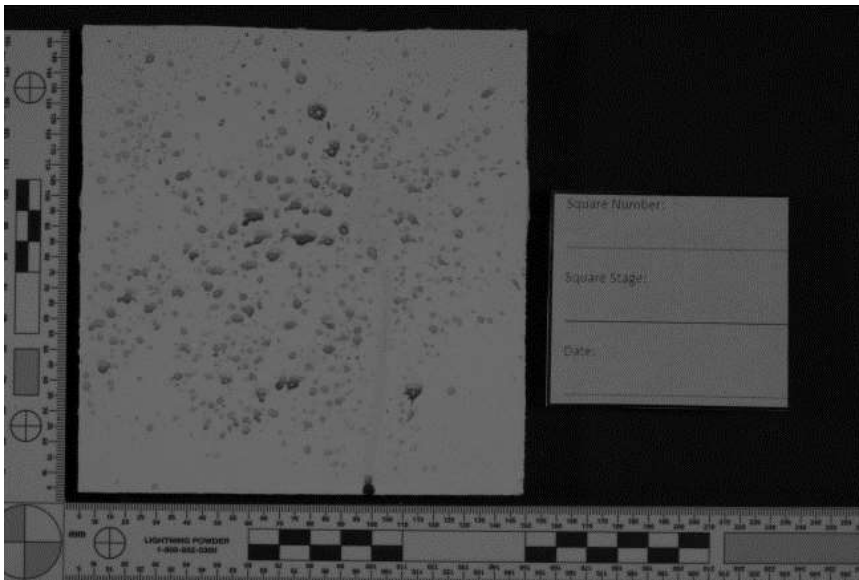
Longpass #70 HDR



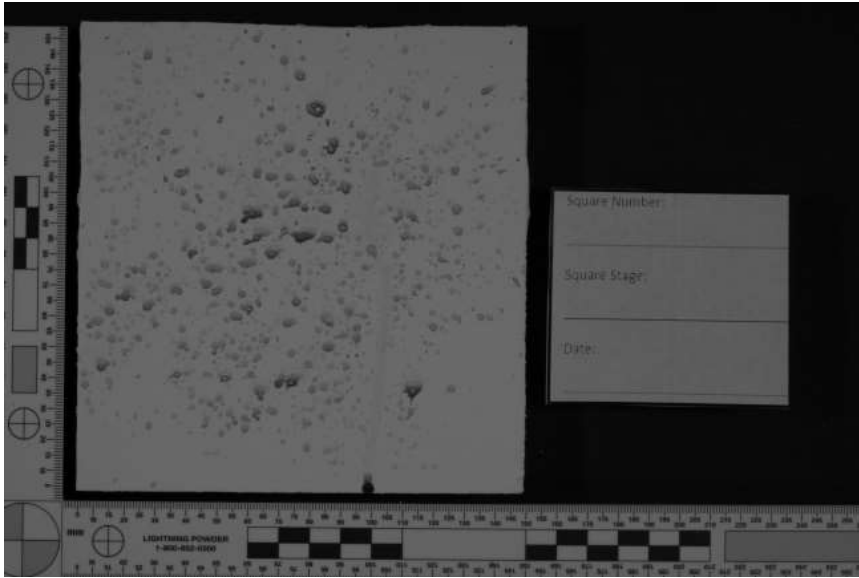
Longpass #70 Single



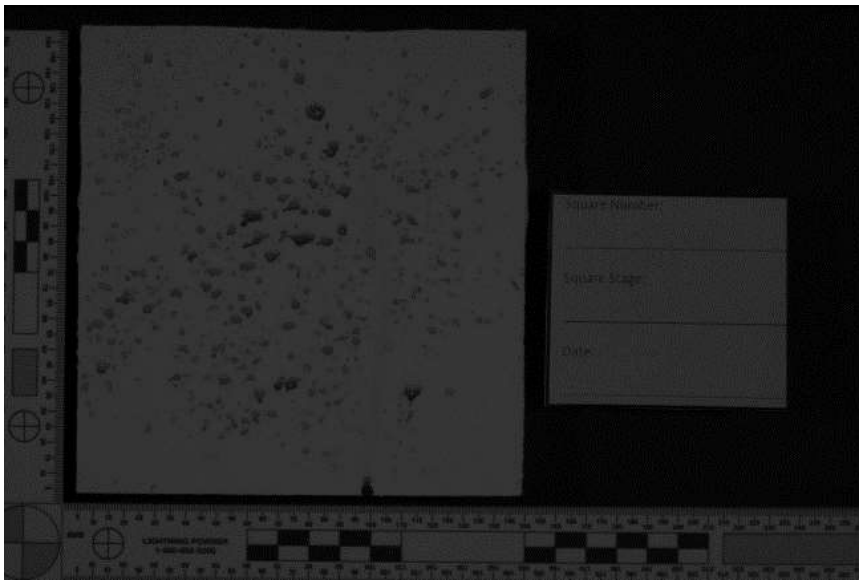
Longpass #87 HDR



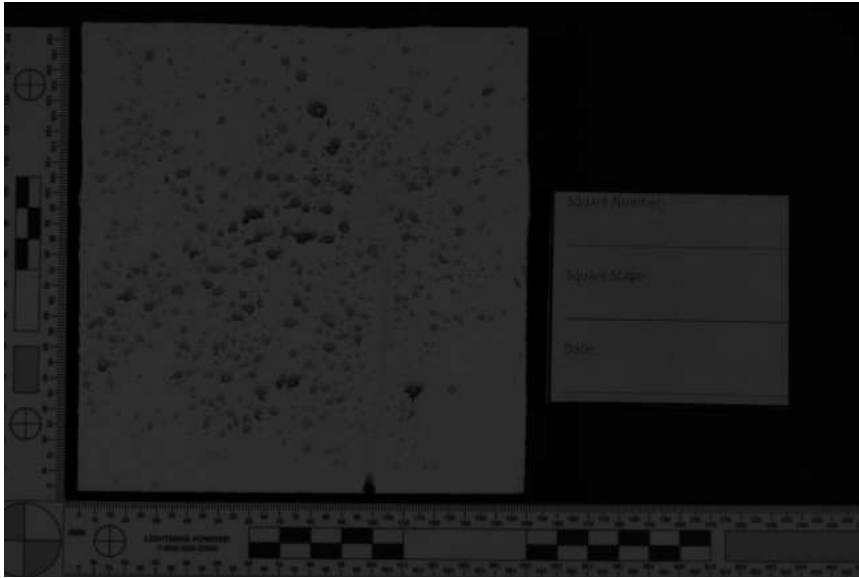
Longpass #87 Single



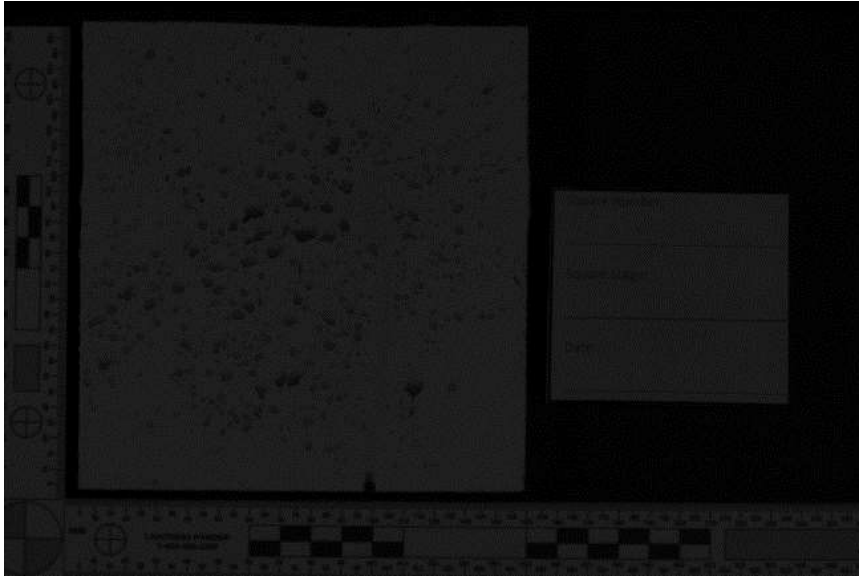
Longpass #87A HDR



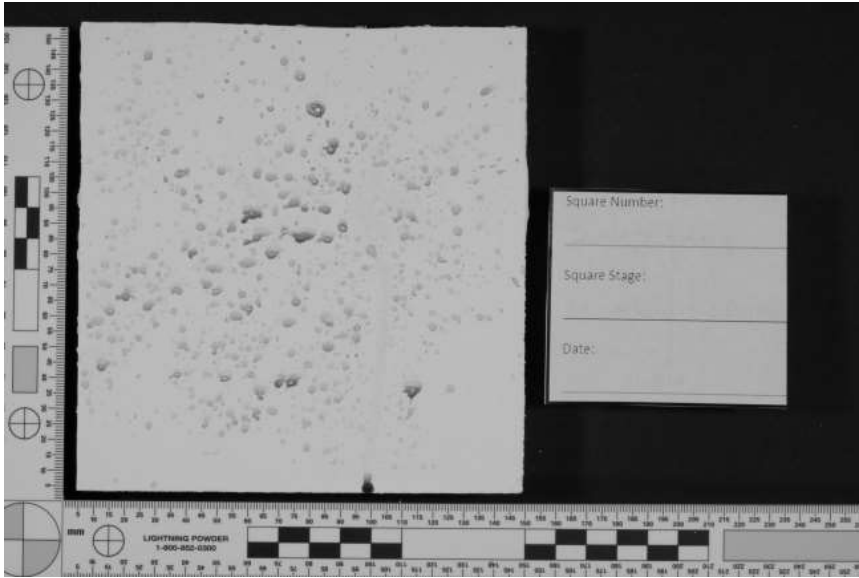
Longpass #87A Single



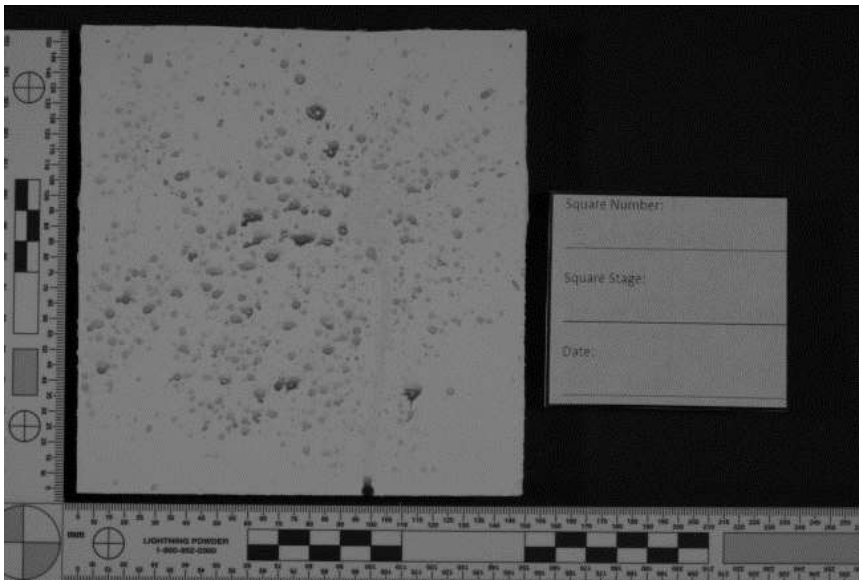
Longpass #87B HDR



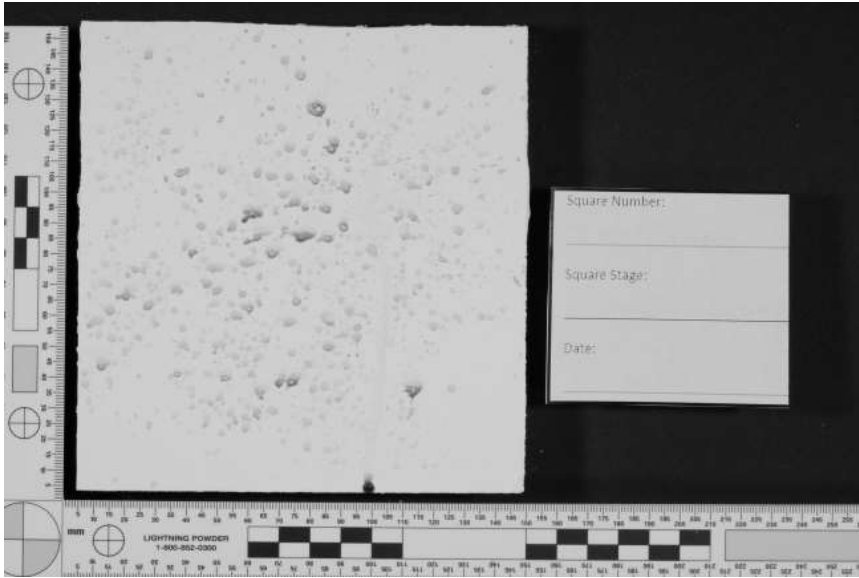
Longpass #87B Single



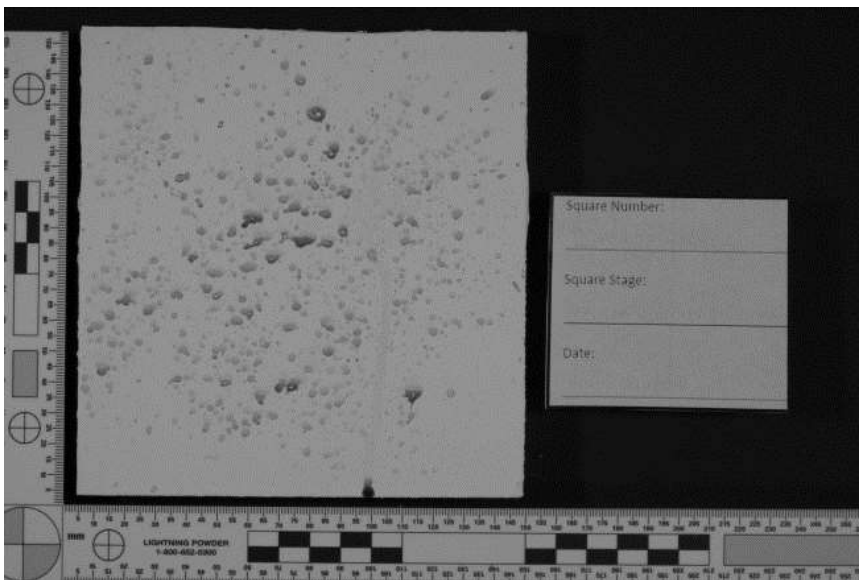
Longpass #88A HDR



Longpass #88A Single

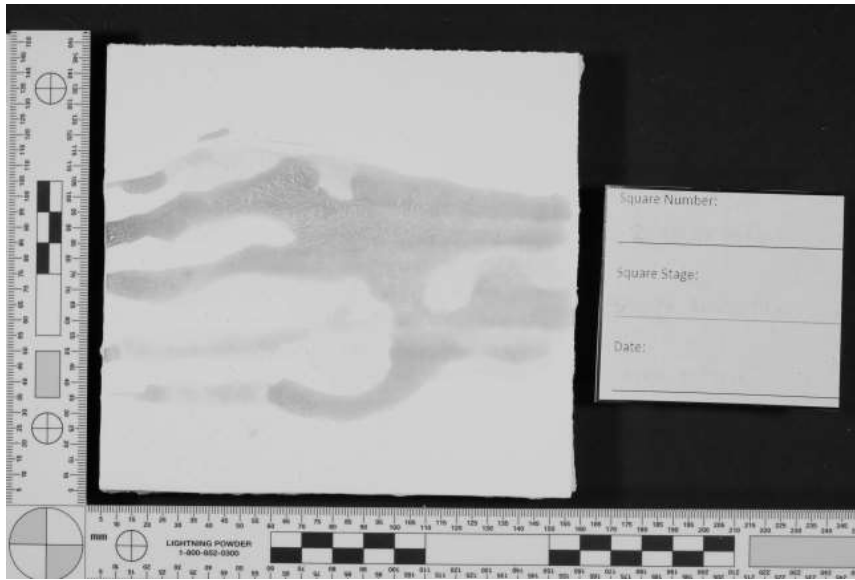


Longpass #89B HDR

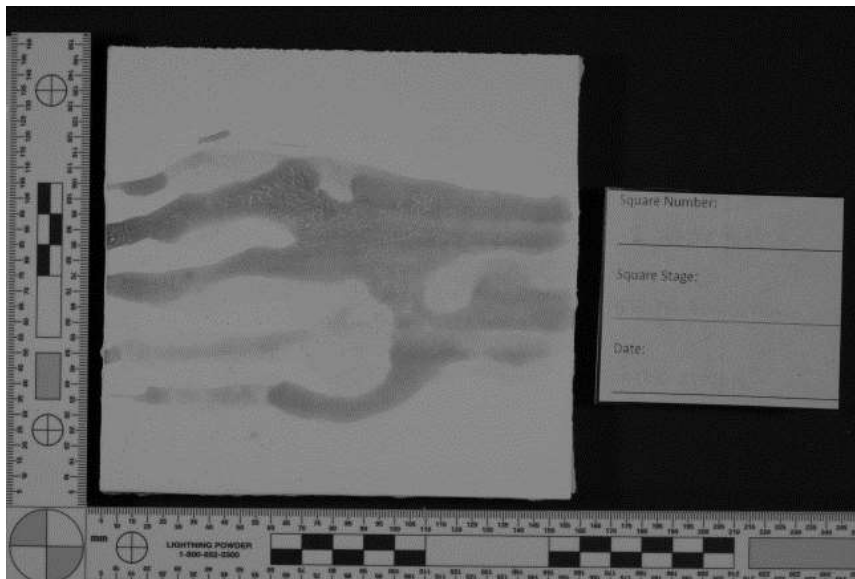


Longpass #89B Single

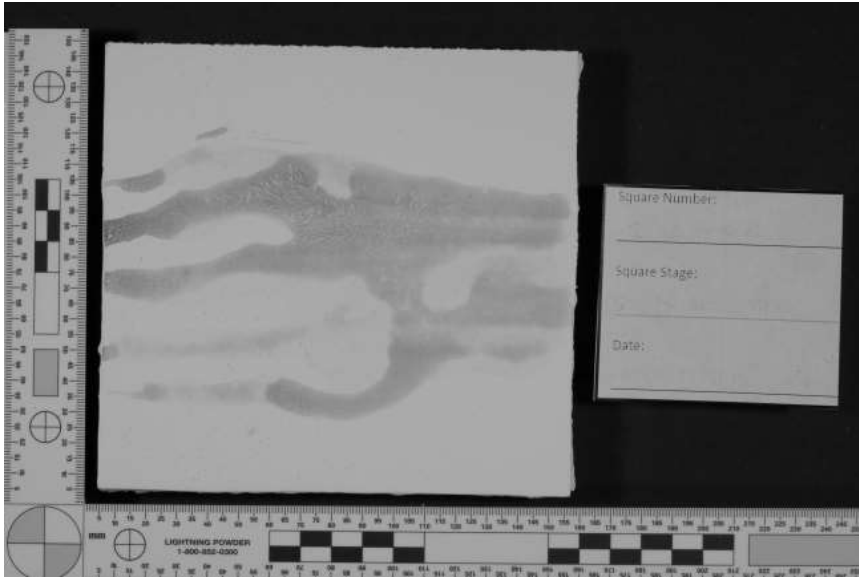
White Acrylic 2 – Swipe



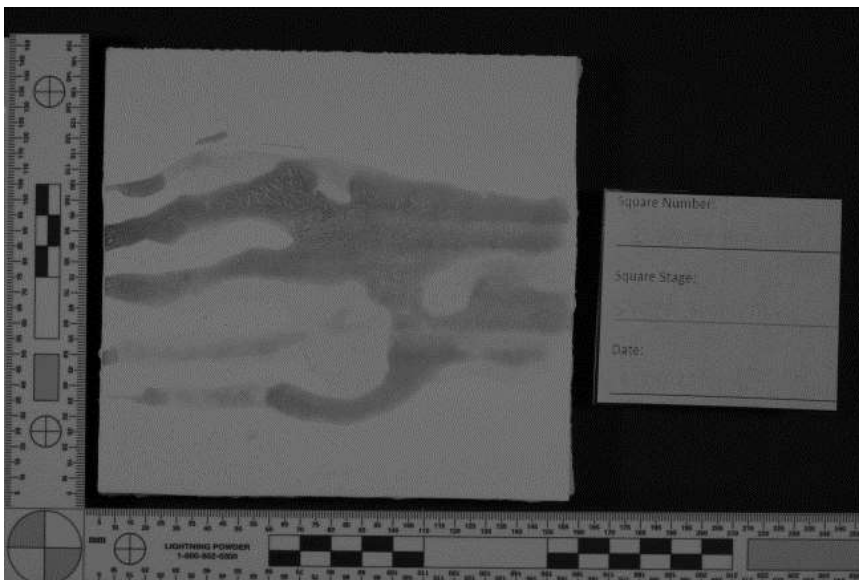
Longpass #70 HDR



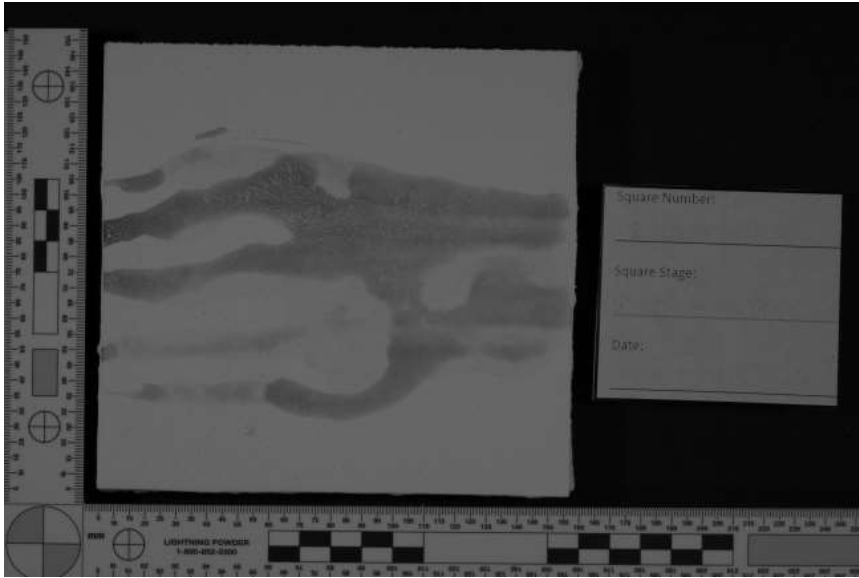
Longpass #70 Single



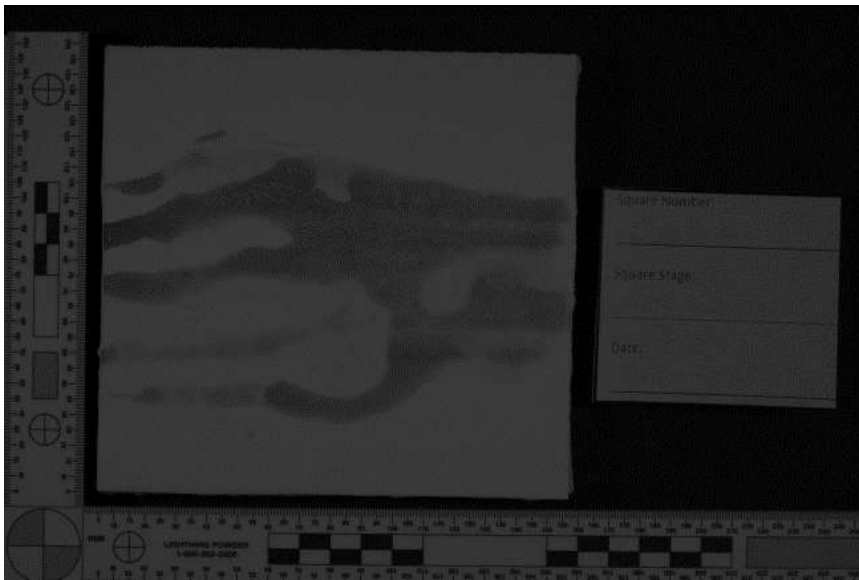
Longpass #87 HDR



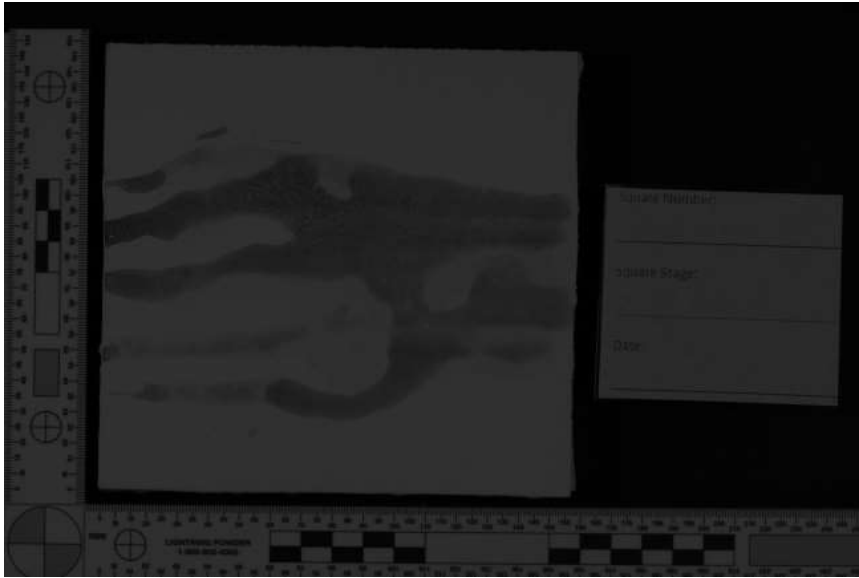
Longpass #87 Single



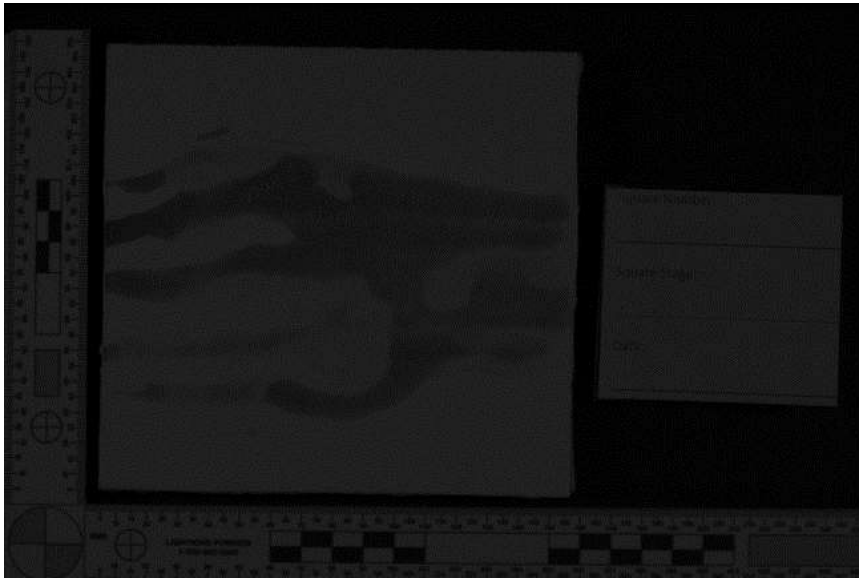
Longpass #87A HDR



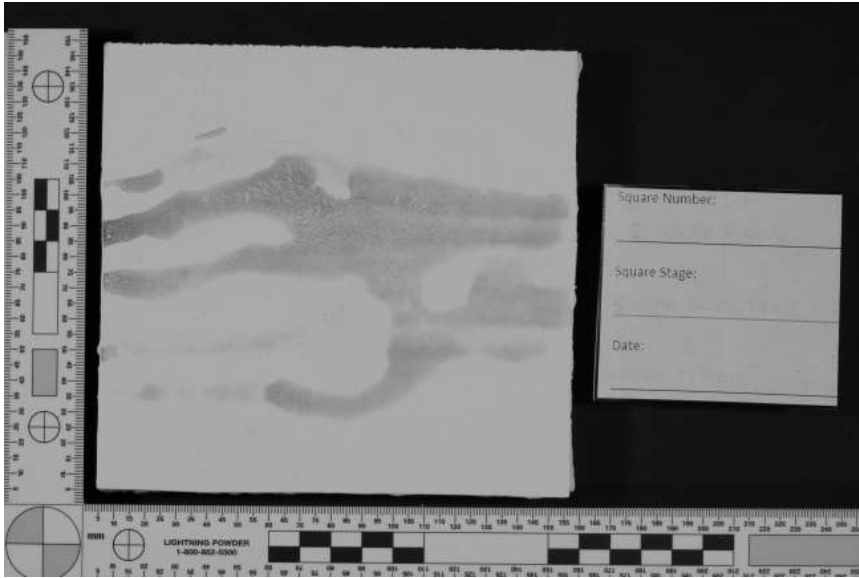
Longpass #87A Single



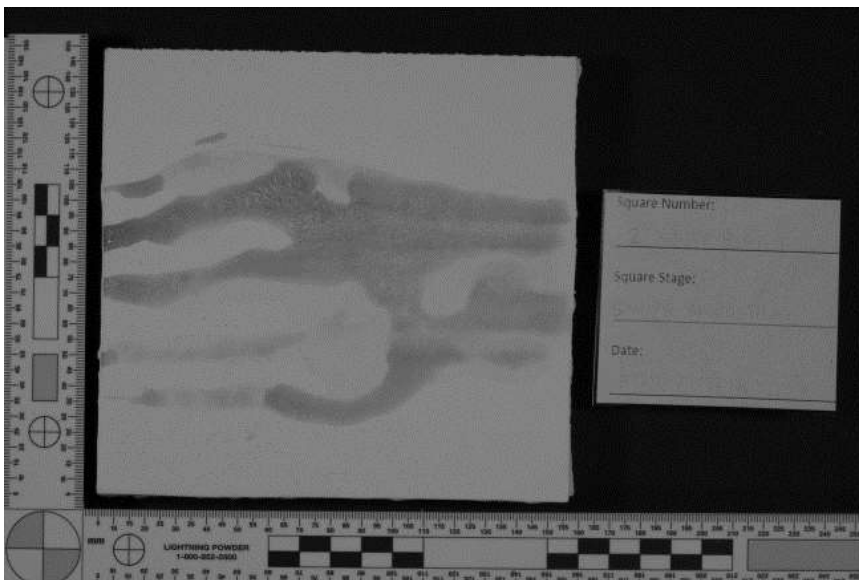
Longpass #87B HDR



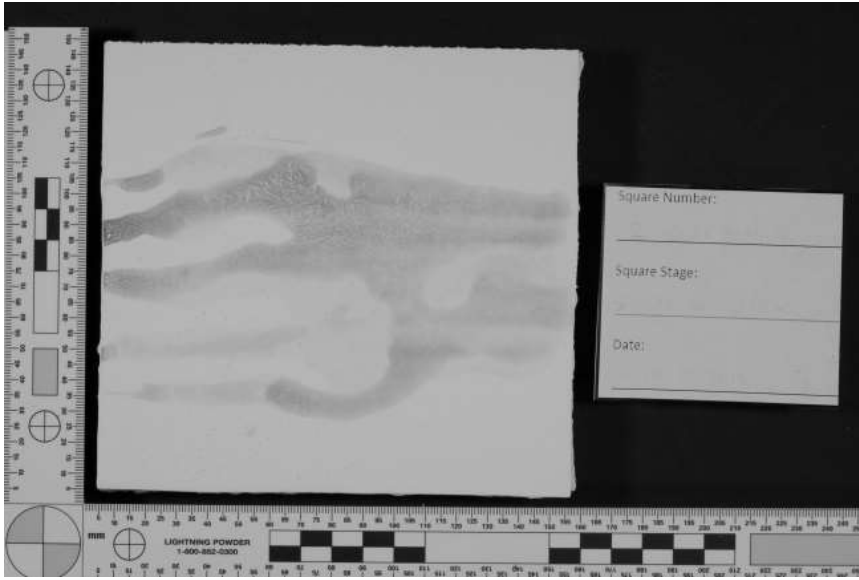
Longpass #87B Single



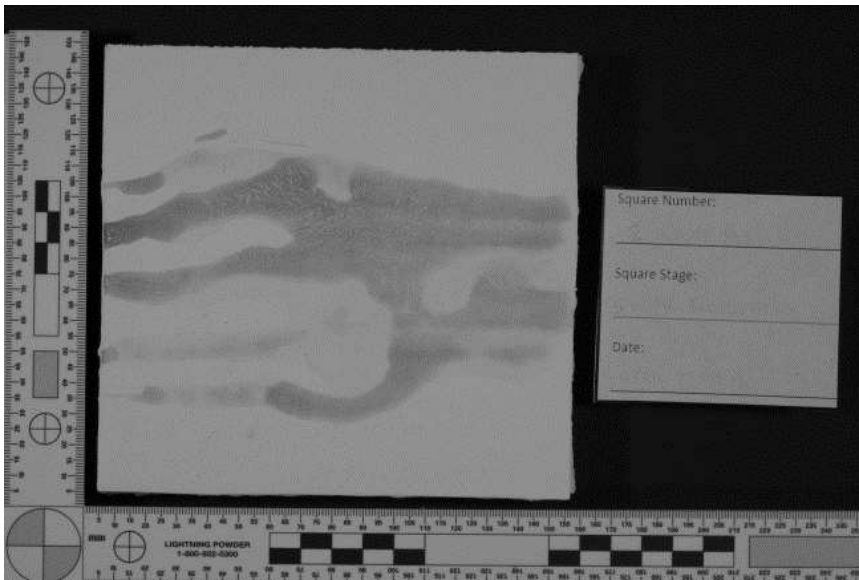
Longpass #88A HDR



Longpass #88A Single

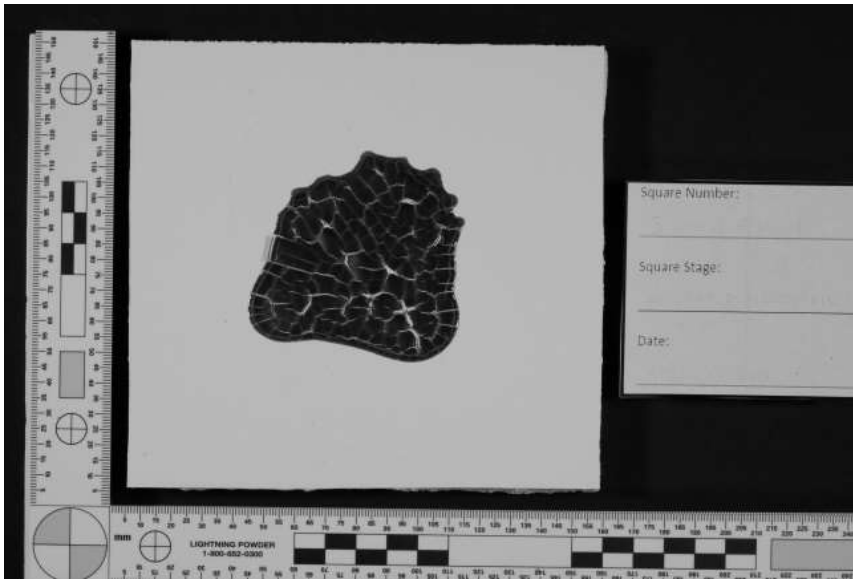


Longpass #89B HDR



Longpass #89B Single

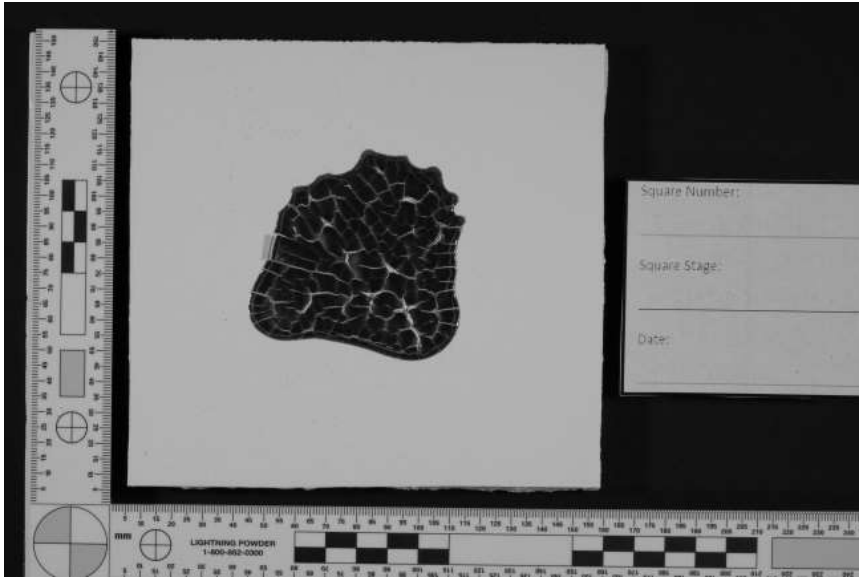
White Acrylic 3 – Saturated



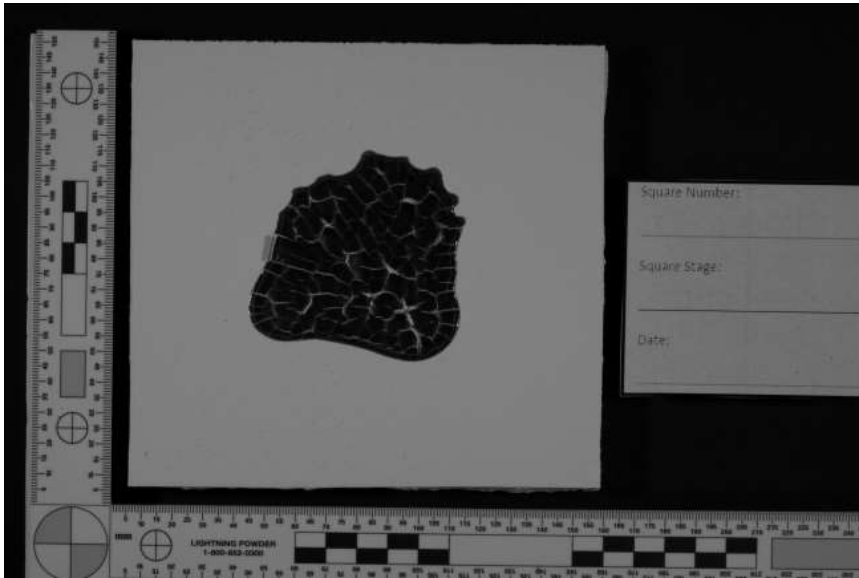
Longpass #70 HDR



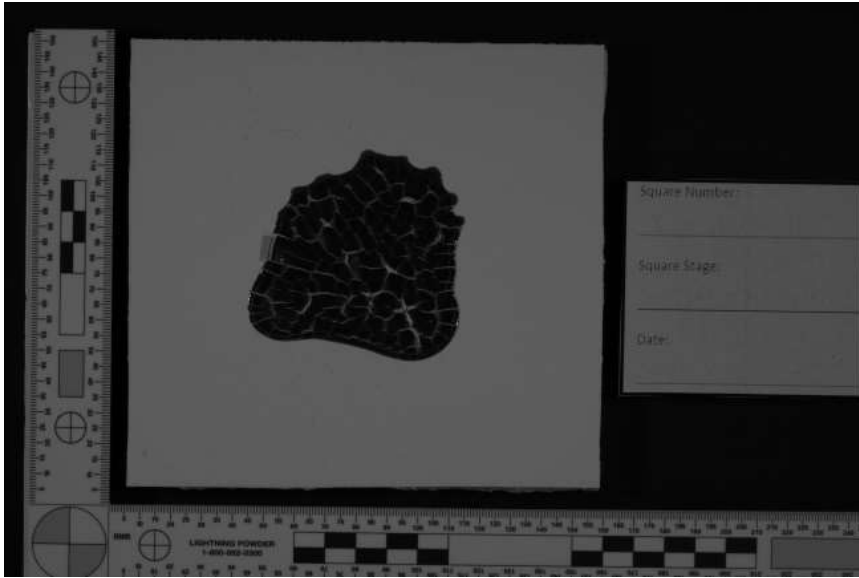
Longpass #70 Single



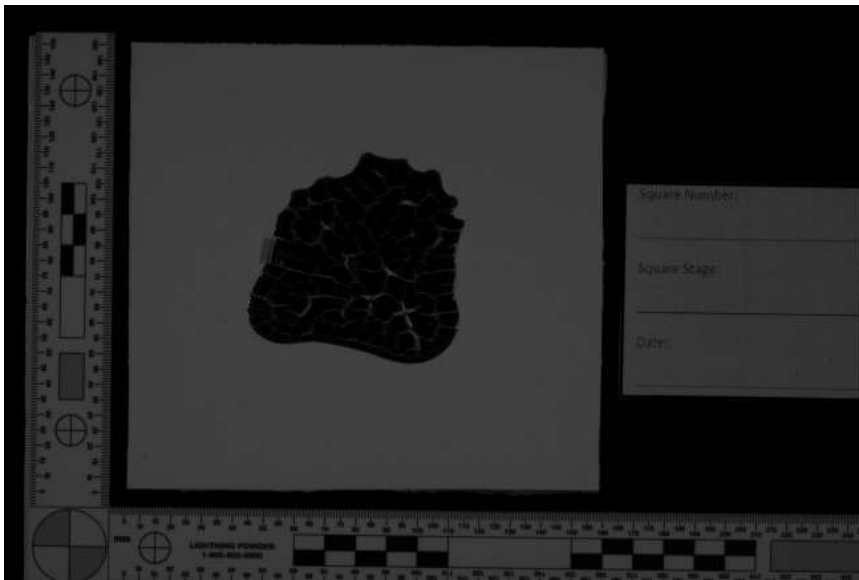
Longpass #87 HDR



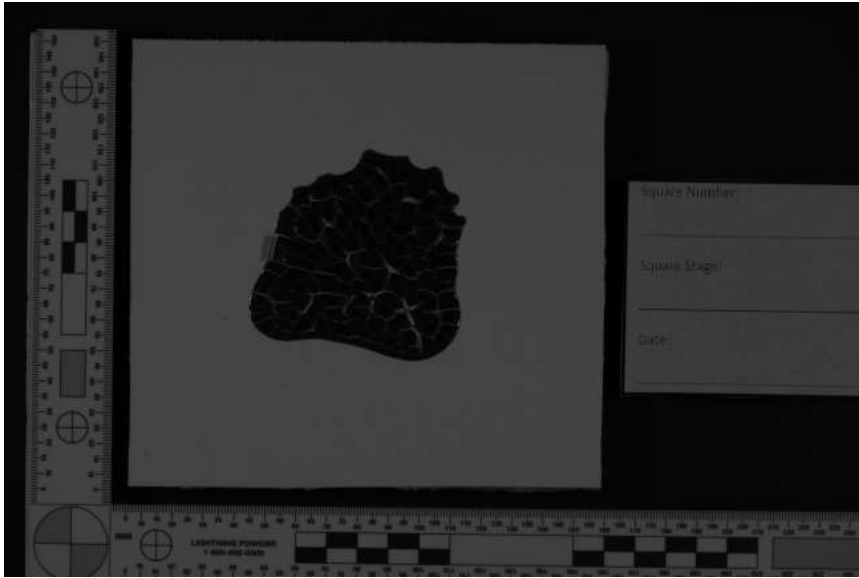
Longpass #87 Single



Longpass #87A HDR



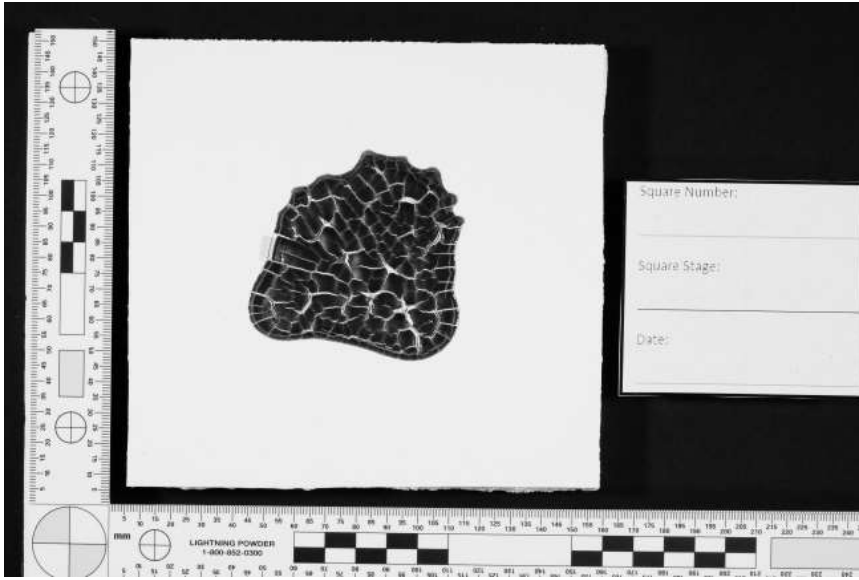
Longpass #87A Single



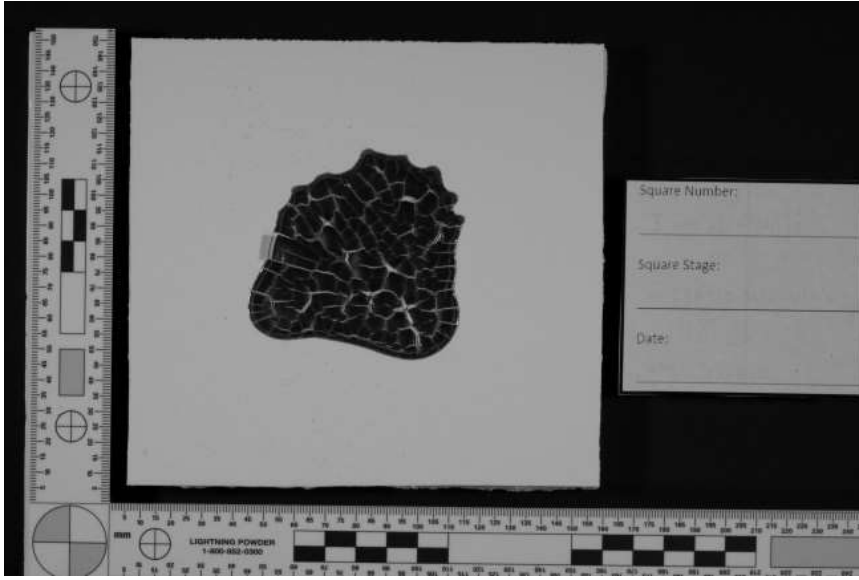
Longpass #87BHDR



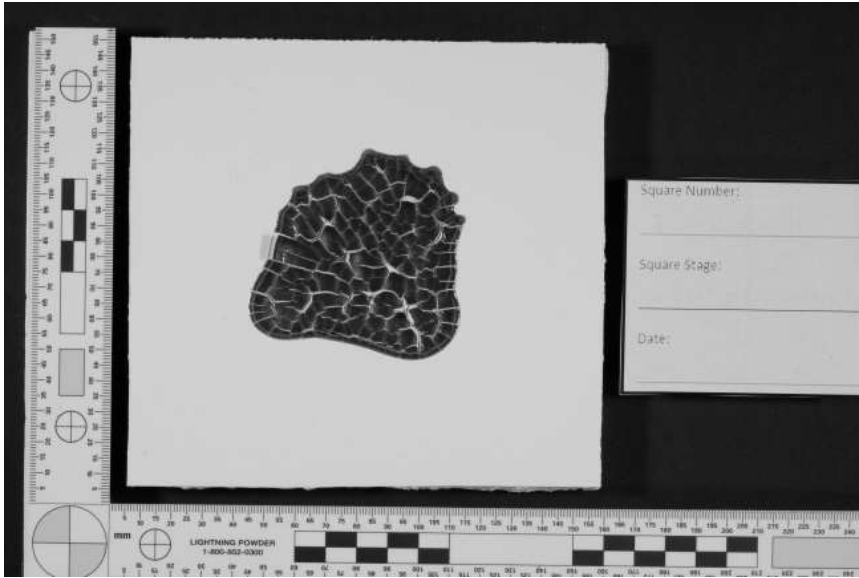
Longpass #87B Single



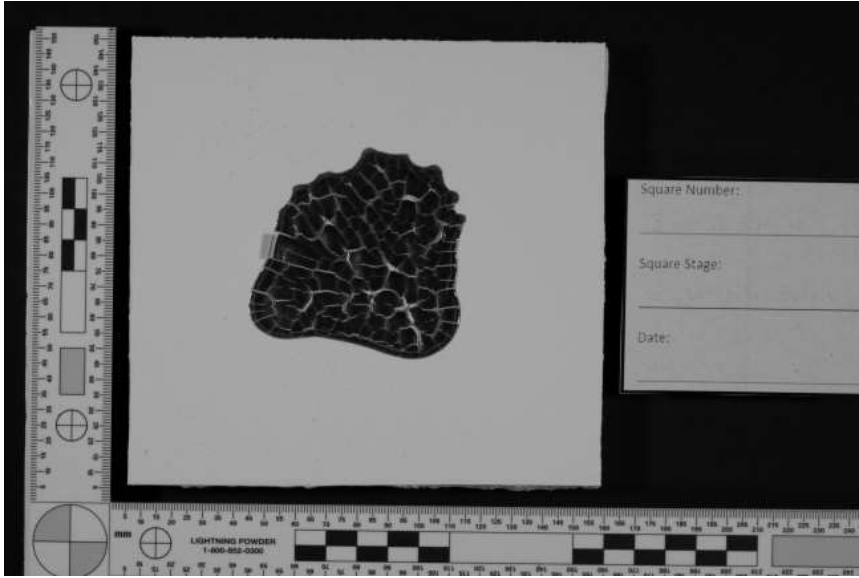
Longpass #88AHDR



Longpass #88A Single

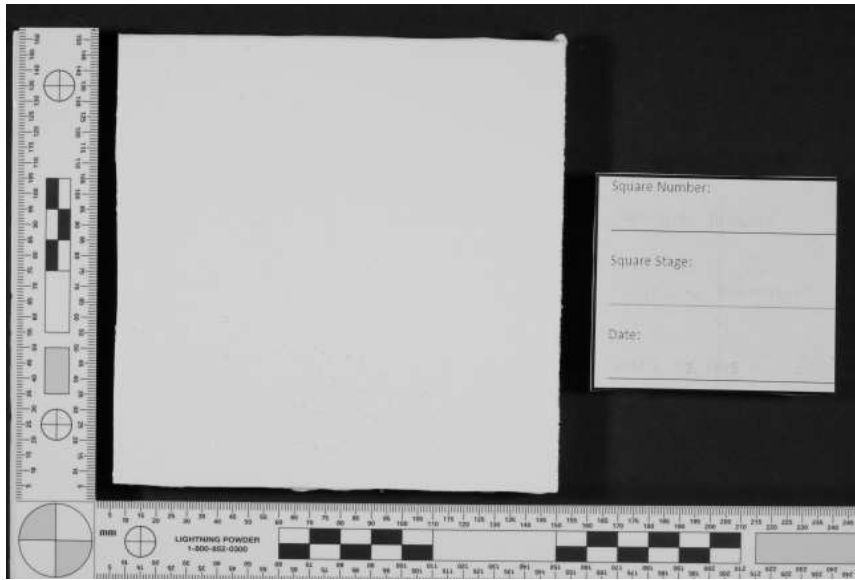


Longpass #89B HDR



Longpass #89B Single

White Acrylic 4 – Control No Blood

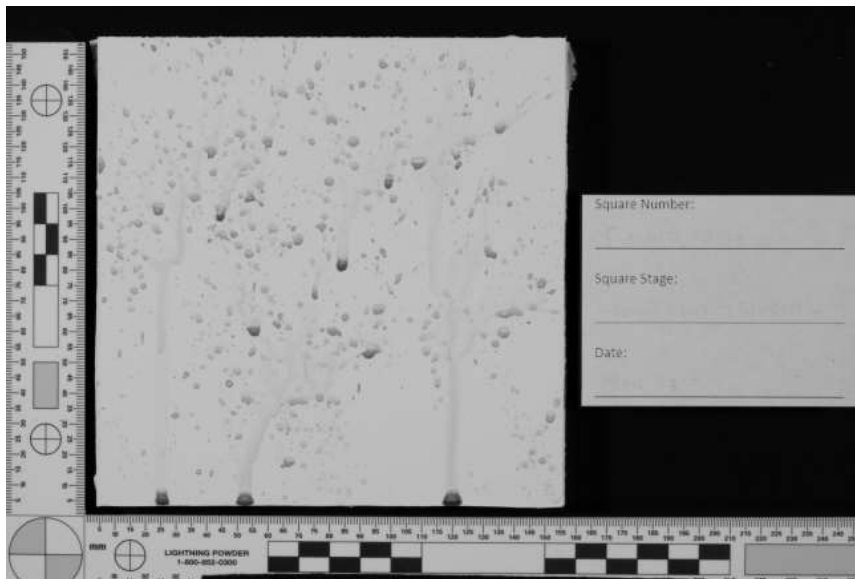


Longpass #70 HDR

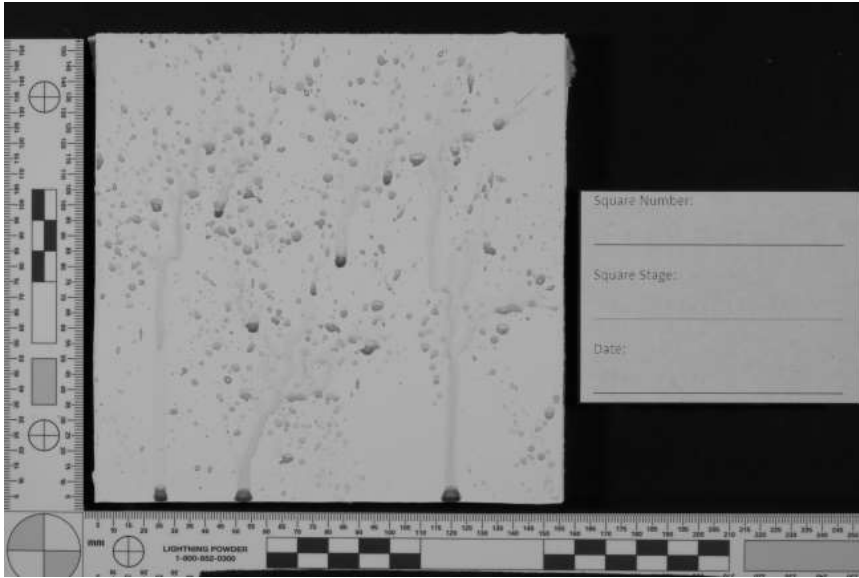
Appendix 4.1.2.2. White Latex – 70, 87, 87A, 87B, 88A, 89B Bloodstain pattern stage
White Latex 5 – Medium Velocity



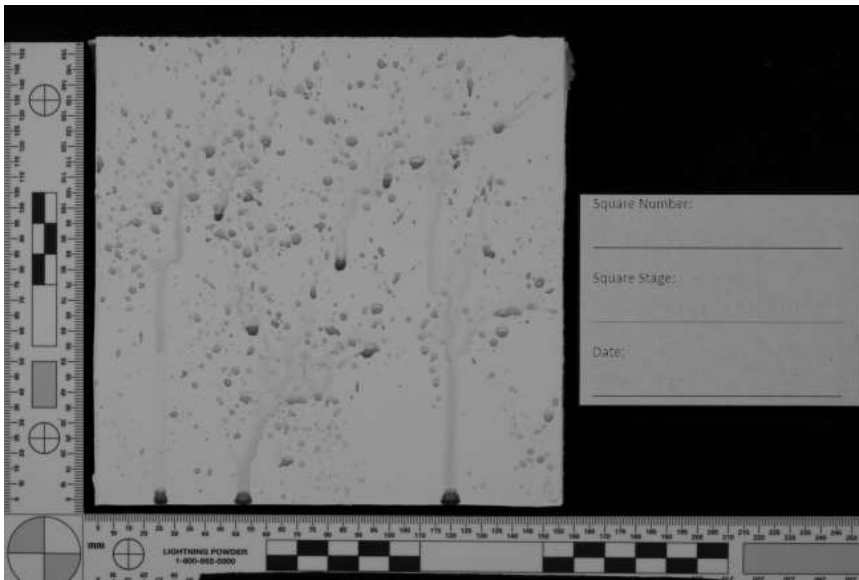
Longpass #70 HDR



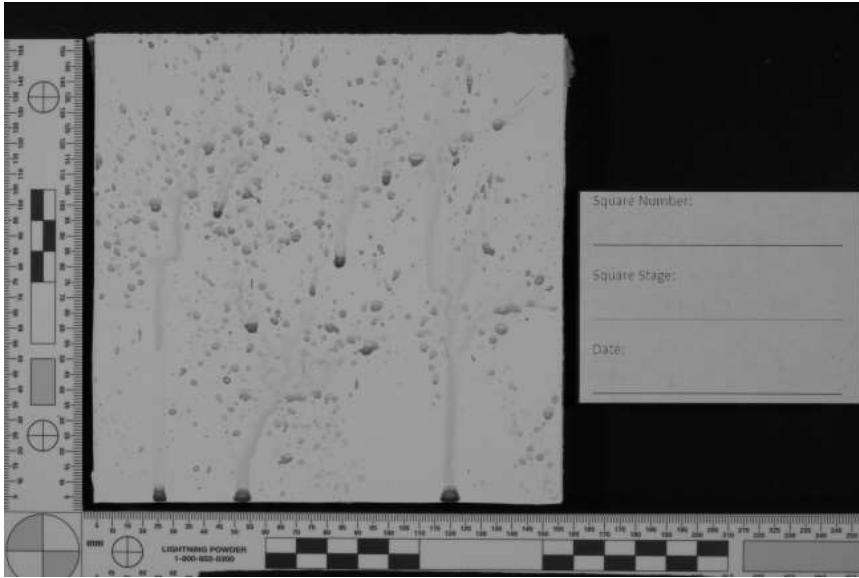
Longpass #70 Single



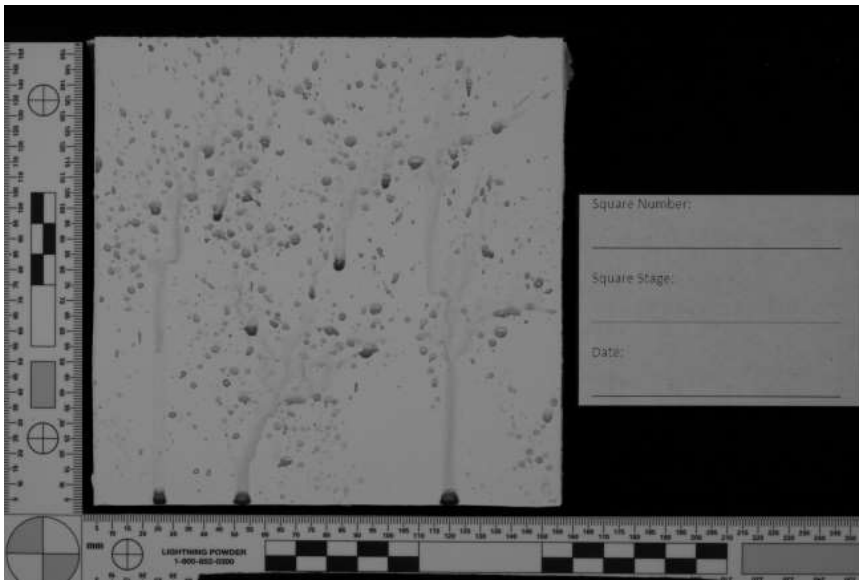
Longpass #87 HDR



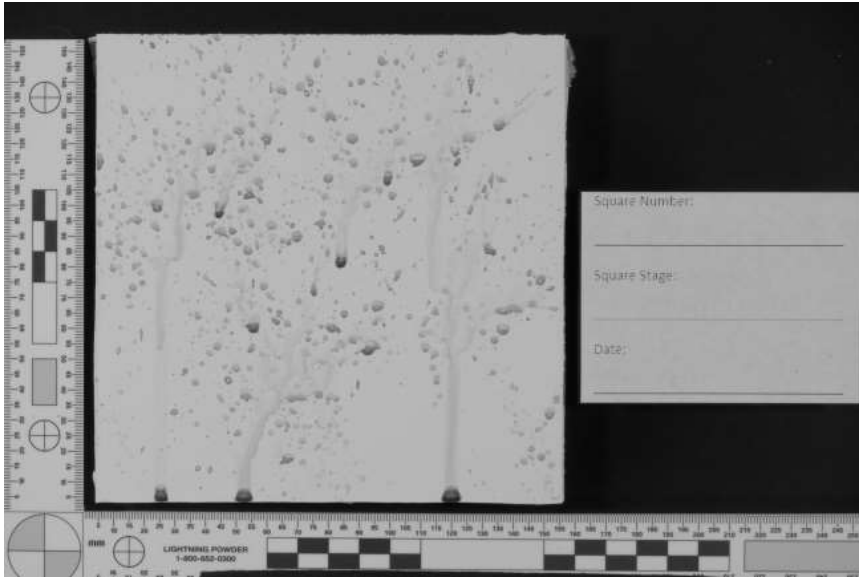
Longpass #87 Single



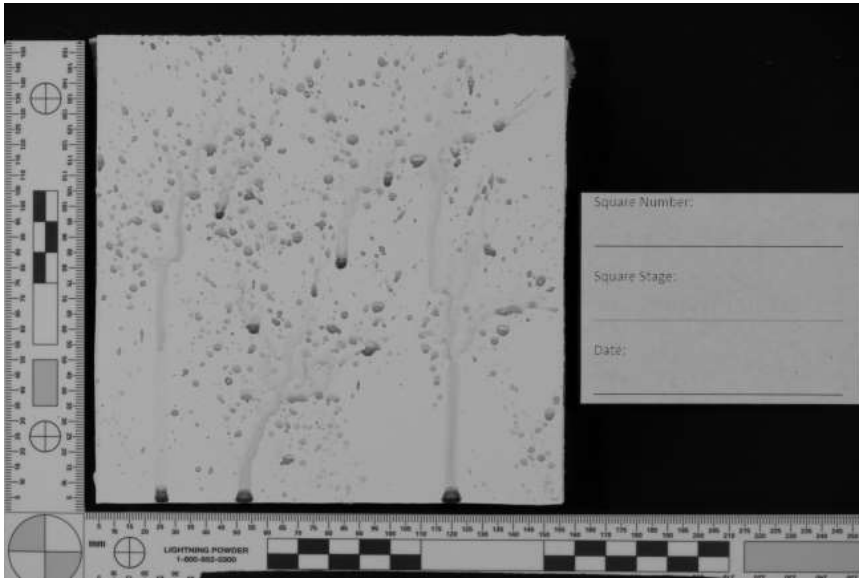
Longpass #87A HDR



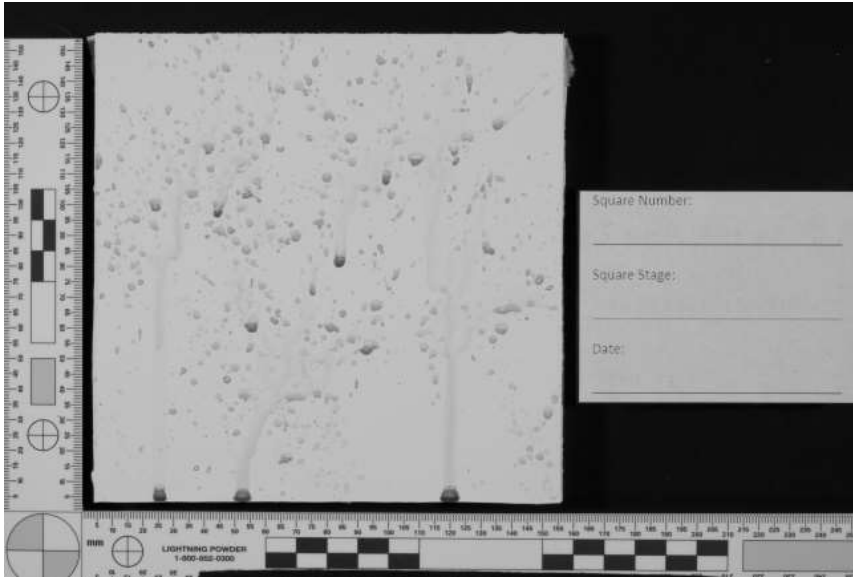
Longpass #87A Single



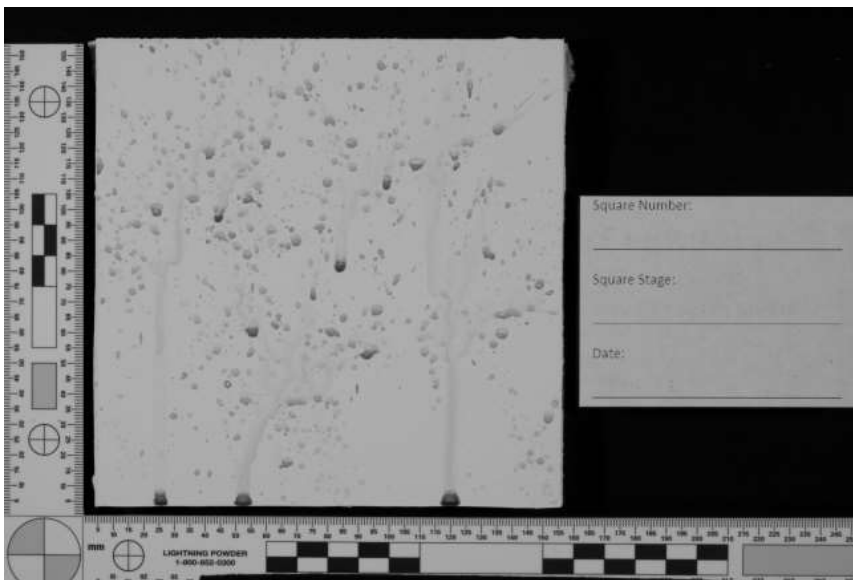
Longpass #87B HDR



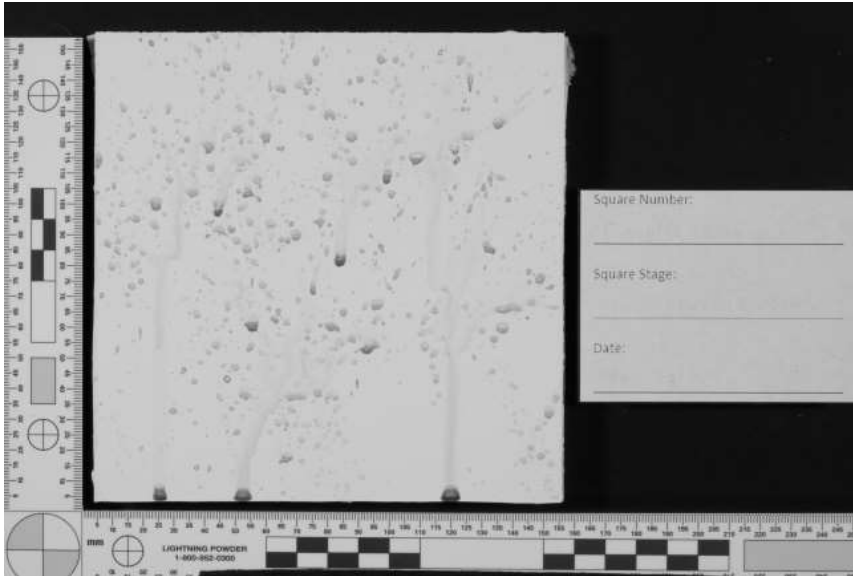
Longpass #87B Single



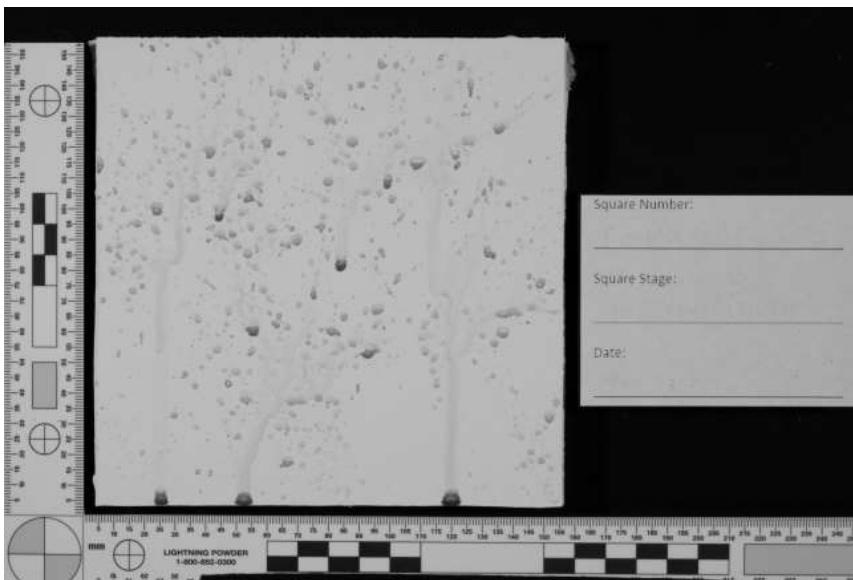
Longpass #88A HDR



Longpass #88A Single

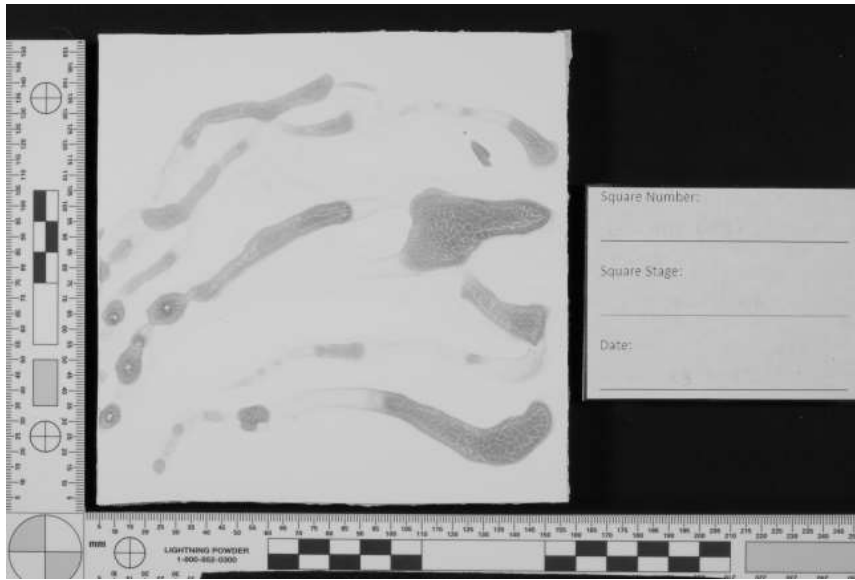


Longpass #89B HDR

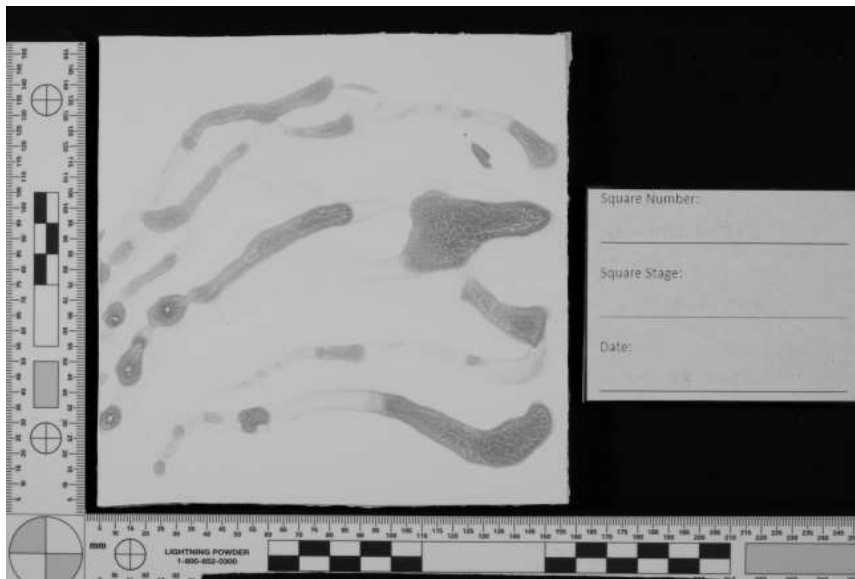


Longpass #89B Single

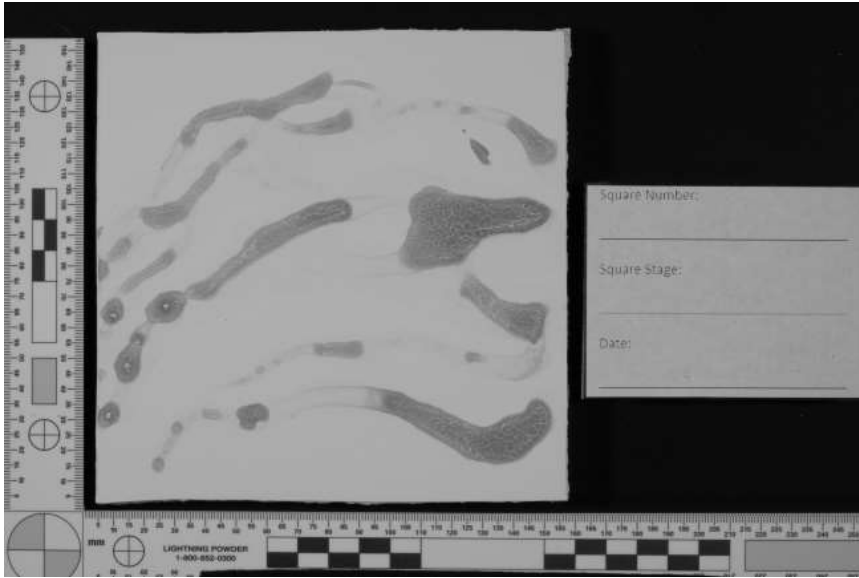
White Latex 6 – Swipe



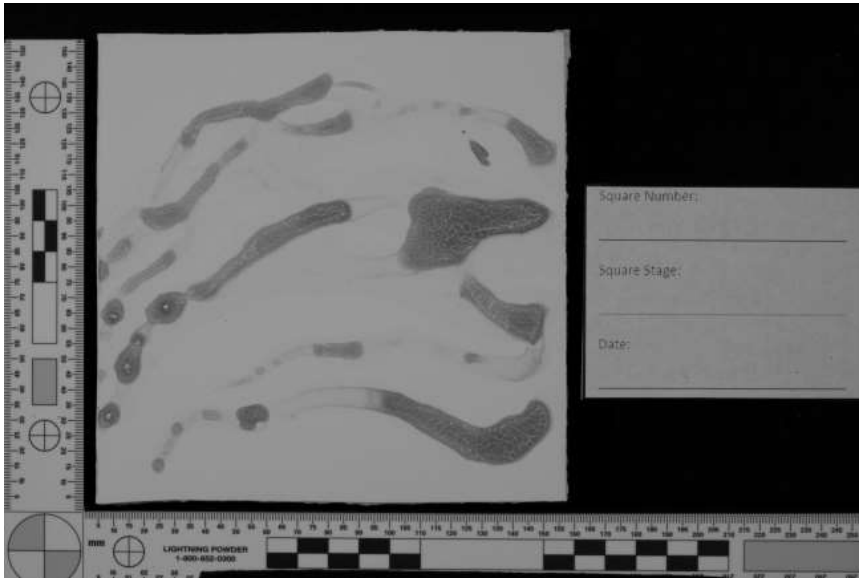
Longpass #70 HDR



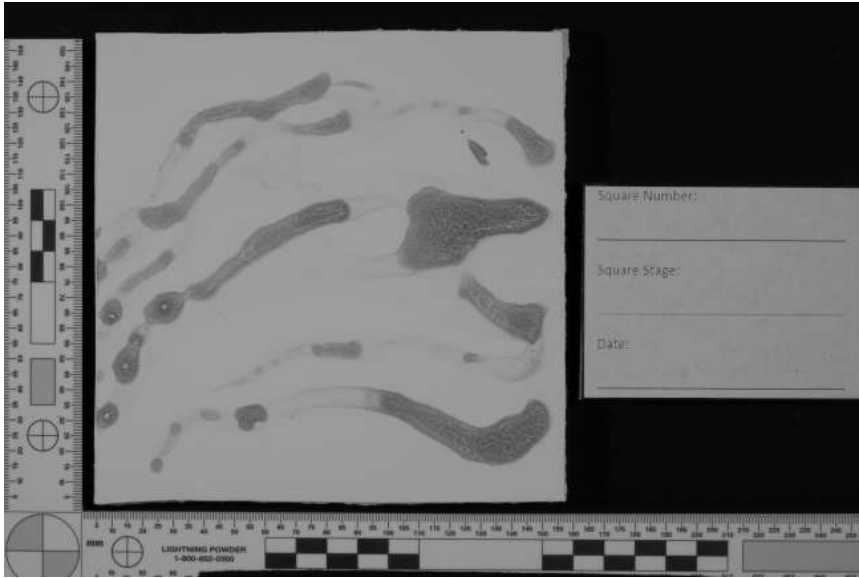
Longpass #70 Single



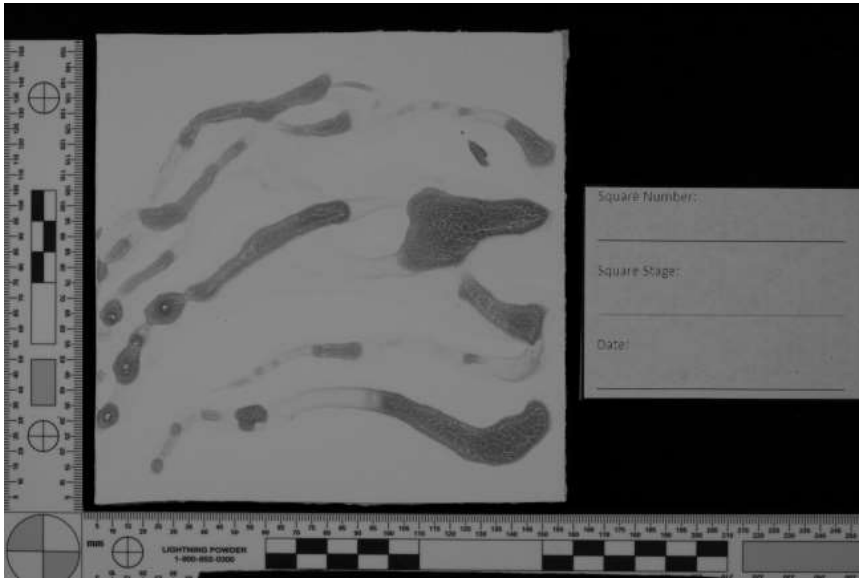
Longpass #87 HDR



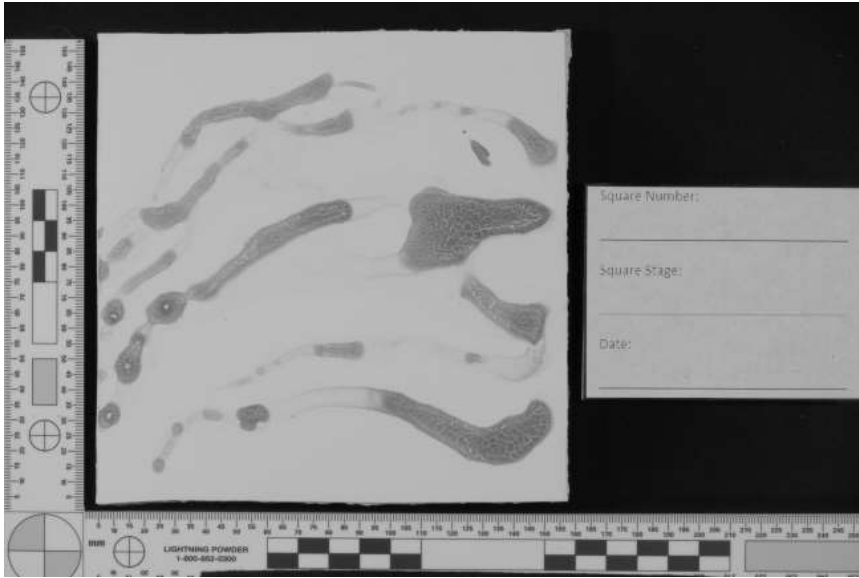
Longpass #87 Single



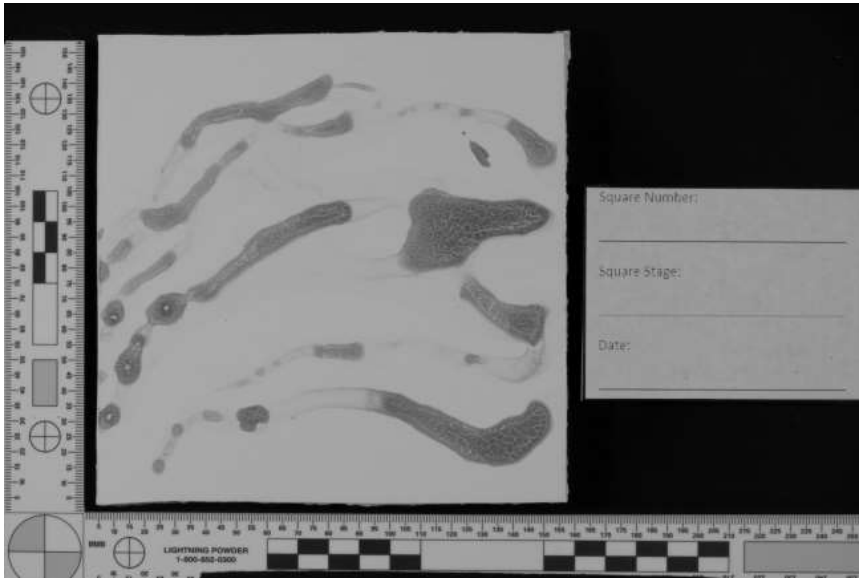
Longpass #87A HDR



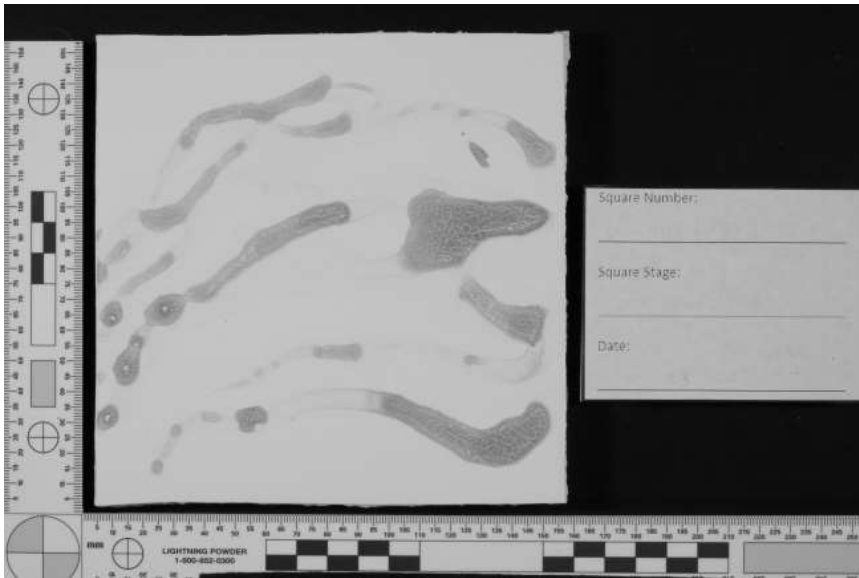
Longpass #87A Single



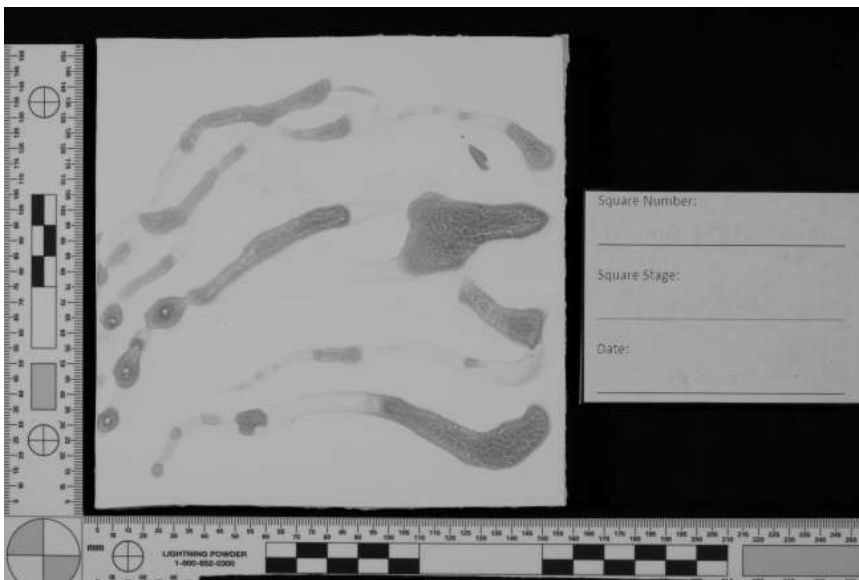
Longpass #87B HDR



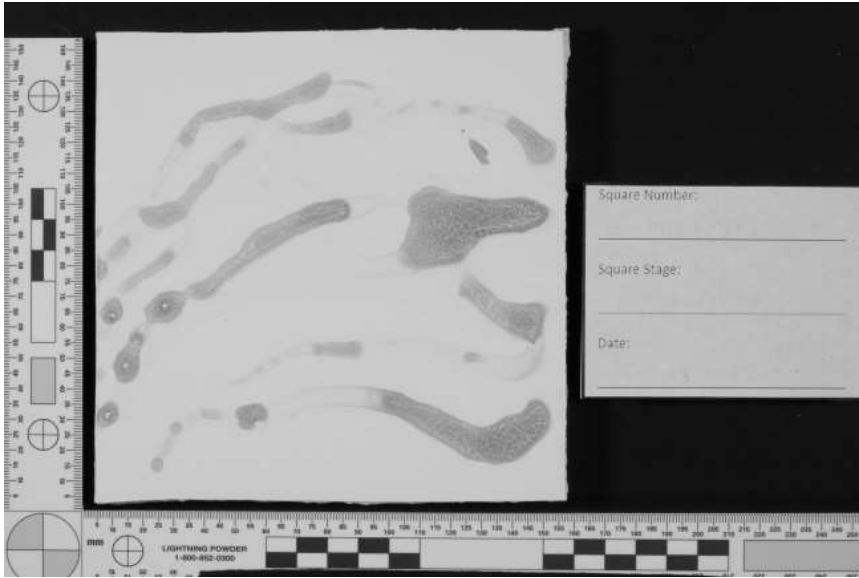
Longpass #87B Single



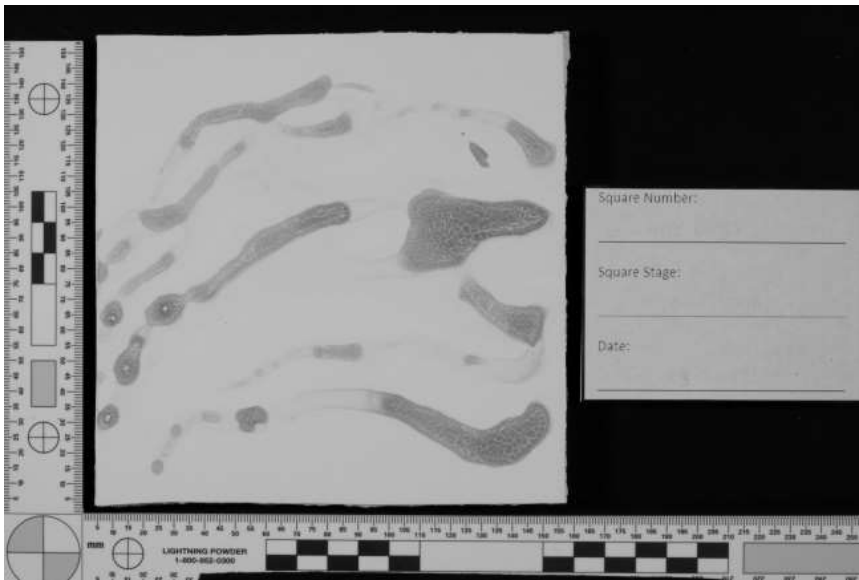
Longpass #88A HDR



Longpass #88A Single

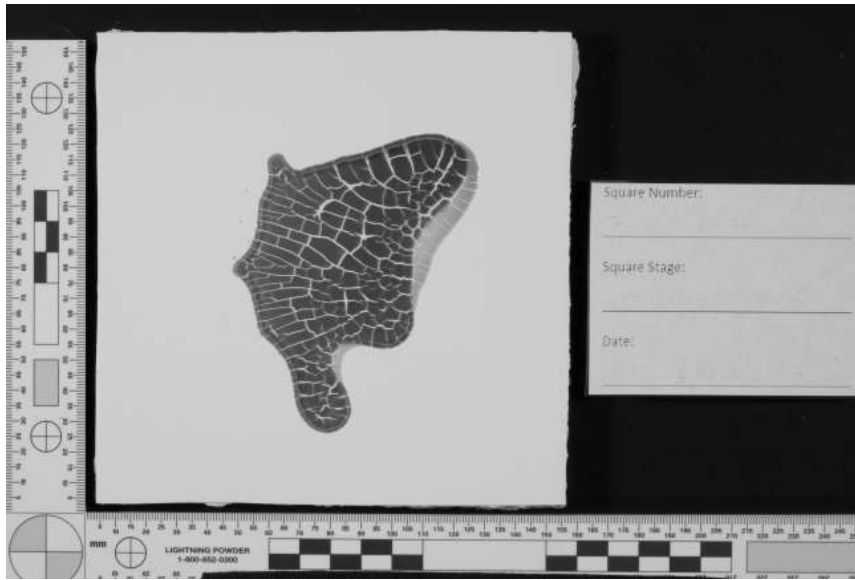


Longpass #89B HDR



Longpass #89B Single

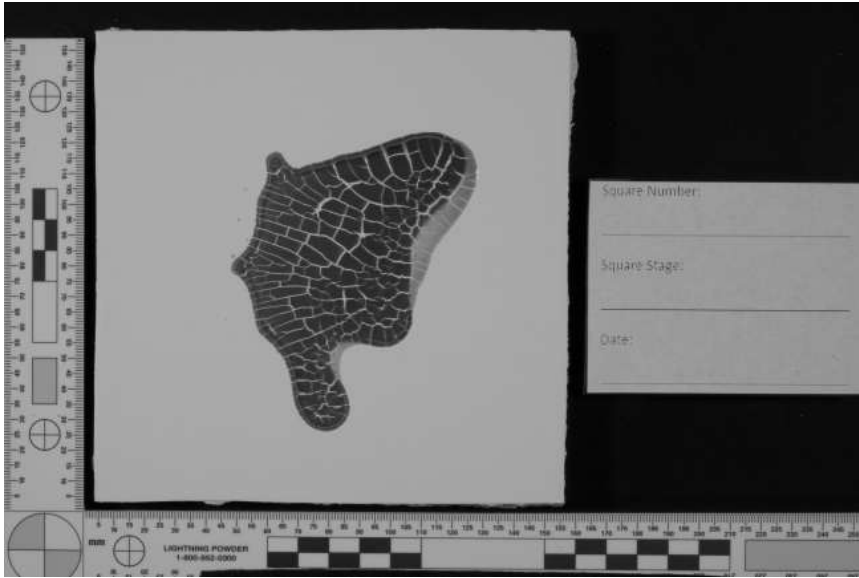
White Latex 7 – Saturated



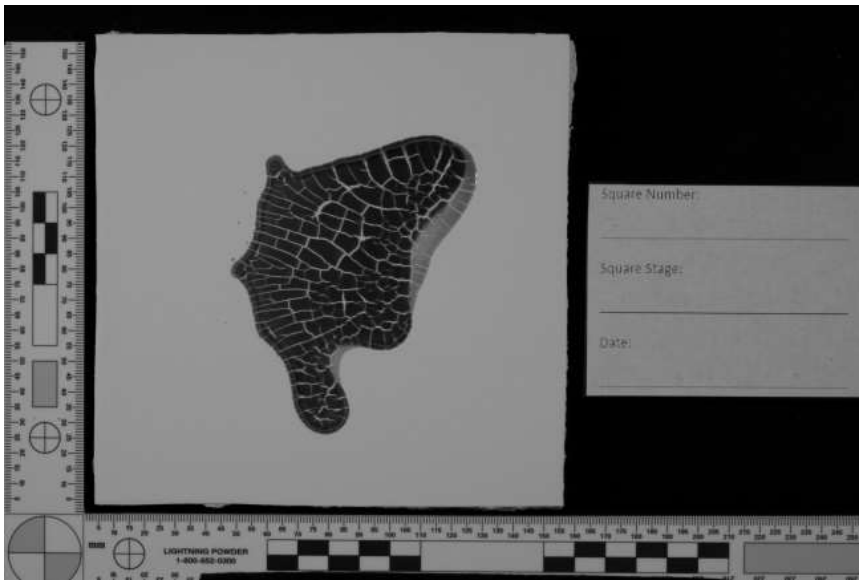
Longpass #70 HDR



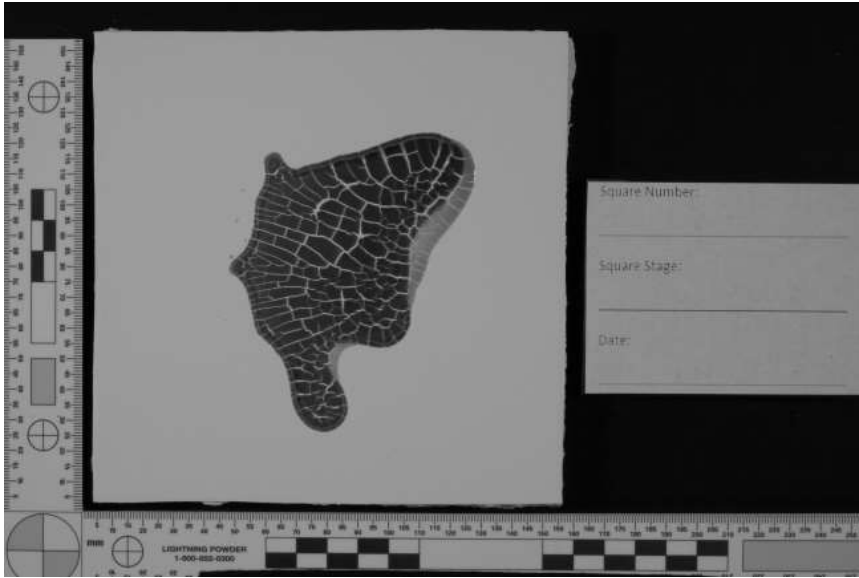
Longpass #70 Single



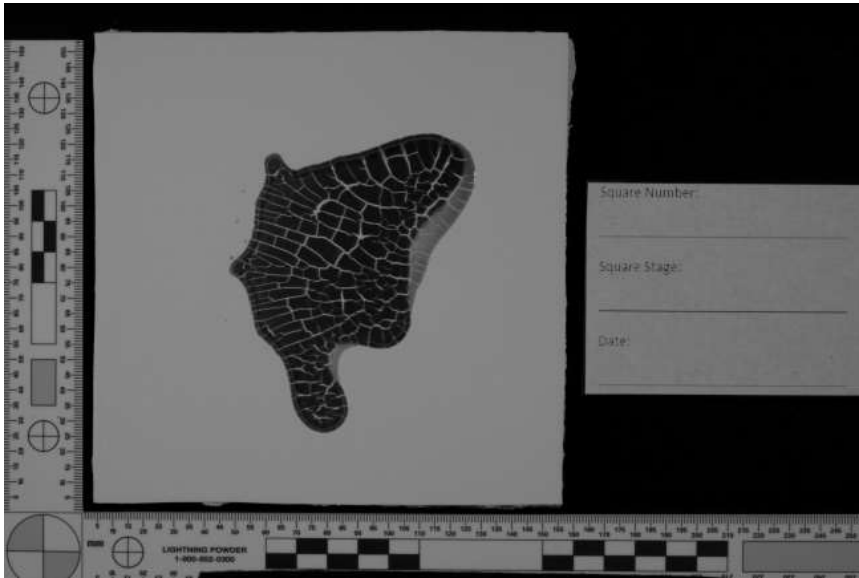
Longpass #87 HDR



Longpass #87 Single



Longpass #87A HDR



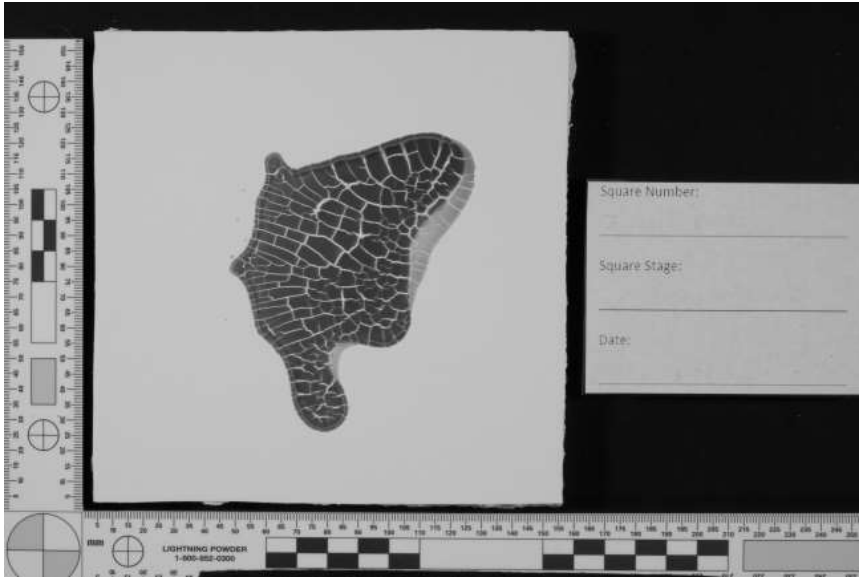
Longpass #87A Single



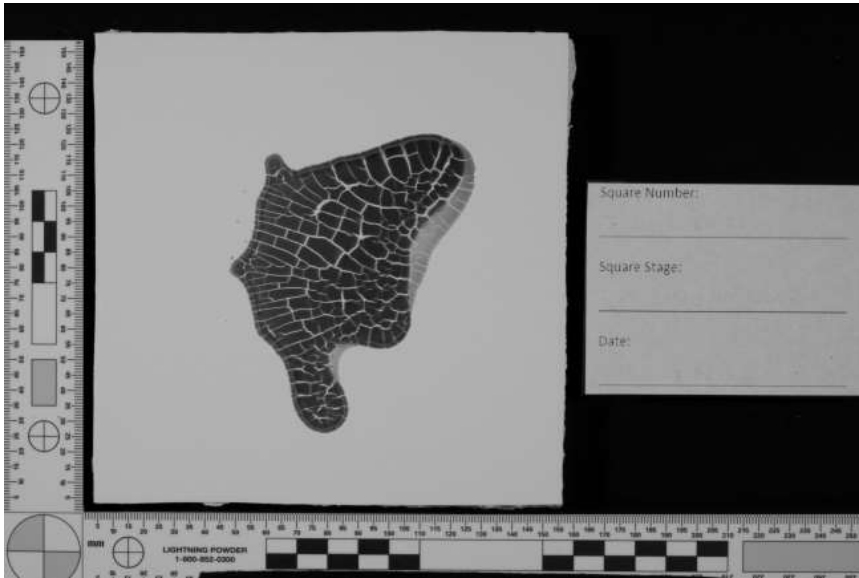
Longpass #87B HDR



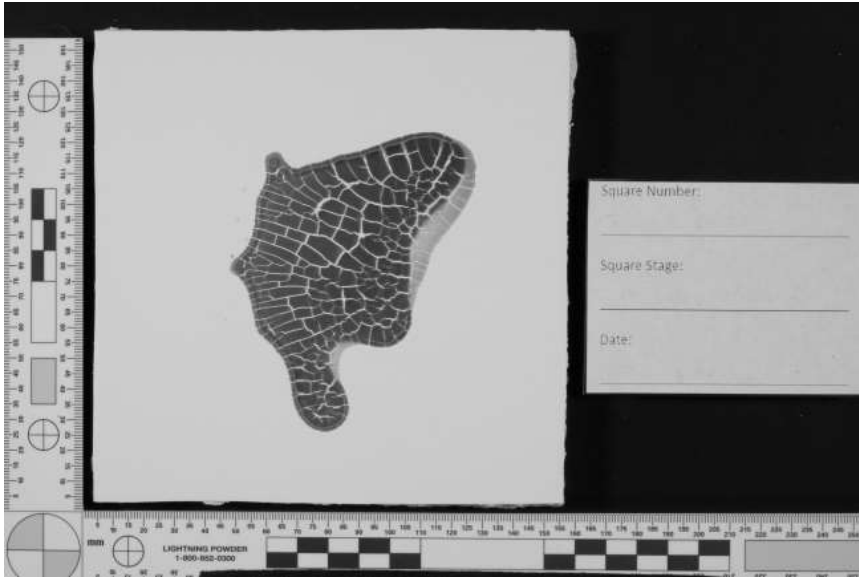
Longpass #87B Single



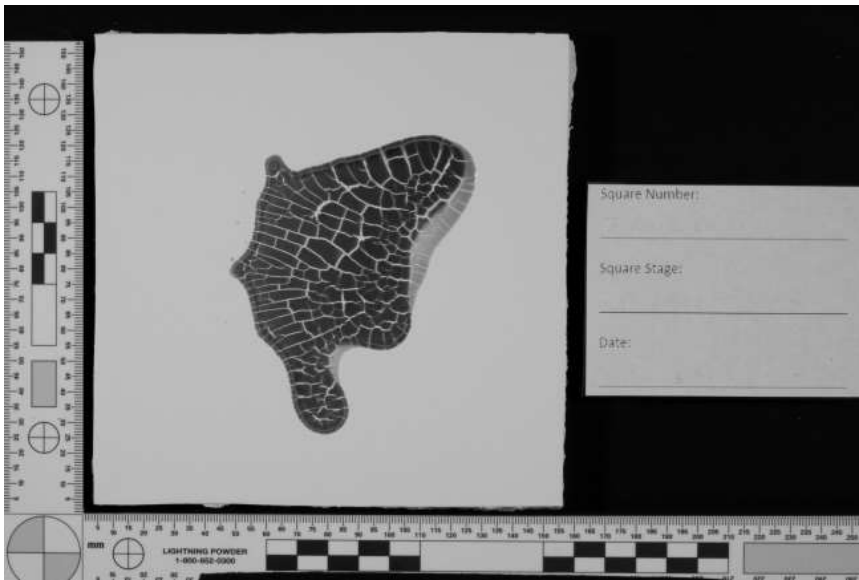
Longpass #88A HDR



Longpass #88A Single



Longpass #89B HDR



Longpass #89B Single

White Latex 8 – Control No Blood



Longpass #70 HDR

Appendix 4.1.2.3. Black Latex – 70, 87, 87A, 87B, 88A, 89B Bloodstain pattern stage
Black Latex 9 – Medium Velocity



Longpass #70 HDR



Longpass #70 Single



Longpass #87 HDR



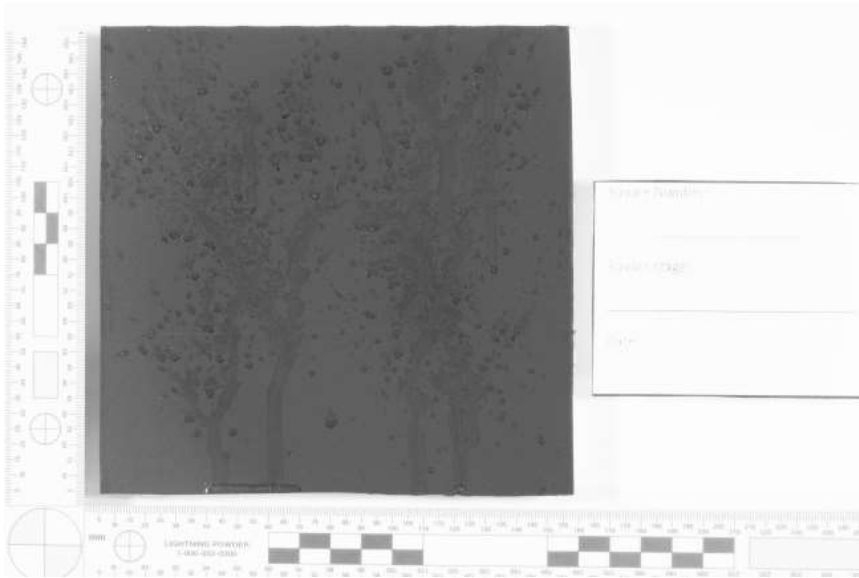
Longpass #87 Single



Longpass #87A HDR



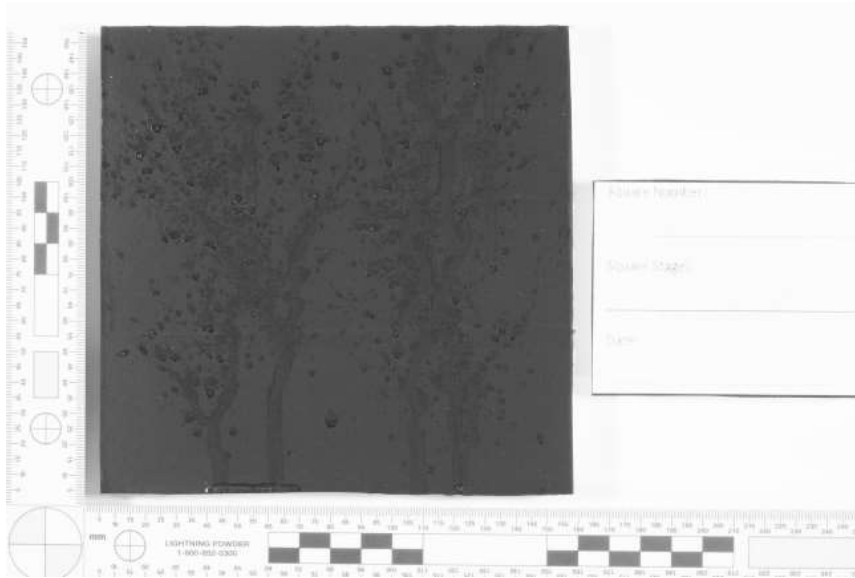
Longpass #87A Single



Longpass #87B HDR



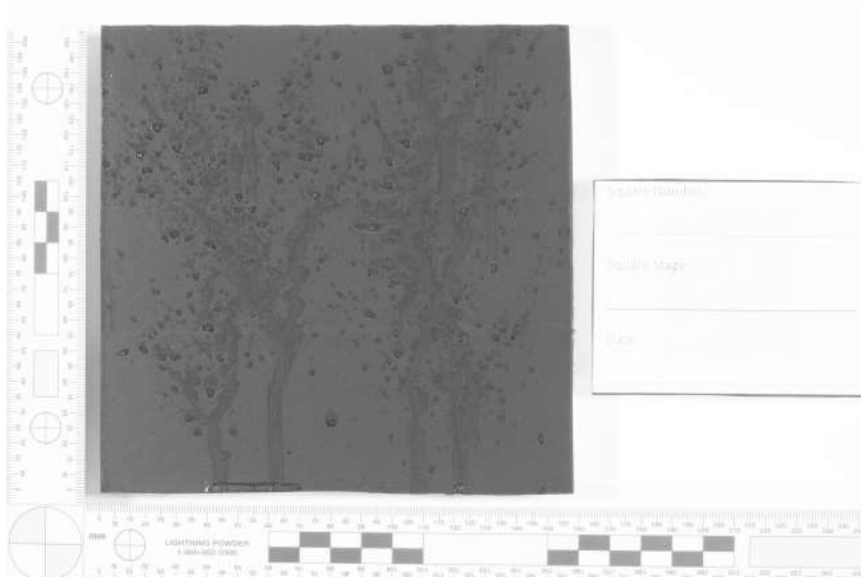
Longpass #87B Single



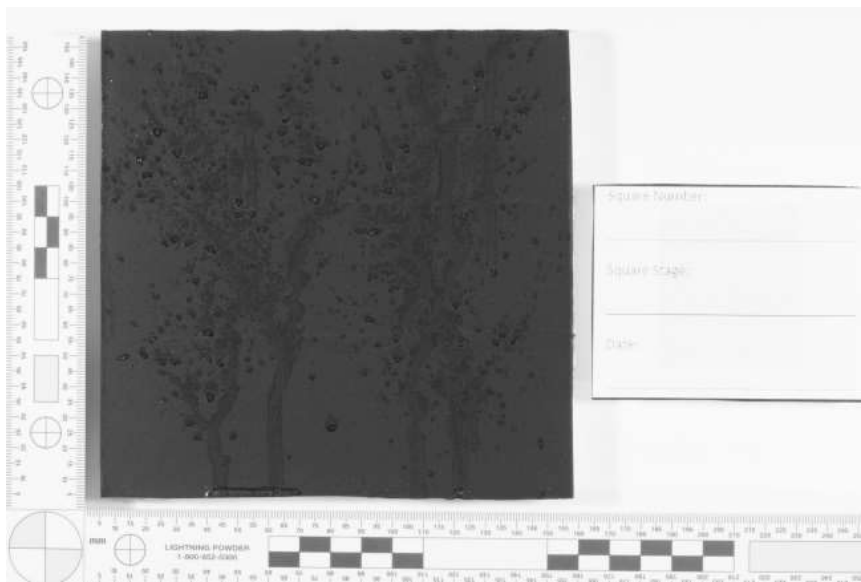
Longpass #88A HDR



Longpass #88A Single

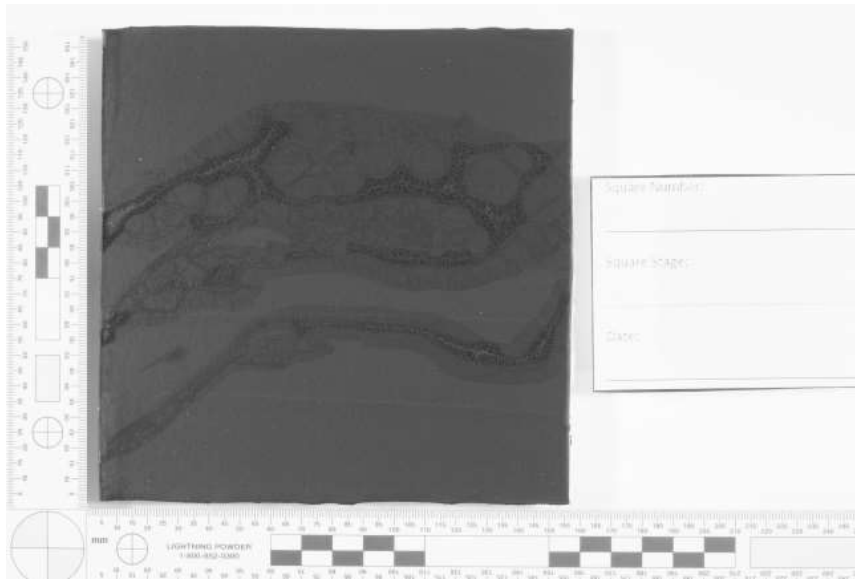


Longpass #89B HDR

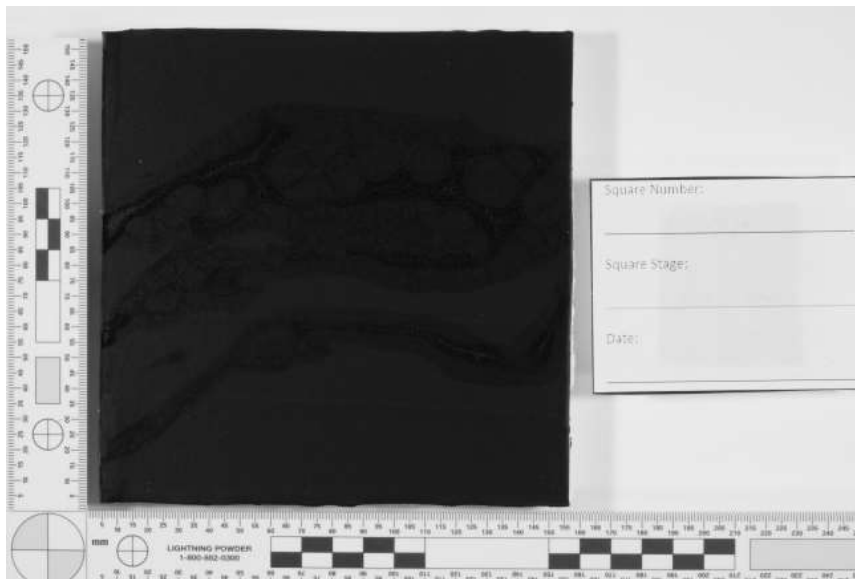


Longpass #89B Single

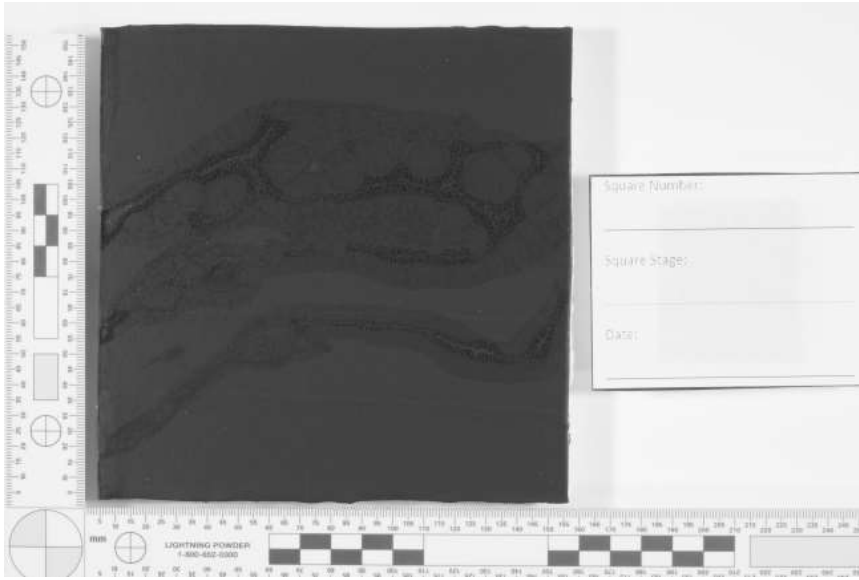
Black Latex 10 – Swipe



Longpass #70 HDR



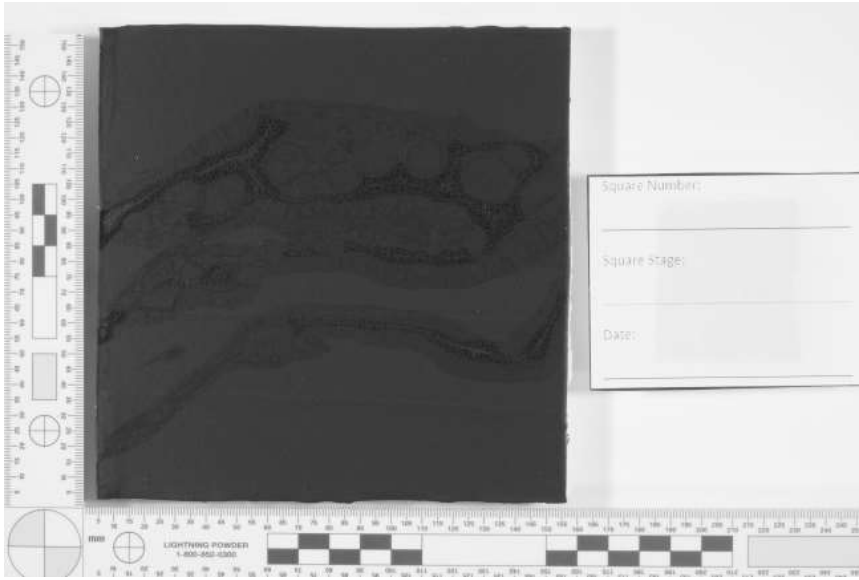
Longpass #70 Single



Longpass #87 HDR



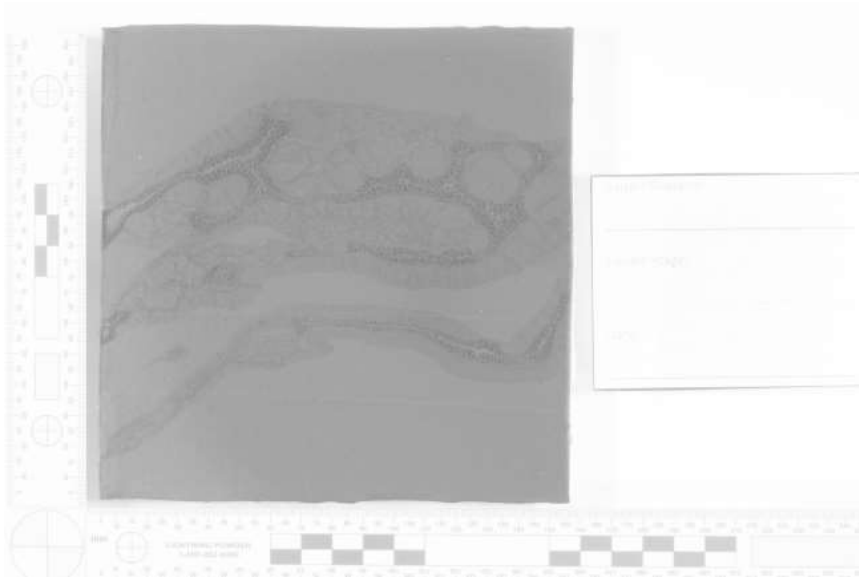
Longpass #87 Single



Longpass #87A HDR



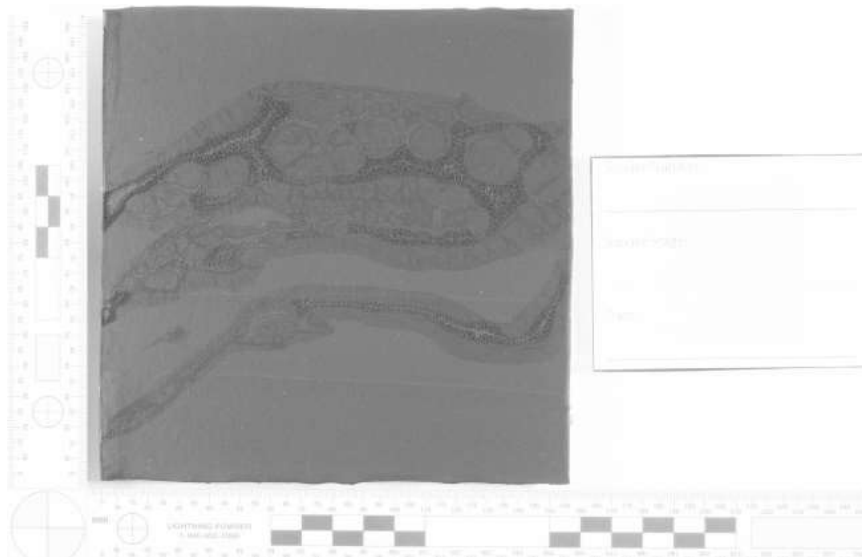
Longpass #87A Single



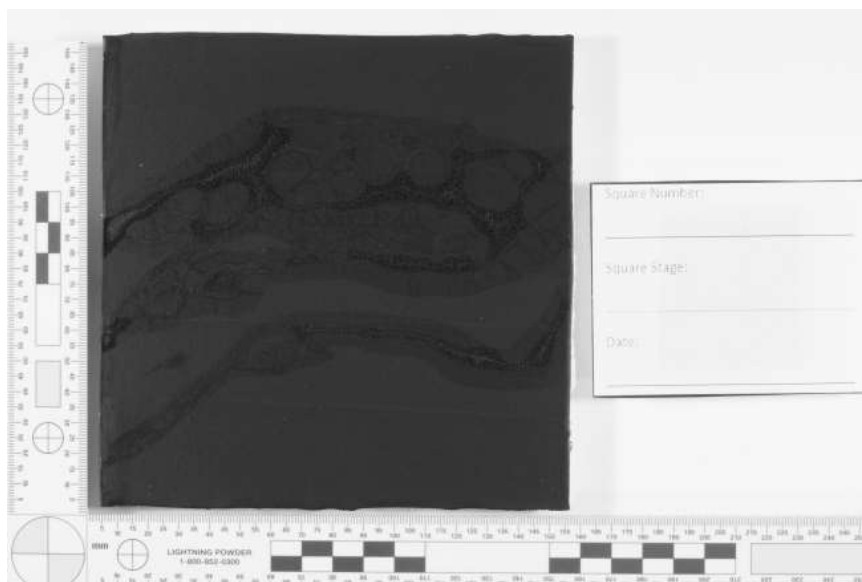
Longpass #87B HDR



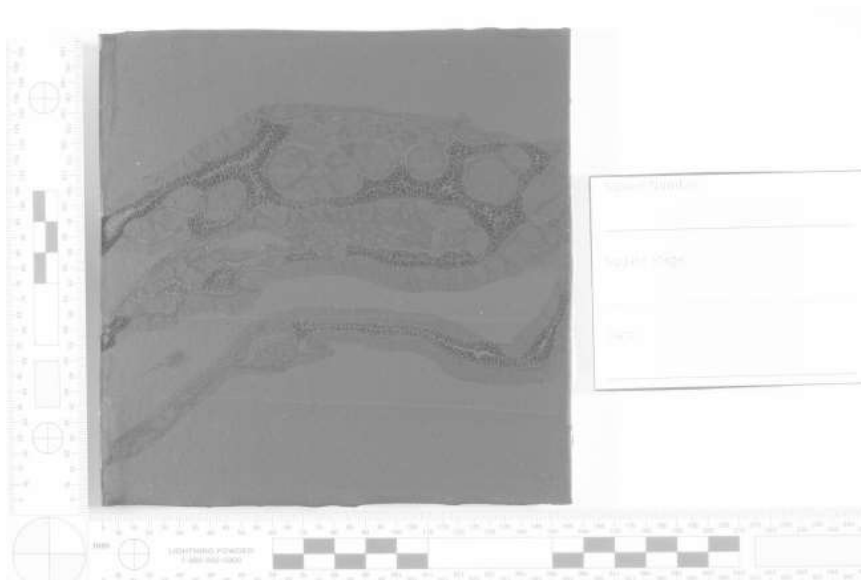
Longpass #87B Single



Longpass #88A HDR



Longpass #88A Single

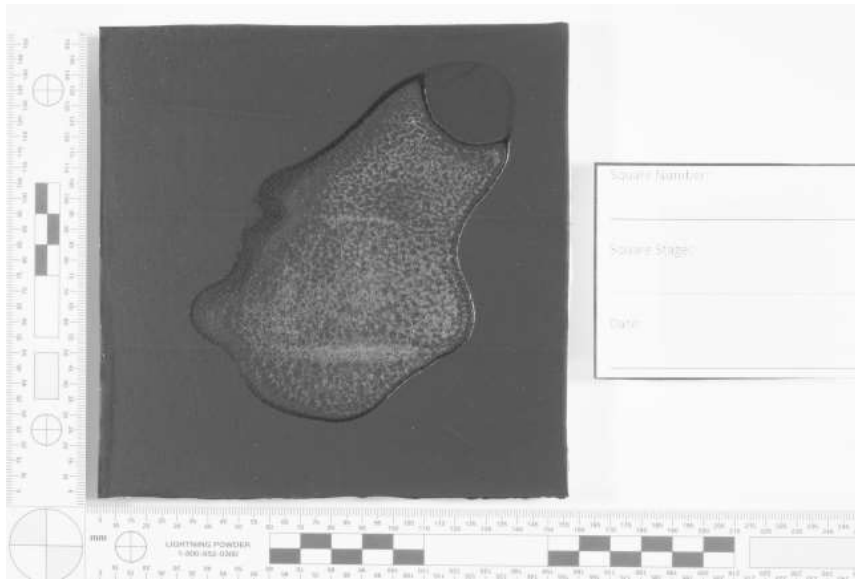


Longpass #89B HDR

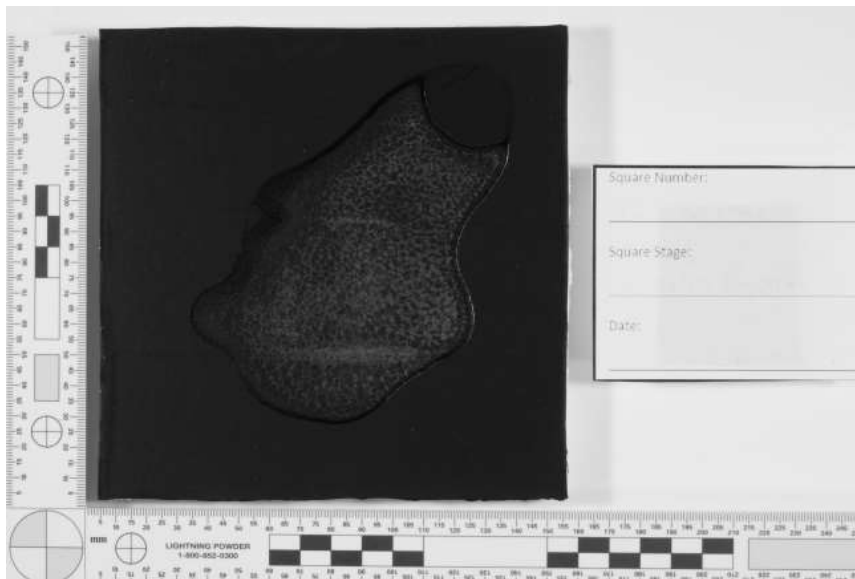


Longpass #89B Single

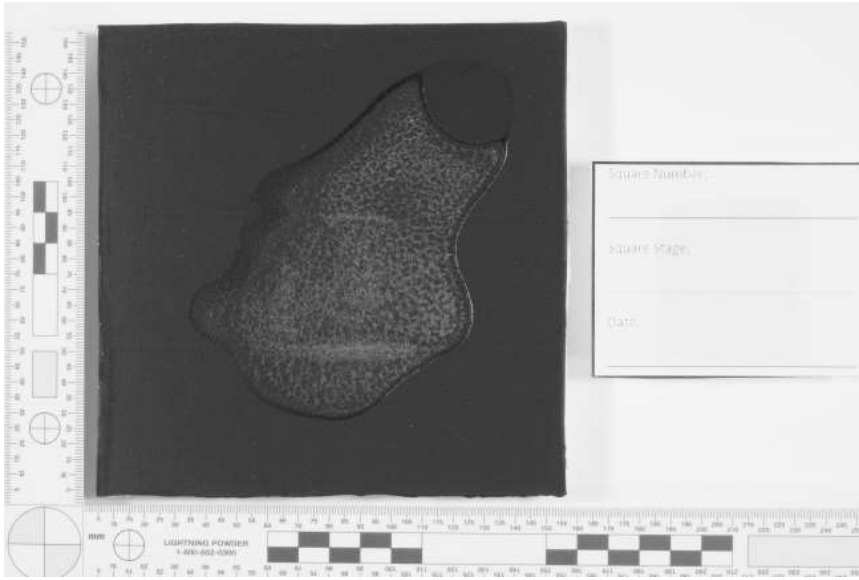
Black Latex 11 – Saturated



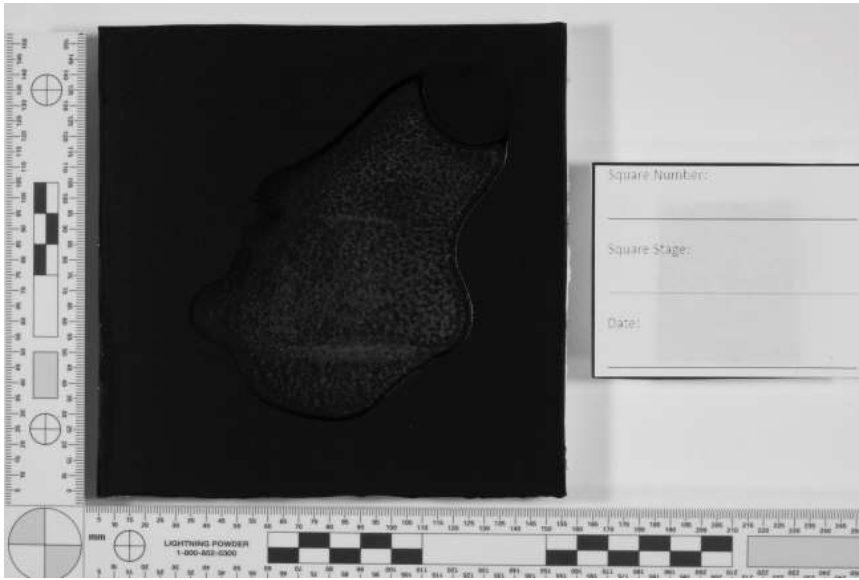
Longpass #70 HDR



Longpass #70 Single



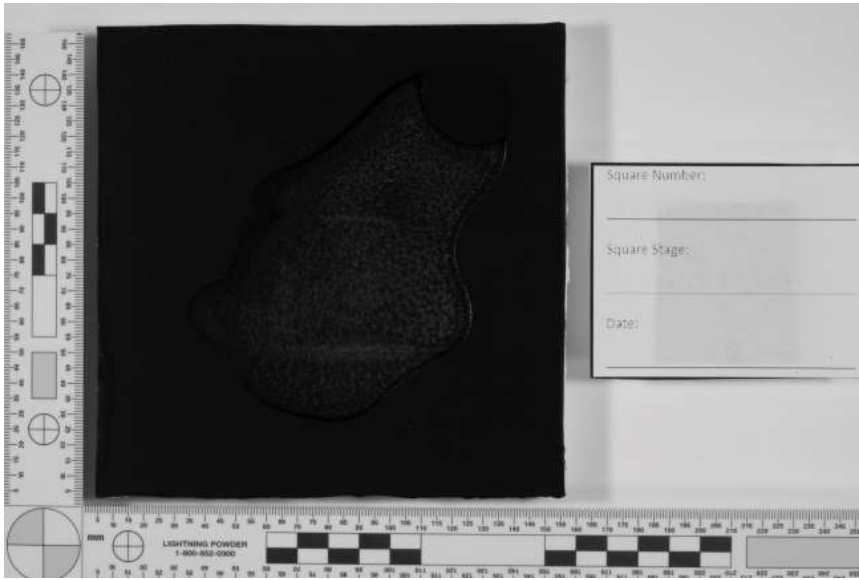
Longpass #87 HDR



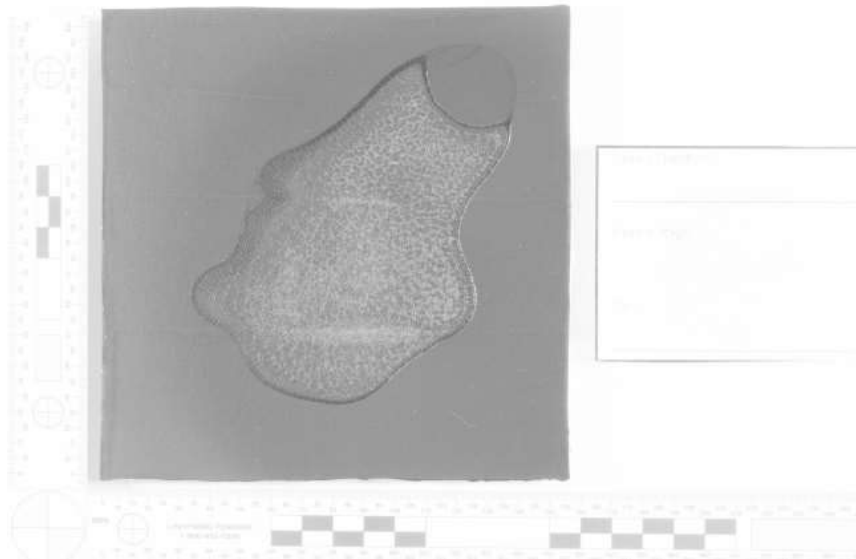
Longpass #87 Single



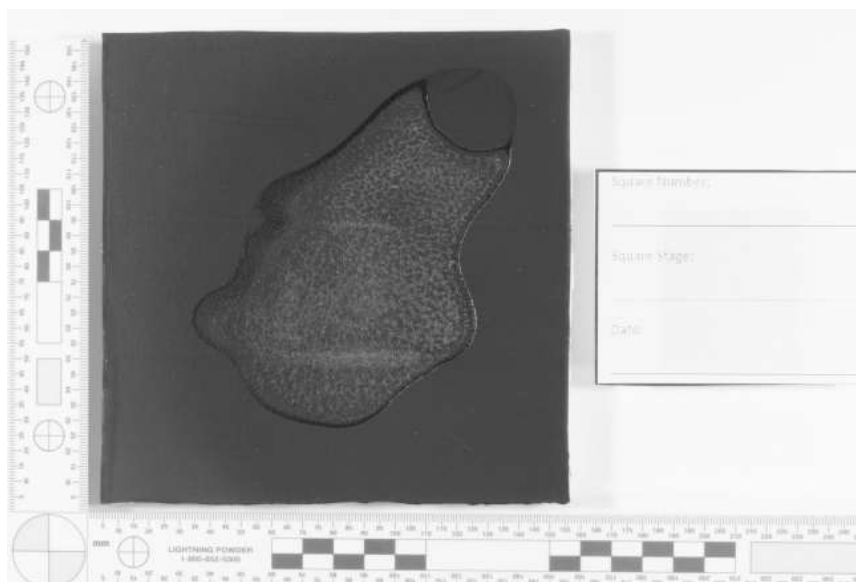
Longpass #87A HDR



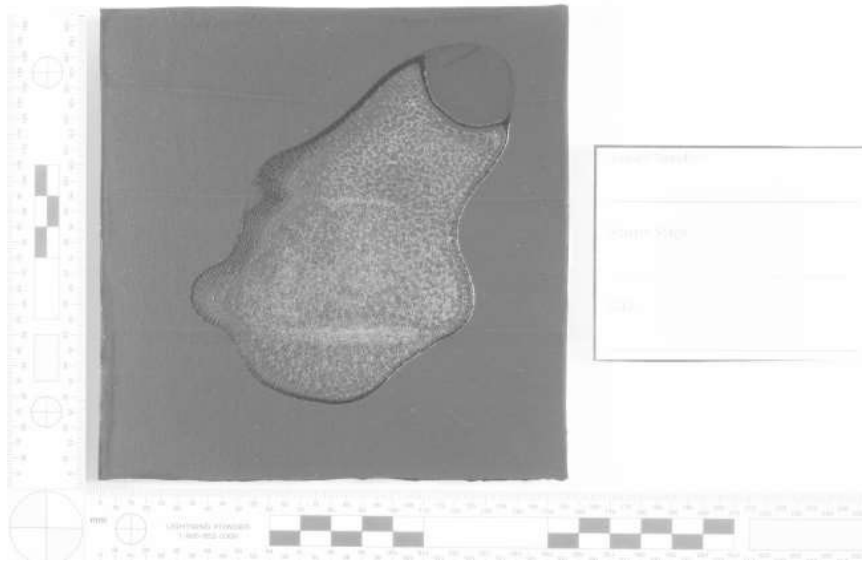
Longpass #87A Single



Longpass #87B HDR



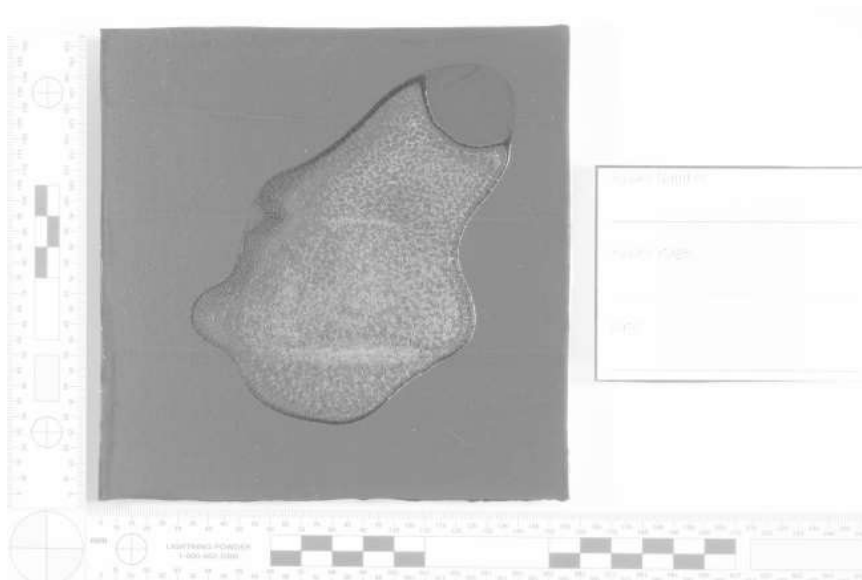
Longpass #87B Single



Longpass #88A HDR



Longpass #88A Single

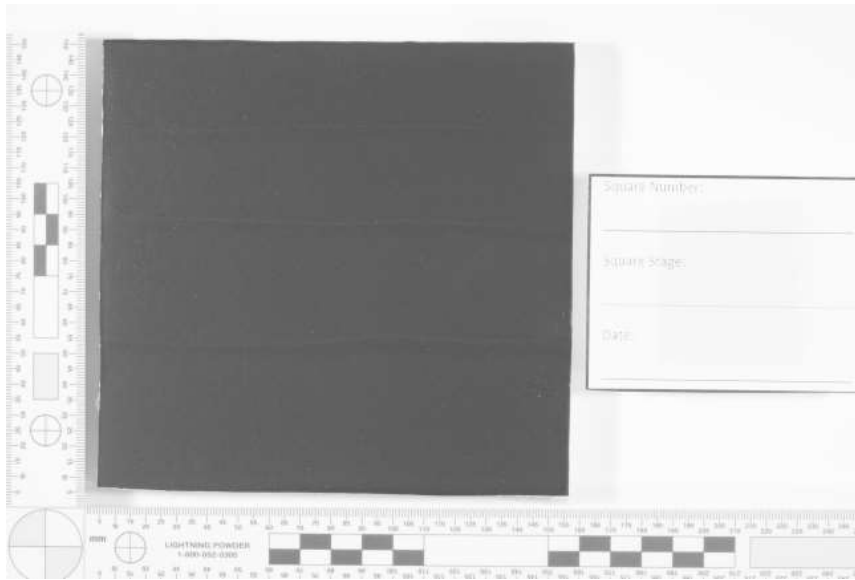


Longpass #89B HDR



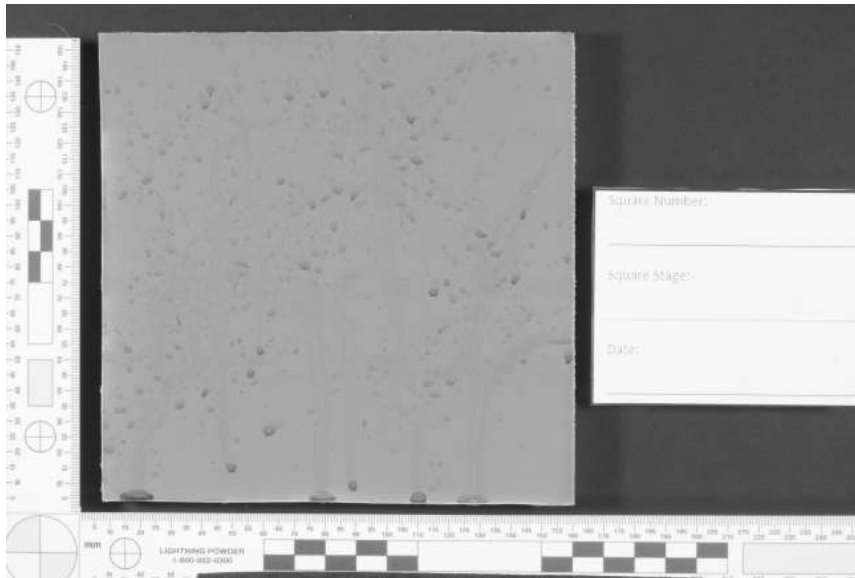
Longpass #89B Single

Black Latex 12 – Control No Blood

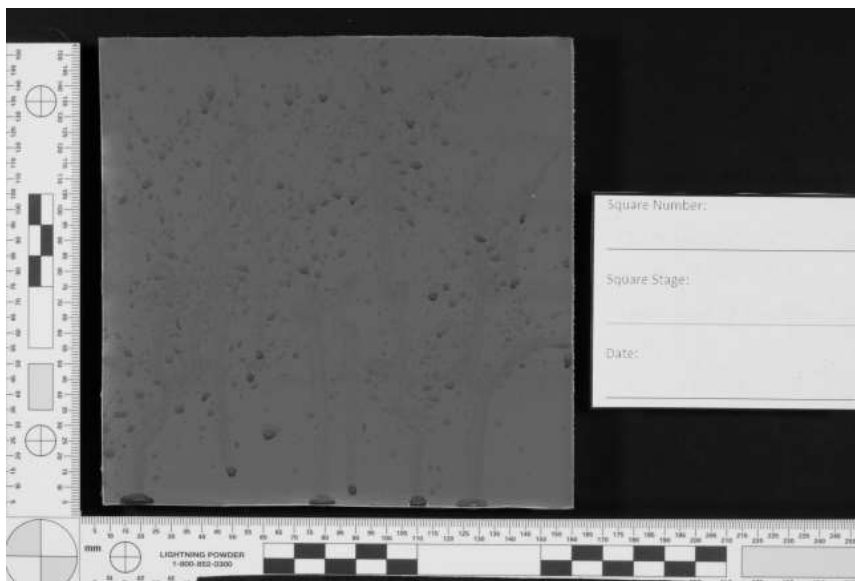


Longpass #70 HDR

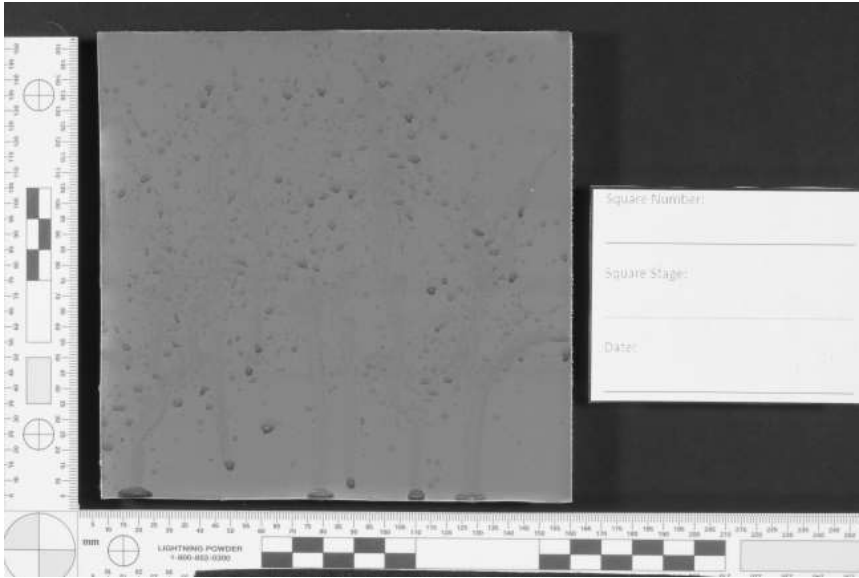
Appendix 4.1.2.4. Maroon Latex – 70, 87, 87A, 87B, 88A, 89B Bloodstain pattern stage
Maroon Latex 13 – Medium Velocity



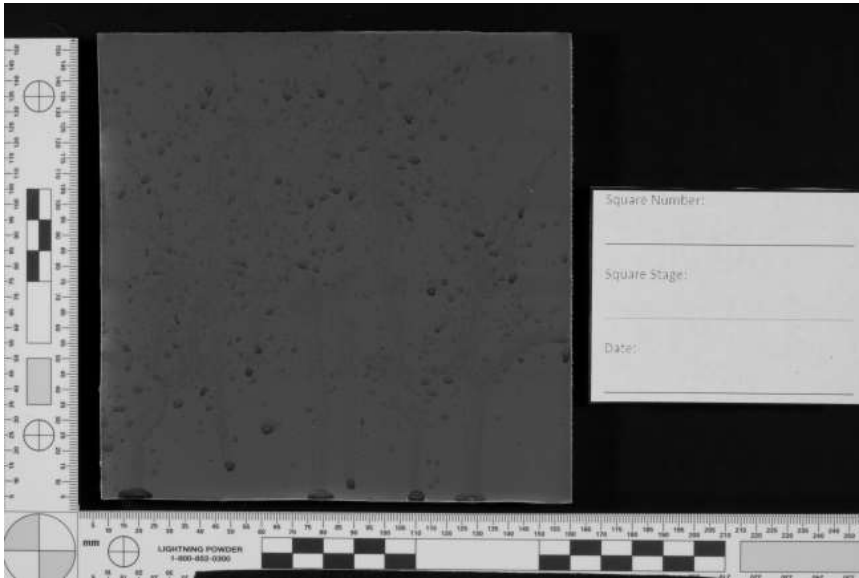
Longpass #70 HDR



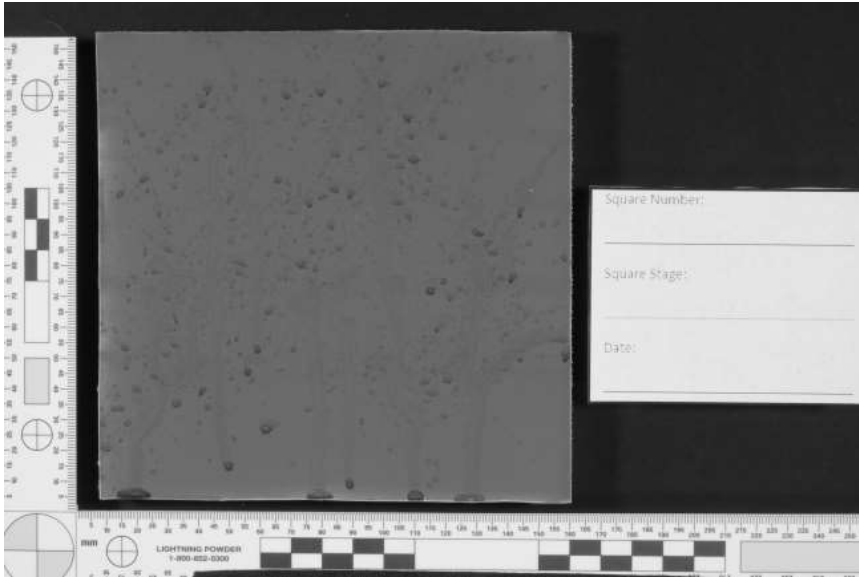
Longpass #70 Single



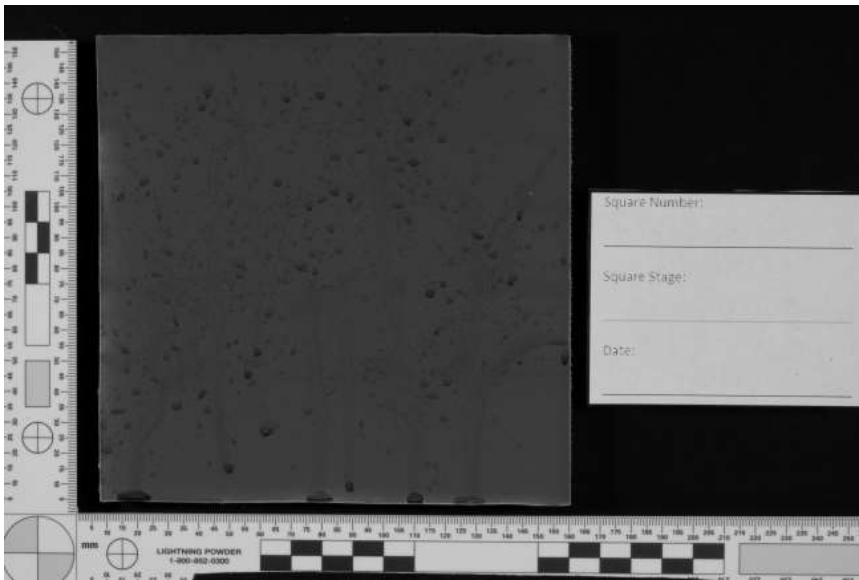
Longpass #87 HDR



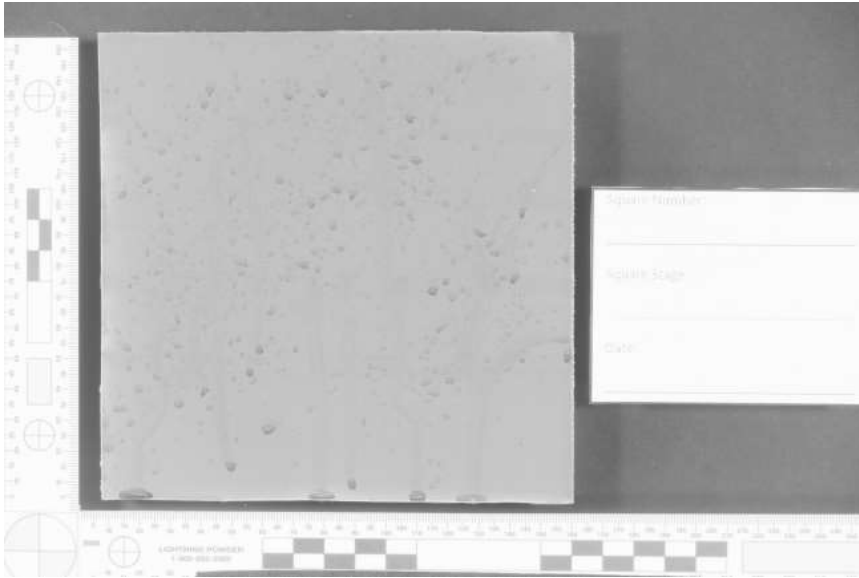
Longpass #87 Single



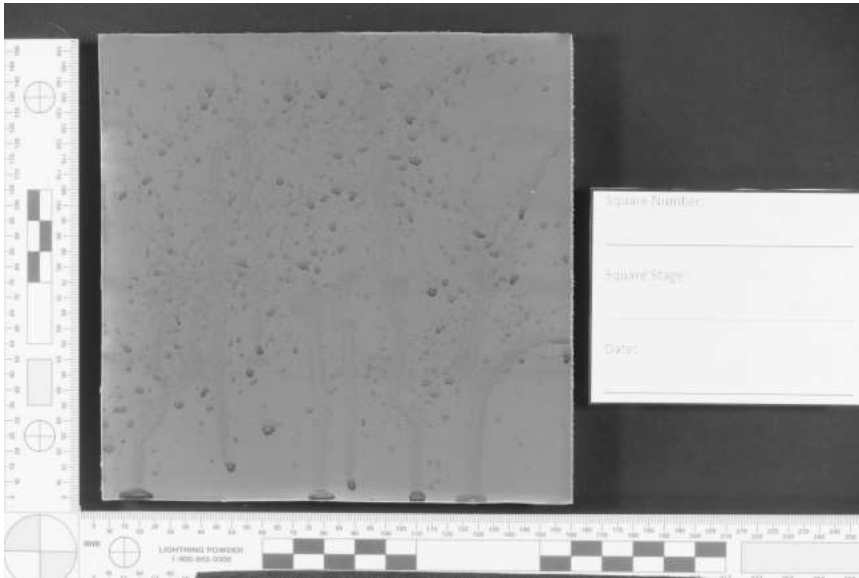
Longpass #87A HDR



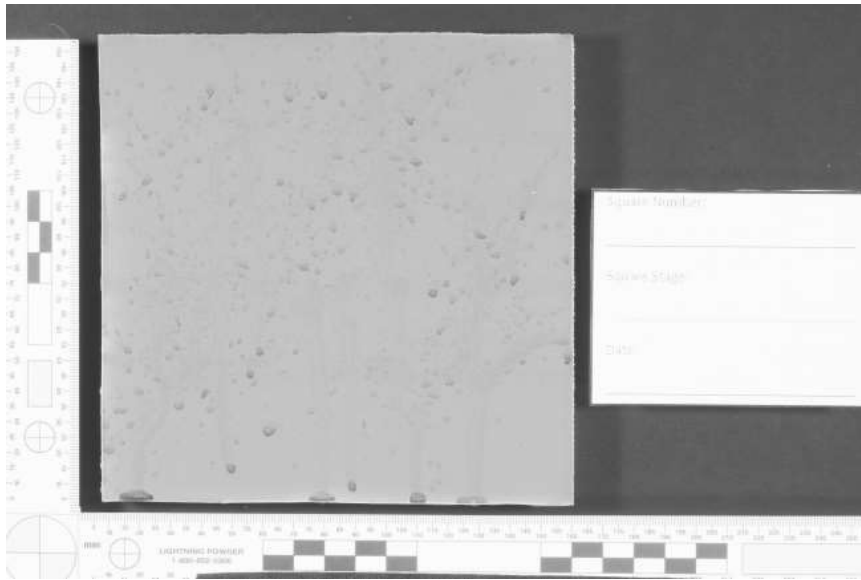
Longpass #87A Single



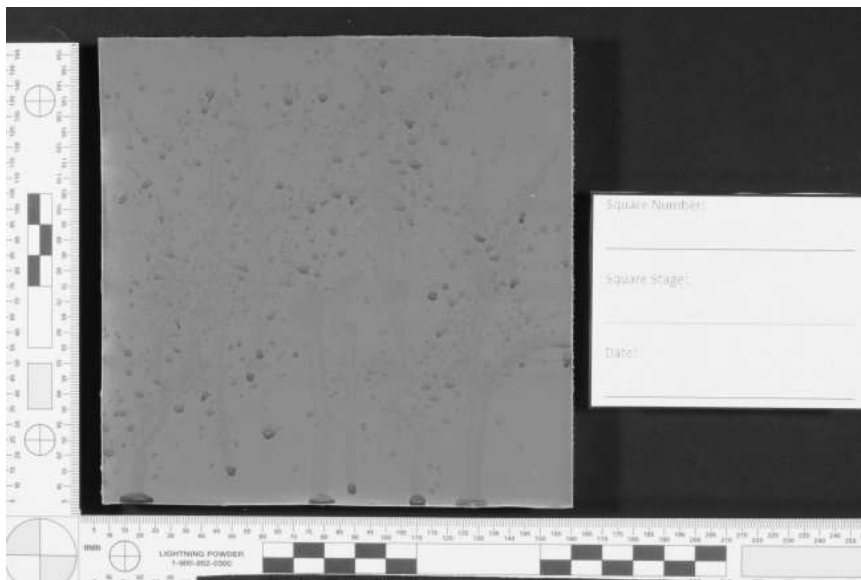
Longpass #87B HDR



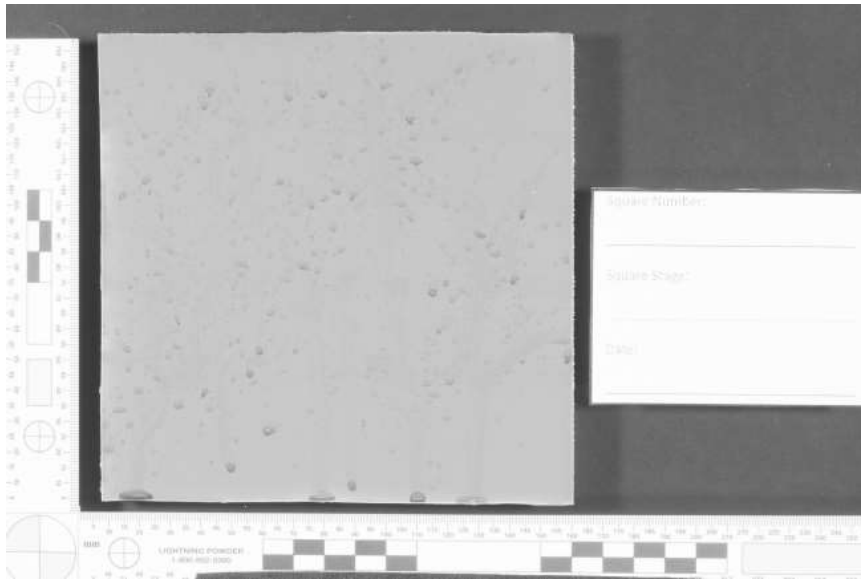
Longpass #87B Single



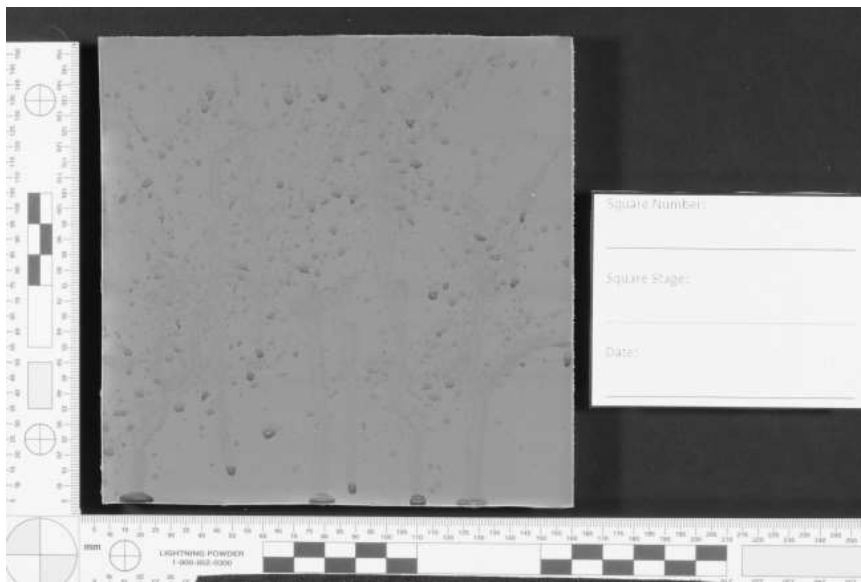
Longpass #88A HDR



Longpass #88A Single



Longpass #89B HDR

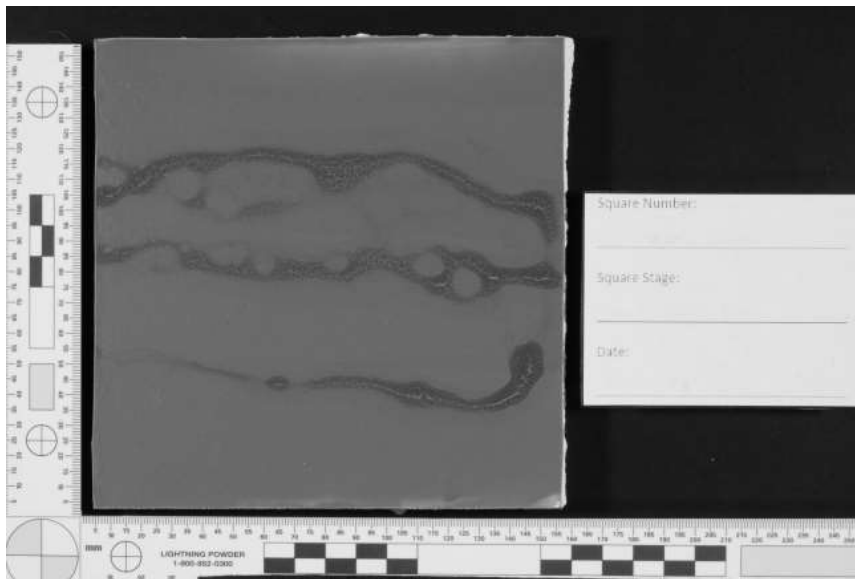


Longpass #89B Single

Maroon Latex 14 – Swipe



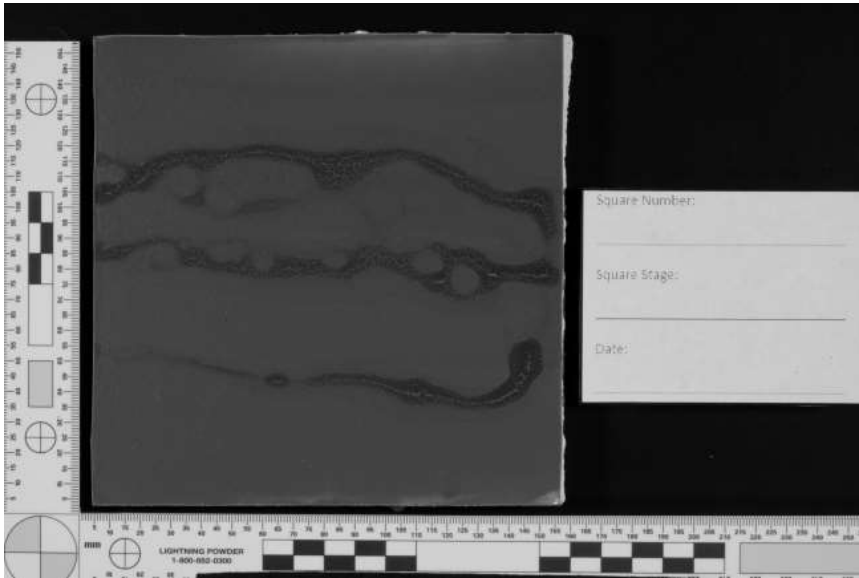
Longpass #70 HDR



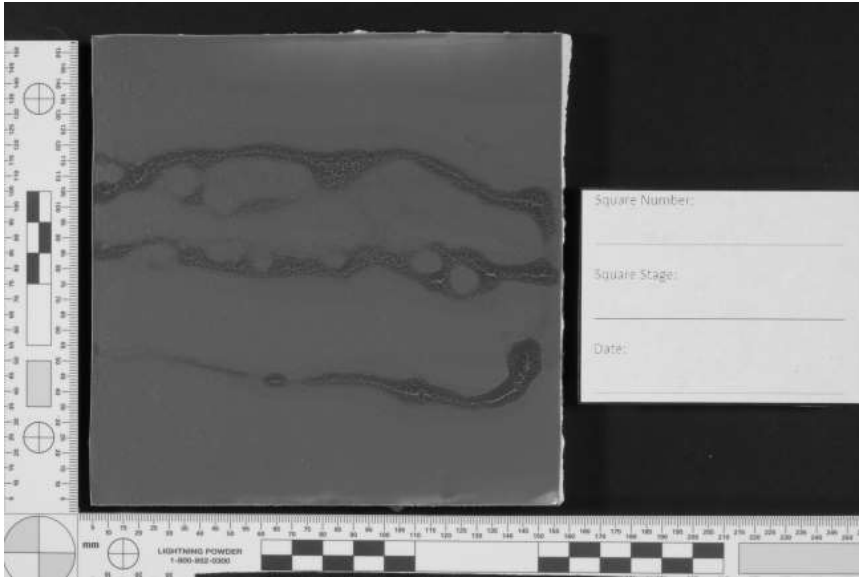
Longpass #70 Single



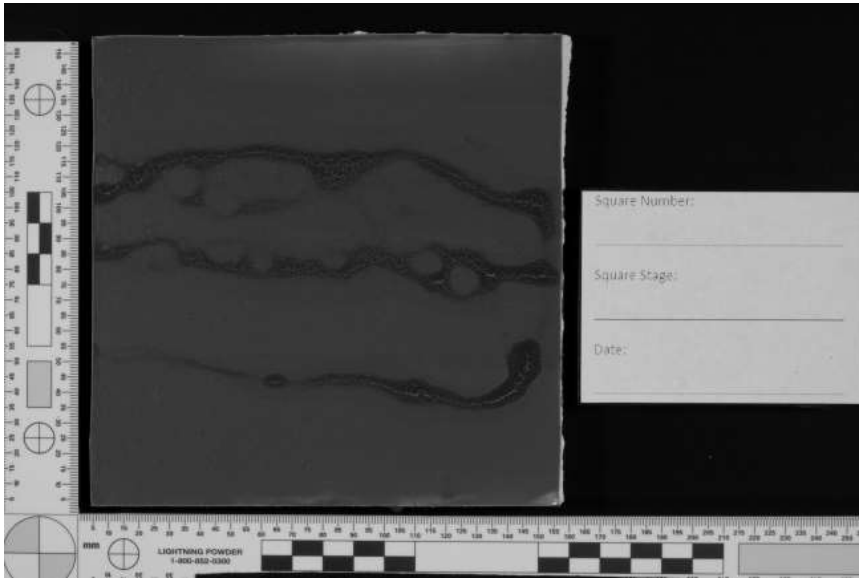
Longpass #87 HDR



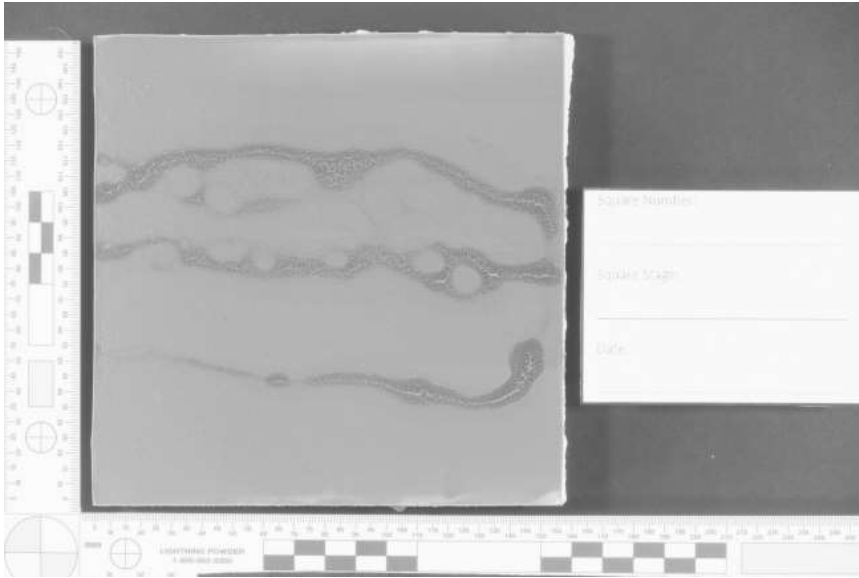
Longpass #87 Single



Longpass #87A HDR



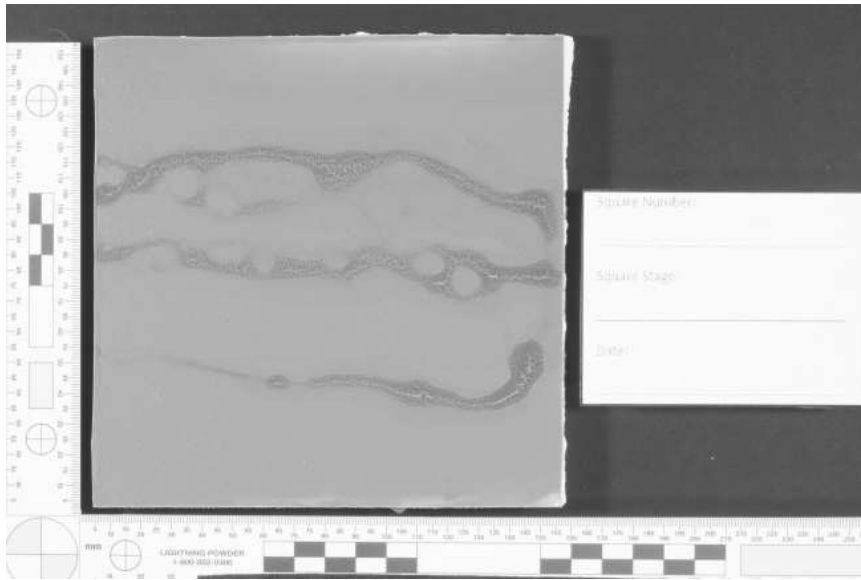
Longpass #87A Single



Longpass #87B HDR



Longpass #87B Single



Longpass #88A HDR



Longpass #88A Single

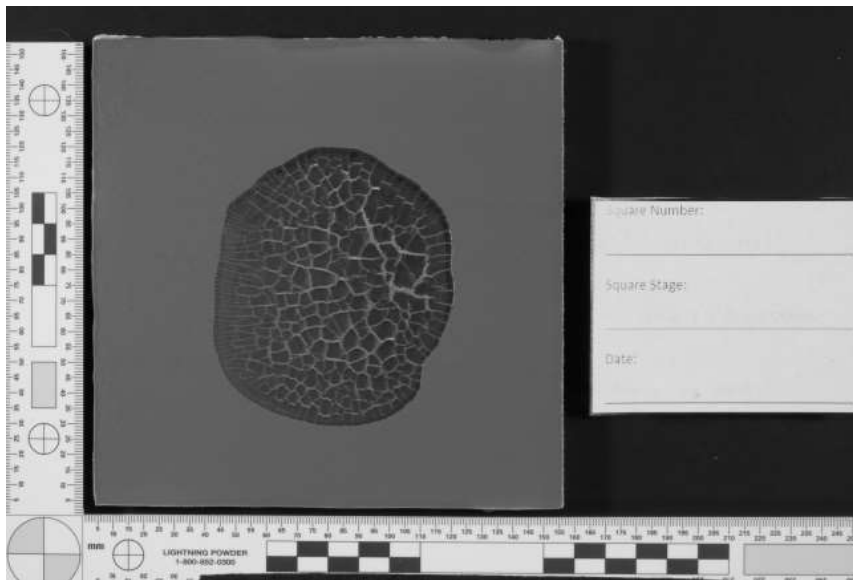


Longpass #89B HDR

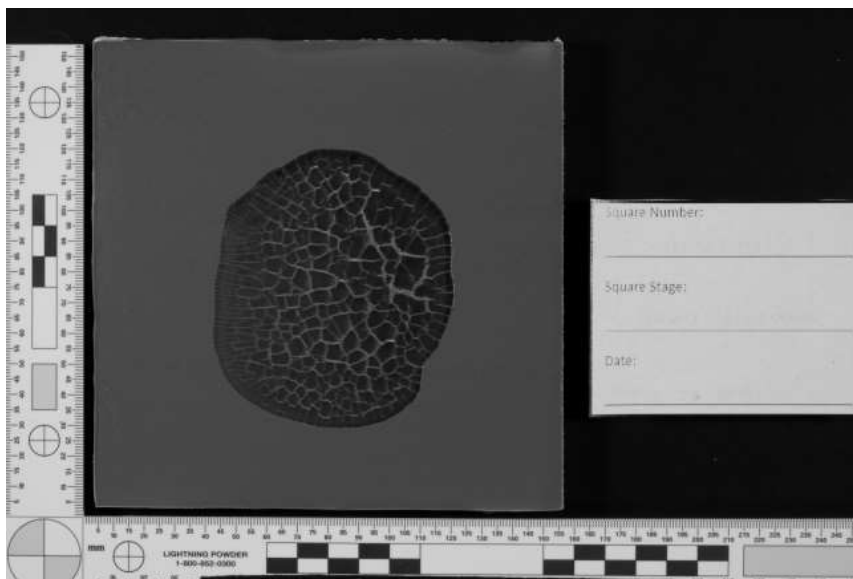


Longpass #89B Single

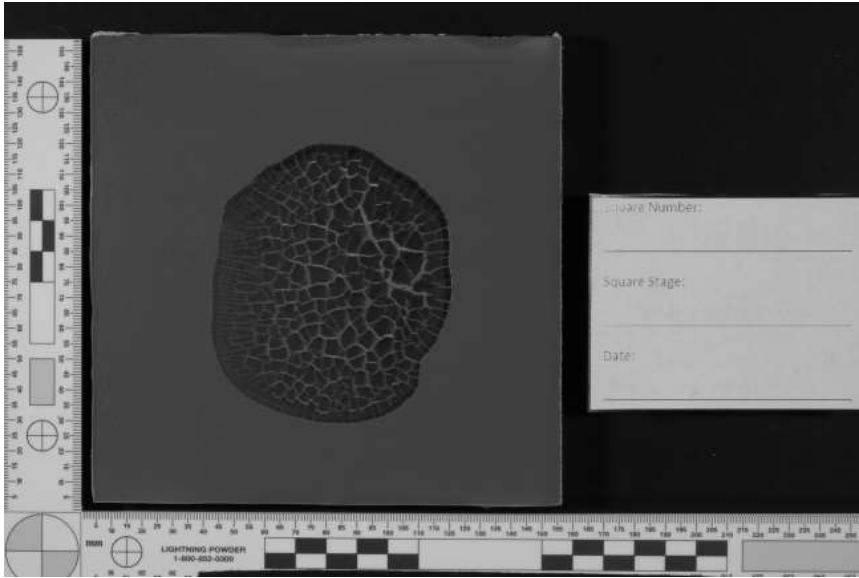
Maroon Latex 15 – Saturated



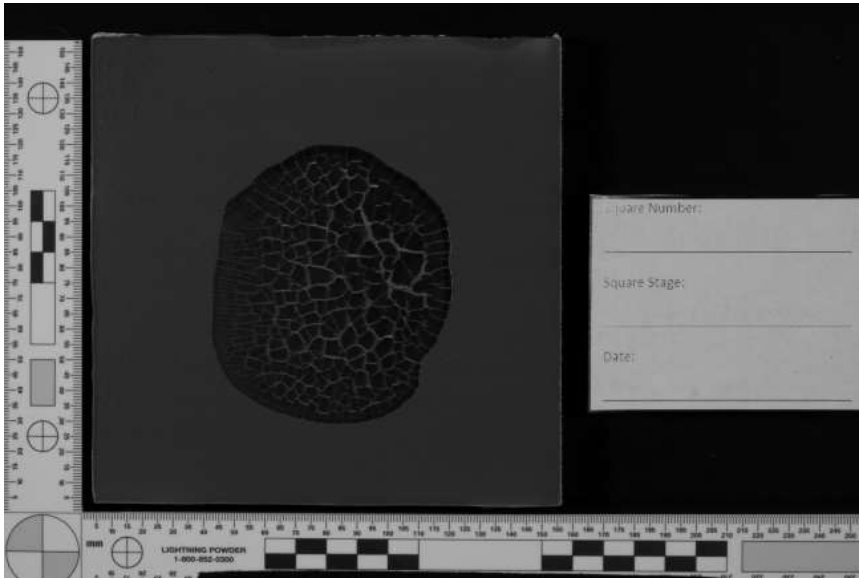
Longpass #70 HDR



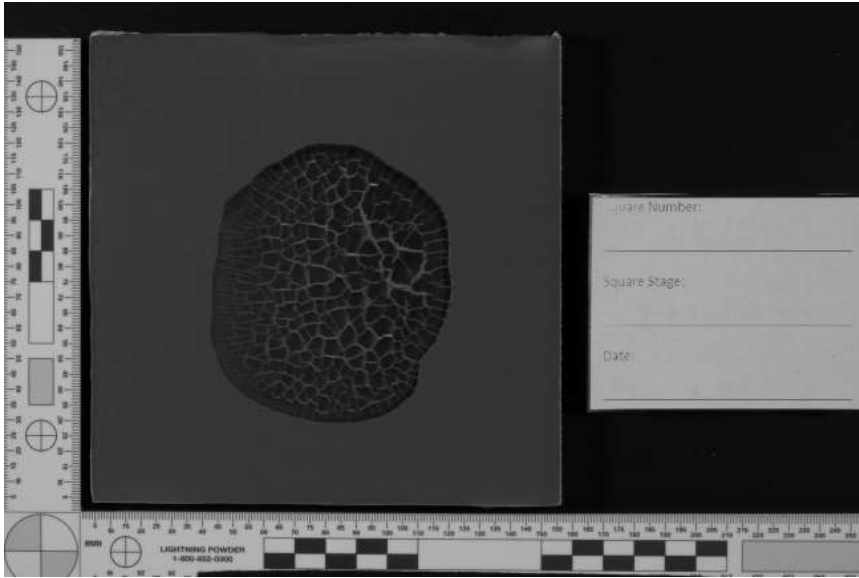
Longpass #70 Single



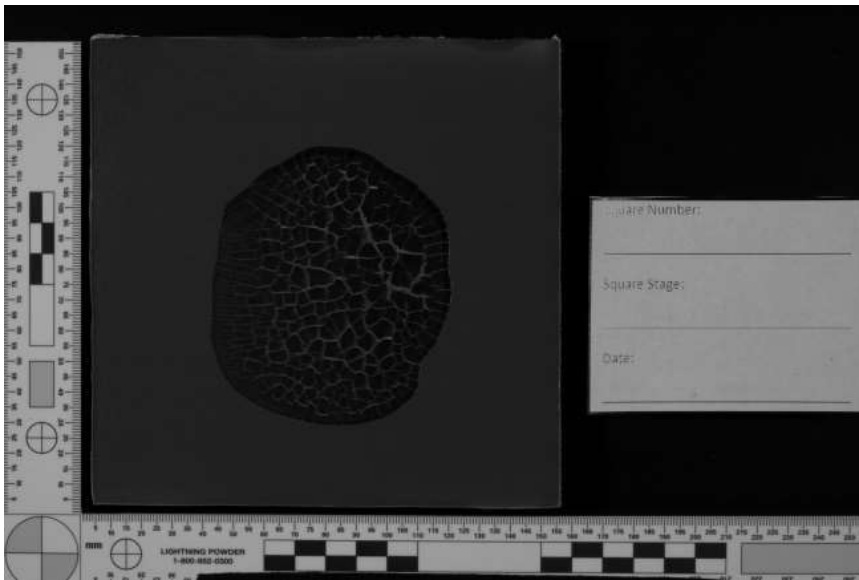
Longpass #87 HDR



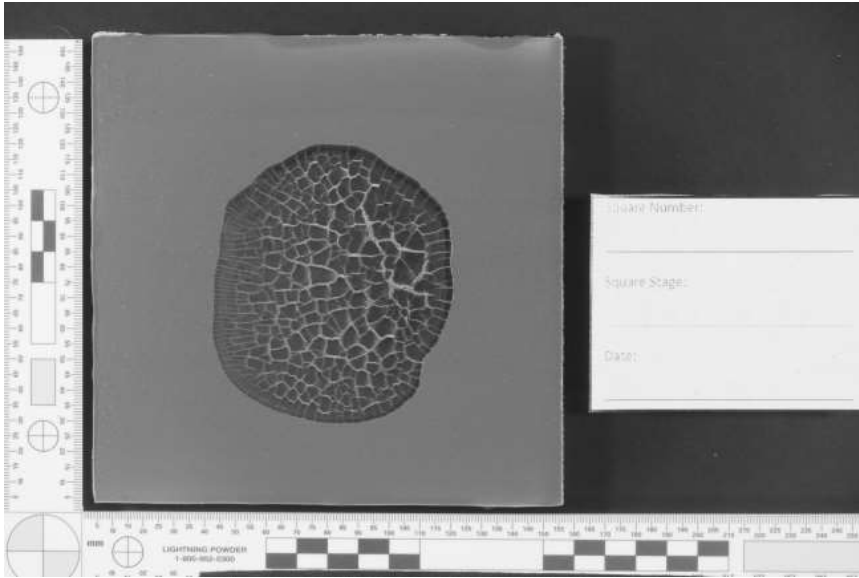
Longpass #87 Single



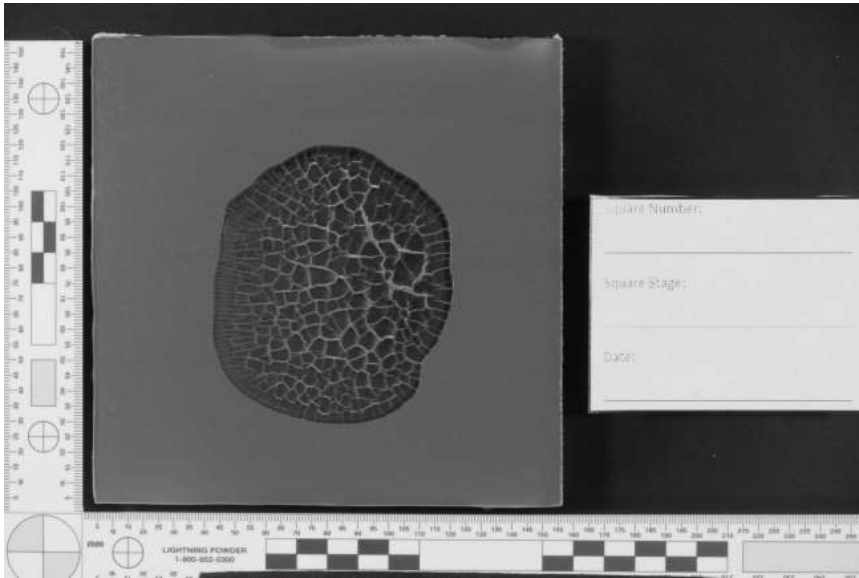
Longpass #87A HDR



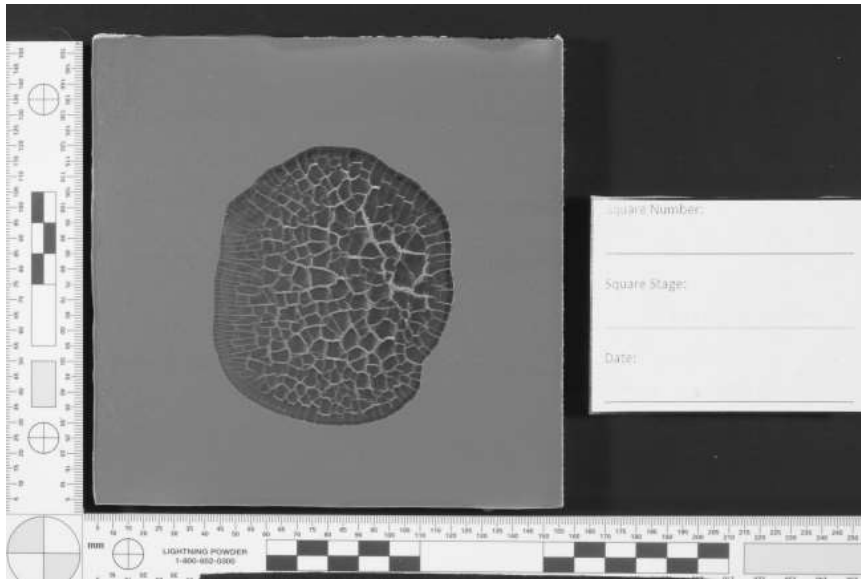
Longpass #87A Single



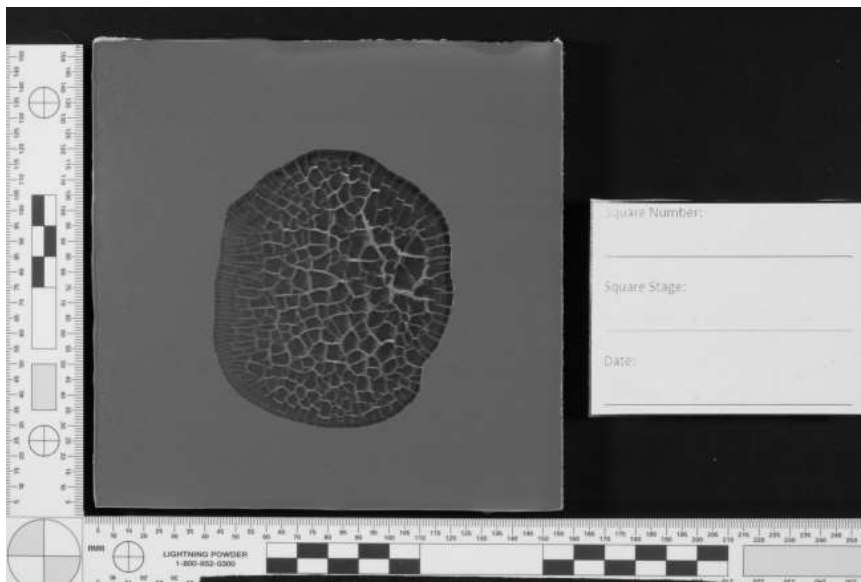
Longpass #87B HDR



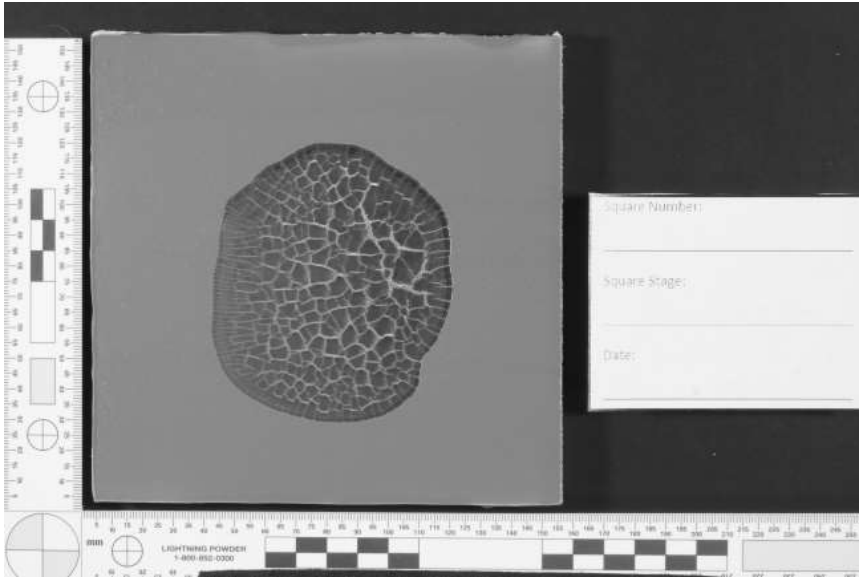
Longpass #87B Single



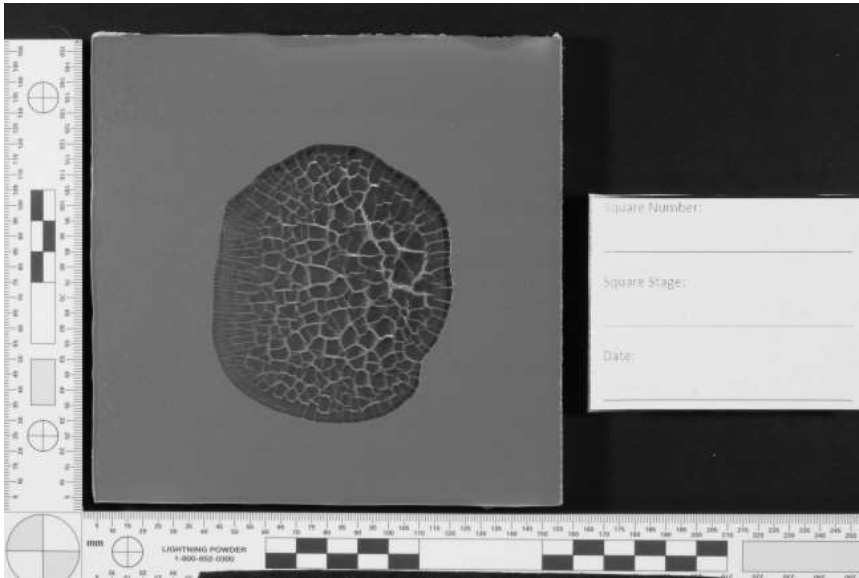
Longpass #88A HDR



Longpass #88A Single

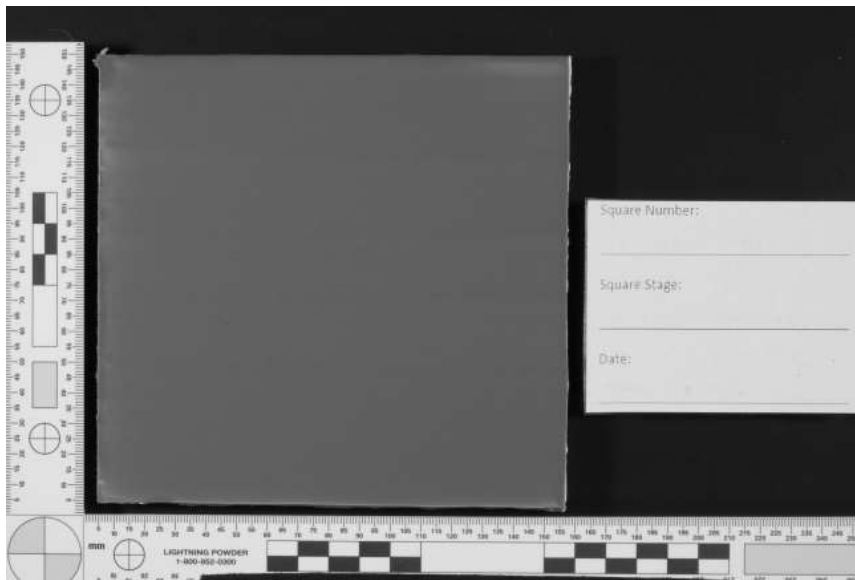


Longpass #89B HDR



Longpass #89B Single

Maroon Latex 16 – Control No Blood



Longpass #70 HDR

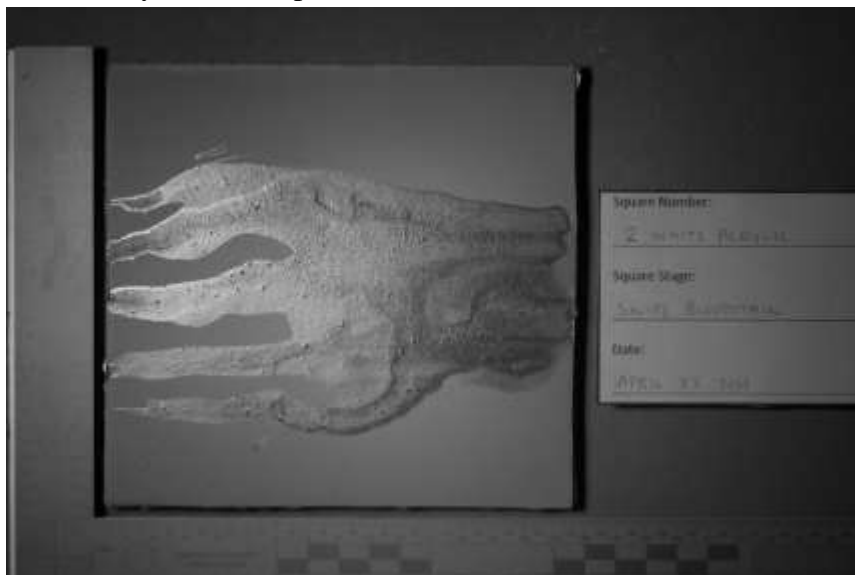
Appendix 4.1.3. Ultraviolet Photography

Appendix 4.1.3.1 White Acrylic Bloodstain pattern stage

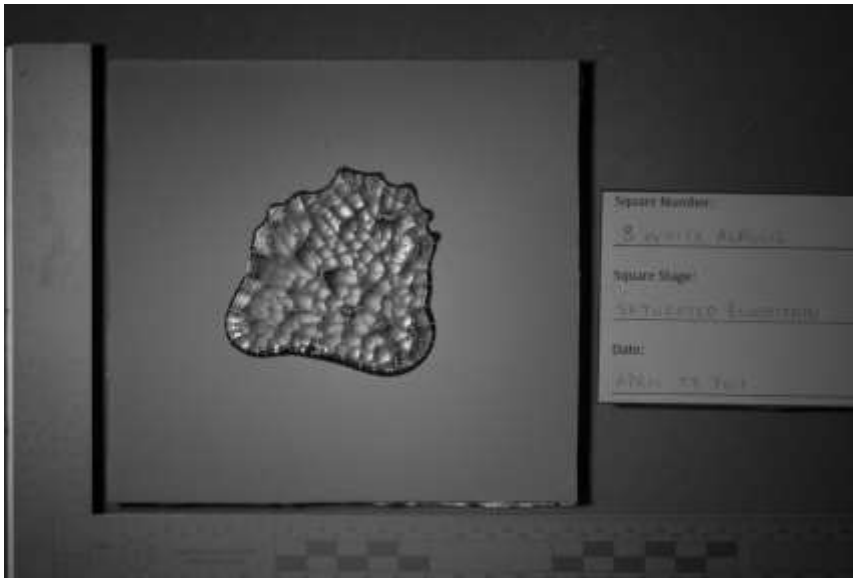
White Acrylic 1 – Medium Velocity



White Acrylic 2 – Swipe



White Acrylic 3 – Saturated



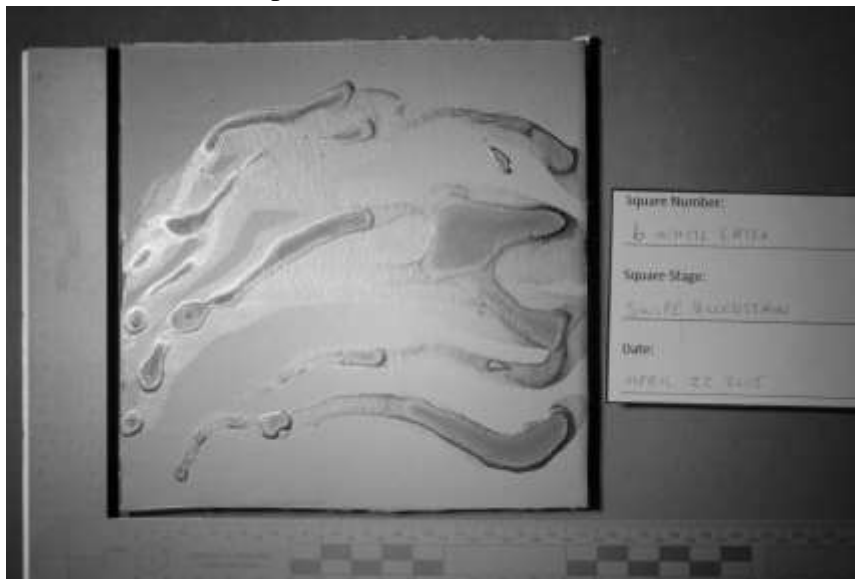
White Acrylic 4 – Control No Bloodstain



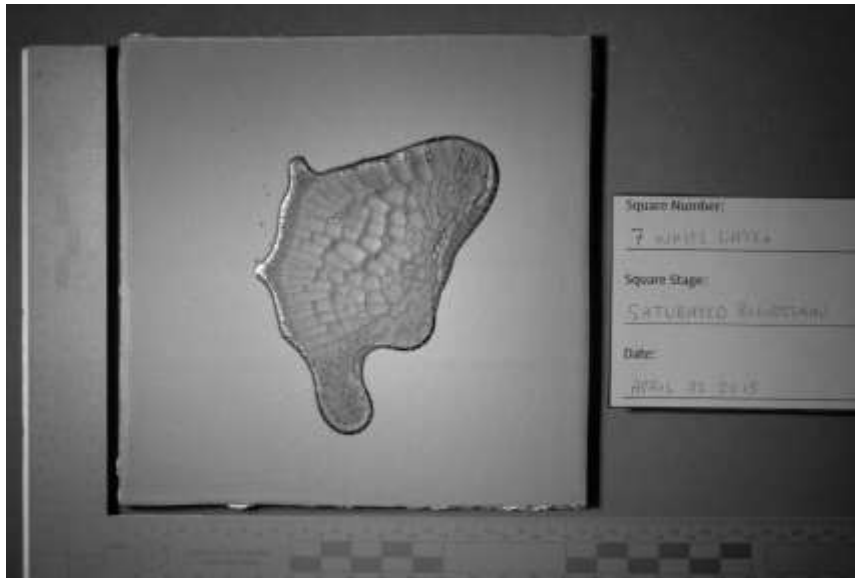
Appendix 4.1.3.2. White Latex Bloodstain pattern stage
White Latex 5 – Medium Velocity



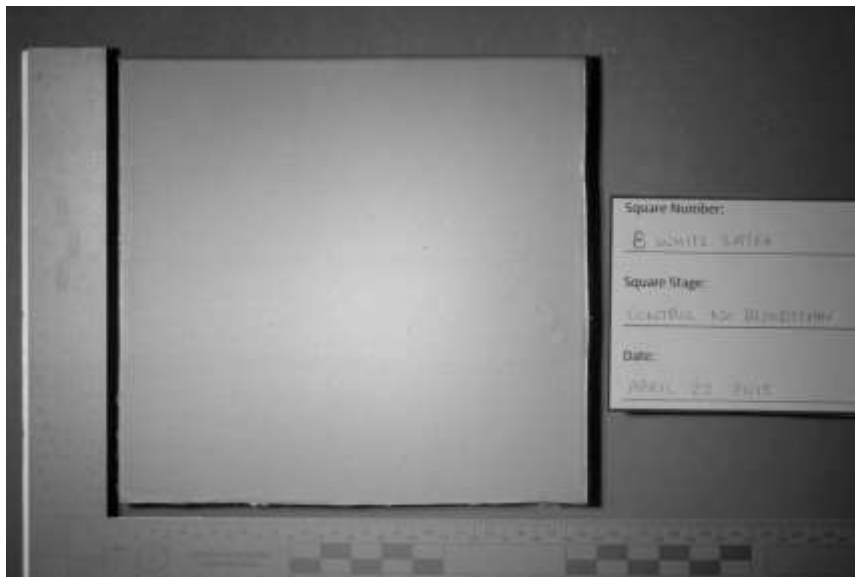
White Latex 6 – Swipe



White Latex 7 – Saturated



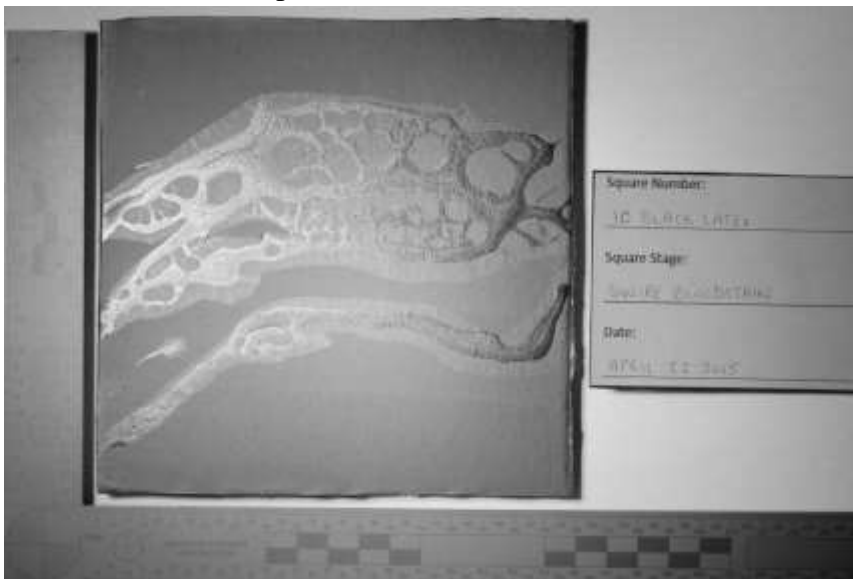
White Latex 8 – Control No Bloodstain



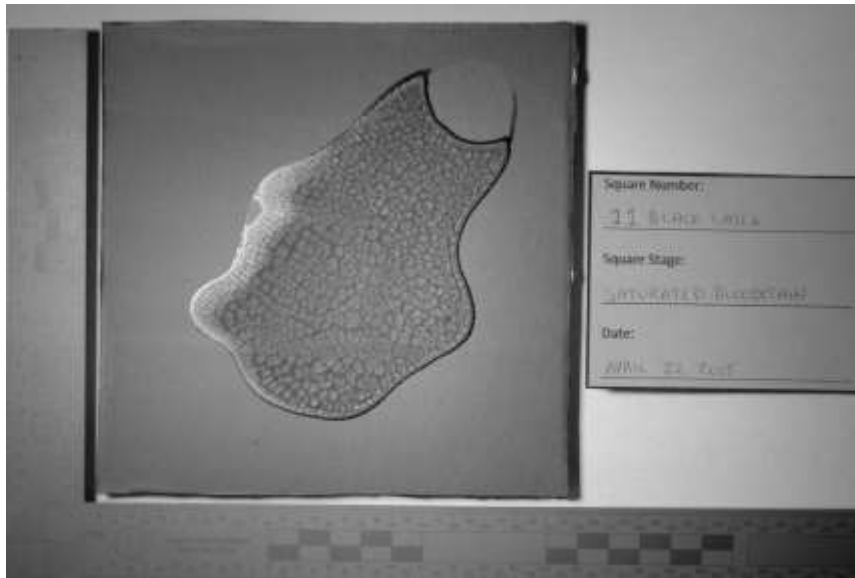
Appendix 4.1.3.3. Black Latex Bloodstain pattern stage
Black Latex 9 – Medium Velocity



Black Latex 10 - Swipe



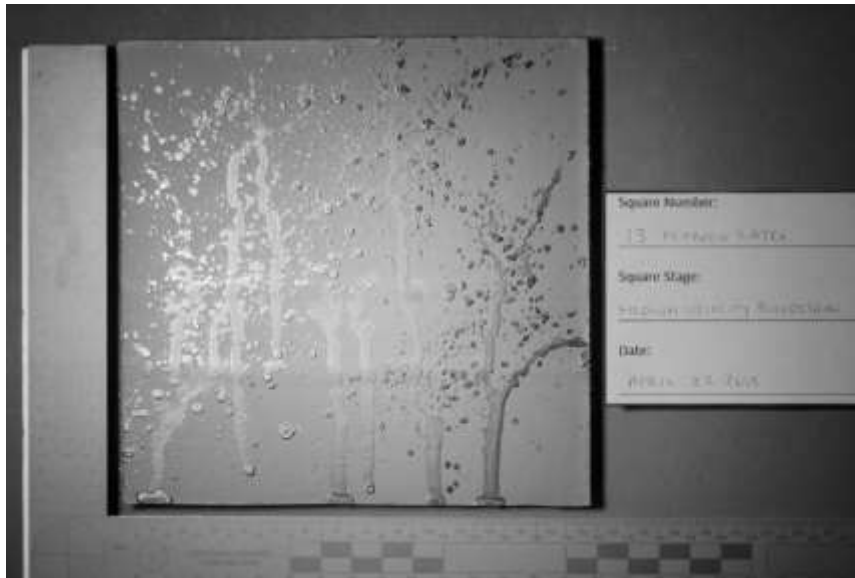
Black Latex 11 – Saturated



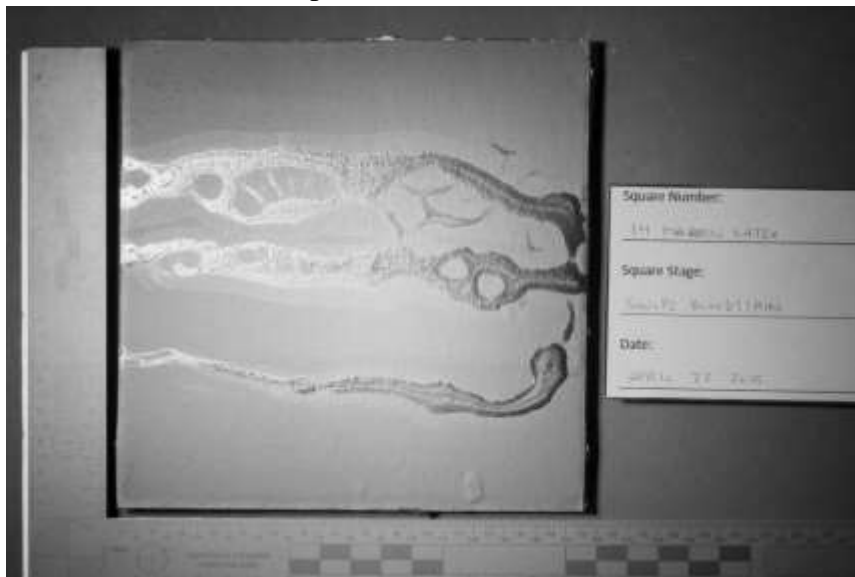
Black Latex 12 – Control No Bloodstain



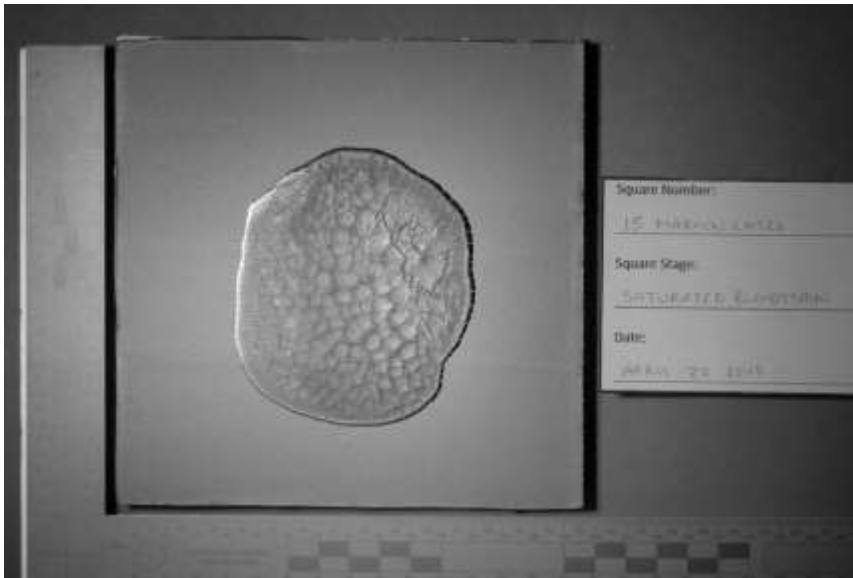
Appendix 4.1.3.4. Maroon Latex Bloodstain pattern stage
Maroon Latex 13 – Medium Velocity



Maroon Latex 14 – Swipe



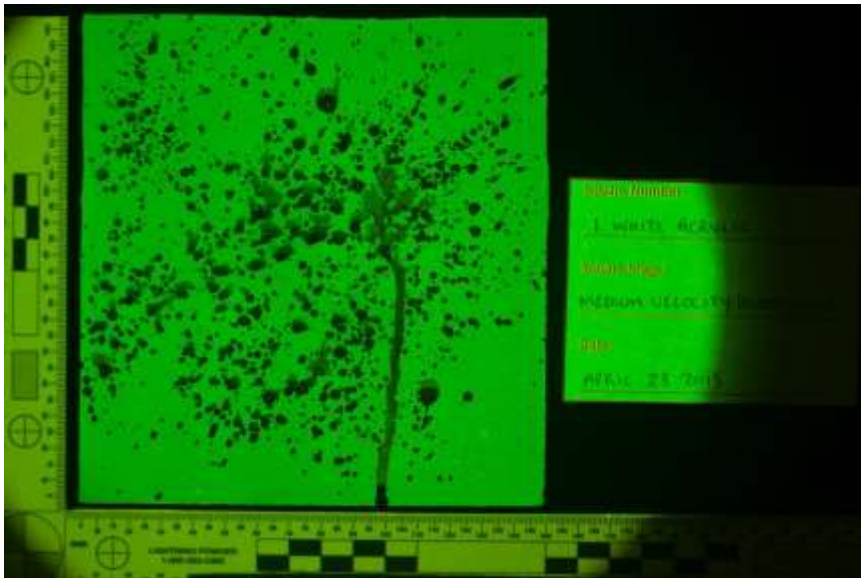
Maroon Latex 15 – Saturated



Maroon Latex 16 – Control No Bloodstain

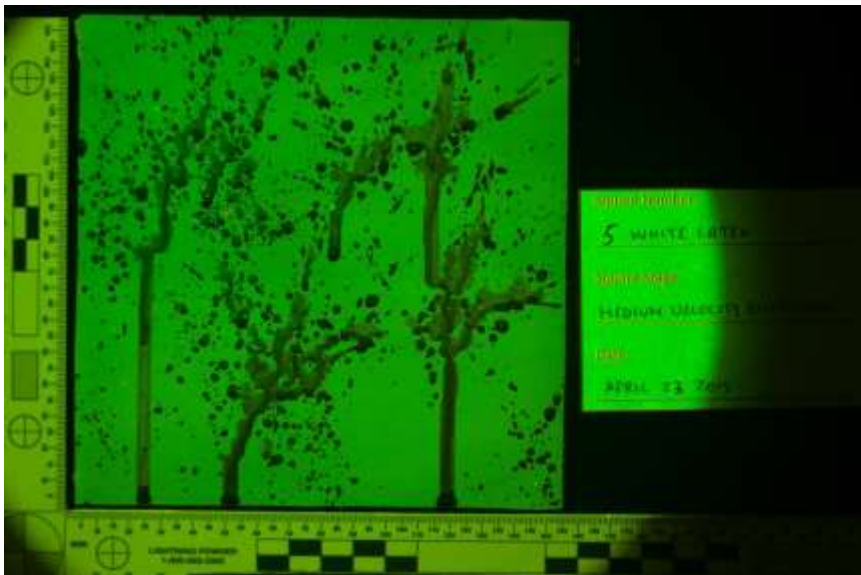


Appendix 4.1.4. Fluorescence Photography Bloodstain pattern stage
Appendix 4.1.4.1. White Acrylic 1 – Medium Velocity



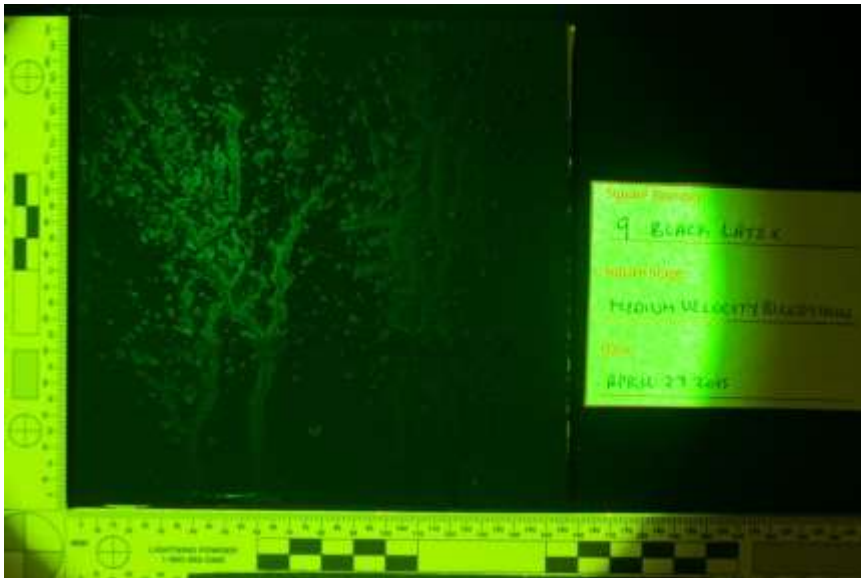
Yellow 445nm

Appendix 4.1.4.2. White Latex 5 – Medium Velocity



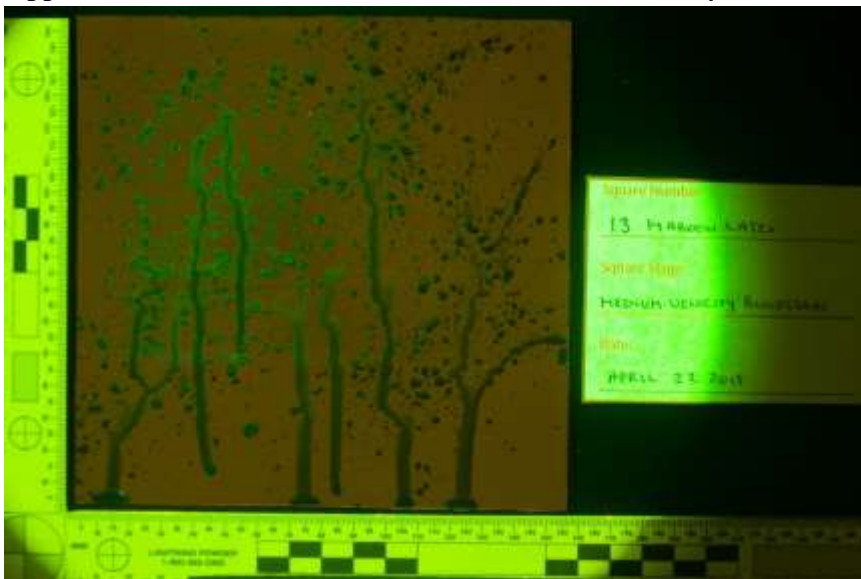
Yellow 445nm

Appendix 4.1.4.3. Black Latex 9 – Medium Velocity



Yellow 445nm

Appendix 4.1.4.4. Maroon Latex 13 – Medium Velocity



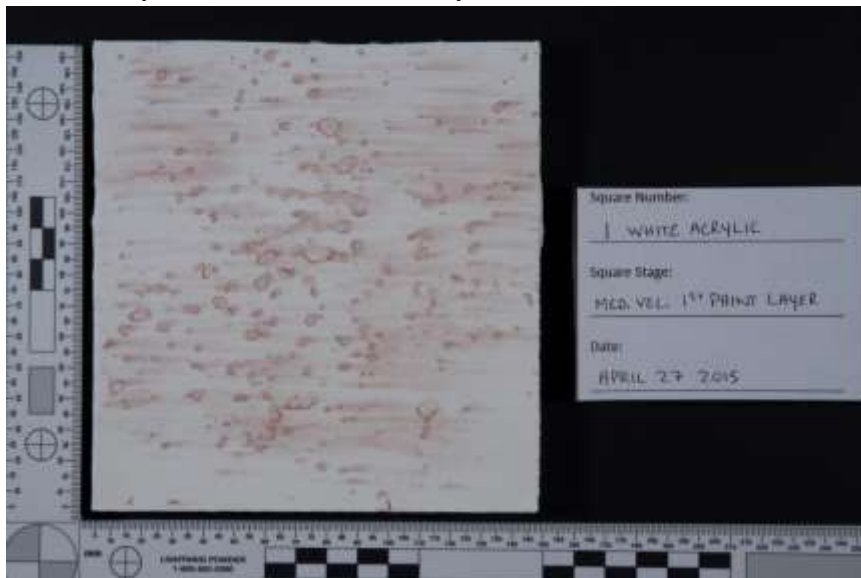
Yellow 445nm

First Layer of Paint over Bloodstain Patterns Stage

Appendix 4.2.2. Standard Photography

Appendix 4.2.2.1. White Acrylic First layer of paint stage

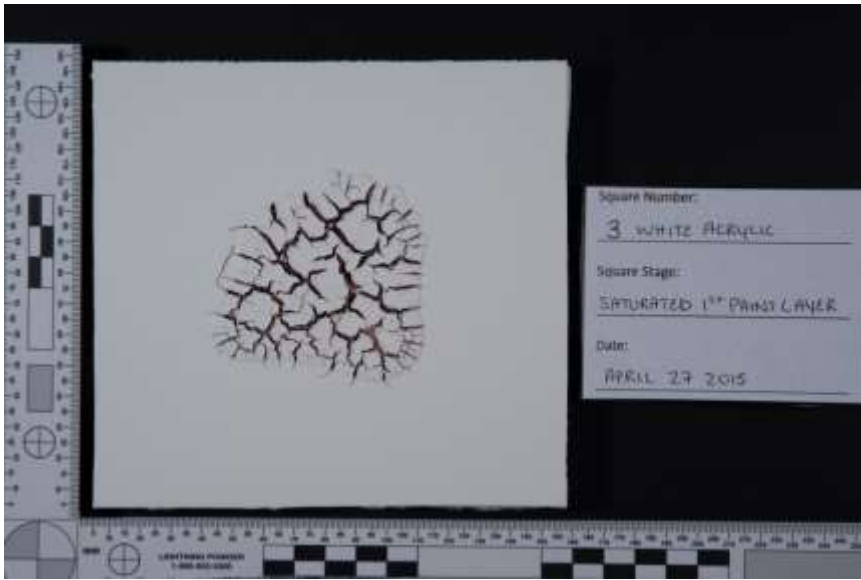
White Acrylic 1 – Medium Velocity



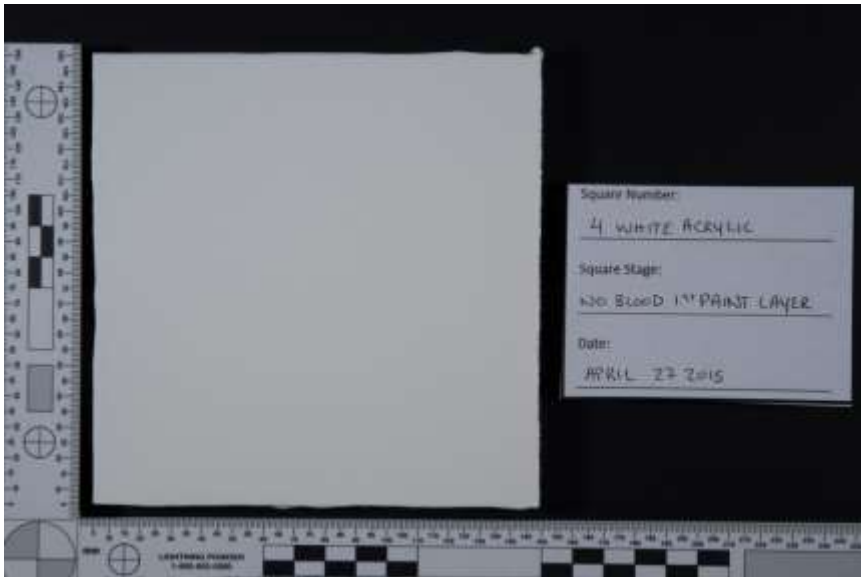
White Acrylic 2 – Swipe



White Acrylic 3 – Saturated



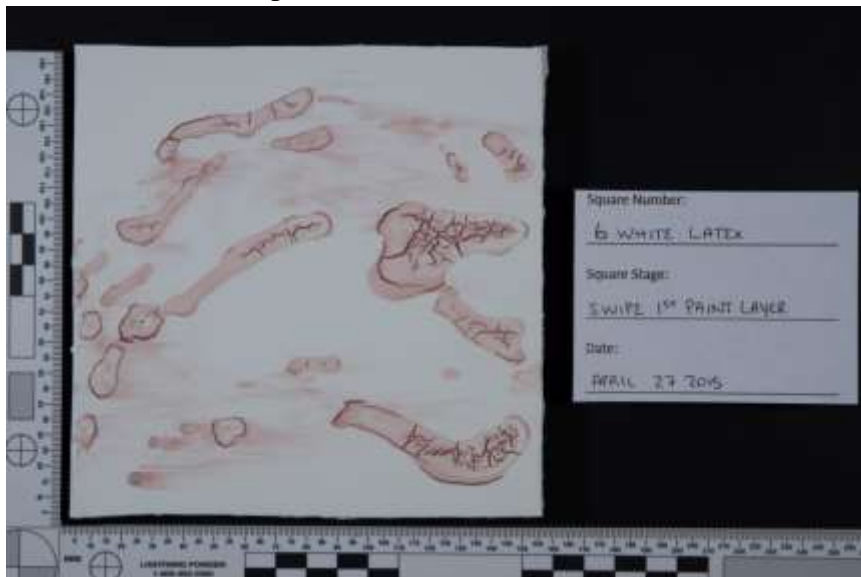
White Acrylic 4 – Control No Bloodstain



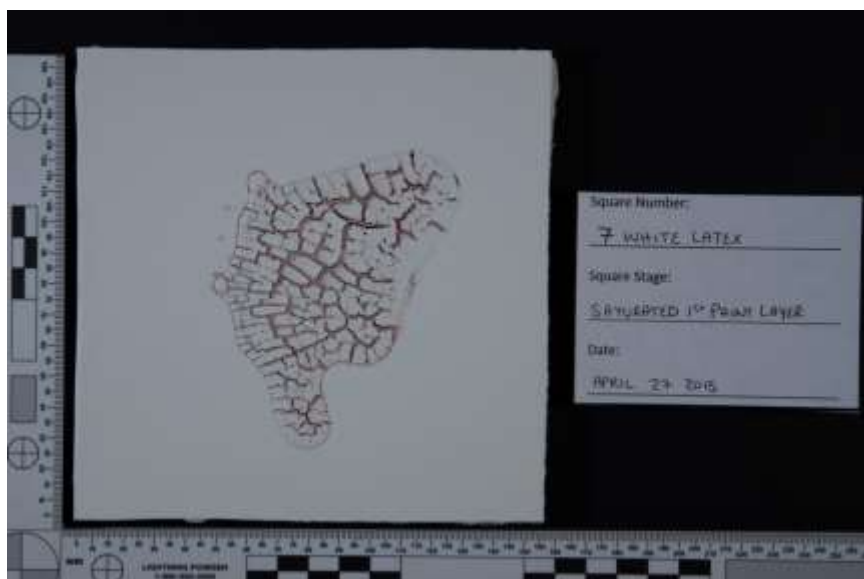
Appendix 4.2.2.2. White Latex First layer of paint stage
White Latex 5 – Medium Velocity



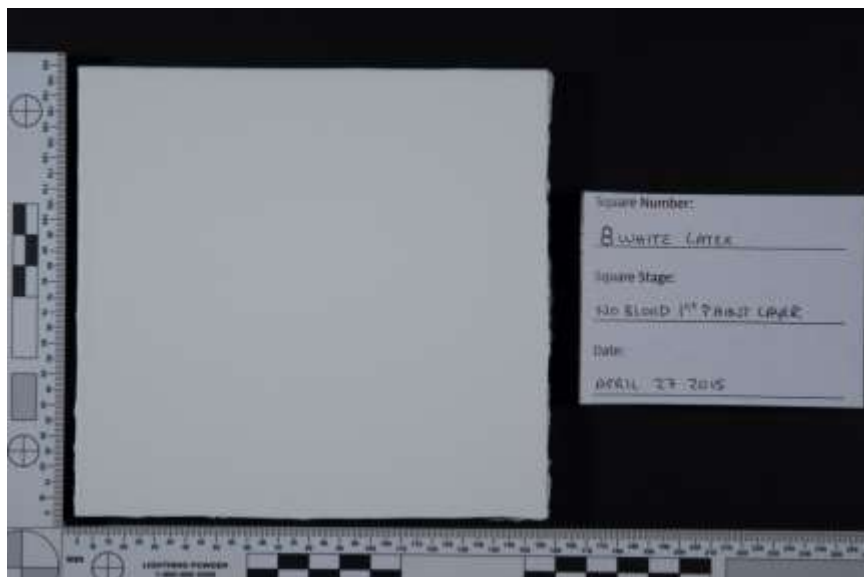
White Latex 6 – Swipe



White Latex 7 – Saturated



White Latex 8 – Control No Bloodstain



Appendix 4.2.2.3. Black Latex First layer of paint stage
Black Latex 9 – Medium Velocity



Black Latex 10 – Swipe



Black Latex 11 – Saturated



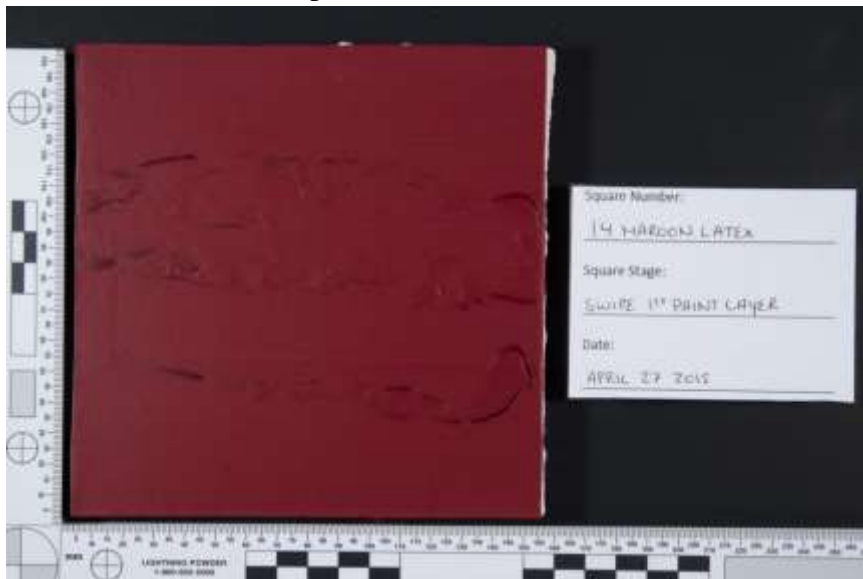
Black Latex 12 – Control No Bloodstain



Appendix 4.2.2.4. Maroon Latex First layer of paint stage
Maroon Latex 13 – Medium Velocity



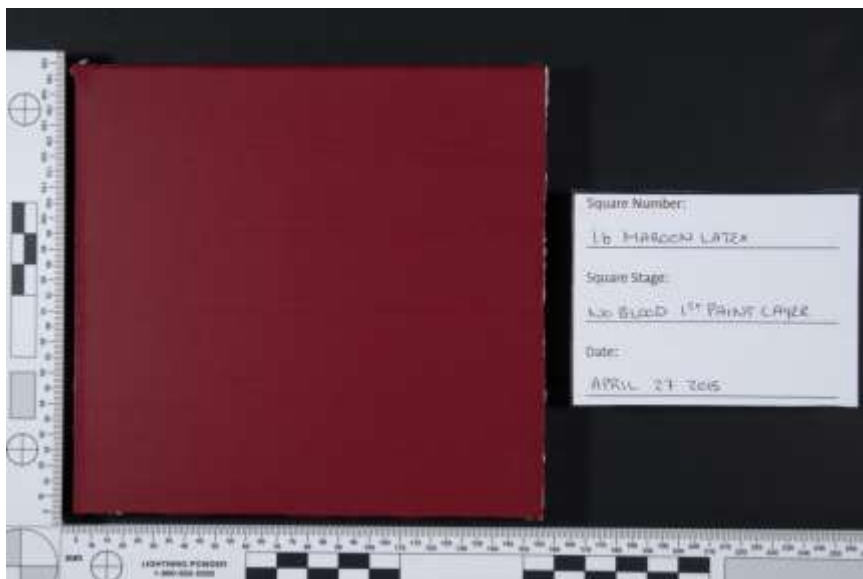
Maroon Latex 14 – Swipe



Maroon Latex 15 – Saturated



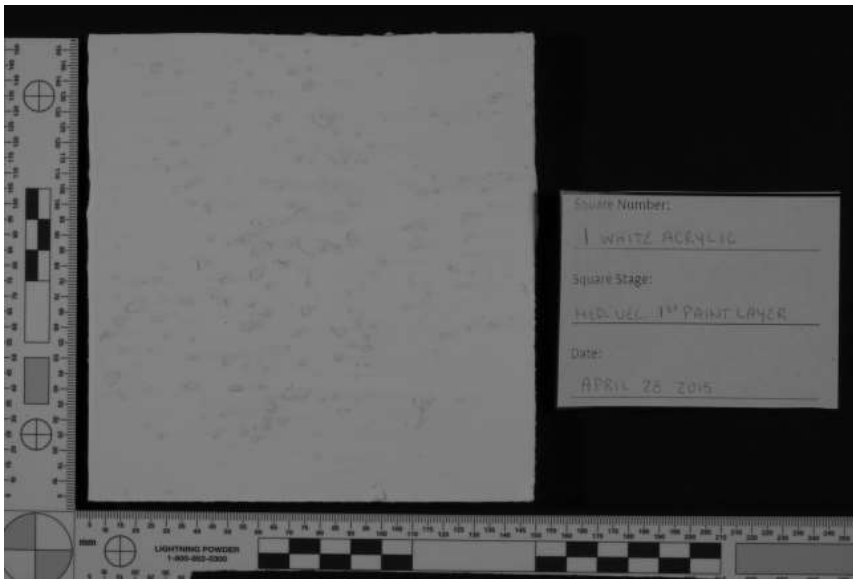
Maroon Latex 16 – Control No Bloodstain



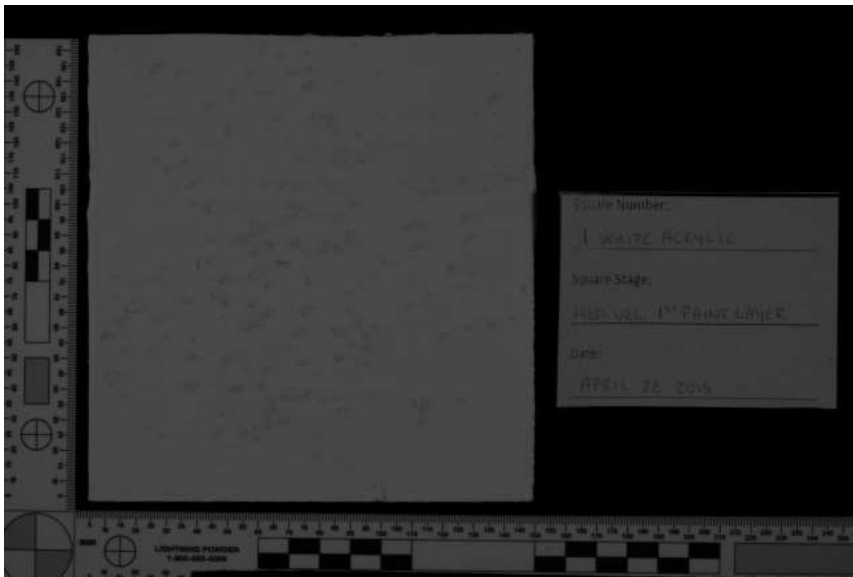
Appendix 4.2.3. Reflective Infrared Photography

Appendix 4.2.3.1. White Acrylic 70, 87, 87A, 87B, 88A, 89B First layer of paint stage

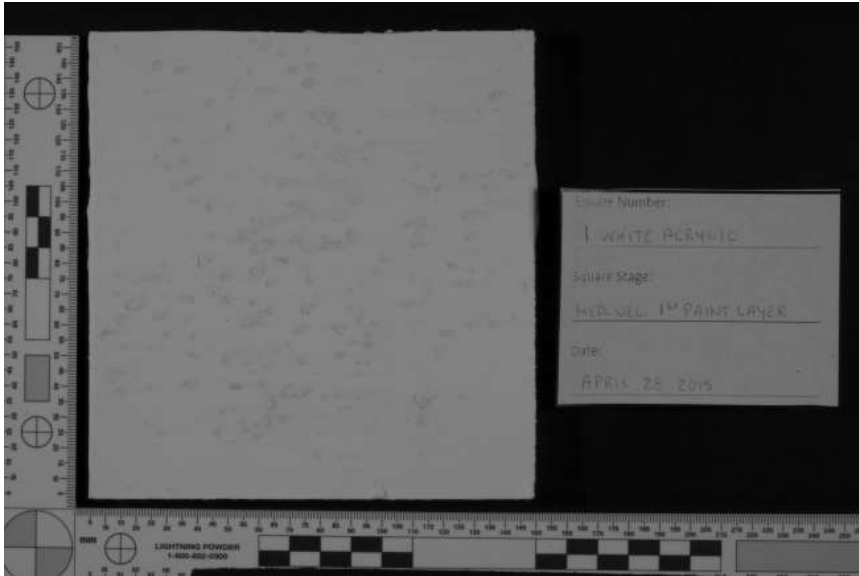
White Acrylic 1 – Medium Velocity



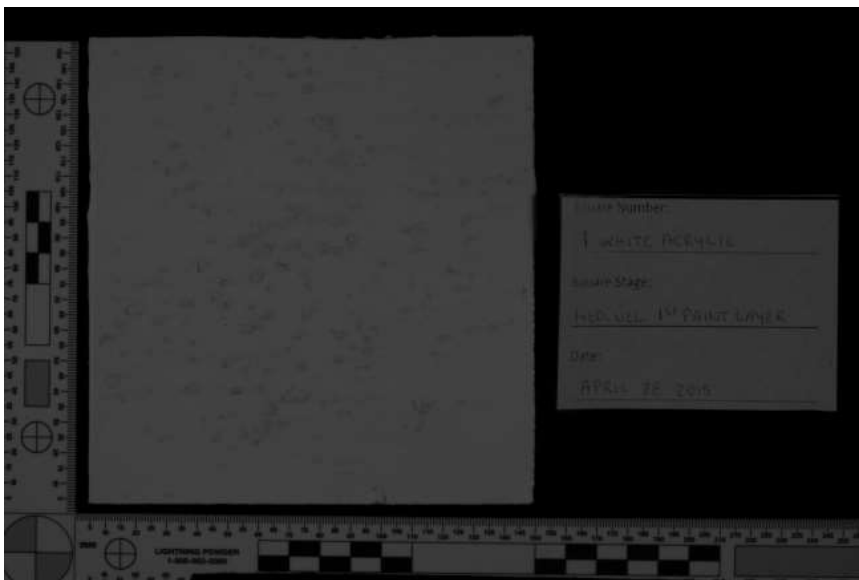
Longpass #70 HDR



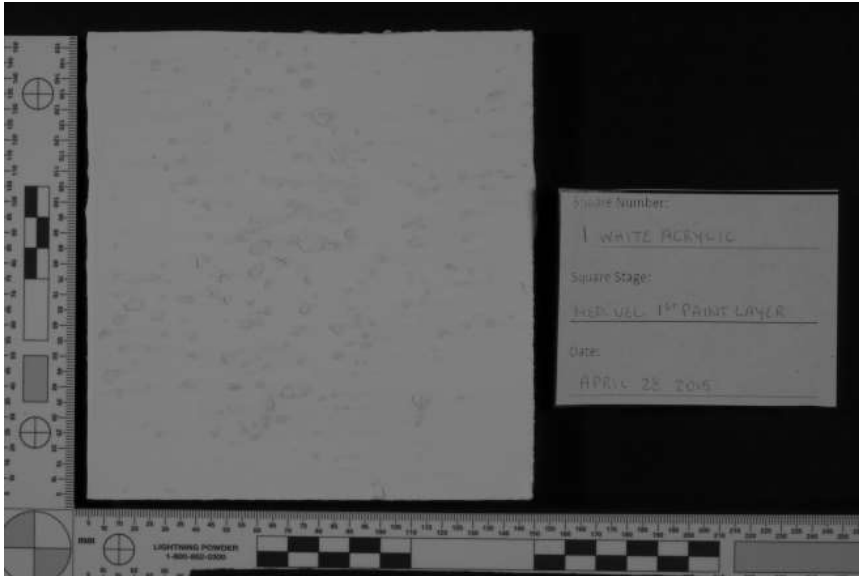
Longpass #70 Single



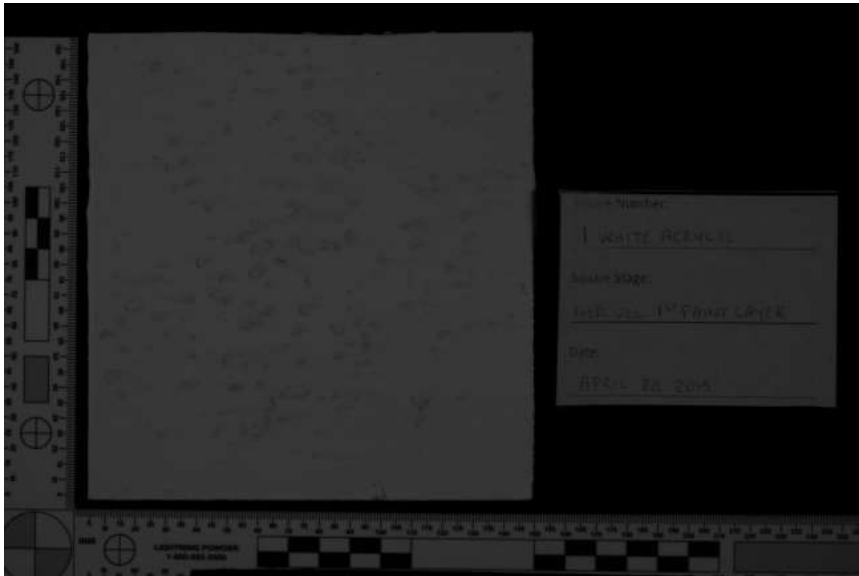
Longpass #87 HDR



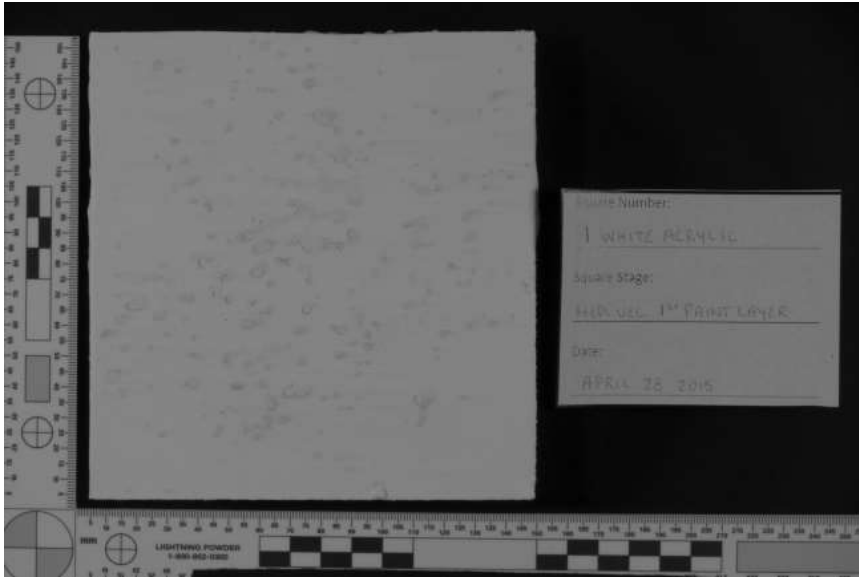
Longpass #87 Single



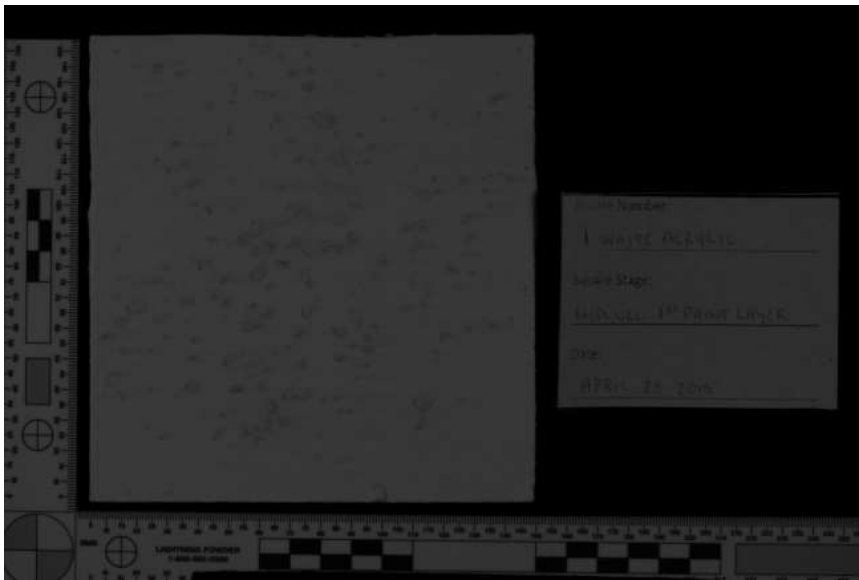
Longpass #87A HDR



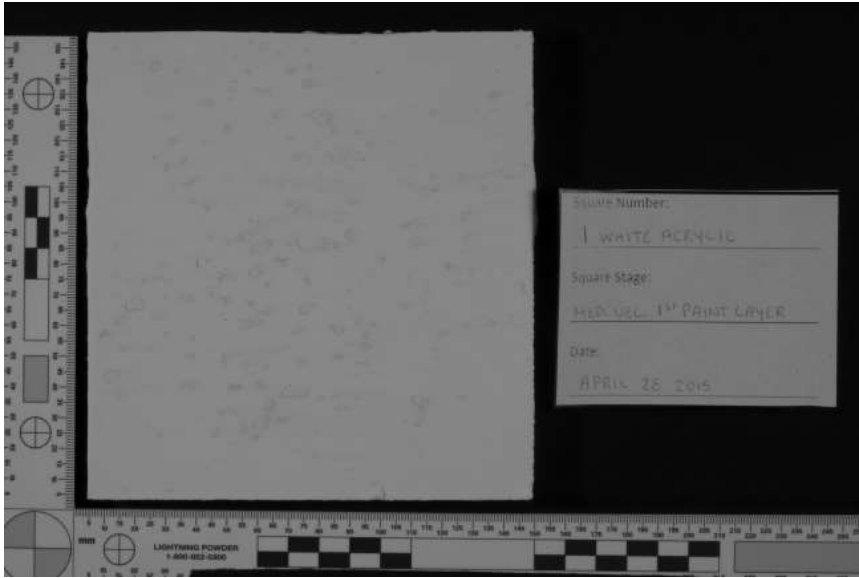
Longpass #87A Single



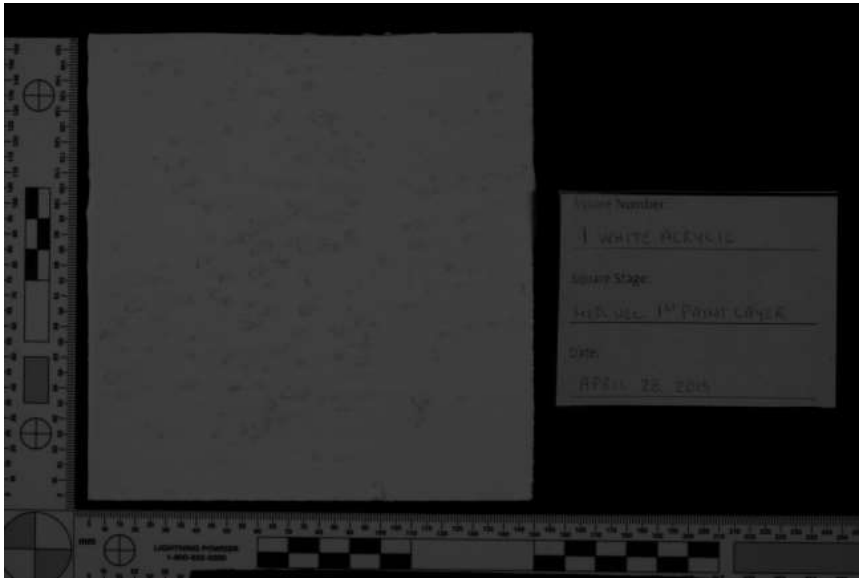
Longpass #87B HDR



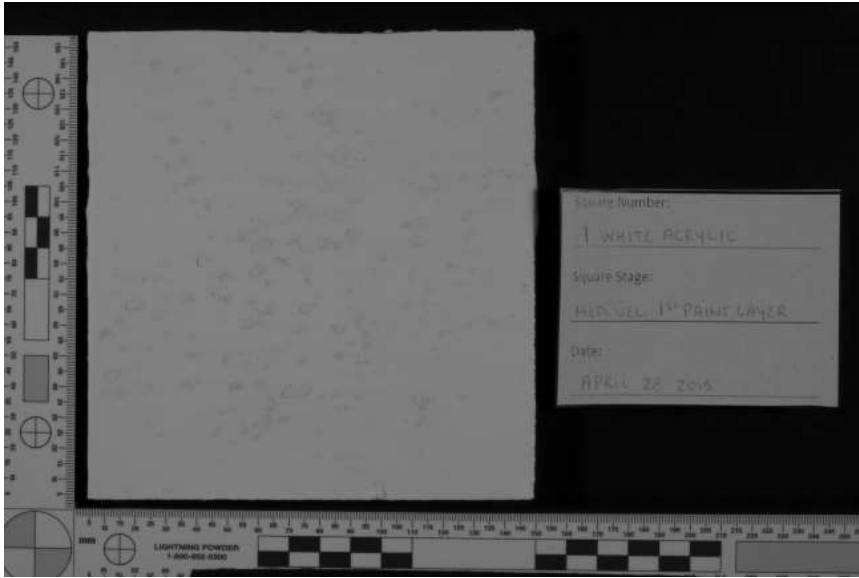
Longpass #87B Single



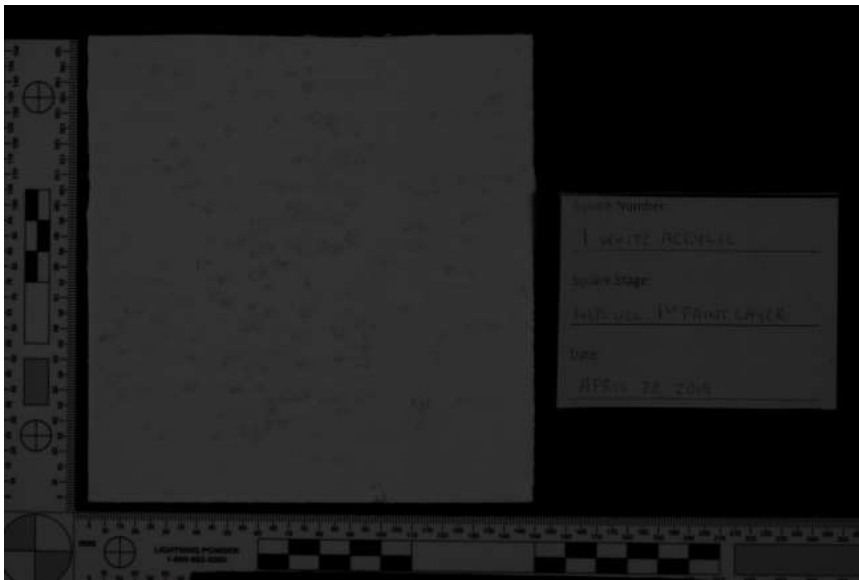
Longpass #88A HDR



Longpass #88A Single

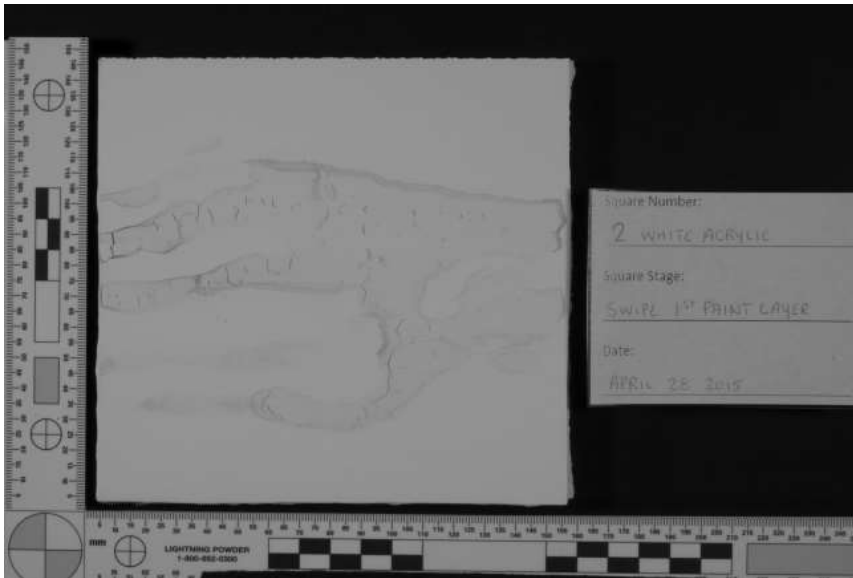


Longpass #89B HDR

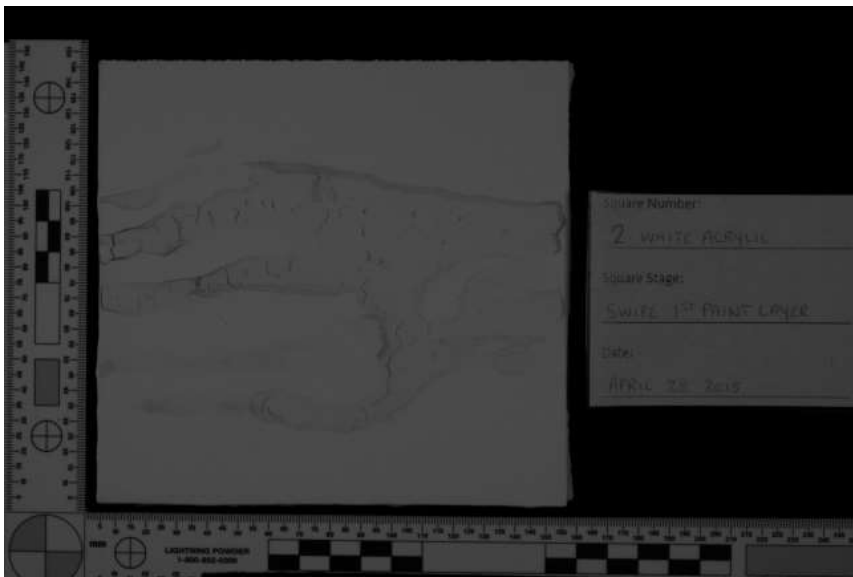


Longpass #89B Single

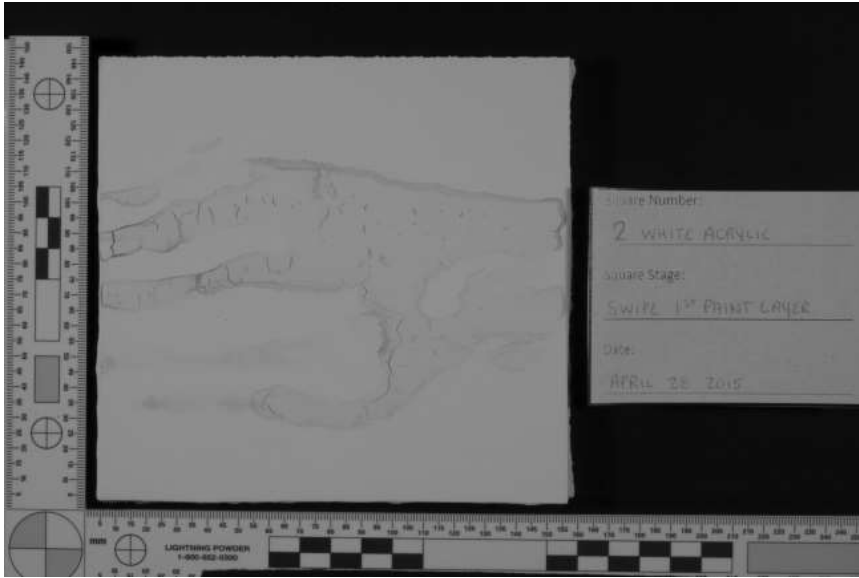
White Acrylic 2 – Swipe



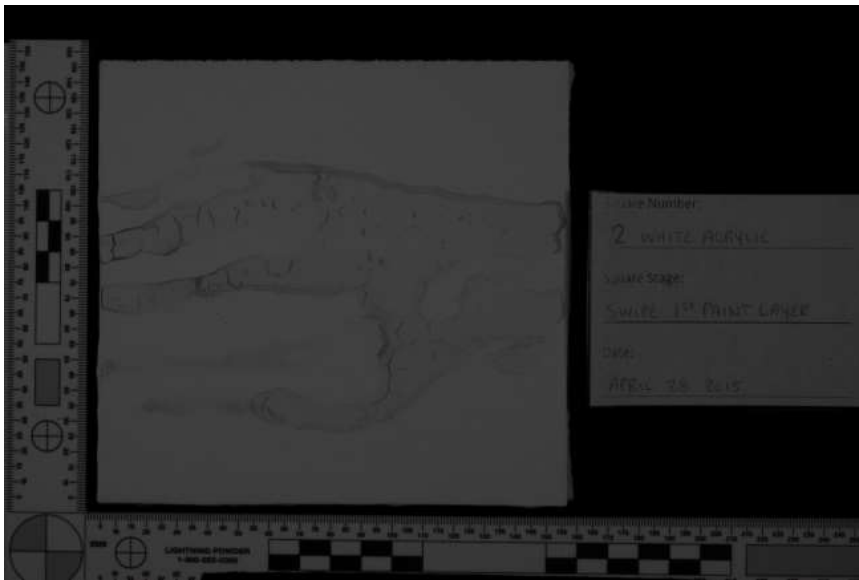
Longpass #70 HDR



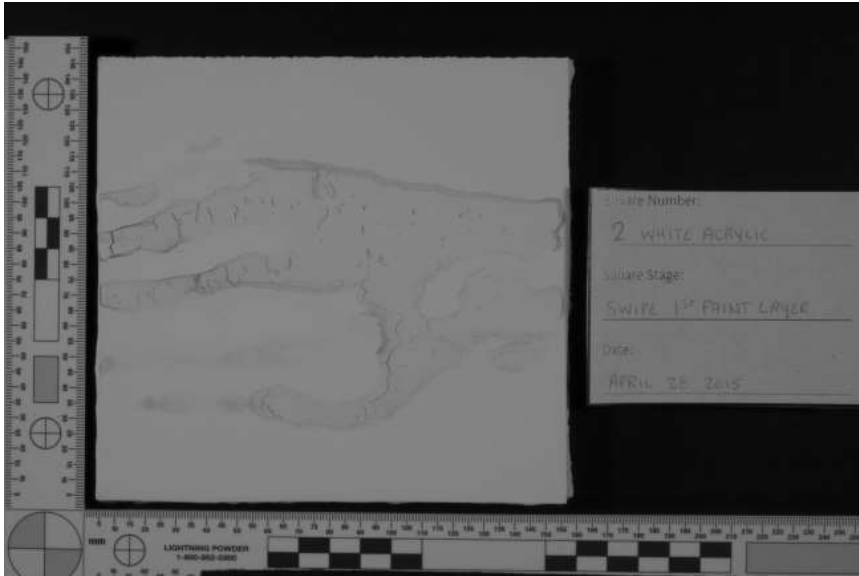
Longpass #70 Single



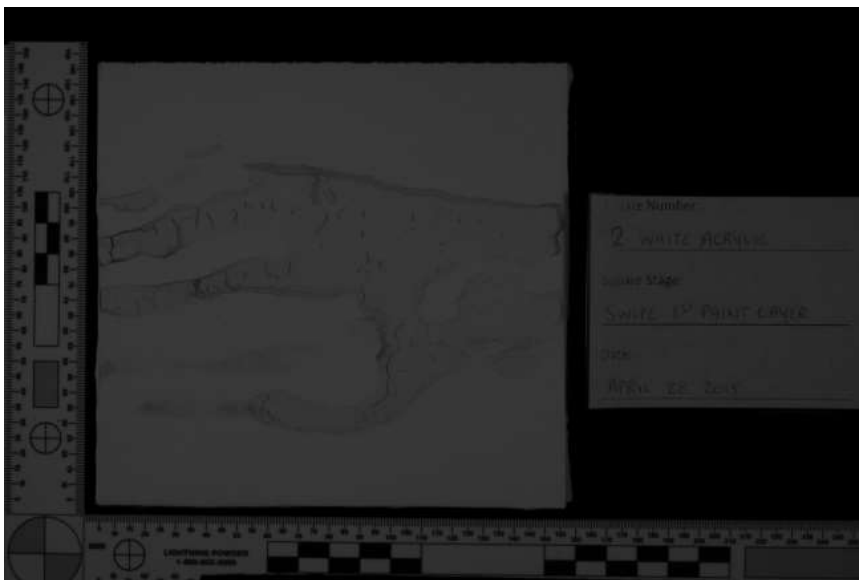
Longpass #87 HDR



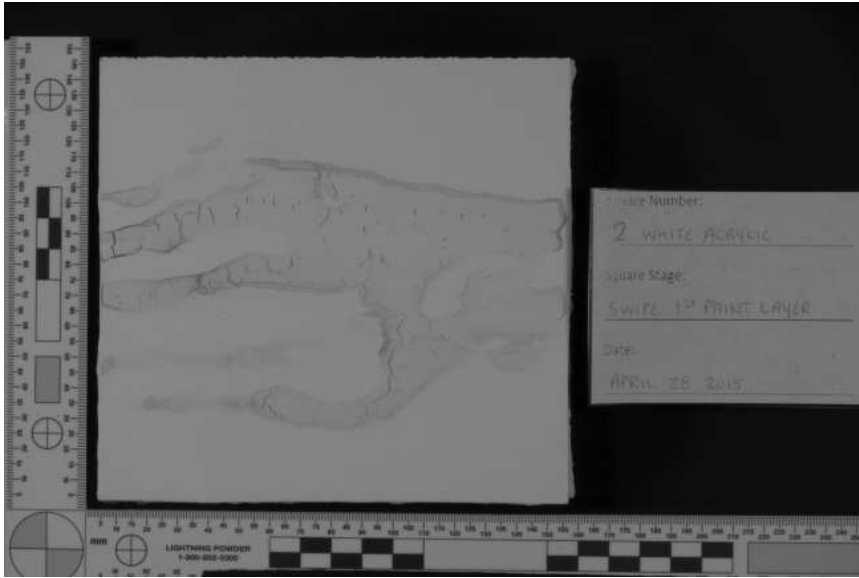
Longpass #87 Single



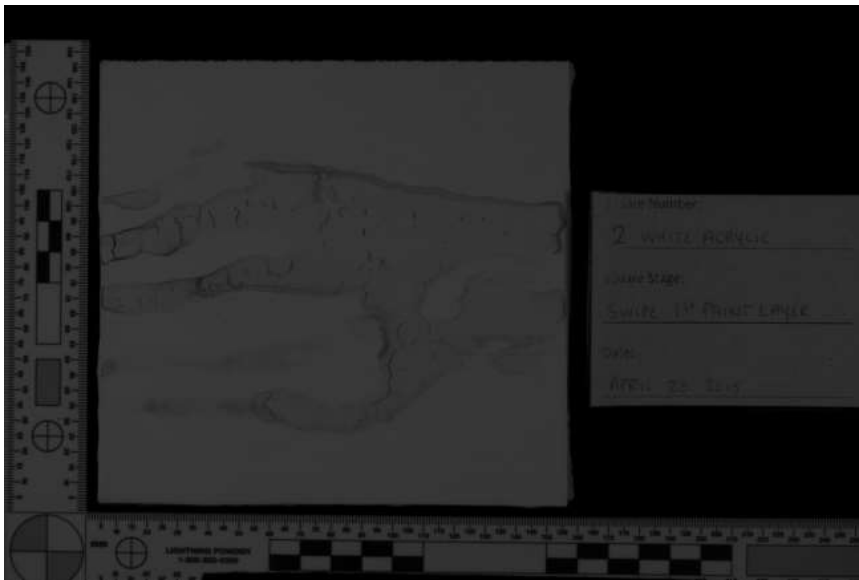
Longpass #87A HDR



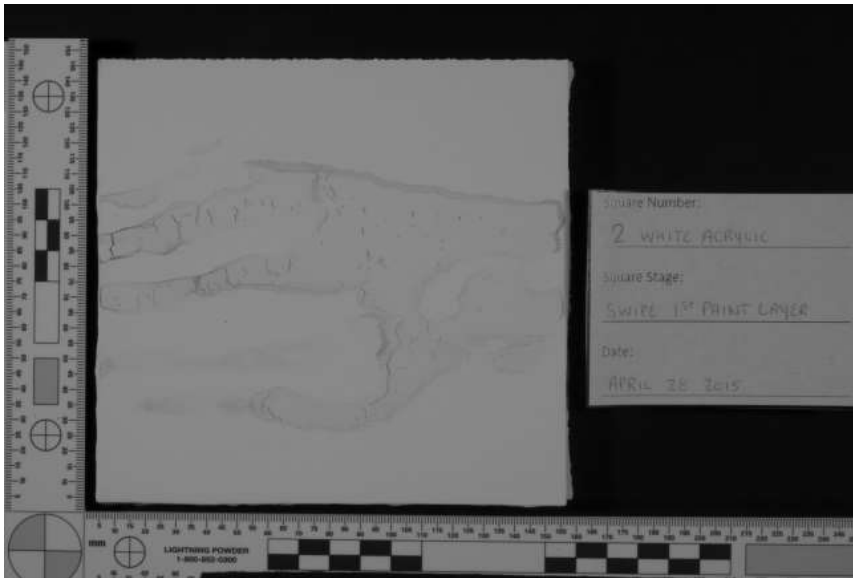
Longpass #87A Single



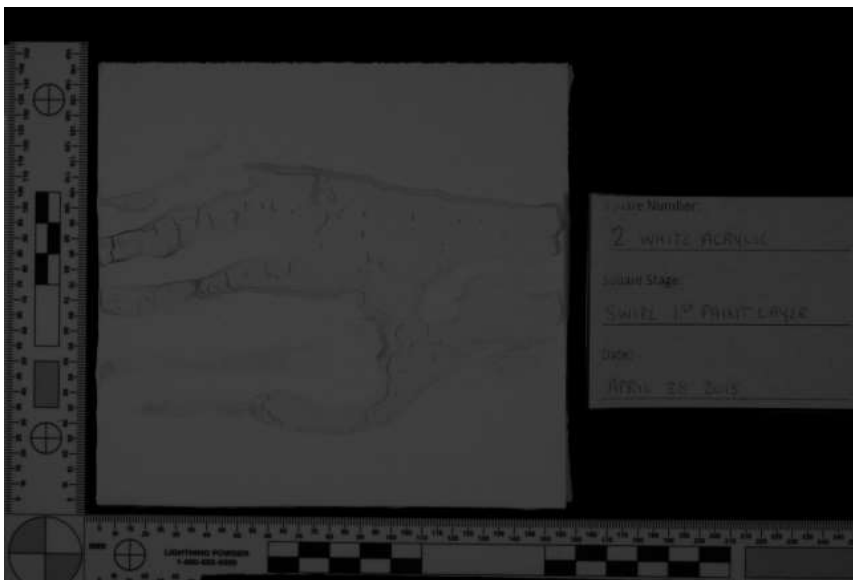
Longpass #87B HDR



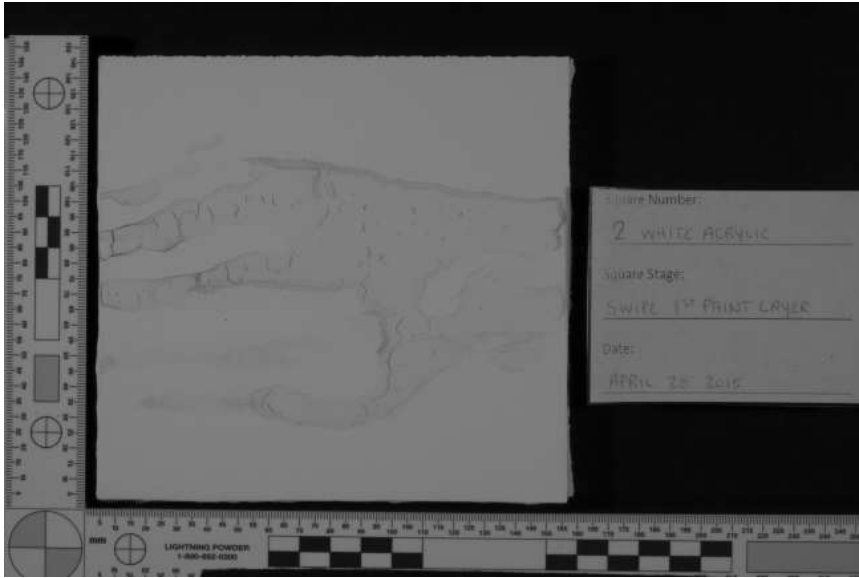
Longpass #87B Single



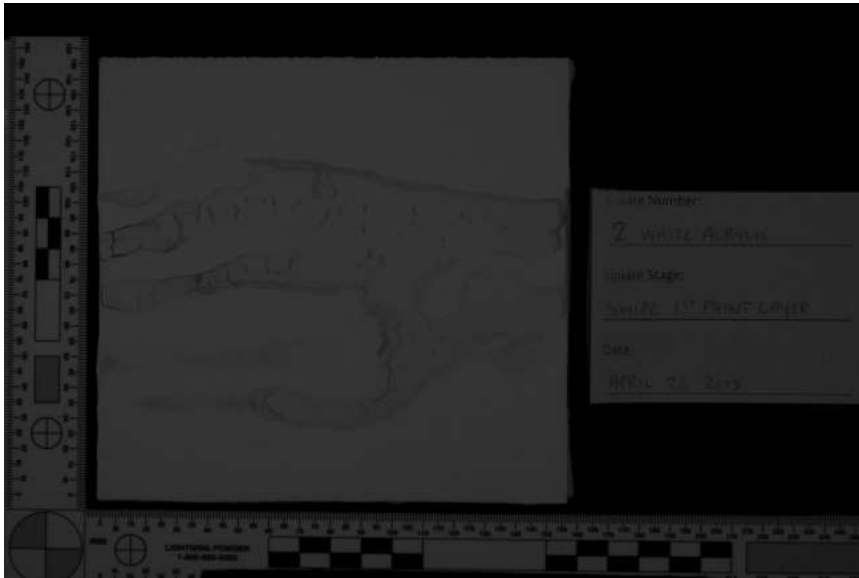
Longpass #88A HDR



Longpass #88A Single

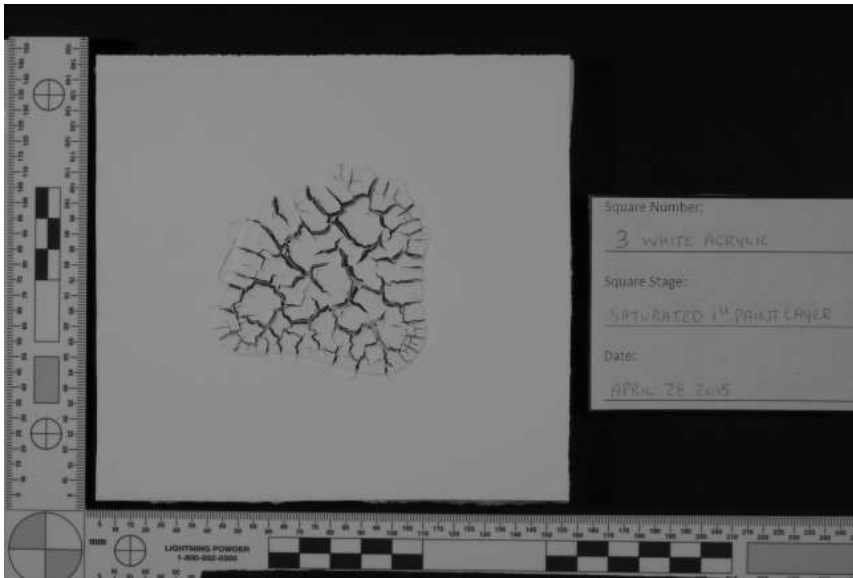


Longpass #89B HDR

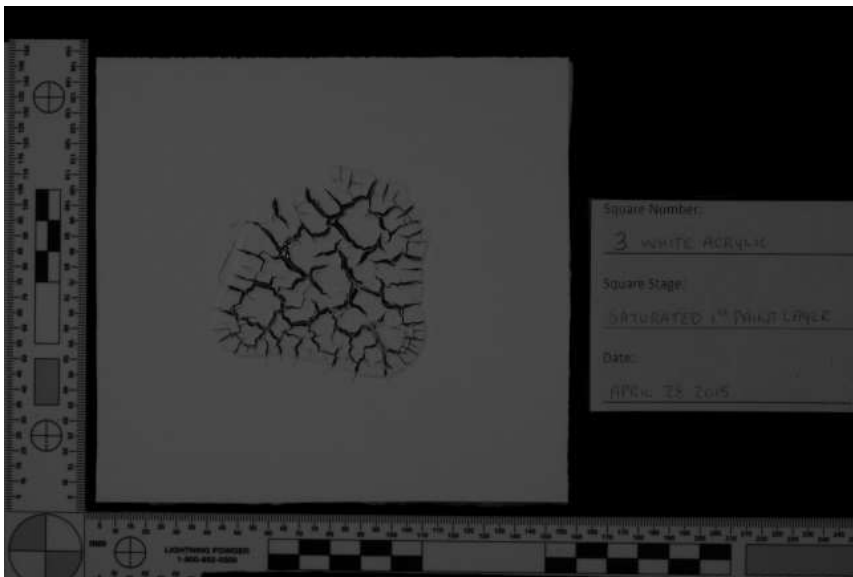


Longpass #89B Single

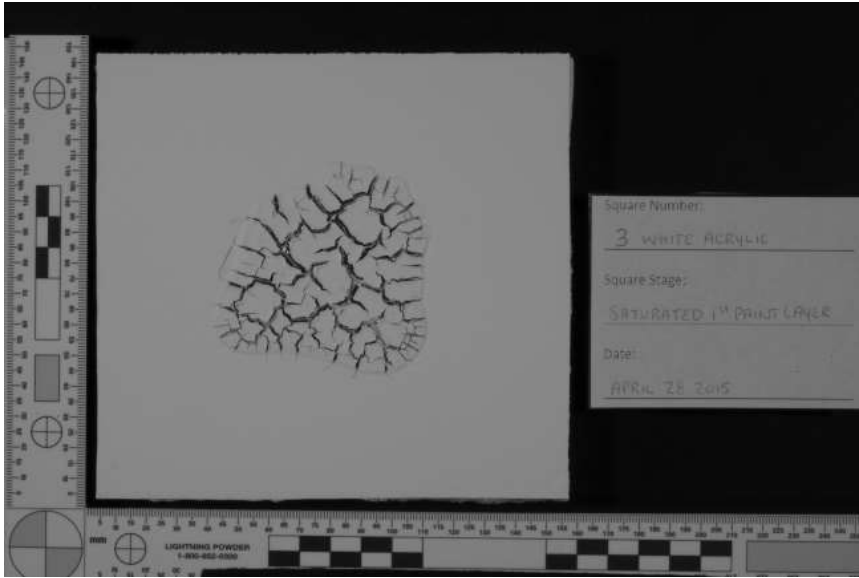
White Acrylic 3 – Saturated



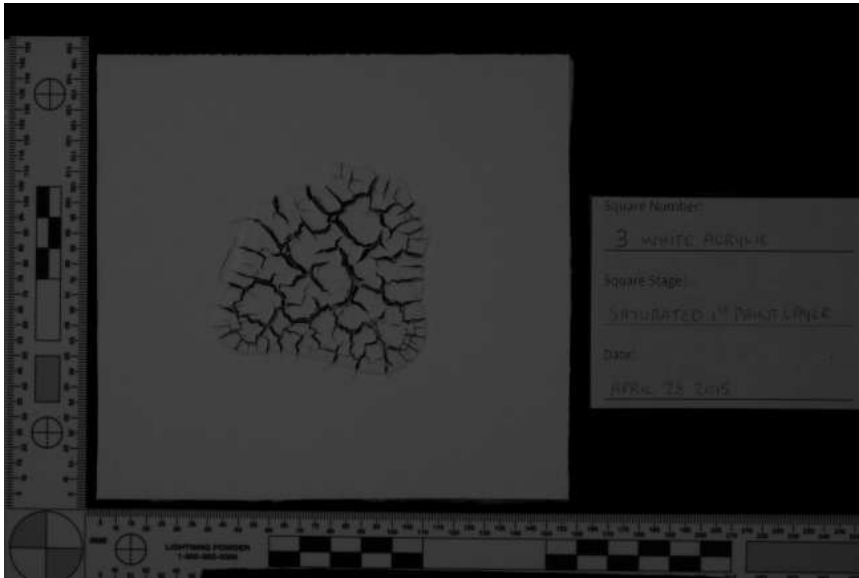
Longpass #70 HDR



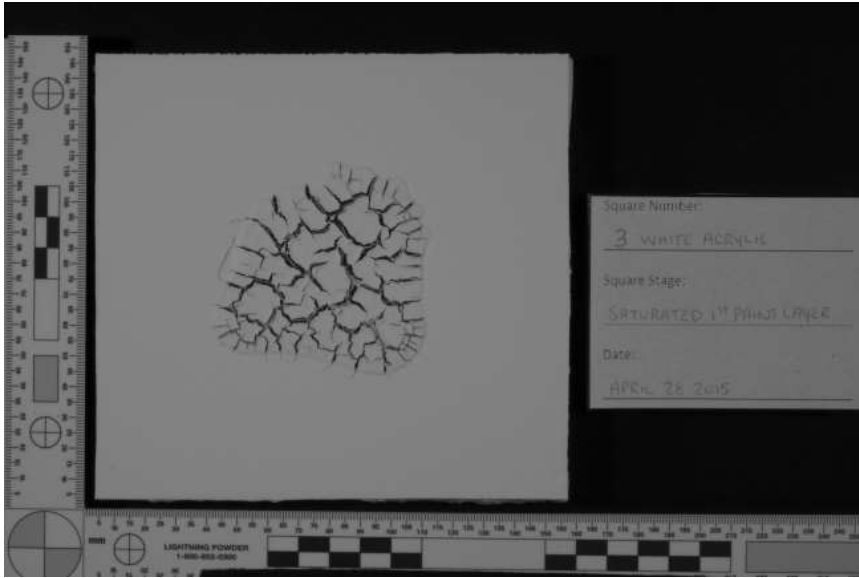
Longpass #70 Single



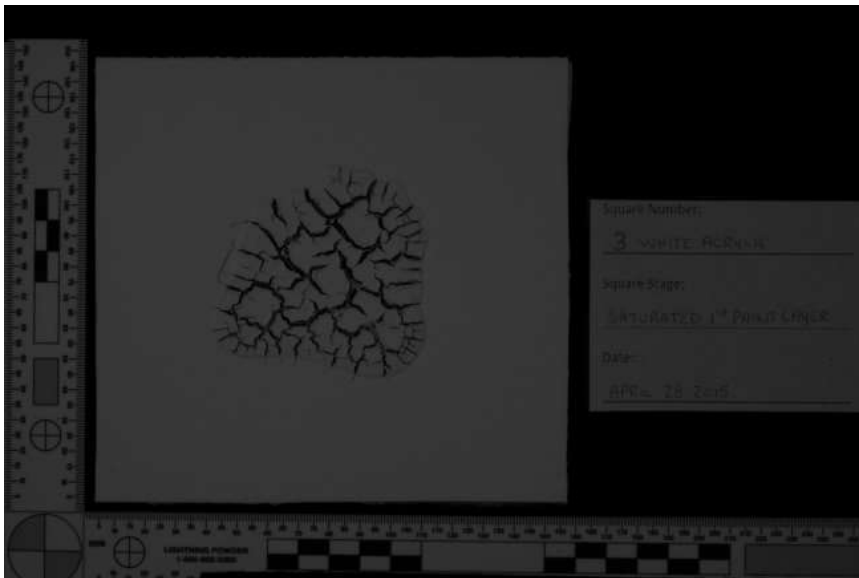
Longpass #87 HDR



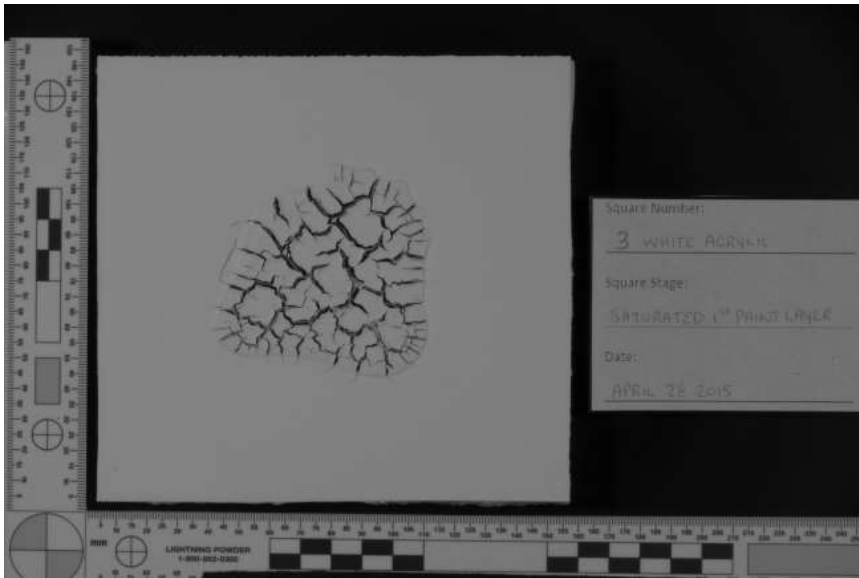
Longpass #87 Single



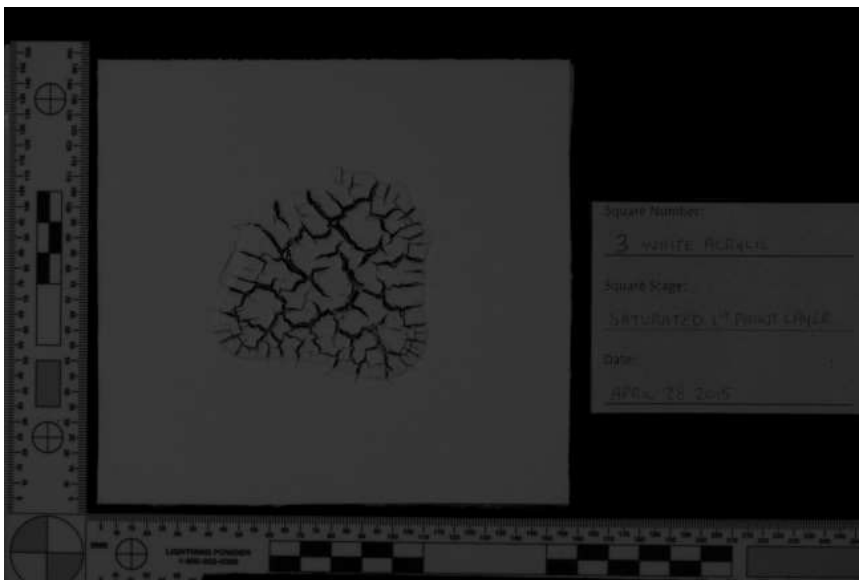
Longpass #87A HDR



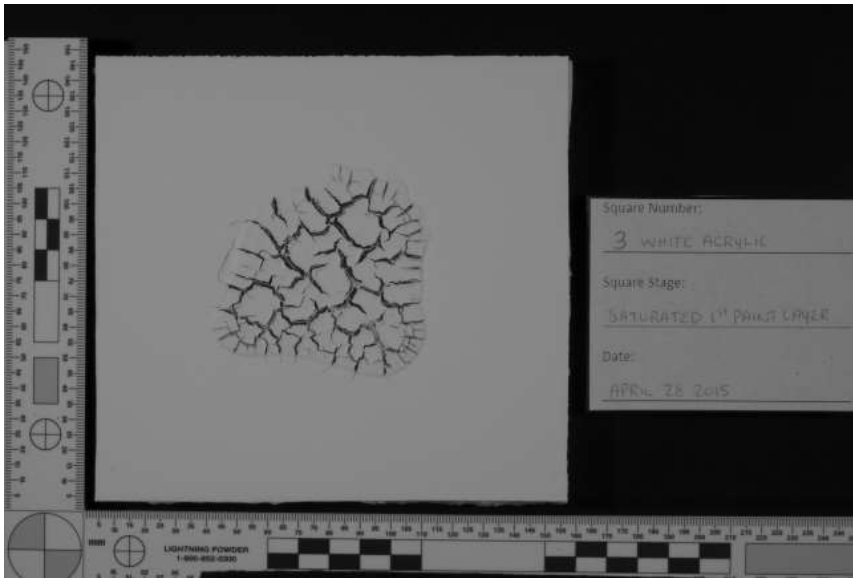
Longpass #87A Single



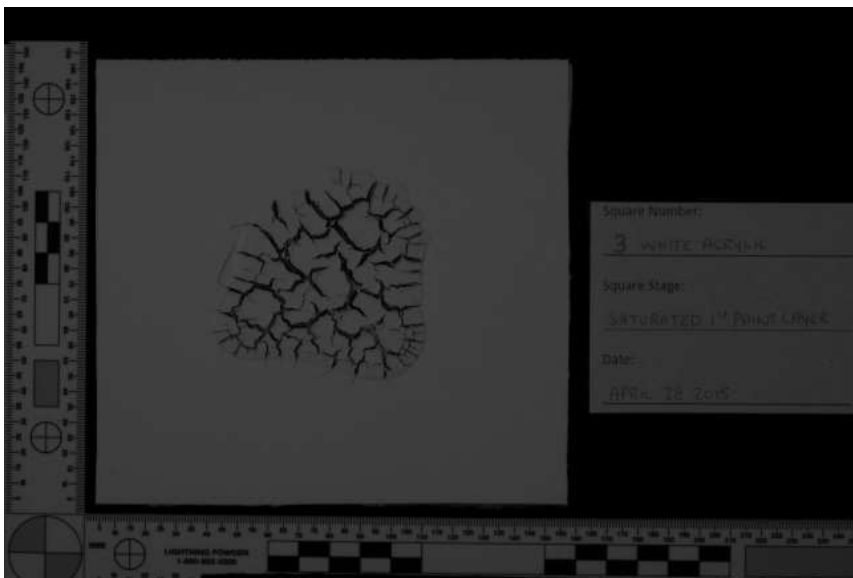
Longpass #87B HDR



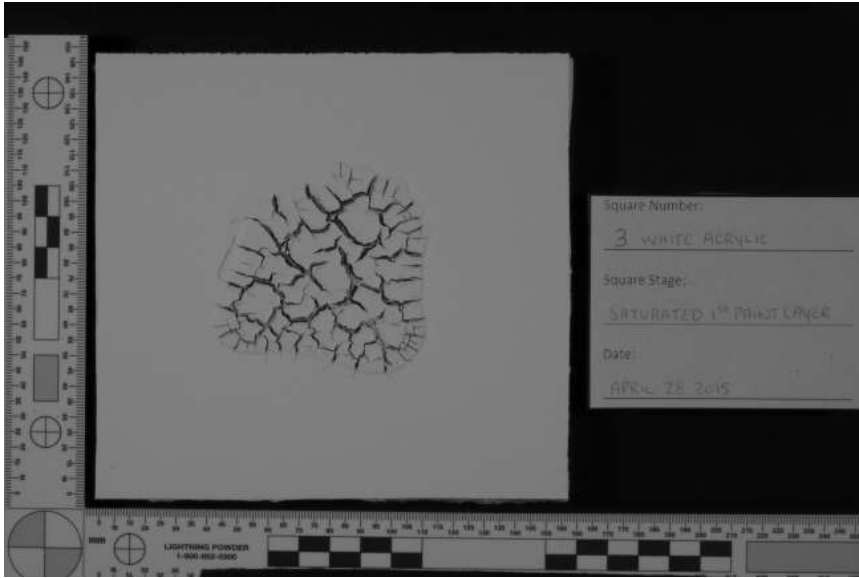
Longpass #87B Single



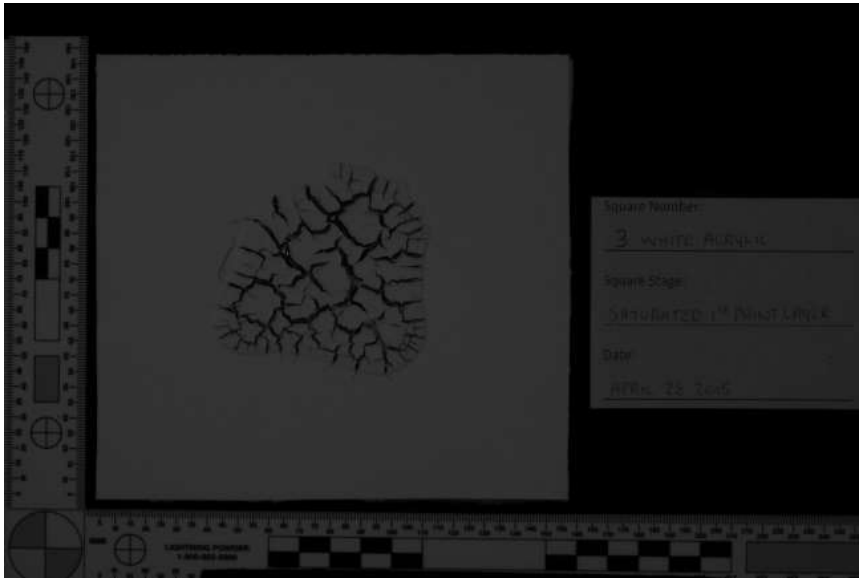
Longpass #88A HDR



Longpass #88A Single

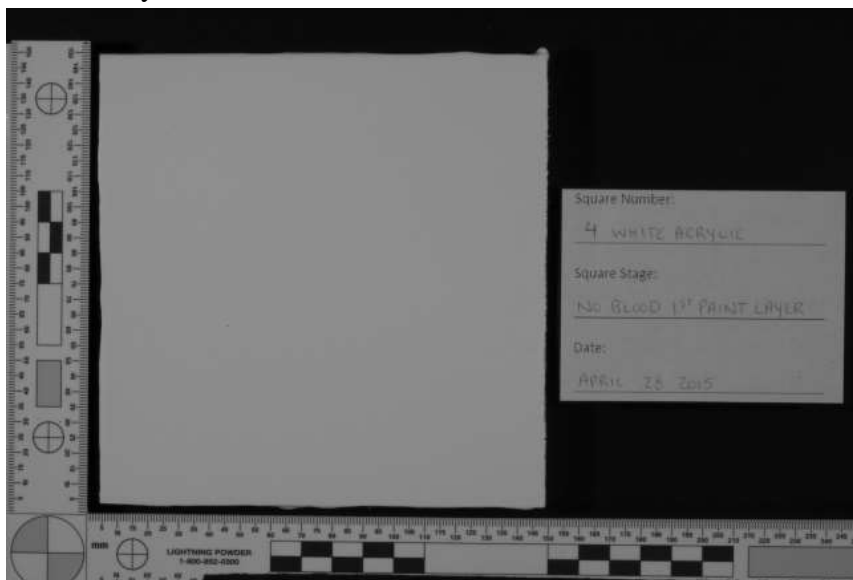


Longpass #89B HDR



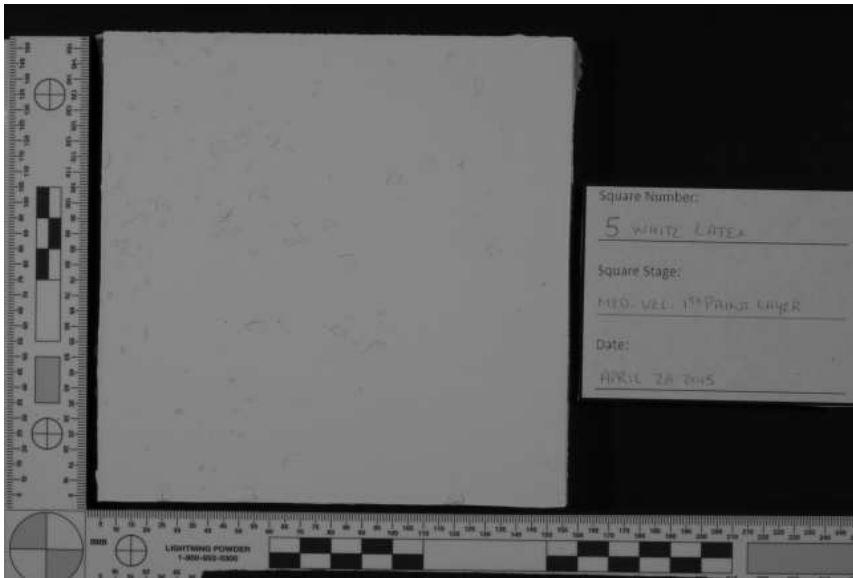
Longpass #89B Single

White Acrylic 4 – Control No Bloodstain



Longpass #70 HDR

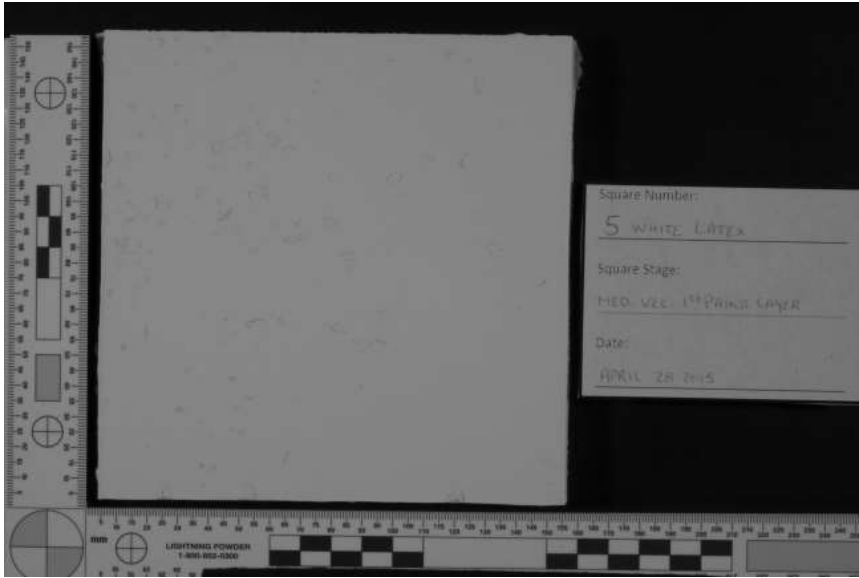
Appendix 4.2.3.2. White Latex 70, 87, 87A, 87B, 88A, 89B First layer of paint stage
White Latex 5 – Medium Velocity



Longpass #70 HDR



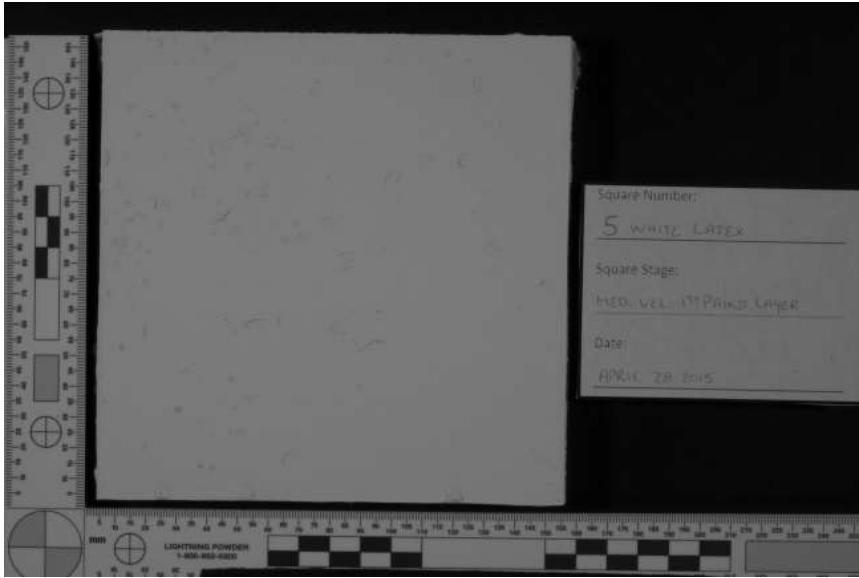
Longpass #70 Single



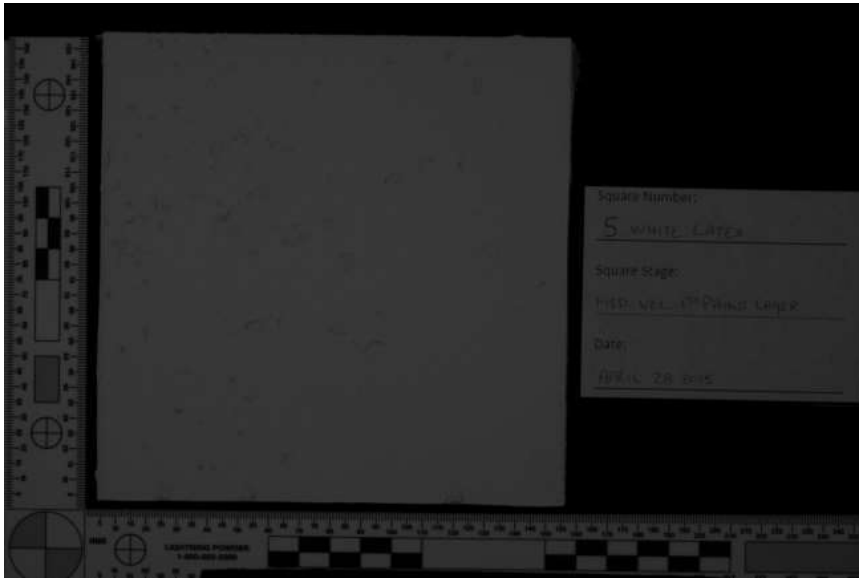
Longpass #87 HDR



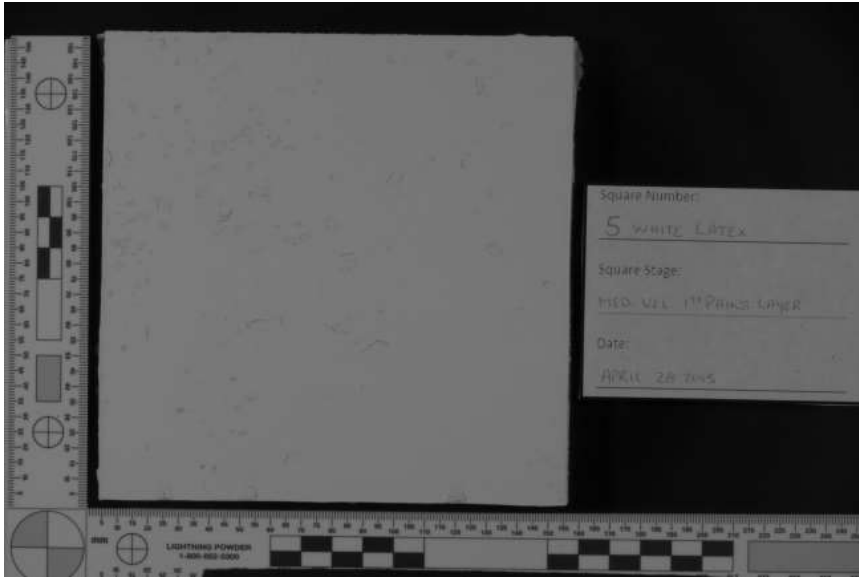
Longpass #87 Single



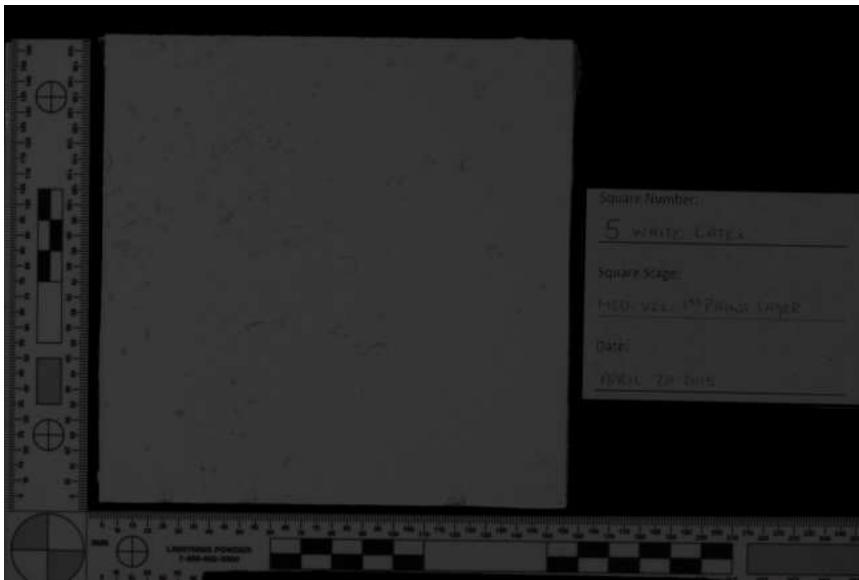
Longpass #87A HDR



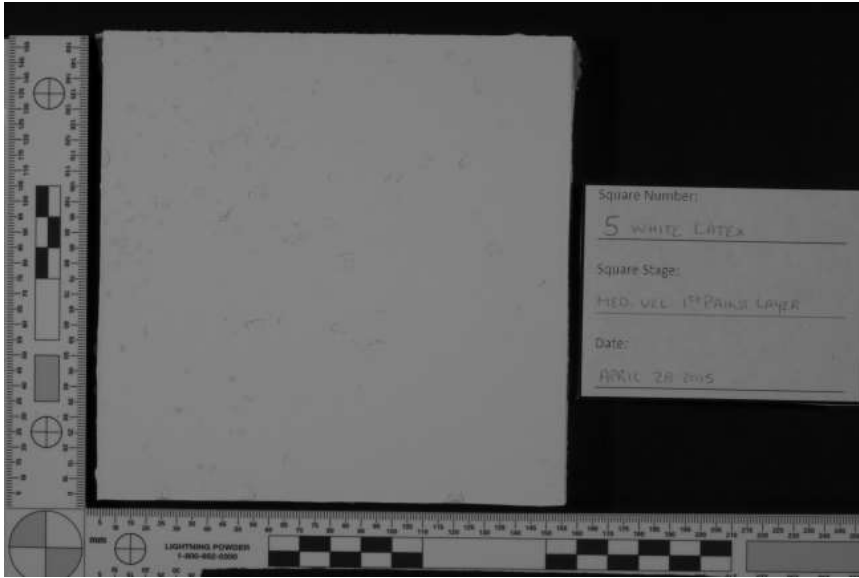
Longpass #87A Single



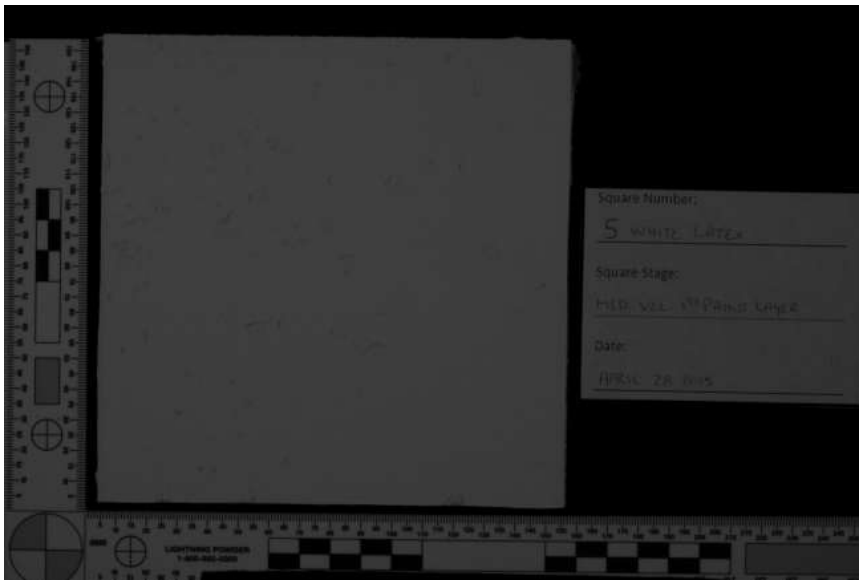
Longpass #87B HDR



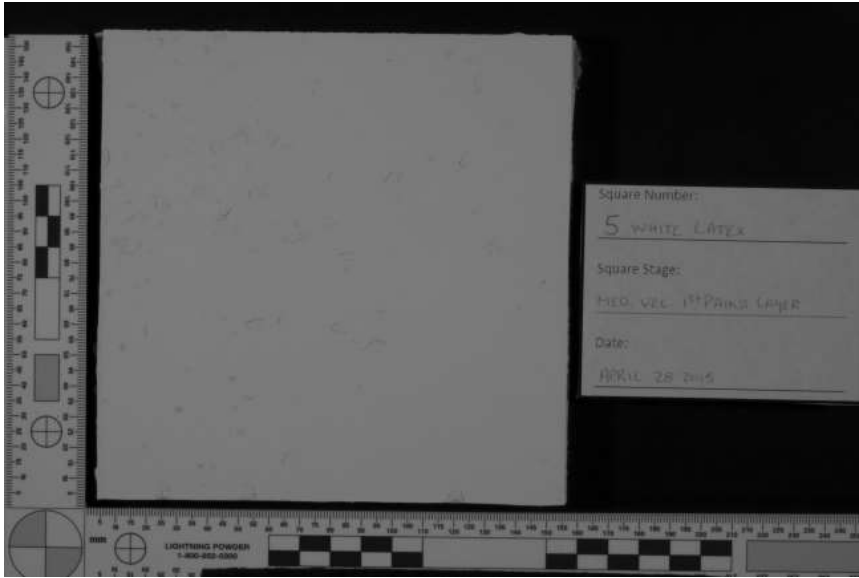
Longpass #87B Single



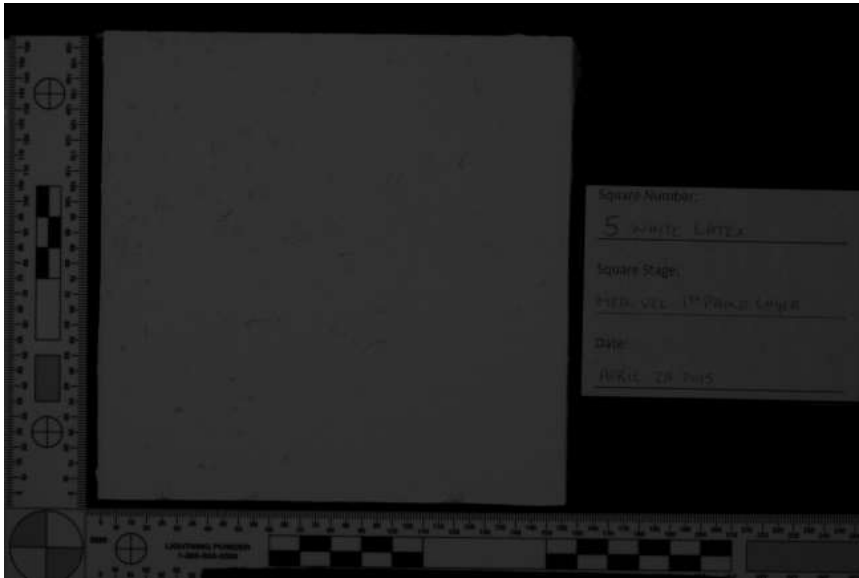
Longpass #88A HDR



Longpass #88A Single

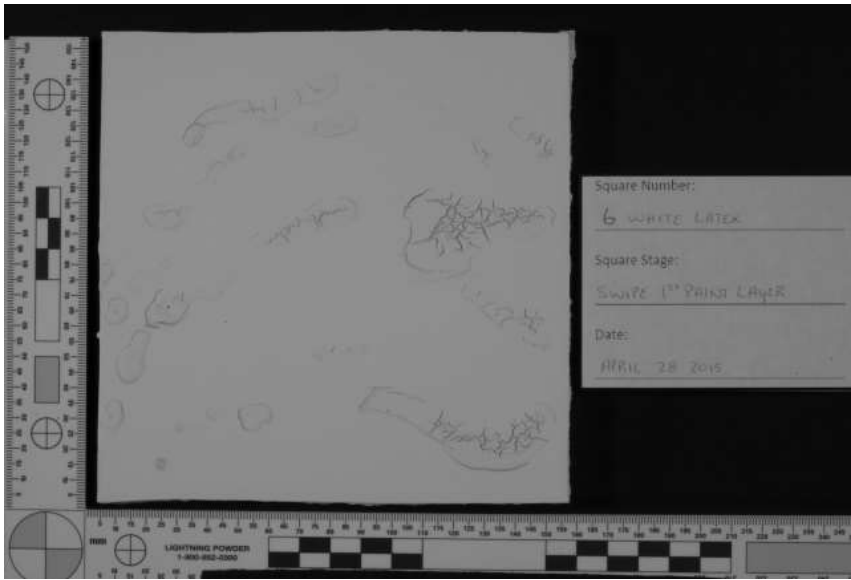


Longpass #89B HDR

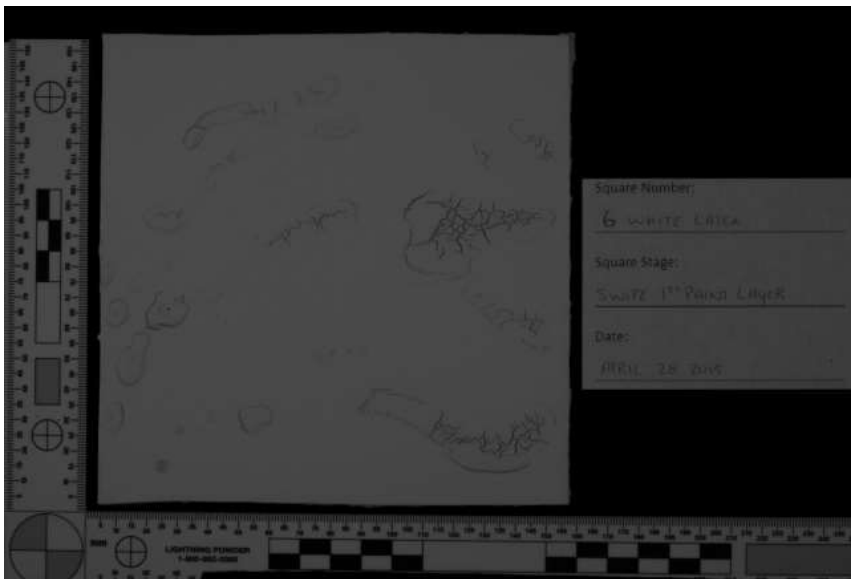


Longpass #89B Single

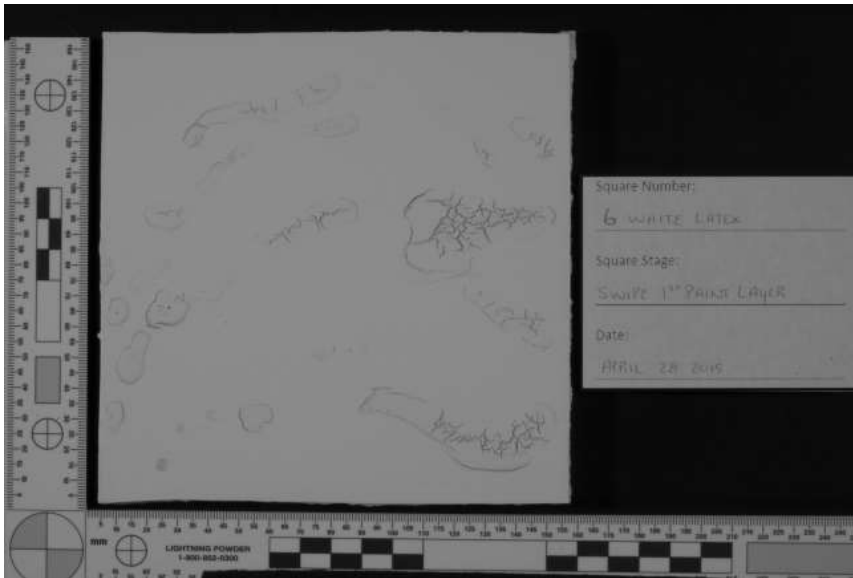
White Latex 6 – Swipe



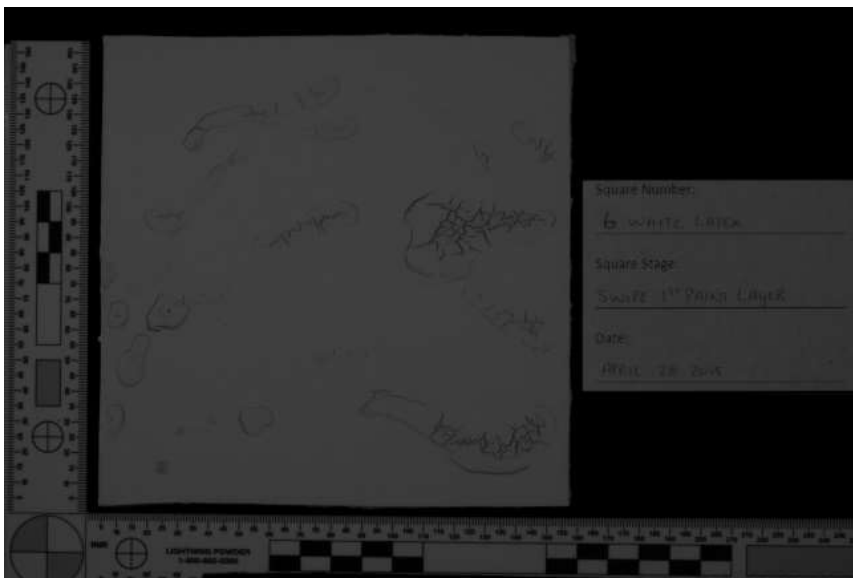
Longpass #70 HDR



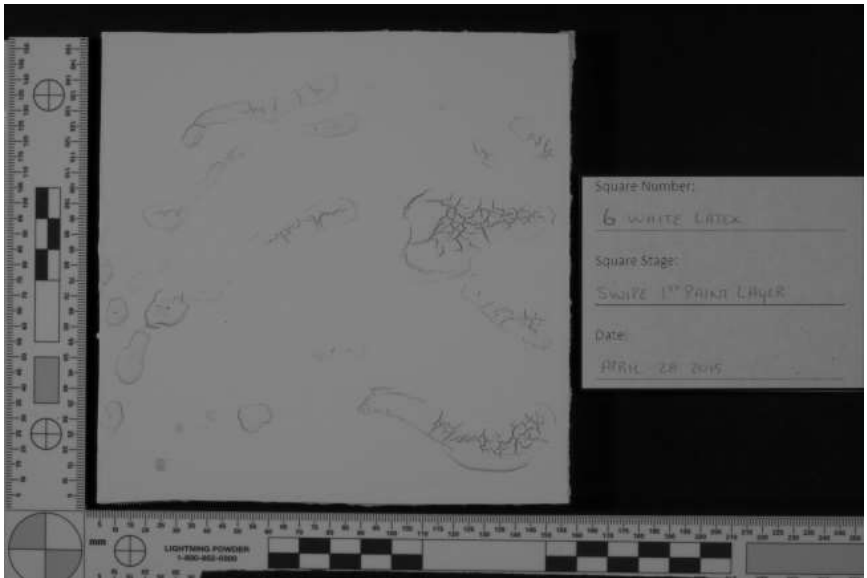
Longpass #70 Single



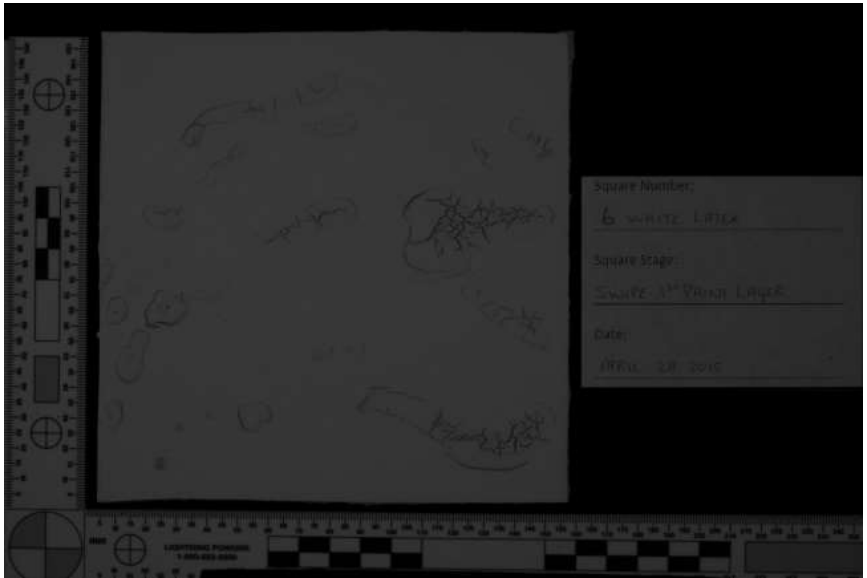
Longpass #87 HDR



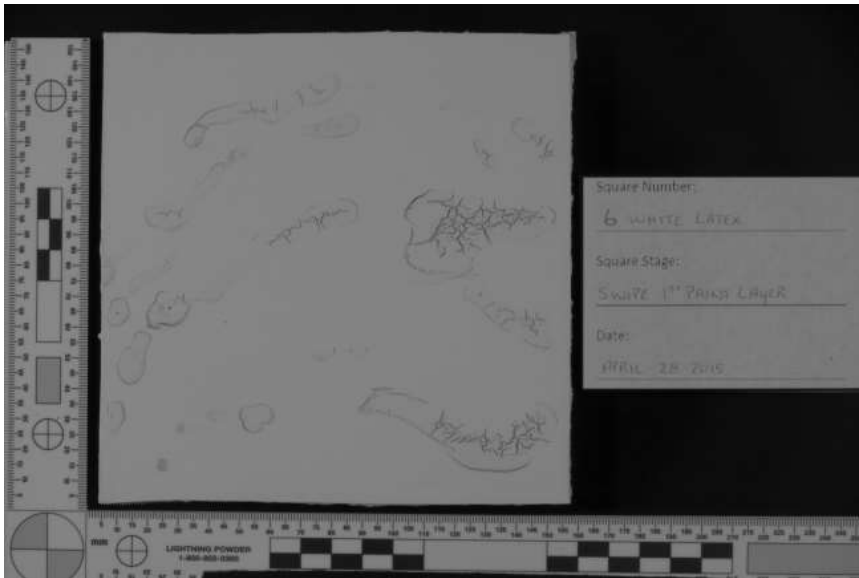
Longpass #87 Single



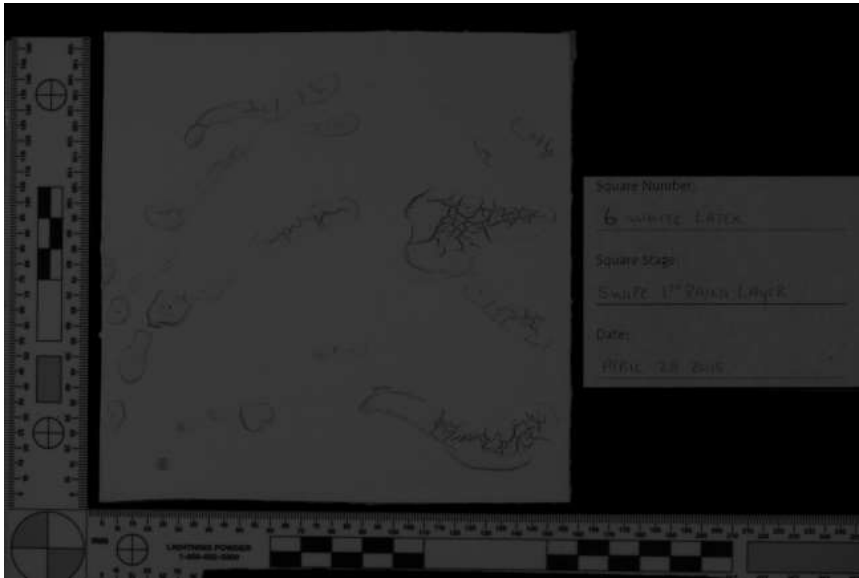
Longpass #87A HDR



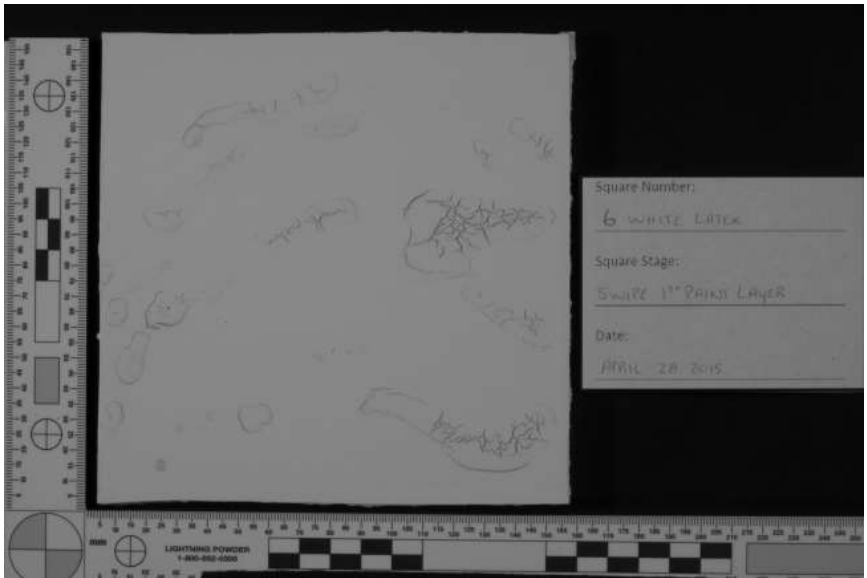
Longpass #87A Single



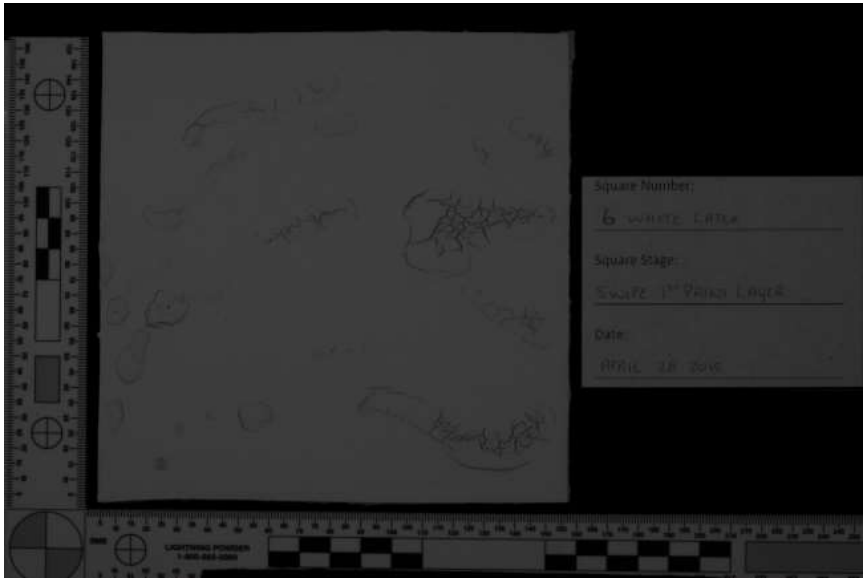
Longpass #87B HDR



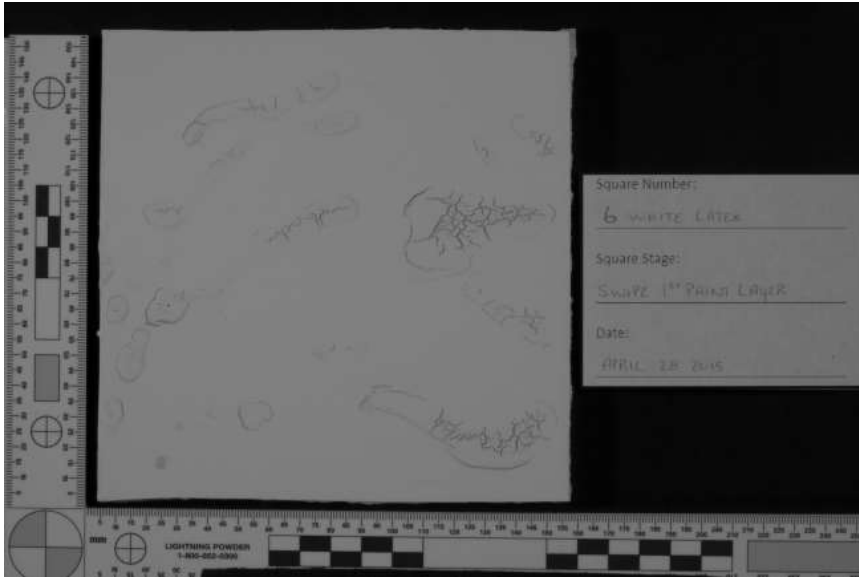
Longpass #87B Single



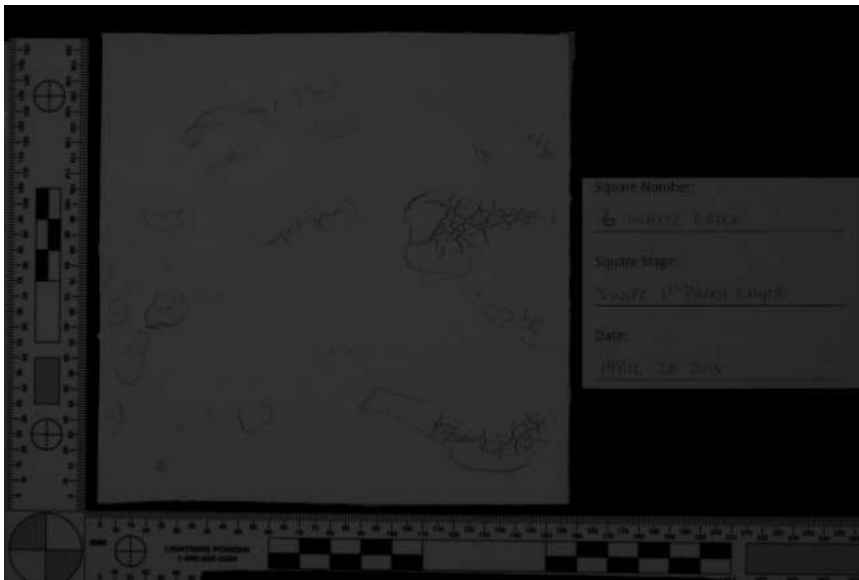
Longpass #88A HDR



Longpass #88A Single

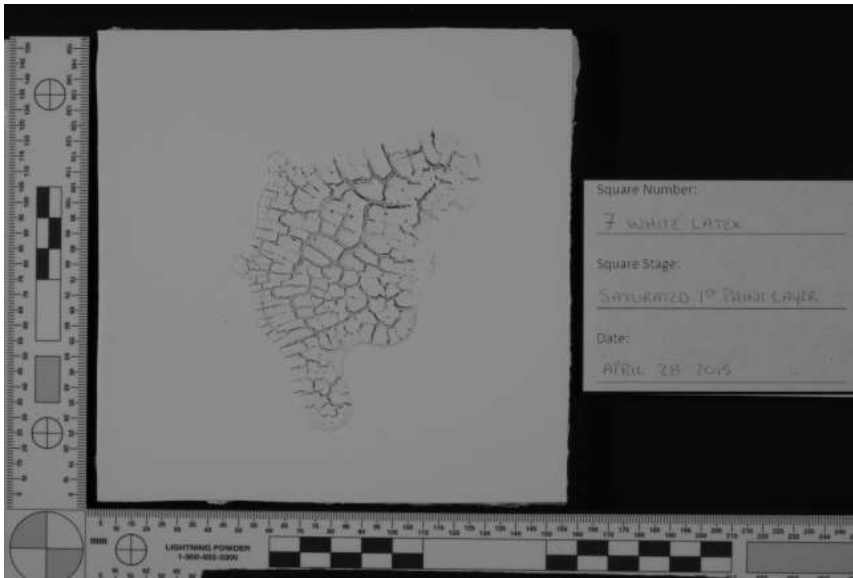


Longpass #89B HDR

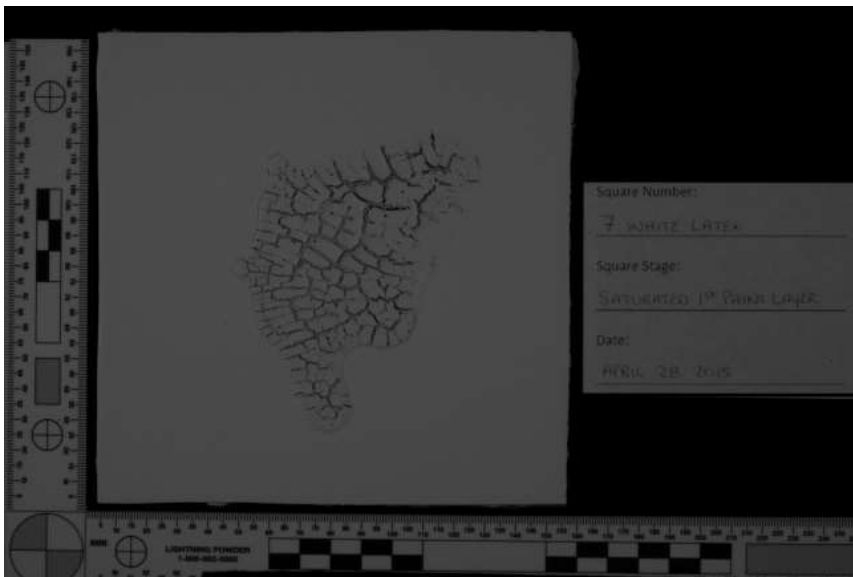


Longpass #89B Single

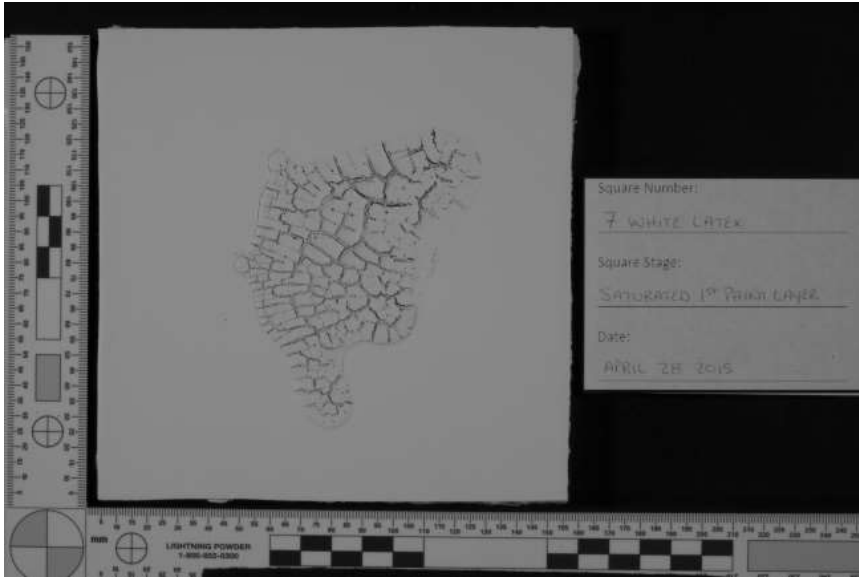
White Latex 7 – Saturated



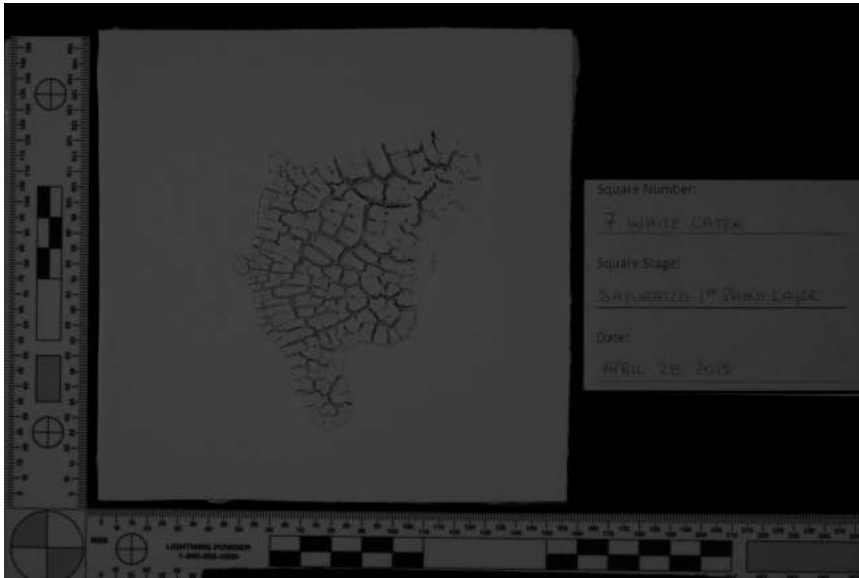
Longpass #70 HDR



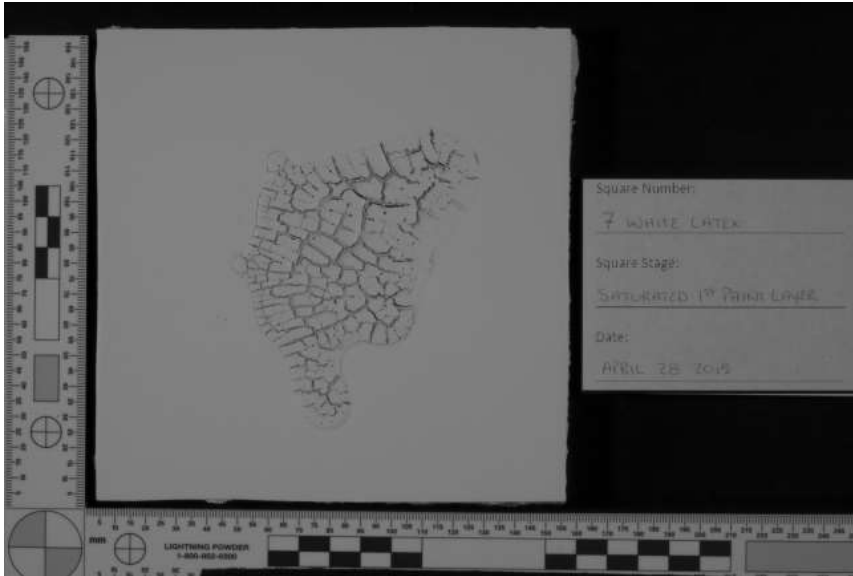
Longpass #70 Single



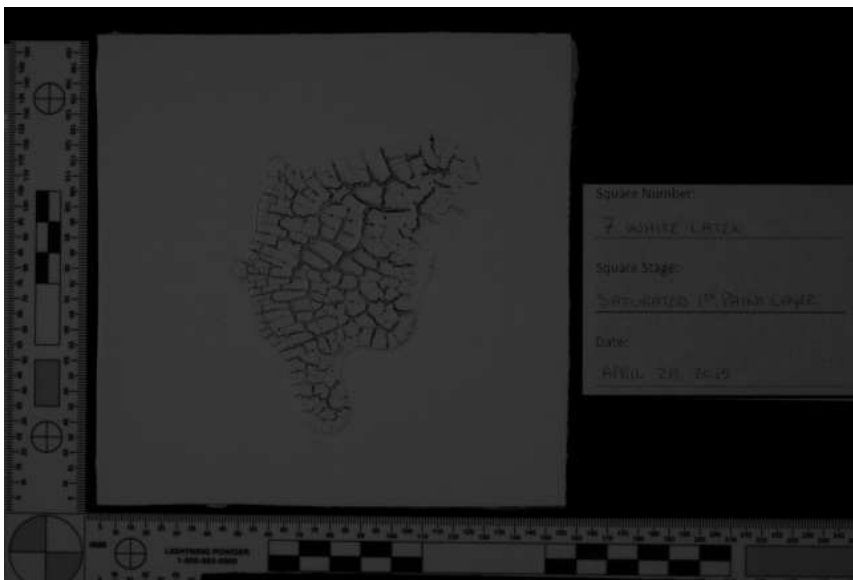
Longpass #87 HDR



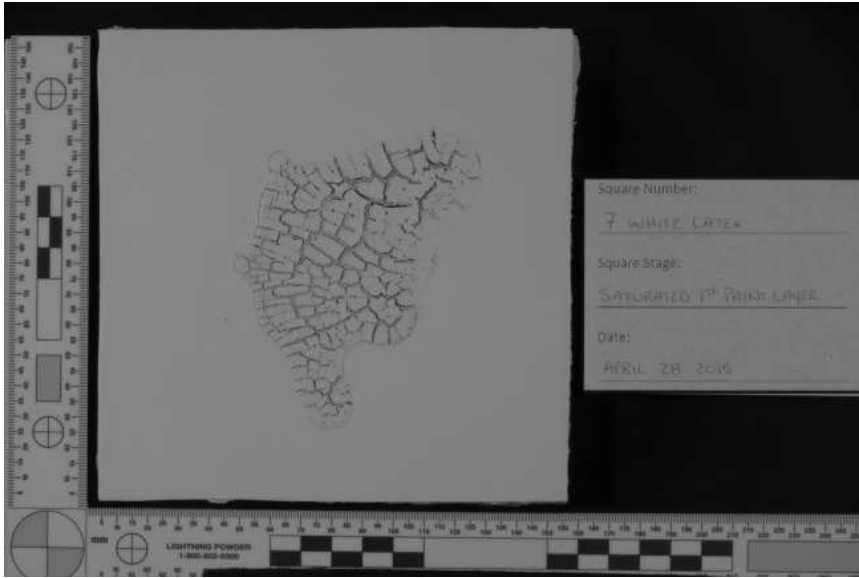
Longpass #87 Single



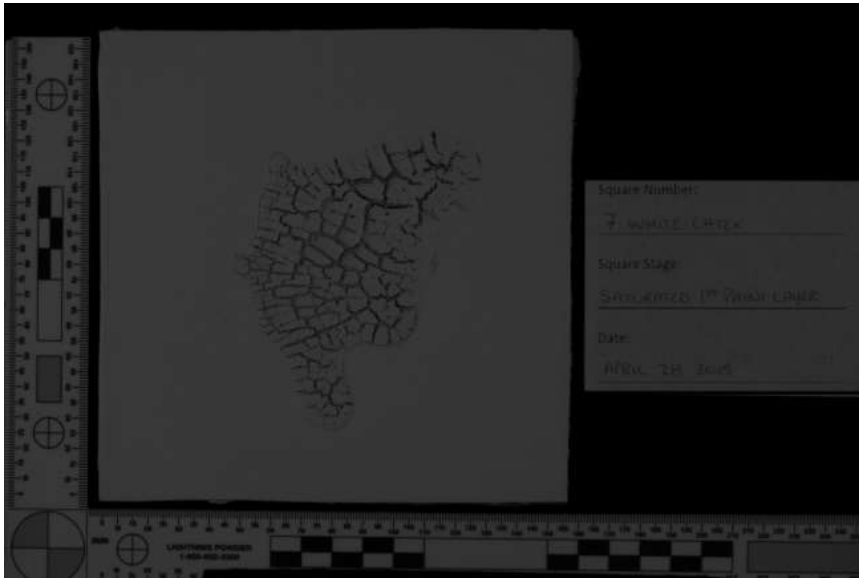
Longpass #87A HDR



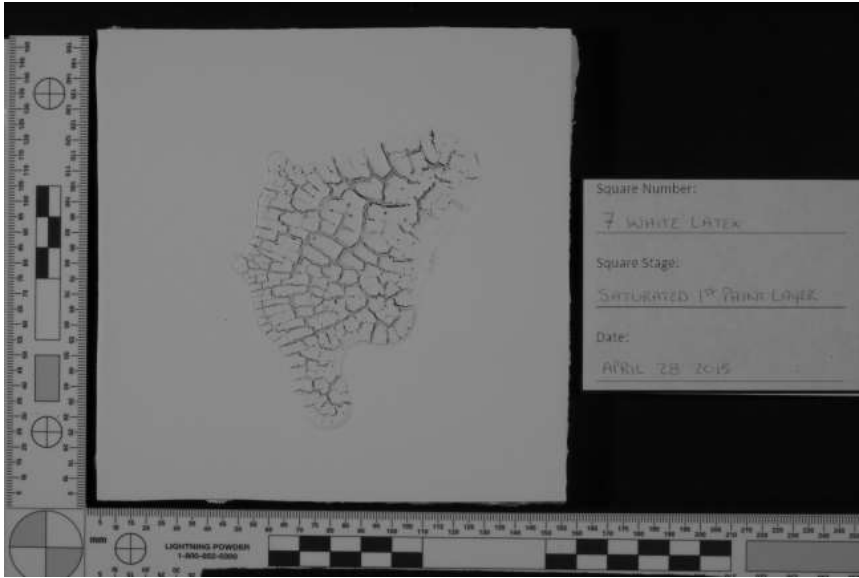
Longpass #87A Single



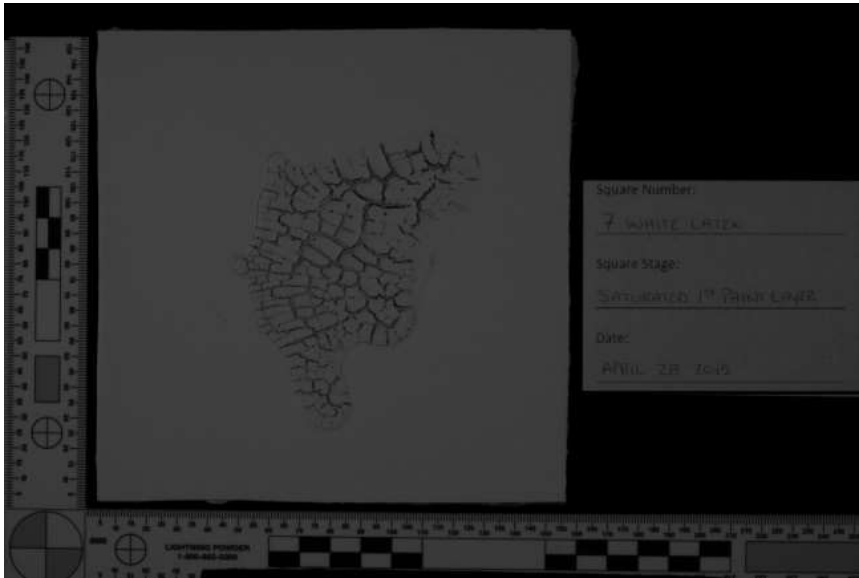
Longpass #87B HDR



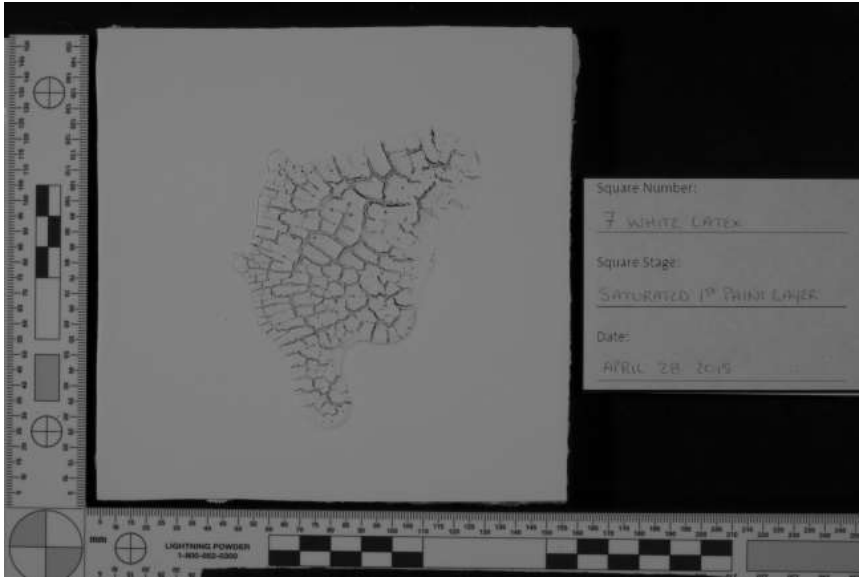
Longpass #87B Single



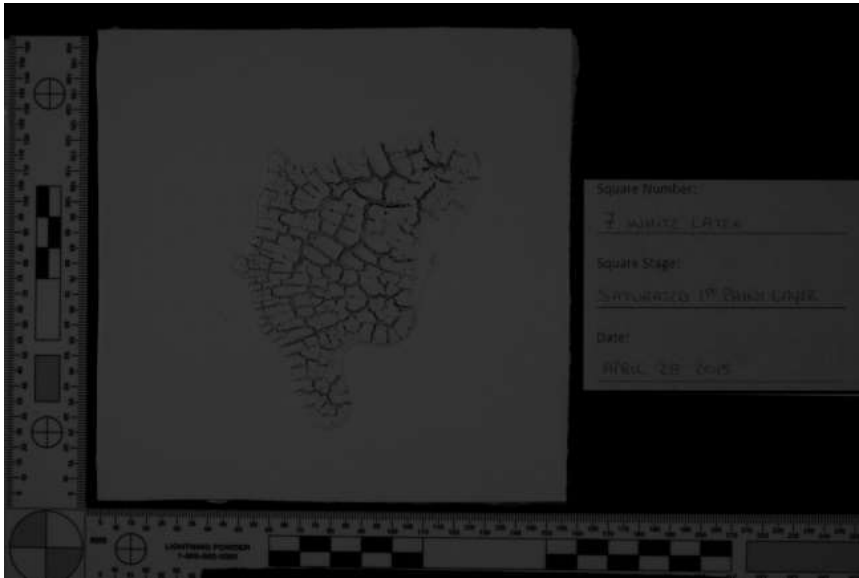
Longpass #88A HDR



Longpass #88A Single

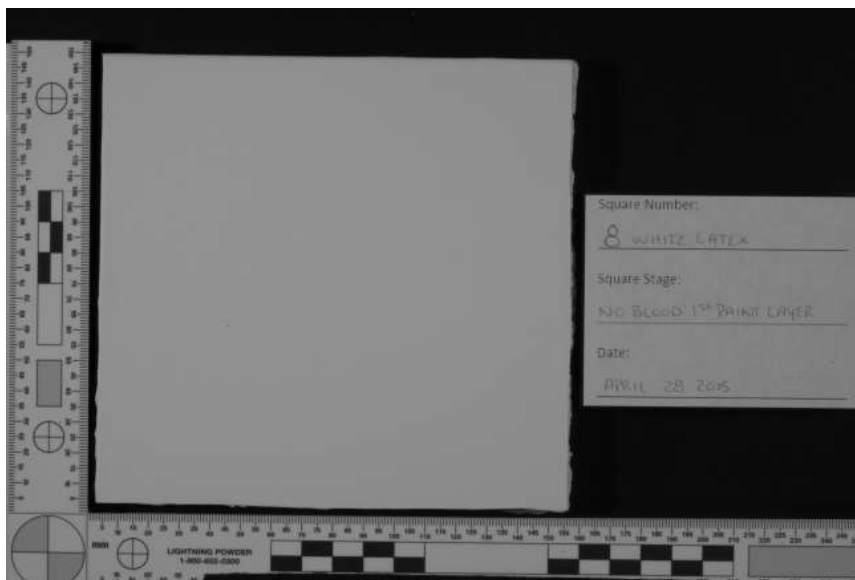


Longpass #89B HDR



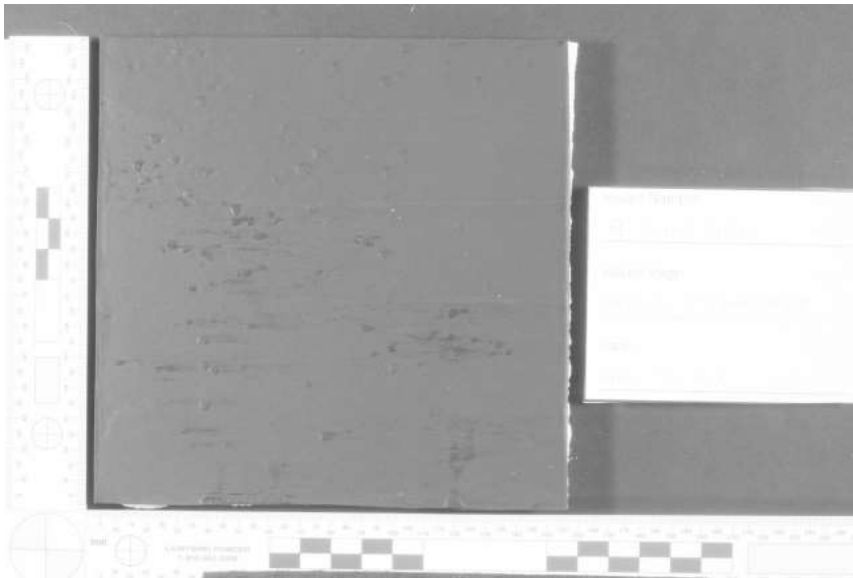
Longpass #89B Single

White Latex 8 – Control No Bloodstain

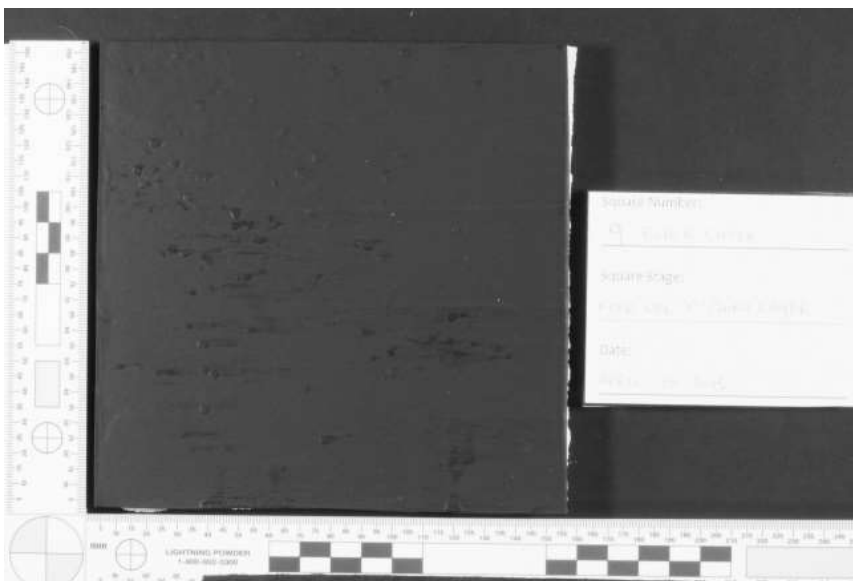


Longpass #70 HDR

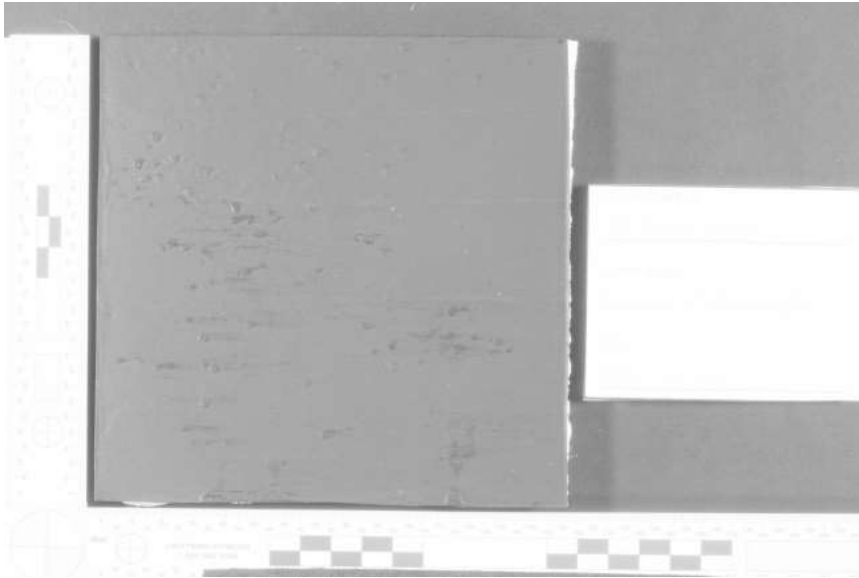
Appendix 4.2.3.3. Black Latex 70, 87, 87A, 87B, 88A, 89B First layer of paint stage
Black Latex 9 – Medium Velocity



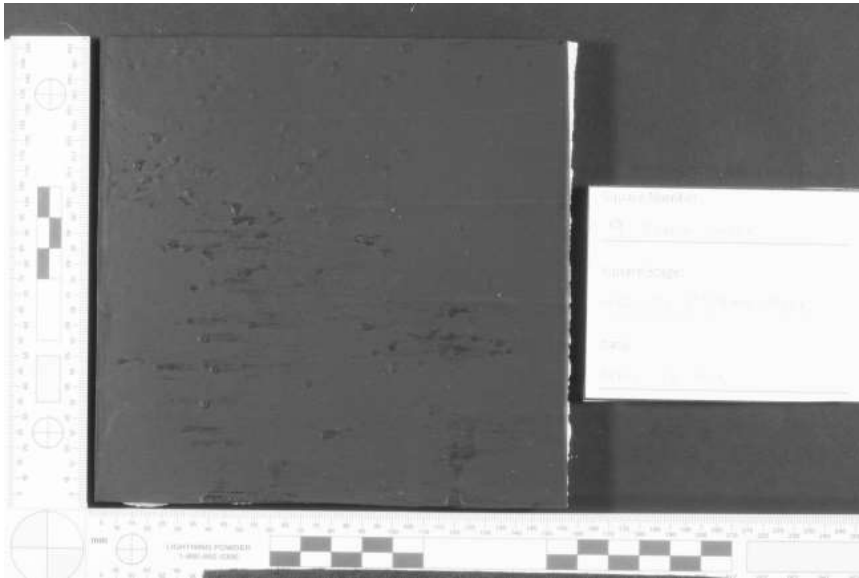
Longpass #70 HDR



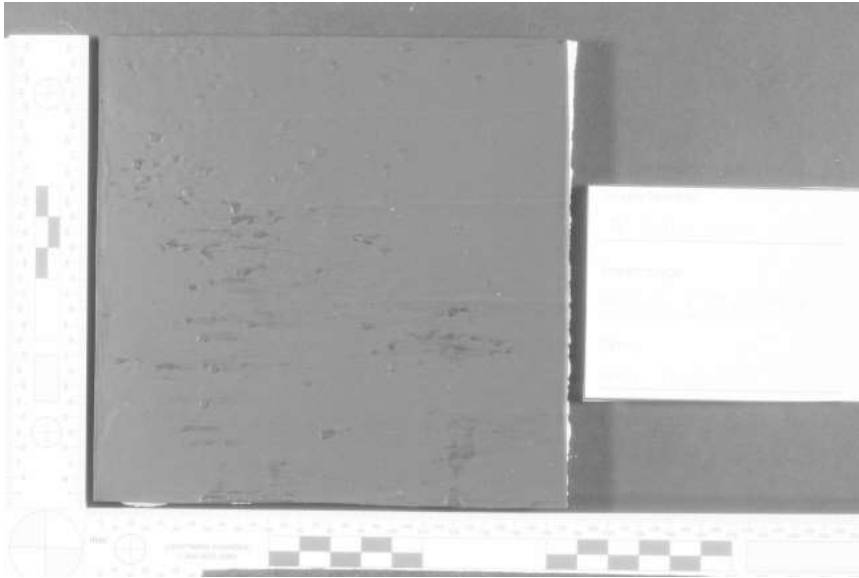
Longpass #70 Single



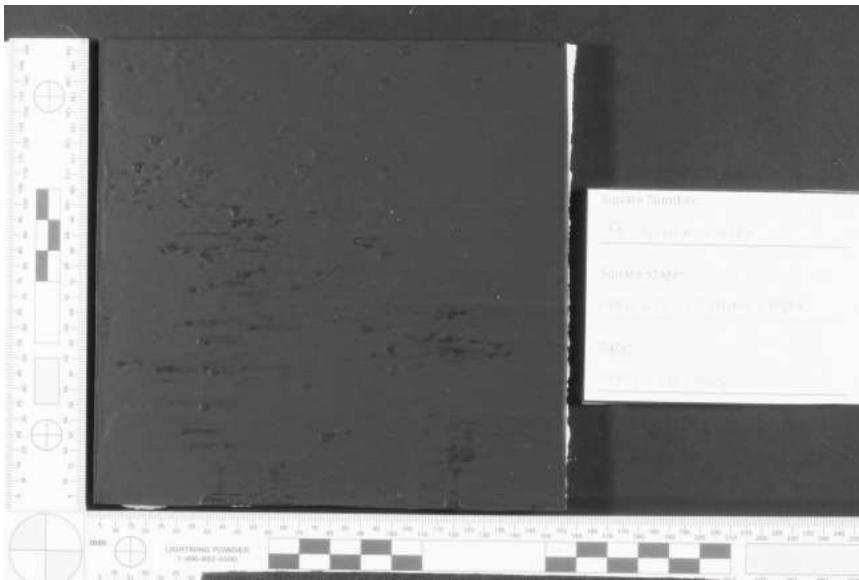
Longpass #87 HDR



Longpass #87 Single



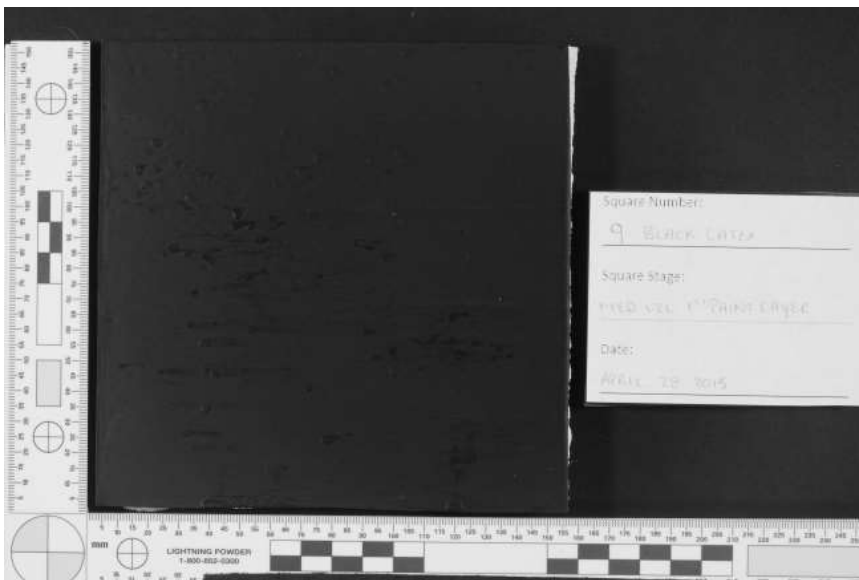
Longpass #87A HDR



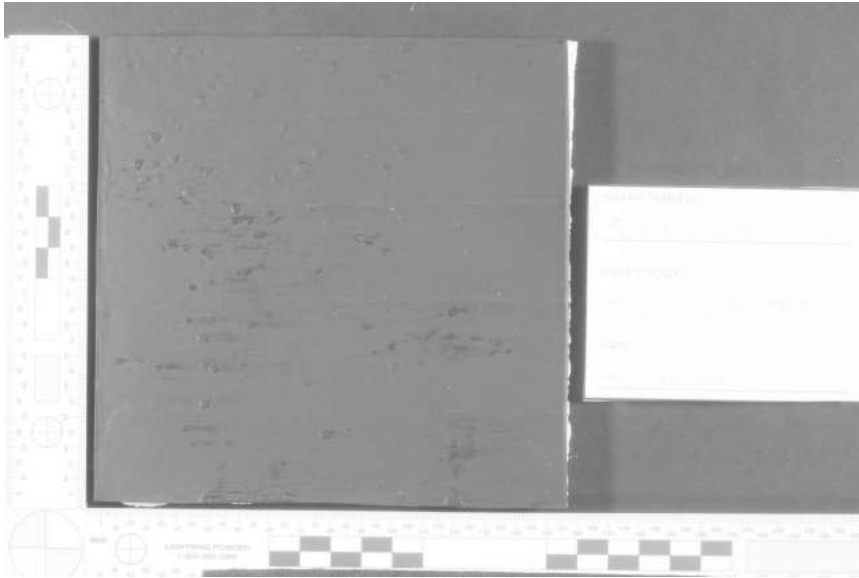
Longpass #87A Single



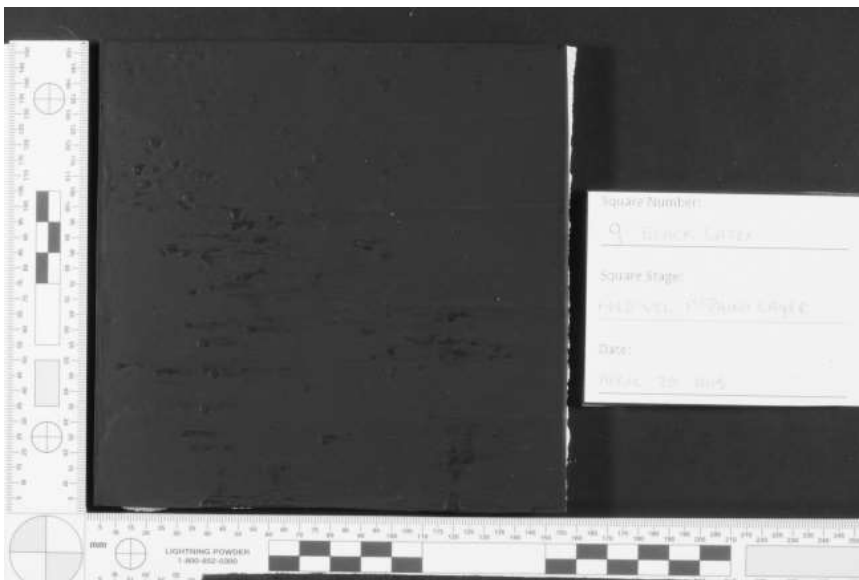
Longpass #87B HDR



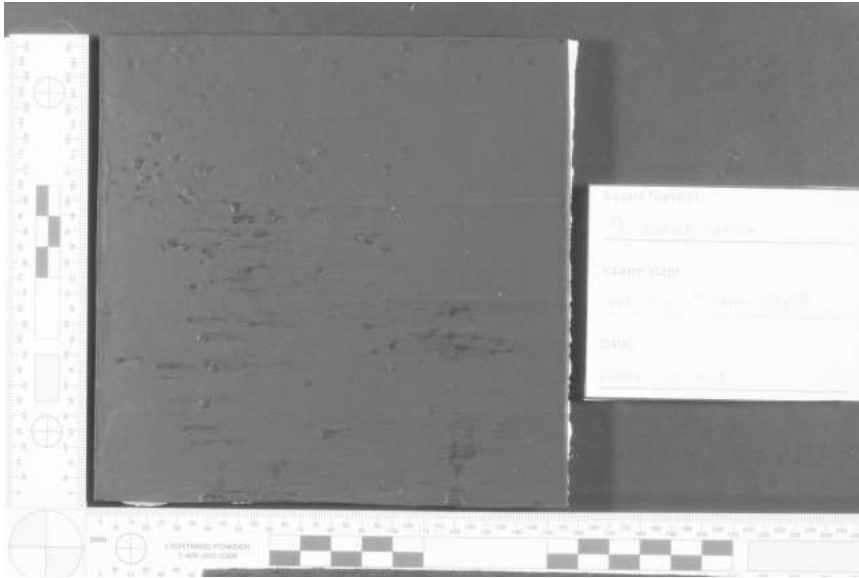
Longpass #87B Single



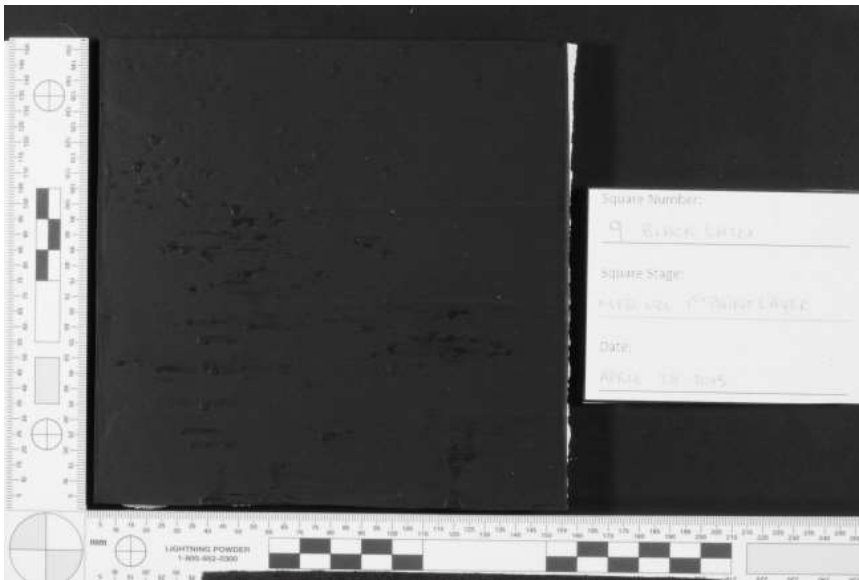
Longpass #88A HDR



Longpass #88A Single

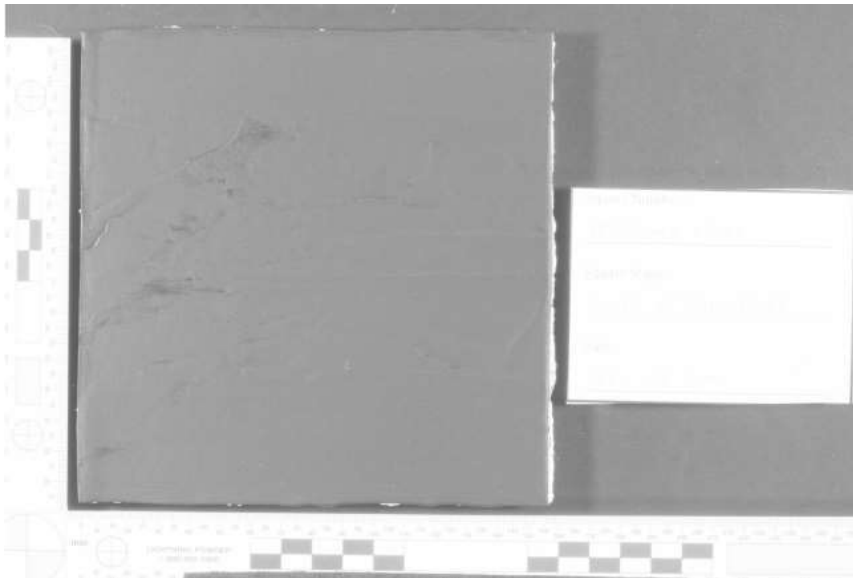


Longpass #89B HDR

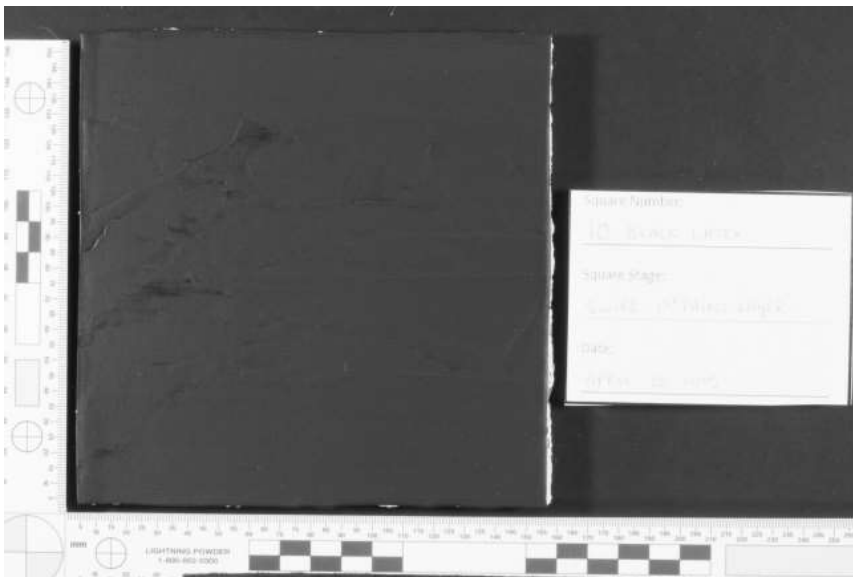


Longpass #89B Single

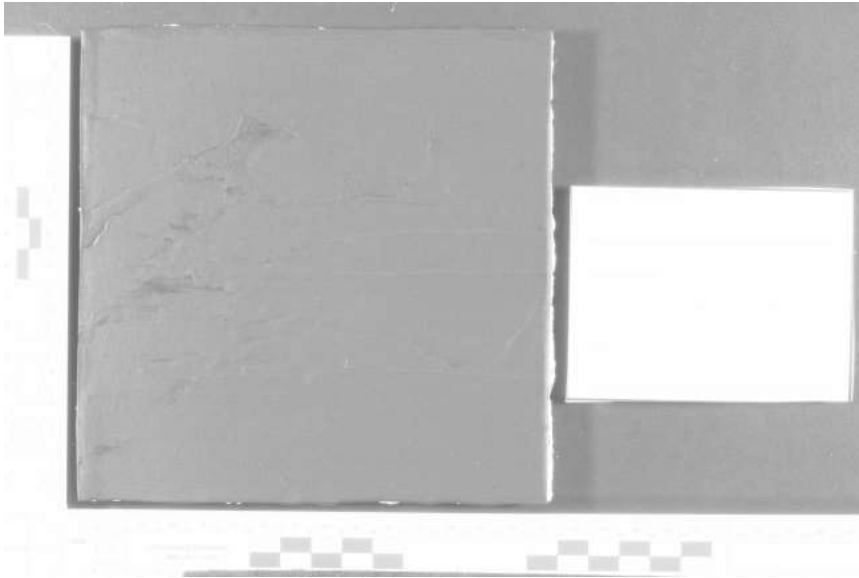
Black Latex 10 – Swipe



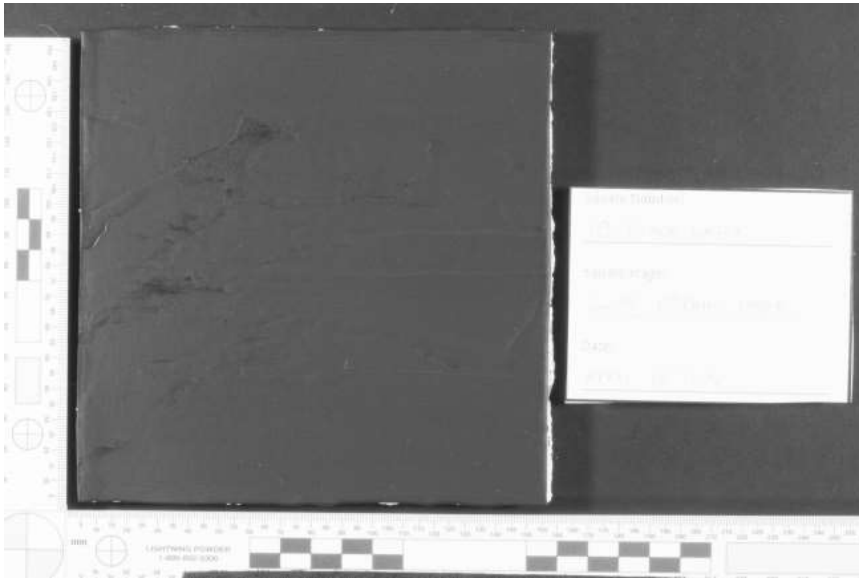
Longpass #70 HDR



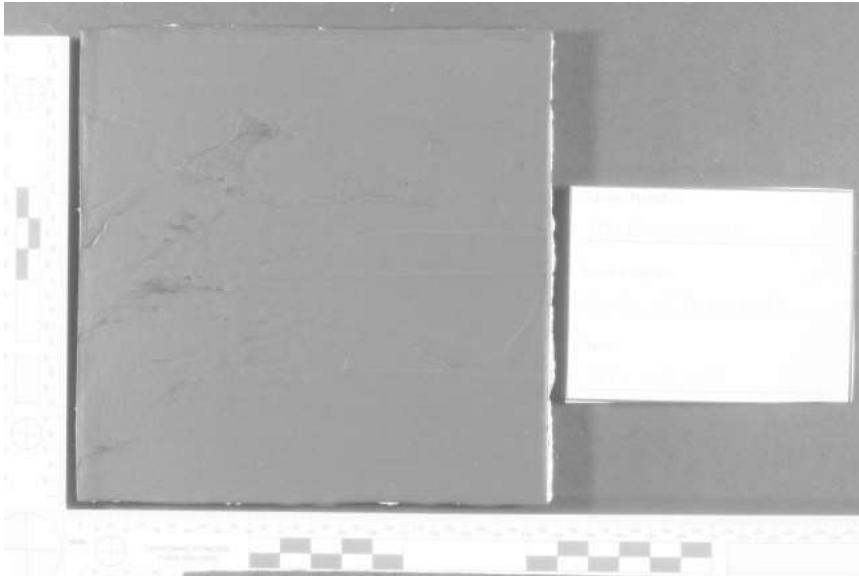
Longpass #70 Single



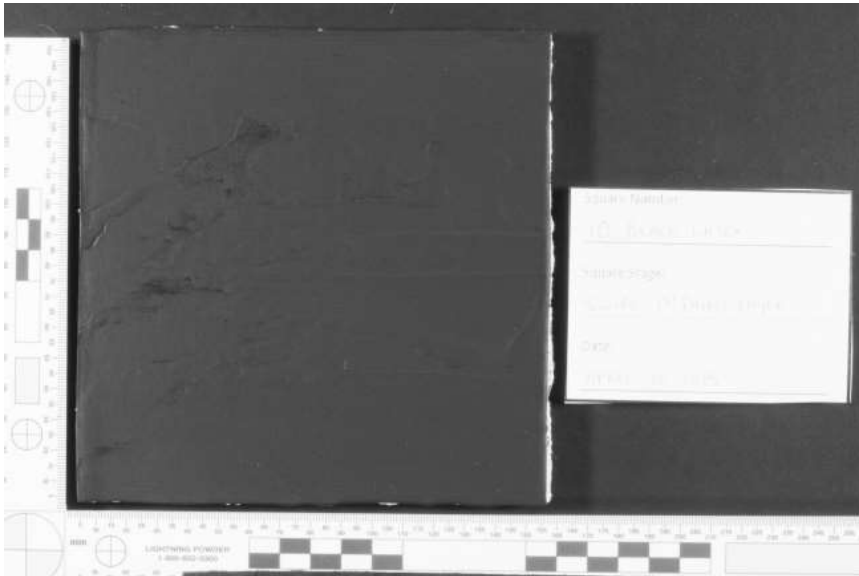
Longpass #87 HDR



Longpass #87 Single



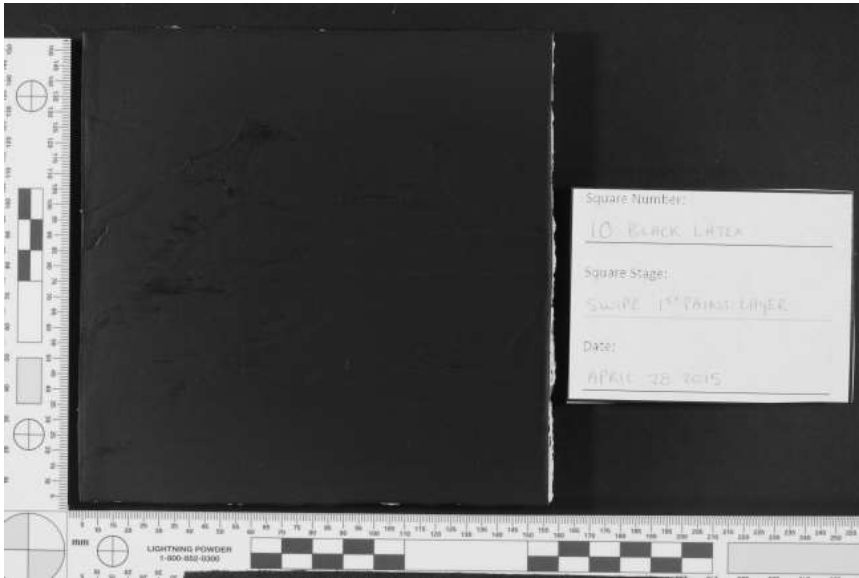
Longpass #87A HDR



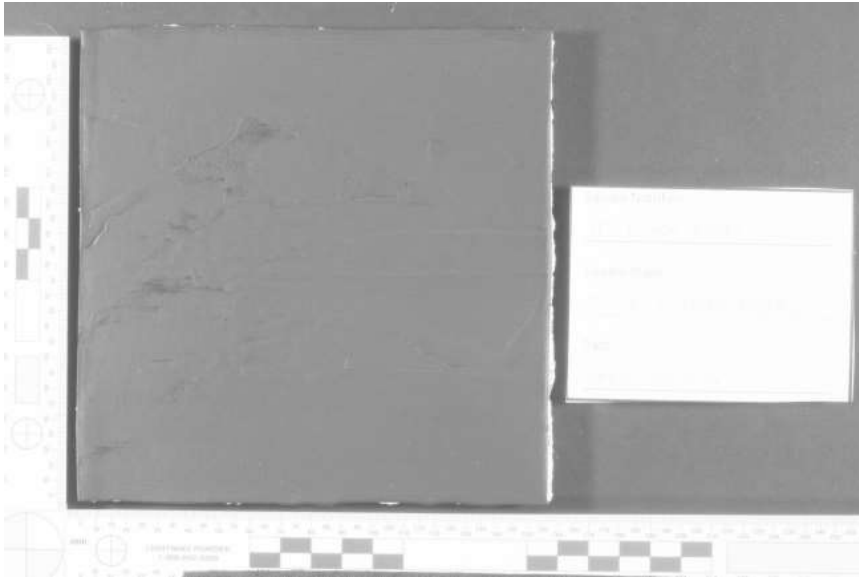
Longpass #87A Single



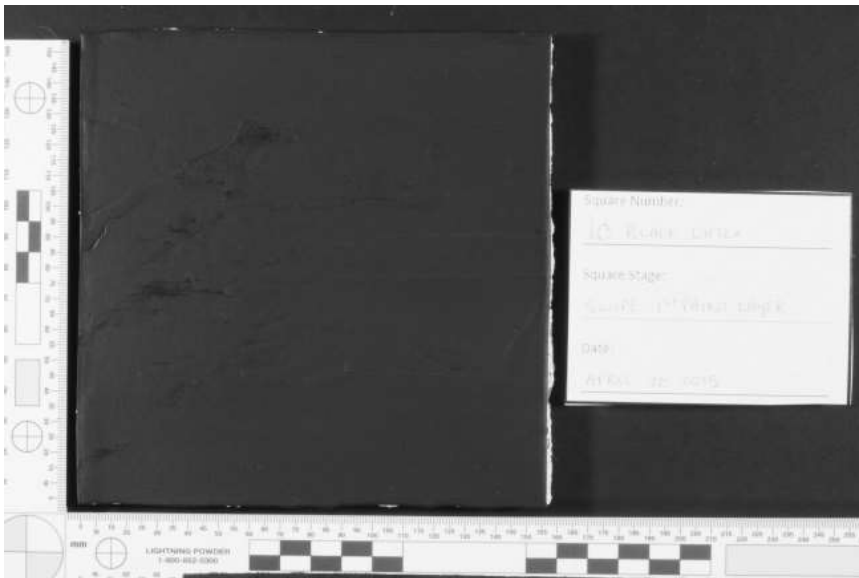
Longpass #87B HDR



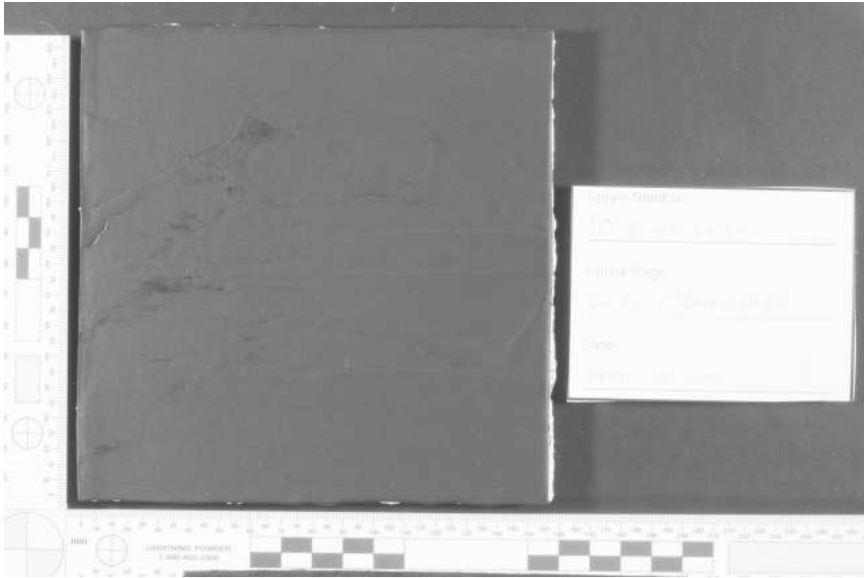
Longpass #87B Single



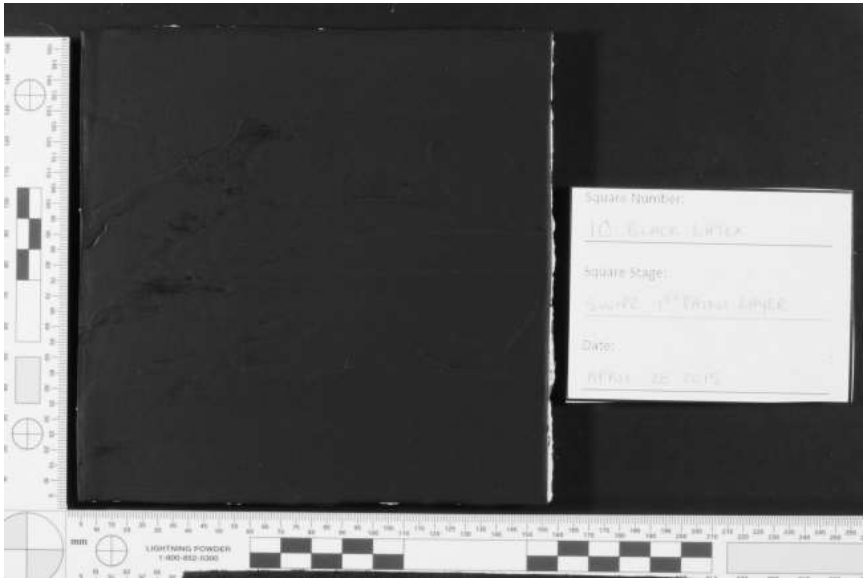
Longpass #88A HDR



Longpass #88A Single

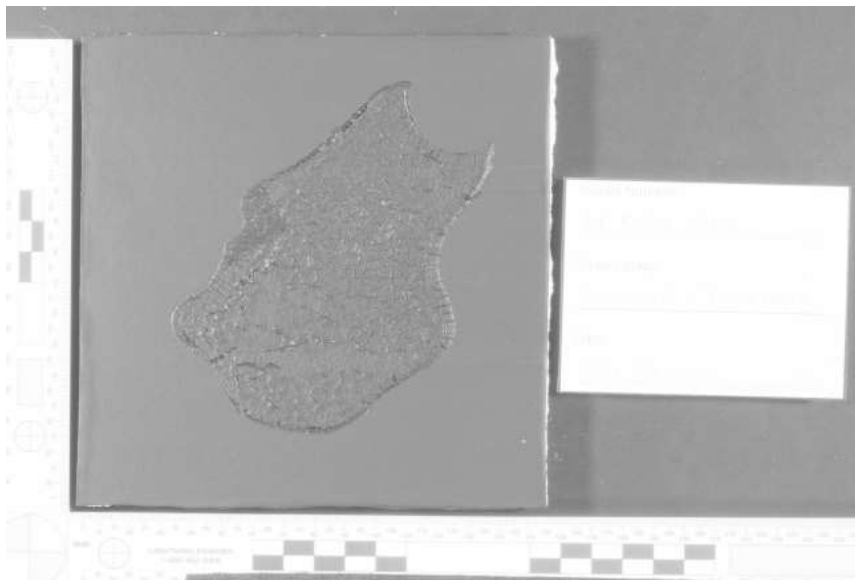


Longpass #89B HDR

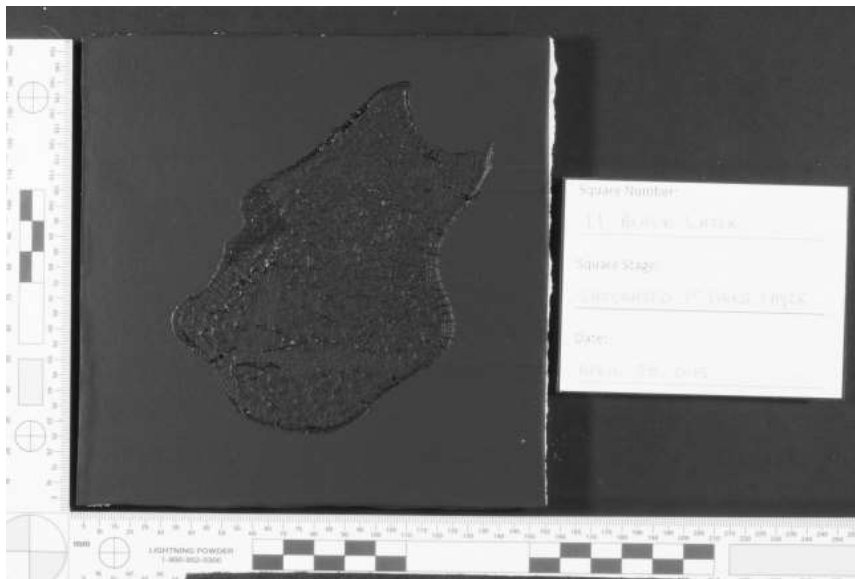


Longpass #89B Single

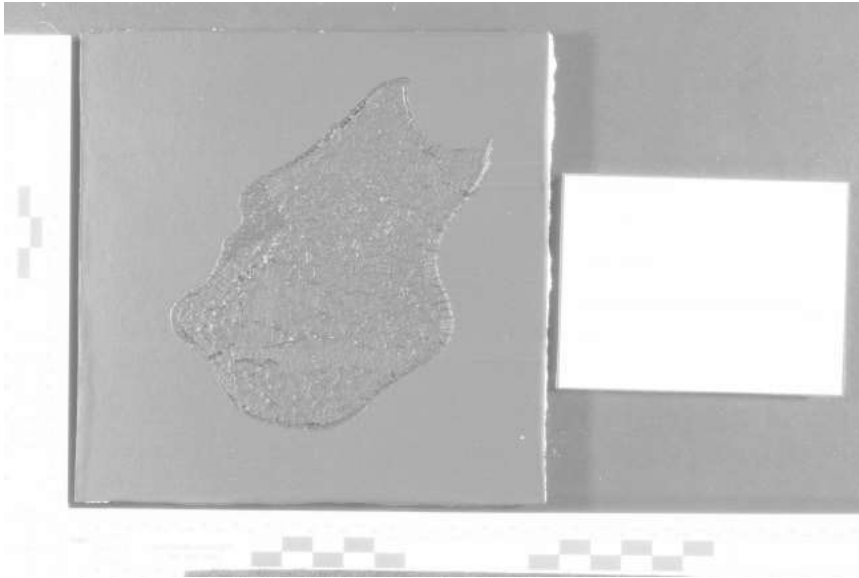
Black Latex 11 – Saturated



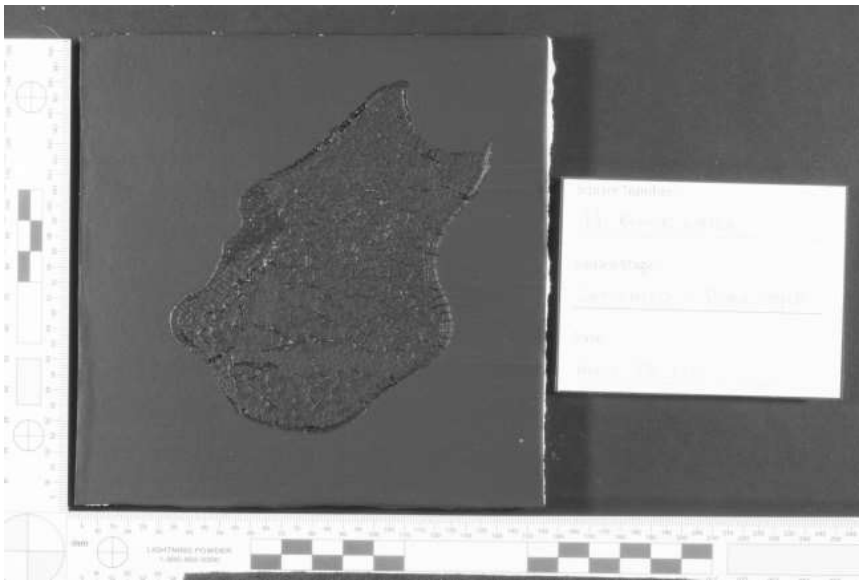
Longpass #70 HDR



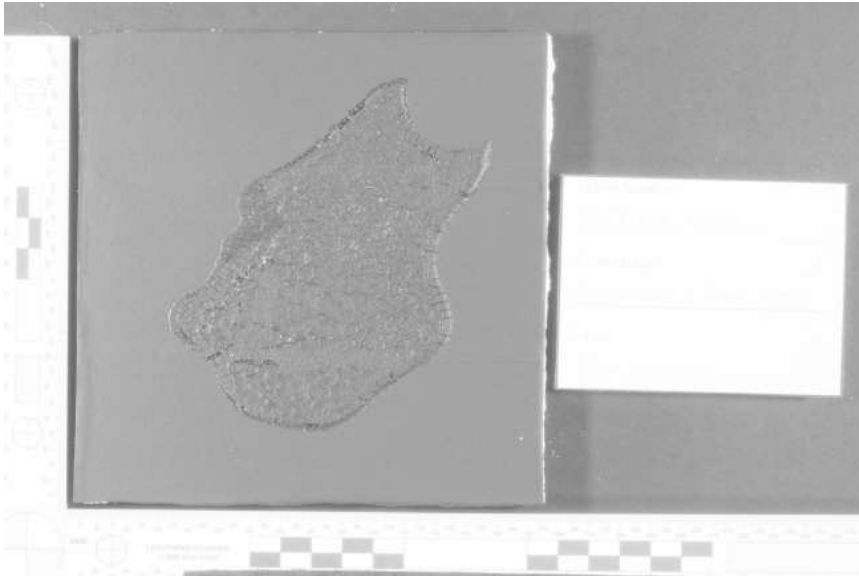
Longpass #70 Single



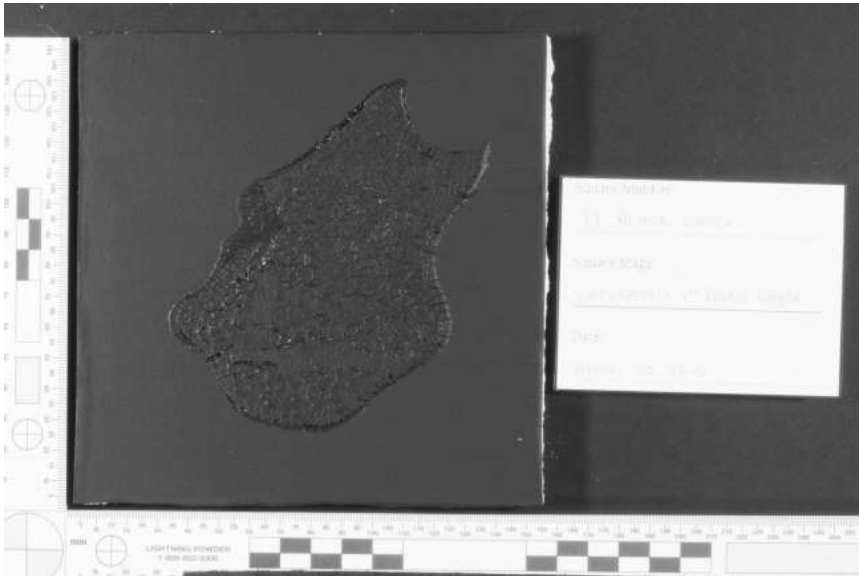
Longpass #87 HDR



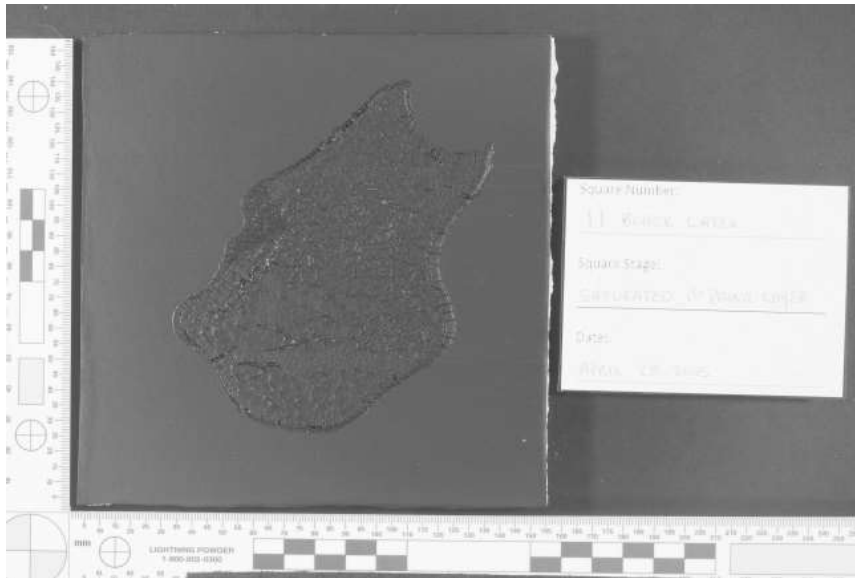
Longpass #87 Single



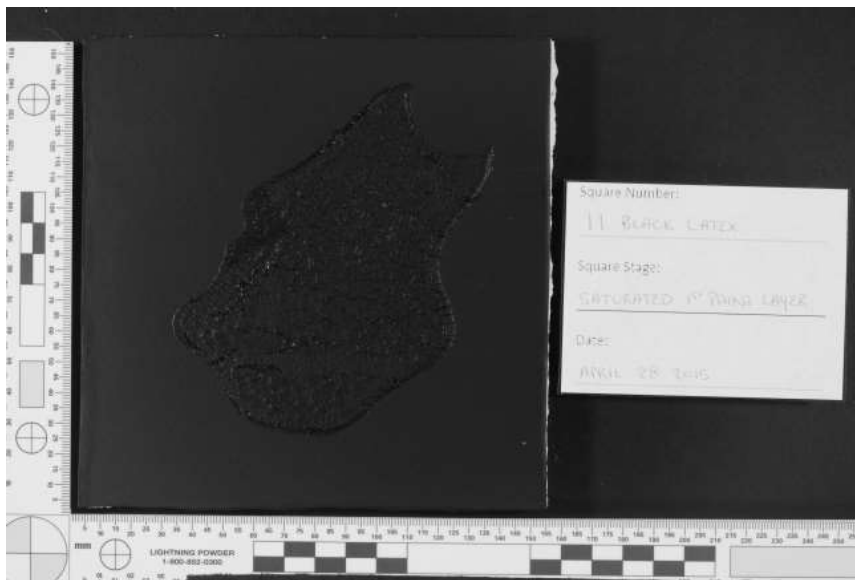
Longpass #87A HDR



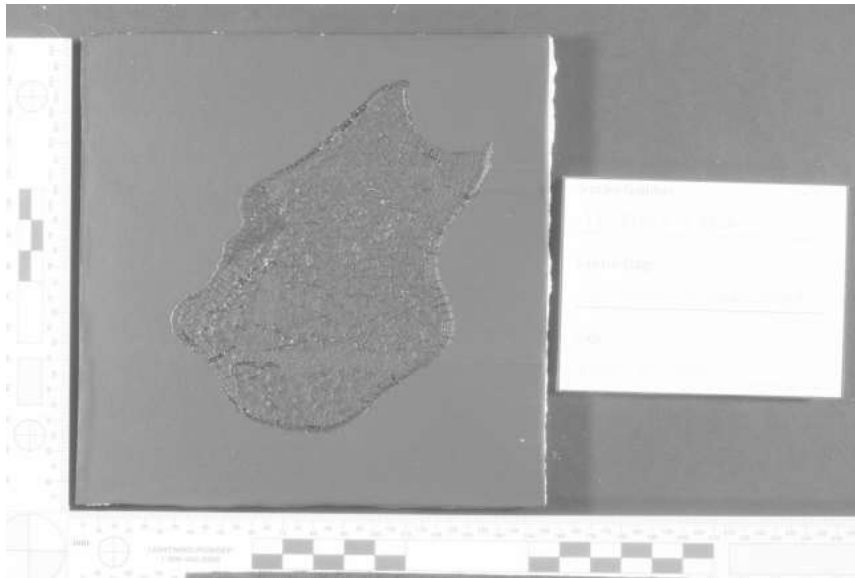
Longpass #87A Single



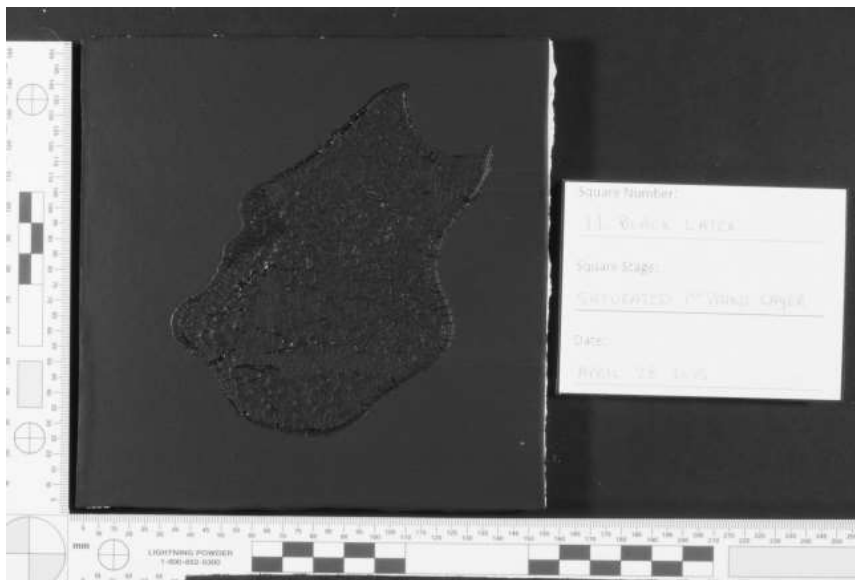
Longpass #87B HDR



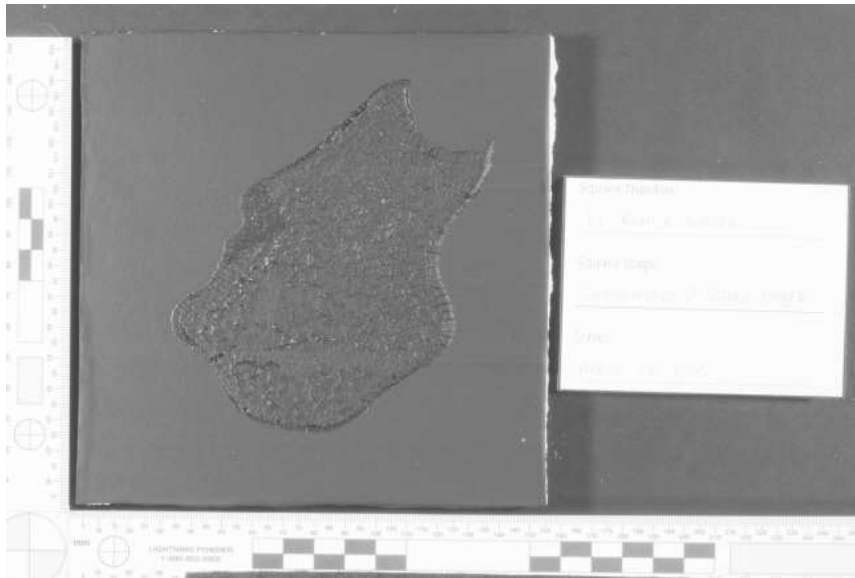
Longpass #87B Single



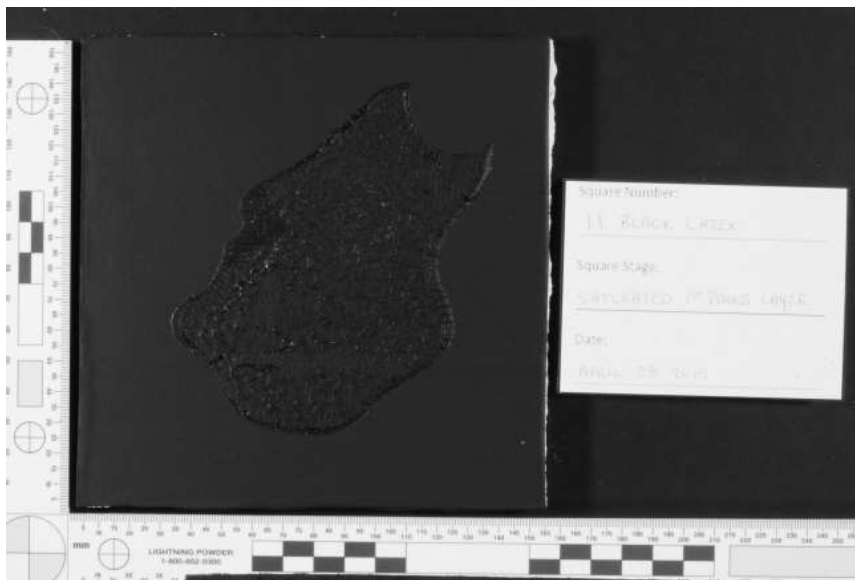
Longpass #88A HDR



Longpass #88A Single

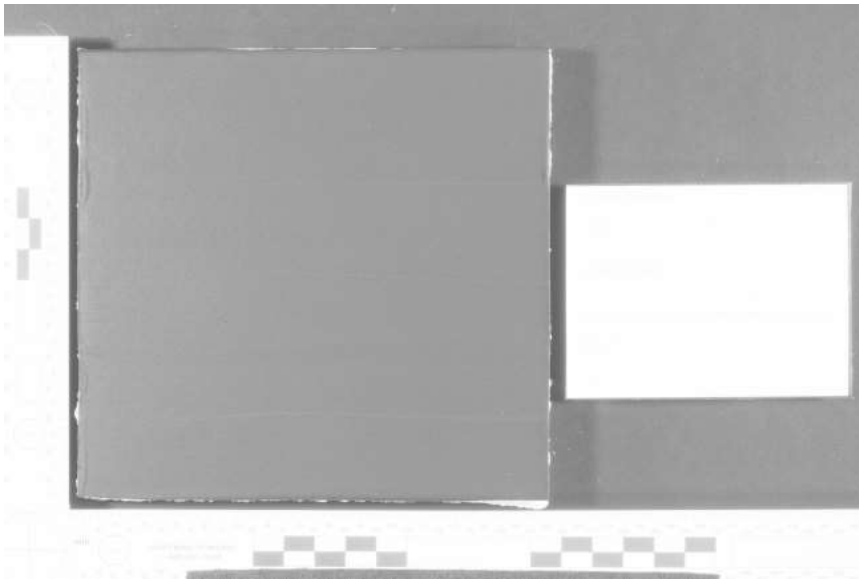


Longpass #89B HDR



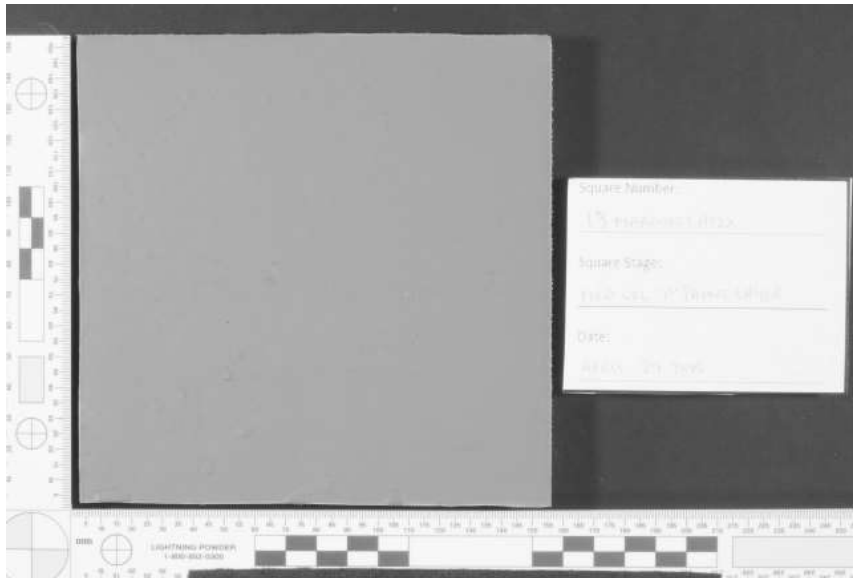
Longpass #89B Single

Black Latex 12 – Control No Bloodstain



Longpass #70 HDR

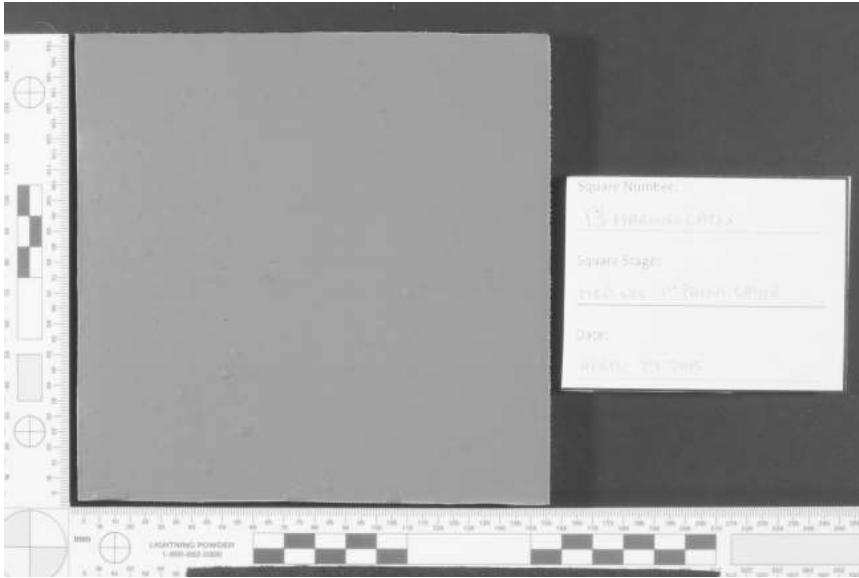
Appendix 4.2.3.4. Maroon Latex 70, 87, 87A, 87B, 88A, 89B First layer of paint stage
Maroon Latex 13 – Medium Velocity



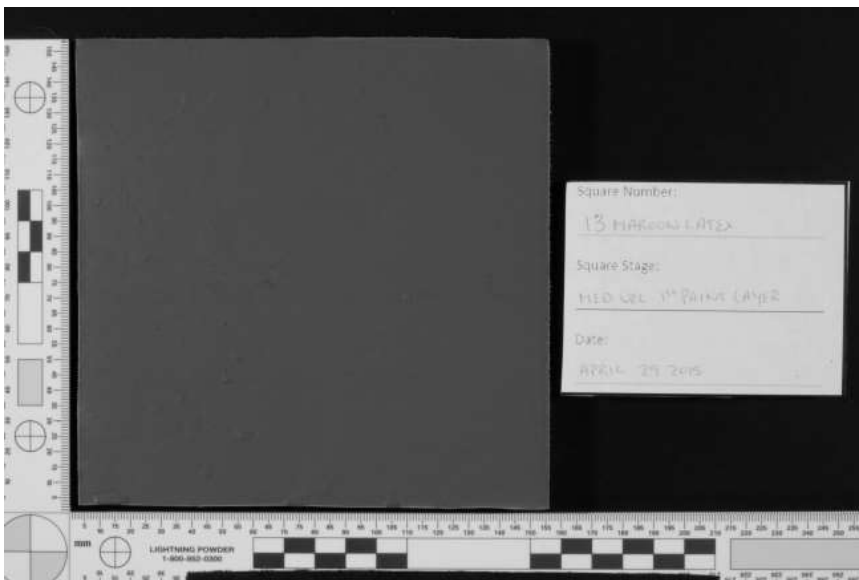
Longpass #70 HDR



Longpass #70 Single



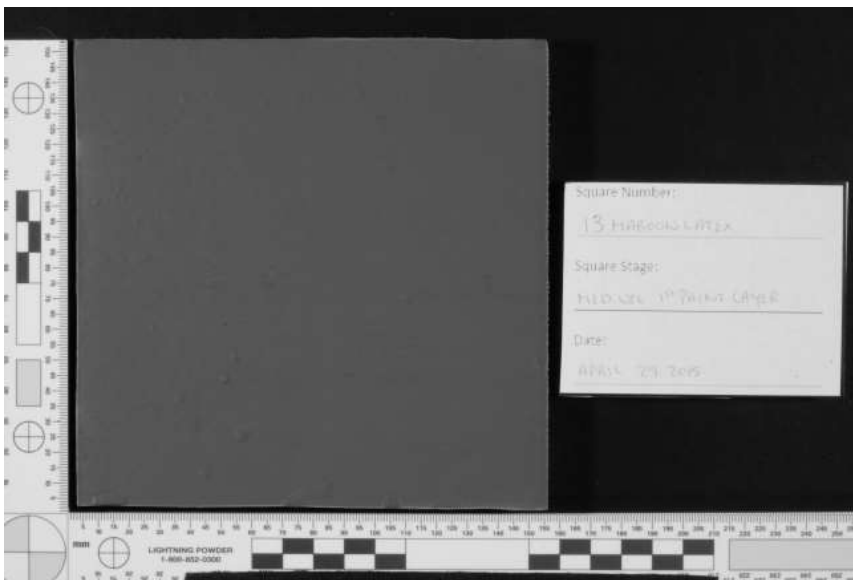
Longpass #87 HDR



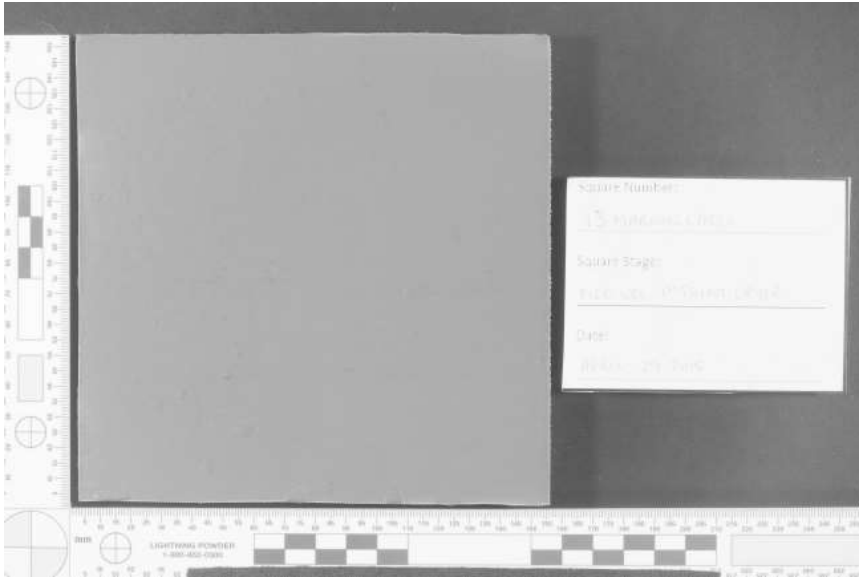
Longpass #87 Single



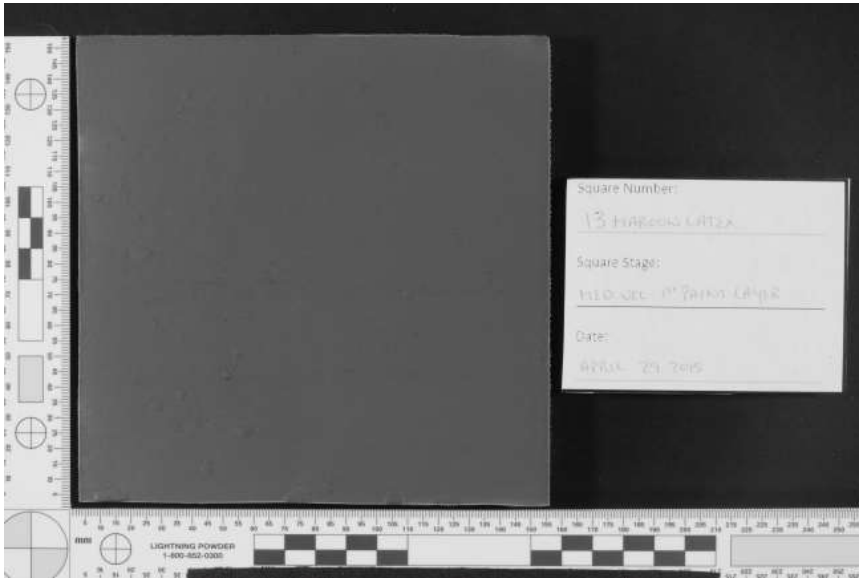
Longpass #87A HDR



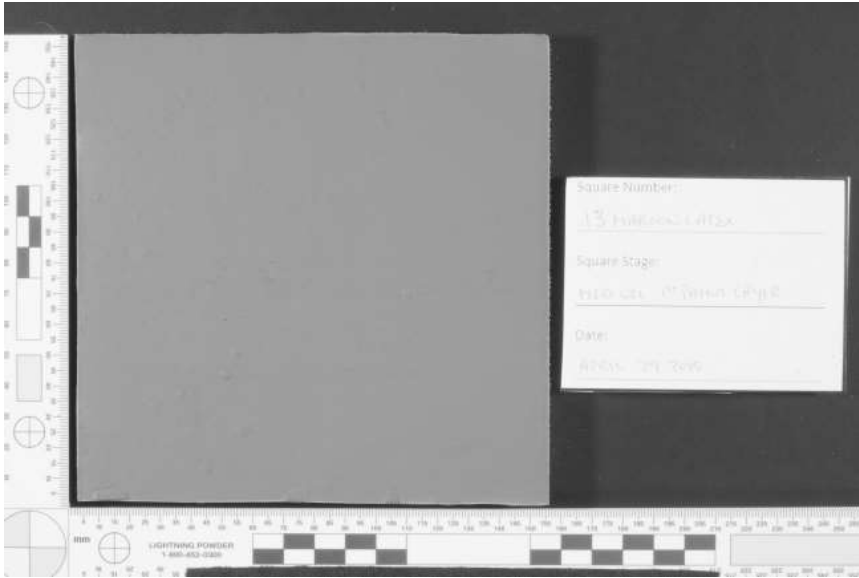
Longpass #87A Single



Longpass #87B HDR



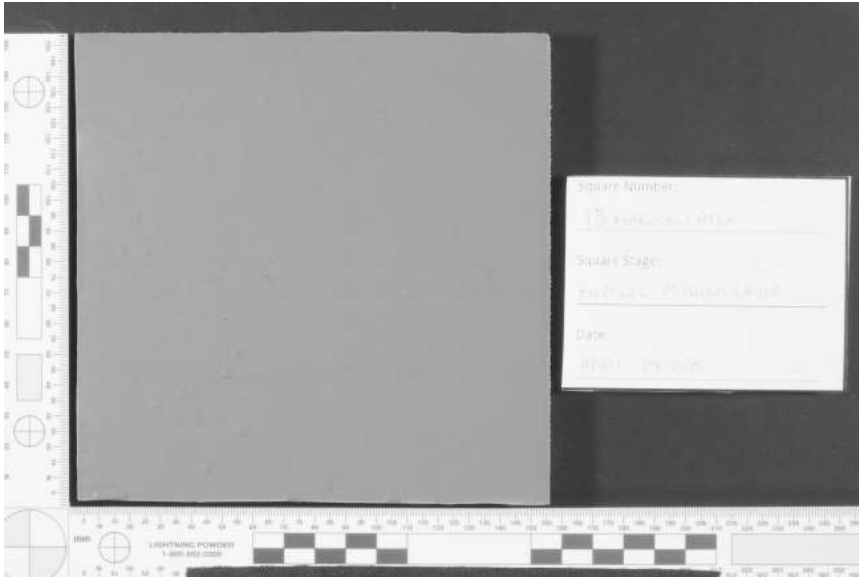
Longpass #87B Single



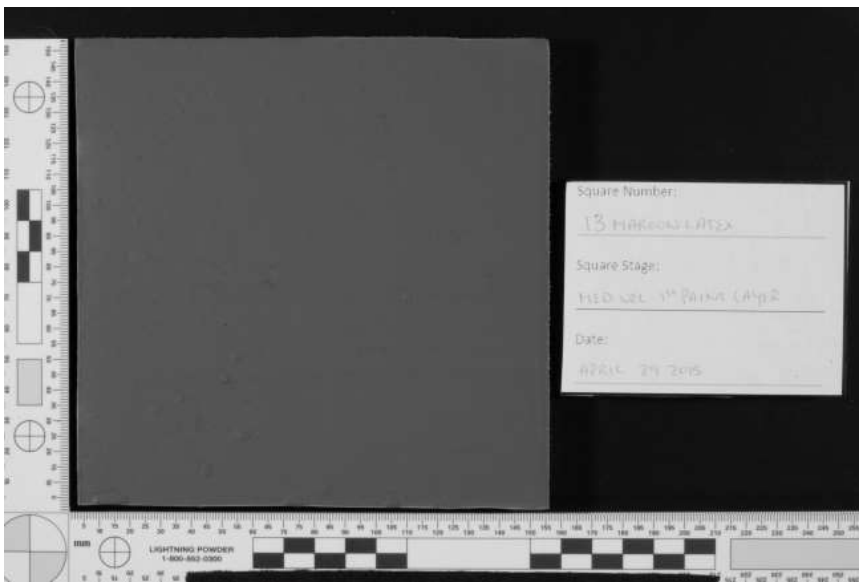
Longpass #88A HDR



Longpass #88A Single

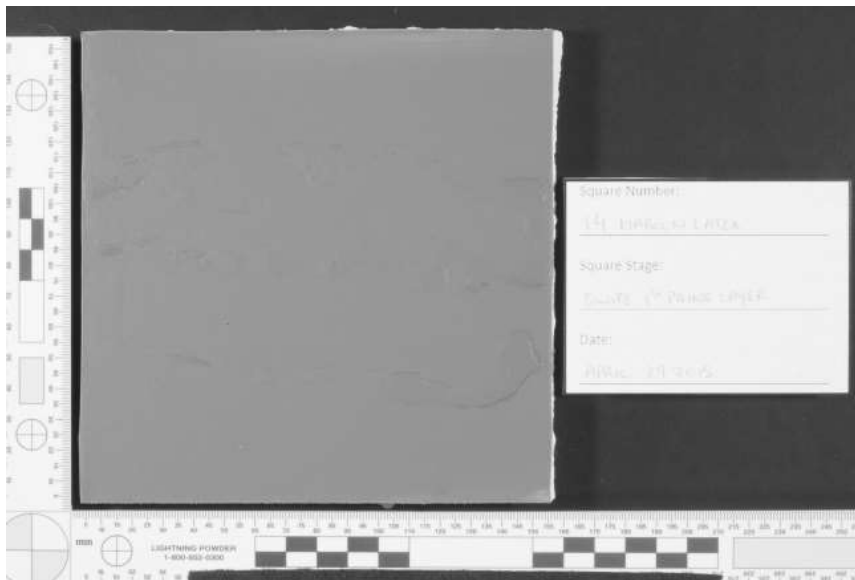


Longpass #89B HDR

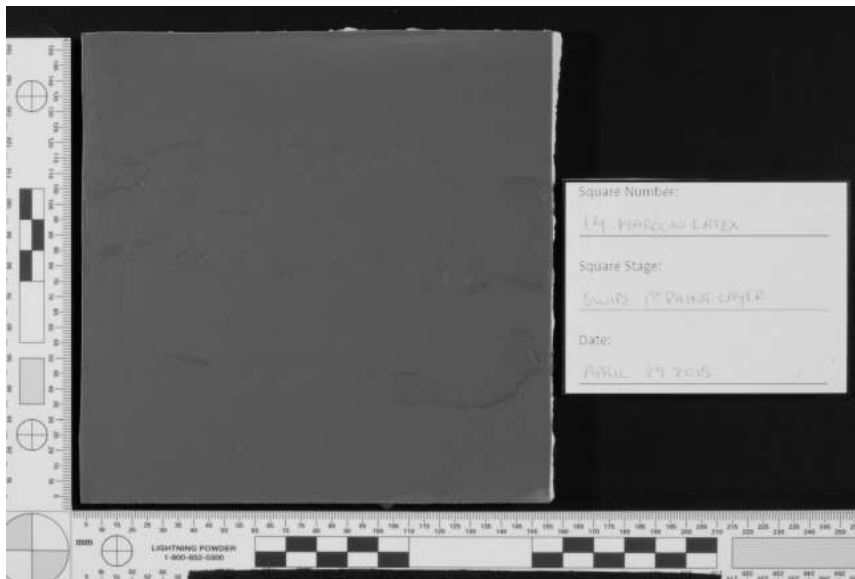


Longpass #89B Single

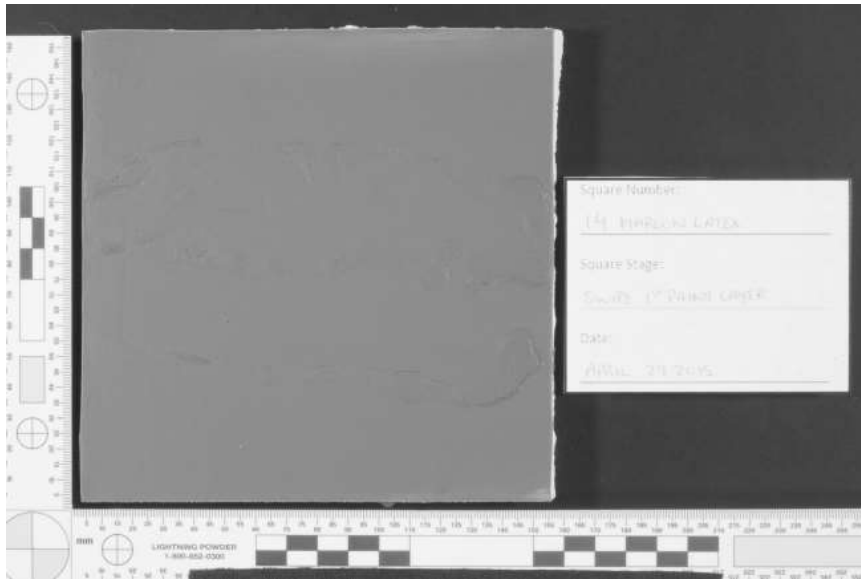
Maroon Latex 14 – Swipe



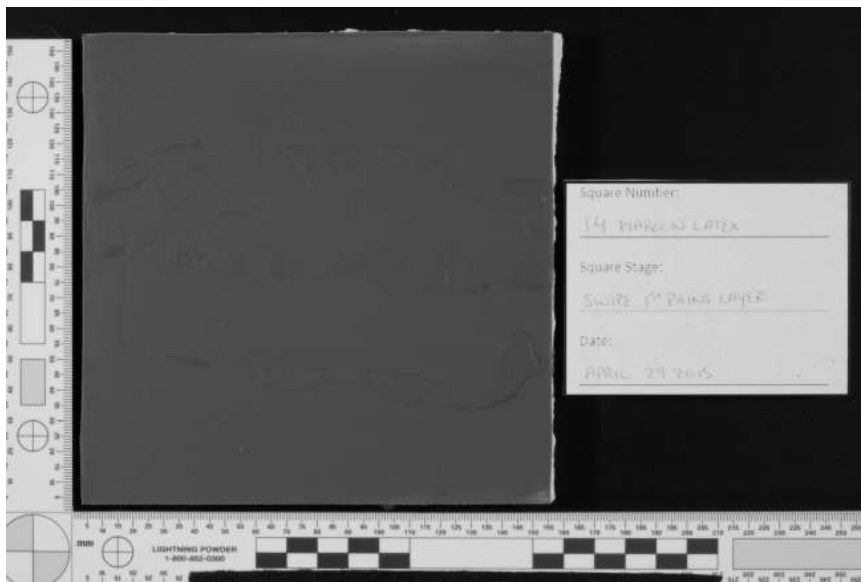
Longpass #70 HDR



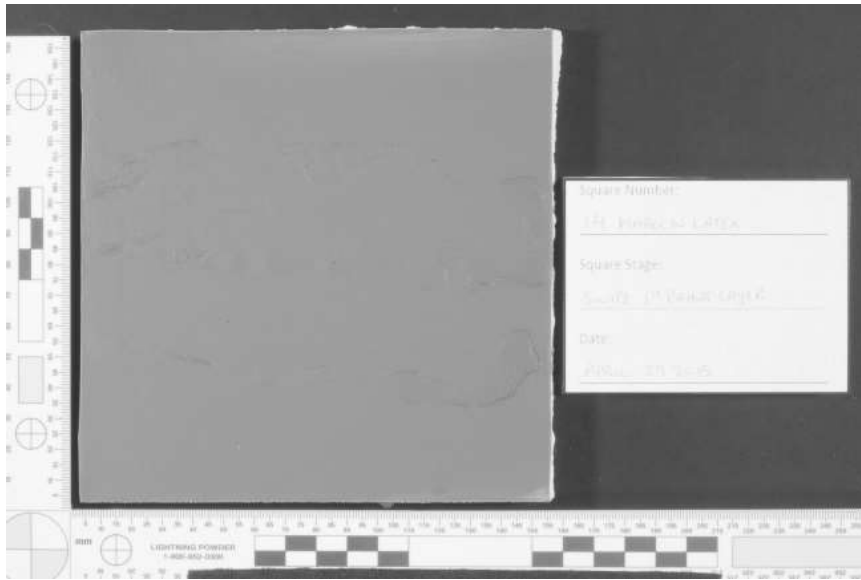
Longpass #70 Single



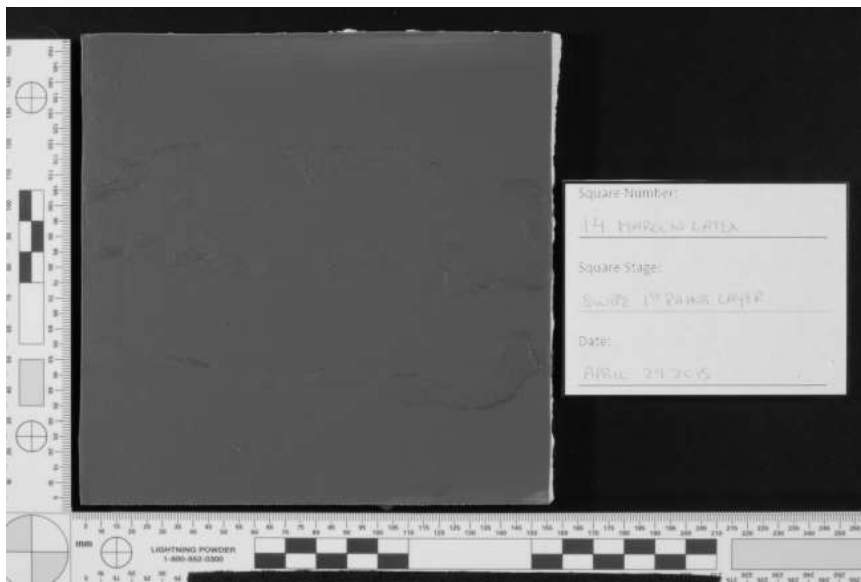
Longpass #87 HDR



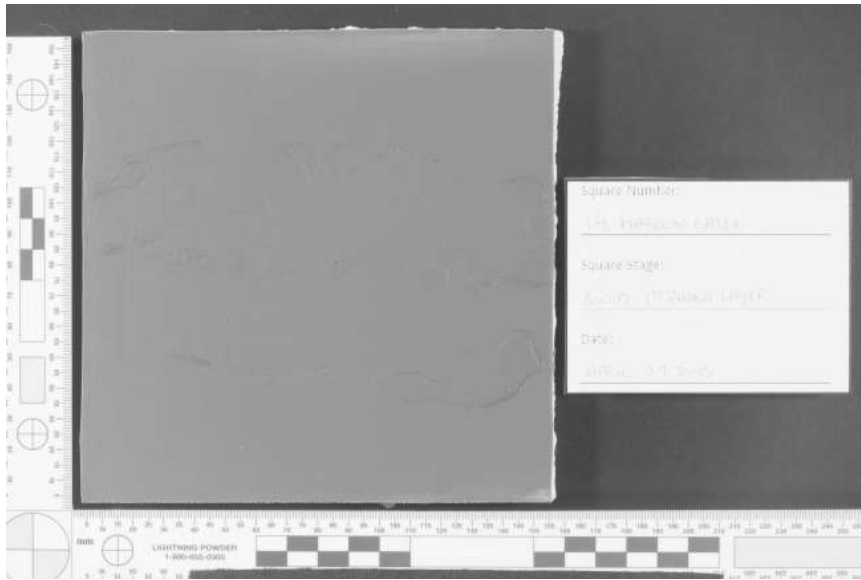
Longpass #87 Single



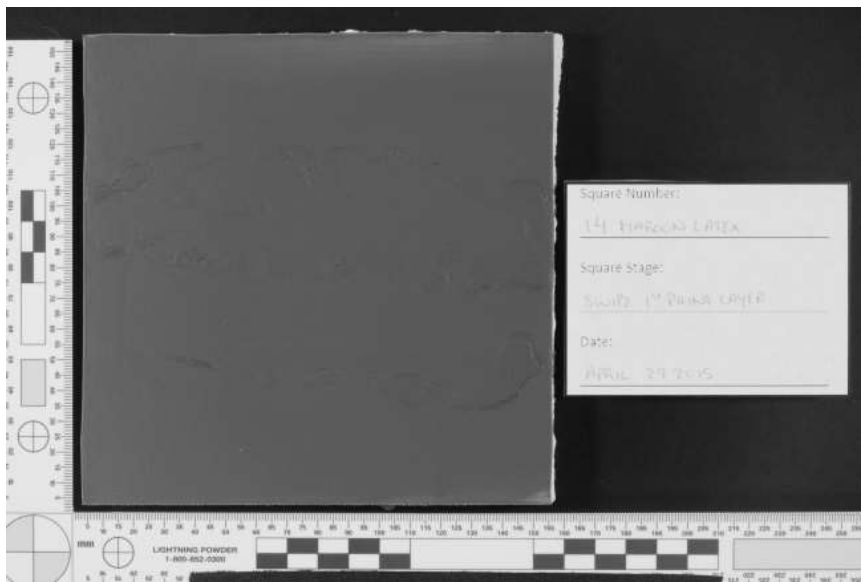
Longpass #87A HDR



Longpass #87A Single



Longpass #87B HDR



Longpass #87B Single



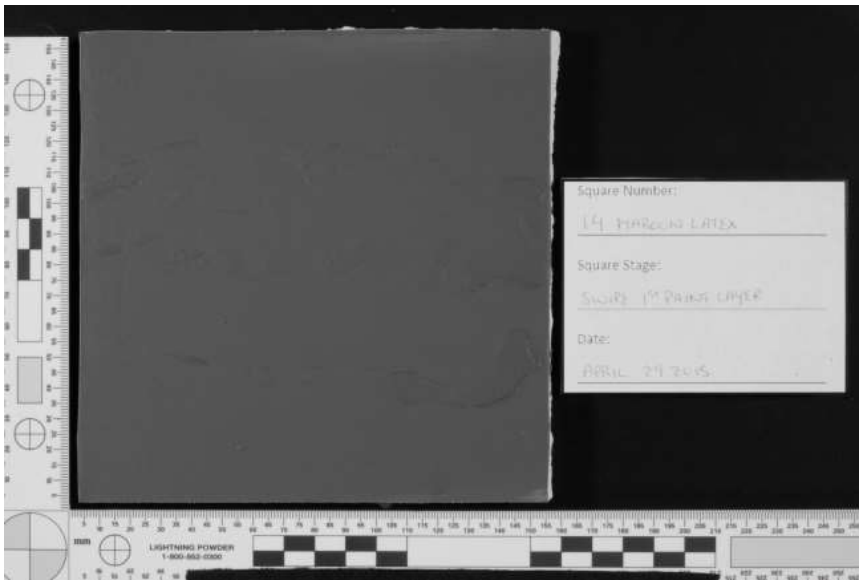
Longpass #88A HDR



Longpass #88A Single



Longpass #89B HDR

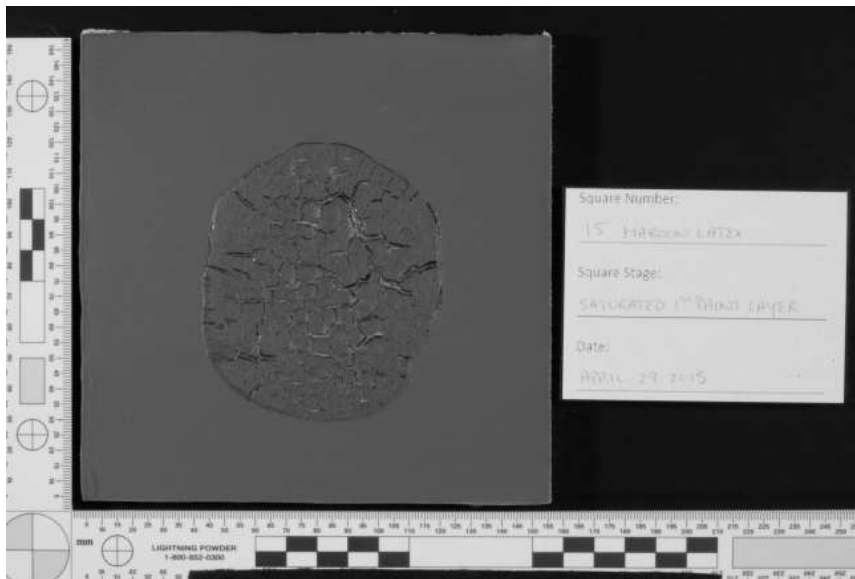


Longpass #89B Single

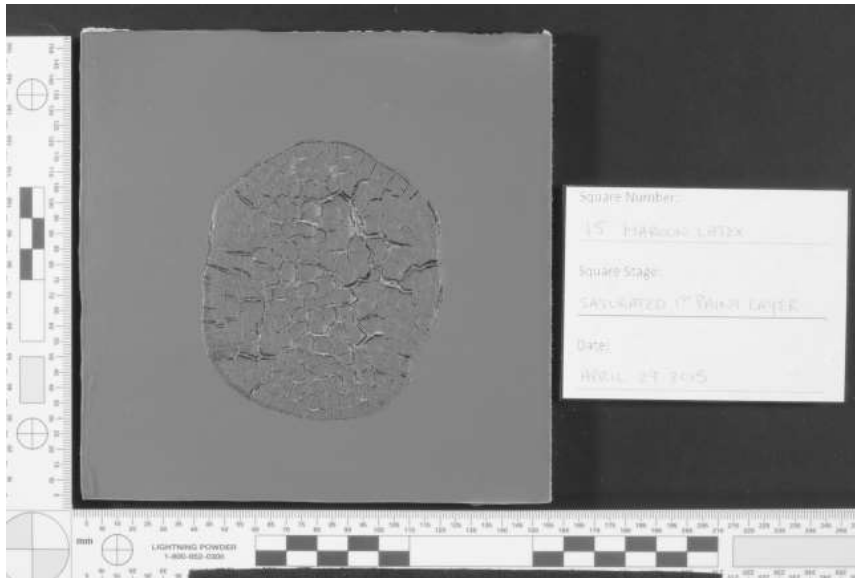
Maroon Latex 15 – Saturated



Longpass #70 HDR



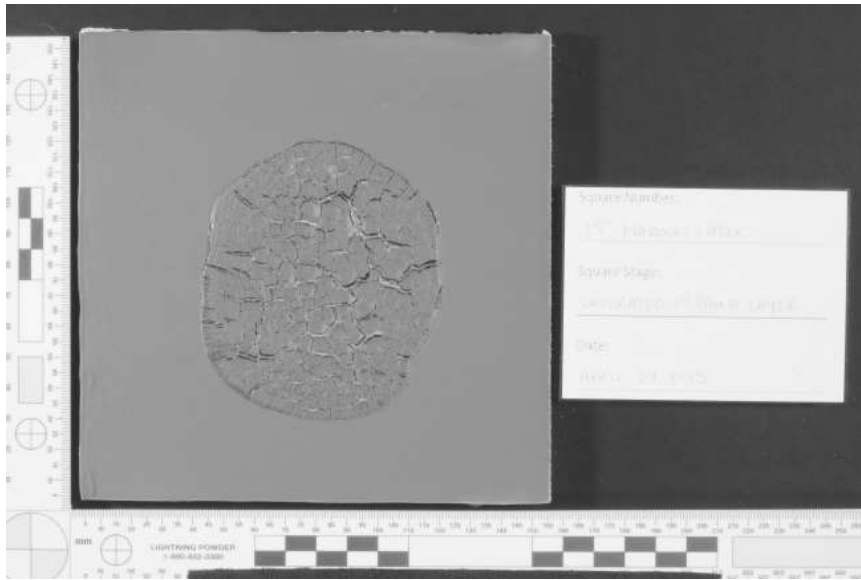
Longpass #70 Single



Longpass #87 HDR



Longpass #87 Single



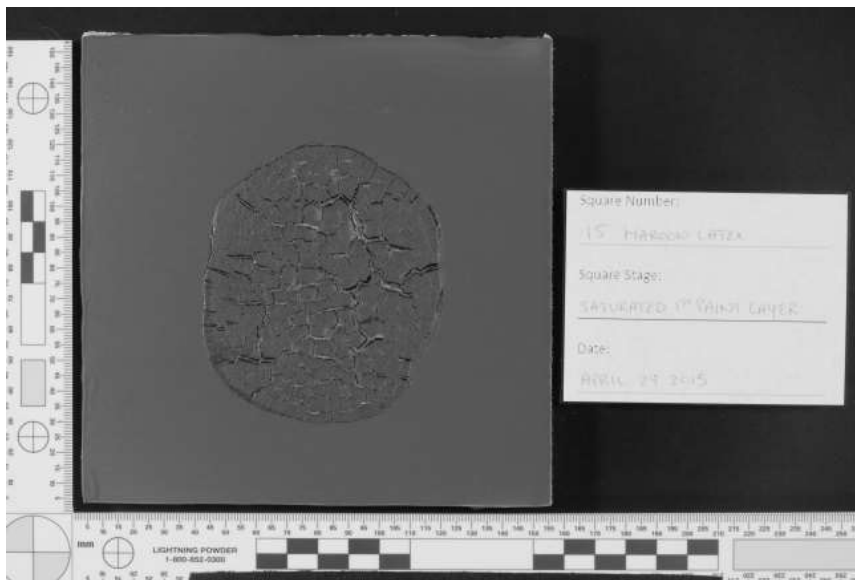
Longpass #87A HDR



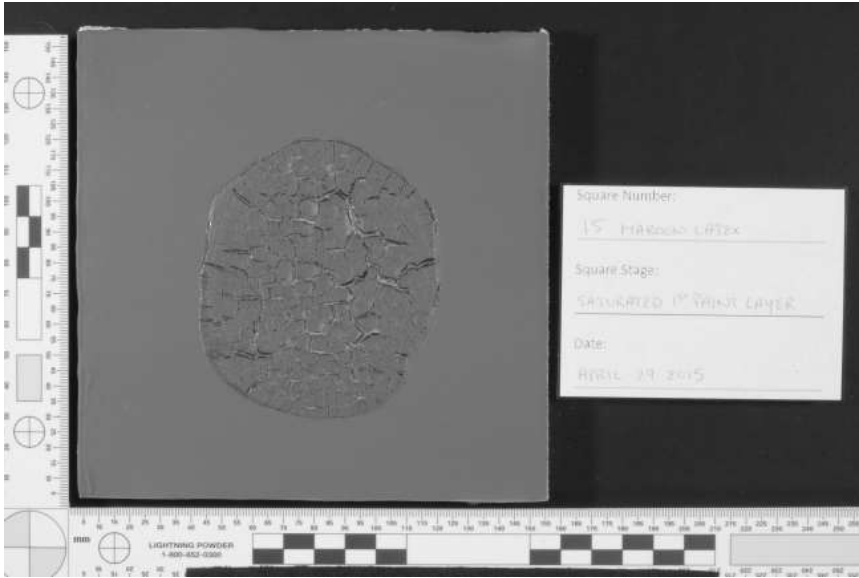
Longpass #87A Single



Longpass #87B HDR



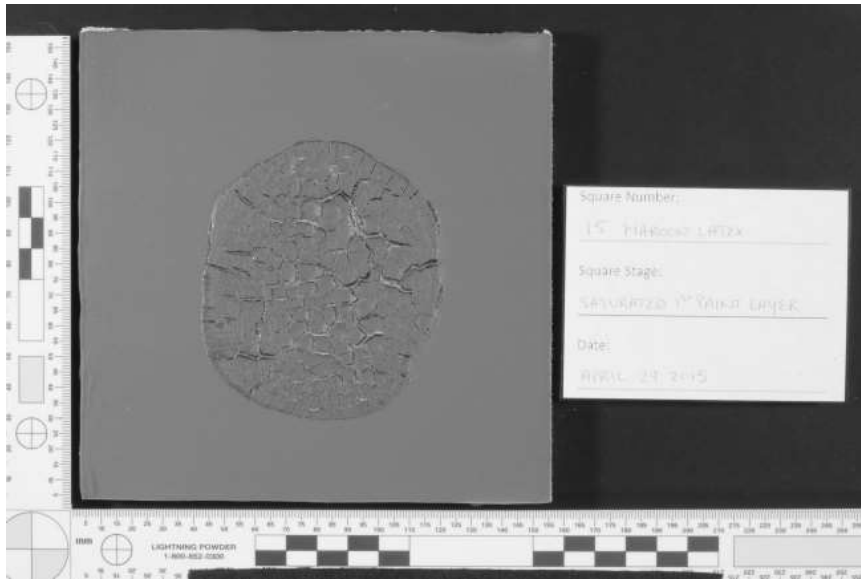
Longpass #87B Single



Longpass #88A HDR



Longpass #88A Single



Longpass #89B HDR



Longpass #89B Single

Maroon Latex 16 – Control No Bloodstain

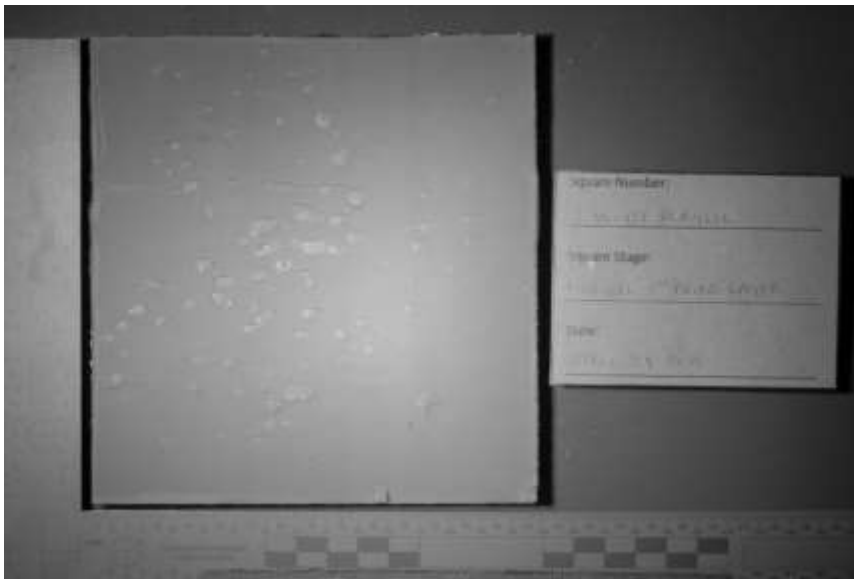


Longpass #70 HDR

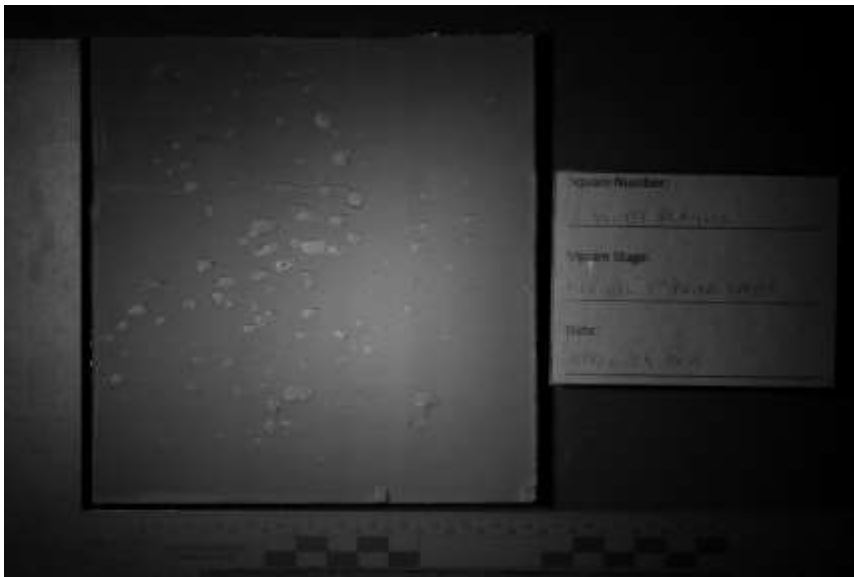
Appendix 4.2.4. Ultraviolet Photography

Appendix 4.2.4.1. White Acrylic First layer of paint stage

White Acrylic 1 – Medium Velocity

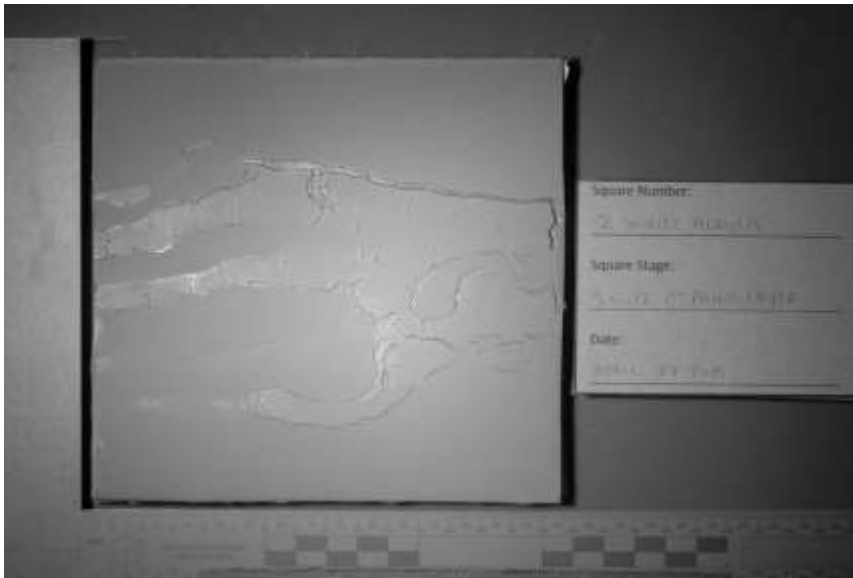


HDR

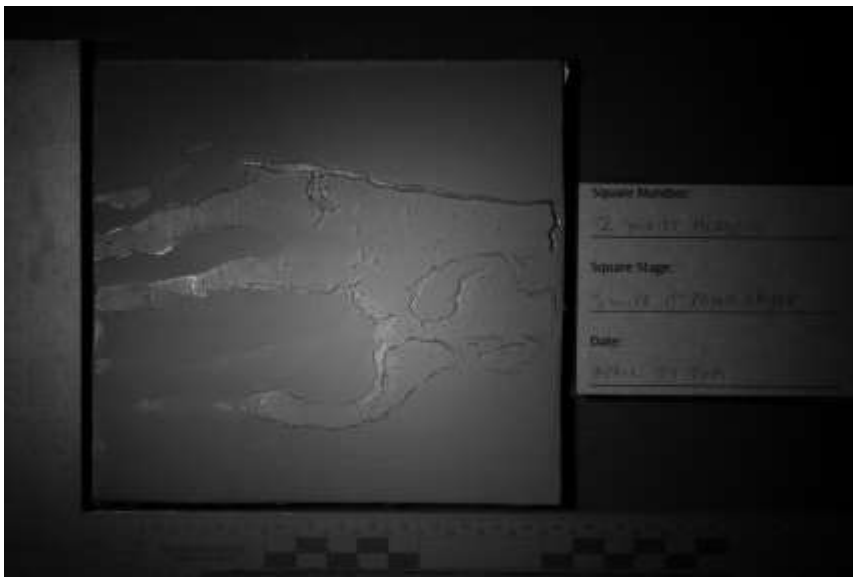


Single

White Acrylic 2 – Swipe

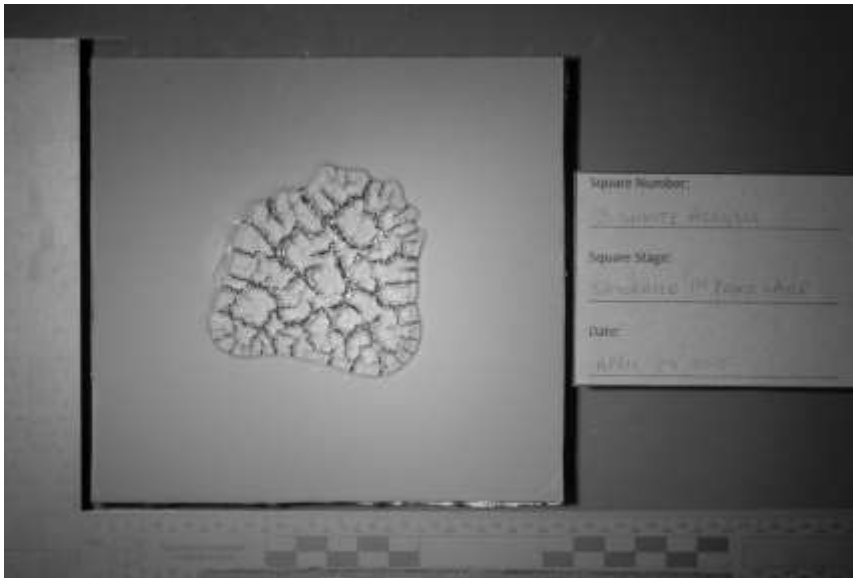


HDR

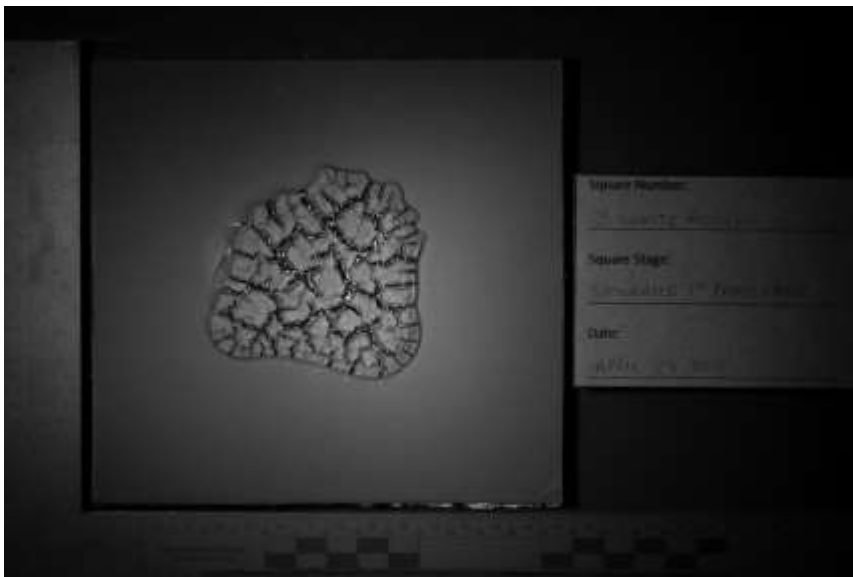


Single

White Acrylic 3 – Saturated



HDR



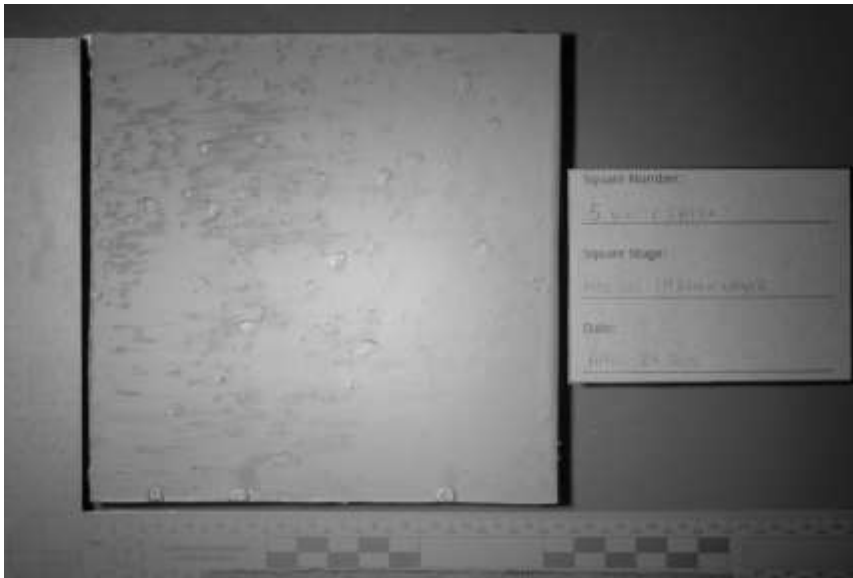
Single

White Acrylic 4 – Control No Bloodstain



HDR

Appendix 4.2.4.2. White Latex First layer of paint stage
White Latex 5 – Medium Velocity

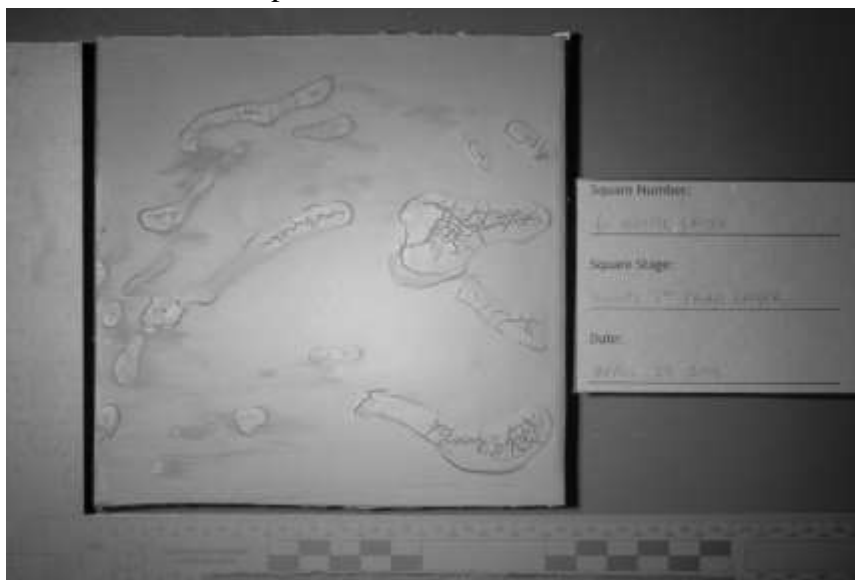


HDR

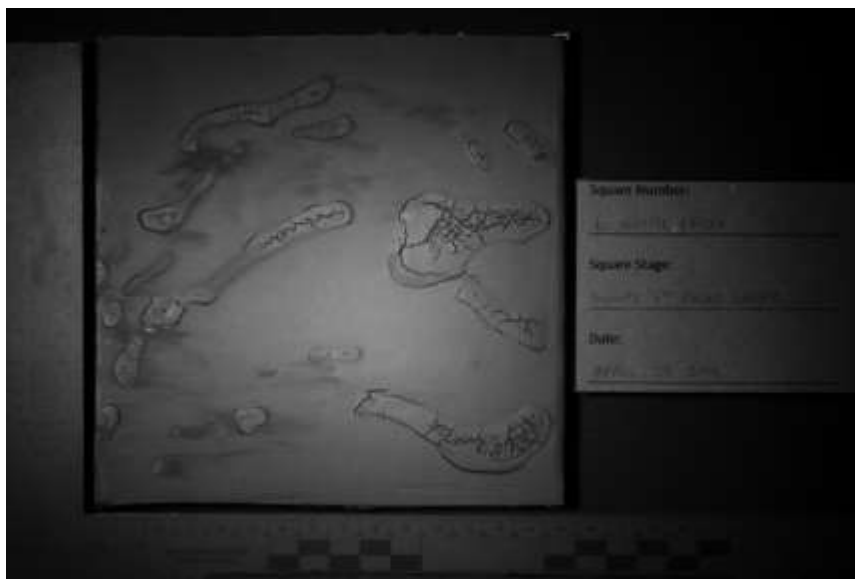


Single

White Latex 6 – Swipe

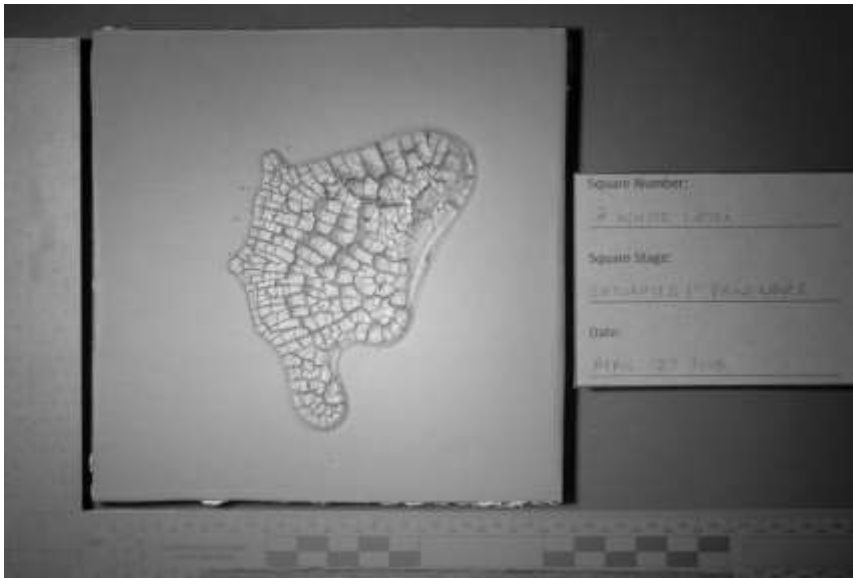


HDR

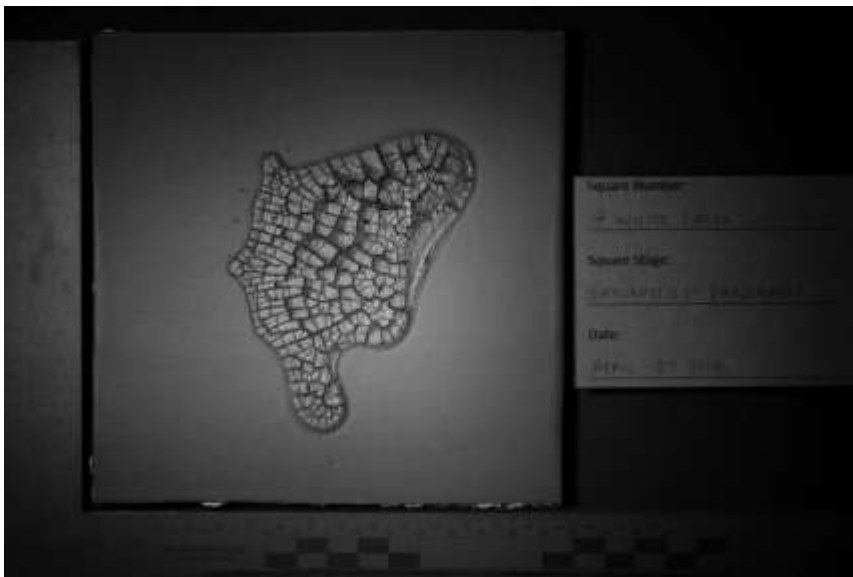


Single

White Latex 7 – Saturated

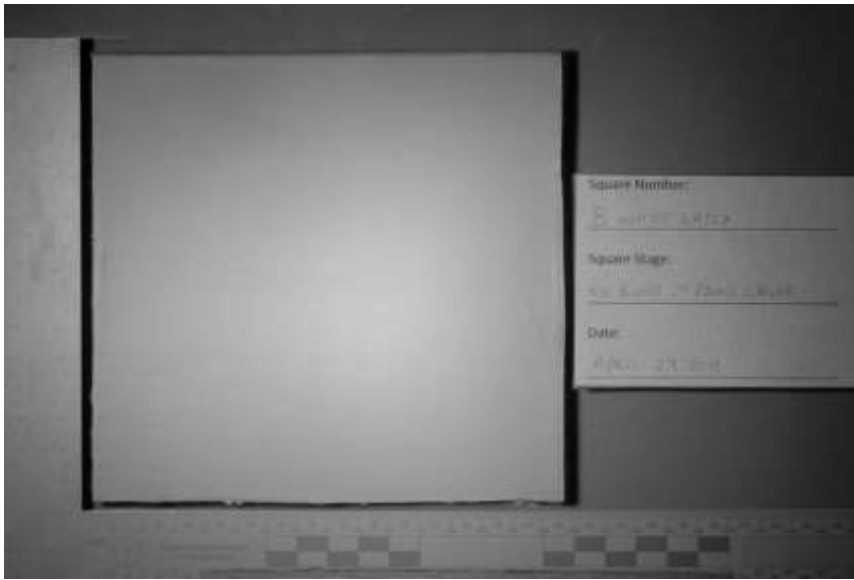


HDR



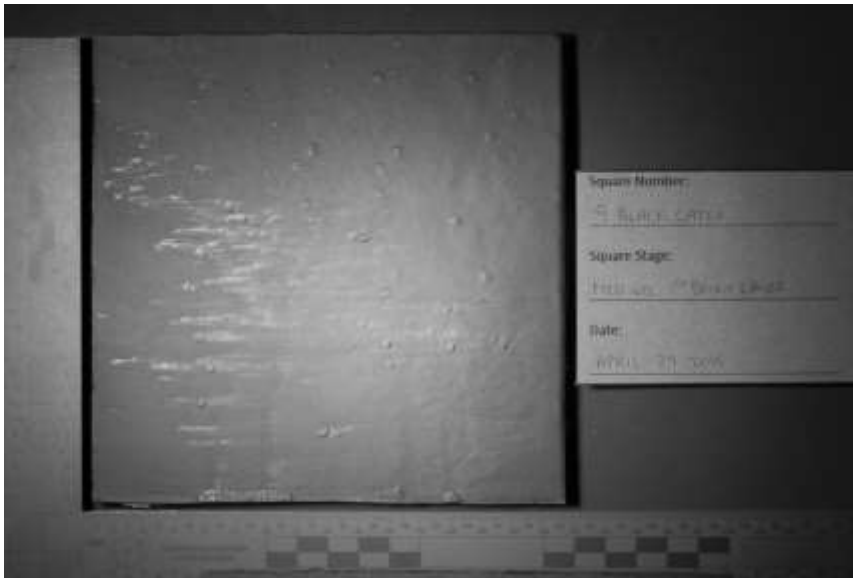
Single

White Latex 8 – Control No Bloodstain



HDR

Appendix 4.2.4.3. Black Latex First layer of paint stage
Black Latex 9 – Medium Velocity

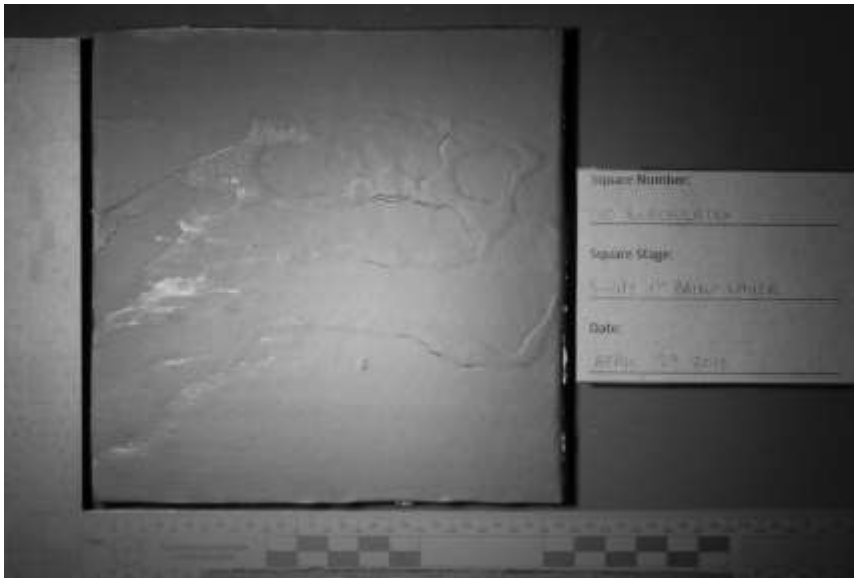


HDR

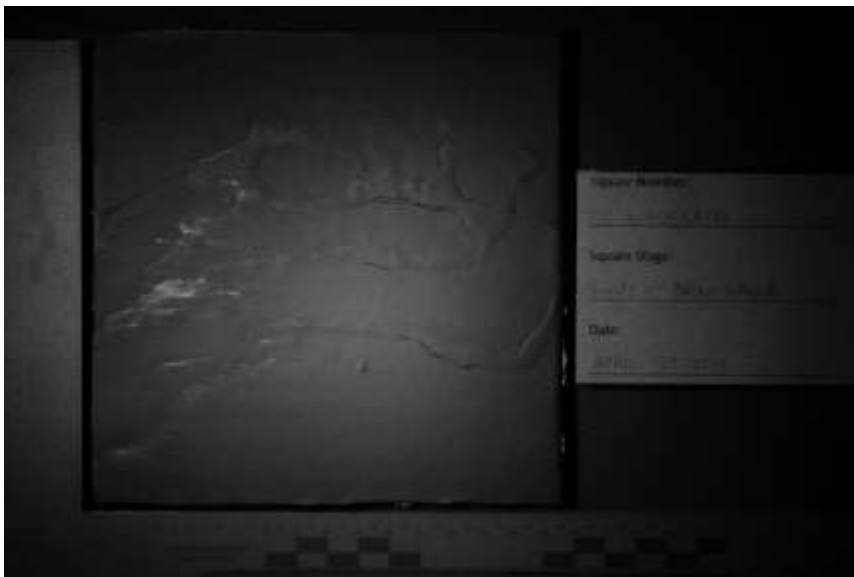


Single

Black Latex 10 – Swipe

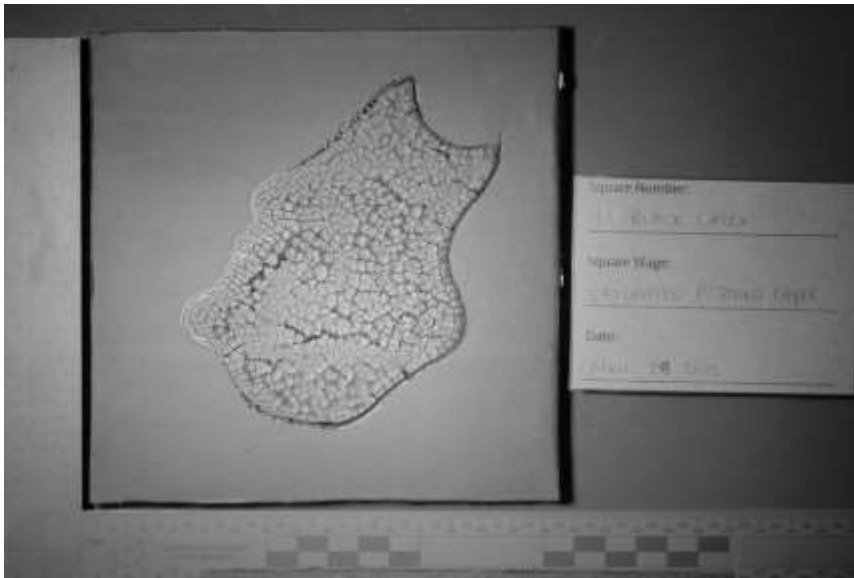


HDR

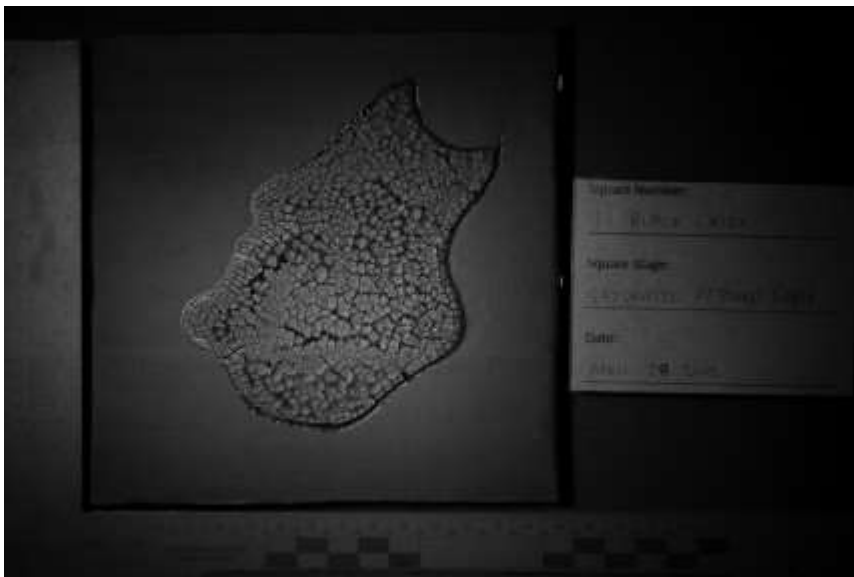


Single

Black Latex 11 – Saturated



HDR



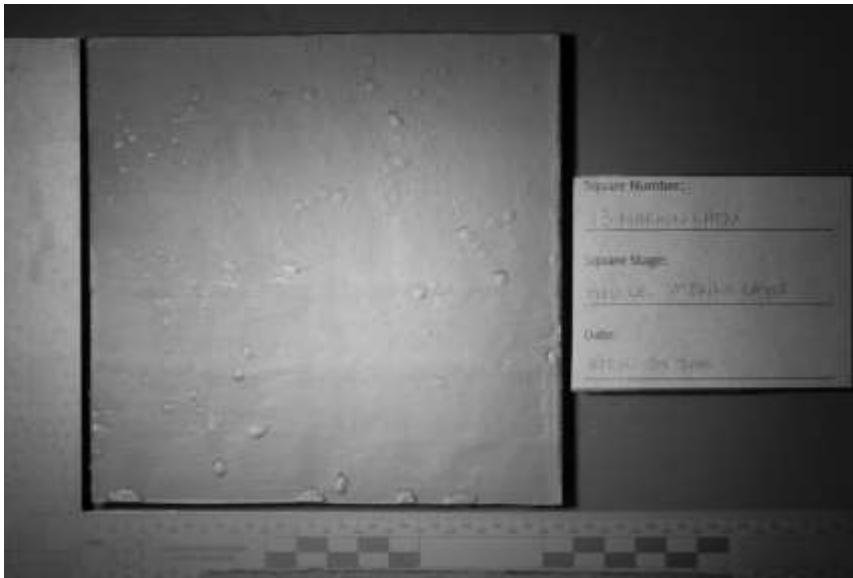
Single

Black Latex 12 – Control No Bloodstain

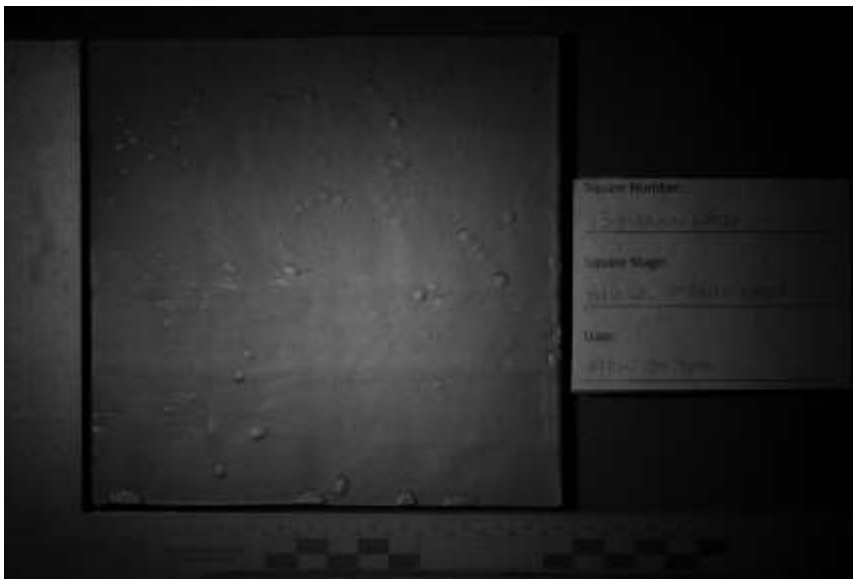


HDR

Appendix 4.2.4.4. Maroon Latex First layer of paint stage
Maroon Latex 13 – Medium Velocity

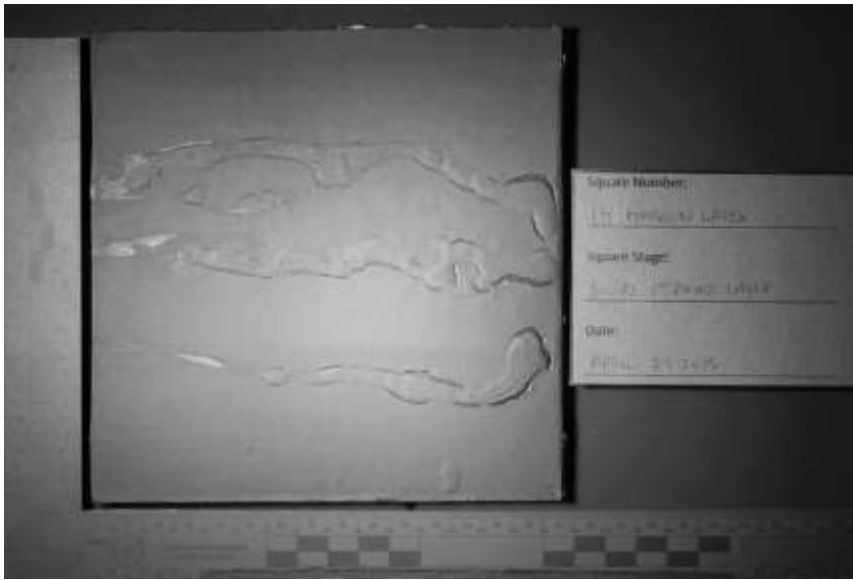


HDR

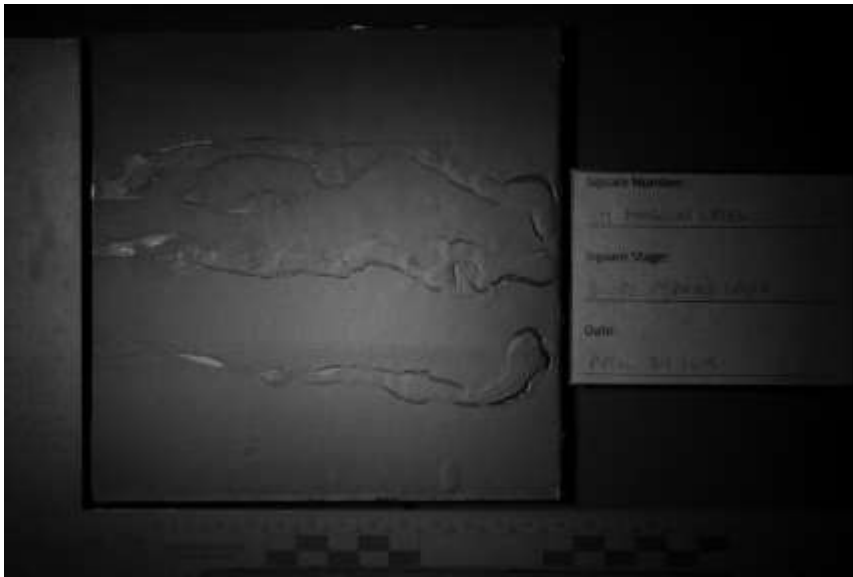


Single

Maroon Latex 14 – Swipe

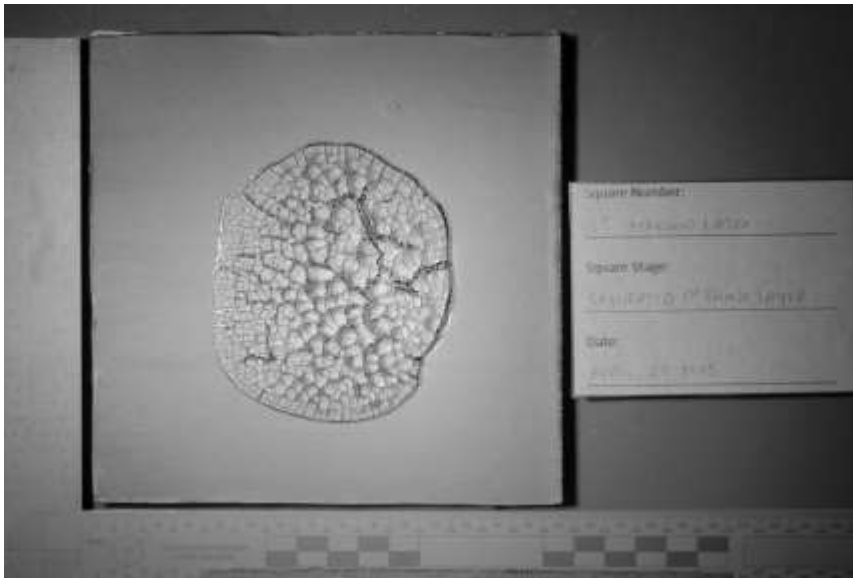


HDR

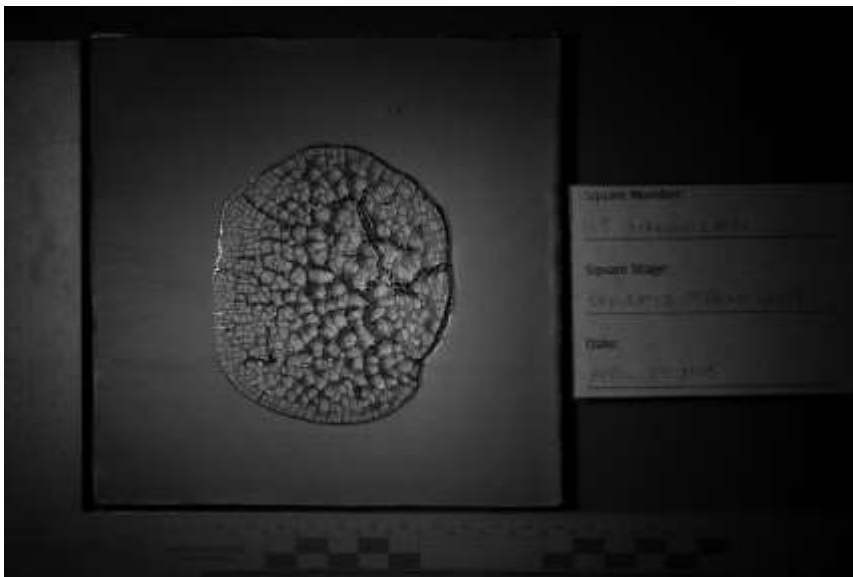


Single

Maroon Latex 15 – Saturated



HDR



Single

Maroon Latex 16 – Control No Bloodstain

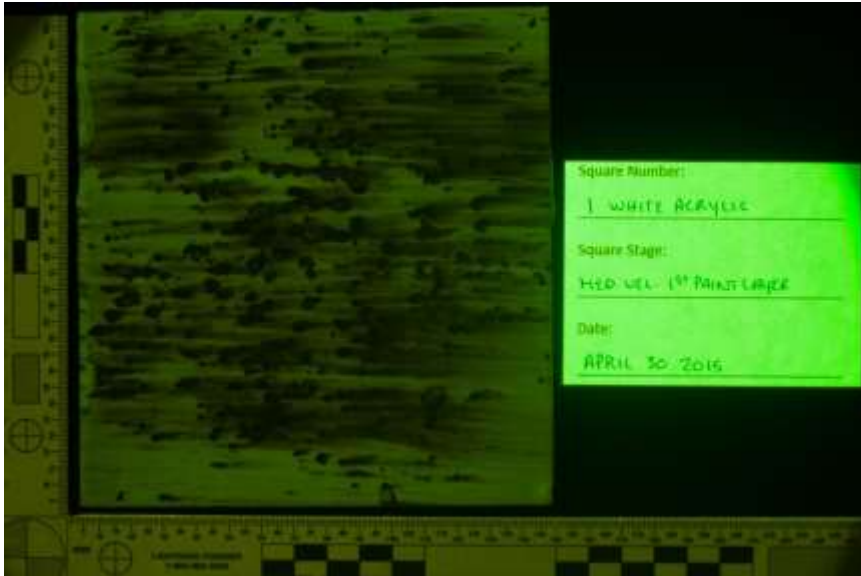


HDR

Appendix 4.2.5. Fluorescence Photography

Appendix 4.2.5.1. White Acrylic – Yellow 415nm, 445nm, 455nm; Orange 445nm, 455nm, 475nm, 495nm, 515nm; Red 575nm First layer of paint stage

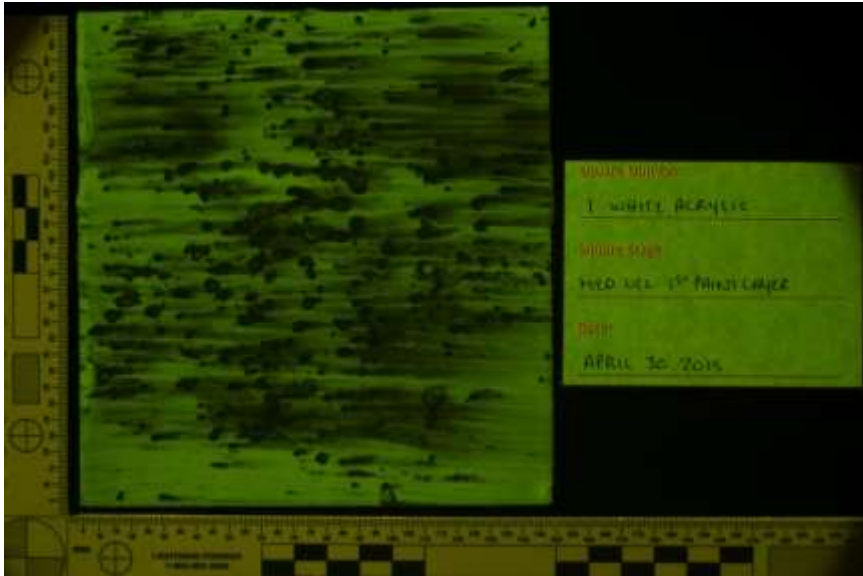
White Acrylic 1 – Medium Velocity



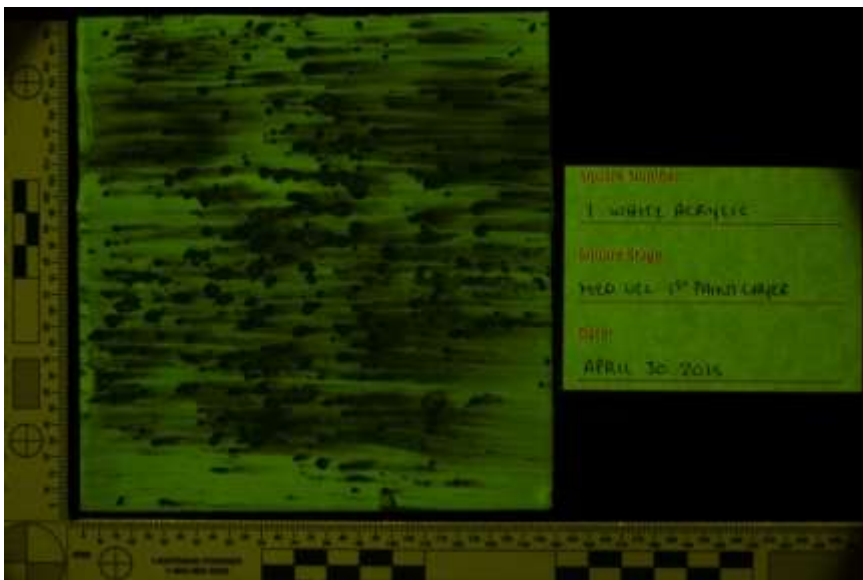
Yellow 415nm HDR



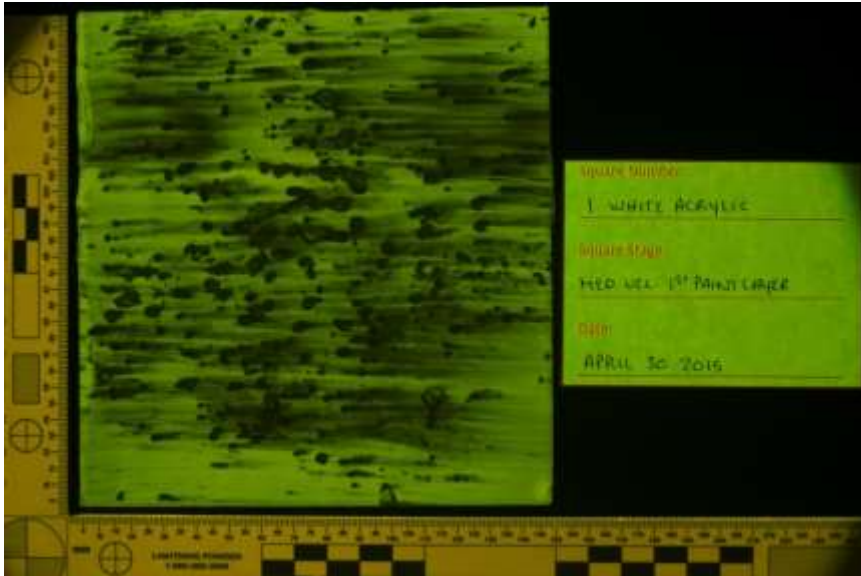
Yellow 415nm Single



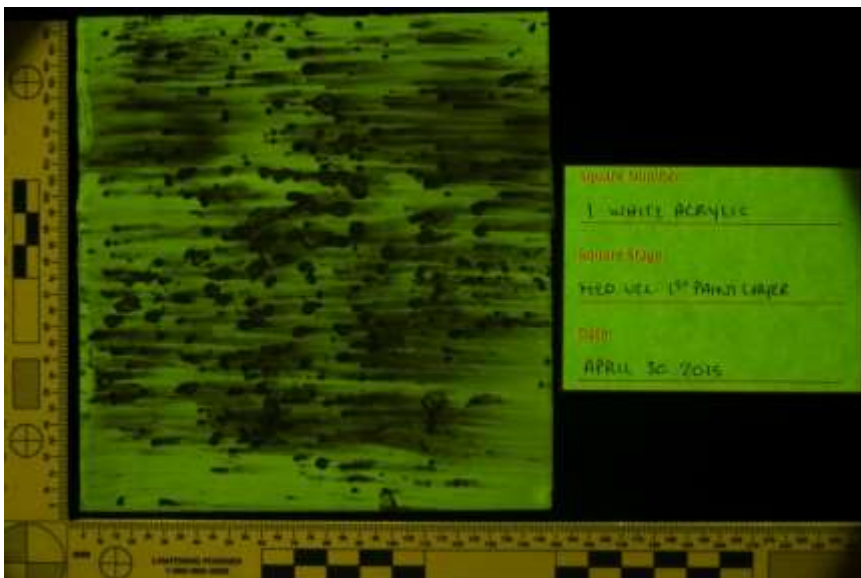
Yellow 445nm HDR



Yellow 445nm Single



Yellow 455nm HDR



Yellow 455nm Single



Orange 445nm HDR



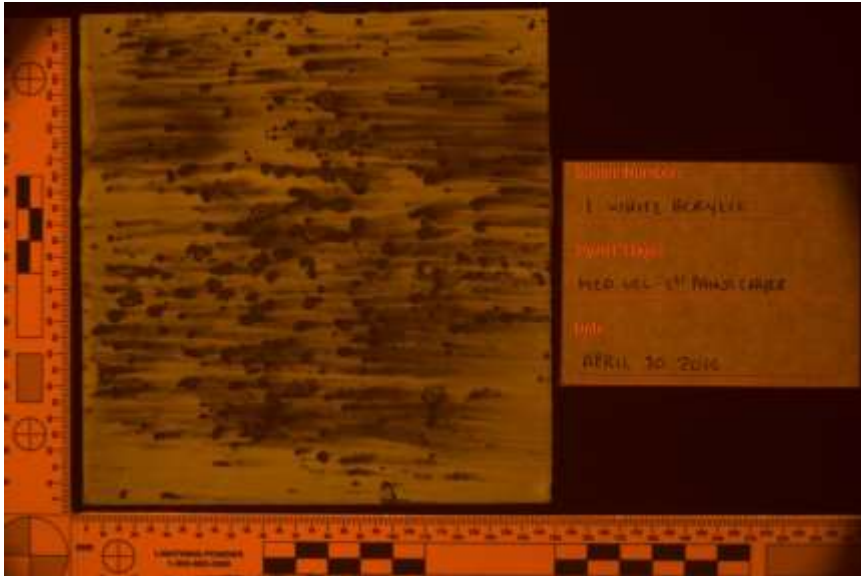
Orange 445nm Single



Orange 455nm HDR



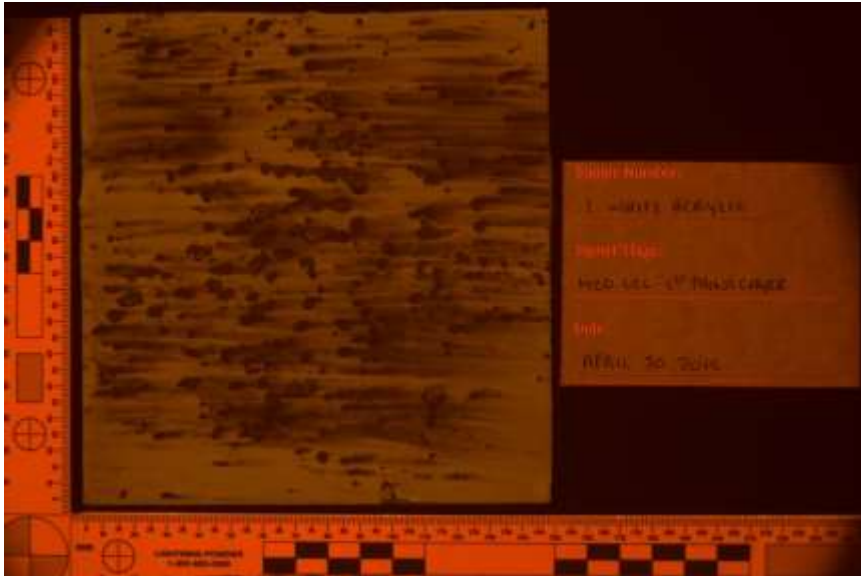
Orange 455nm Single



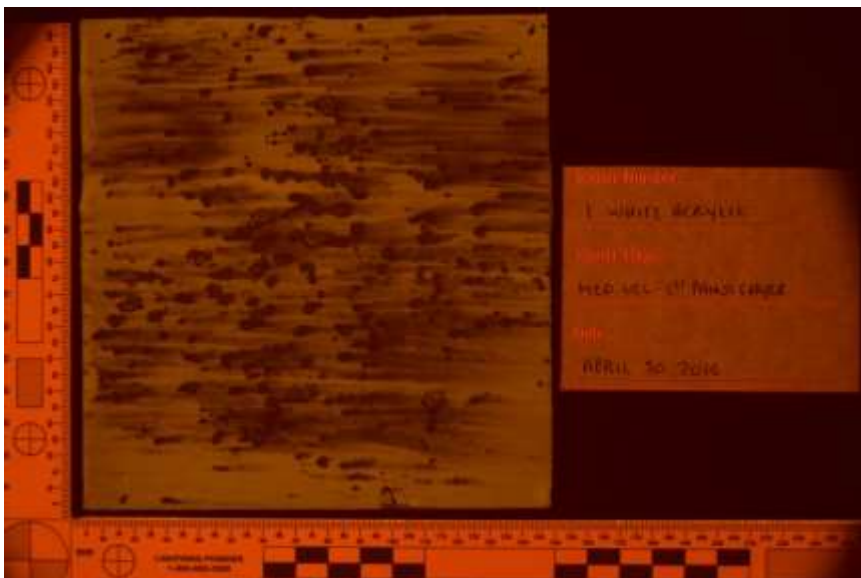
Orange 475nm HDR



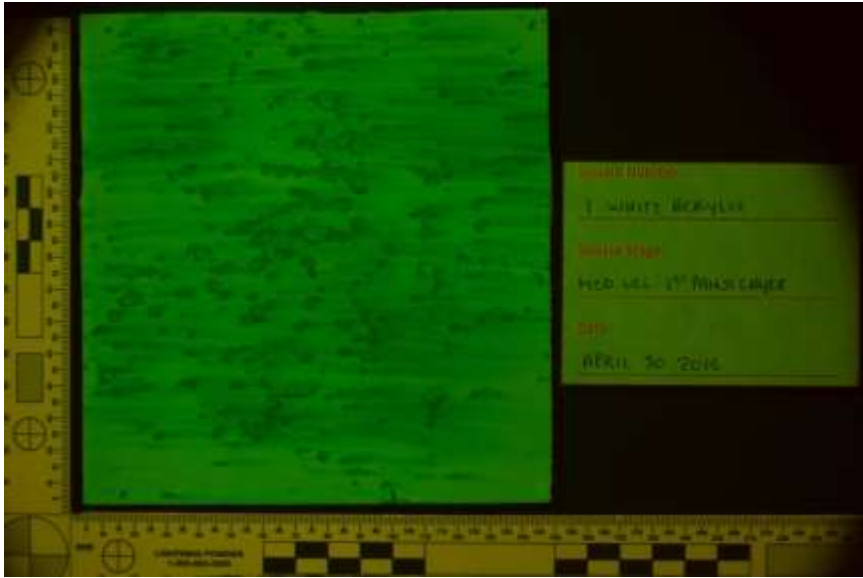
Orange 475nm Single



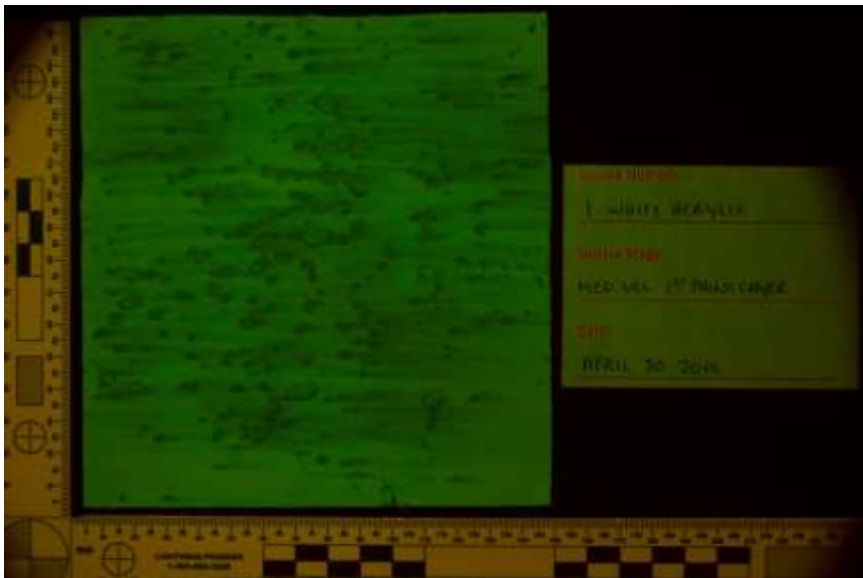
Orange 495nm HDR



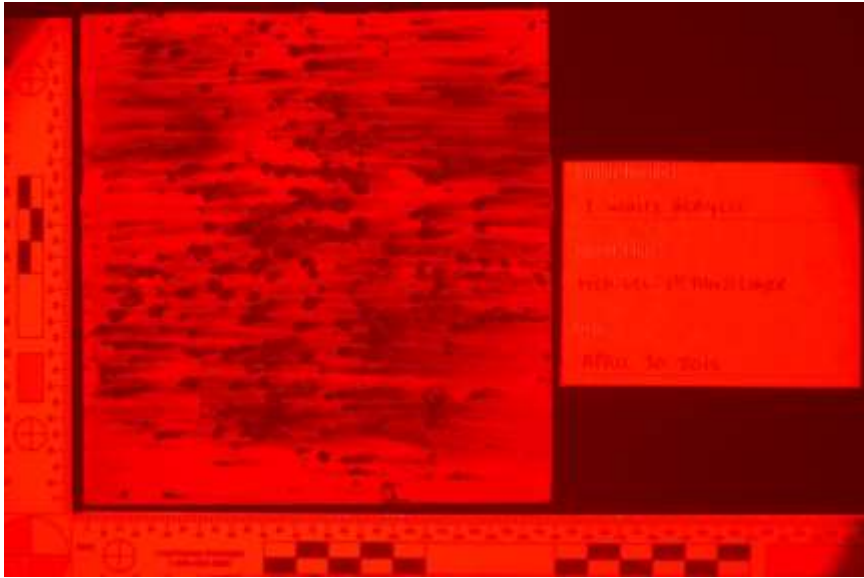
Orange 495nm Single



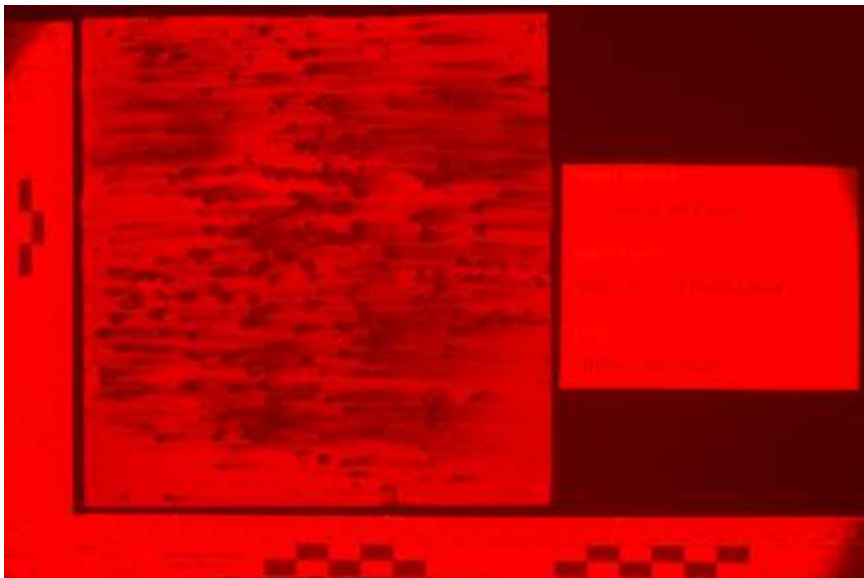
Orange 515nm HDR



Orange 515nm Single

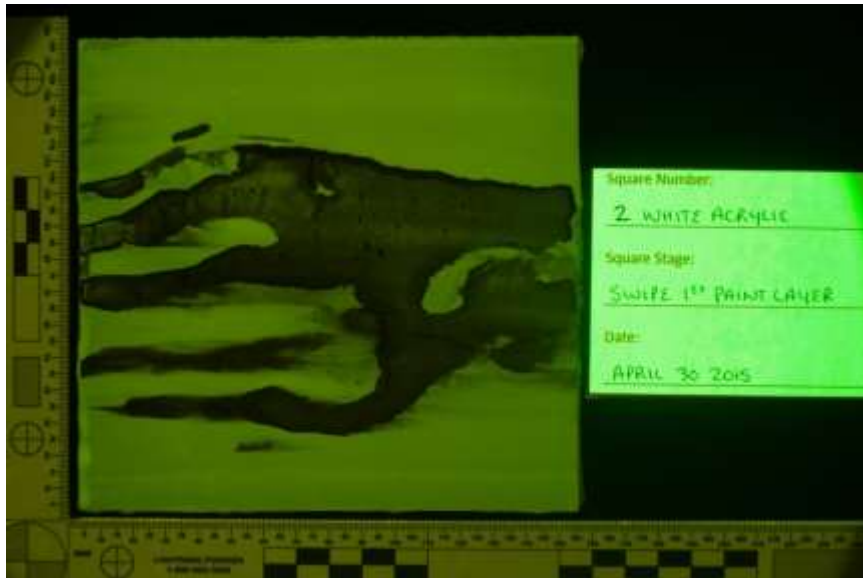


Red 575nm HDR

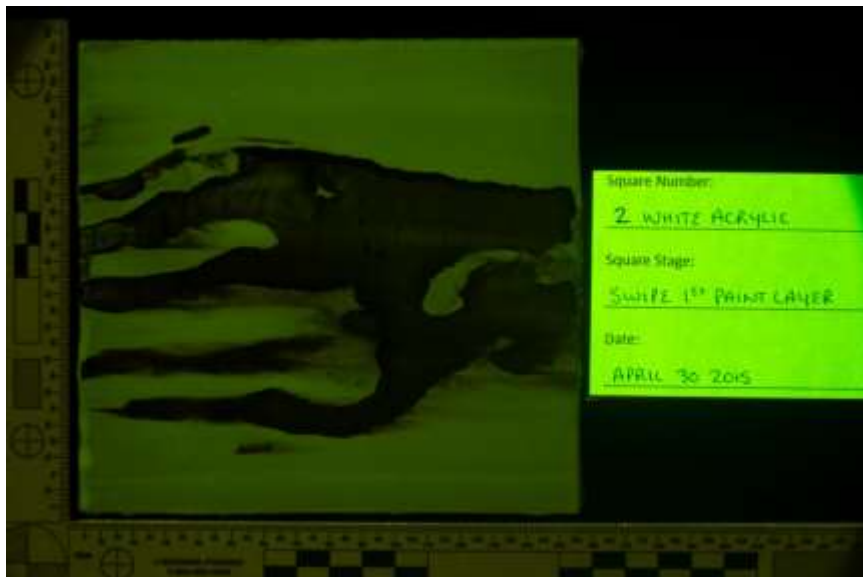


Red 575nm Single

White Acrylic 2 – Swipe



Yellow 415nm HDR



Yellow 415nm Single



Yellow 445nm HDR



Yellow 445nm Single



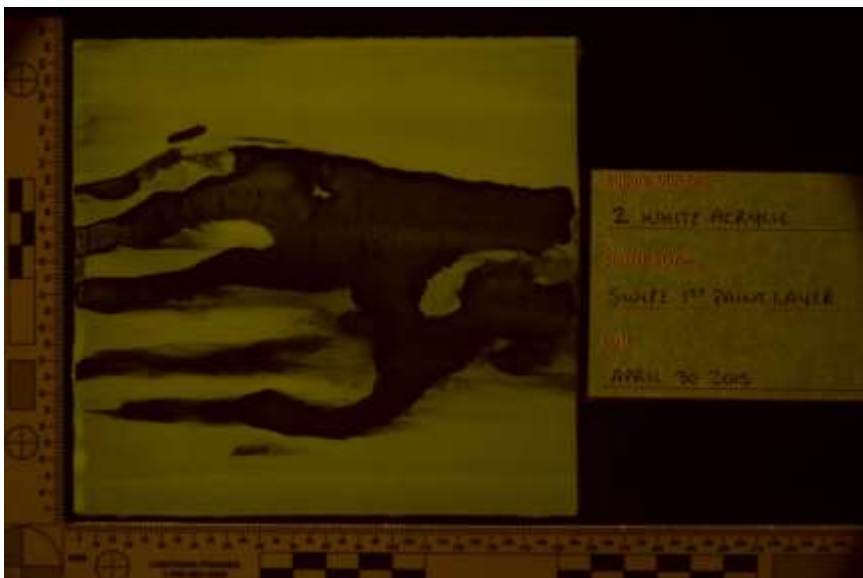
Yellow 455nm HDR



Yellow 455nm Single



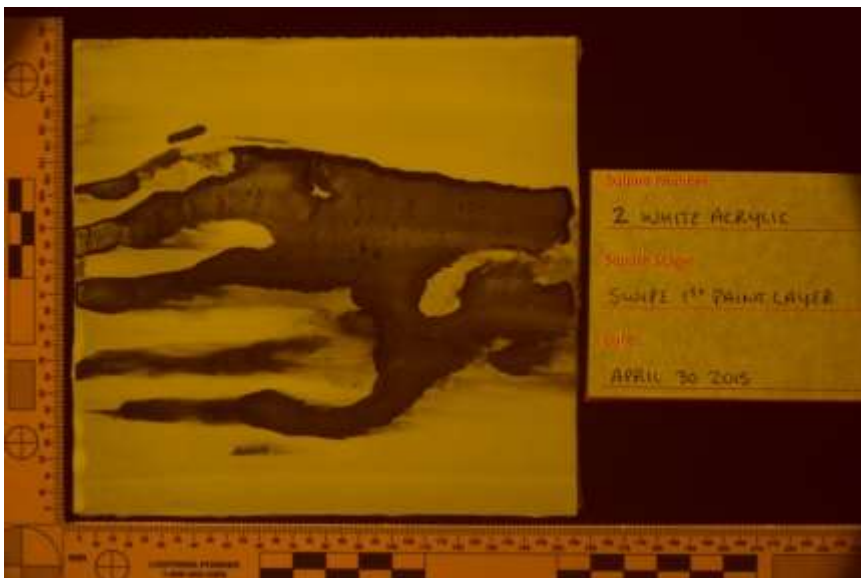
Orange 445nm HDR



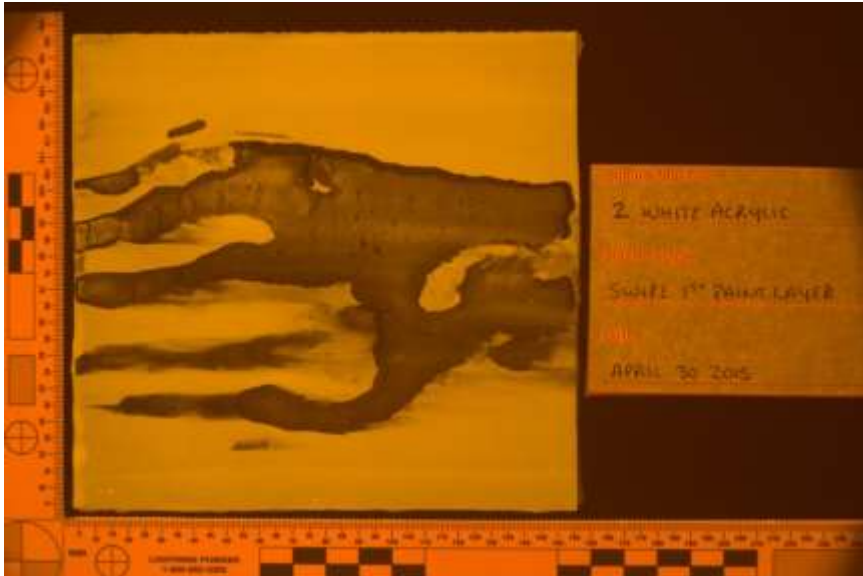
Orange 445nm Single



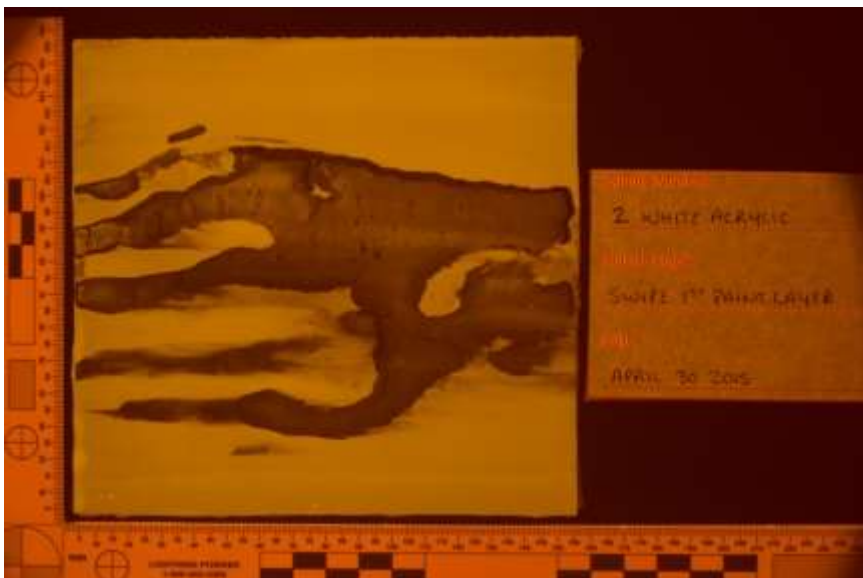
Orange 455nm HDR



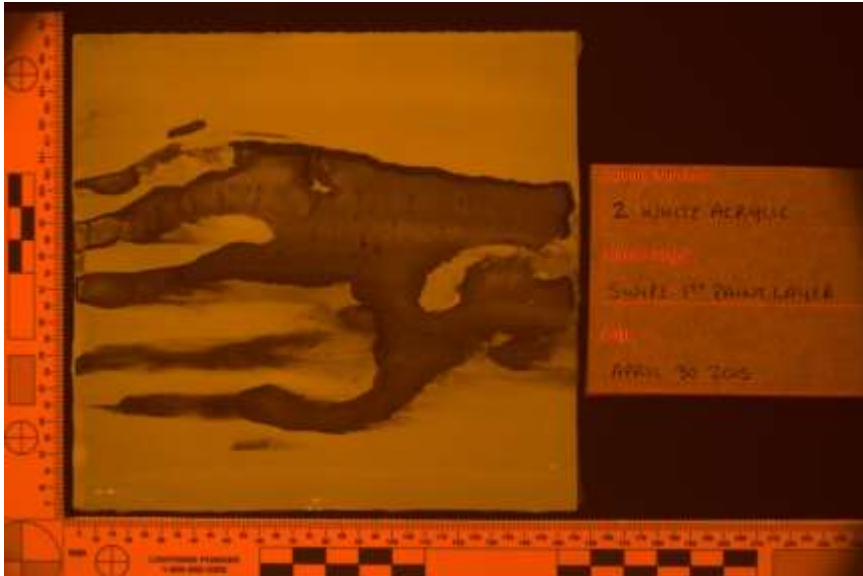
Orange 455nm Single



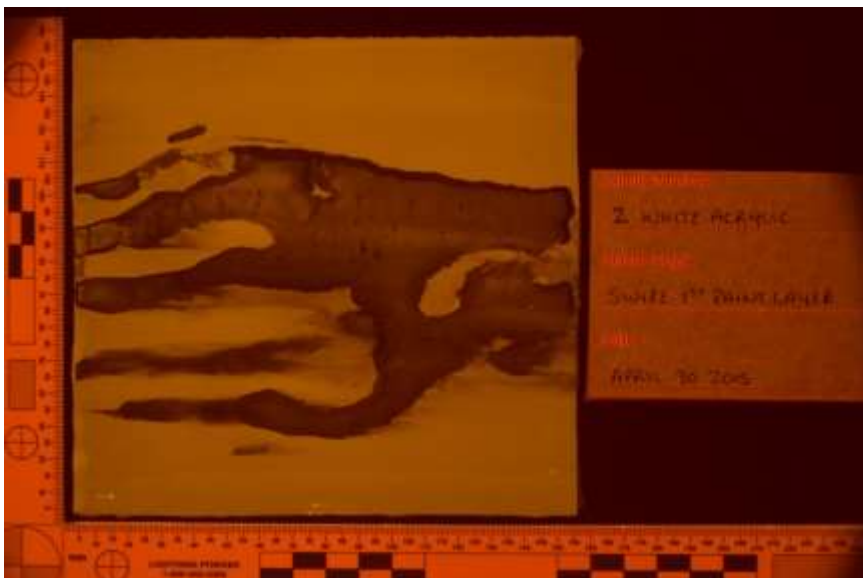
Orange 475nm HDR



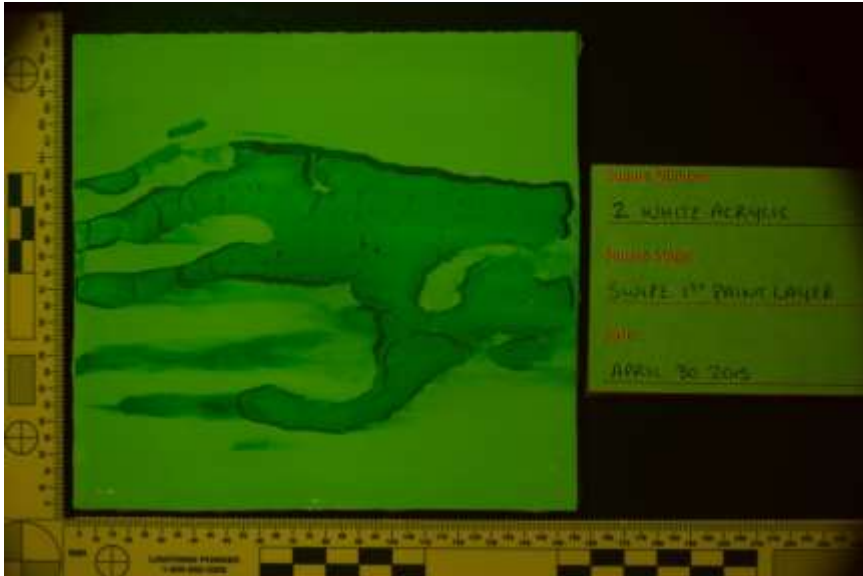
Orange 475nm Single



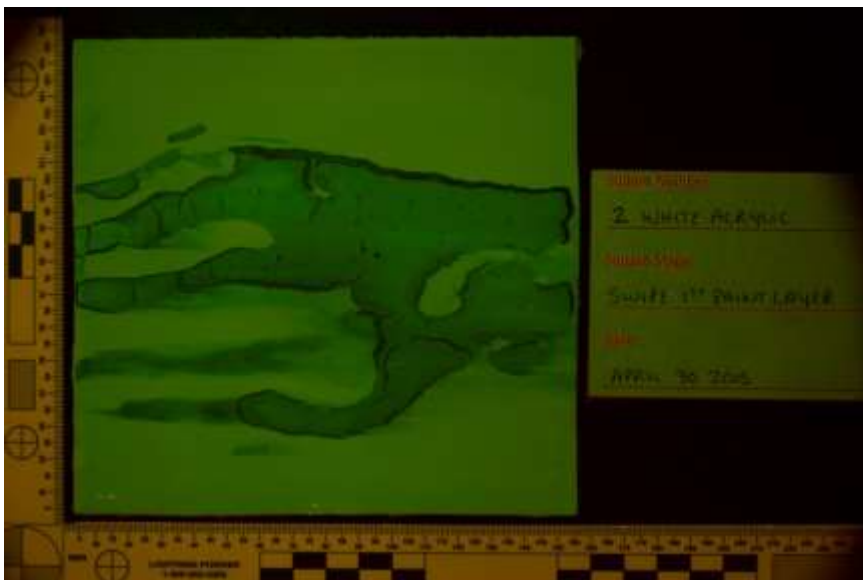
Orange 495nm HDR



Orange 495nm Single



Orange 515nm HDR



Orange 515nm Single

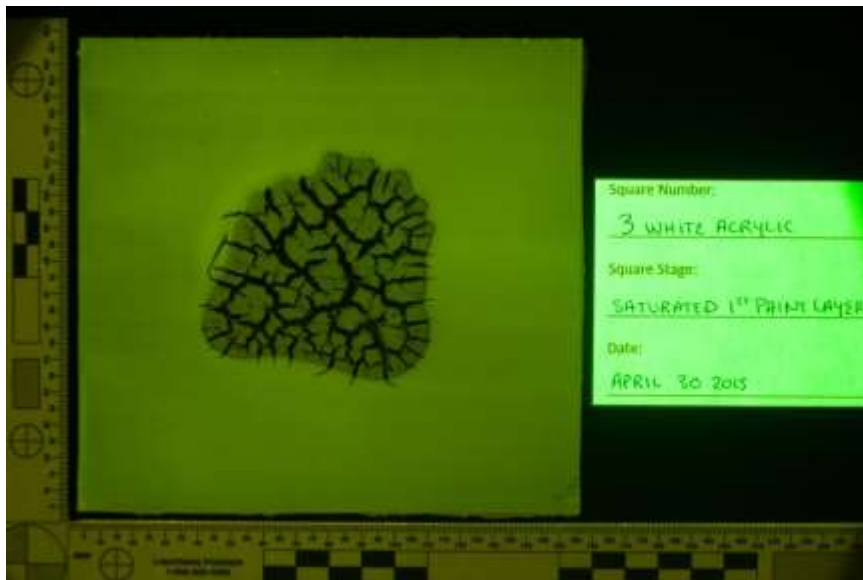


Red 575nm HDR

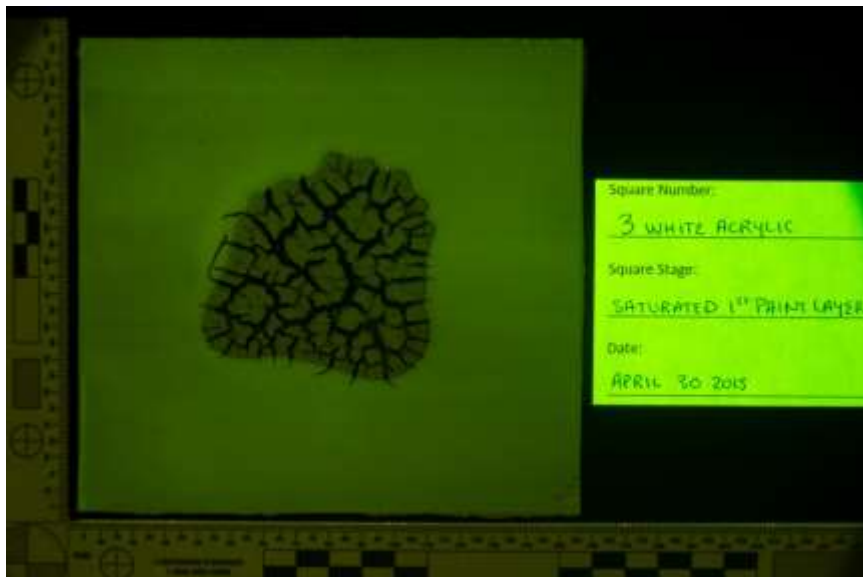


Red 575nm Single

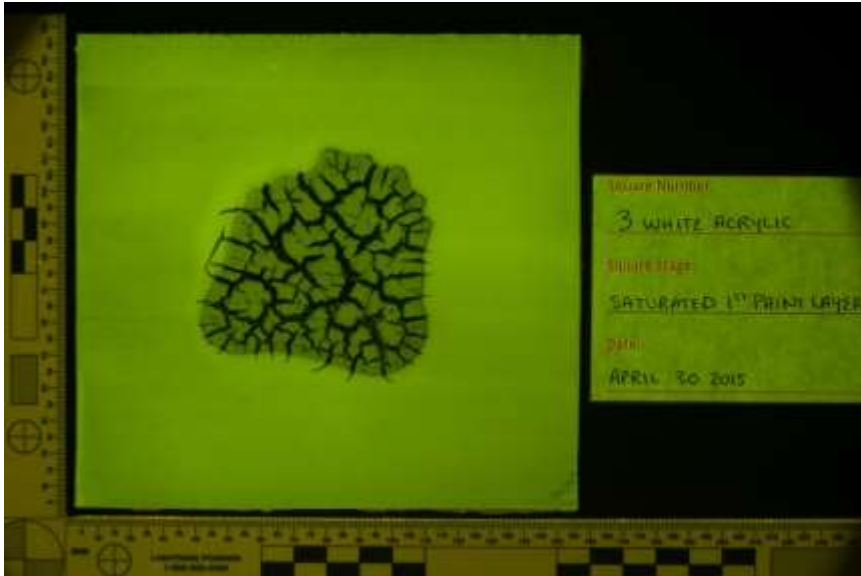
White Acrylic 3 – Saturated



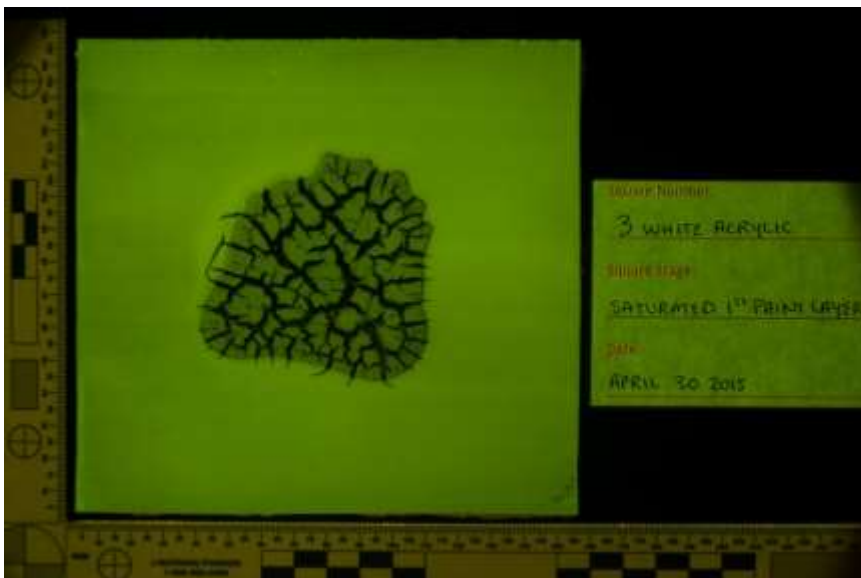
Yellow 415nm HDR



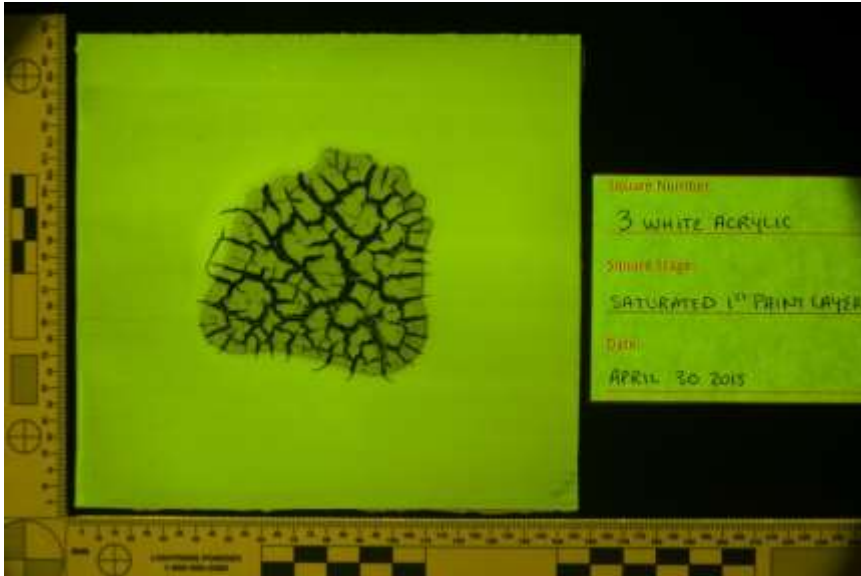
Yellow 415nm Single



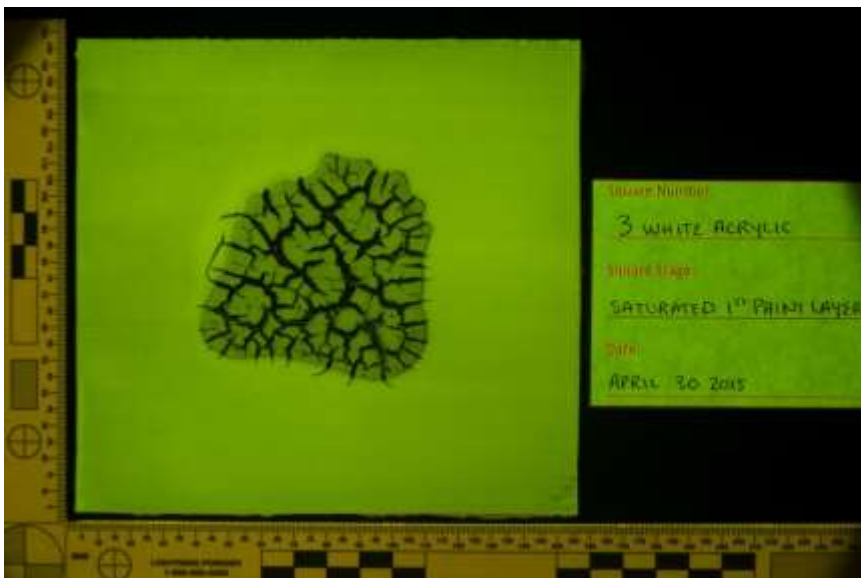
Yellow 445nm HDR



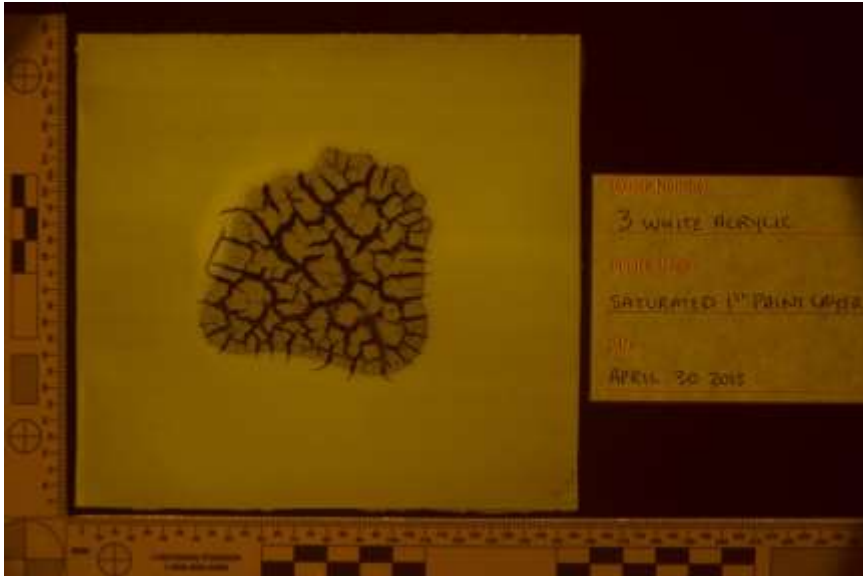
Yellow 445nm Single



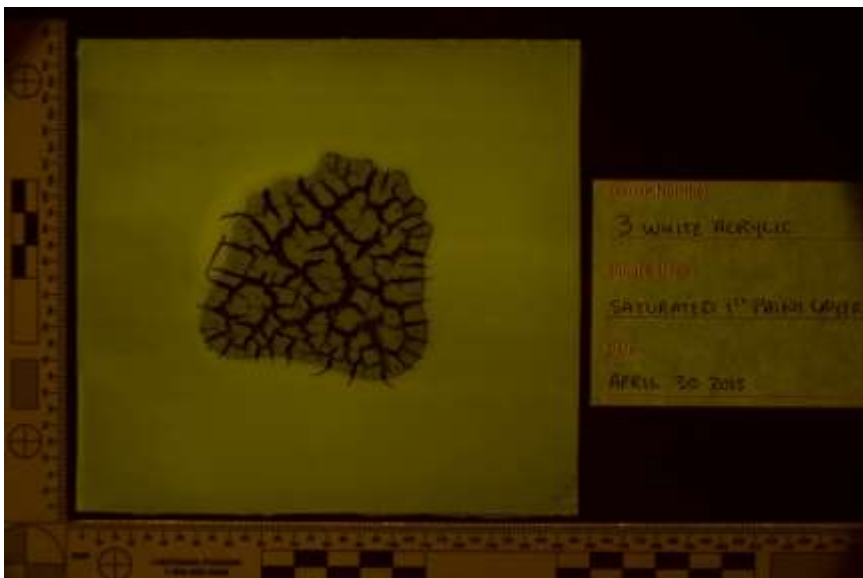
Yellow 455nm HDR



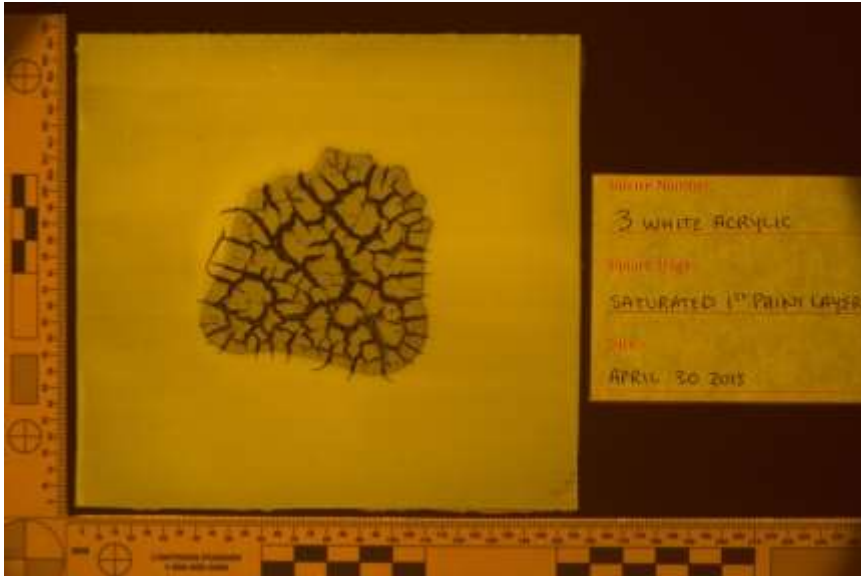
Yellow 455nm Single



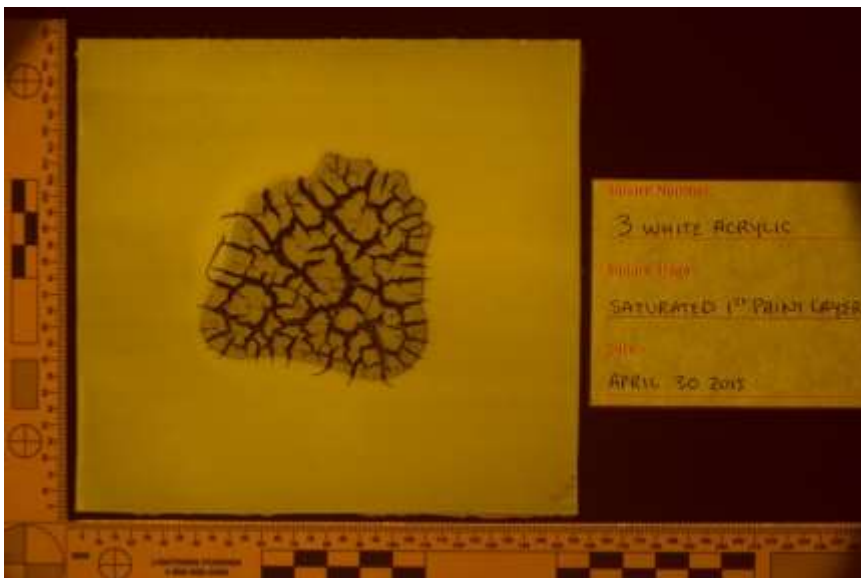
Orange 445nm HDR



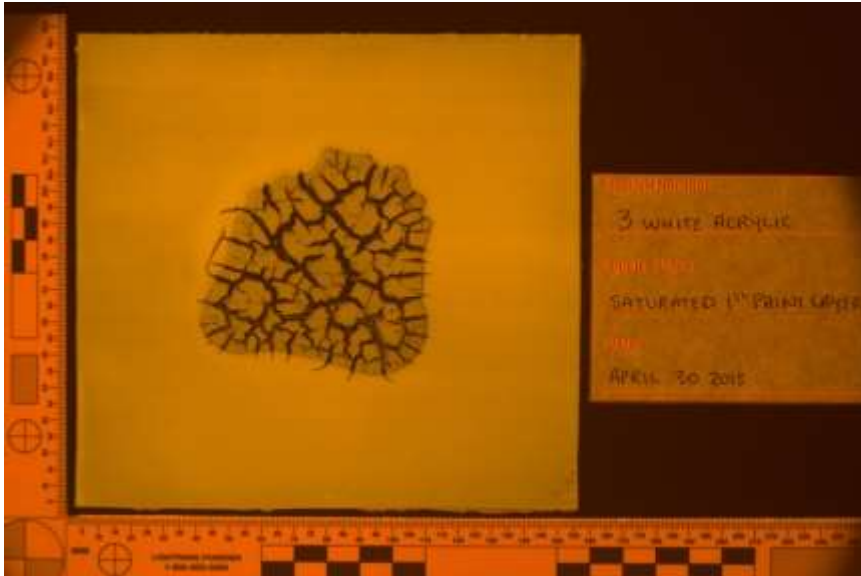
Orange 445nm Single



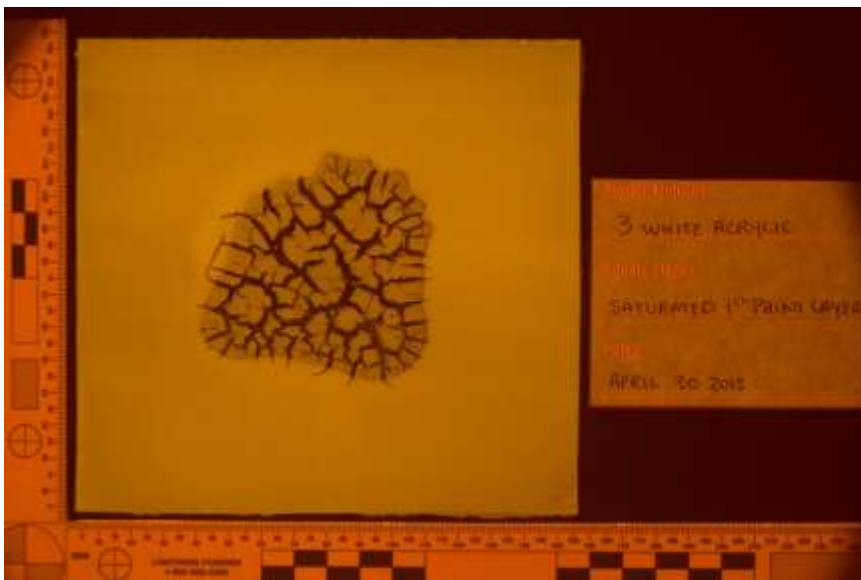
Orange 455nm HDR



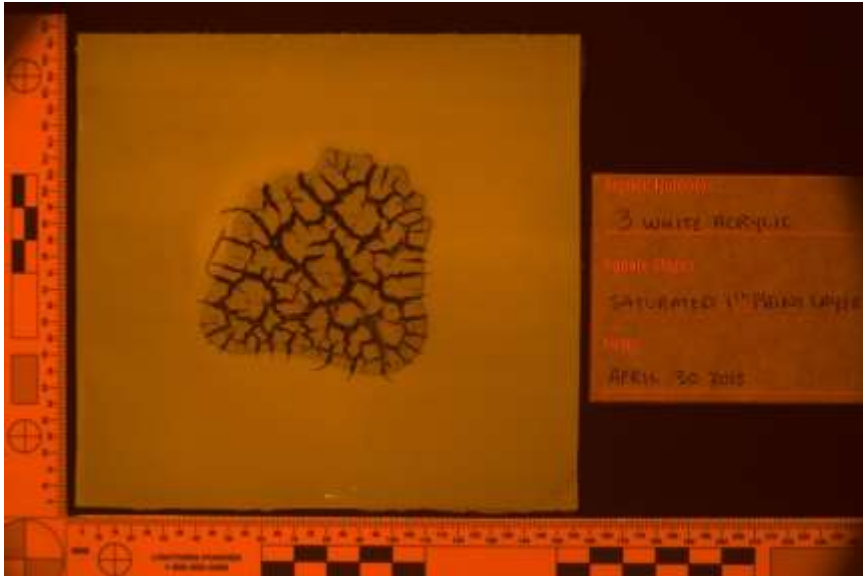
Orange 455nm Single



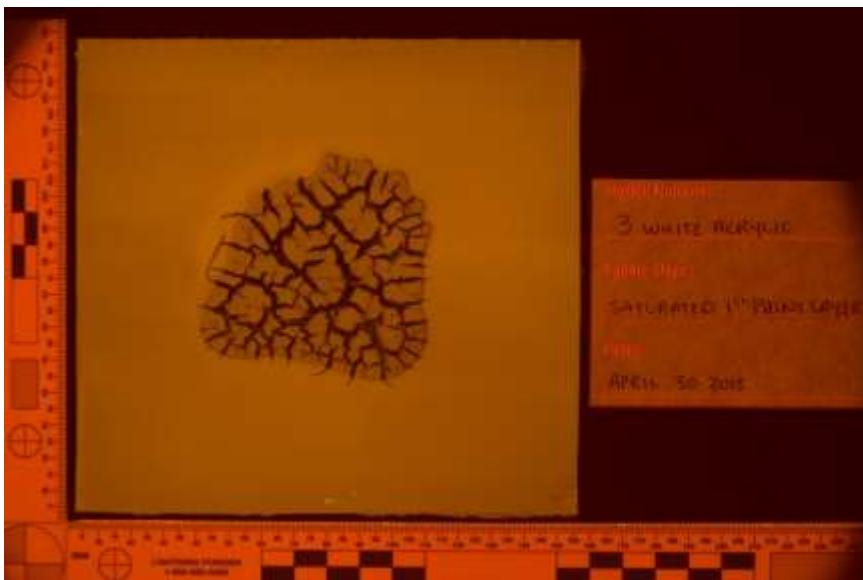
Orange 475nm HDR



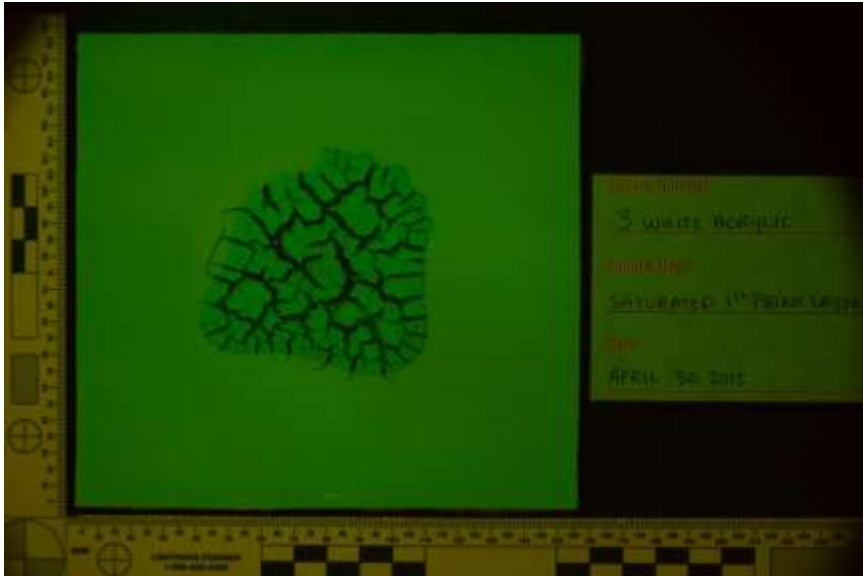
Orange 475nm Single



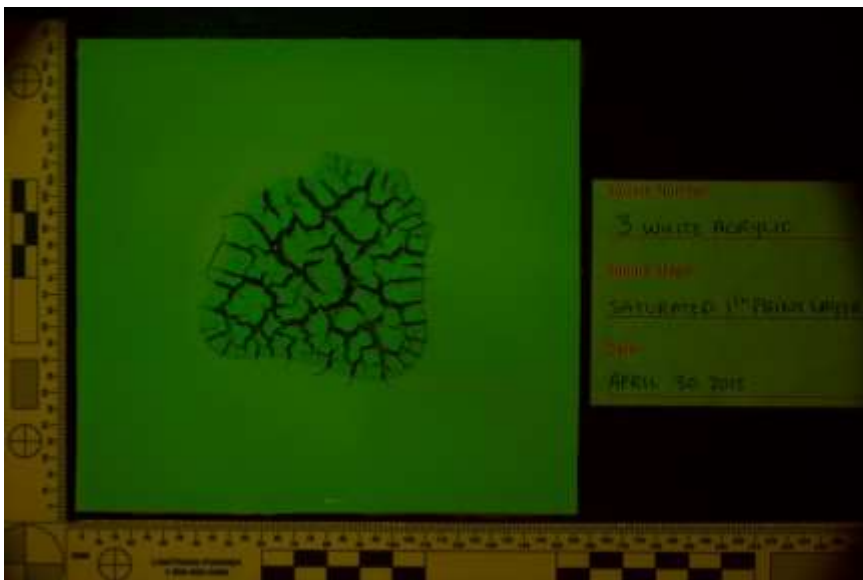
Orange 495nm HDR



Orange 495nm Single



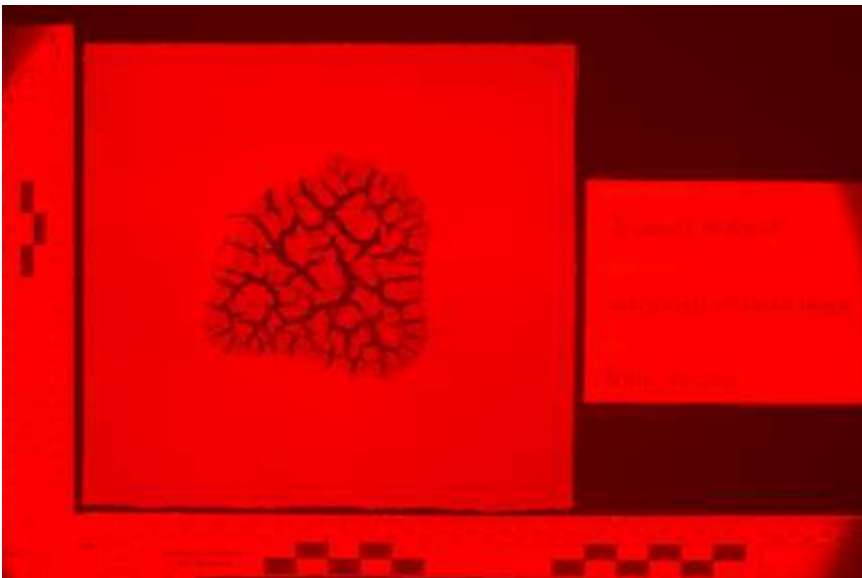
Orange 515nm HDR



Orange 515nm Single

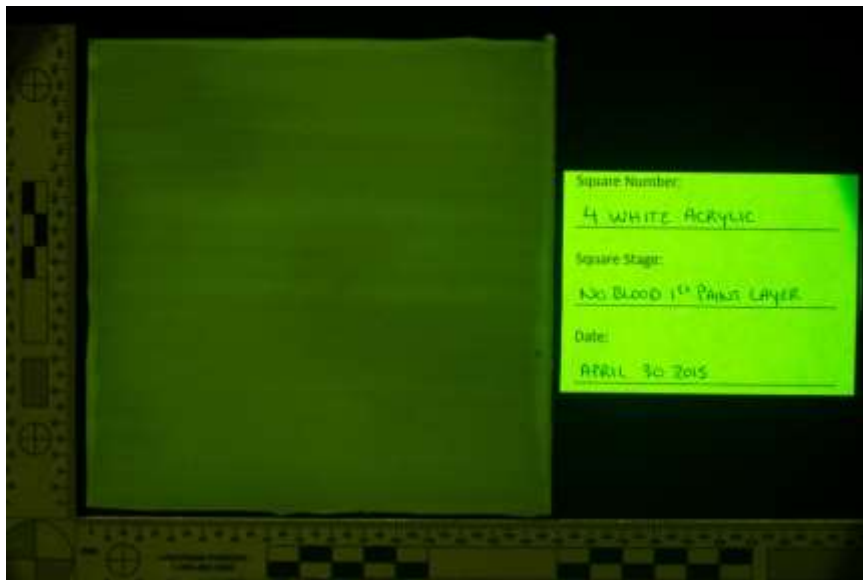


Red 575nm HDR

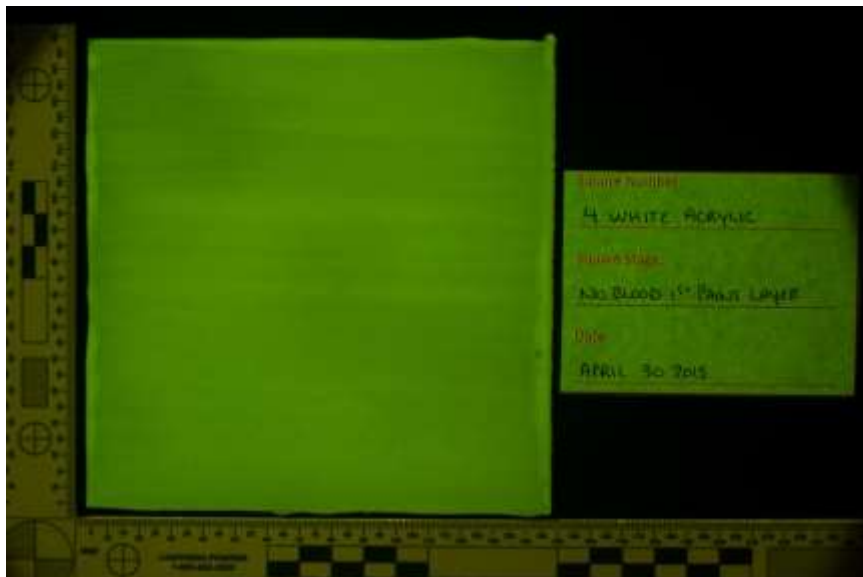


Red 575nm Single

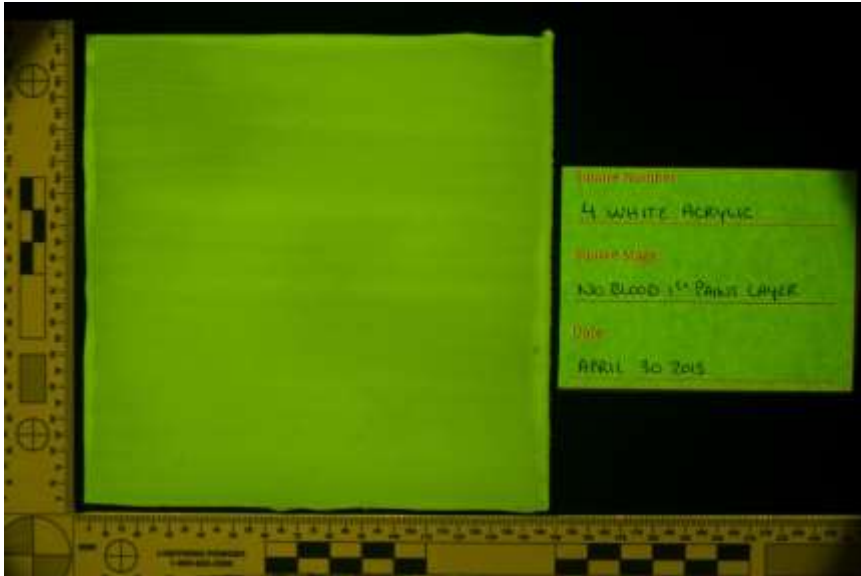
White Acrylic 4 – Control No Bloodstain



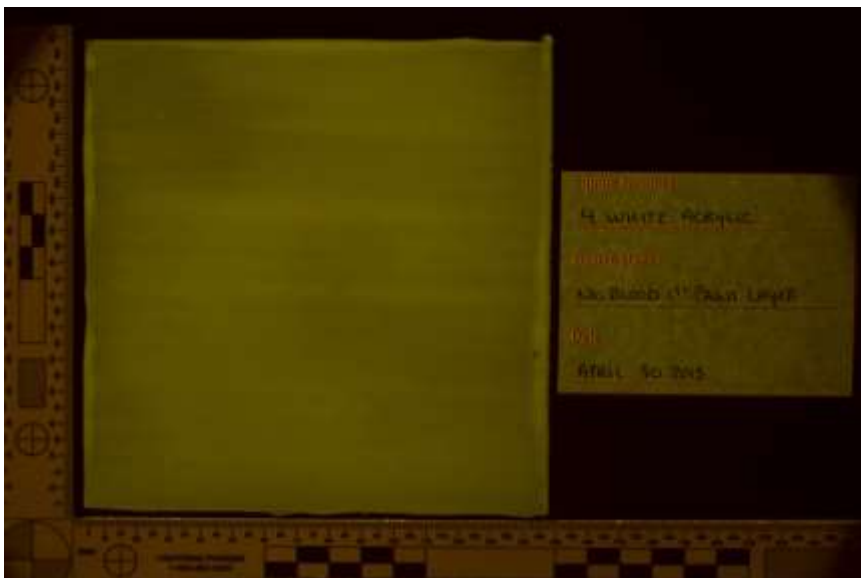
Yellow 415nm HDR



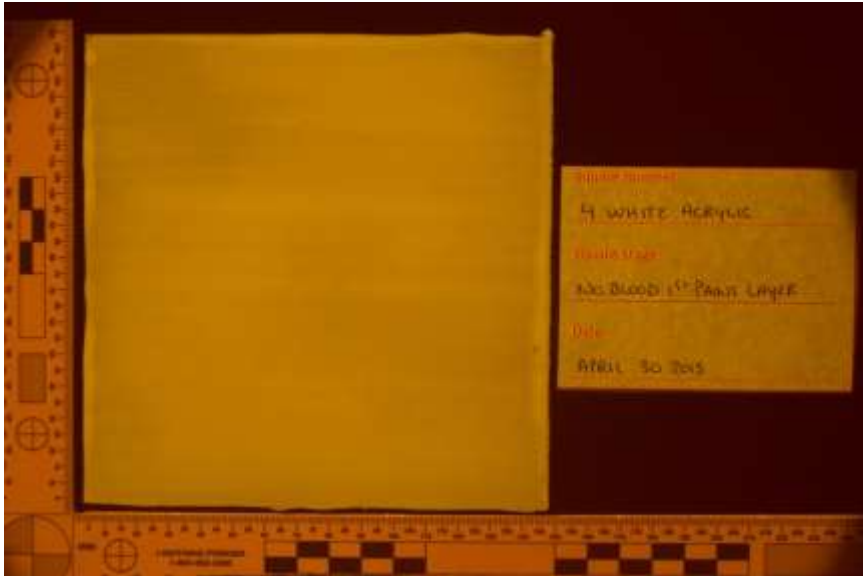
Yellow 445nm HDR



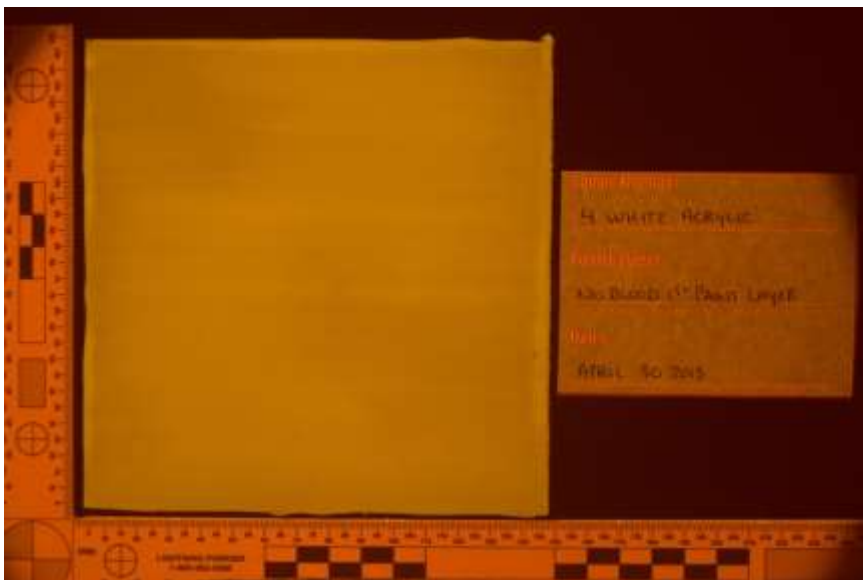
Yellow 455nm HDR



Orange 445nm HDR



Orange 455nm HDR



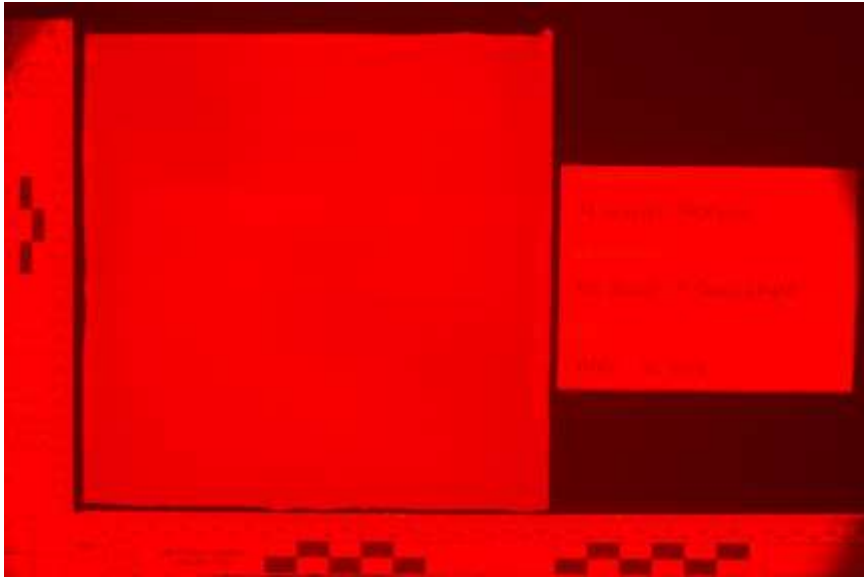
Orange 475nm HDR



Orange 495nm HDR

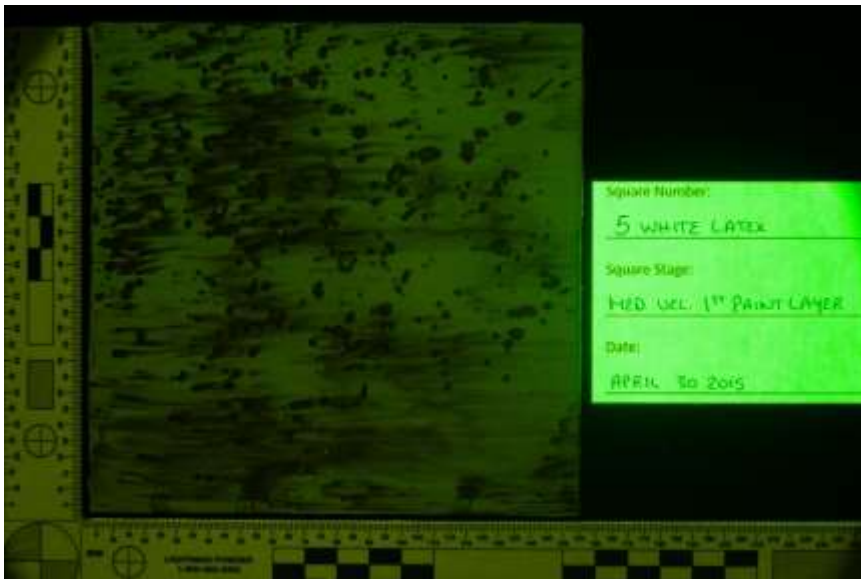


Orange 515nm HDR



Red 575nm HDR

Appendix 4.2.5.2. White Latex – Yellow 415nm, 445nm, 455nm; Orange 445nm, 455nm, 475nm, 495nm, 515nm; Red 575nm First layer of paint stage
White Latex 5 – Medium Velocity



Yellow 415nm HDR



Yellow 415nm Single



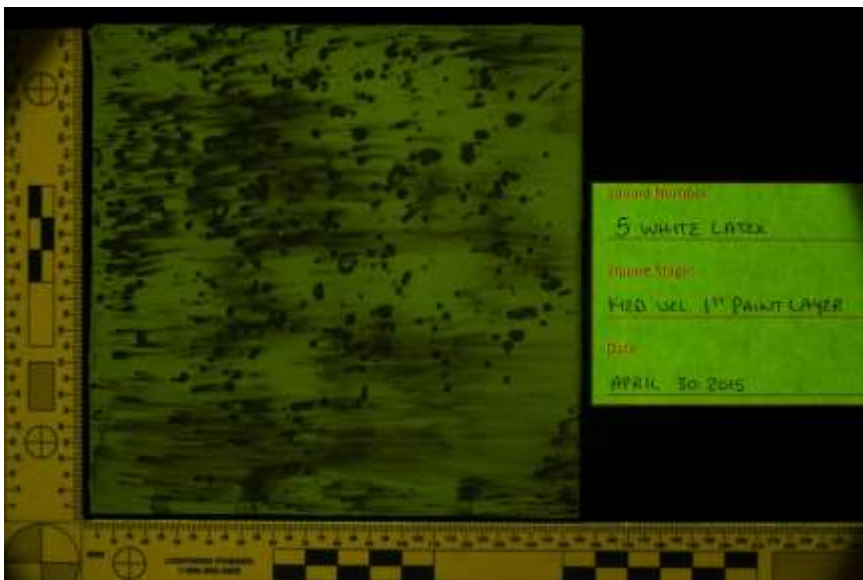
Yellow 445nm HDR



Yellow 445nm Single



Yellow 455nm HDR



Yellow 455nm Single



Orange 445nm HDR



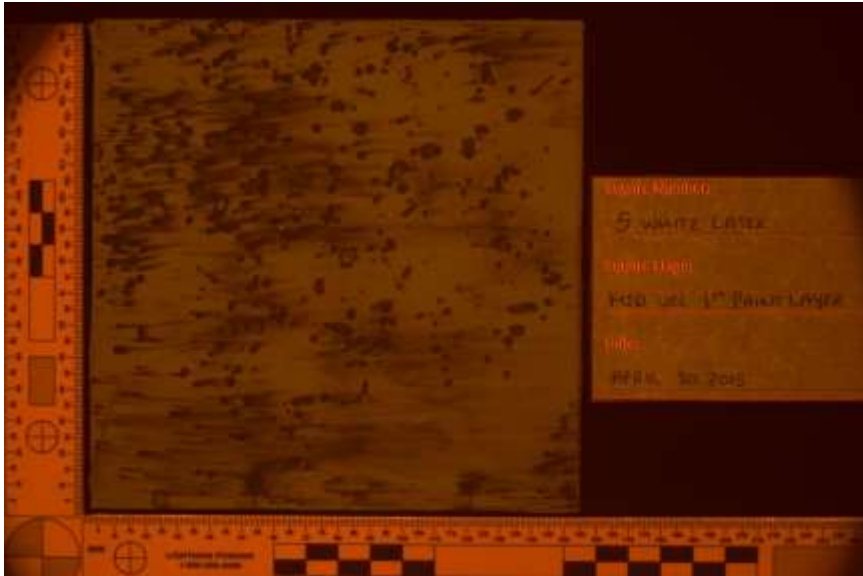
Orange 445nm Single



Orange 455nm HDR



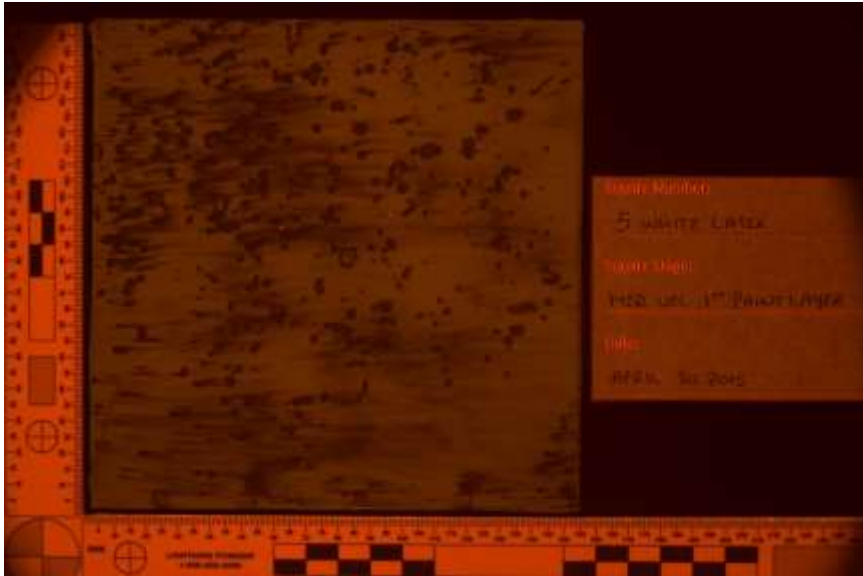
Orange 455nm Single



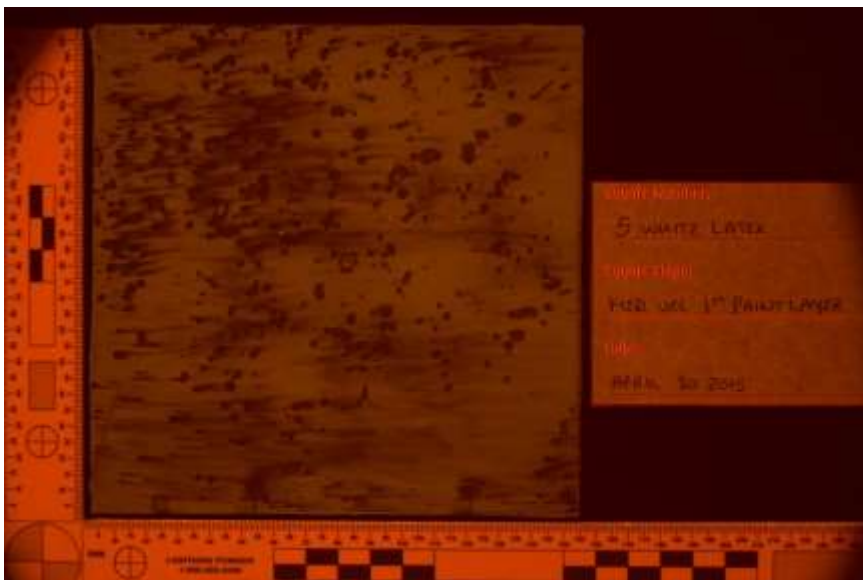
Orange 475nm HDR



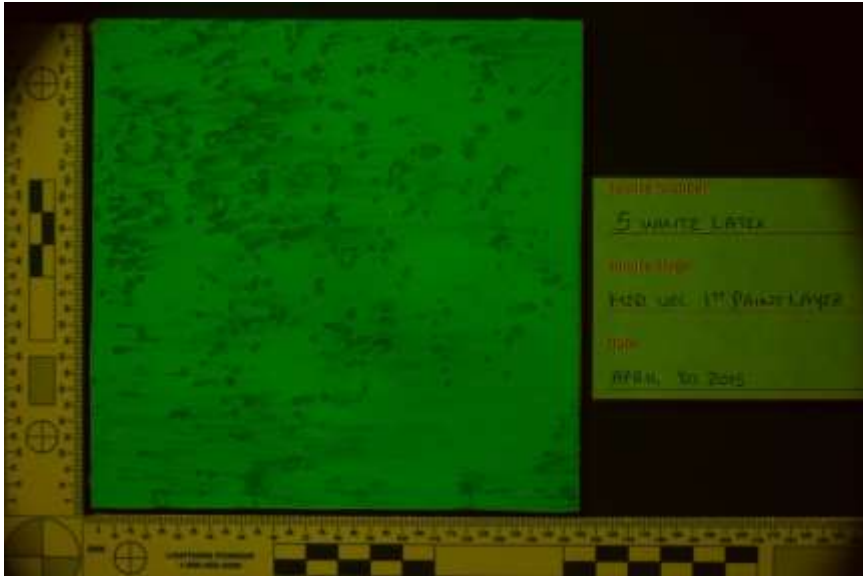
Orange 475nm Single



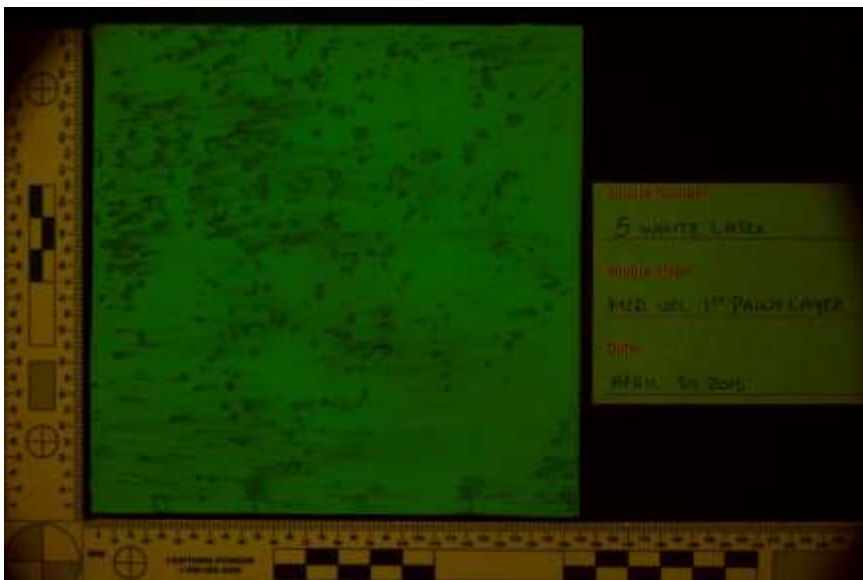
Orange 495nm HDR



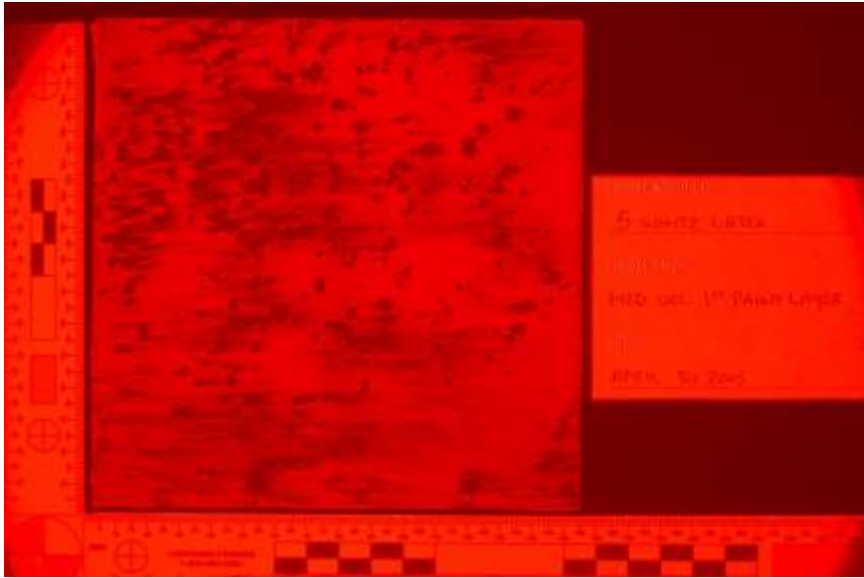
Orange 495nm Single



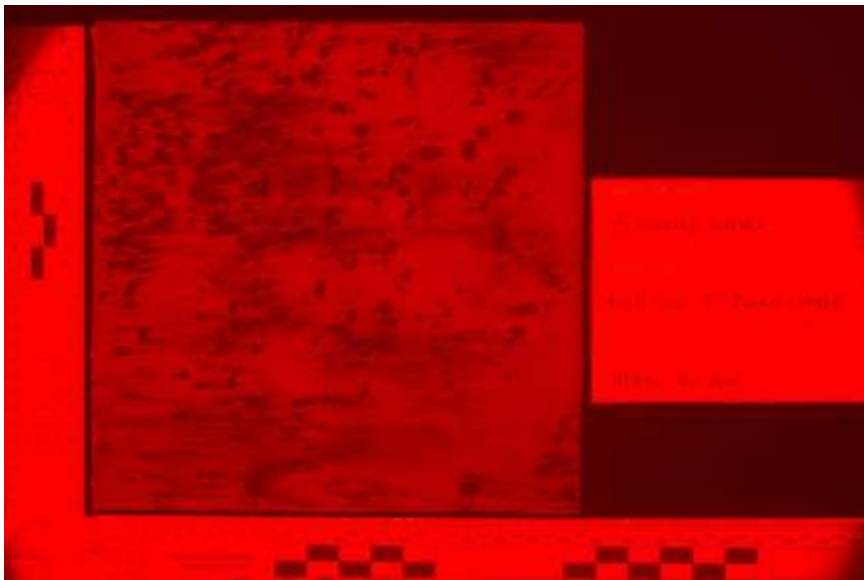
Orange 515nm HDR



Orange 515nm Single

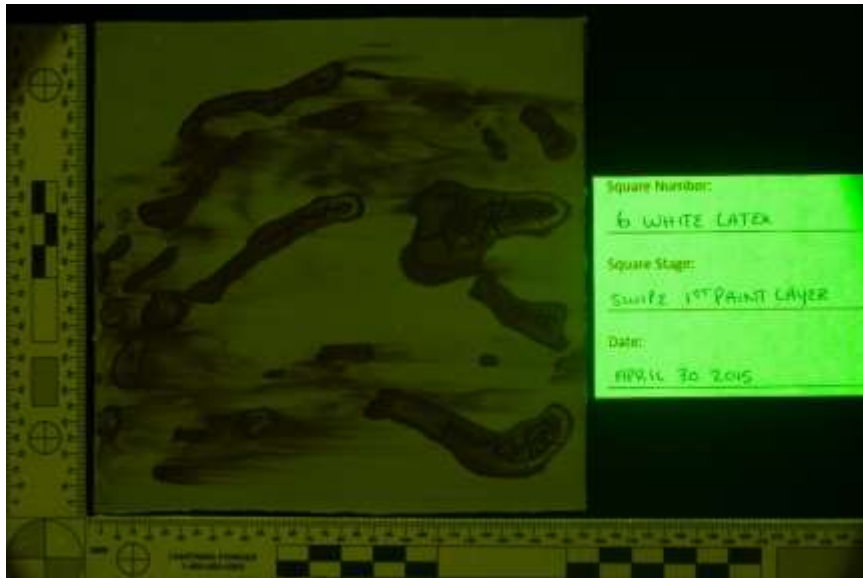


Red 575nm HDR

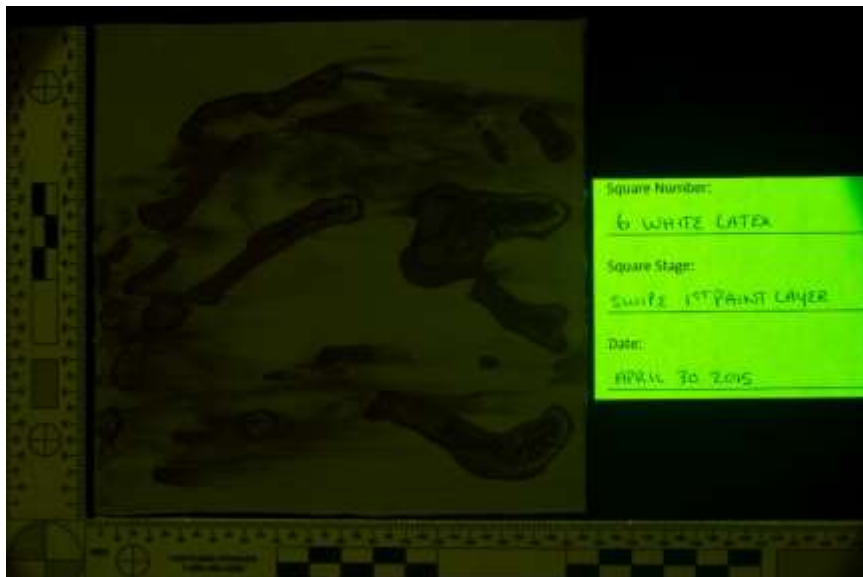


Red 575nm Single

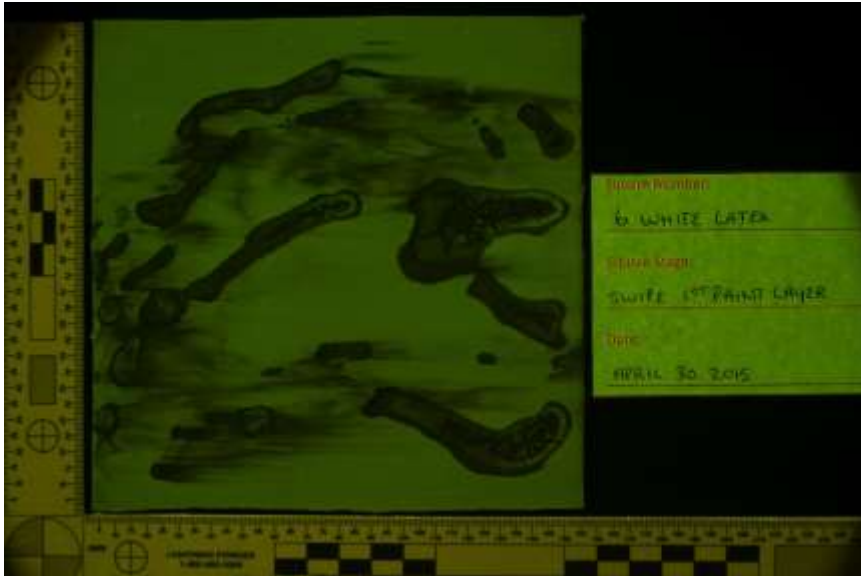
White Latex 6 – Swipe



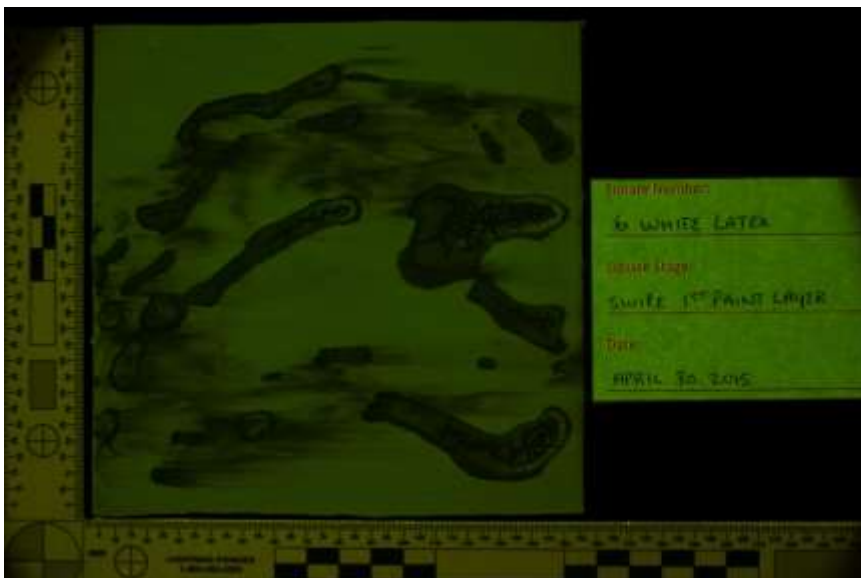
Yellow 415nm HDR



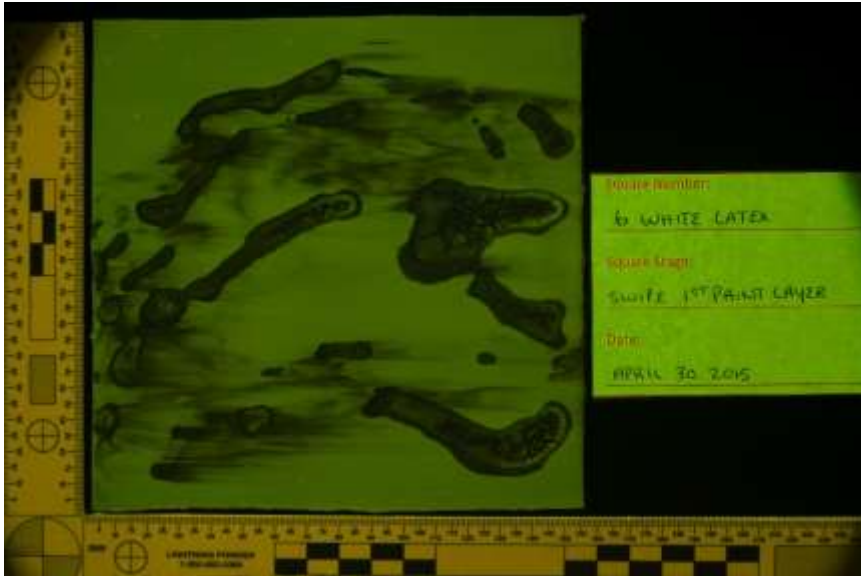
Yellow 415nm Single



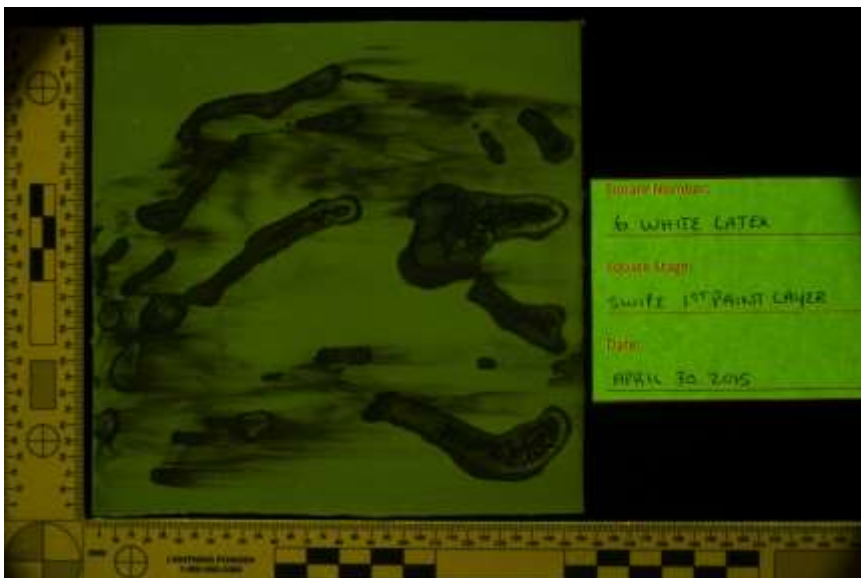
Yellow 445nm HDR



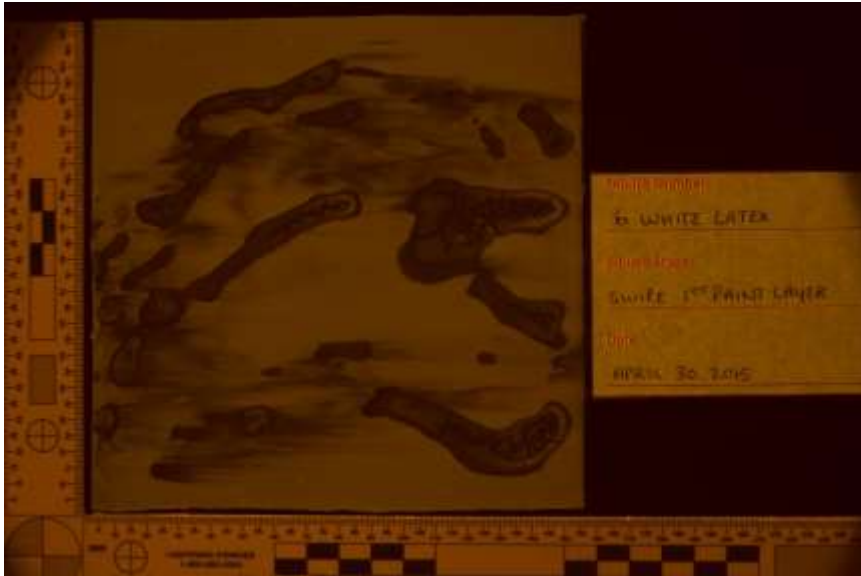
Yellow 445nm Single



Yellow 455nm HDR



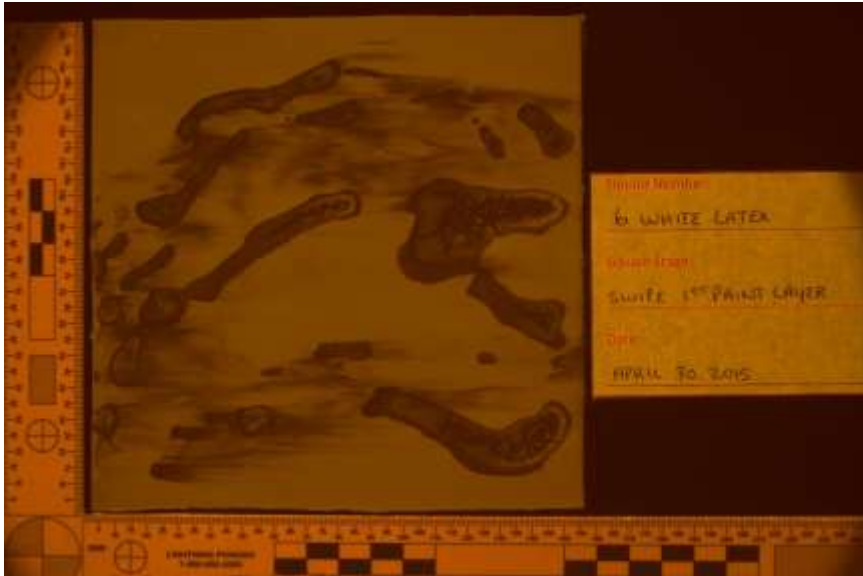
Yellow 455nm Single



Orange 445nm HDR



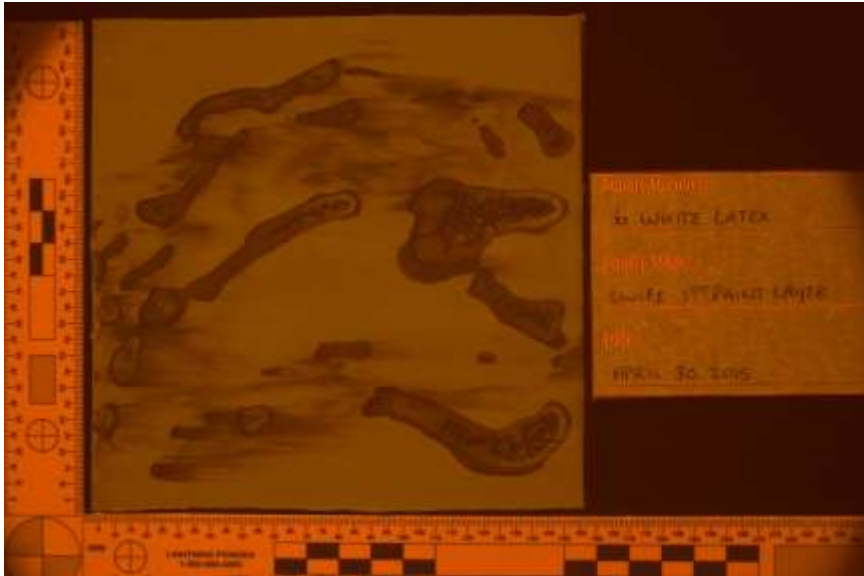
Orange 445nm Single



Orange 455nm HDR



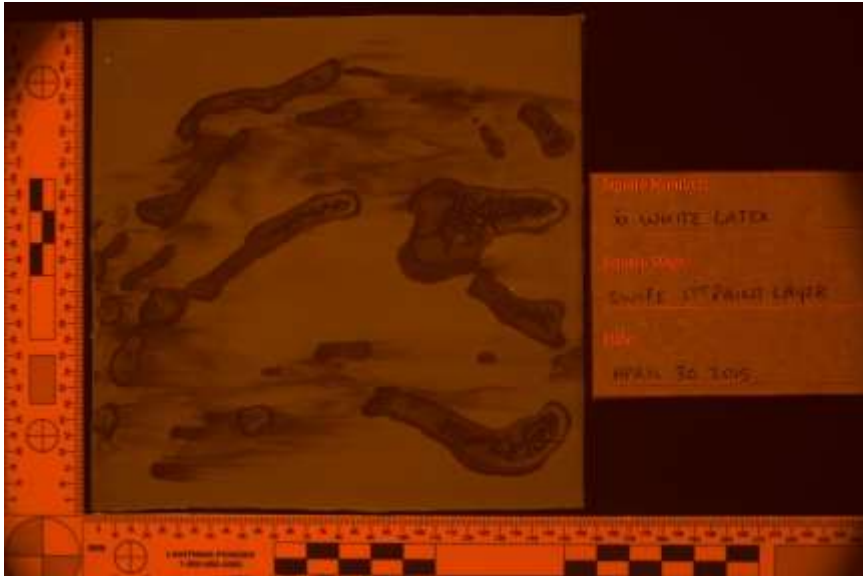
Orange 455nm Single



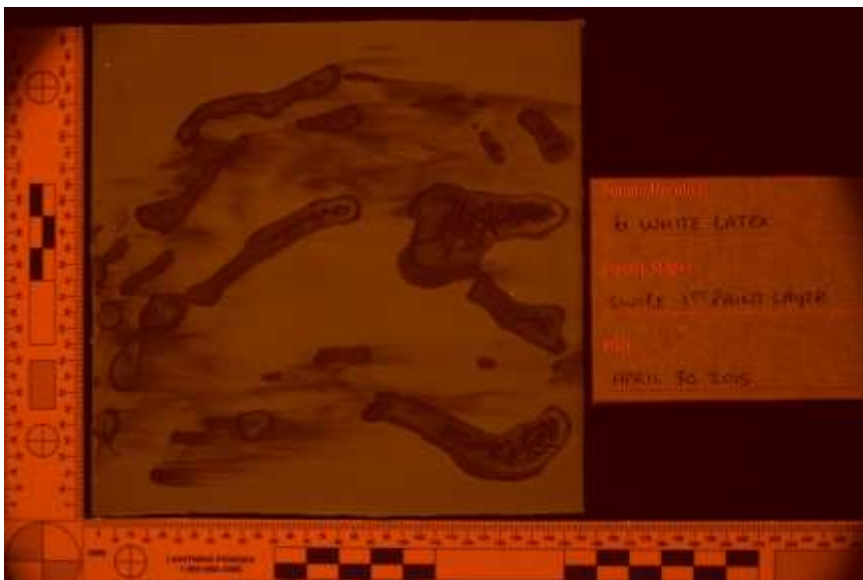
Orange 475nm HDR



Orange 475nm Single



Orange 495nm HDR



Orange 495nm Single



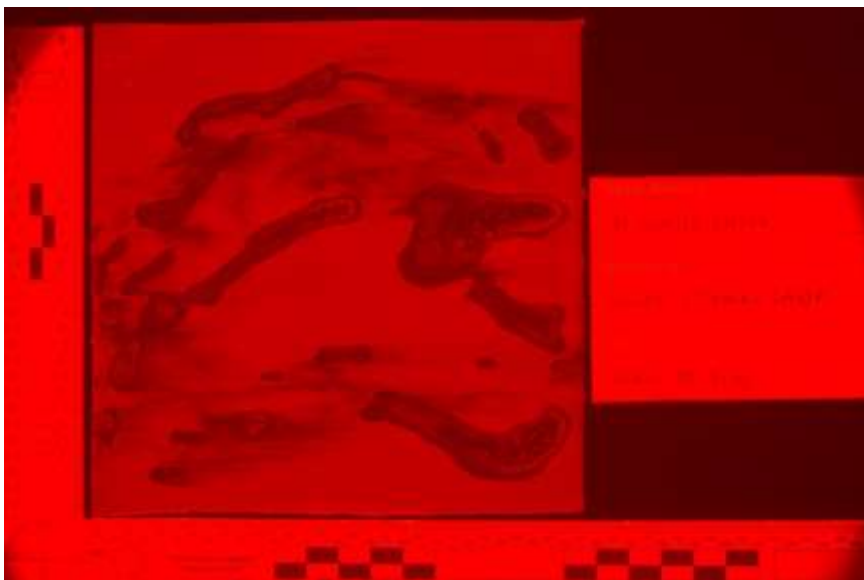
Orange 515nm HDR



Orange 515nm Single

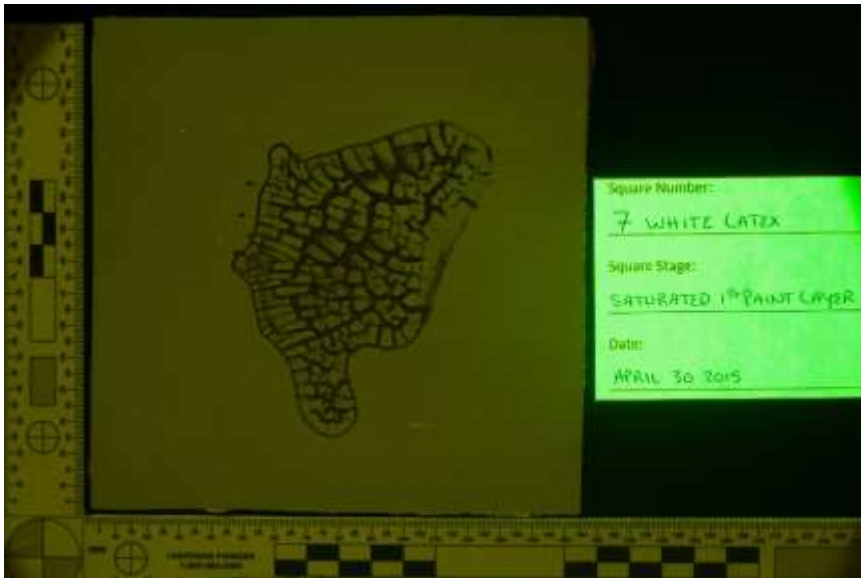


Red 575nm HDR

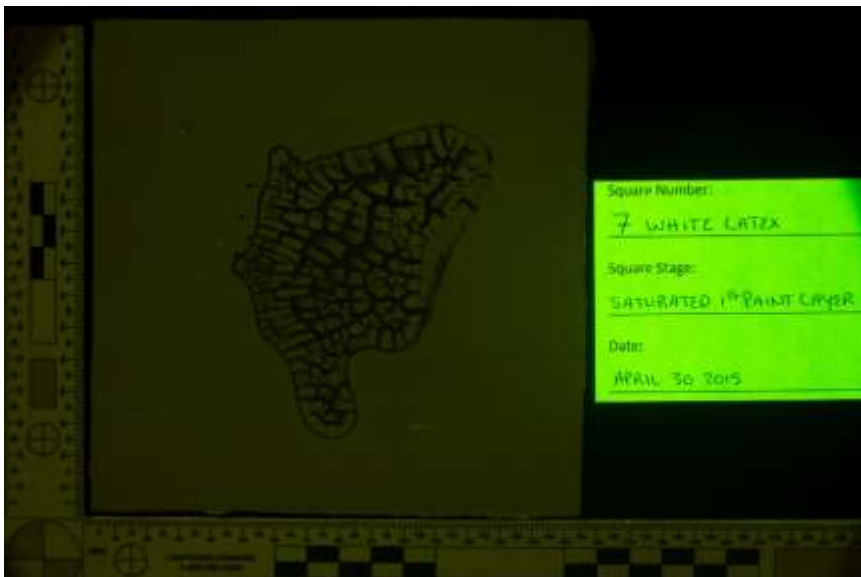


Red 575nm Single

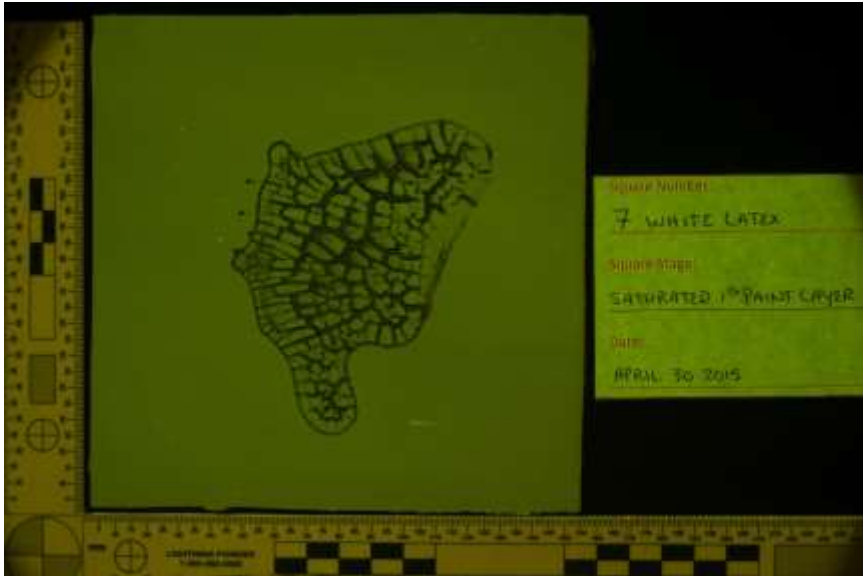
White Latex 7 – Saturated



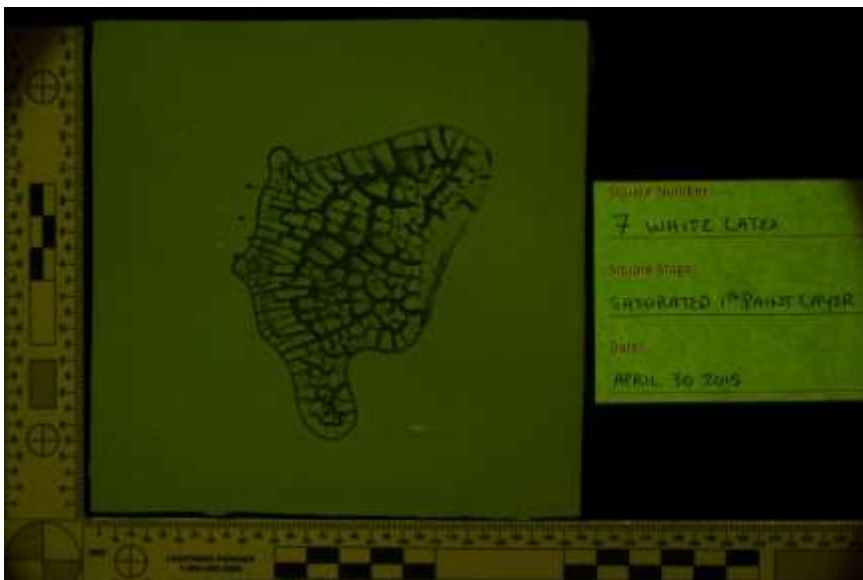
Yellow 415nm HDR



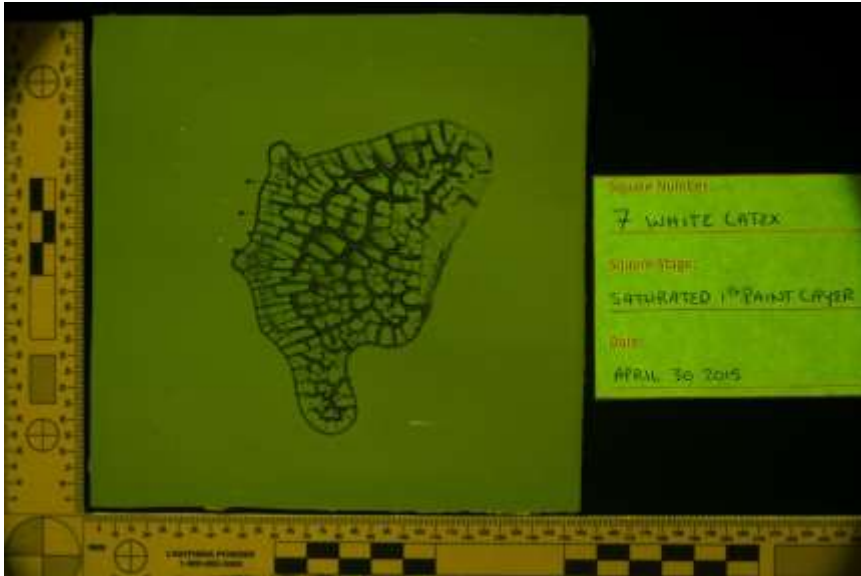
Yellow 415nm Single



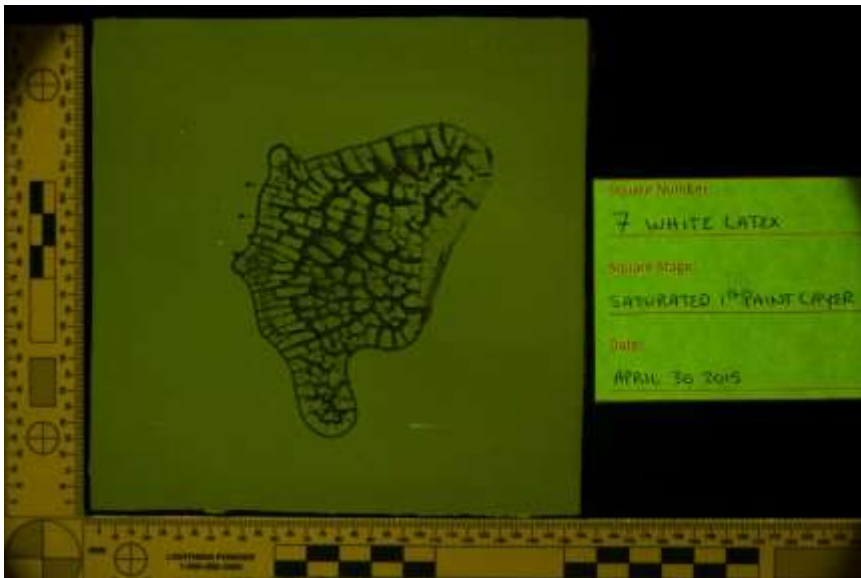
Yellow 445nm HDR



Yellow 445nm Single



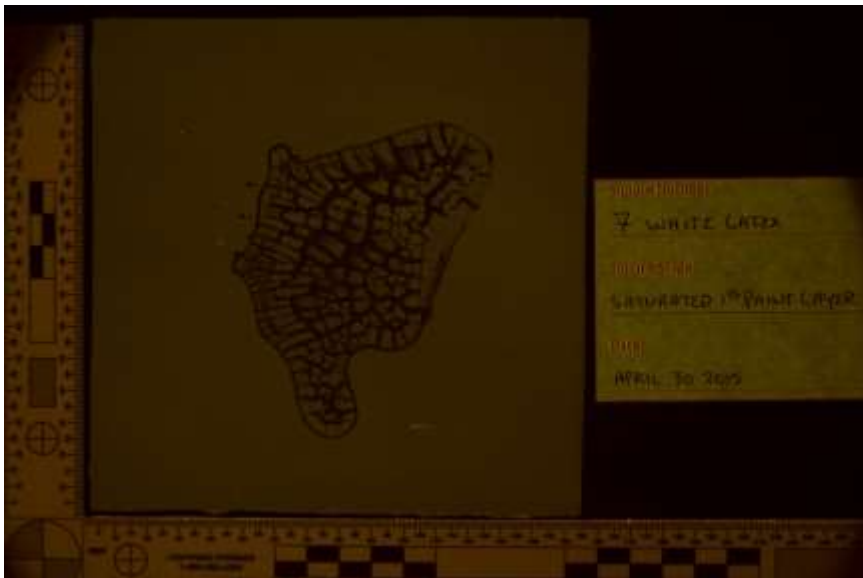
Yellow 455nm HDR



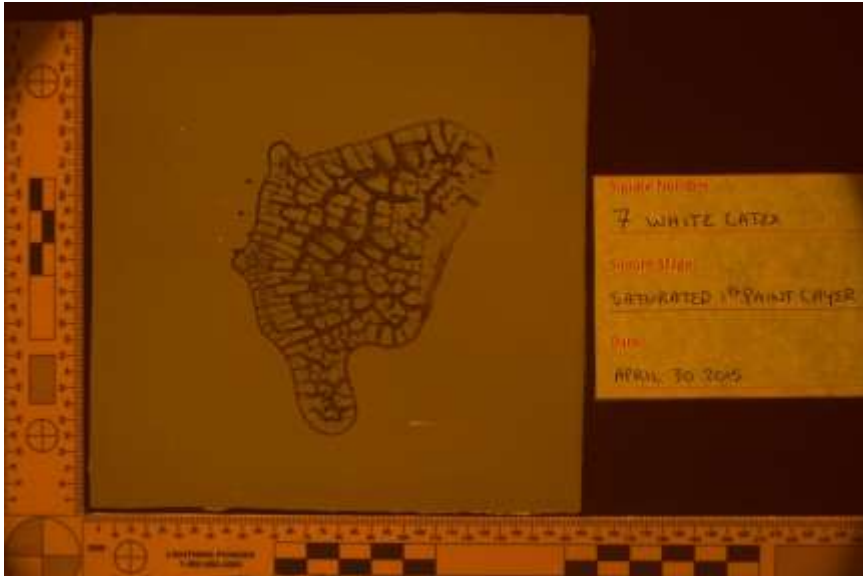
Yellow 455nm Single



Orange 445nm HDR



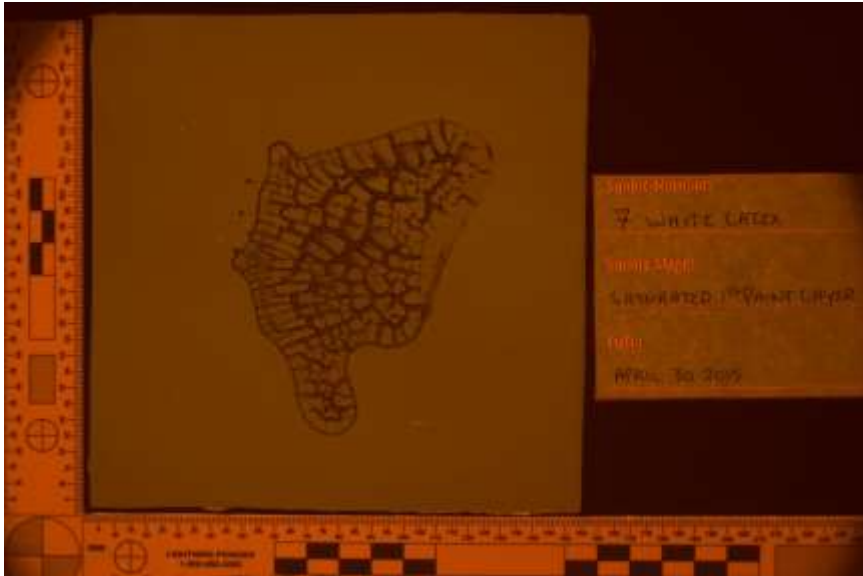
Orange 445nm Single



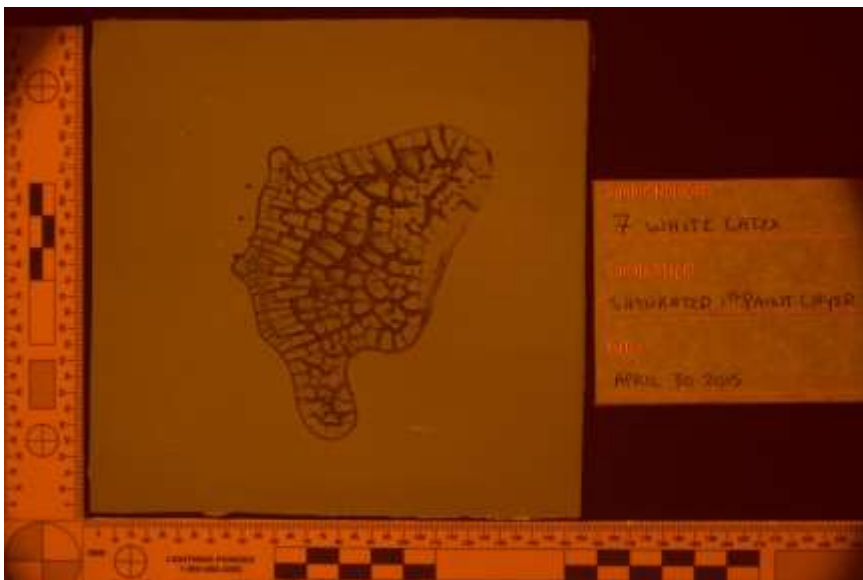
Orange 455nm HDR



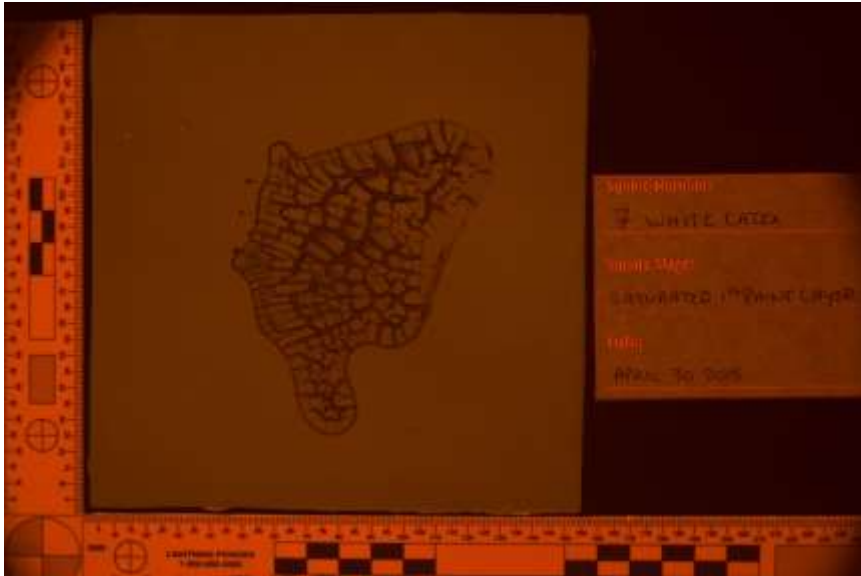
Orange 455nm Single



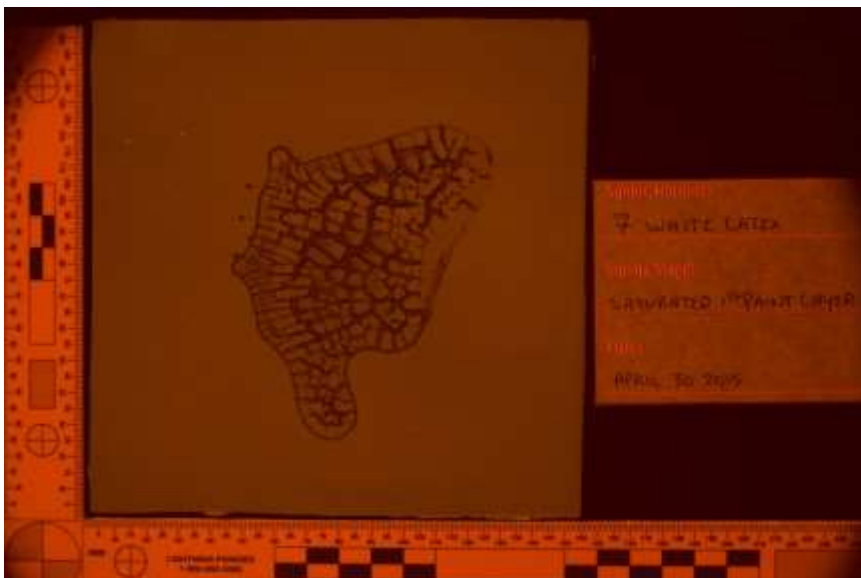
Orange 475nm HDR



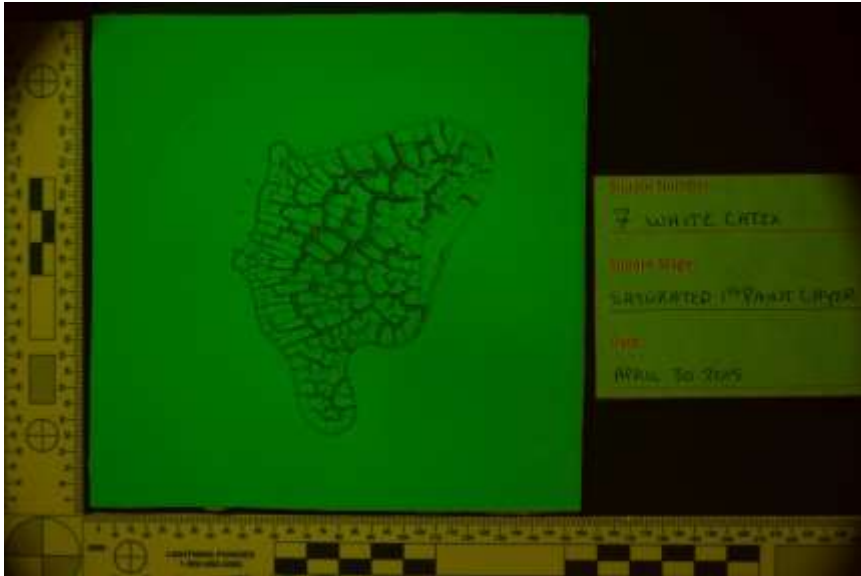
Orange 475nm Single



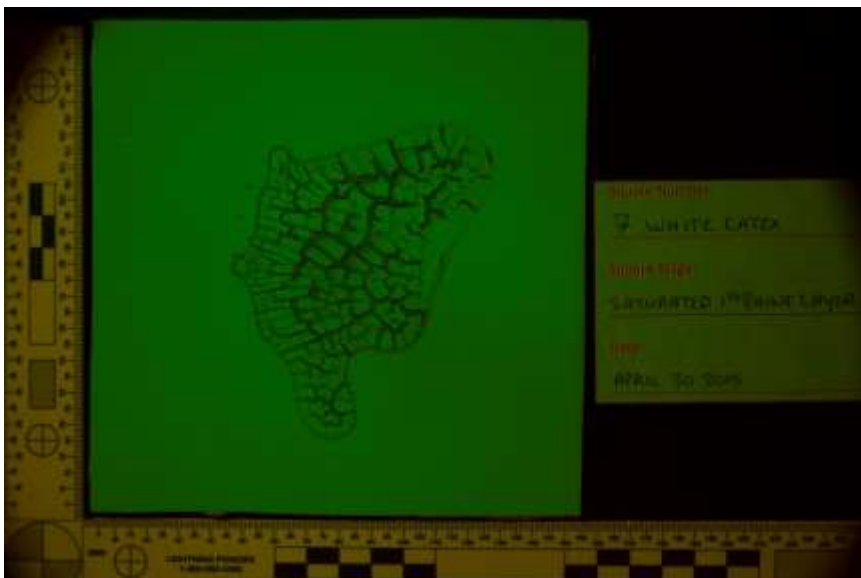
Orange 495nm HDR



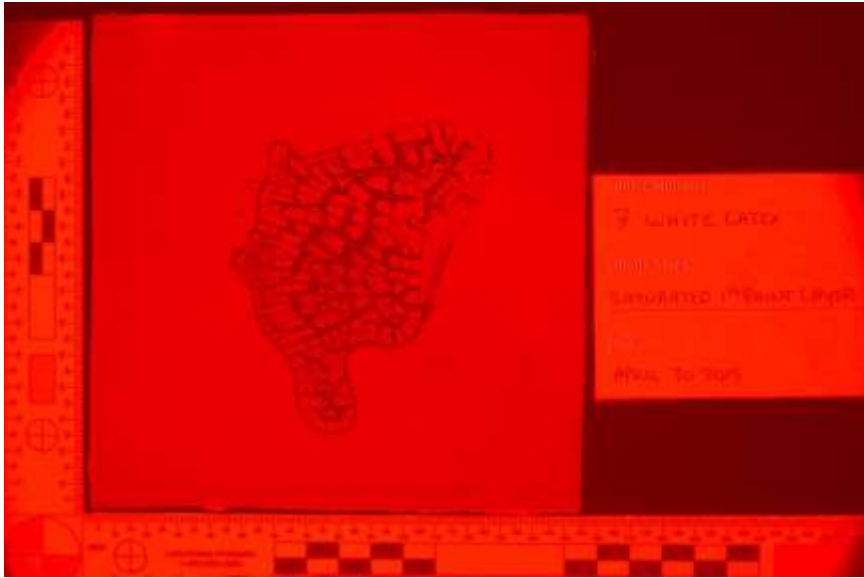
Orange 495nm Single



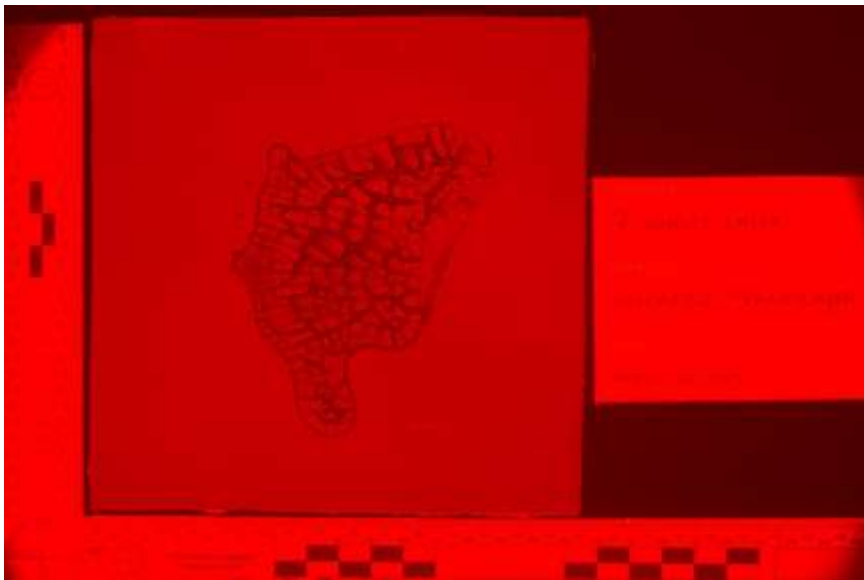
Orange 515nm HDR



Orange 515nm Single



Red 575nm HDR

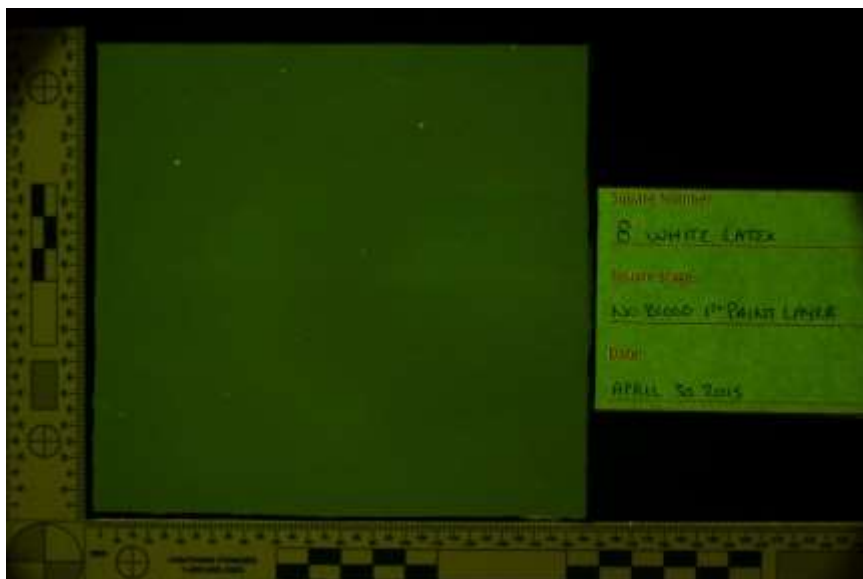


Red 575nm Single

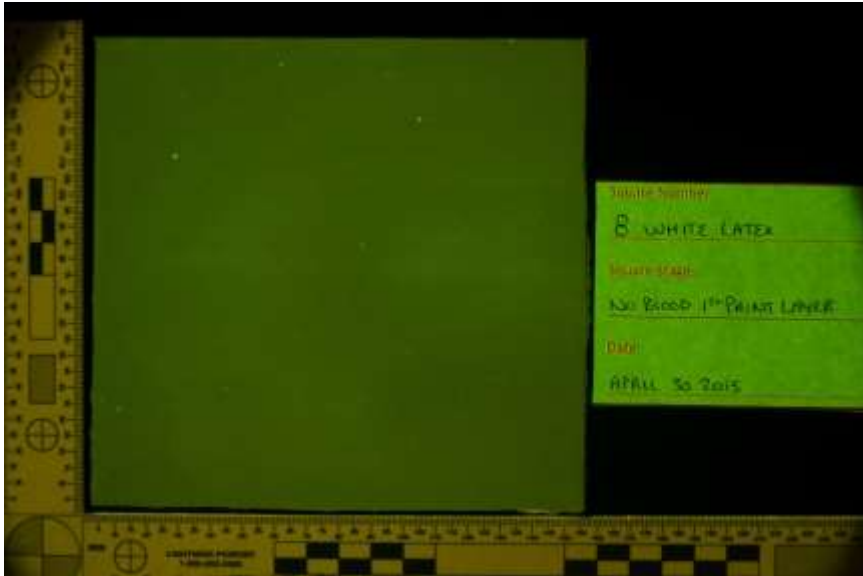
White Latex 8 – Control No Bloodstain



Yellow 415nm HDR



Yellow 445nm HDR



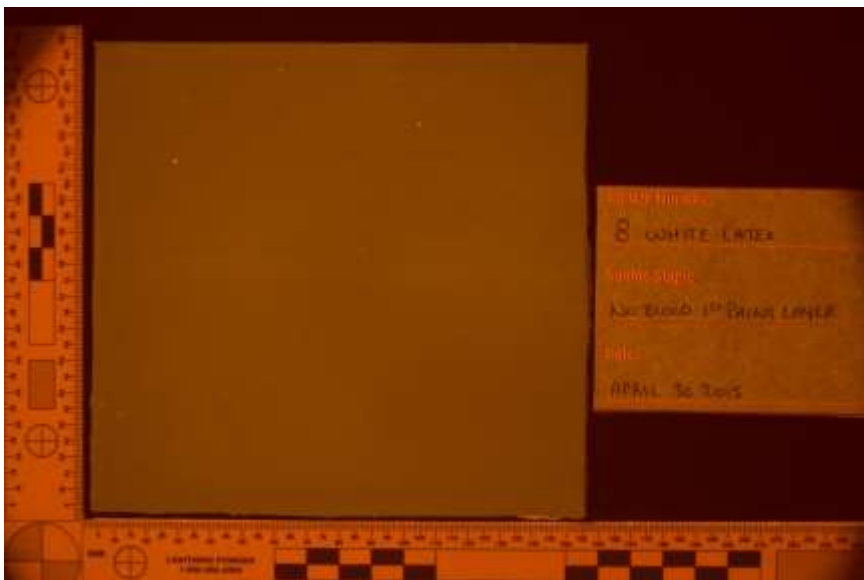
Yellow 455nm HDR



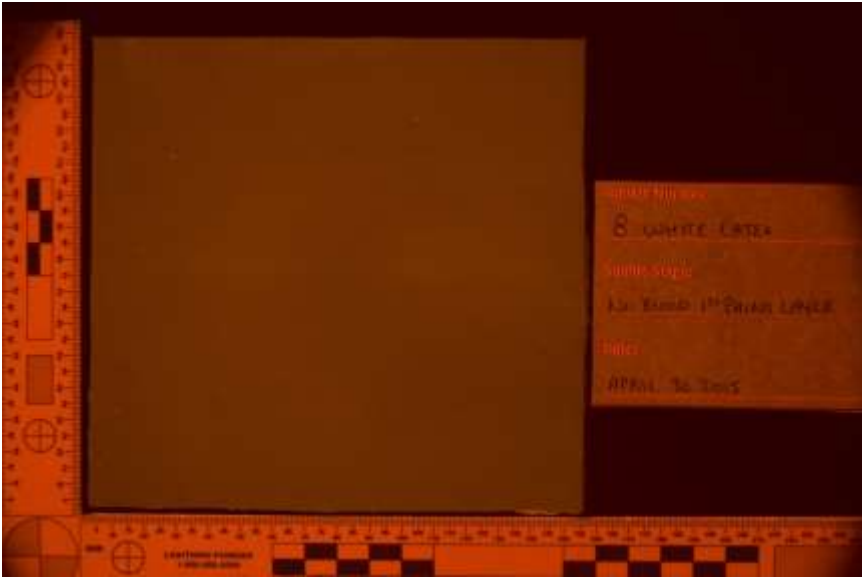
Orange 445nm HDR



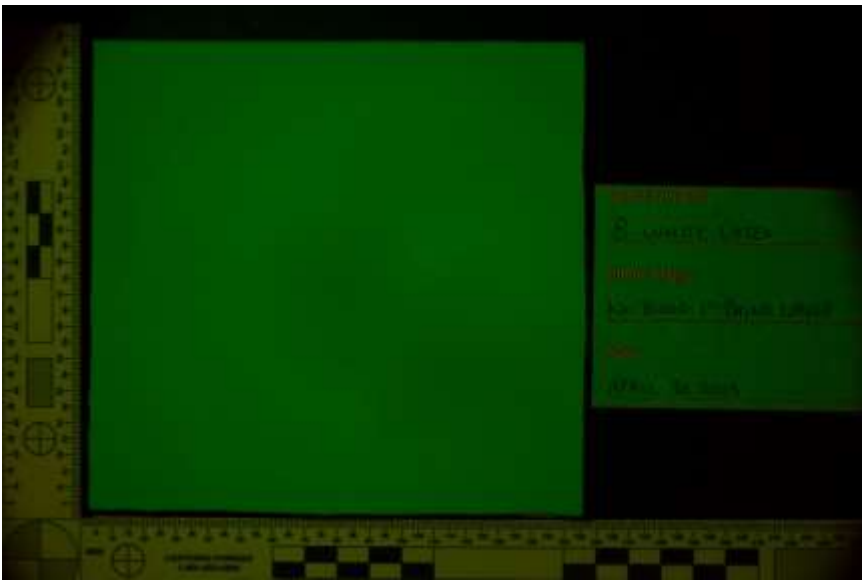
Orange 455nm HDR



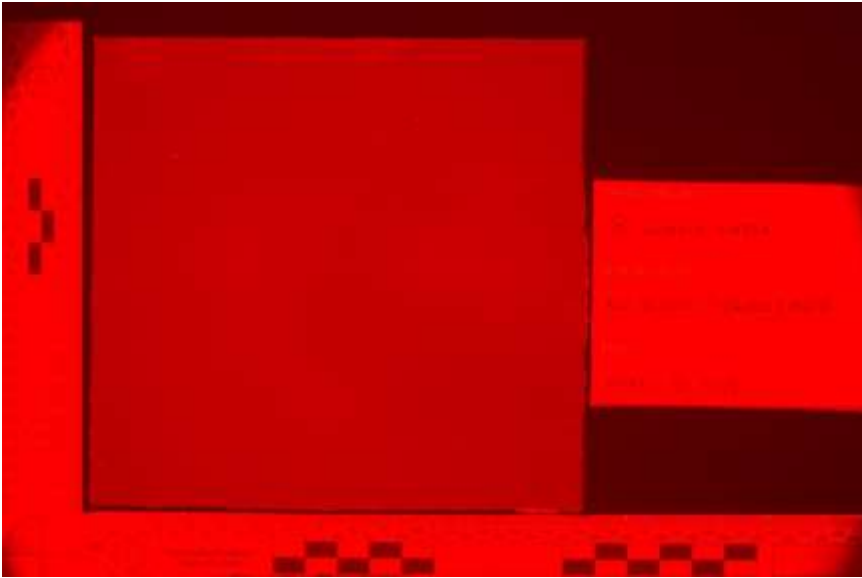
Orange 475nm HDR



Orange 495nm HDR

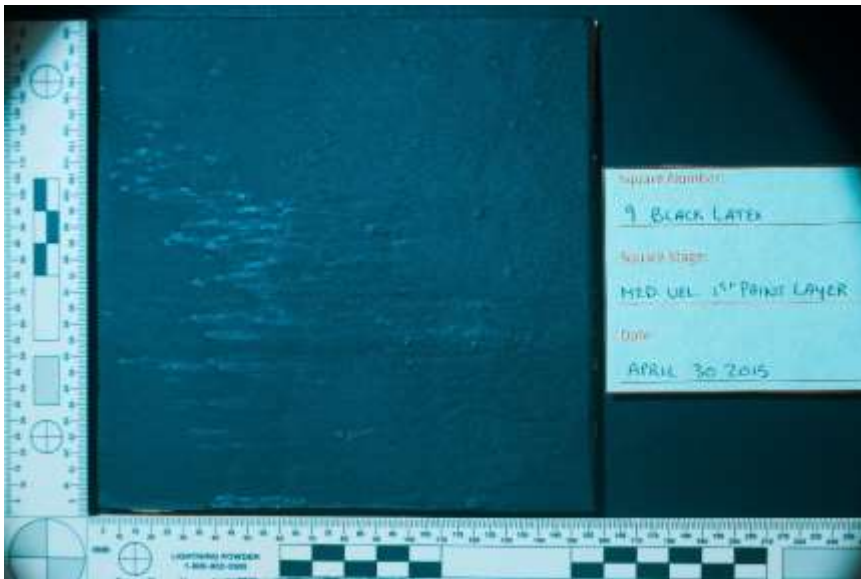


Orange 515nm HDR



Red 575nm HDR

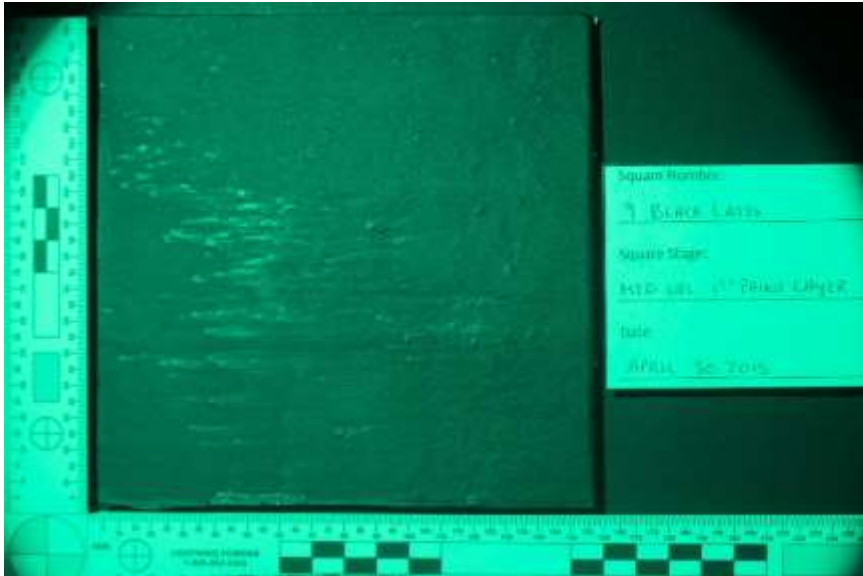
Appendix 4.2.5.3. Black Latex – Yellow 475nm, 495nm, 670nm; Orange 555nm, 600nm, 670nm; Red 600nm First layer of paint stage
Black Latex 9 – Medium Velocity



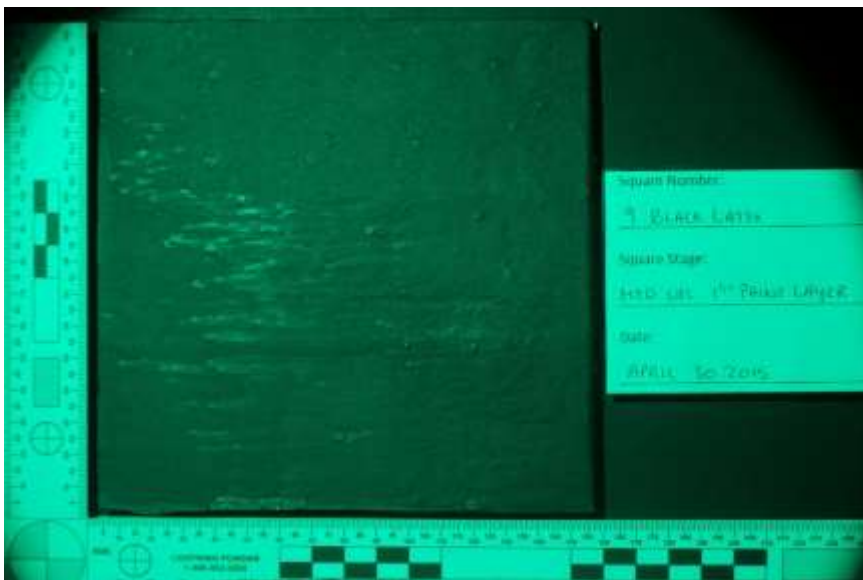
Yellow 475nm HDR



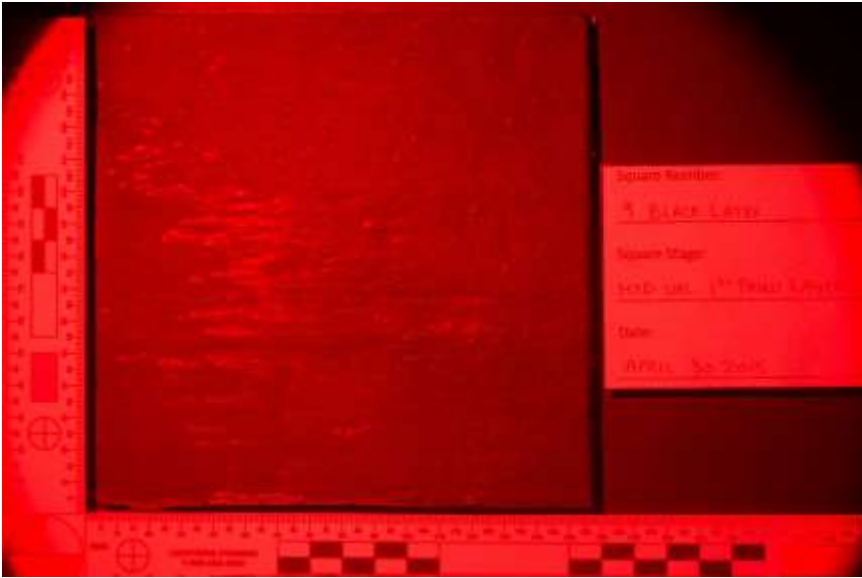
Yellow 475nm Single



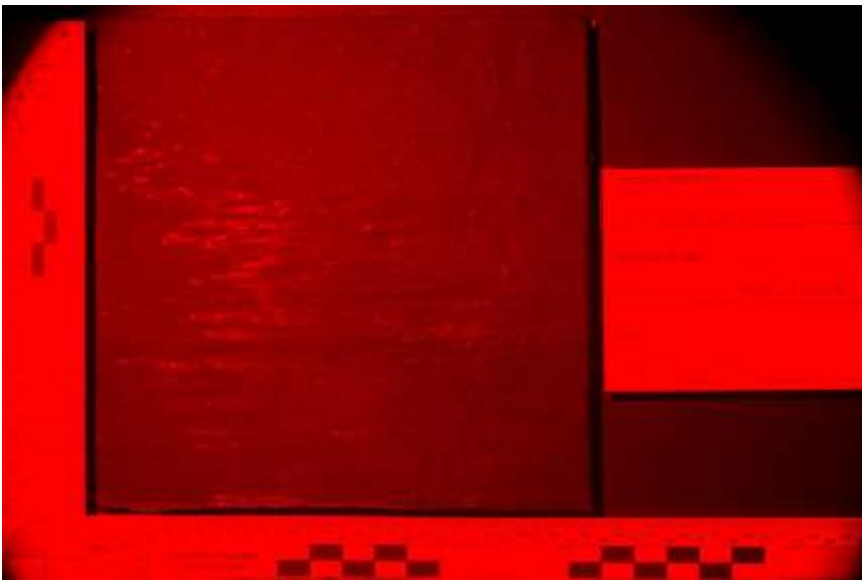
Yellow 495nm HDR



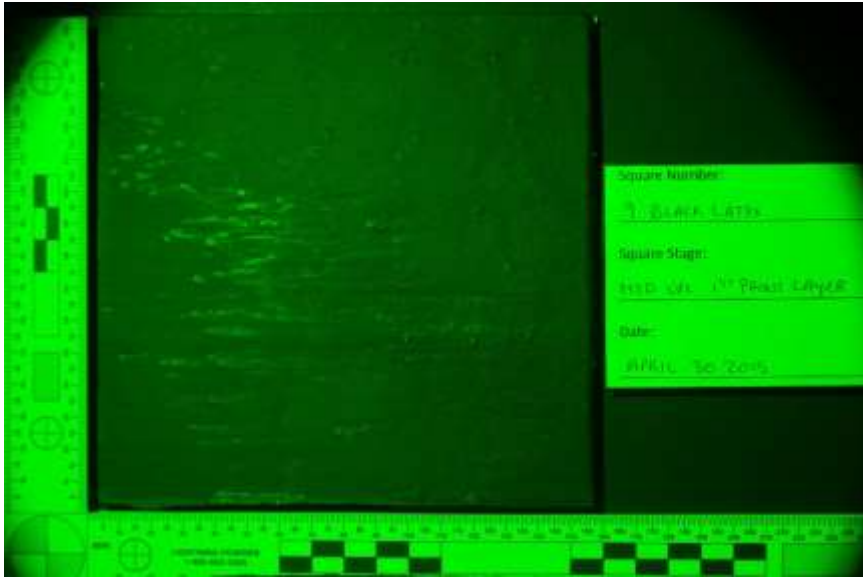
Yellow 495nm Single



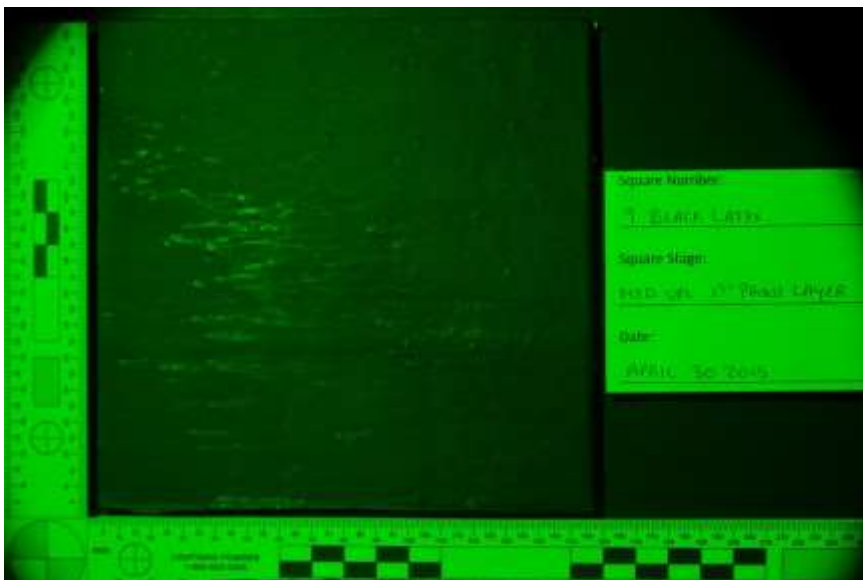
Yellow 670nm HDR



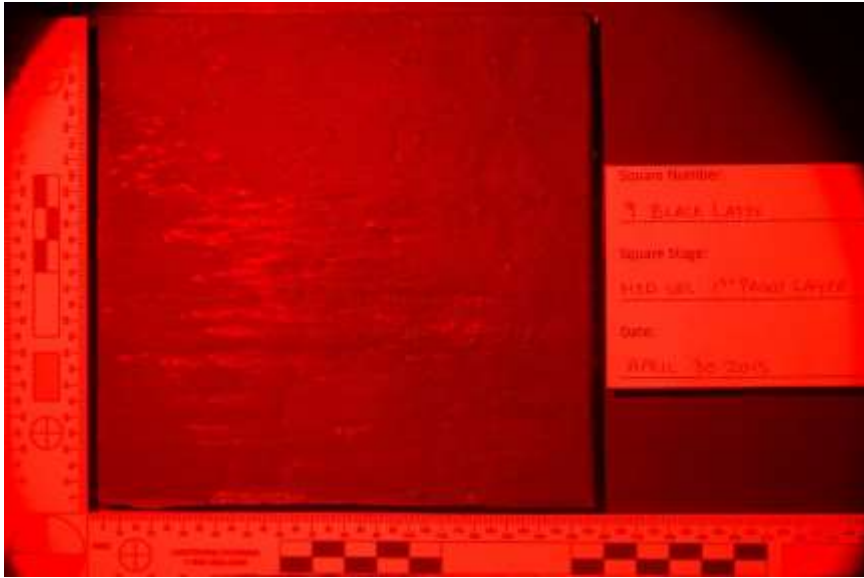
Yellow 670nm Single



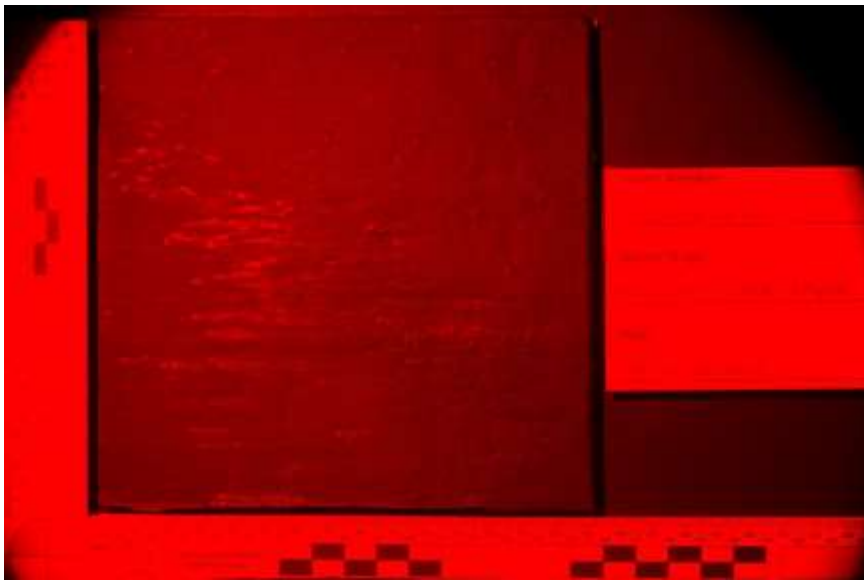
Orange 555nm HDR



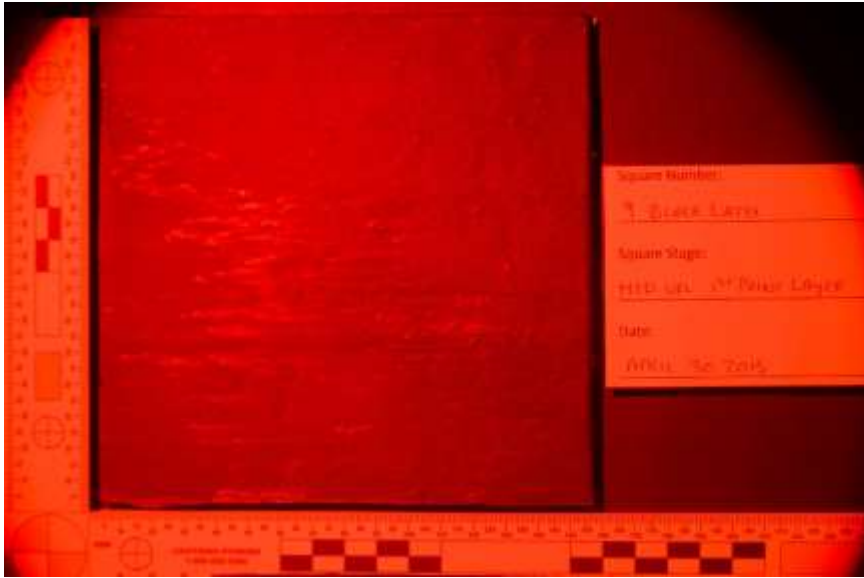
Orange 555nm Single



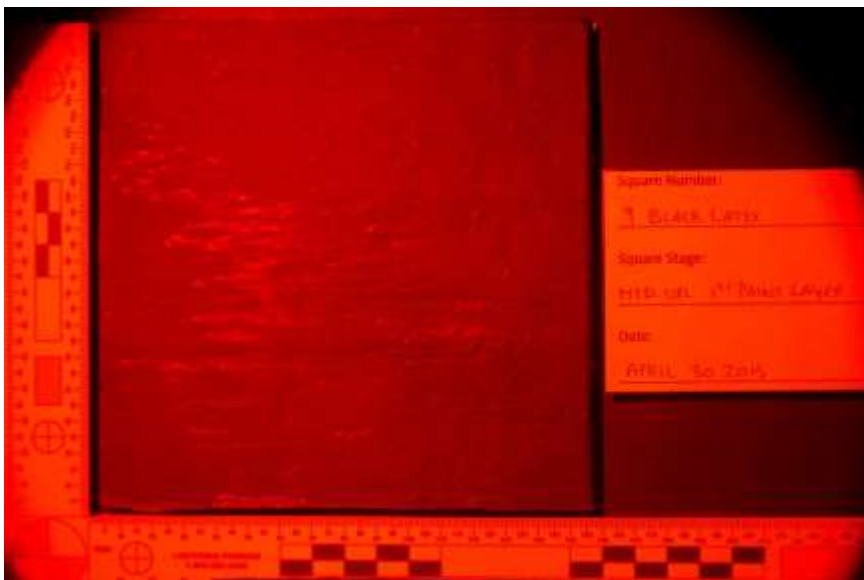
Orange 670nm HDR



Orange 670nm Single

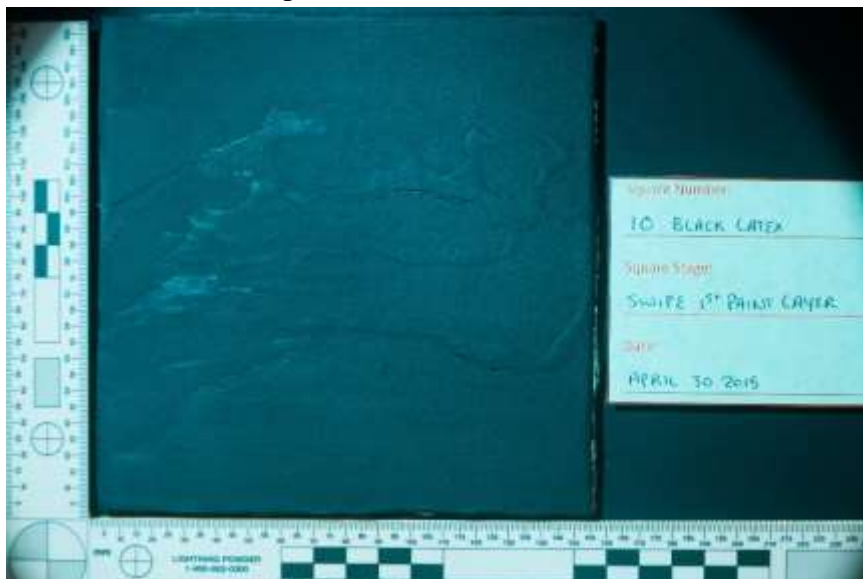


Red 600nm HDR

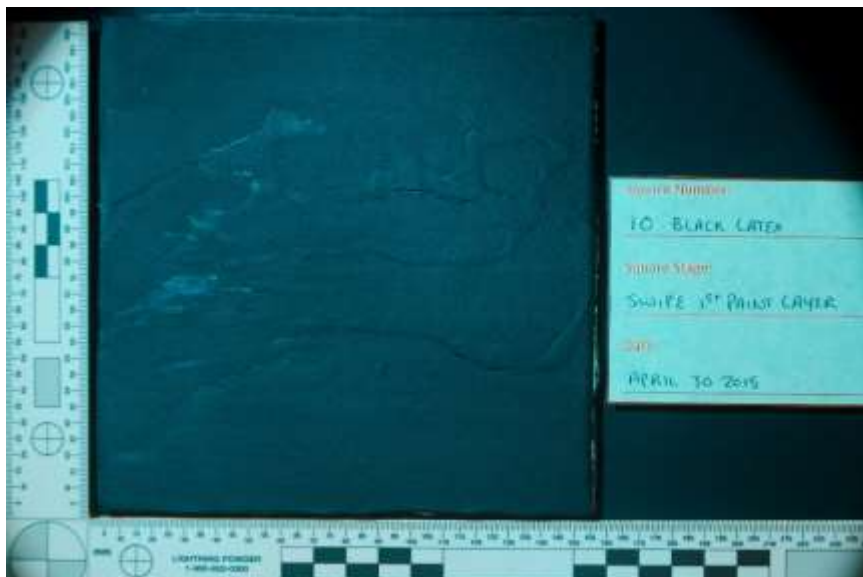


Red 600nm Single

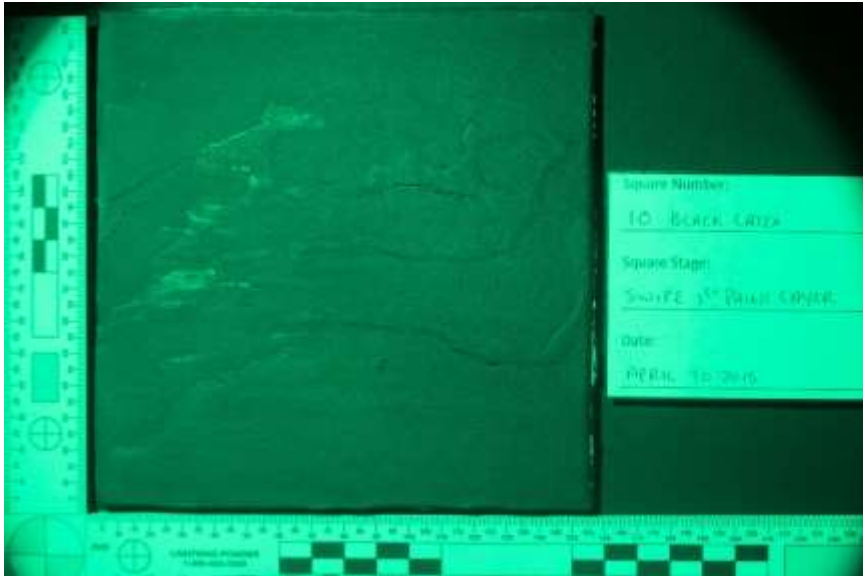
Black Latex 10 – Swipe



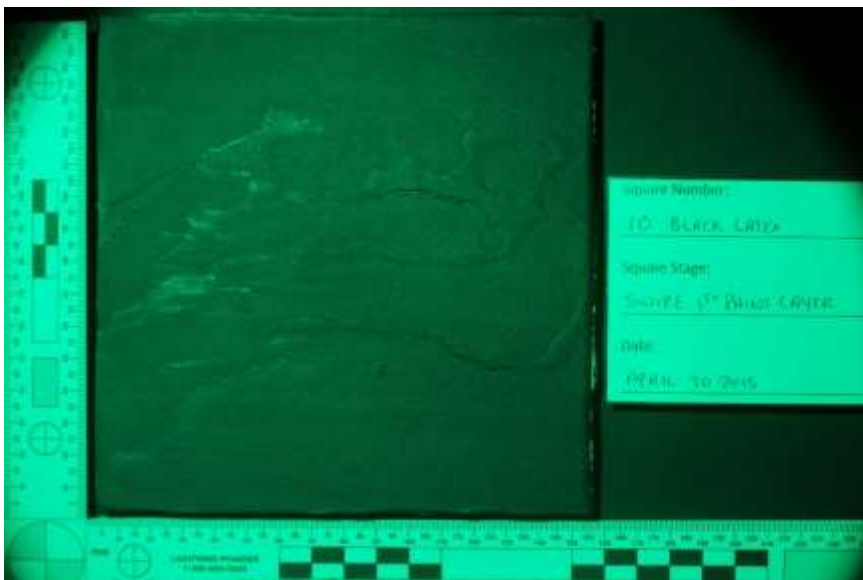
Yellow 475nm HDR



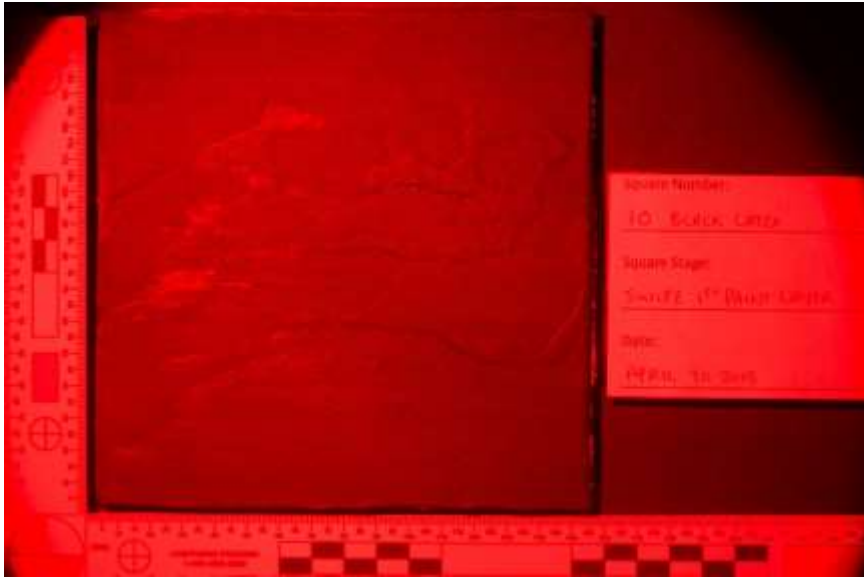
Yellow 475nm Single



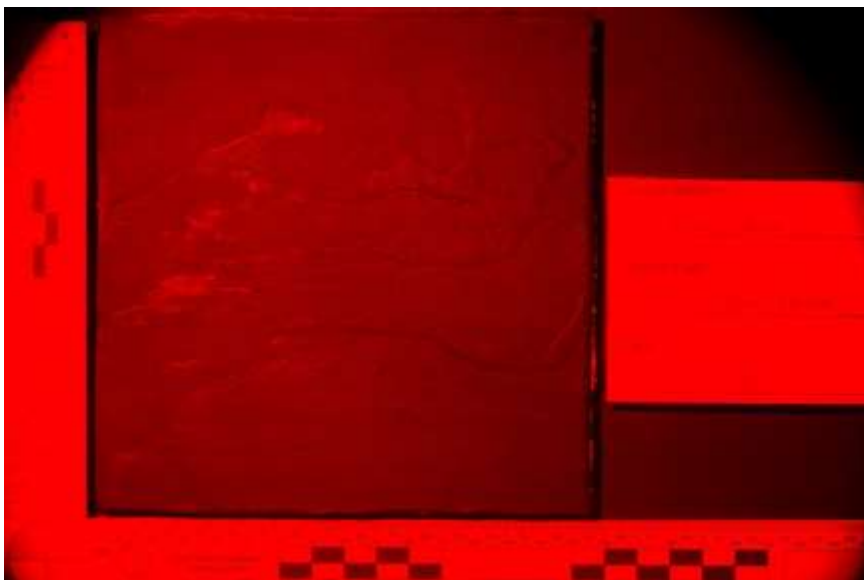
Yellow 495nm HDR



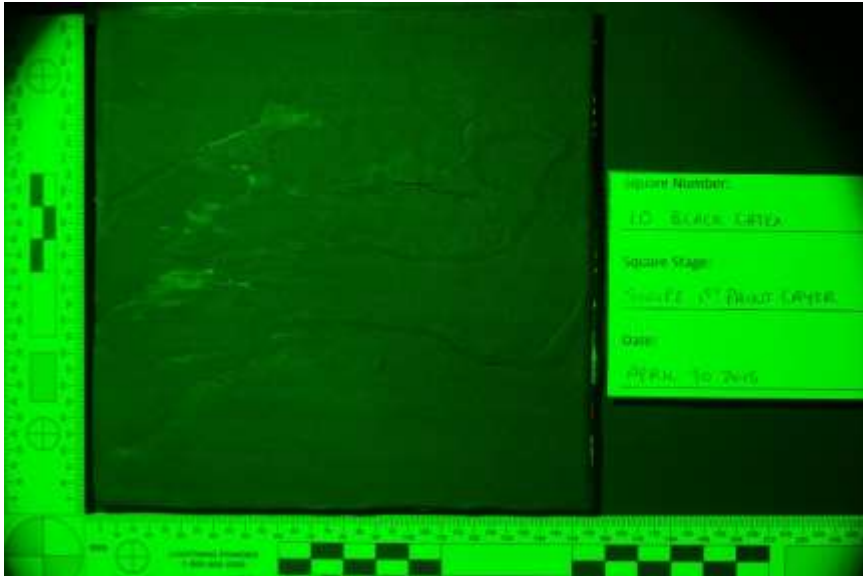
Yellow 495nm Single



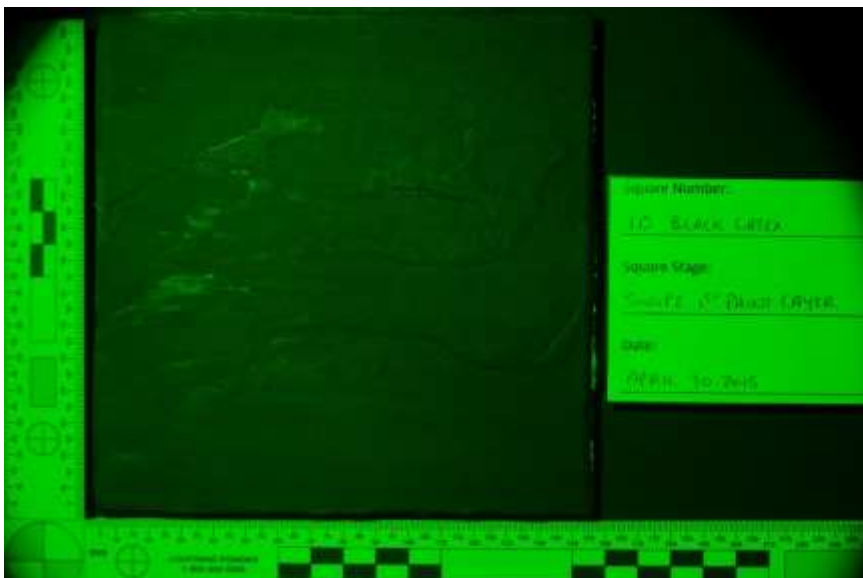
Yellow 670nm HDR



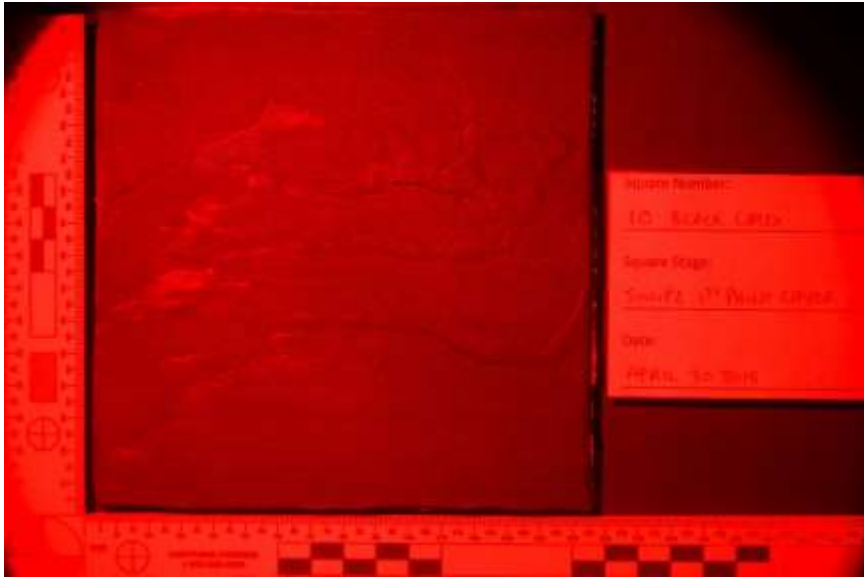
Yellow 670nm Single



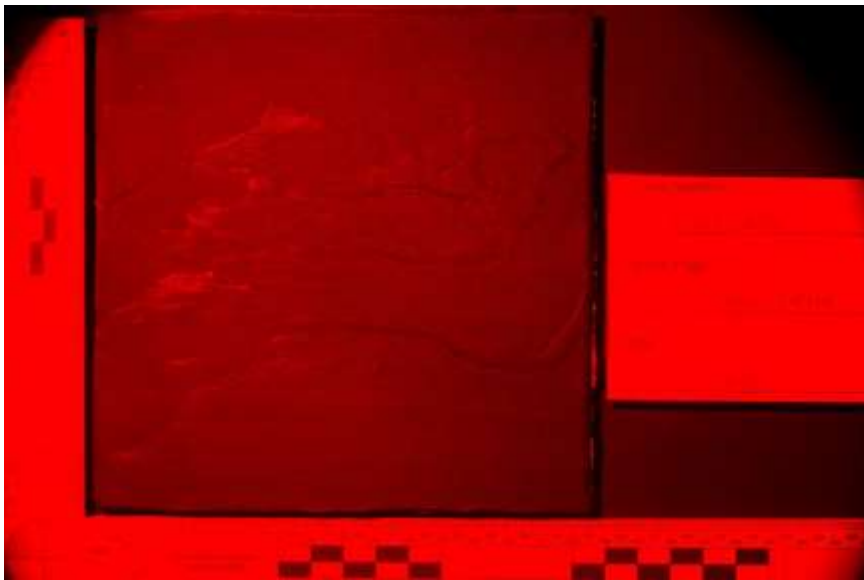
Orange 555nm HDR



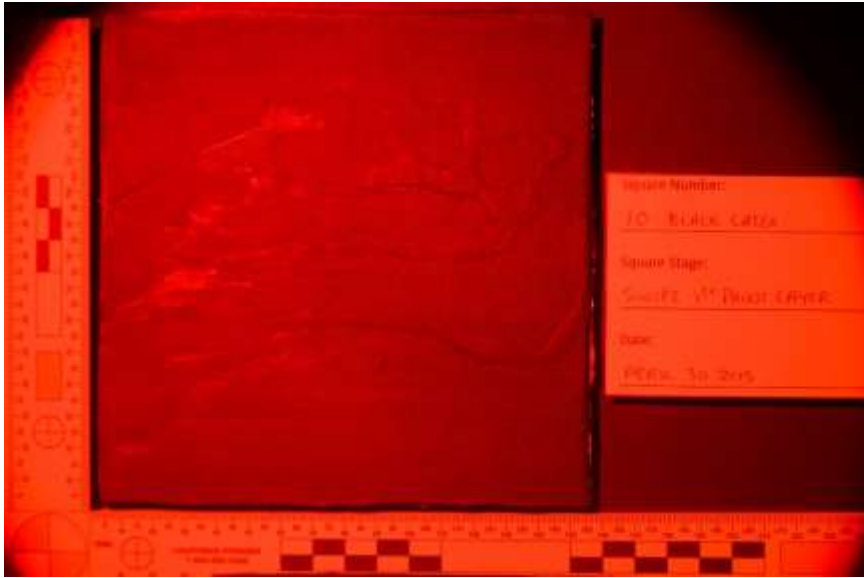
Orange 555nm Single



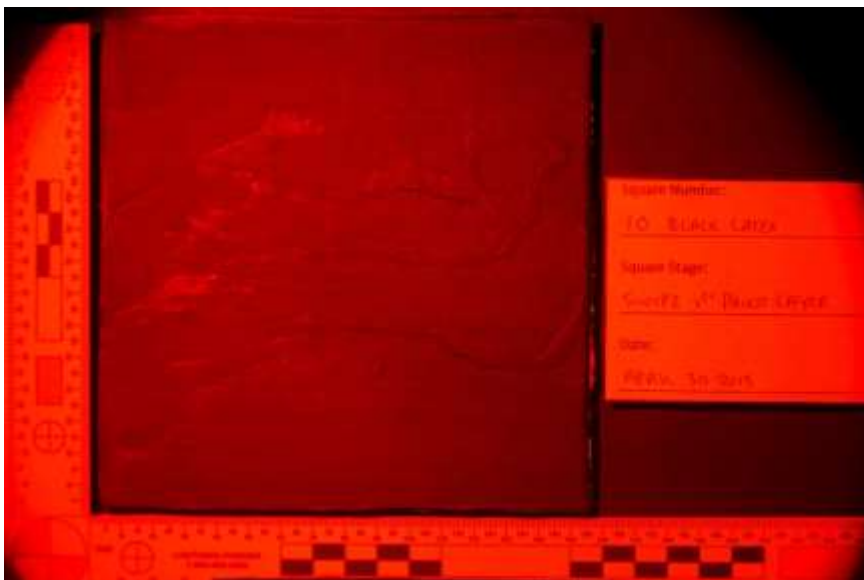
Orange 670nm HDR



Orange 670nm Single

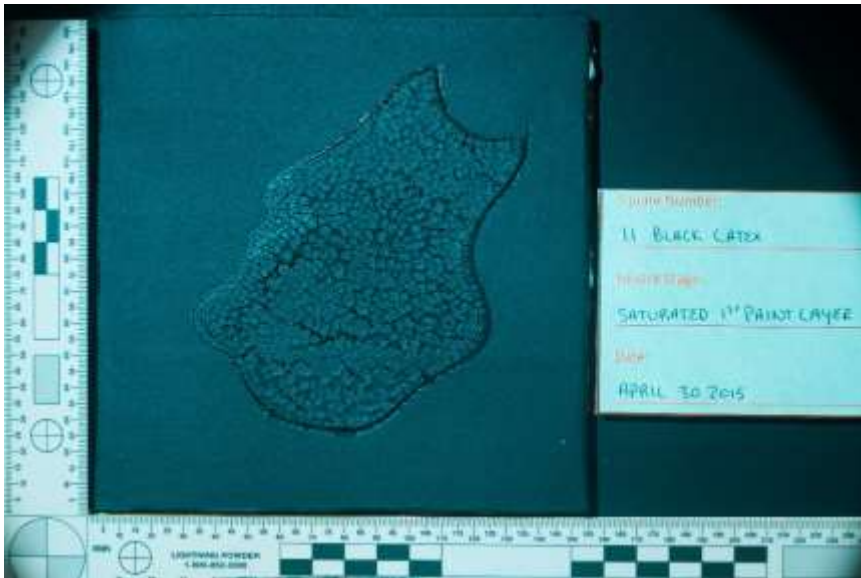


Red 600nm HDR

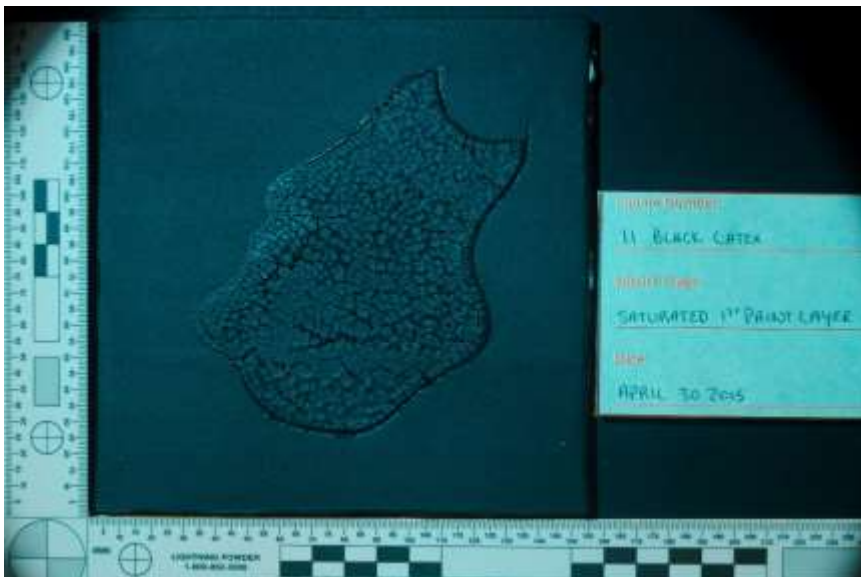


Red 600nm Single

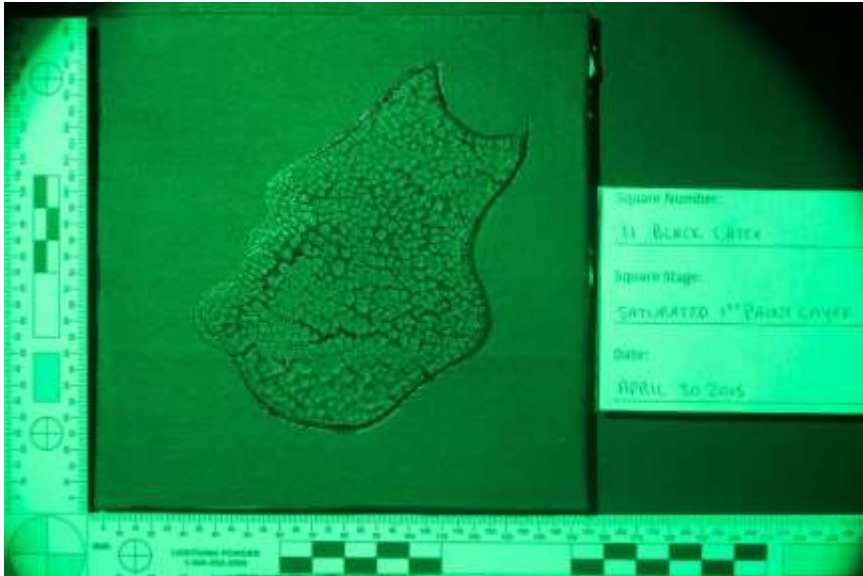
Black Latex 11 – Saturated



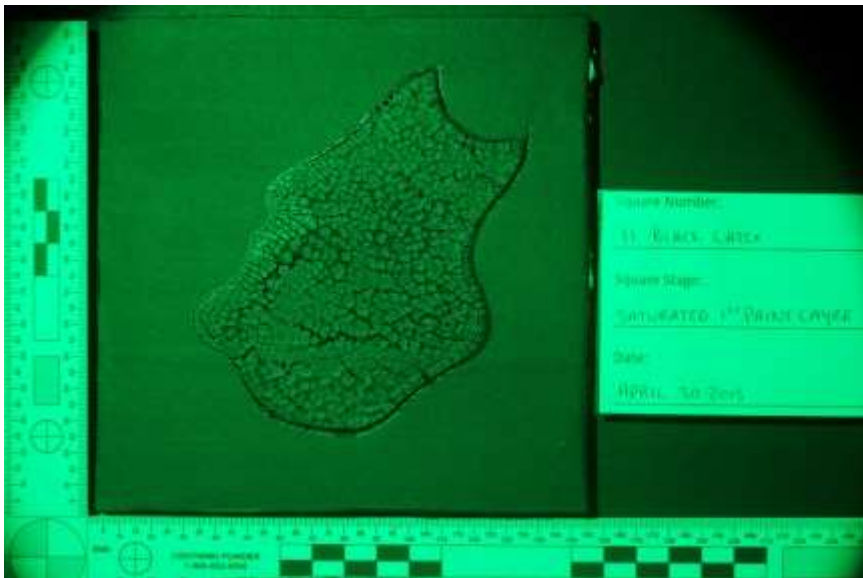
Yellow 475nm HDR



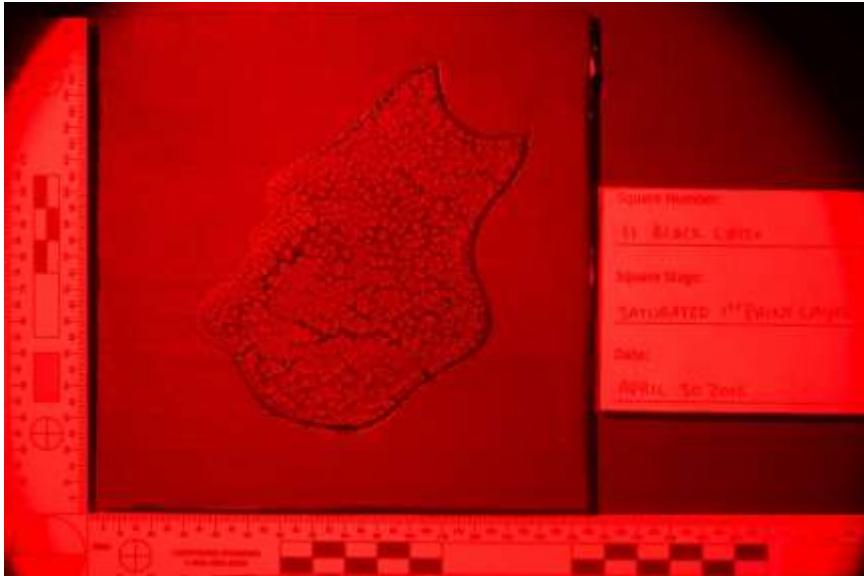
Yellow 475nm Single



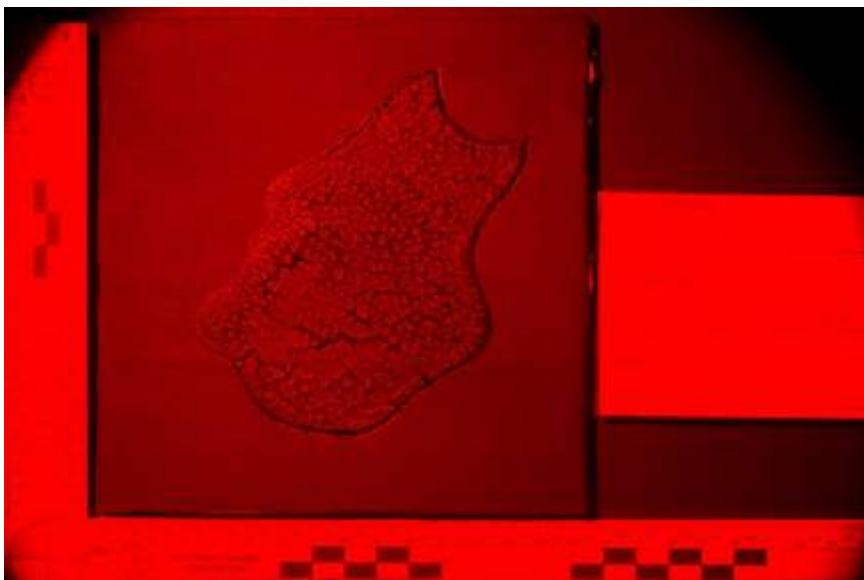
Yellow 495nm HDR



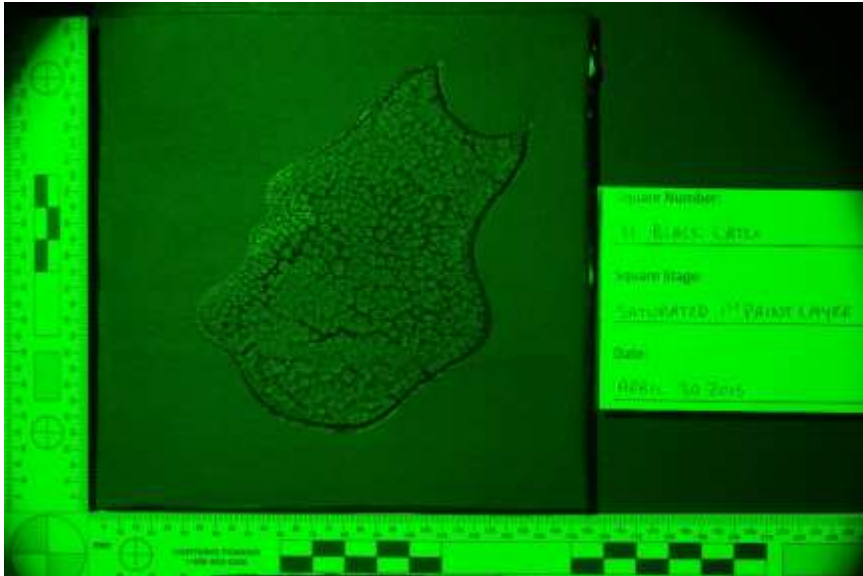
Yellow 495nm Single



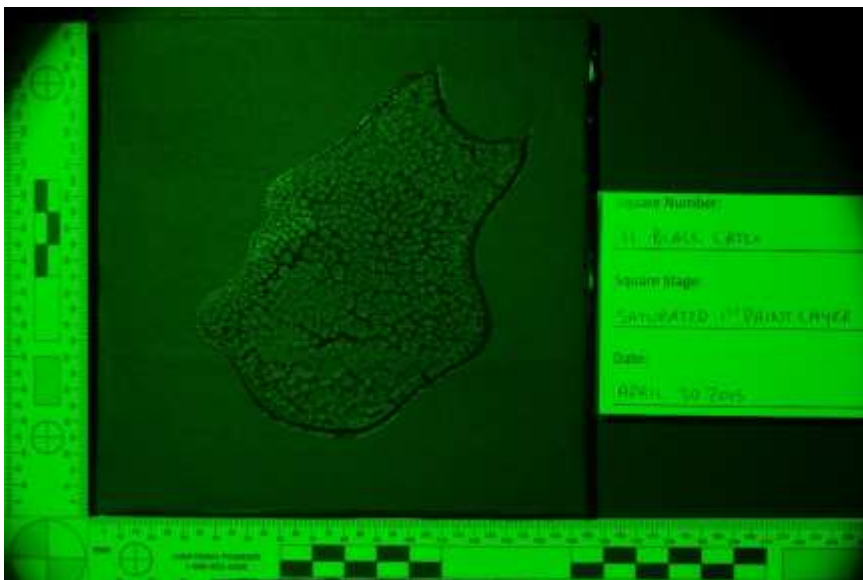
Yellow 670nm HDR



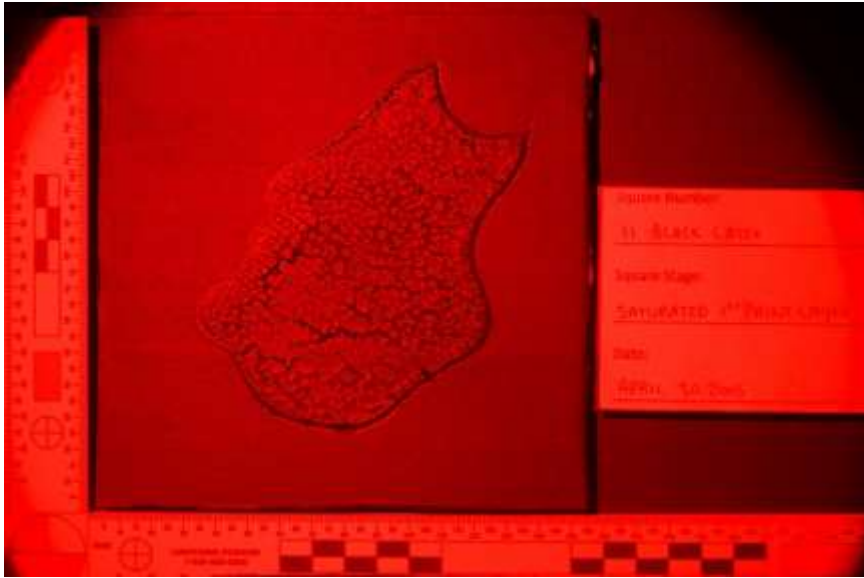
Yellow 670nm Single



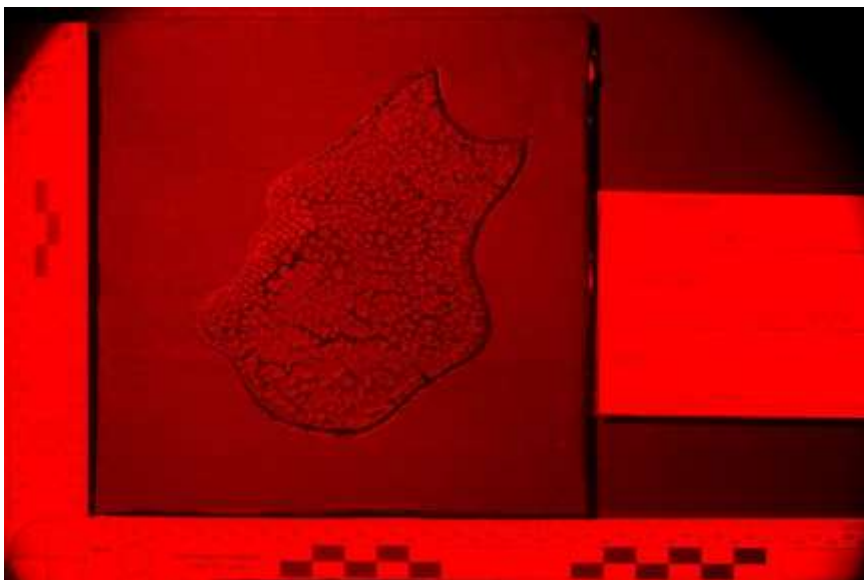
Orange 555nm HDR



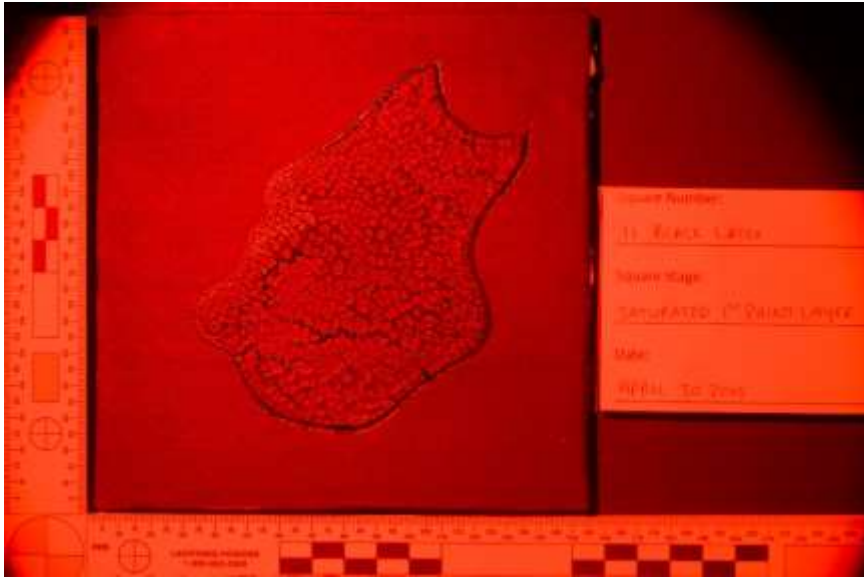
Orange 555nm Single



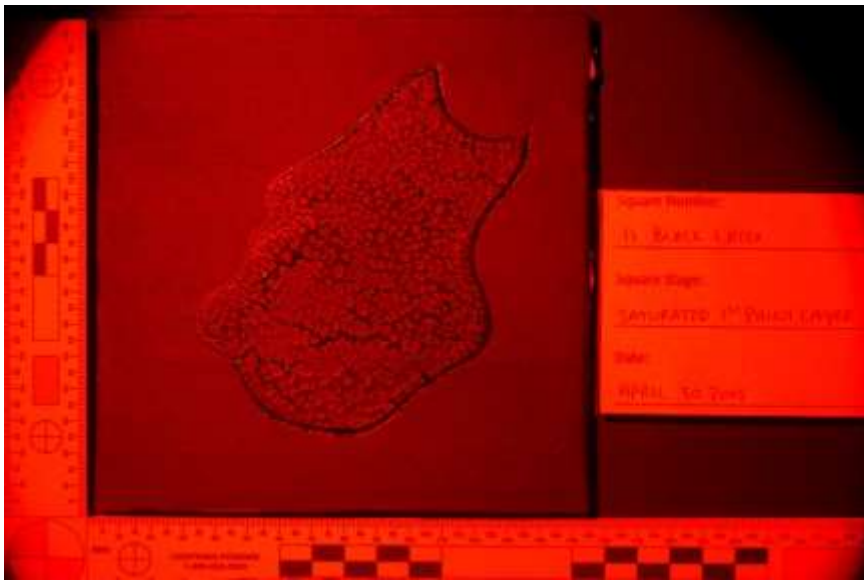
Orange 670nm HDR



Orange 670nm Single



Red 600nm HDR

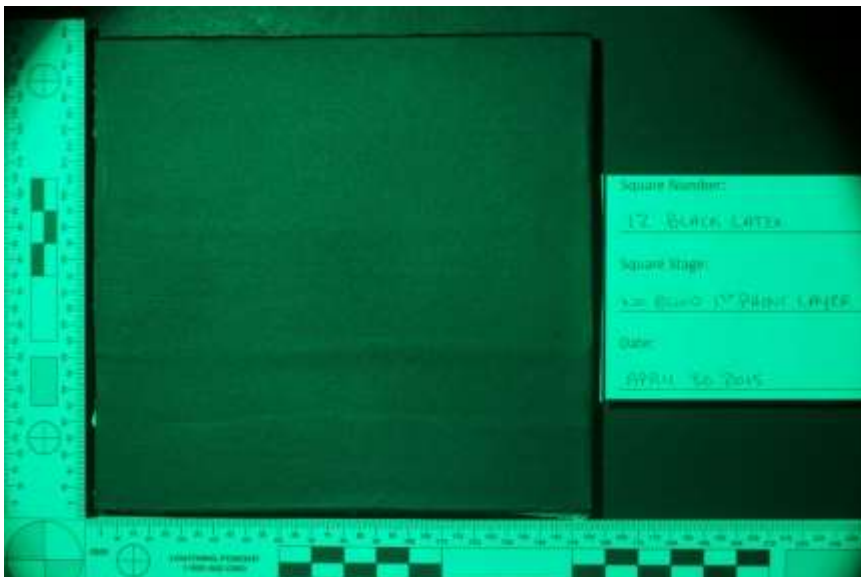


Red 600nm Single

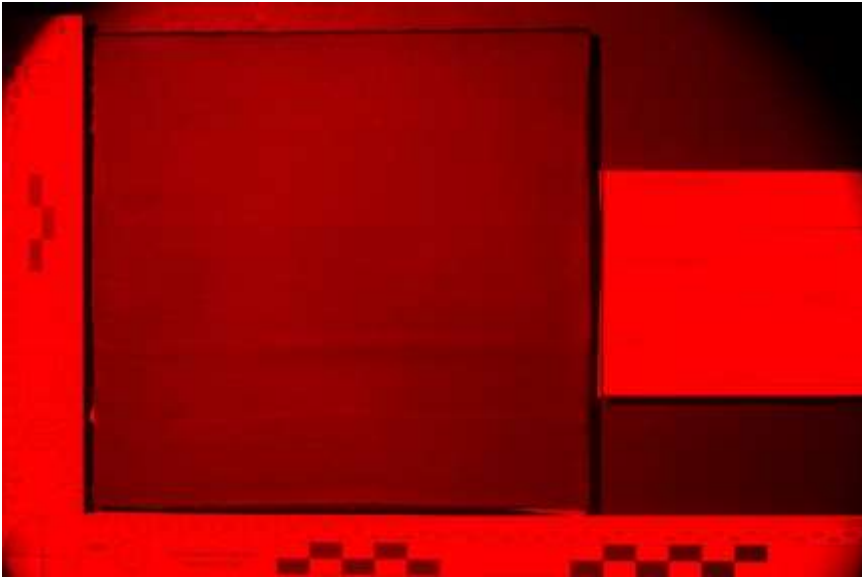
Black Latex 12 – Control No Bloodstain



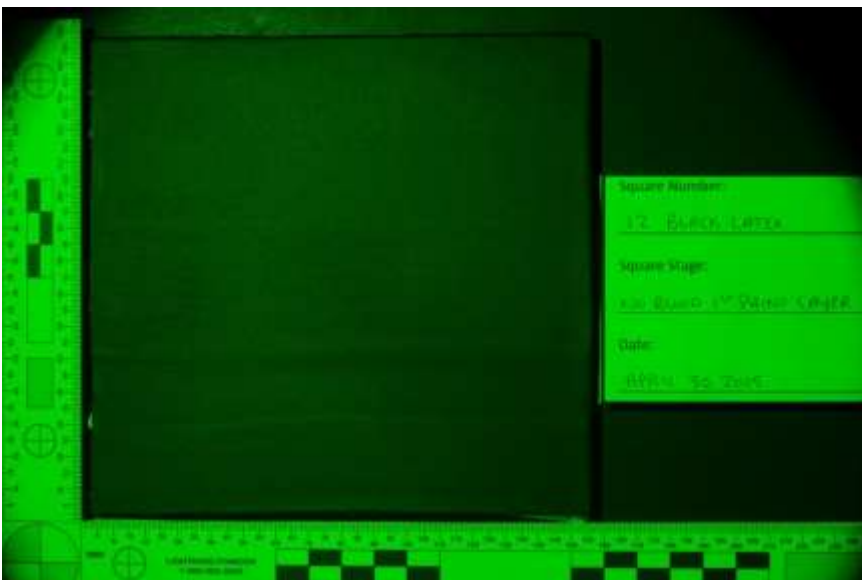
Yellow 475nm HDR



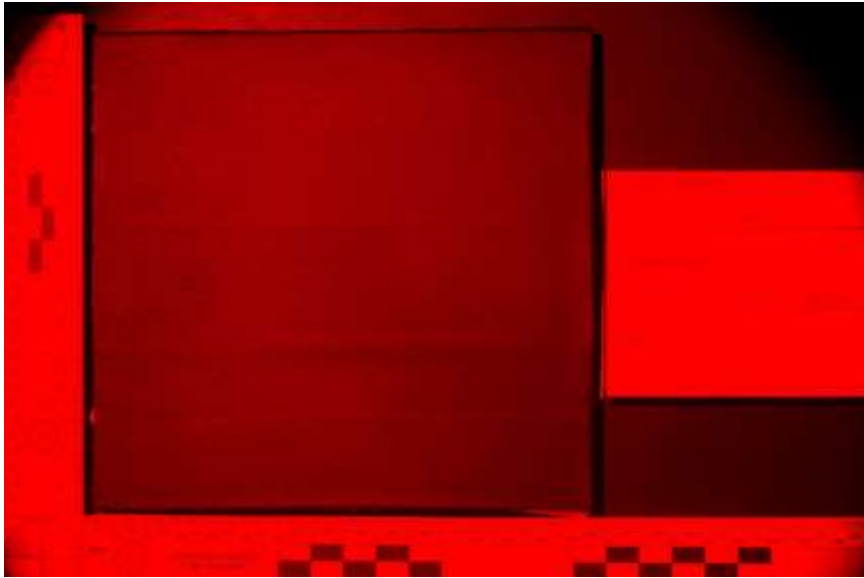
Yellow 495nm HDR



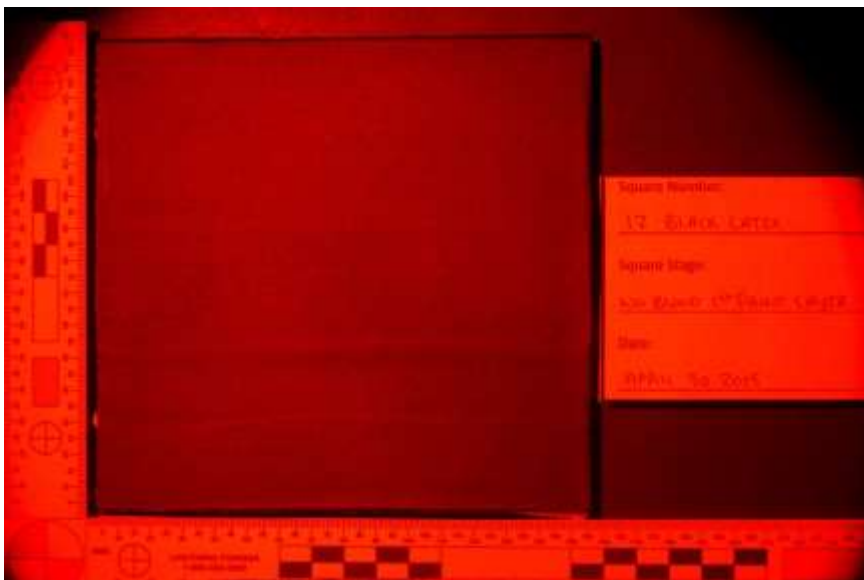
Yellow 670nm HDR



Orange 555nm HDR

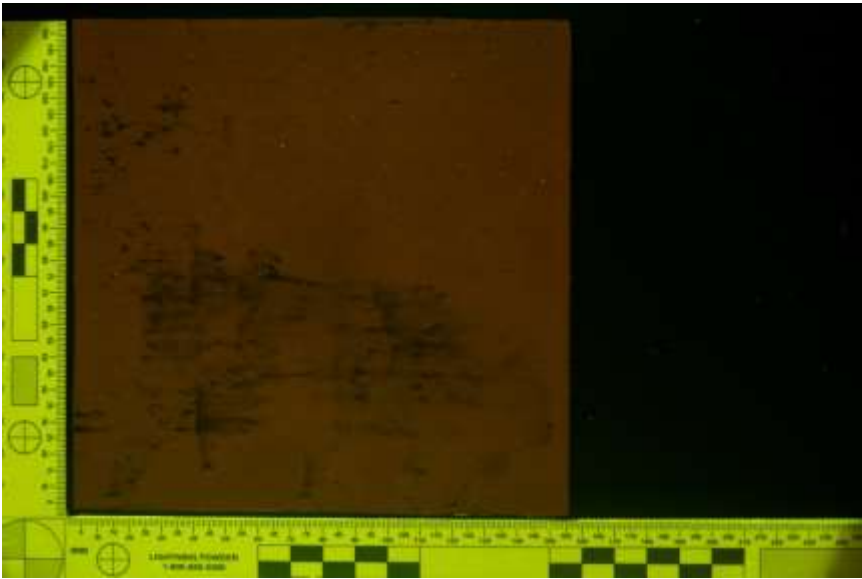


Orange 670nm HDR

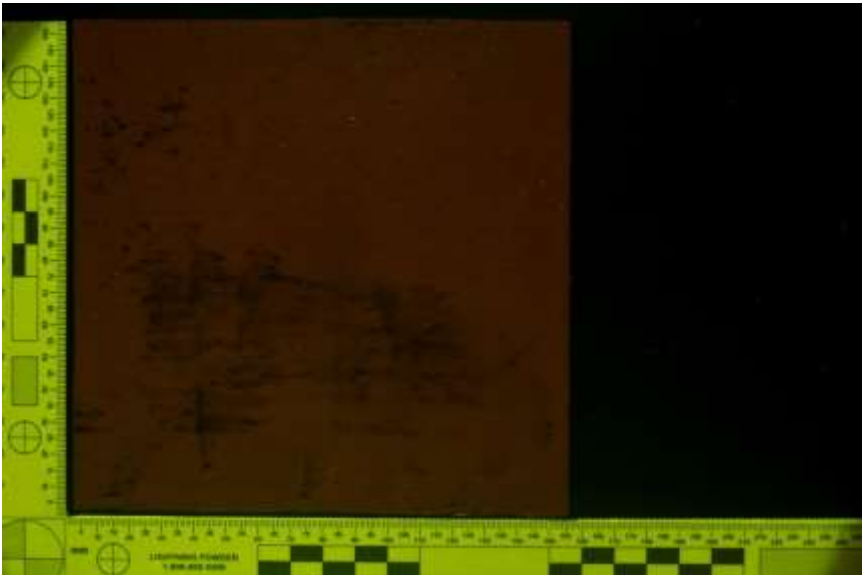


Red 600nm HDR

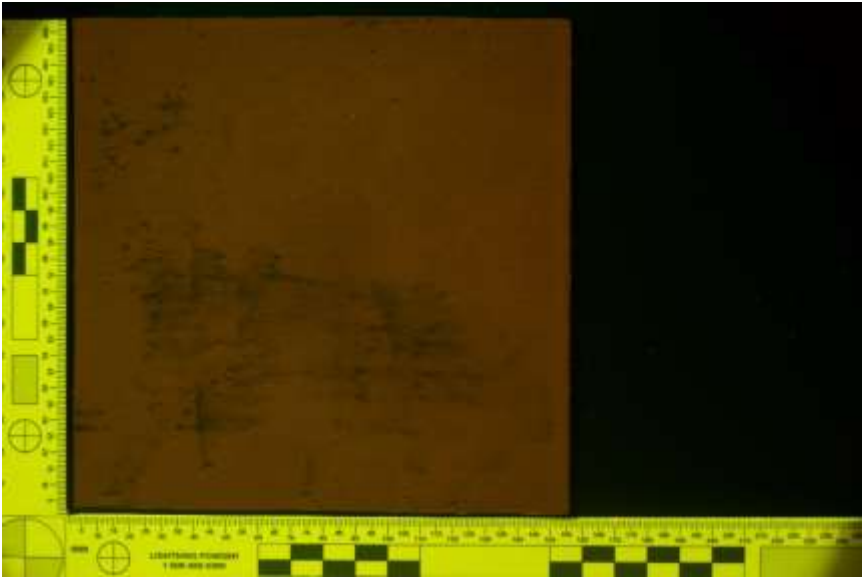
Appendix 4.2.5.4. Maroon Latex – Yellow 415nm, 445nm, 455nm; Orange 415nm, 445nm; Red 415nm, 445nm, 455nm, 575nm First layer of paint stage
Maroon Latex 13 – Medium Velocity



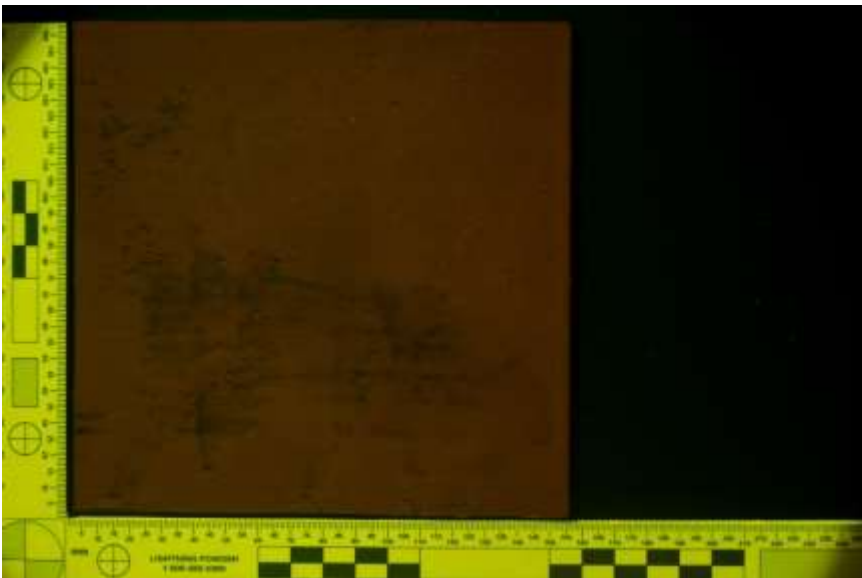
Yellow 415nm HDR



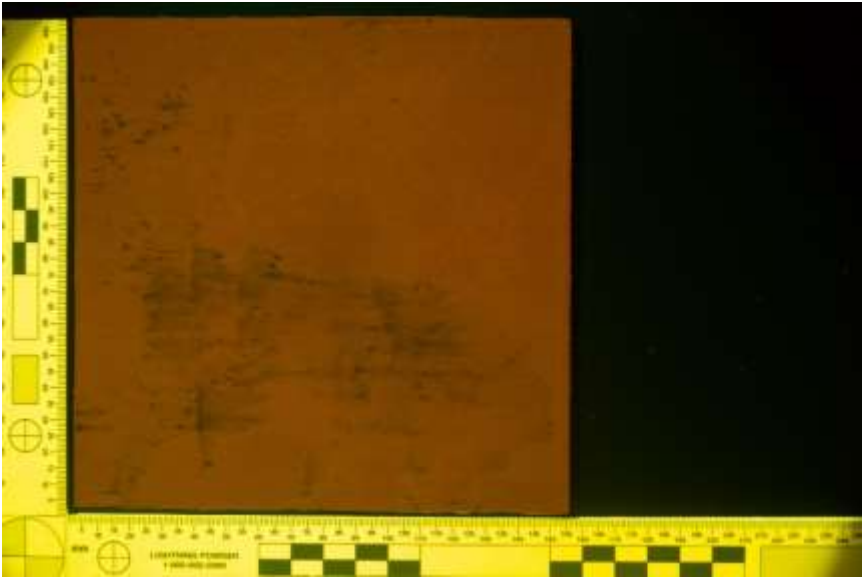
Yellow 415nm Single



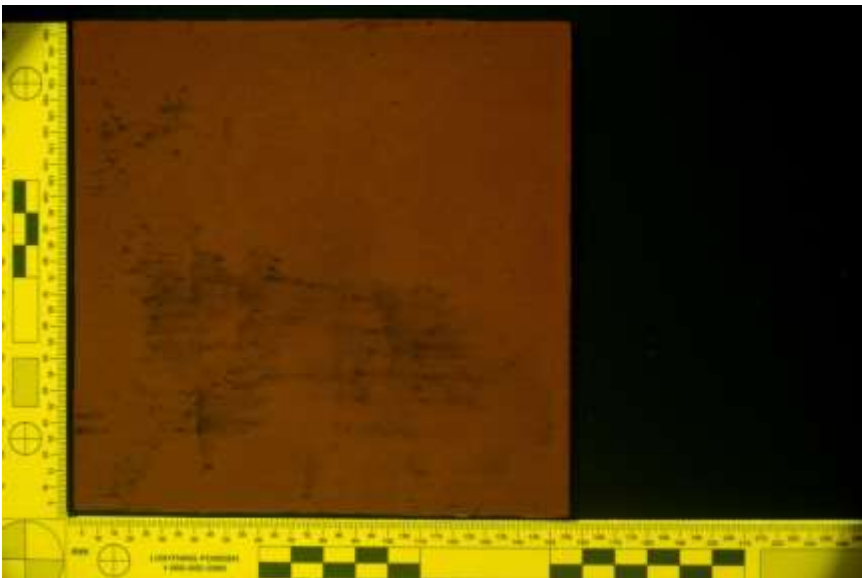
Yellow 445nm HDR



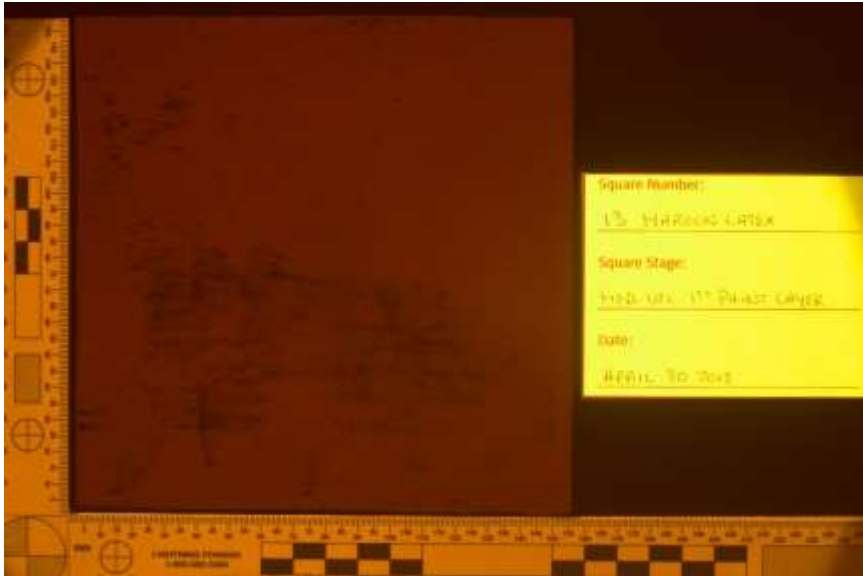
Yellow 445nm Single



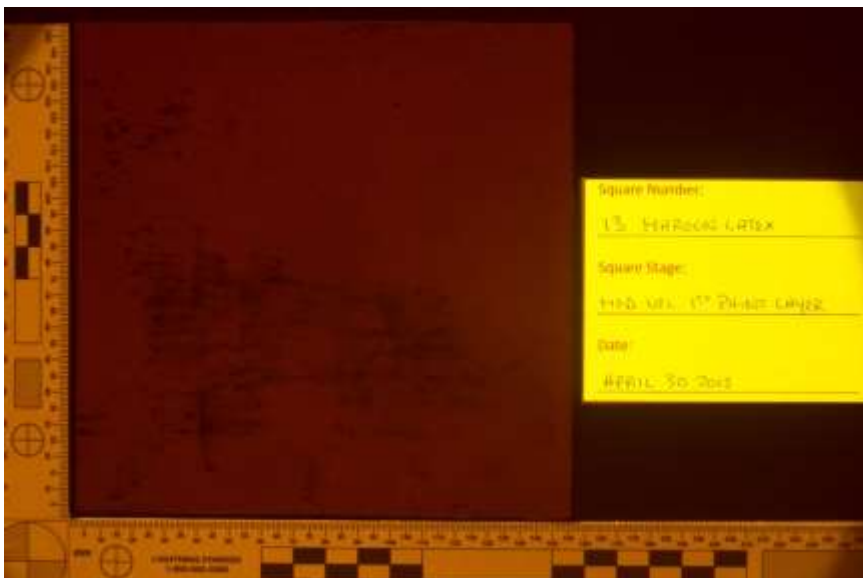
Yellow 455nm HDR



Yellow 455nm Single



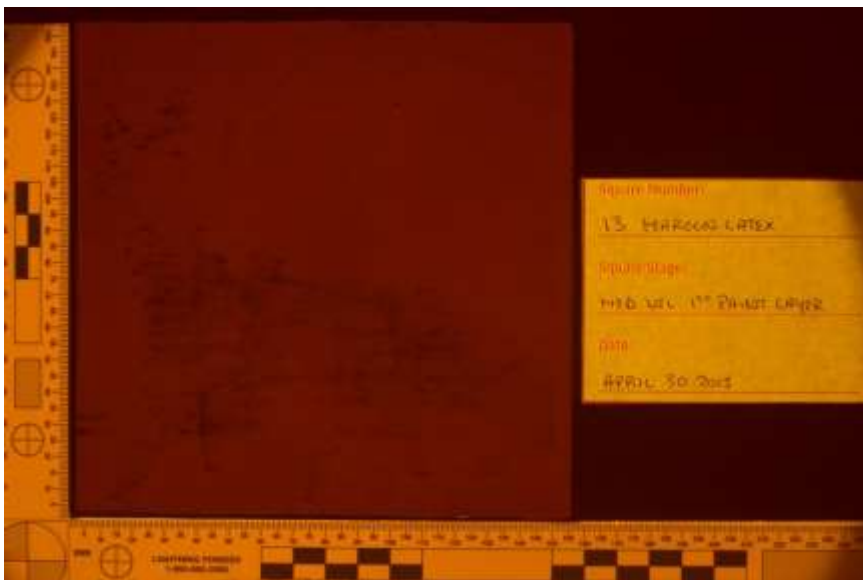
Orange 415nm HDR



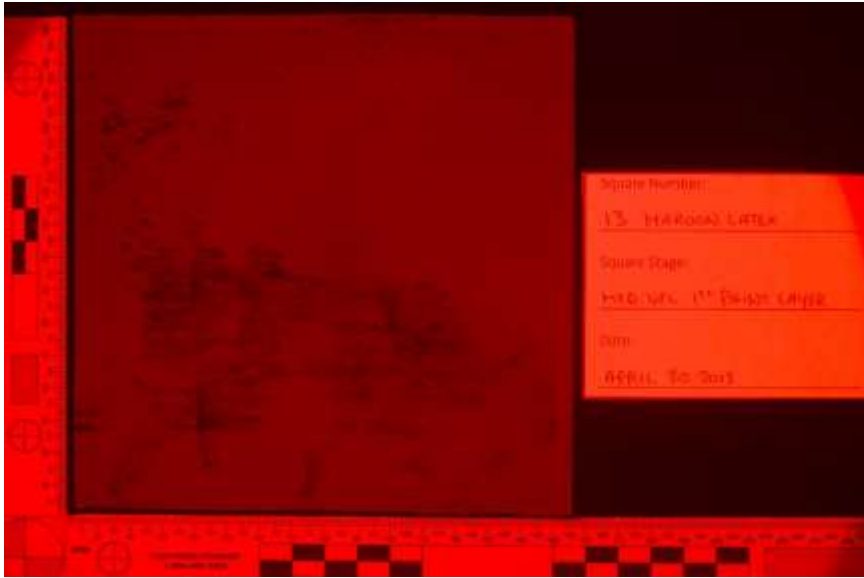
Orange 415nm Single



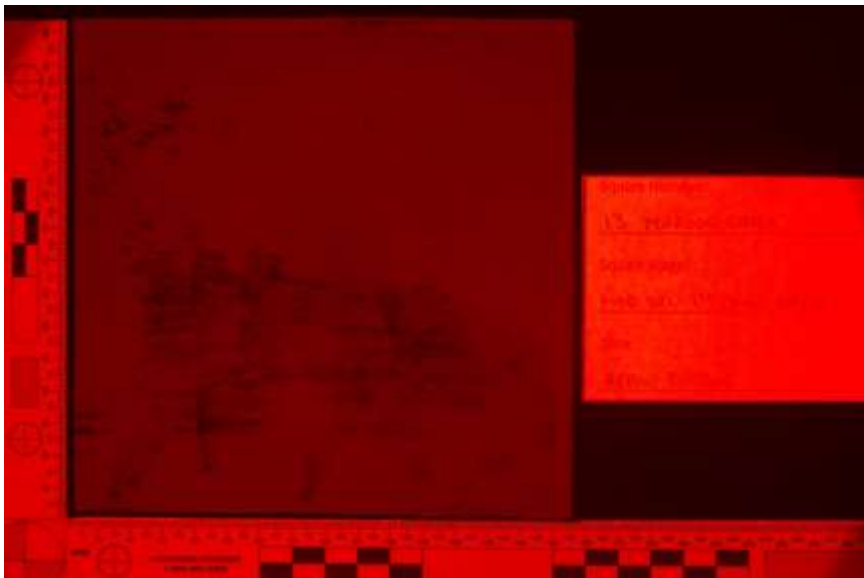
Orange 445nm HDR



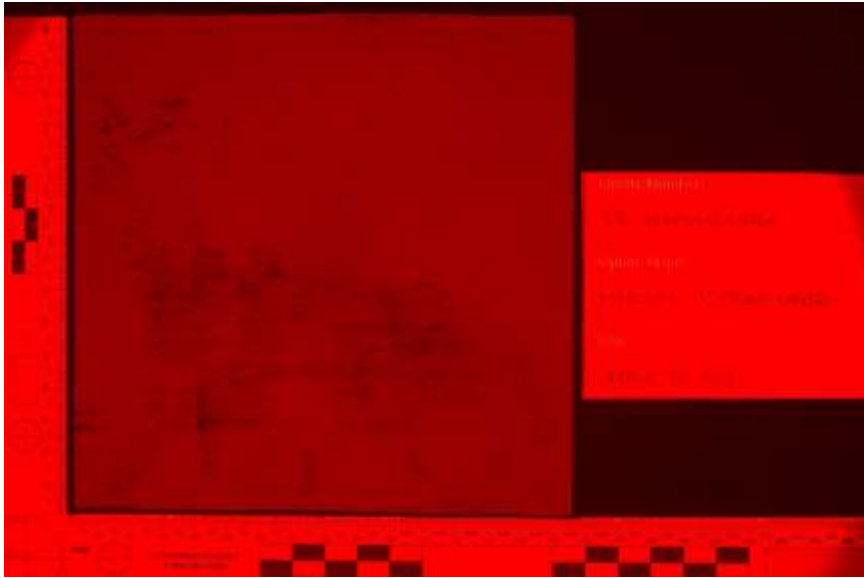
Orange 445nm Single



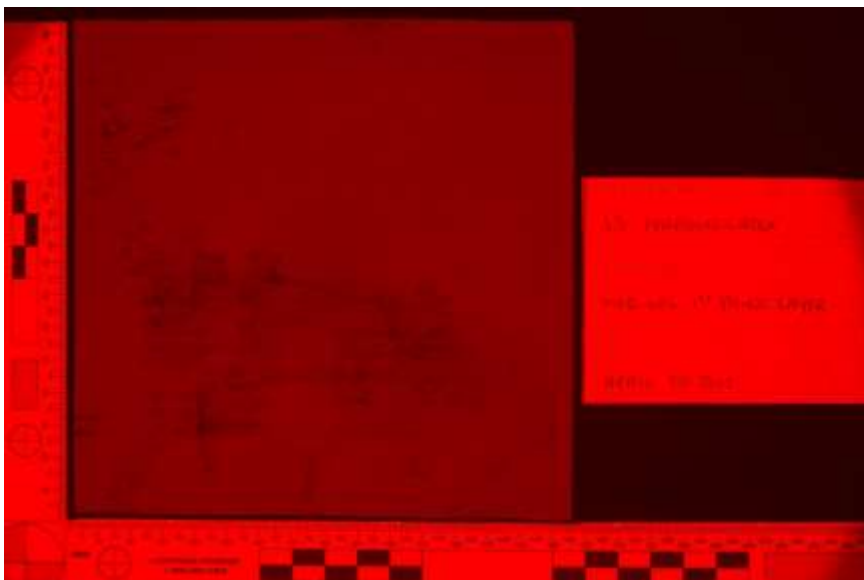
Red 415nm HDR



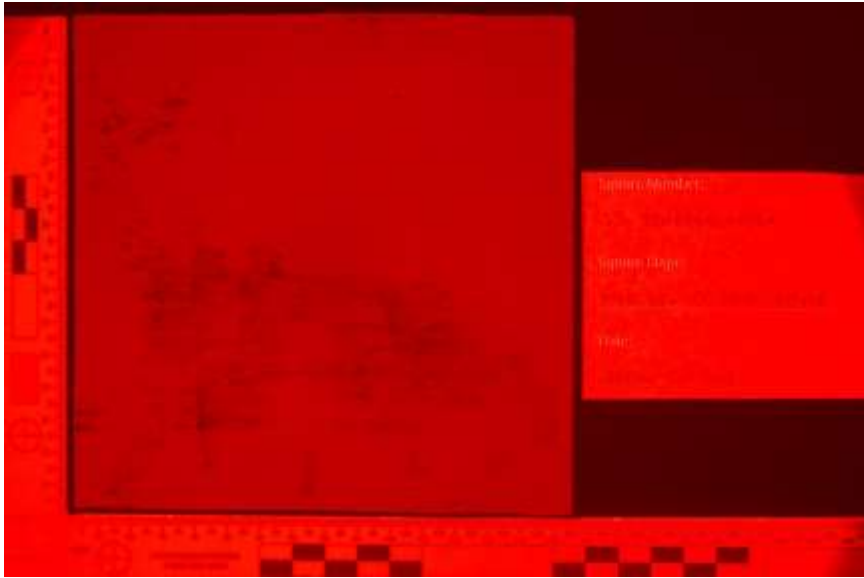
Red 415nm Single



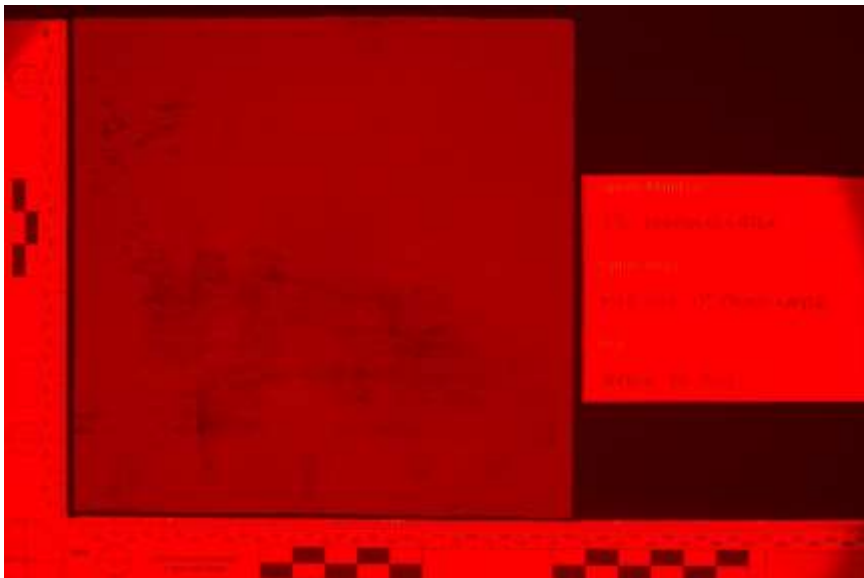
Red 445nm HDR



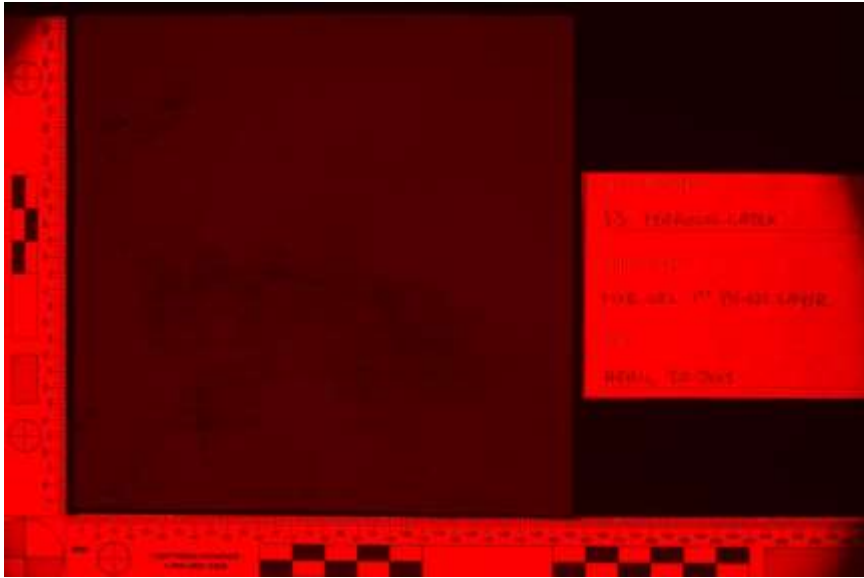
Red 445nm Single



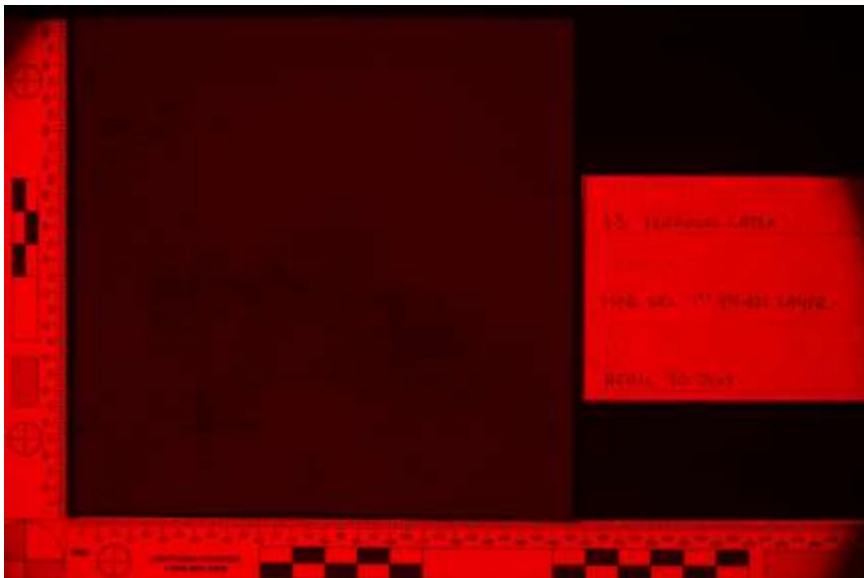
Red 455nm HDR



Red 455nm Single

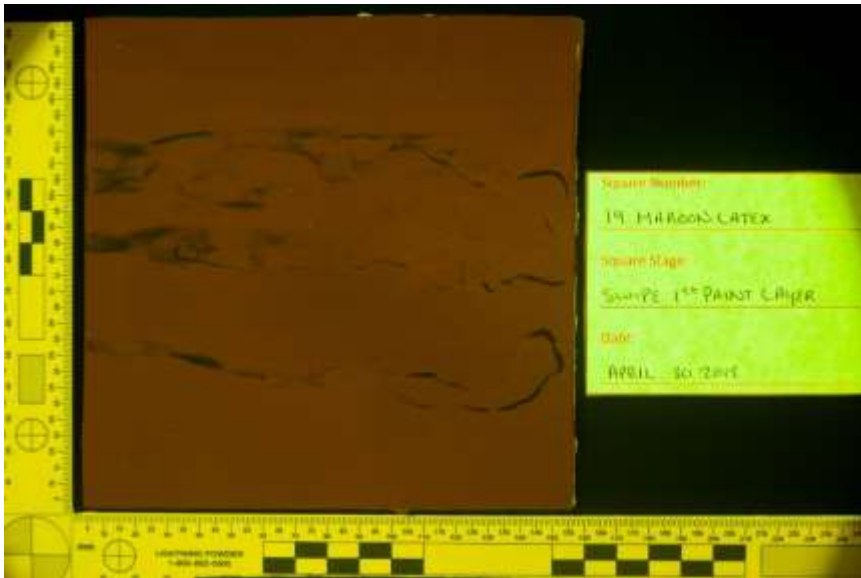


Red 575nm HDR



Red 575nm Single

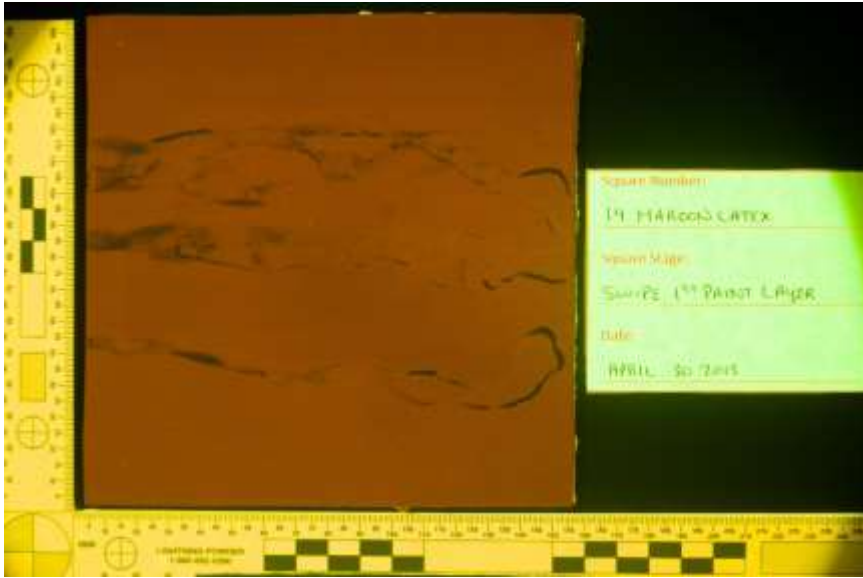
Maroon Latex 14 – Swipe



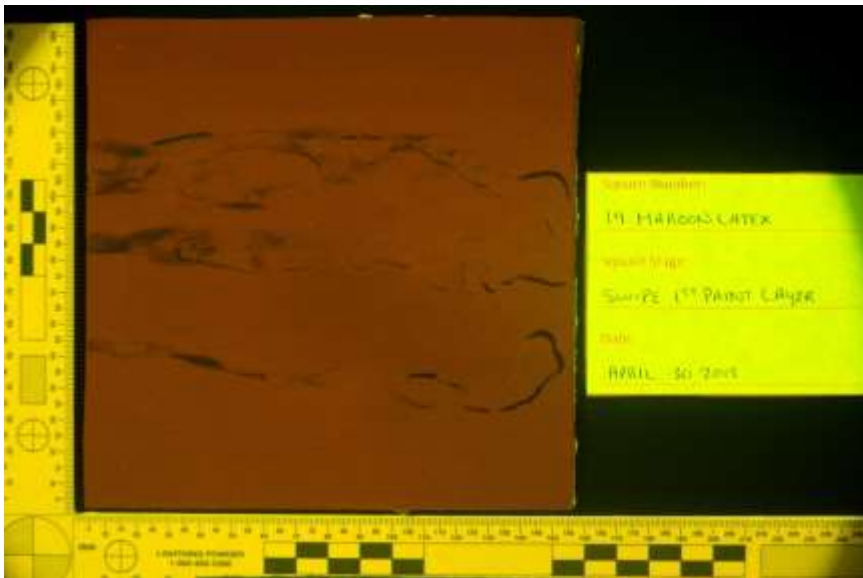
Yellow 415nm HDR



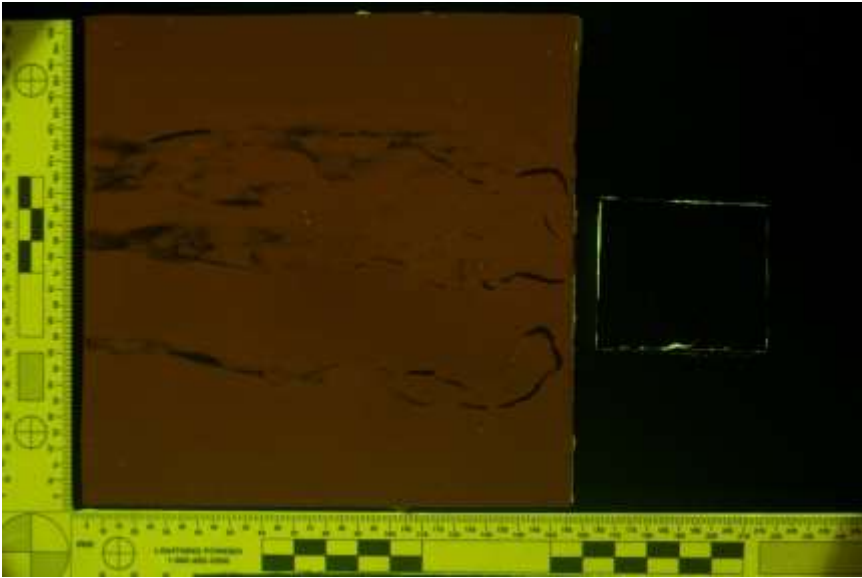
Yellow 415nm Single



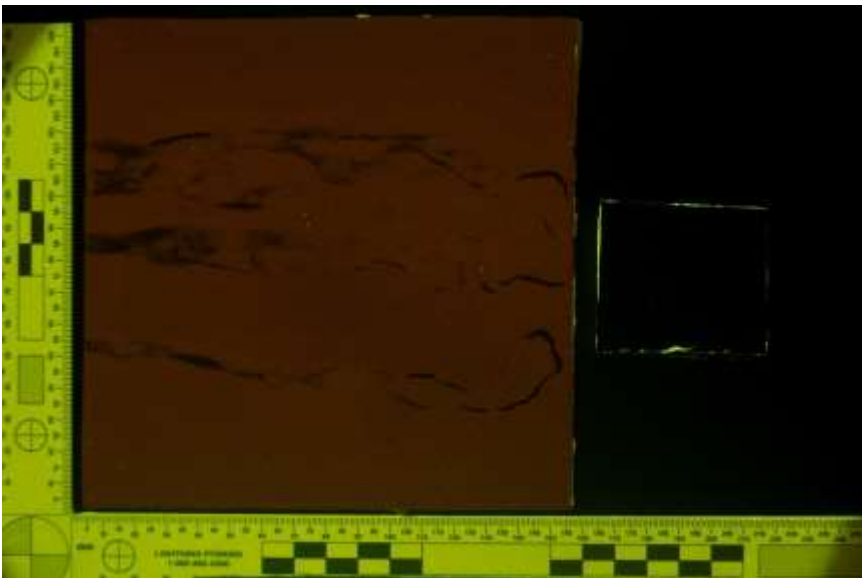
Yellow 445nm HDR



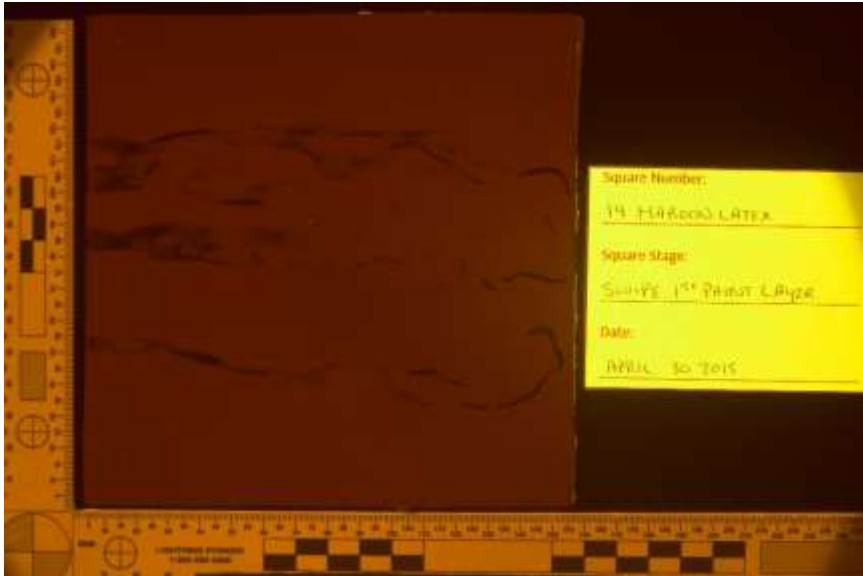
Yellow 445nm Single



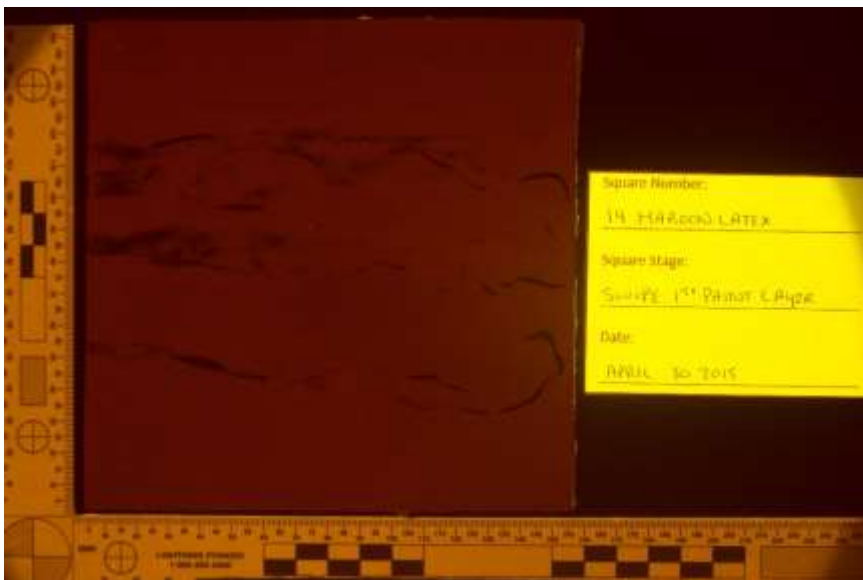
Yellow 455nm HDR



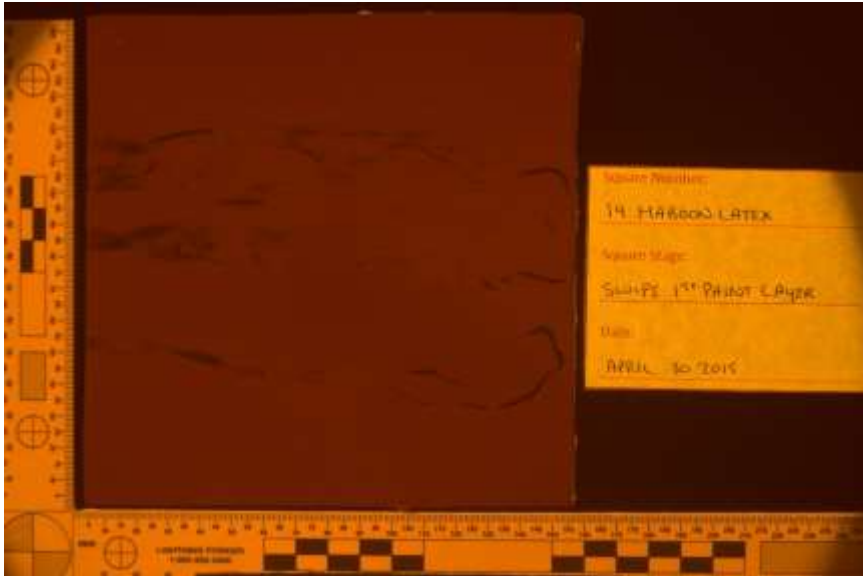
Yellow 455nm Single



Orange 415nm HDR



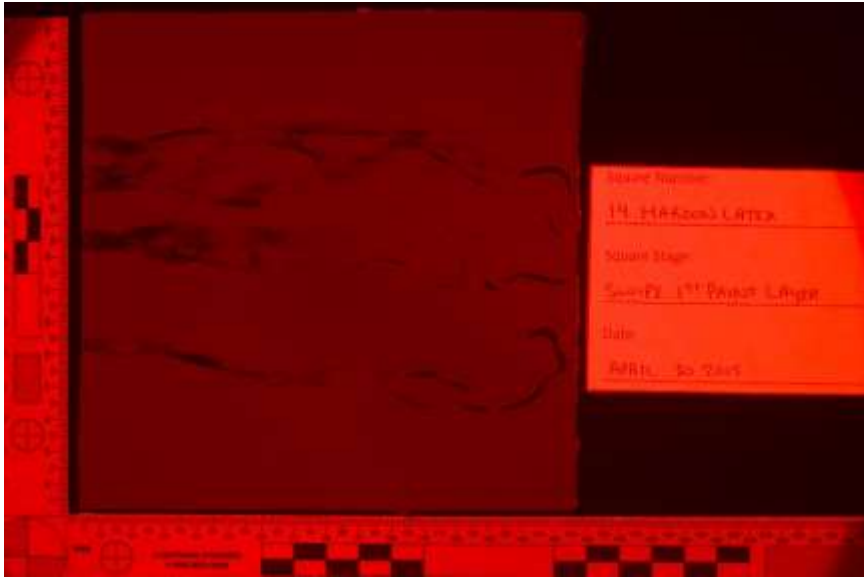
Orange 415nm Single



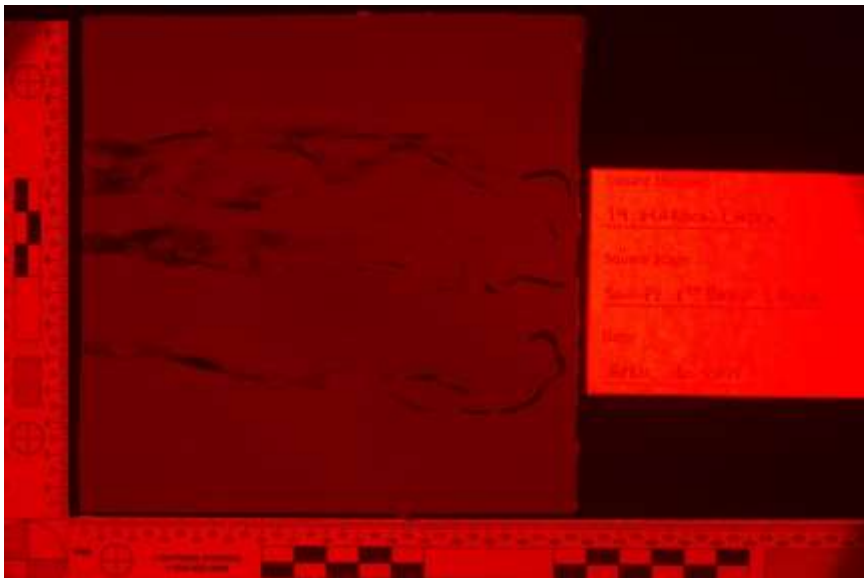
Orange 445nm HDR



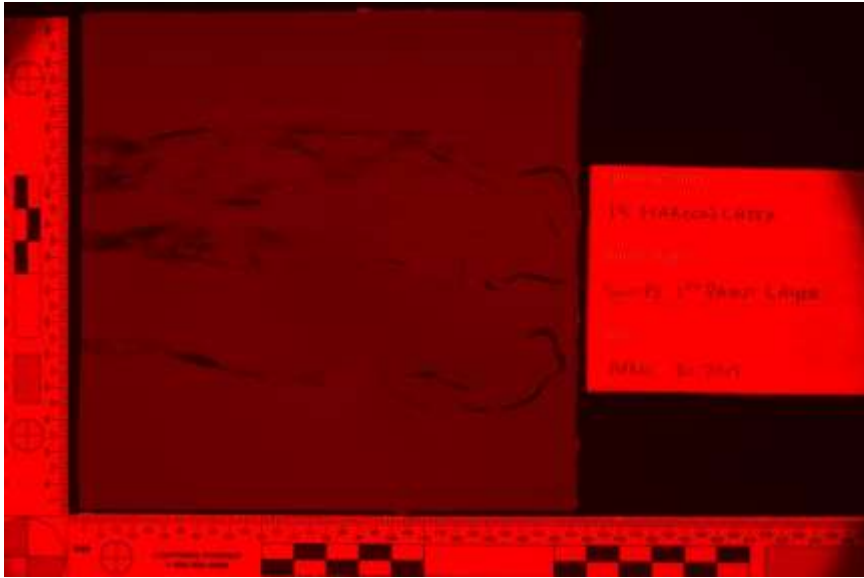
Orange 445nm Single



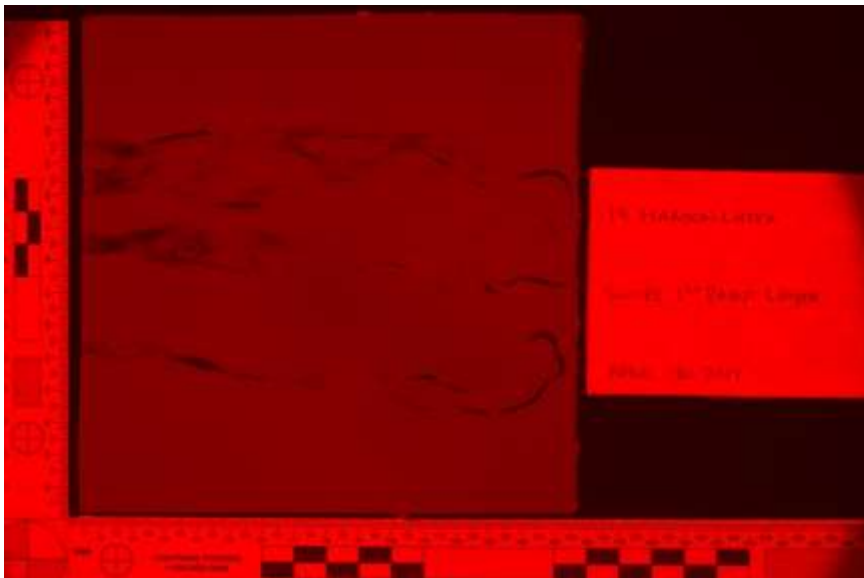
Red 415nm HDR



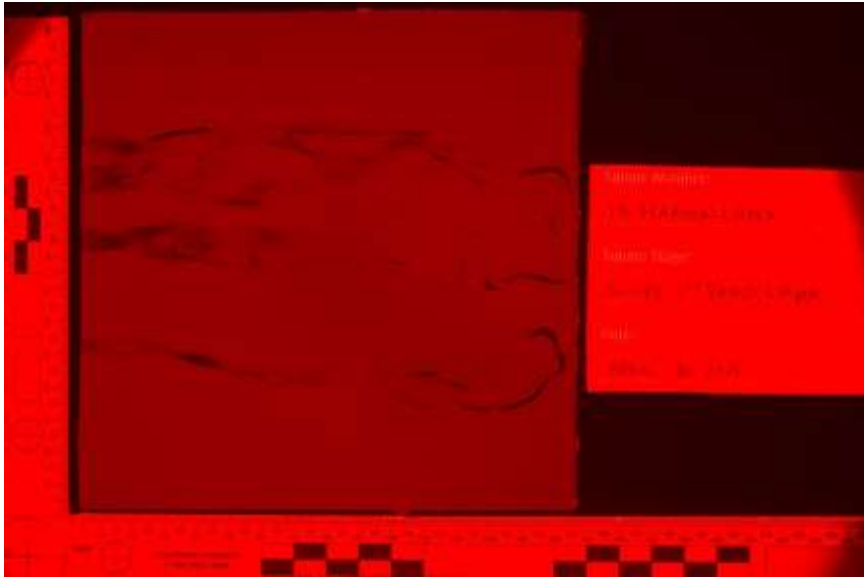
Red 415nm Single



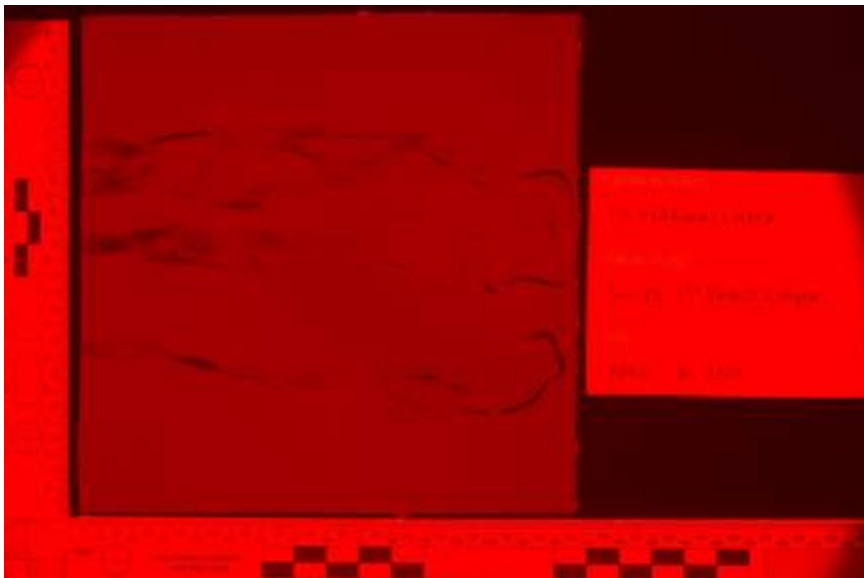
Red 445nm HDR



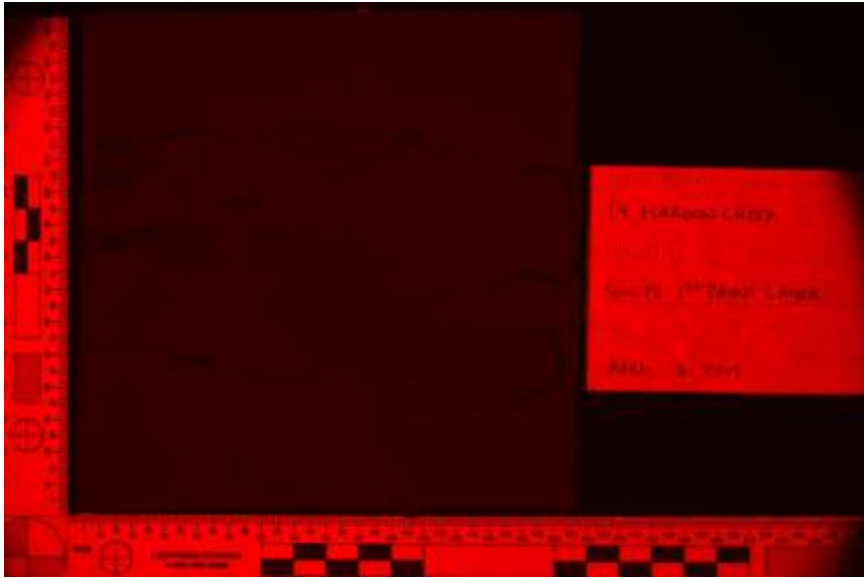
Red 445nm Single



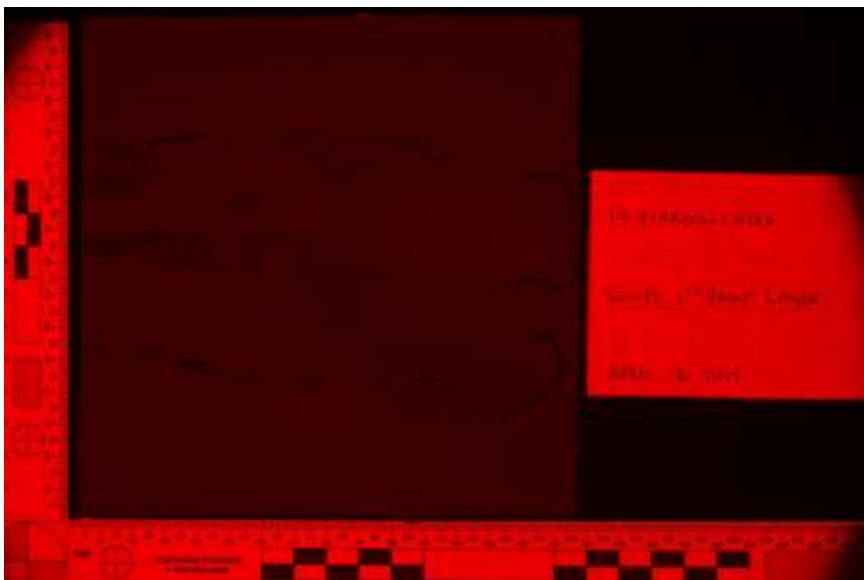
Red 455nm HDR



Red 455nm Single

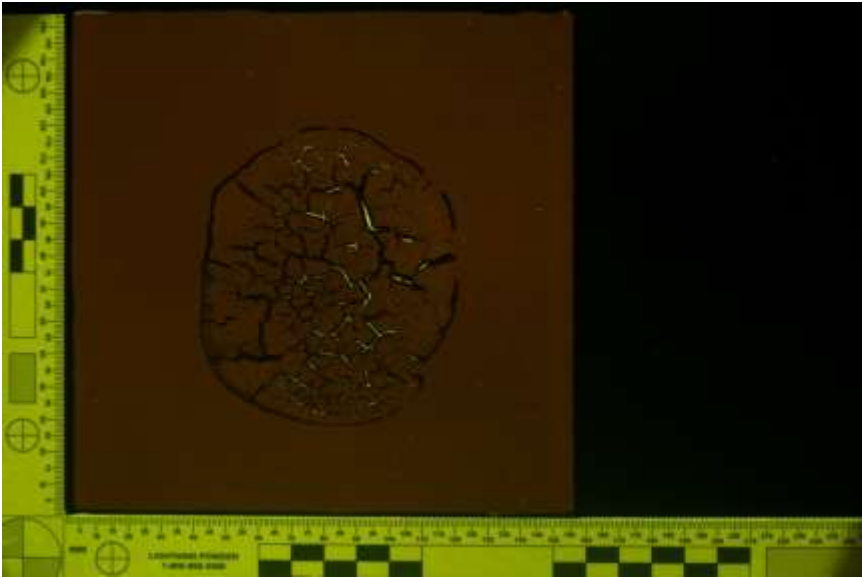


Red 575nm HDR

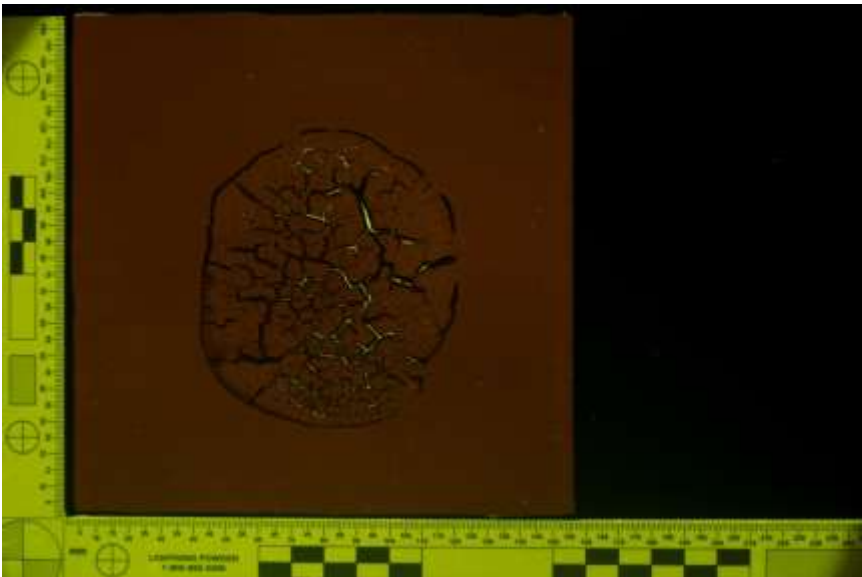


Red 575nm Single

Maroon Latex 15 – Saturated



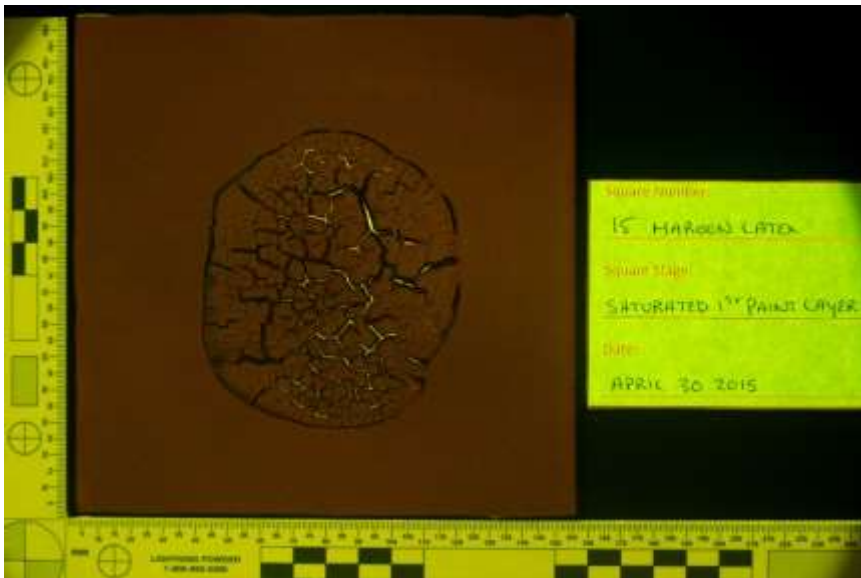
Yellow 415nm HDR



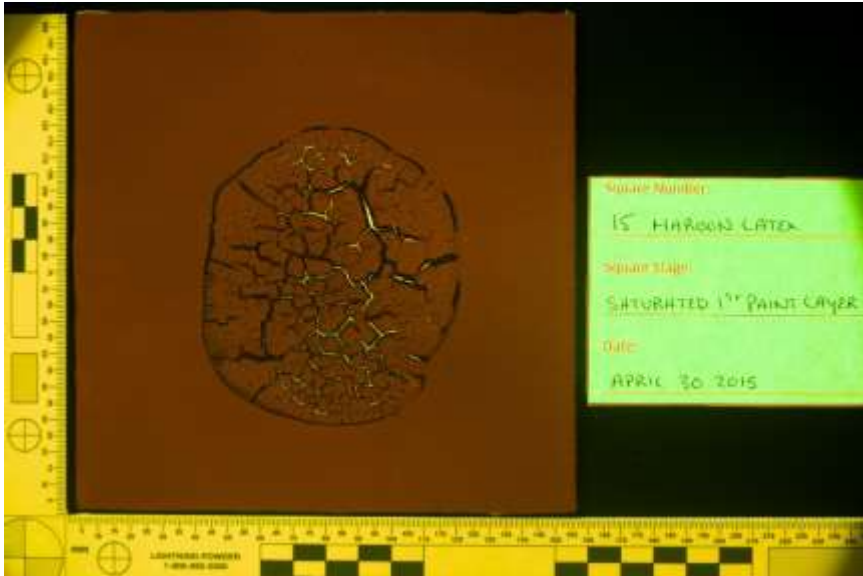
Yellow 415nm Single



Yellow 445nm HDR



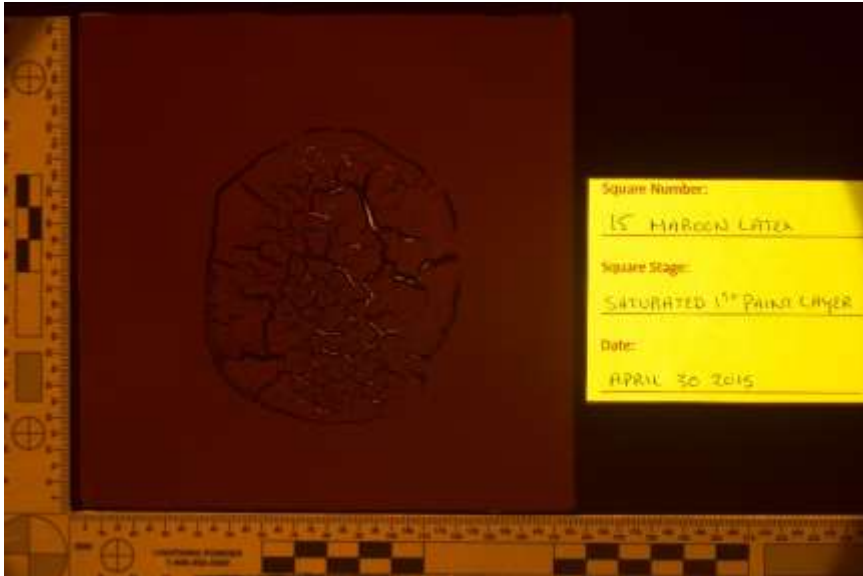
Yellow 445nm Single



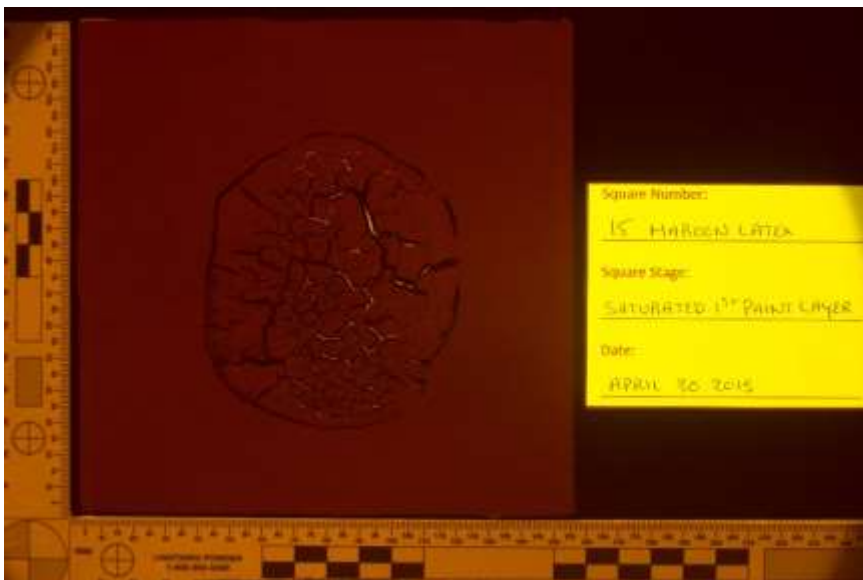
Yellow 455nm HDR



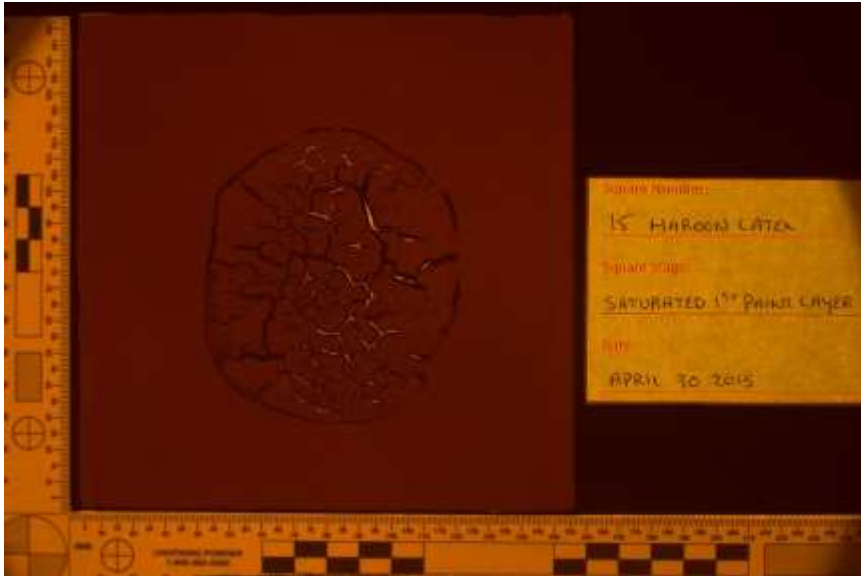
Yellow 455nm Single



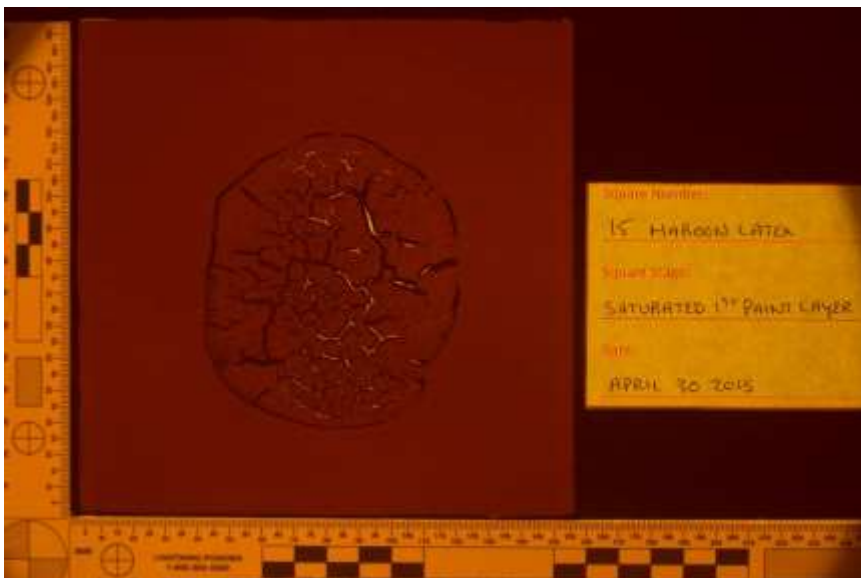
Orange 415nm HDR



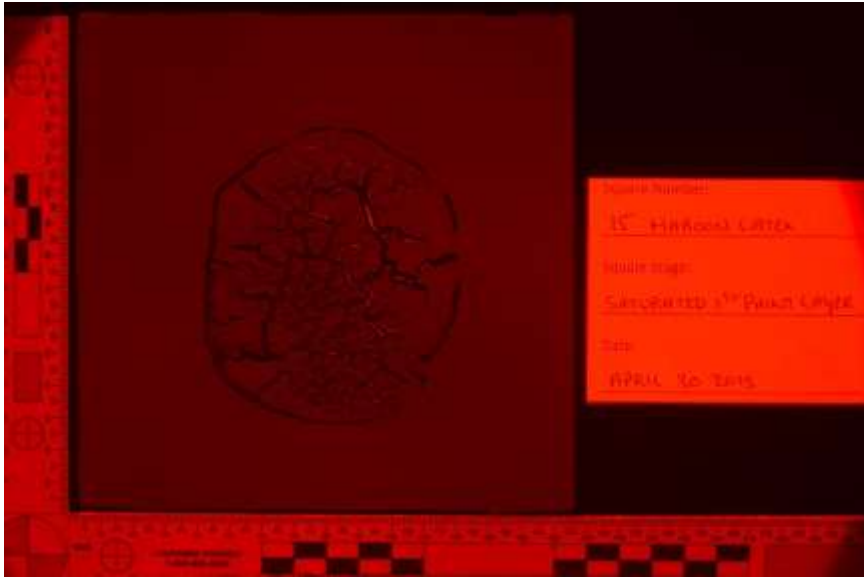
Orange 415nm Single



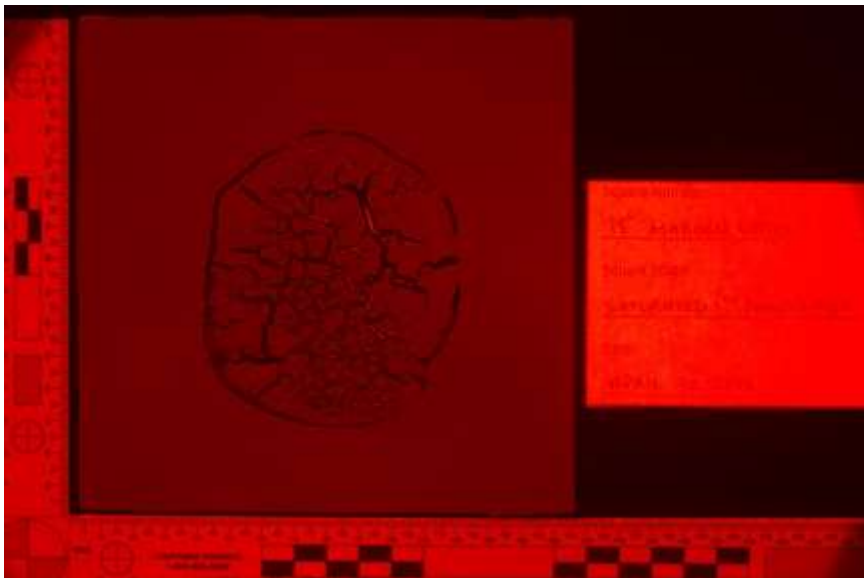
Orange 445nm HDR



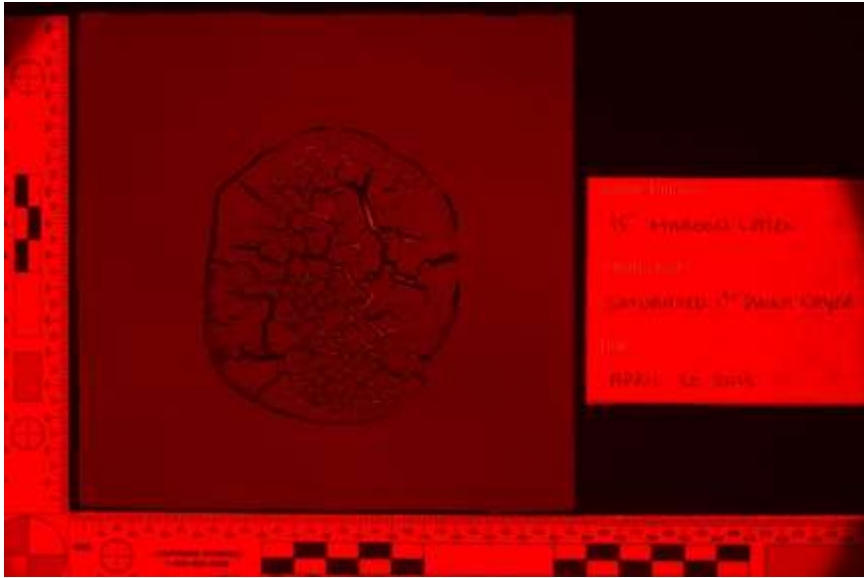
Orange 445nm Single



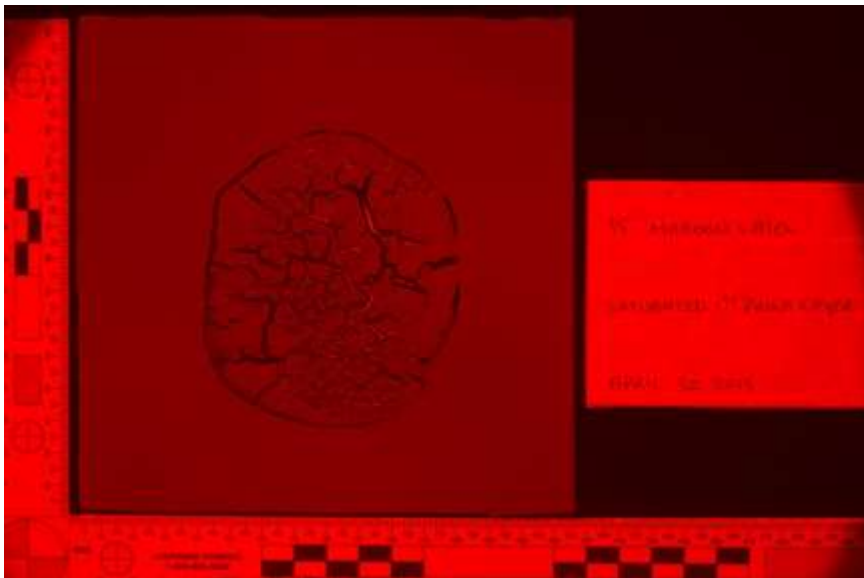
Red 415nm HDR



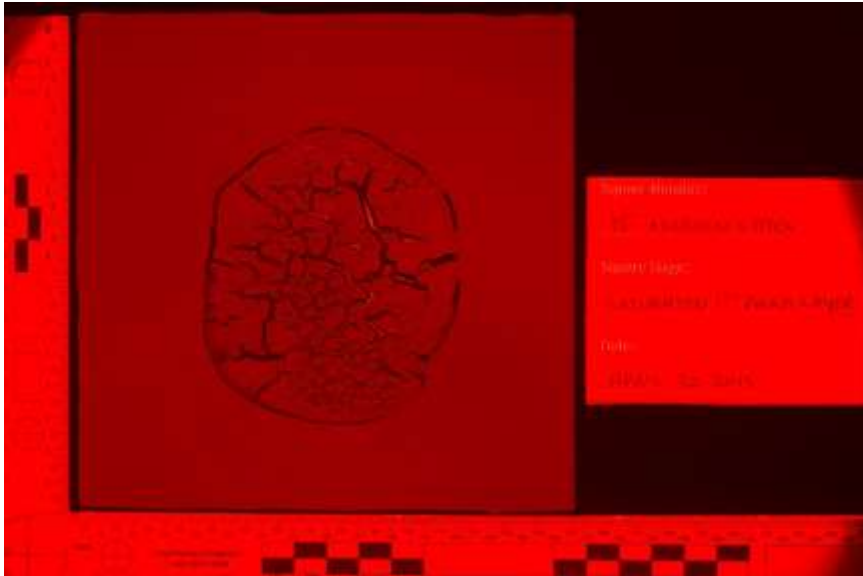
Red 415nm Single



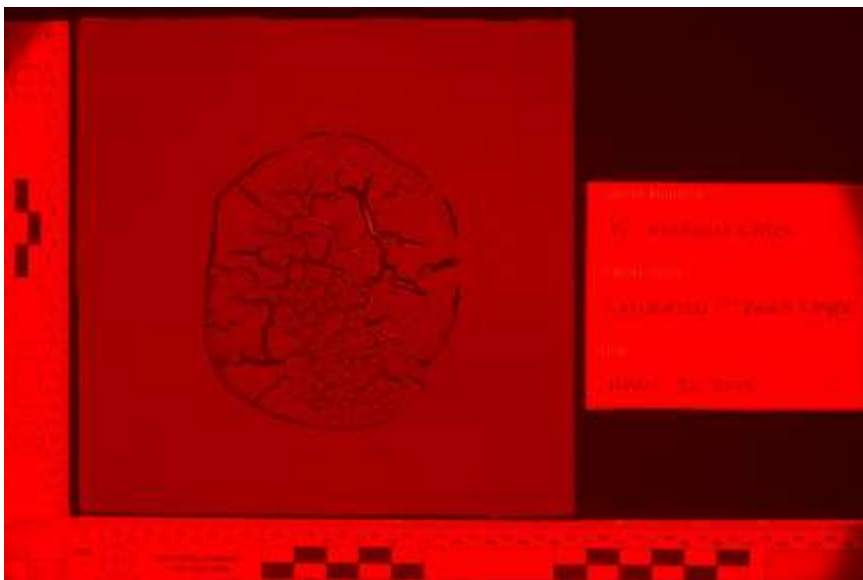
Red 445nm HDR



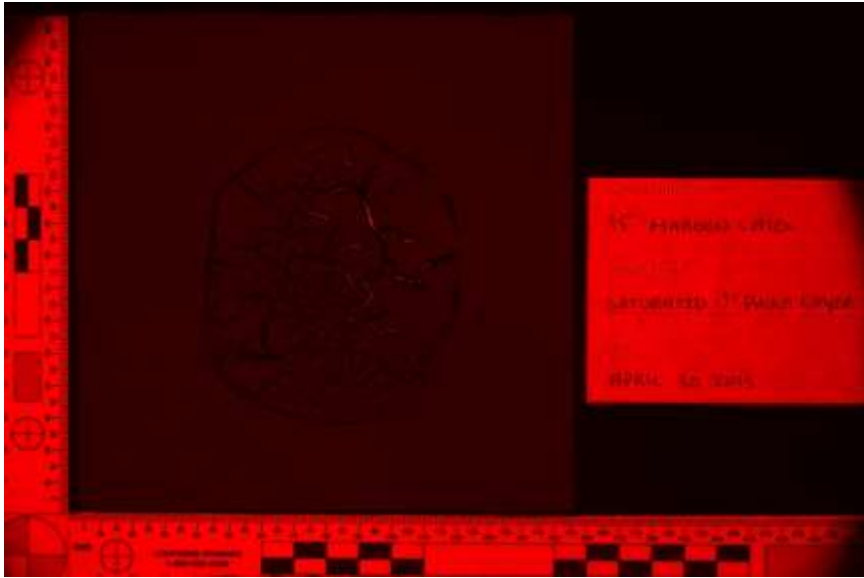
Red 445nm Single



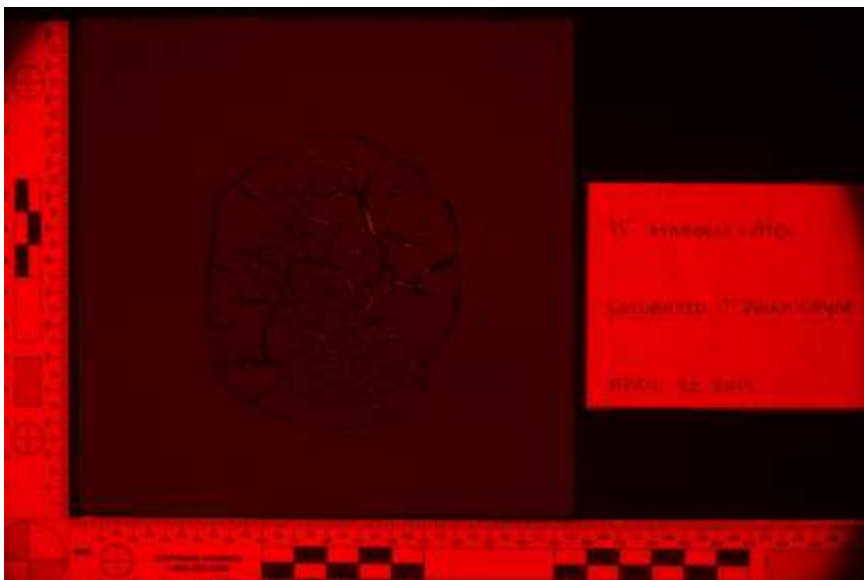
Red 455nm HDR



Red 455nm Single



Red 575nm HDR

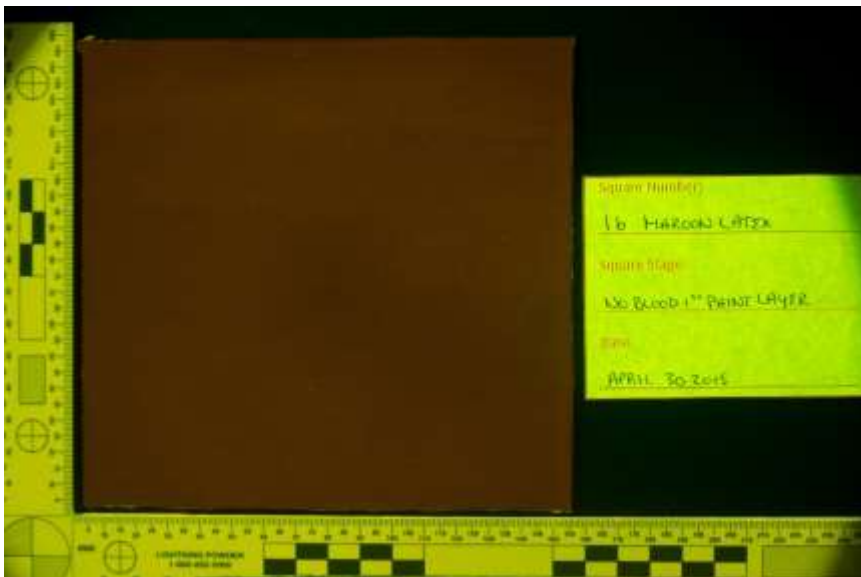


Red 575nm Single

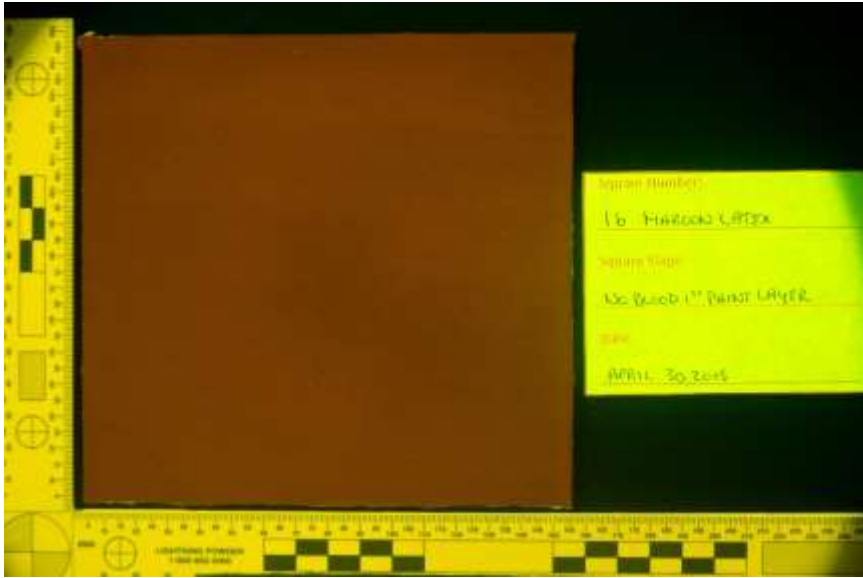
Maroon Latex 16 – Control No Bloodstain



Yellow 415nm HDR



Yellow 445nm HDR



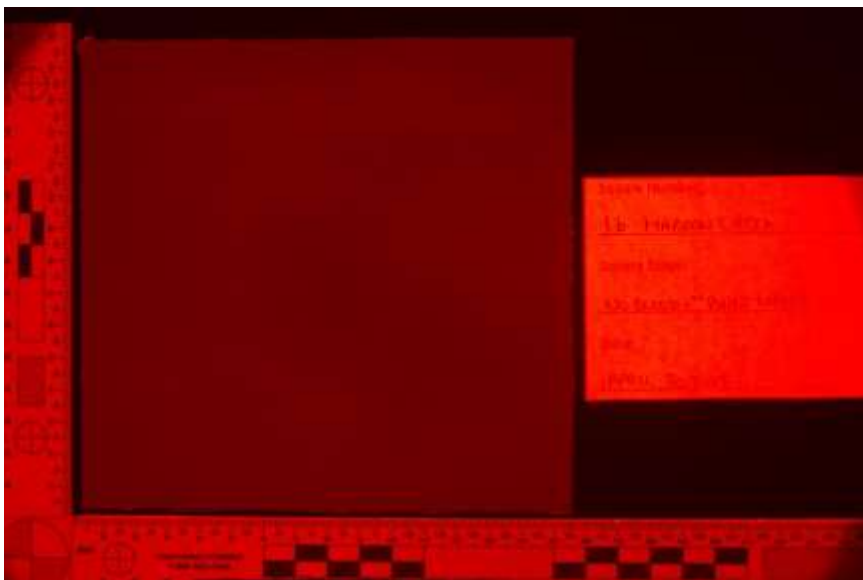
Yellow 455nm HDR



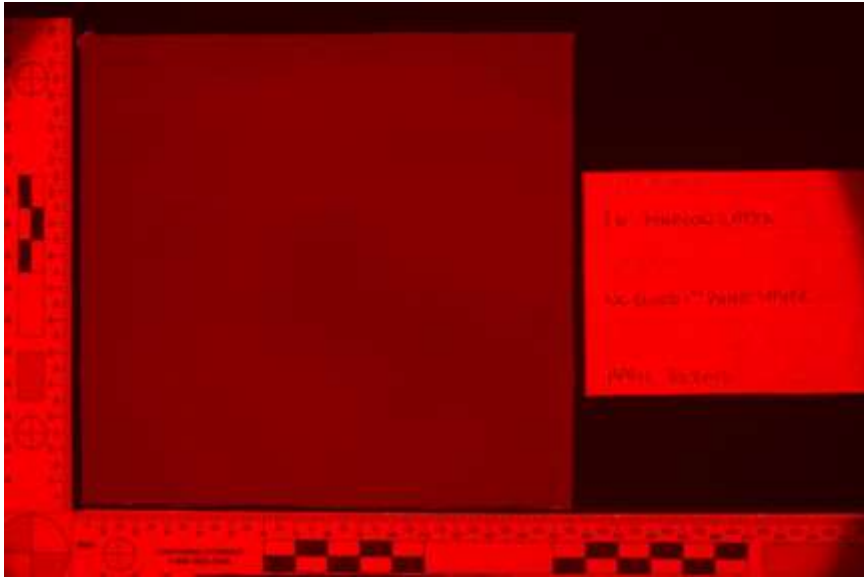
Orange 415nm HDR



Orange 445nm HDR



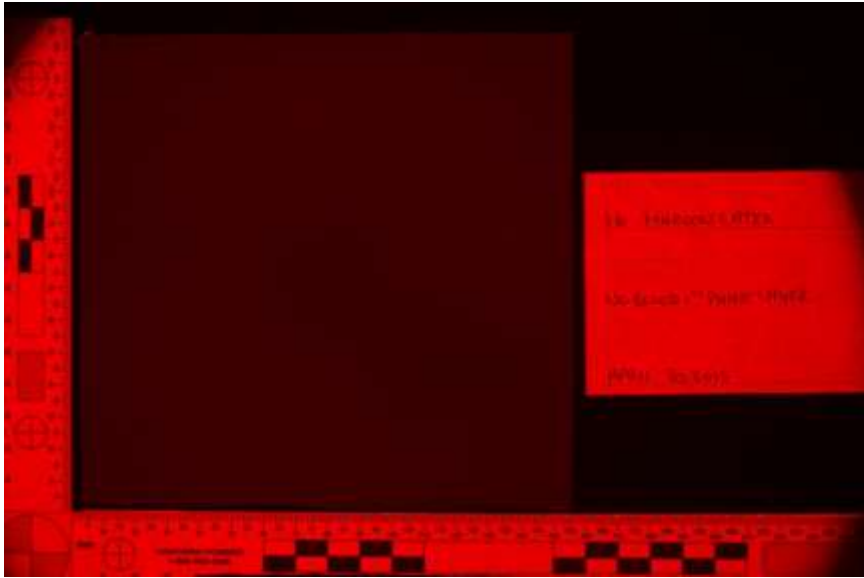
Red 415nm HDR



Red 445nm HDR



Red 455nm HDR



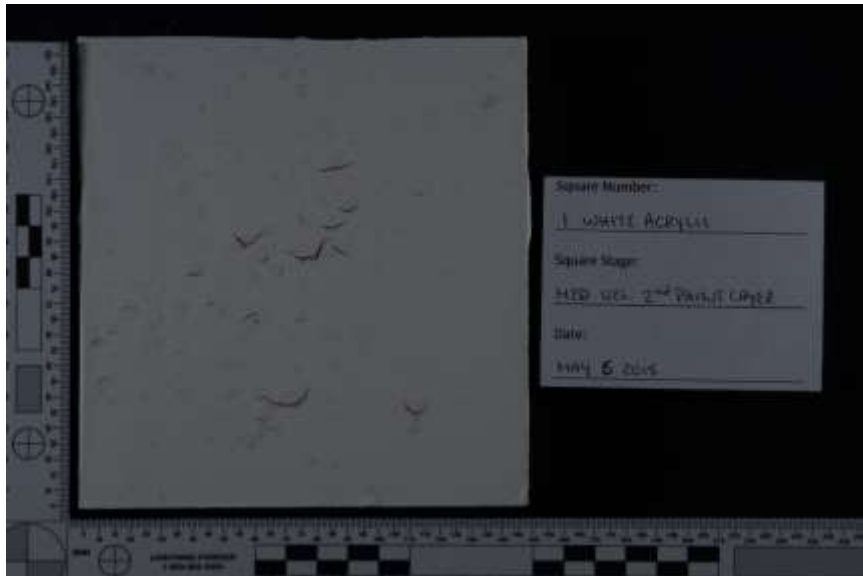
Red 575nm HDR

Second Layer of Paint over Bloodstain Patterns Stage

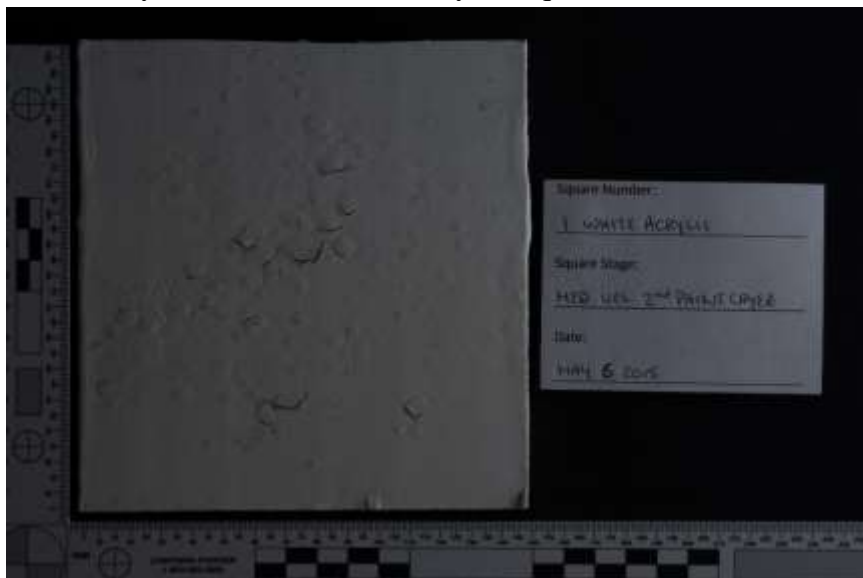
Appendix 4.3.2. Standard Photography

Appendix 4.3.2.1. White Acrylic

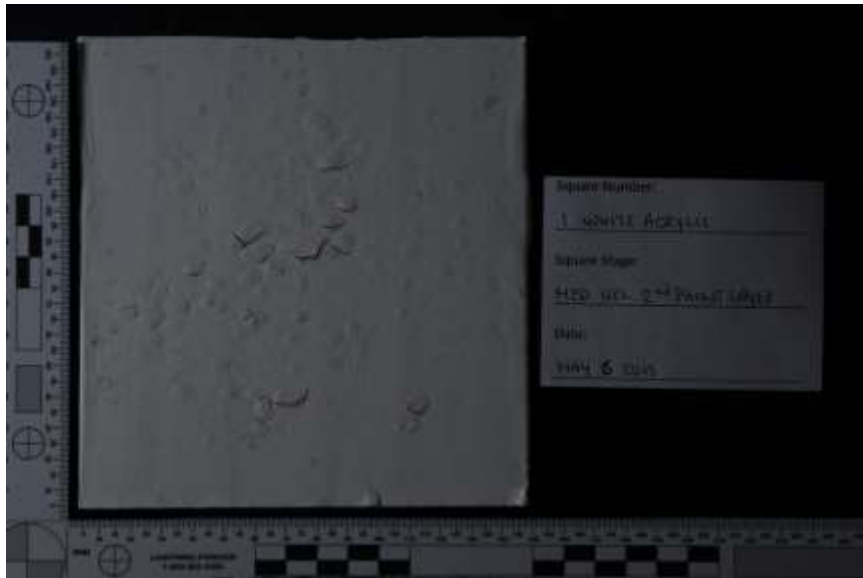
White Acrylic 1 – Medium Velocity



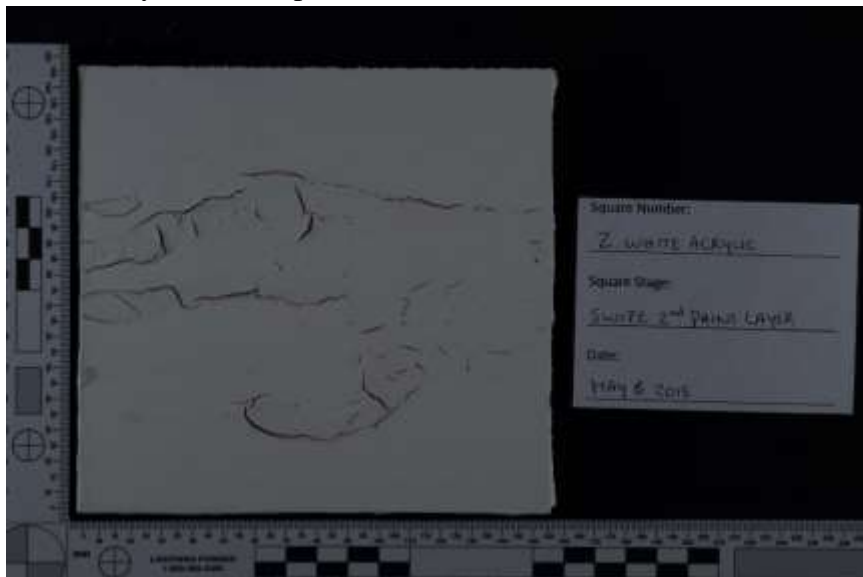
White Acrylic 1 – Medium Velocity Oblique Left



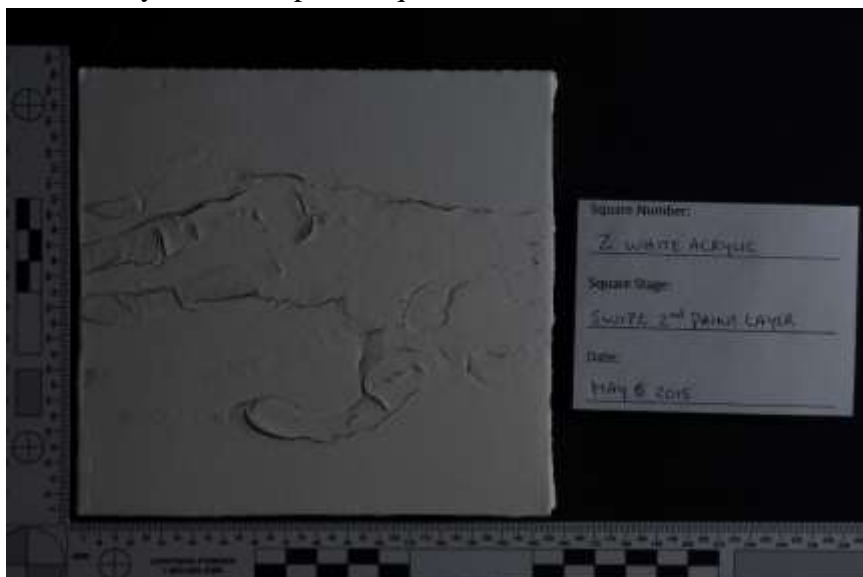
White Acrylic 1 – Medium Velocity Oblique Right



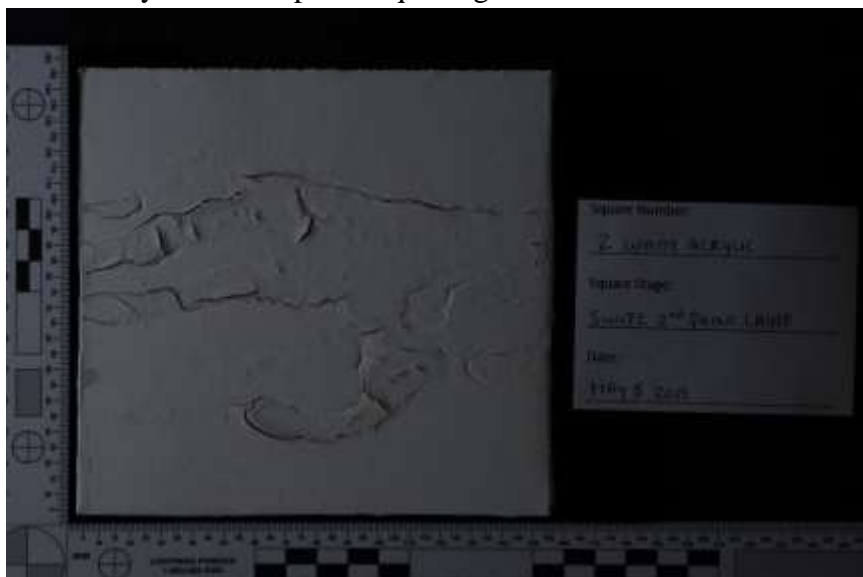
White Acrylic 2 – Swipe



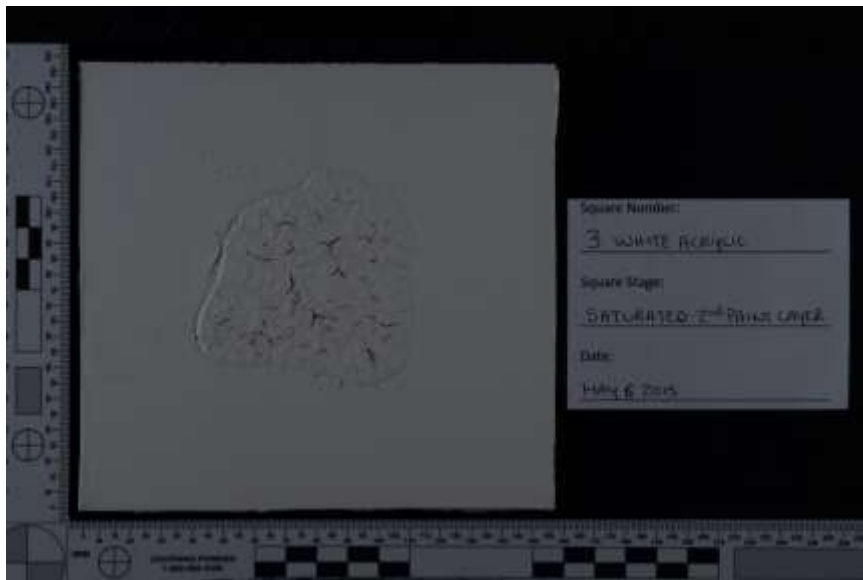
White Acrylic 2 – Swipe Oblique Left



White Acrylic 2 – Swipe Oblique Right



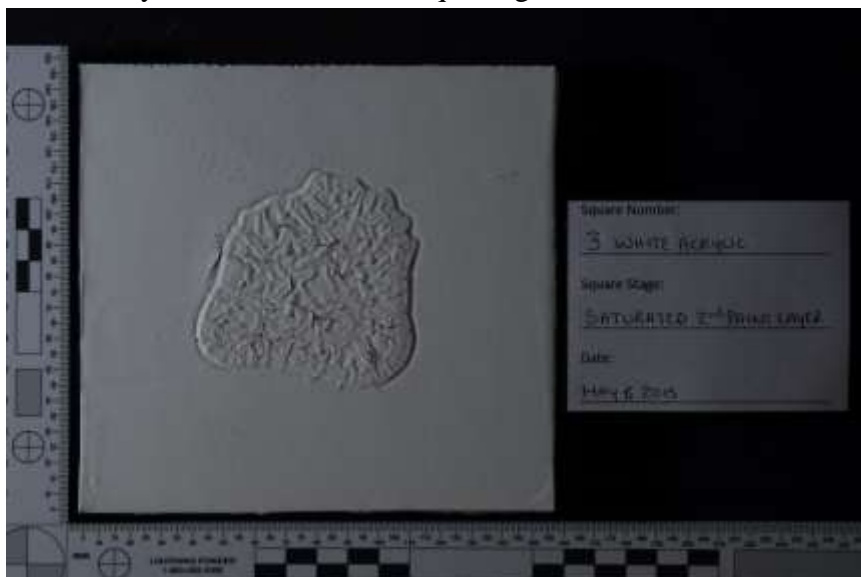
White Acrylic 3 – Saturated



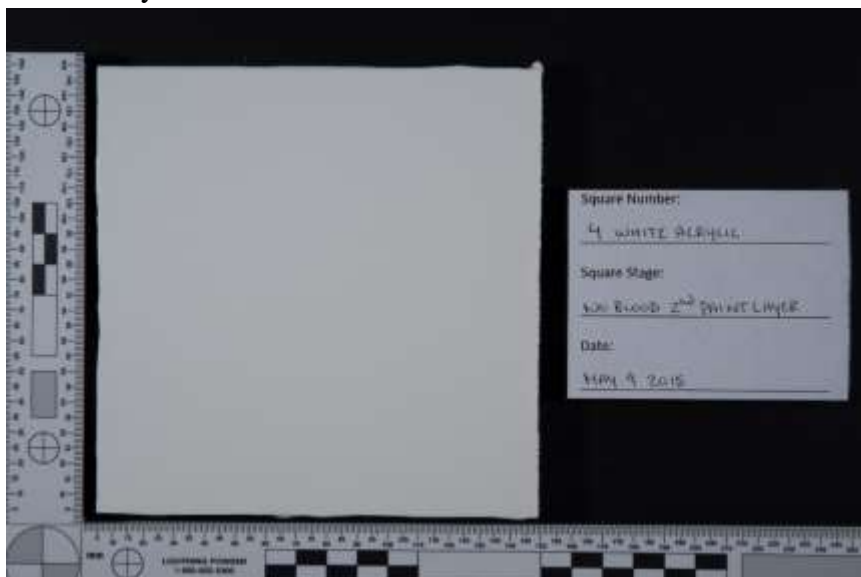
White Acrylic 3 – Saturated Oblique Left



White Acrylic 3 – Saturated Oblique Right



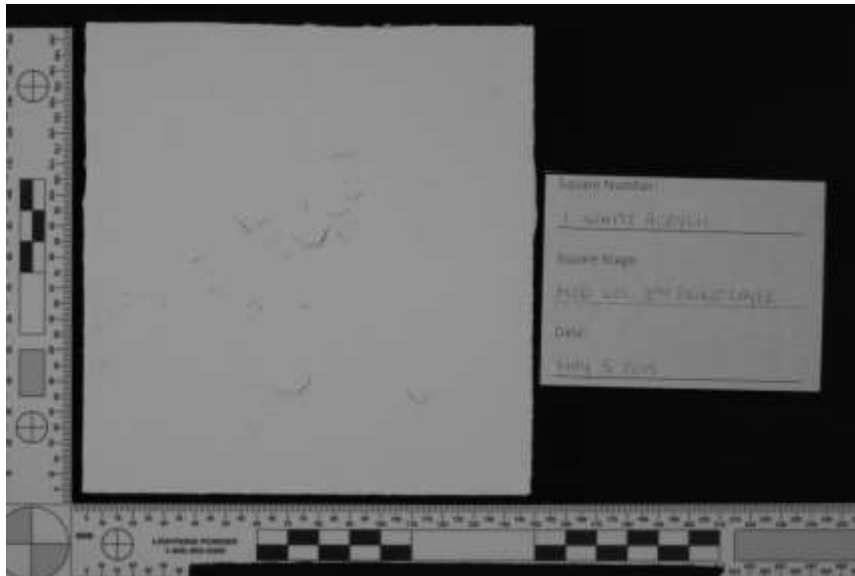
White Acrylic 4 – Control No Bloodstain



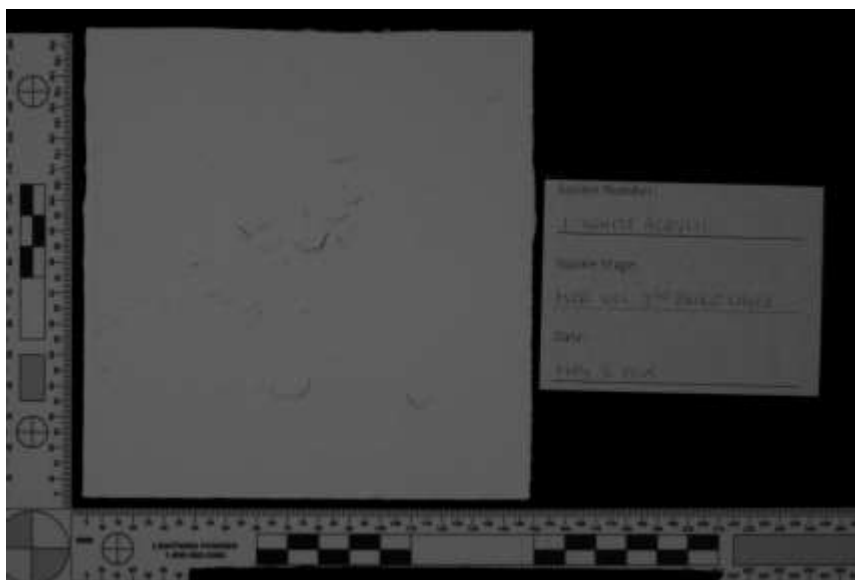
Appendix 4.3.3. Reflective Infrared Photography

Appendix 4.3.3.1. White Acrylic 87A, 87B, 88A, 89B Oblique Second layer of paint stage

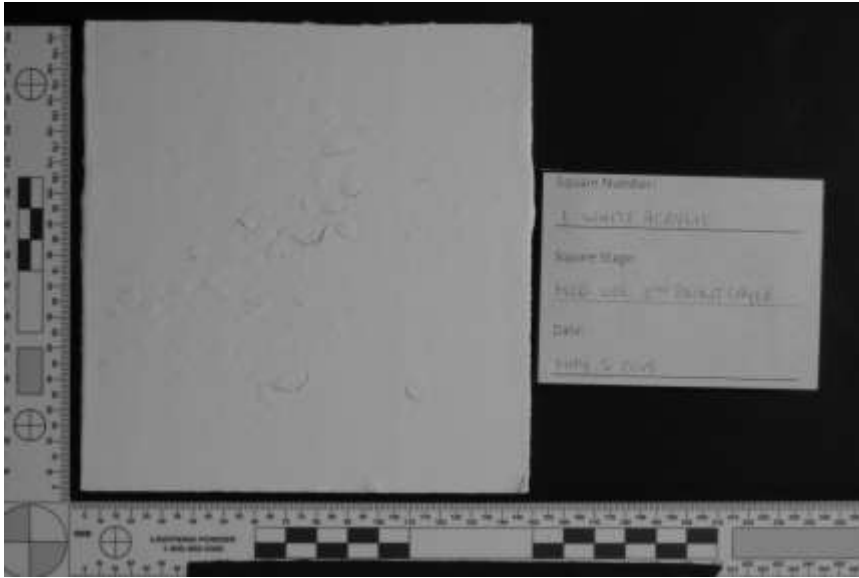
White Acrylic 1 – Medium Velocity



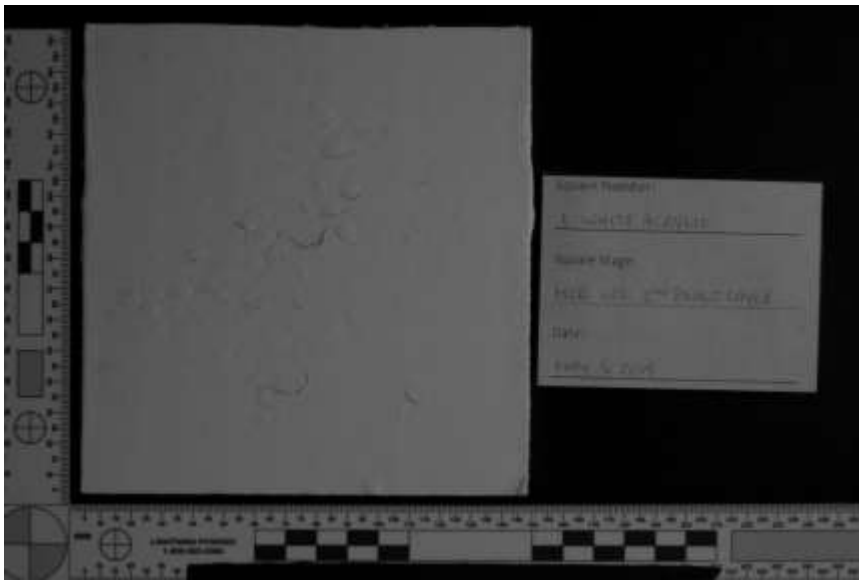
Longpass 87A HDR



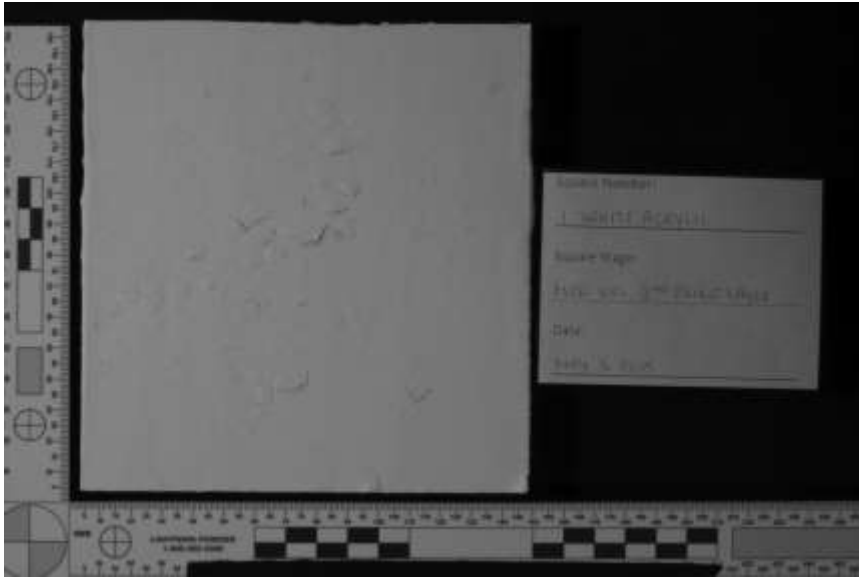
Longpass 87A Single



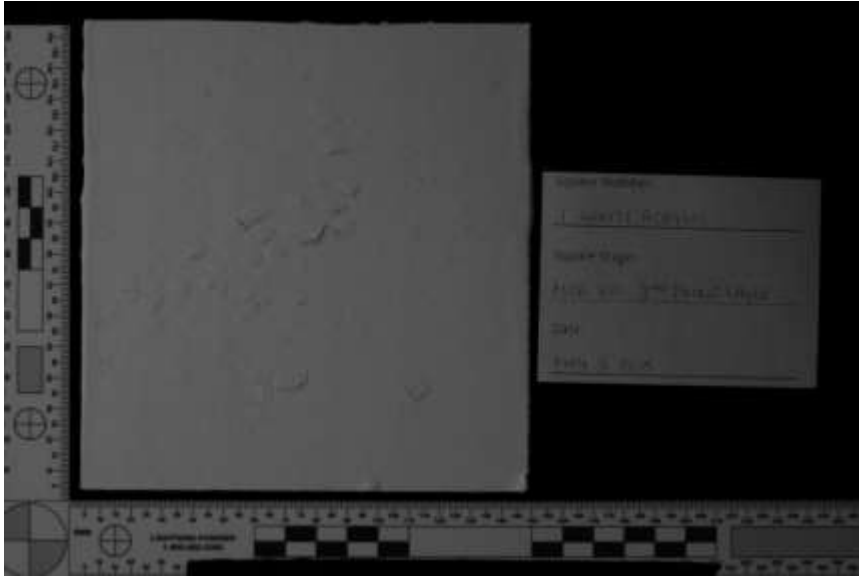
Longpass 87A HDR Left Oblique



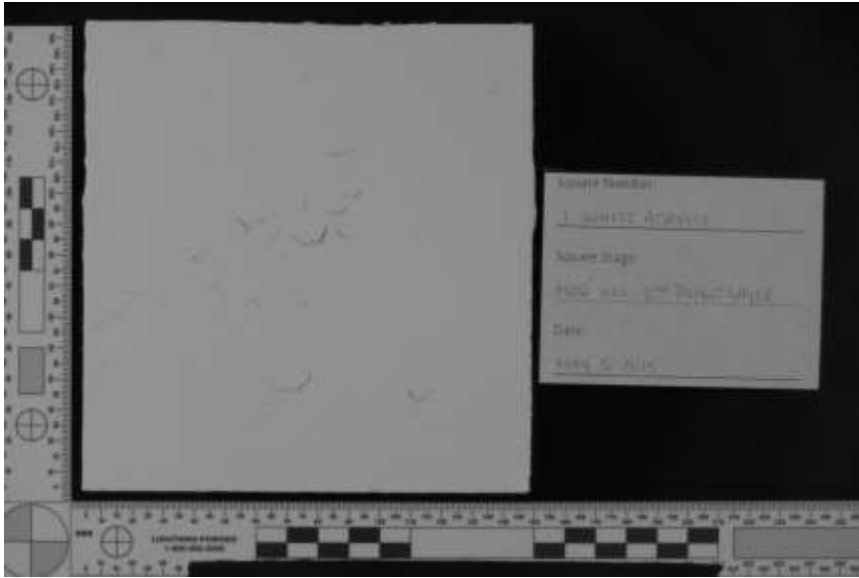
Longpass 87A Single Left Oblique



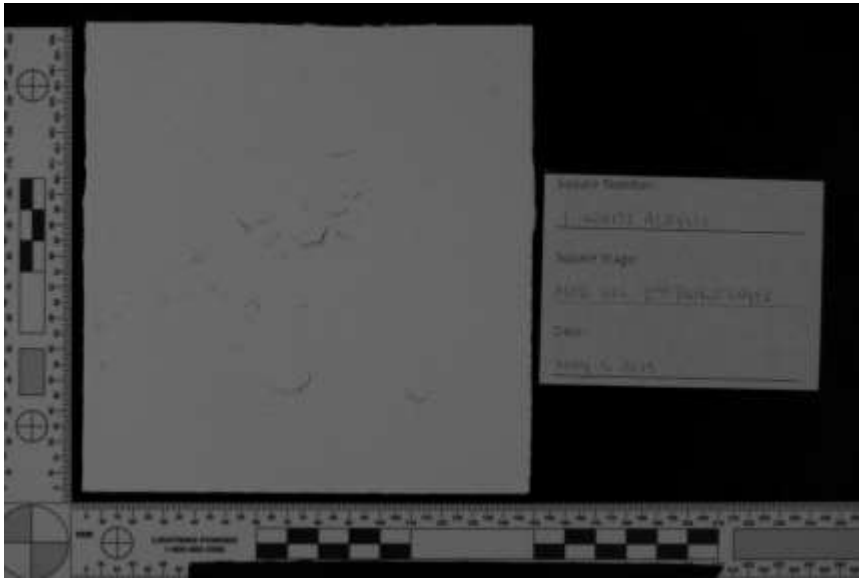
Longpass 87A HDR Right Oblique



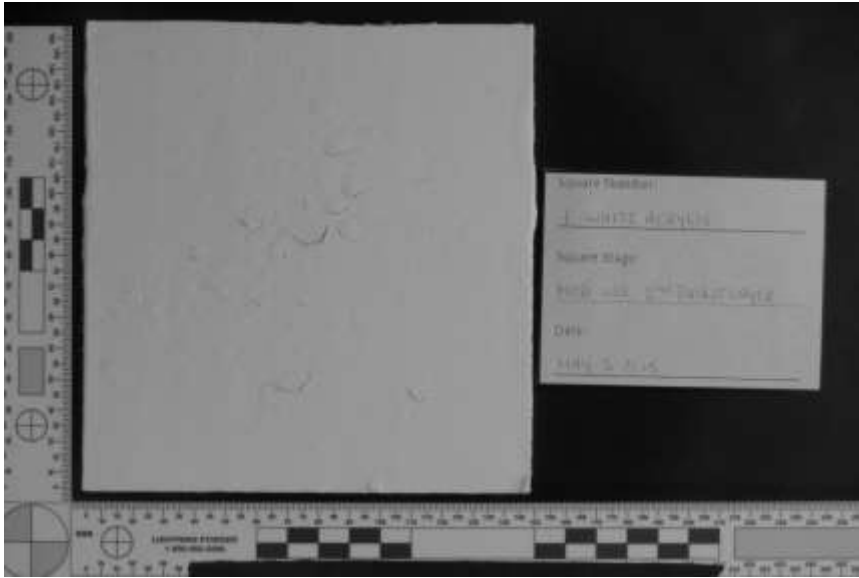
Longpass 87A Single Right Oblique



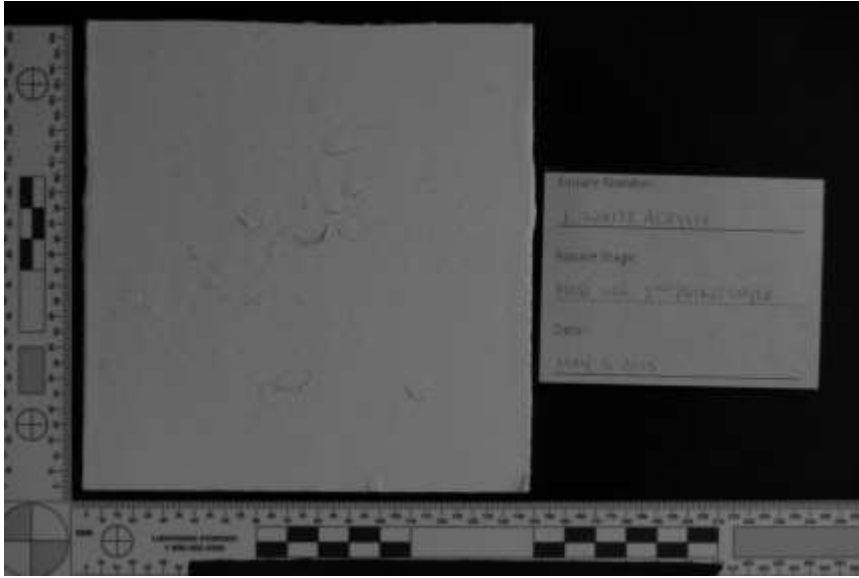
Longpass 87B HDR



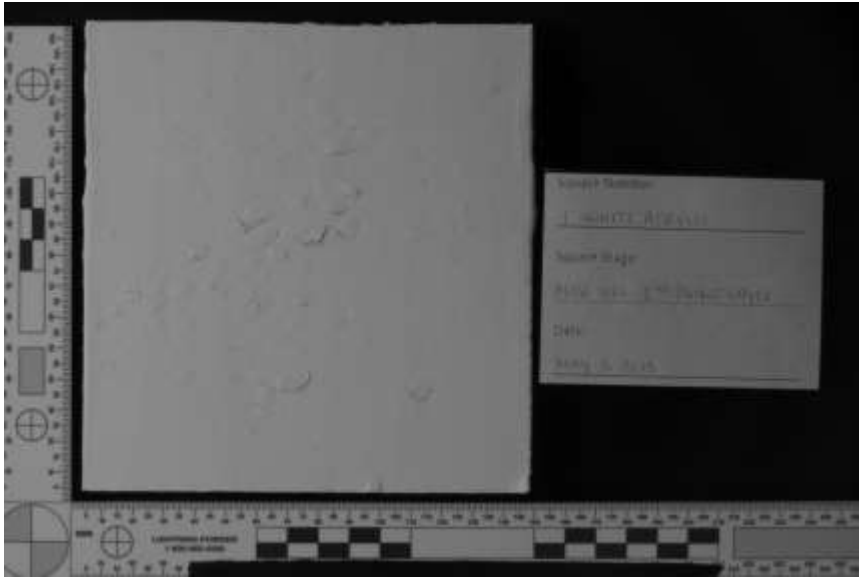
Longpass 87B Single



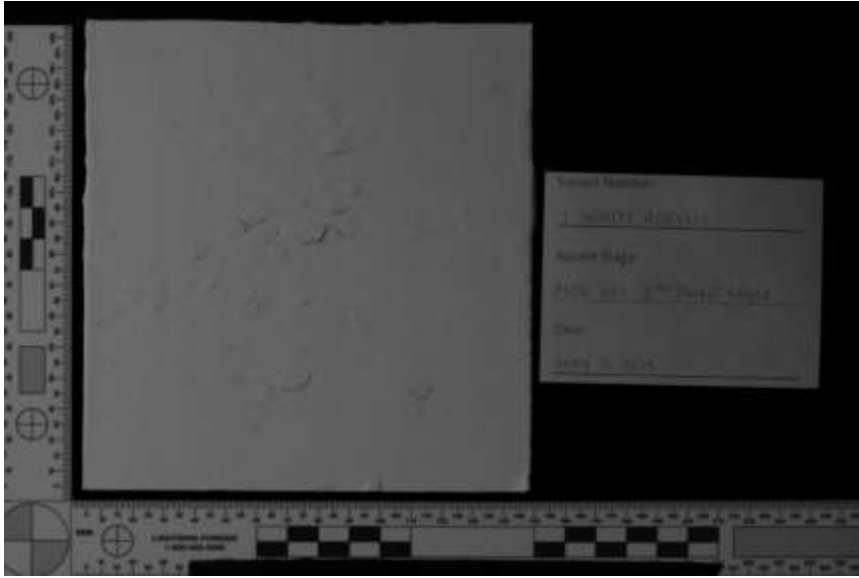
Longpass 87B HDR Left Oblique



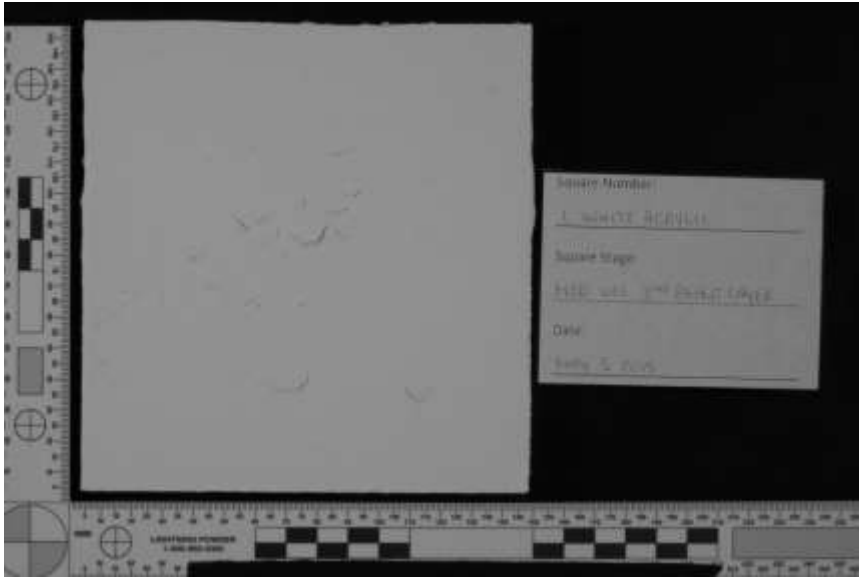
Longpass 87B Single Left Oblique



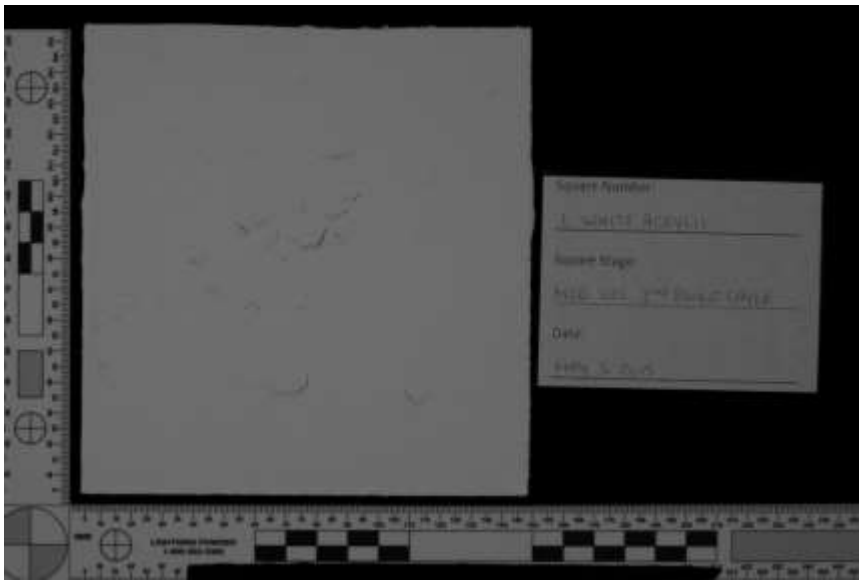
Longpass 87B HDR Right Oblique



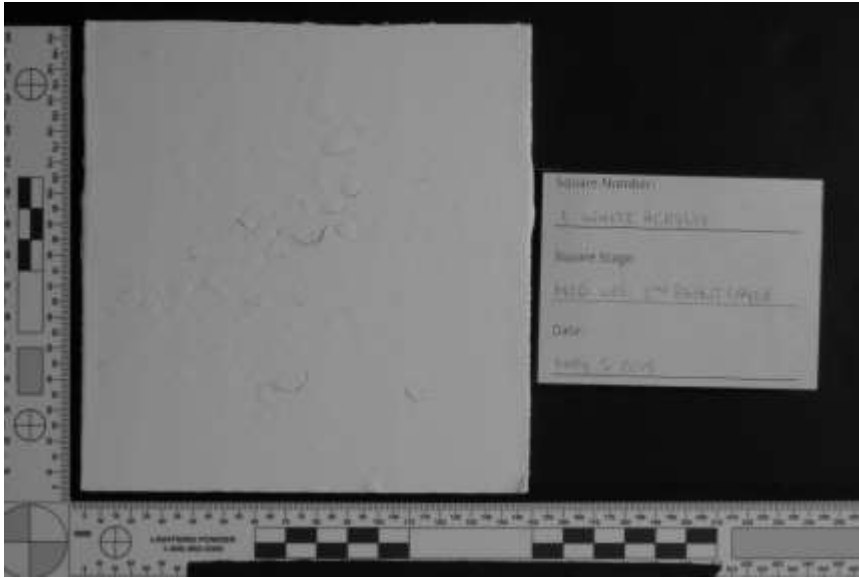
Longpass 87B Single Right Oblique



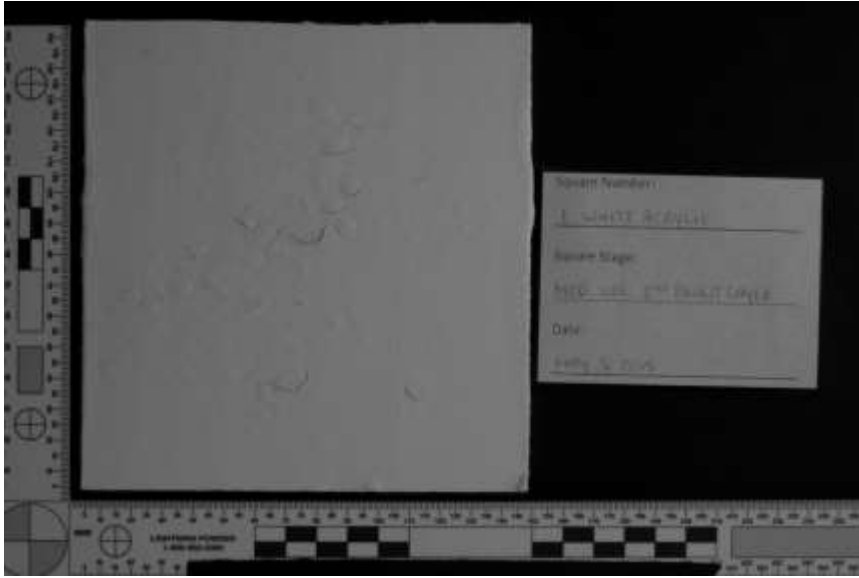
Longpass 88A HDR



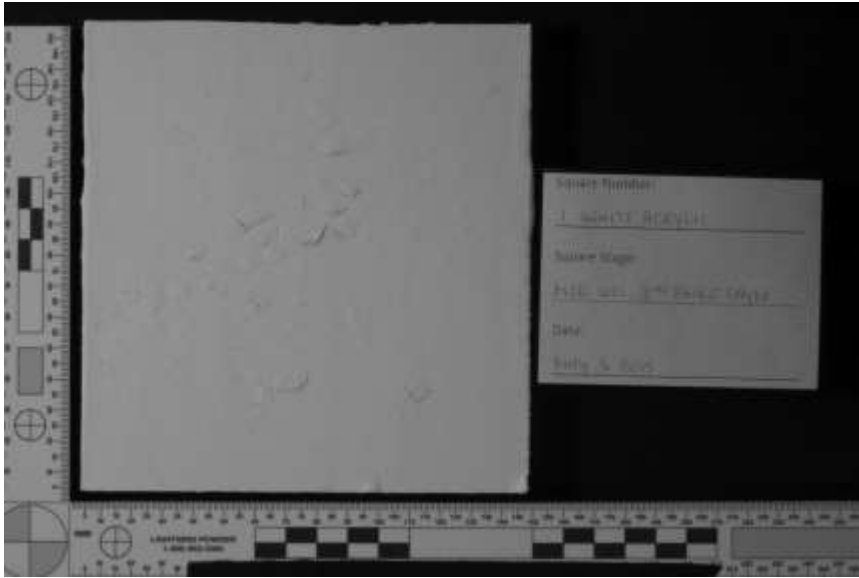
Longpass 88A Single



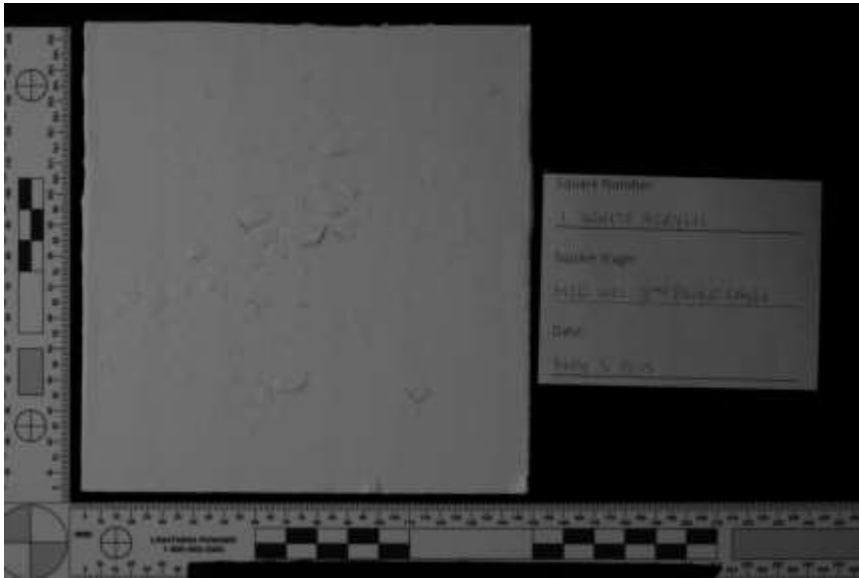
Longpass 88A HDR Left Oblique



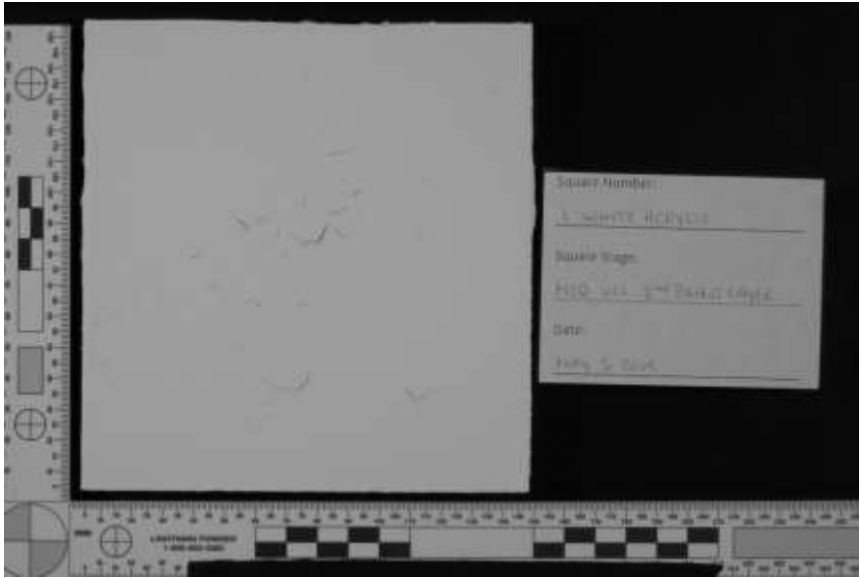
Longpass 88A Single Left Oblique



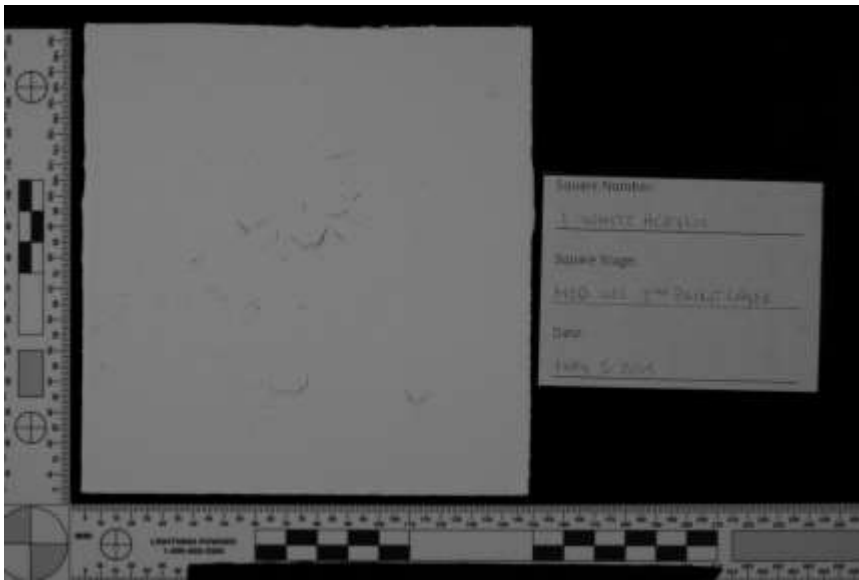
Longpass 88A HDR Right Oblique



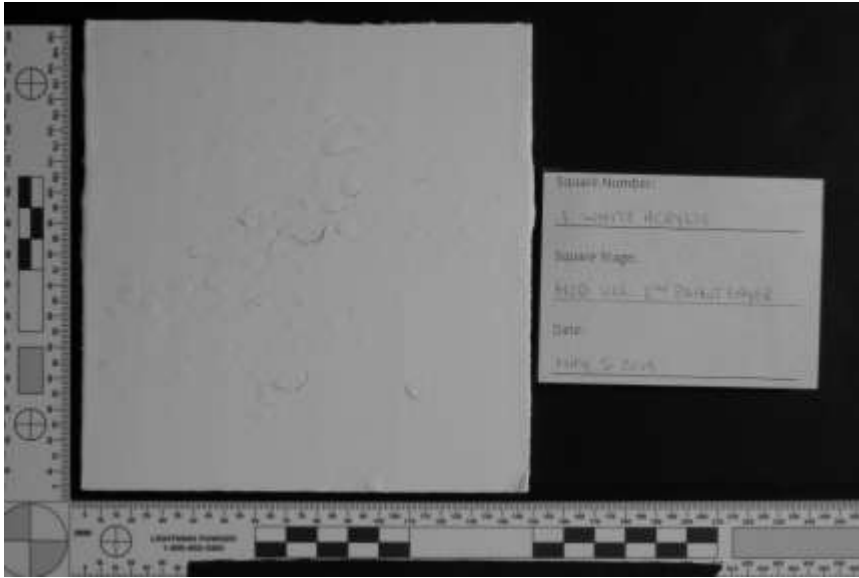
Longpass 88A Single Right Oblique



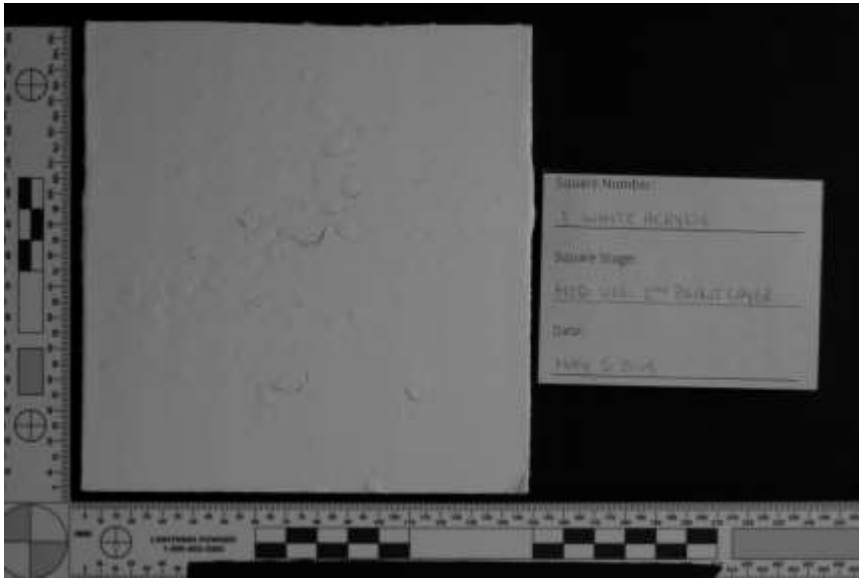
Longpass 89B HDR



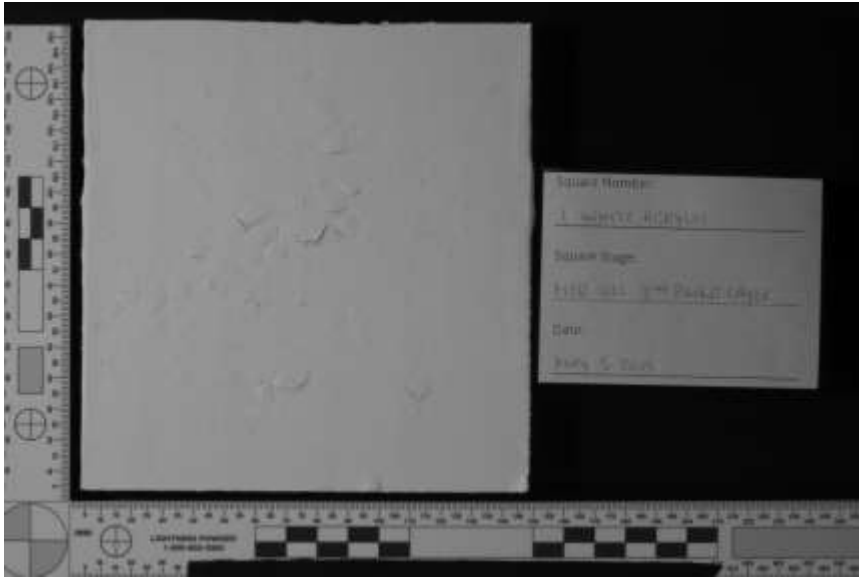
Longpass 89B Single



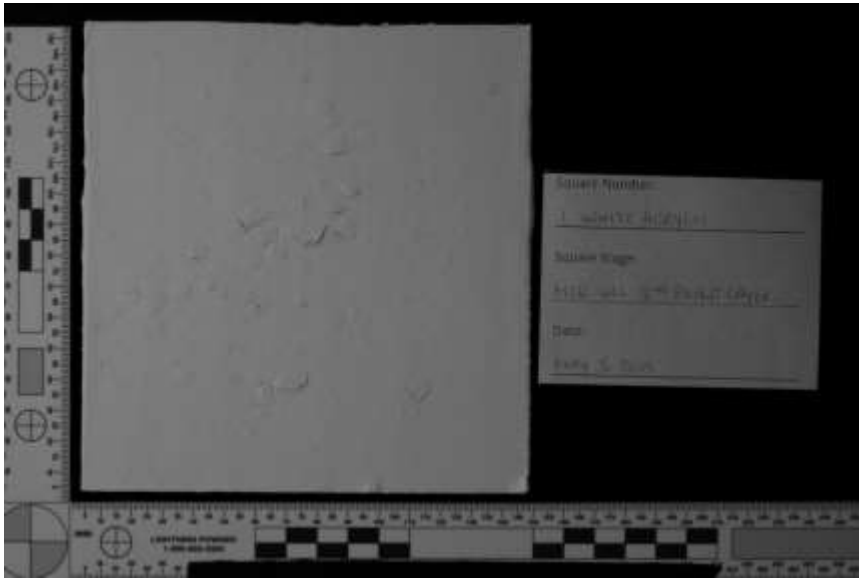
Longpass 89B HDR Left Oblique



Longpass 89B Single Left Oblique

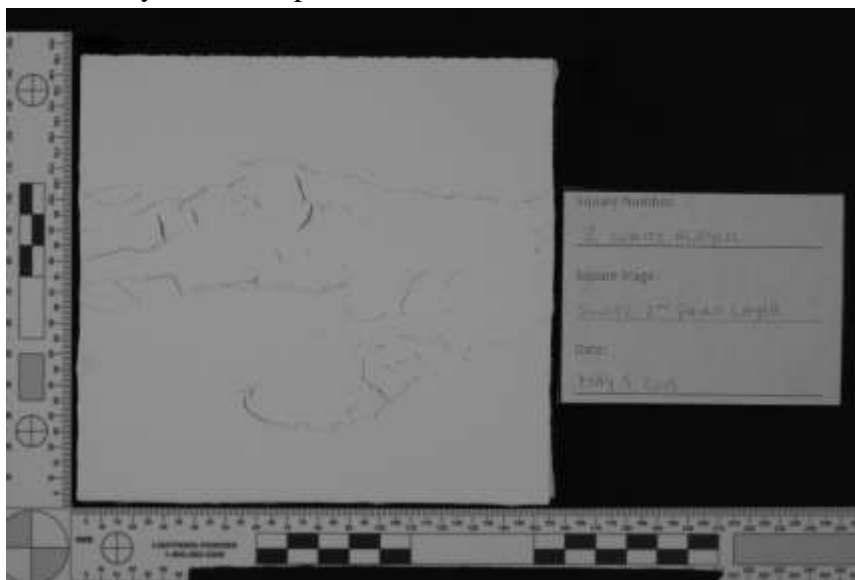


Longpass 89B HDR Right Oblique

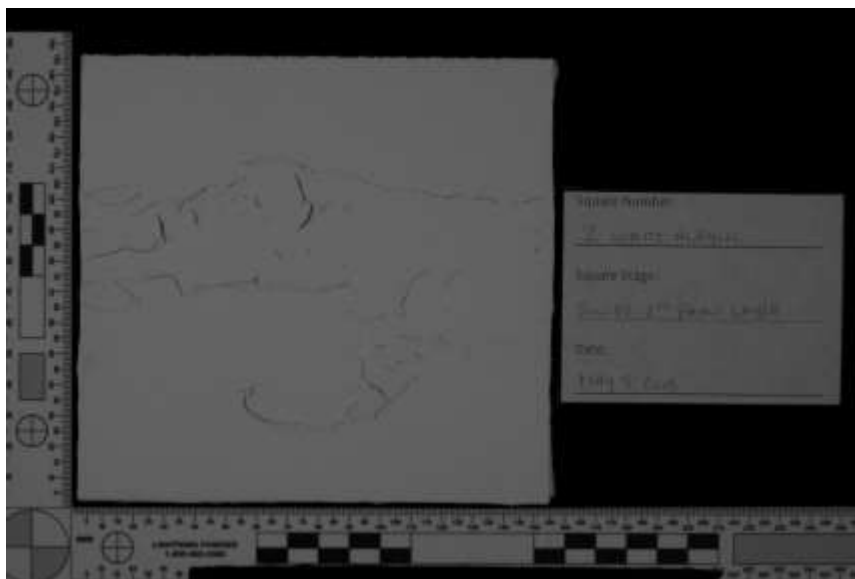


Longpass 89B Single Right Oblique

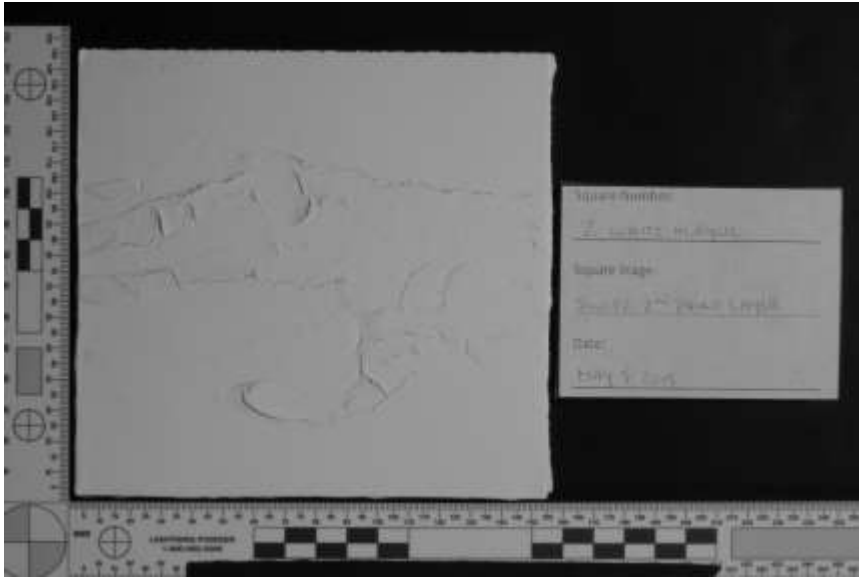
White Acrylic 2 – Swipe



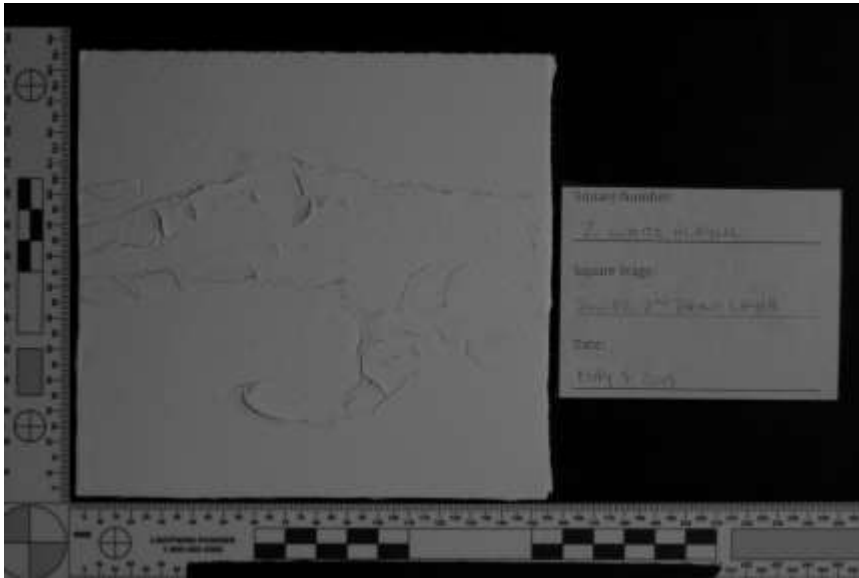
Longpass 87A HDR



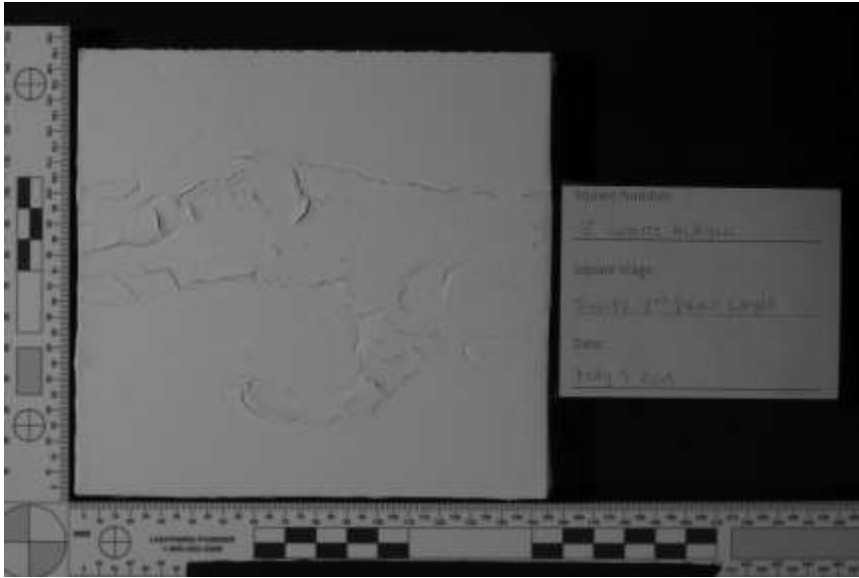
Longpass 87A Single



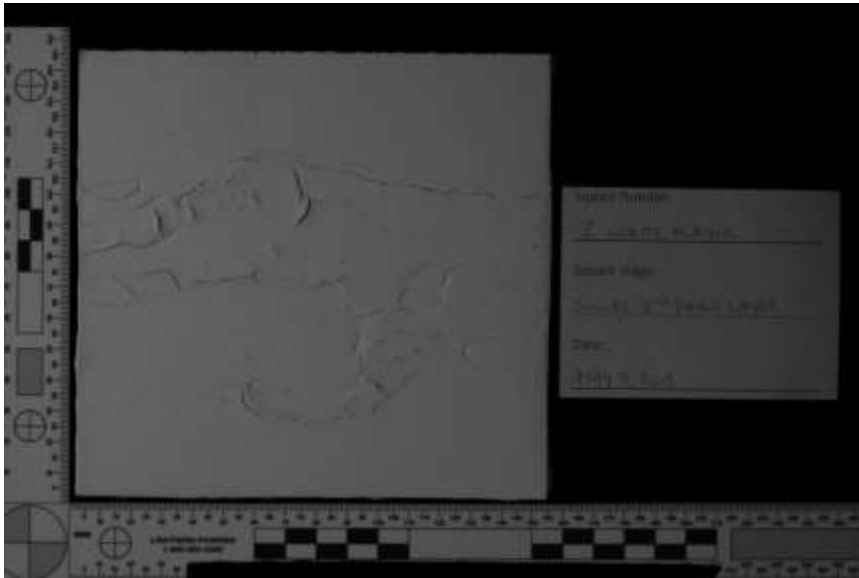
Longpass 87A HDR Left Oblique



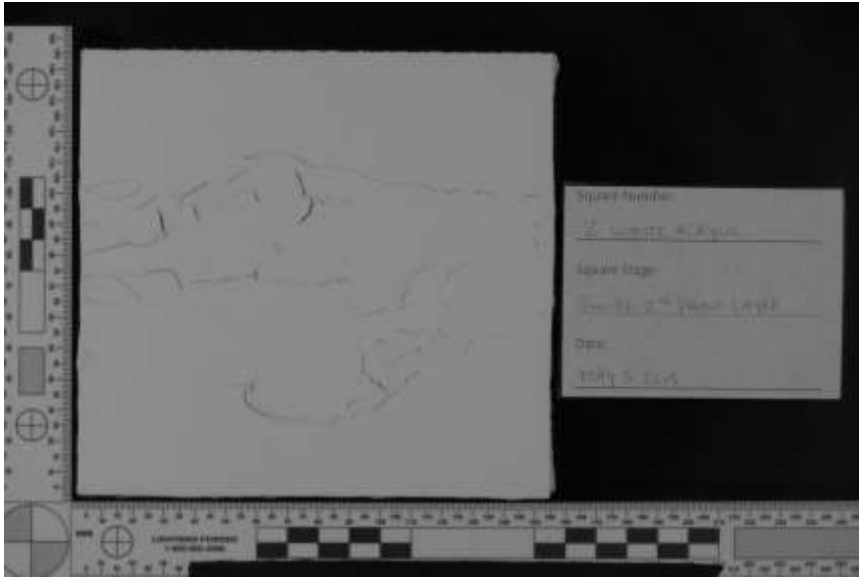
Longpass 87A Single Left Oblique



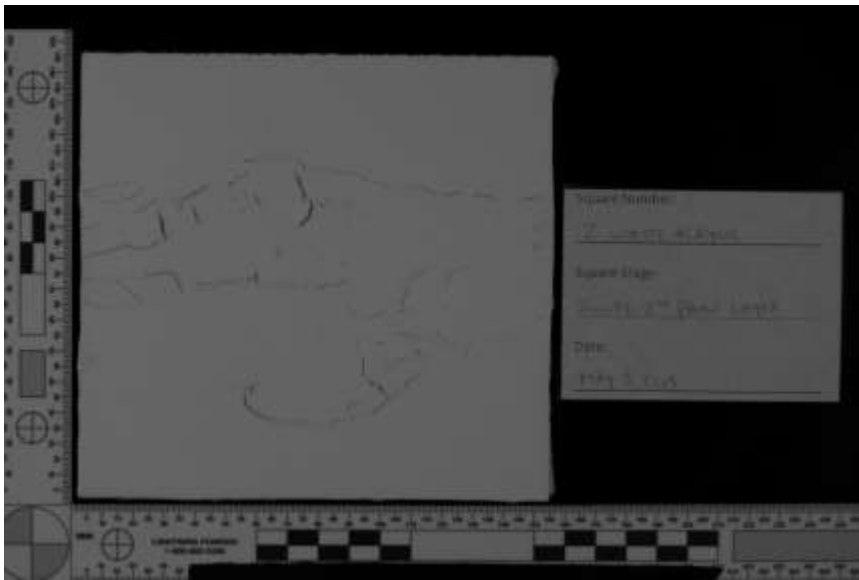
Longpass 87A HDR Right Oblique



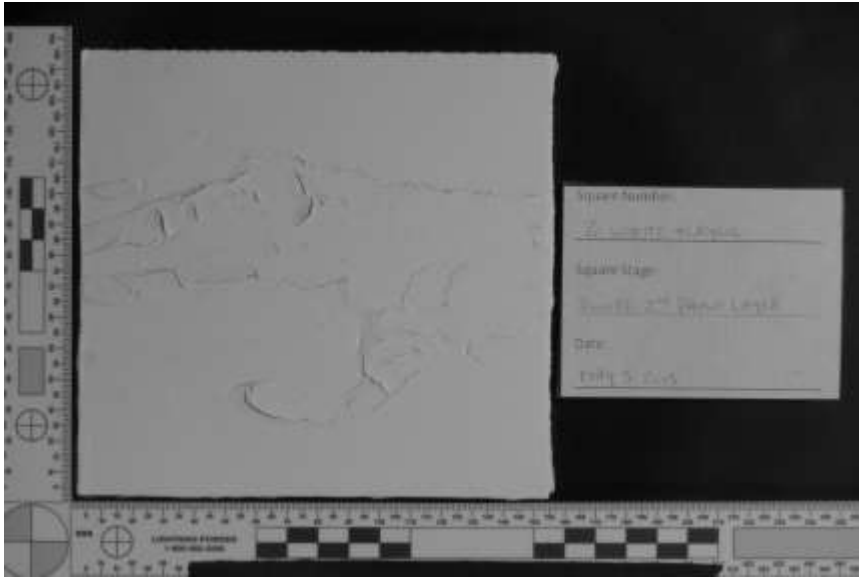
Longpass 87A Single Right Oblique



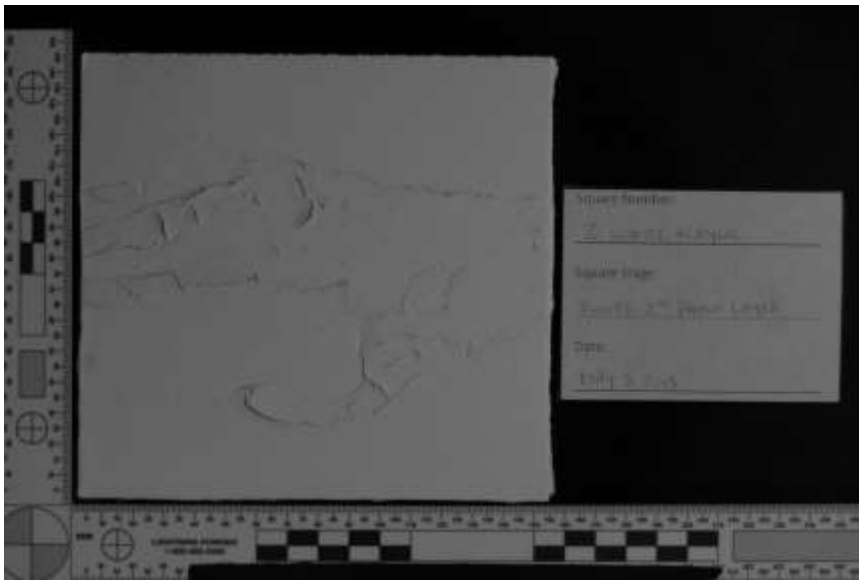
Longpass 87B HDR



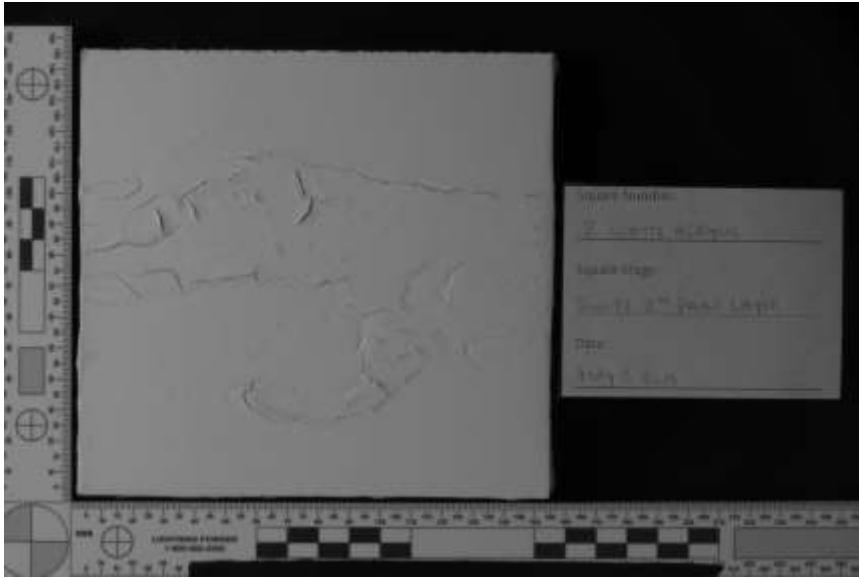
Longpass 87B Single



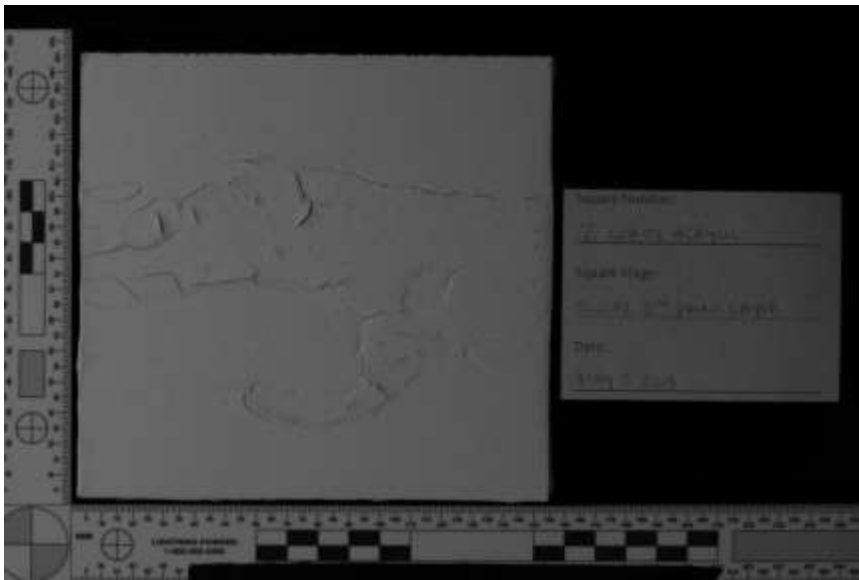
Longpass 87B HDR Left Oblique



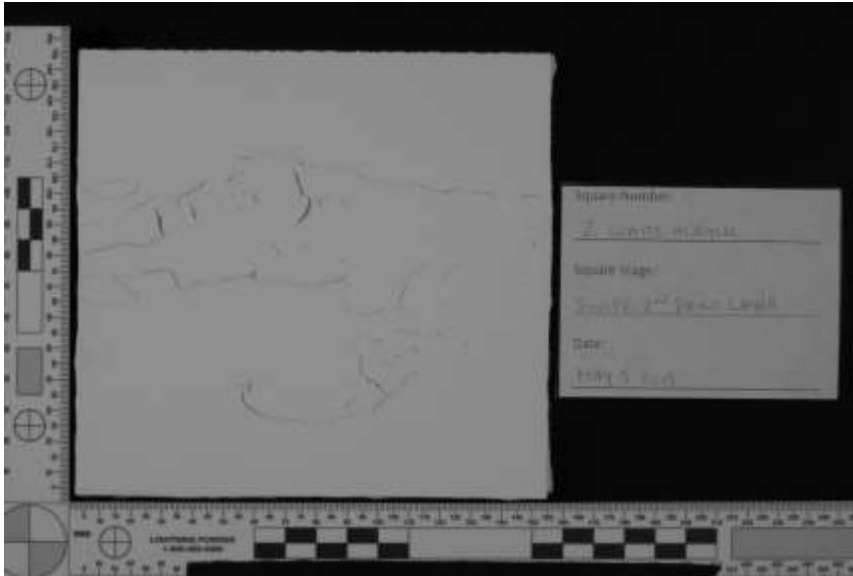
Longpass 87B Single Left Oblique



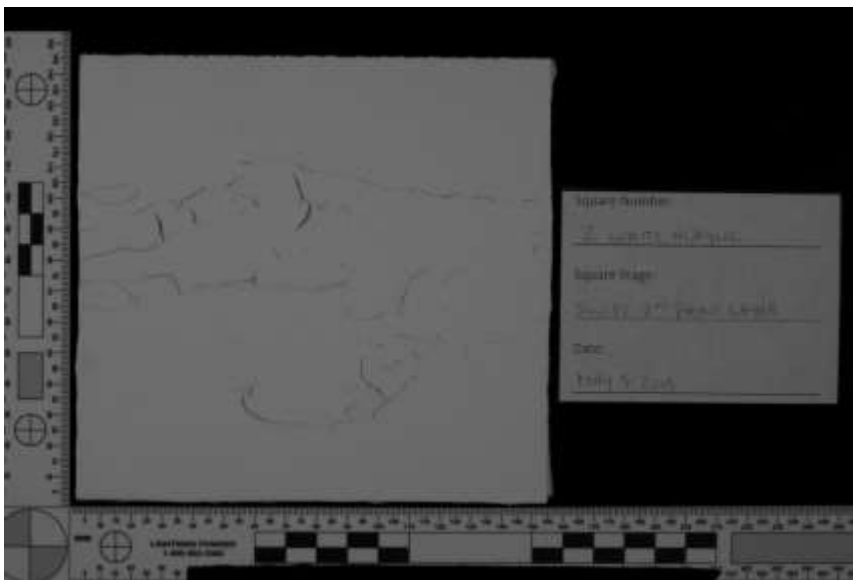
Longpass 87B HDR Right Oblique



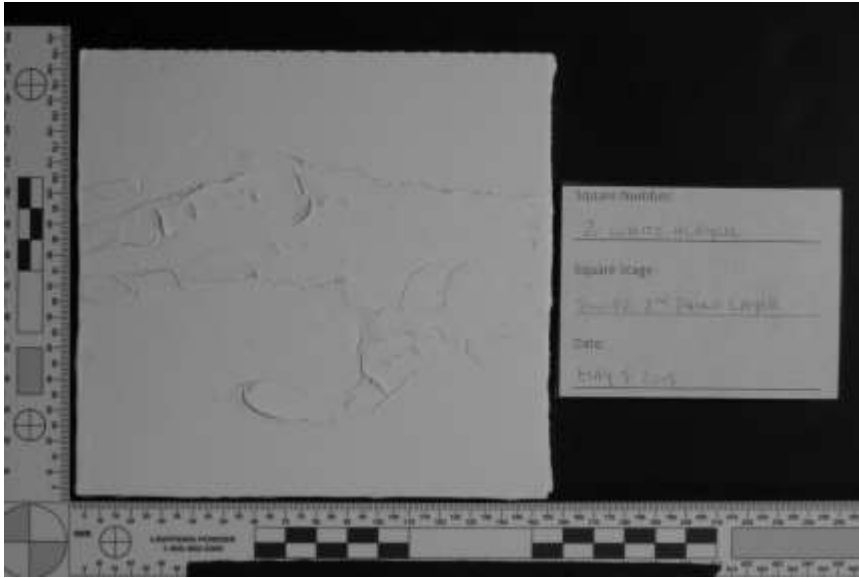
Longpass 87B Single Right Oblique



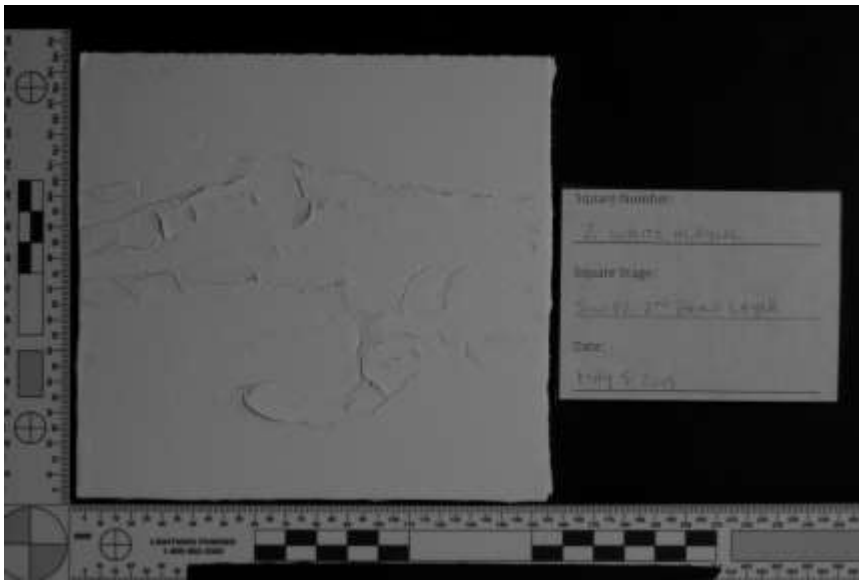
Longpass 88A HDR



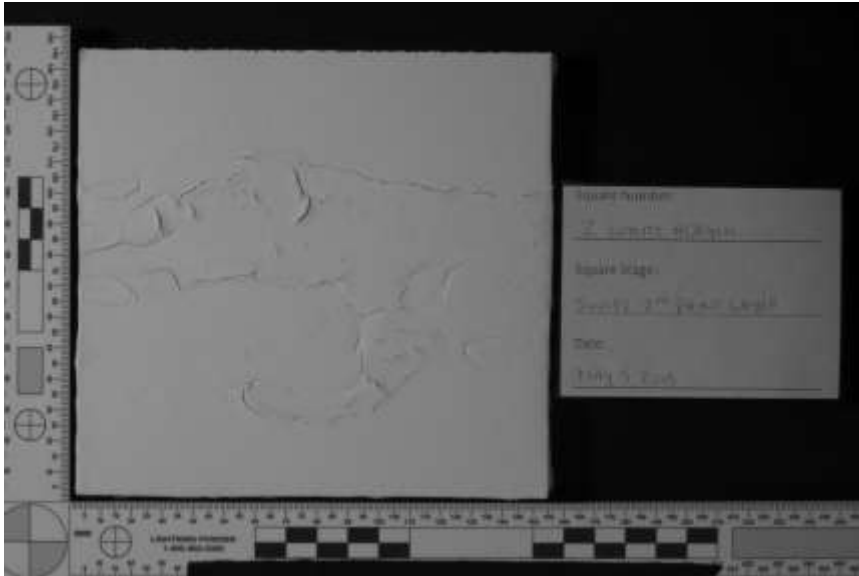
Longpass 88A Single



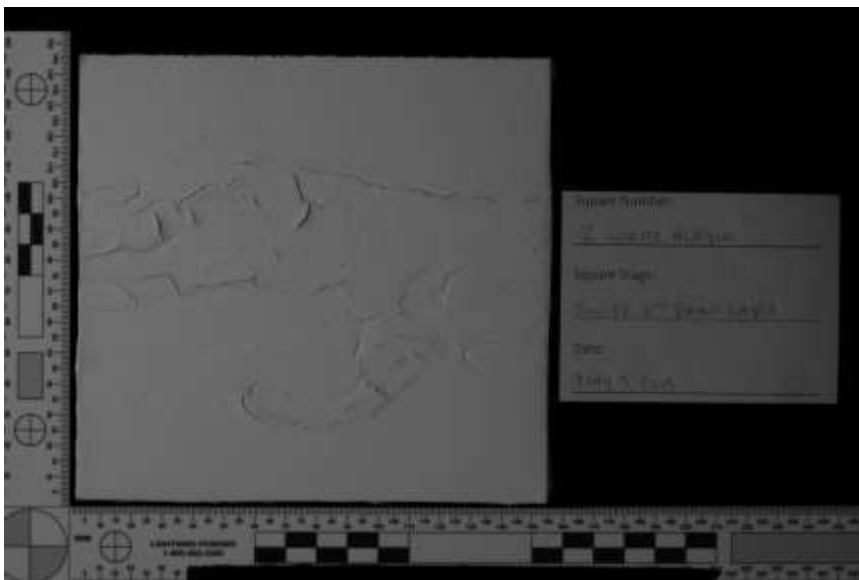
Longpass 88A HDR Left Oblique



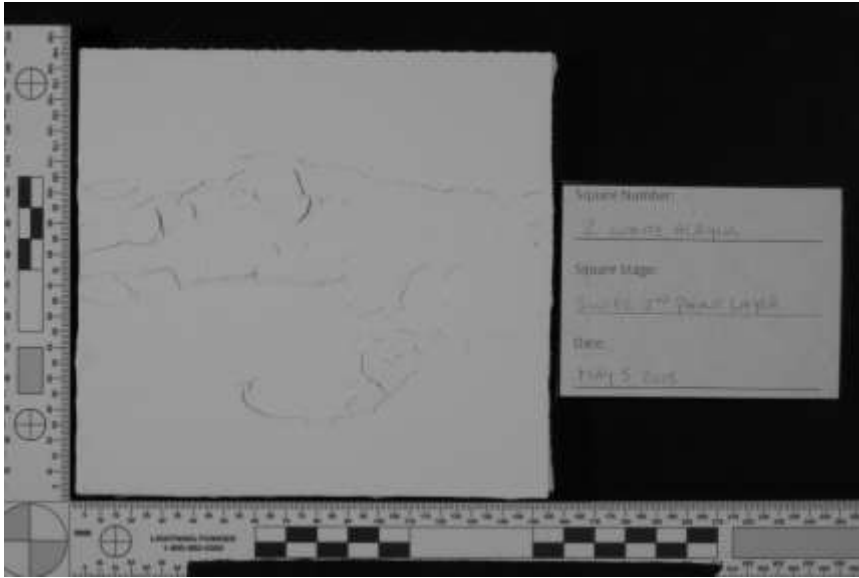
Longpass 88A Single Left Oblique



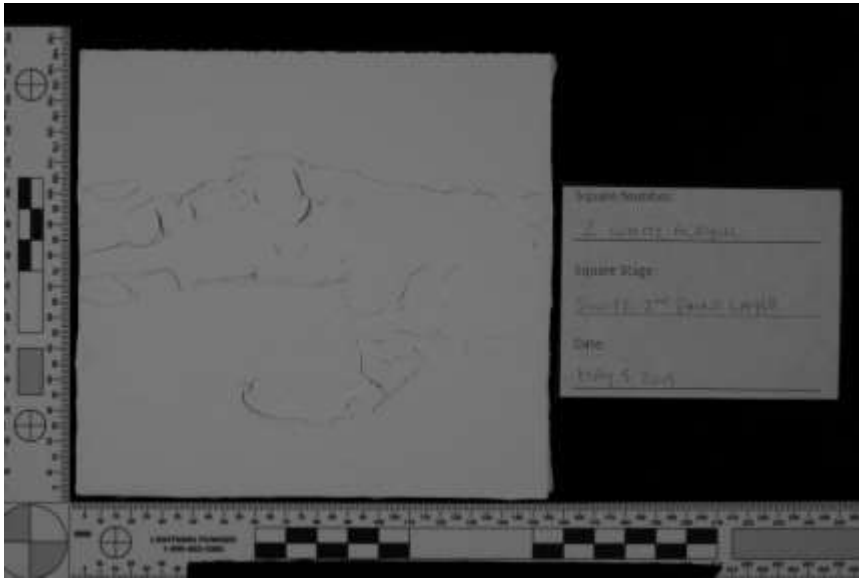
Longpass 88A HDR Right Oblique



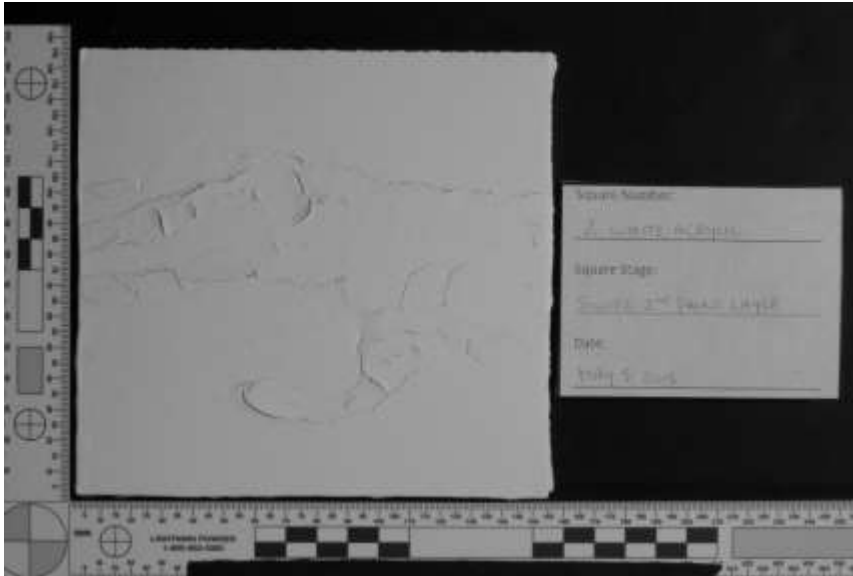
Longpass 88A Single Right Oblique



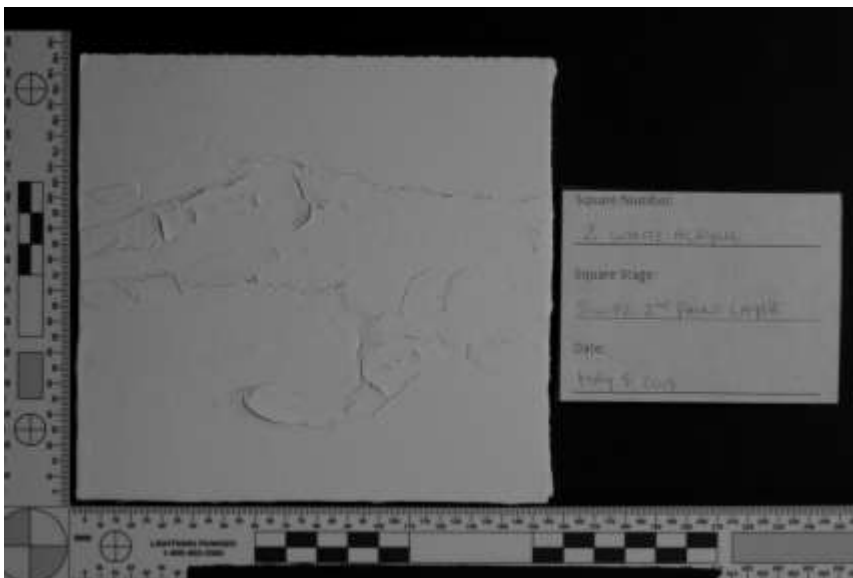
Longpass 89B HDR



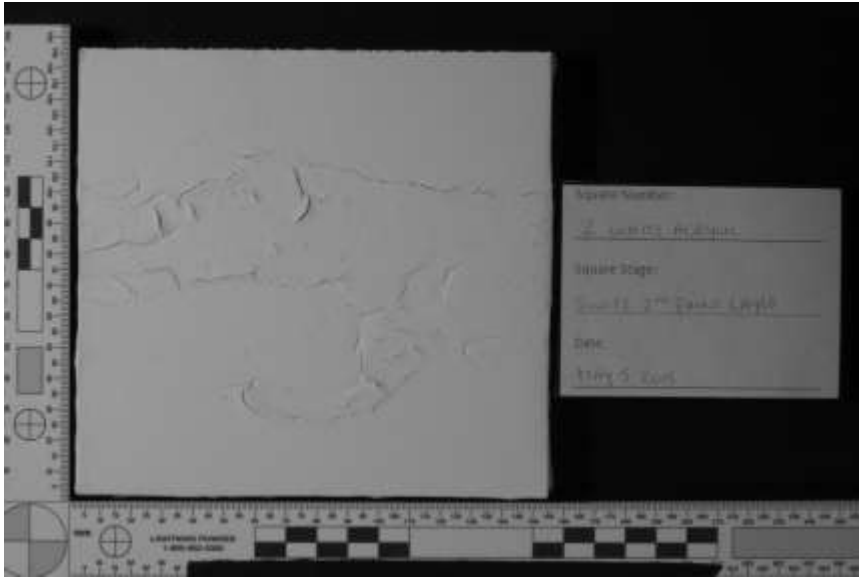
Longpass 89B Single



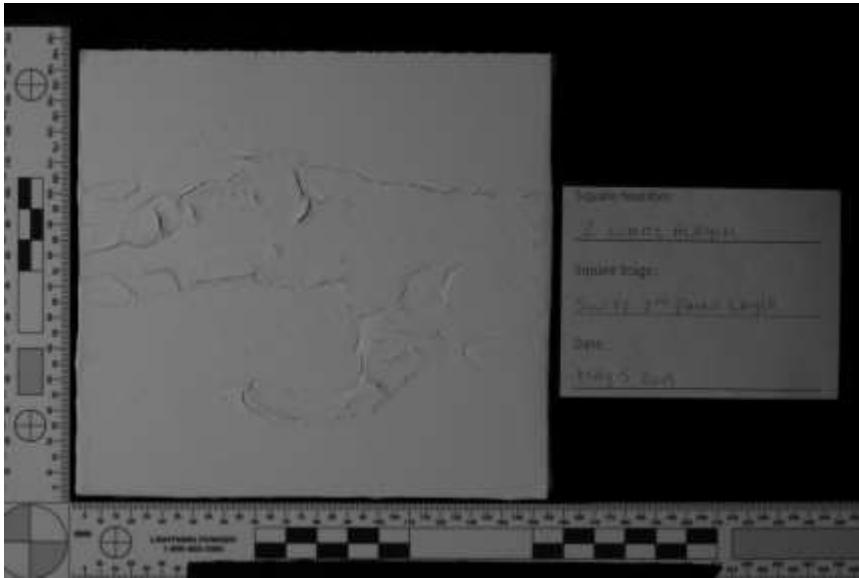
Longpass 89B HDR Left Oblique



Longpass 89B Single Left Oblique

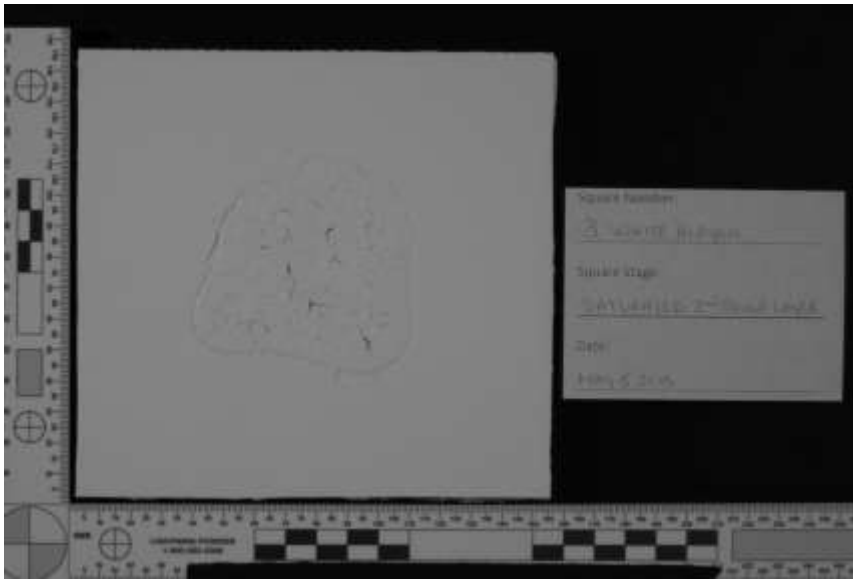


Longpass 89B HDR Right Oblique

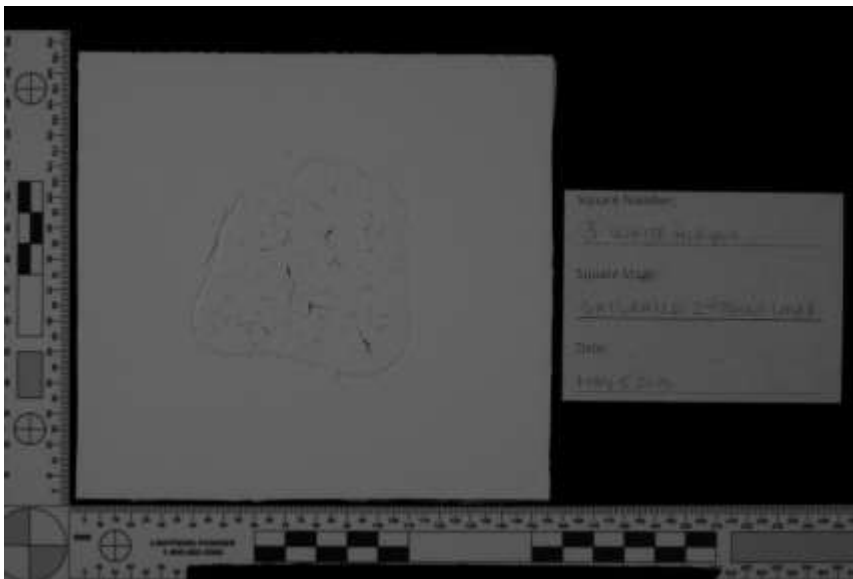


Longpass 89B Single Right Oblique

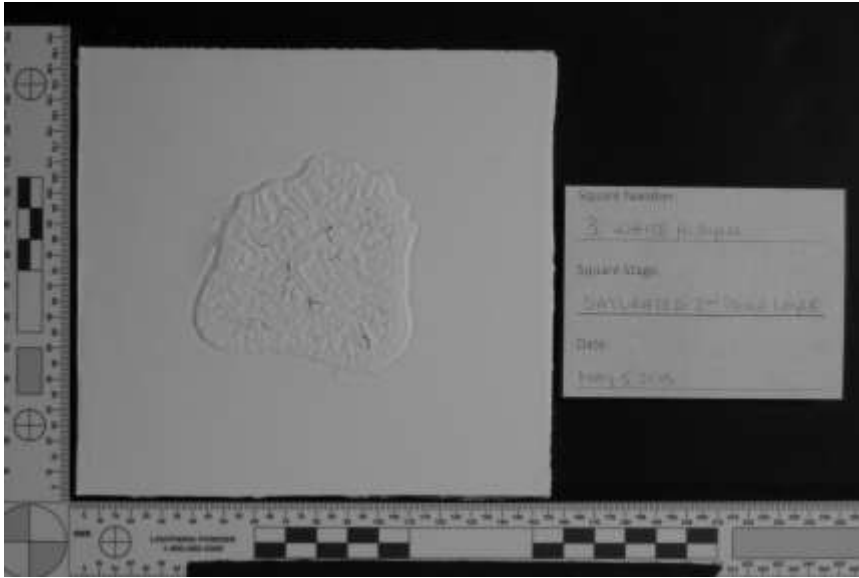
White Acrylic 3 – Saturated



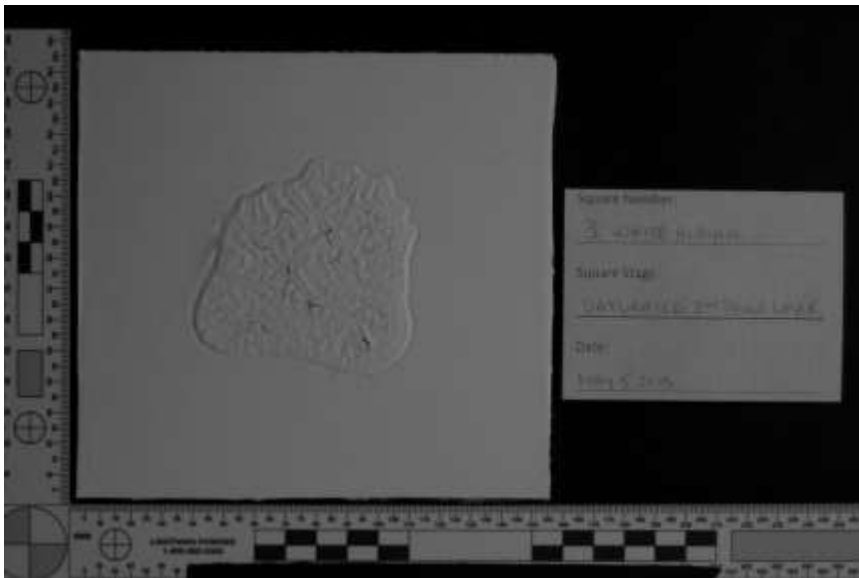
Longpass 87A HDR



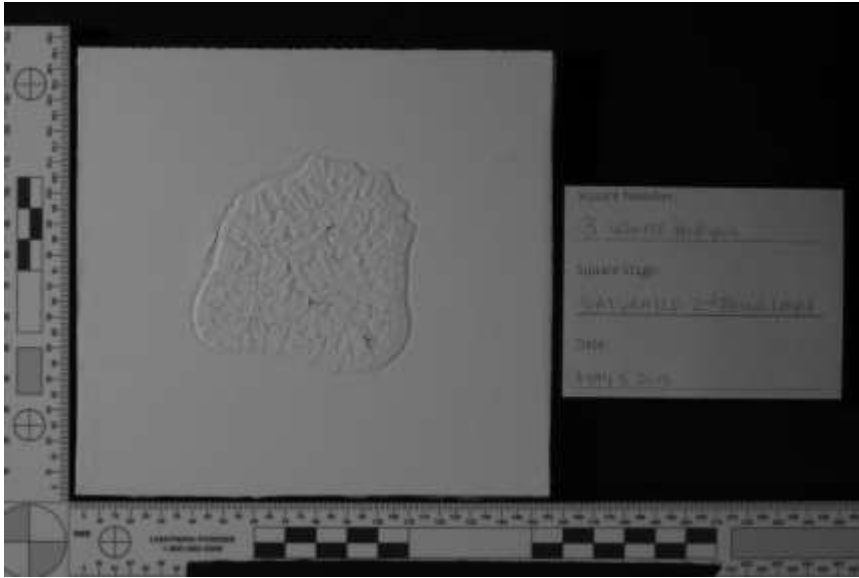
Longpass 87A Single



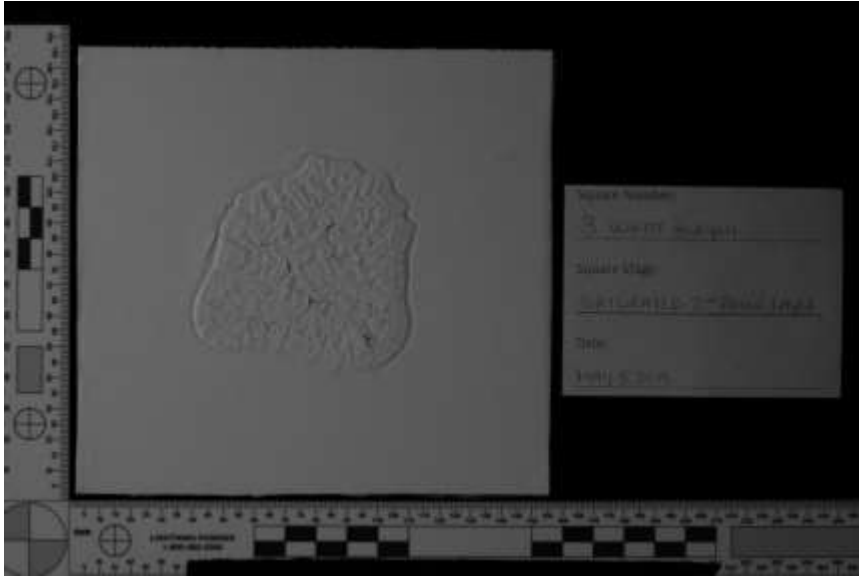
Longpass 87A HDR Left Oblique



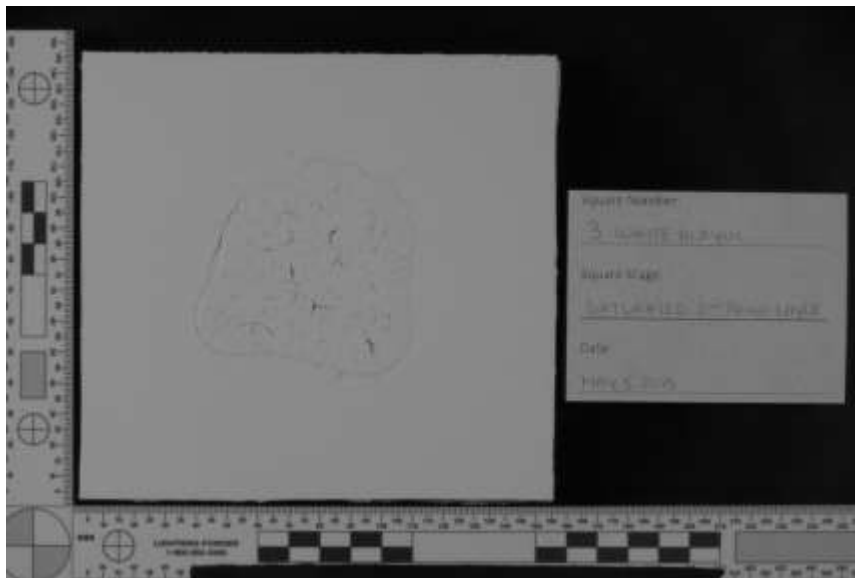
Longpass 87A Single Left Oblique



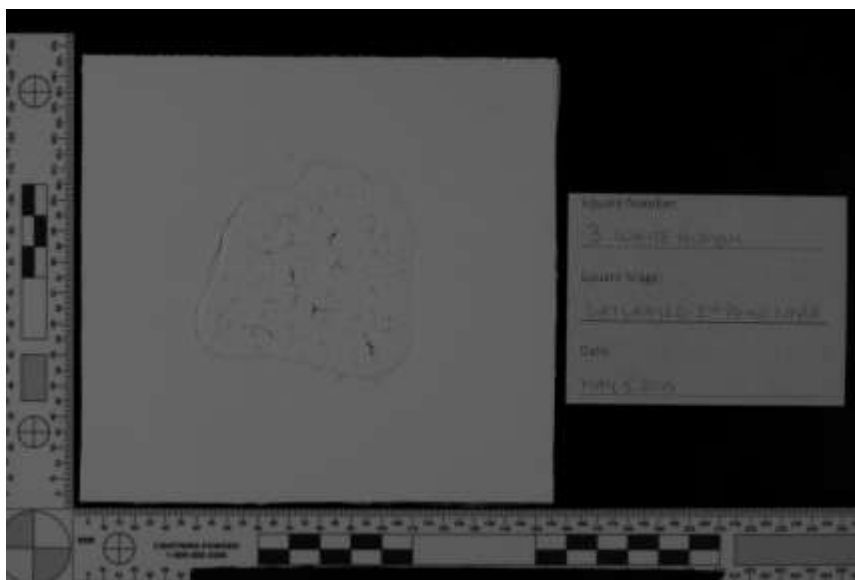
Longpass 87A HDR Right Oblique



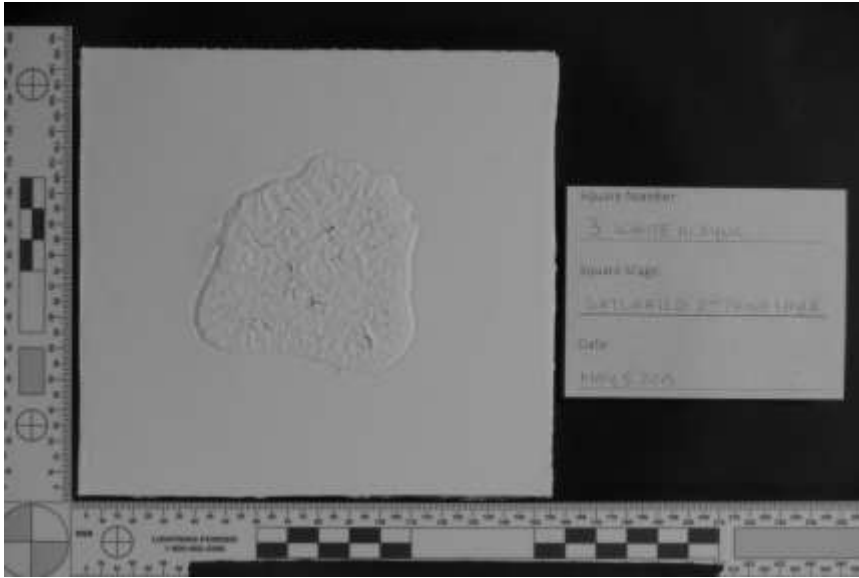
Longpass 87A Single Right Oblique



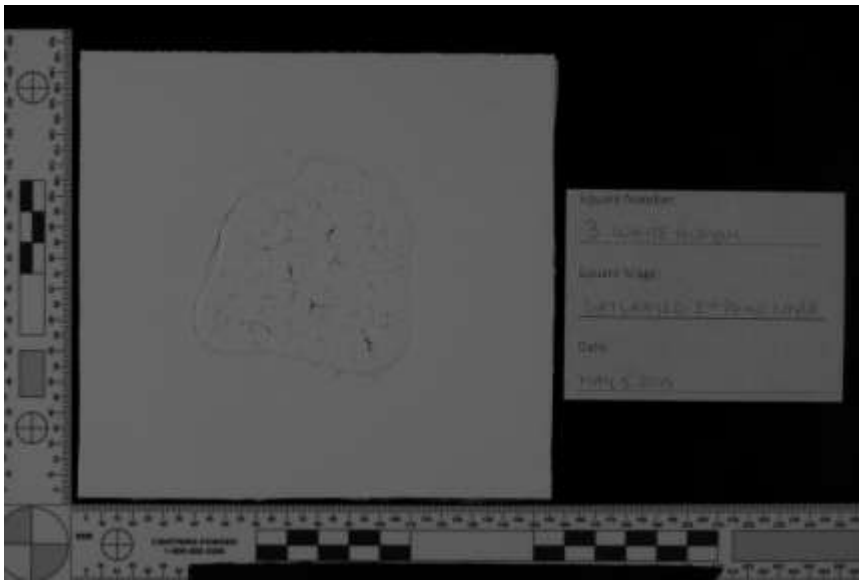
Longpass 87B HDR



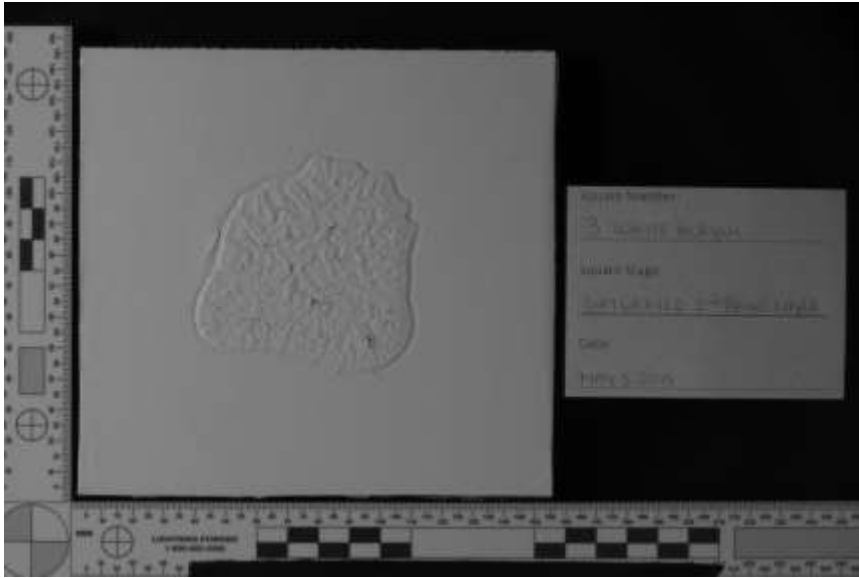
Longpass 87B Single



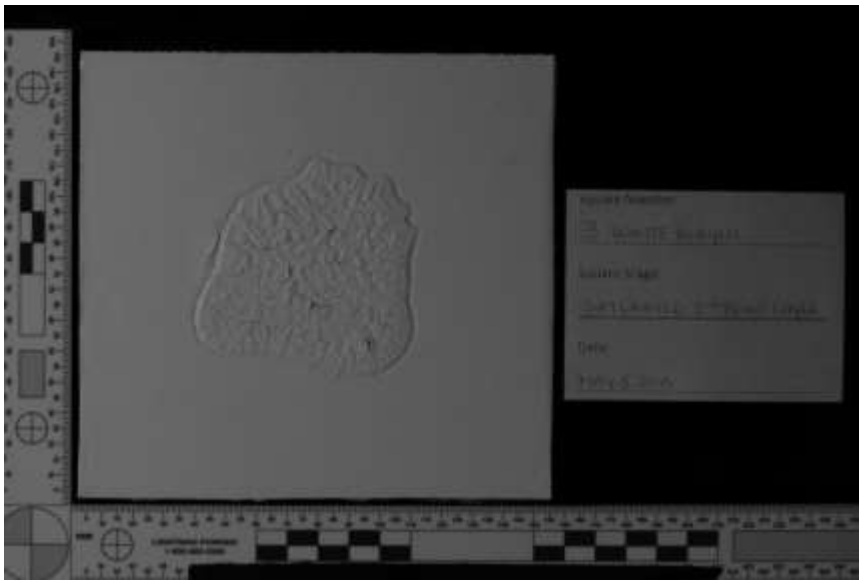
Longpass 87B HDR Left Oblique



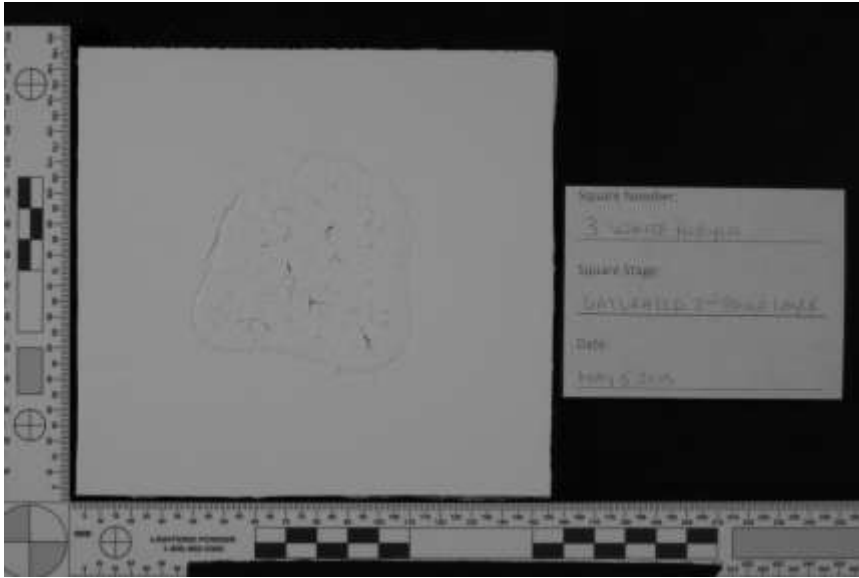
Longpass 87B Single Left Oblique



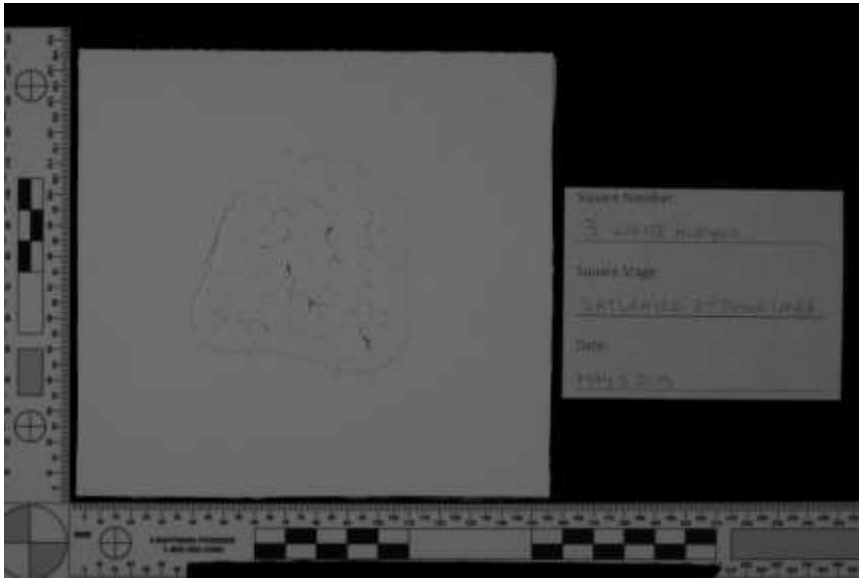
Longpass 87B HDR Right Oblique



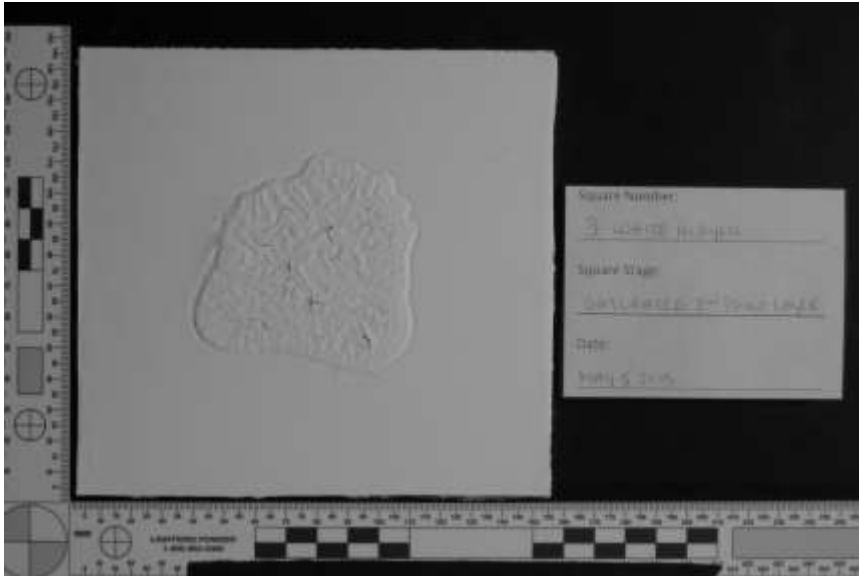
Longpass 87B Single Right Oblique



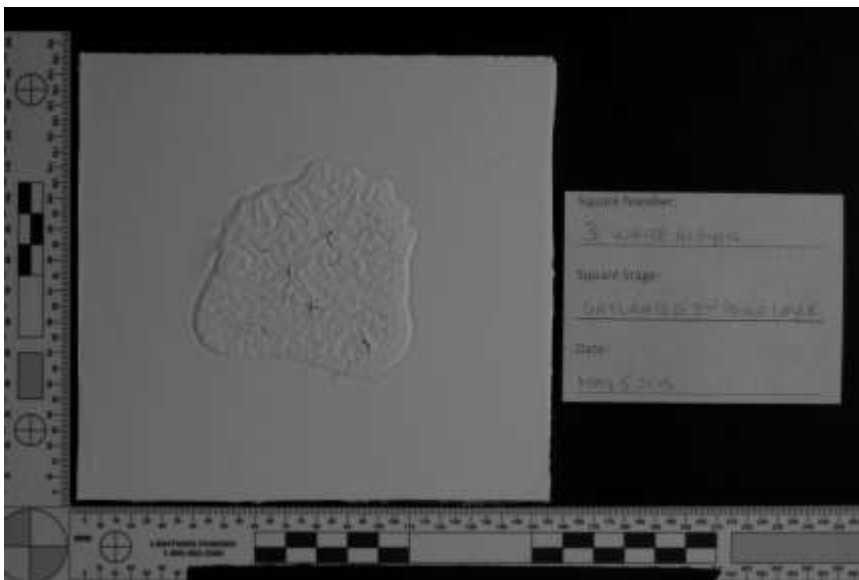
Longpass 88A HDR



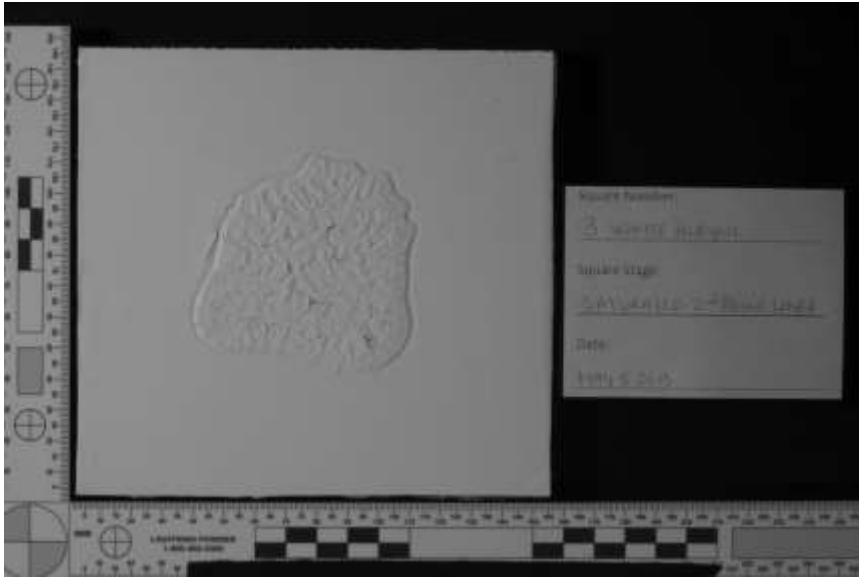
Longpass 88A Single



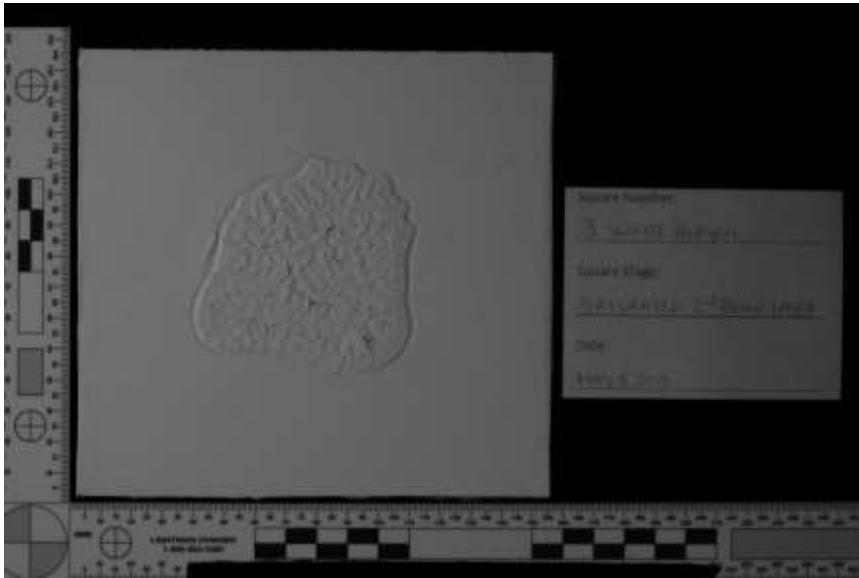
Longpass 88A HDR Left Oblique



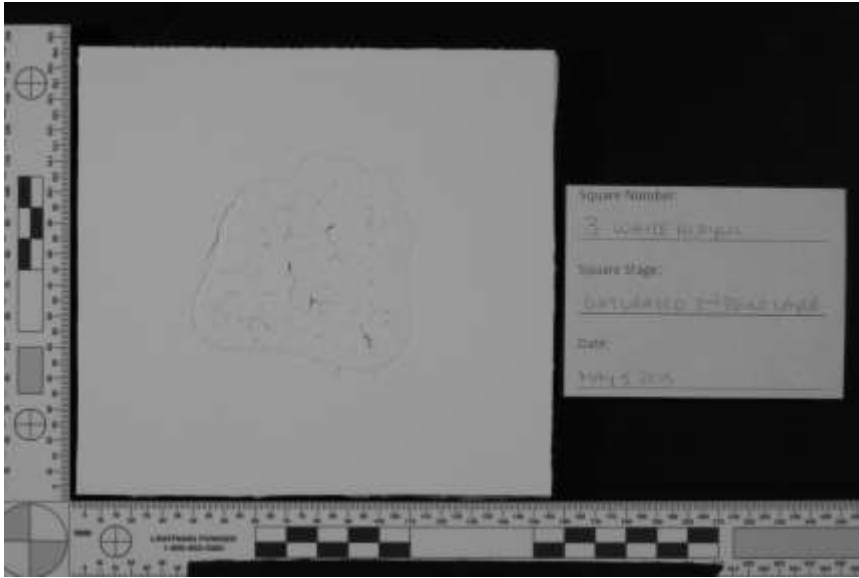
Longpass 88A Single Left Oblique



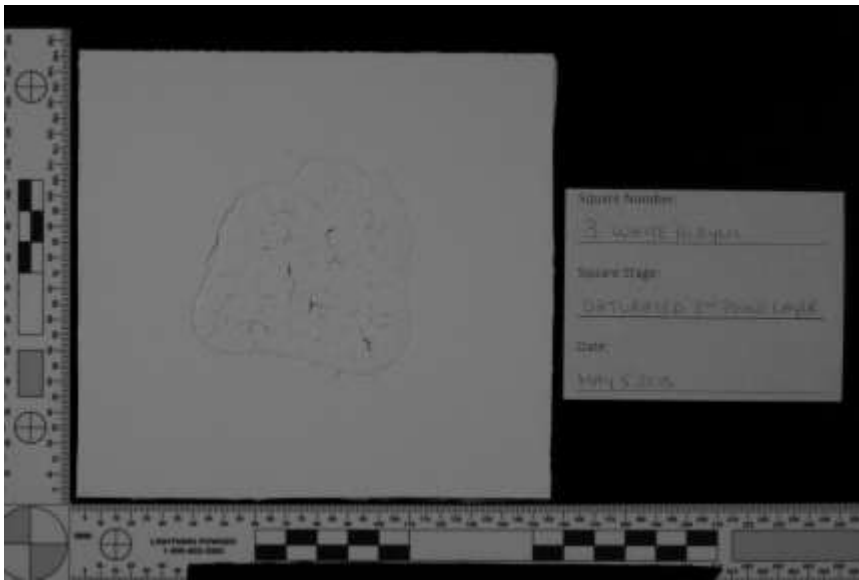
Longpass 88A HDR Right Oblique



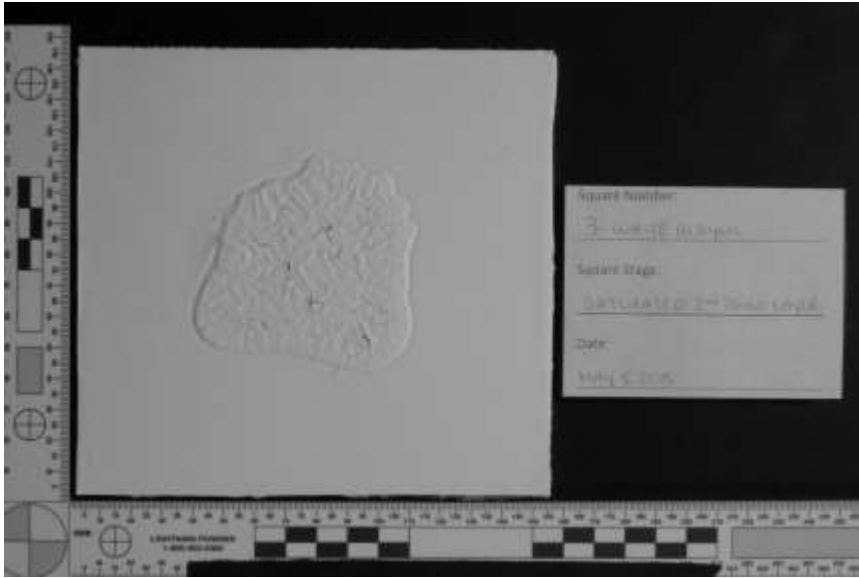
Longpass 88A Single Right Oblique



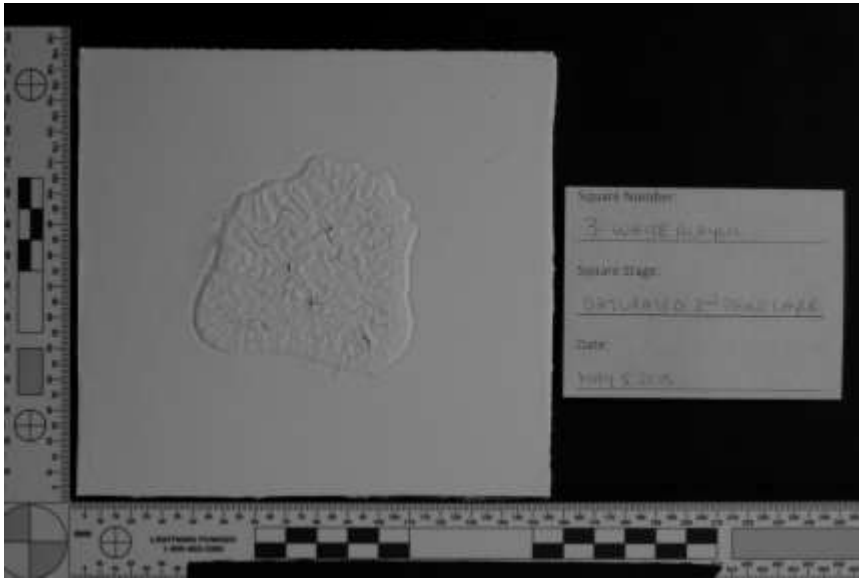
Longpass 89B HDR



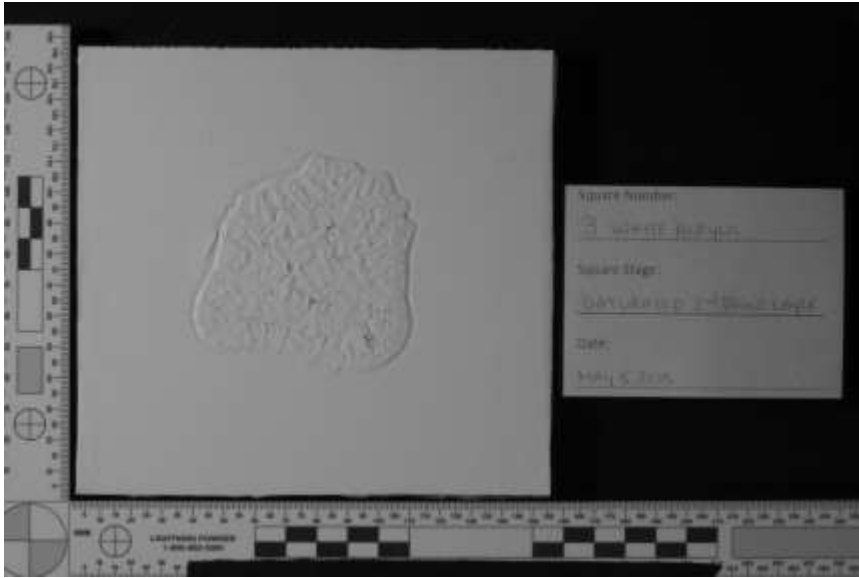
Longpass 89B Single



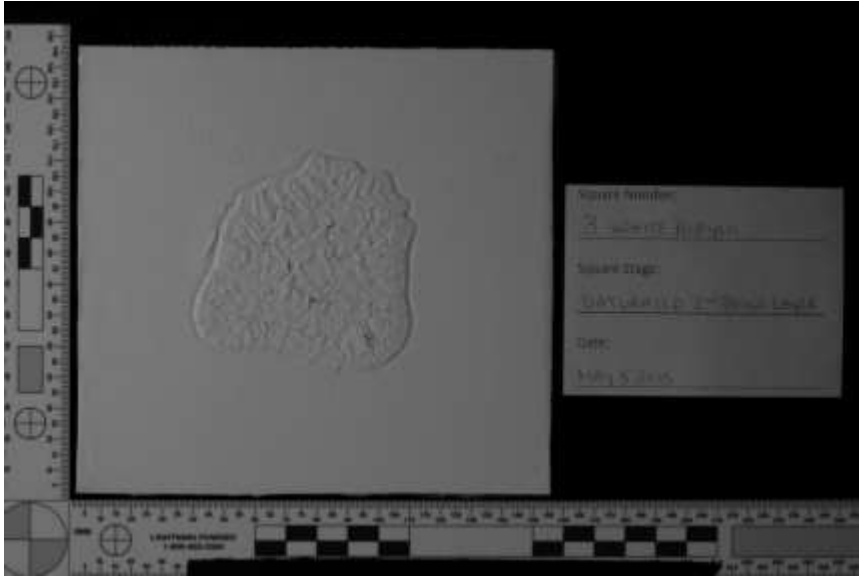
Longpass 89B HDR Left Oblique



Longpass 89B Single Left Oblique



Longpass 89B HDR Right Oblique

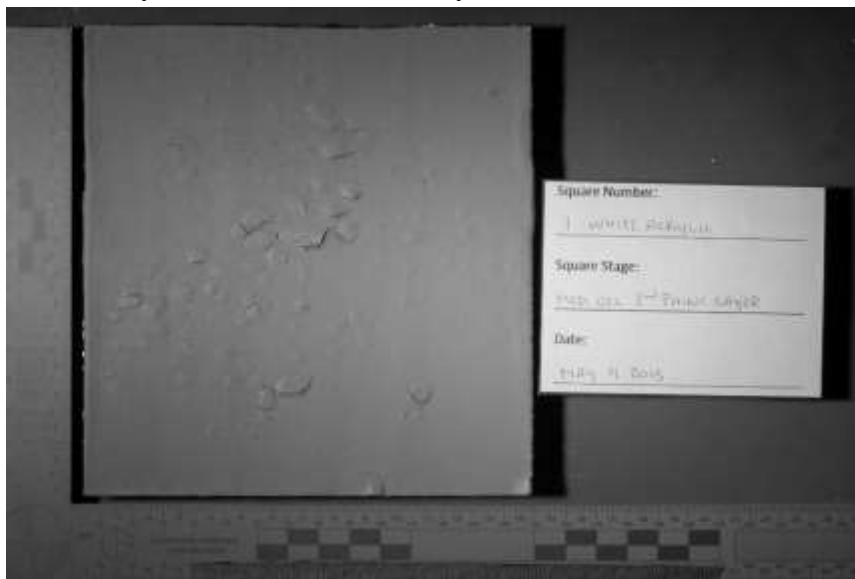


Longpass 89B Single Right Oblique

Appendix 4.3.4. Ultraviolet Photography

Appendix 4.3.4.1. White Acrylic Second layer of paint stage

White Acrylic 1 – Medium Velocity

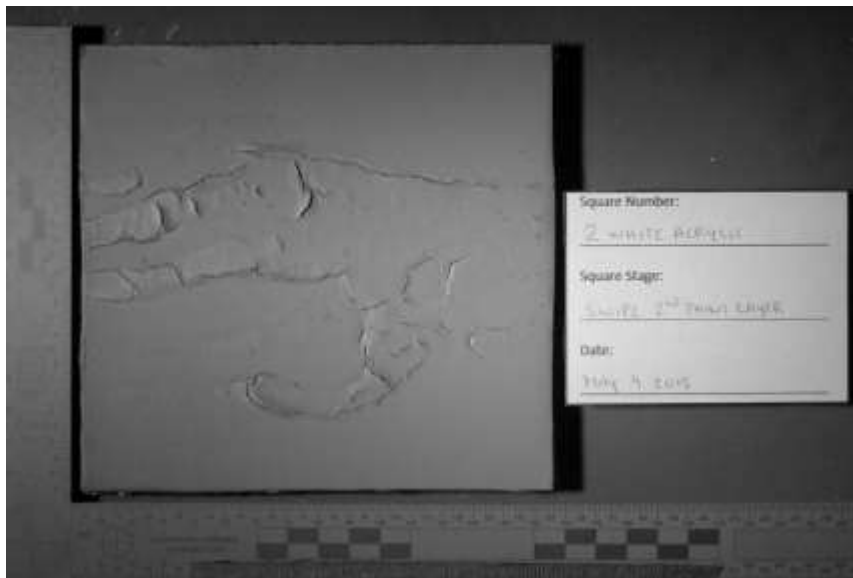


HDR



Single

White Acrylic 2 – Swipe

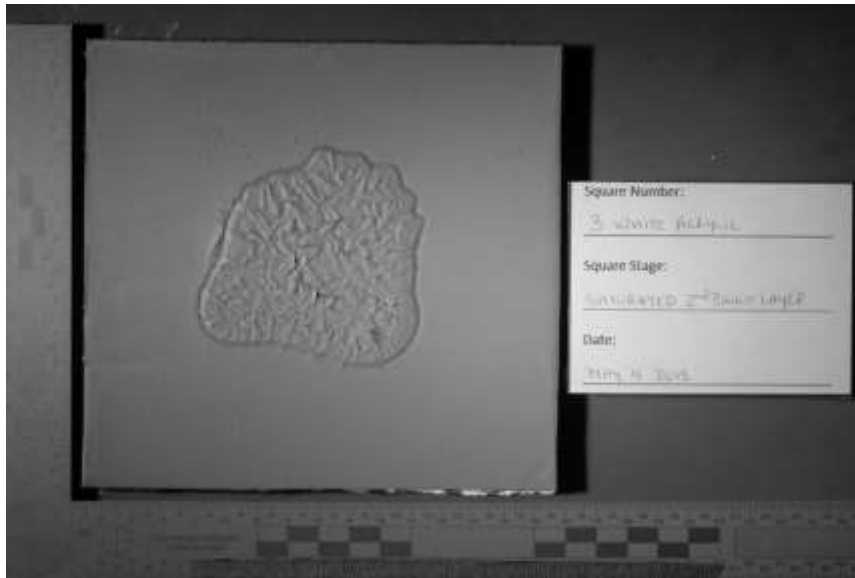


HDR

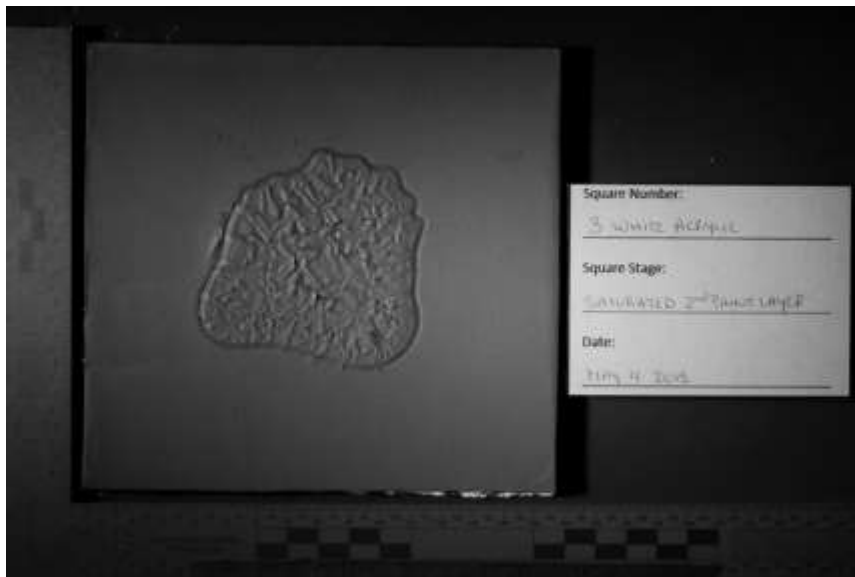


Single

White Acrylic 3 – Saturated



HDR



Single

Appendix 4.3.4.2. White Latex Second layer of paint stage
White Latex 5 – Medium Velocity



Square Number:
5 WHITE LATEX

Square Stage:
MED VEL 2ND COAT LAYER

Date:
MAY 9 2015

HDR



Square Number:
5 WHITE LATEX

Square Stage:
MED VEL 2ND COAT LAYER

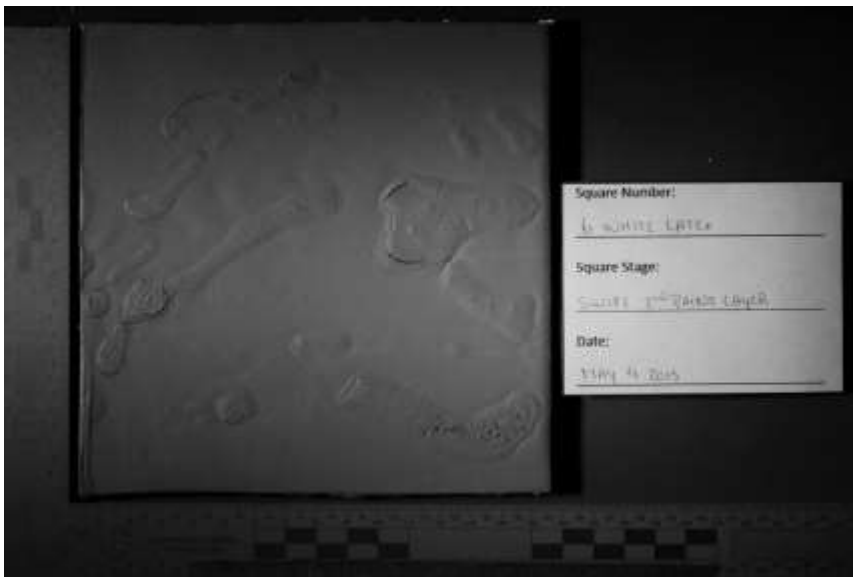
Date:
MAY 9 2015

Single

White Latex 6 – Swipe

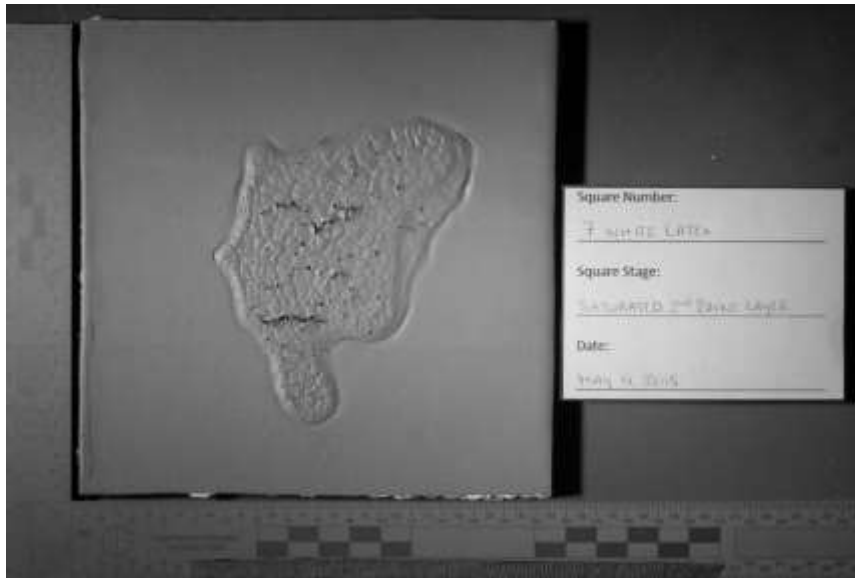


HDR

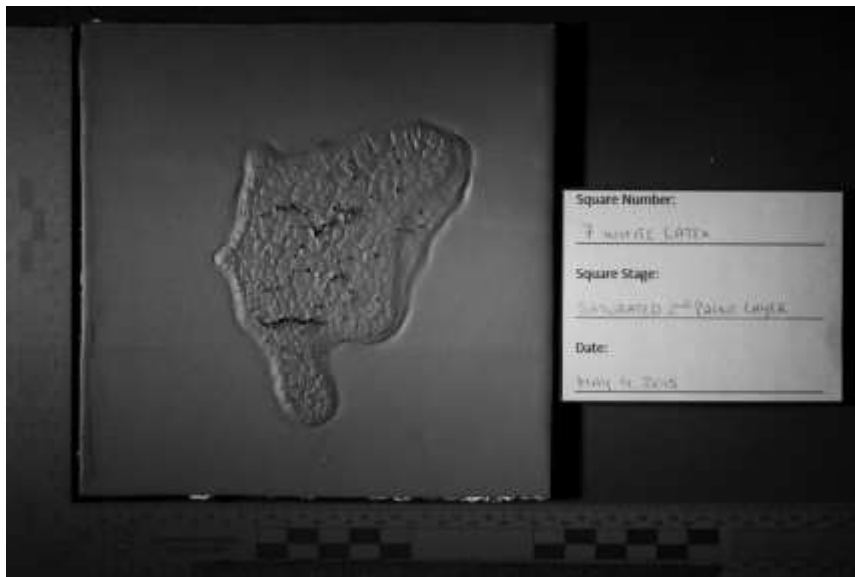


Single

White Latex 7 – Saturated



HDR



Single

Appendix 4.3.4.3. Black Latex Second layer of paint stage
Black Latex 9 – Medium Velocity

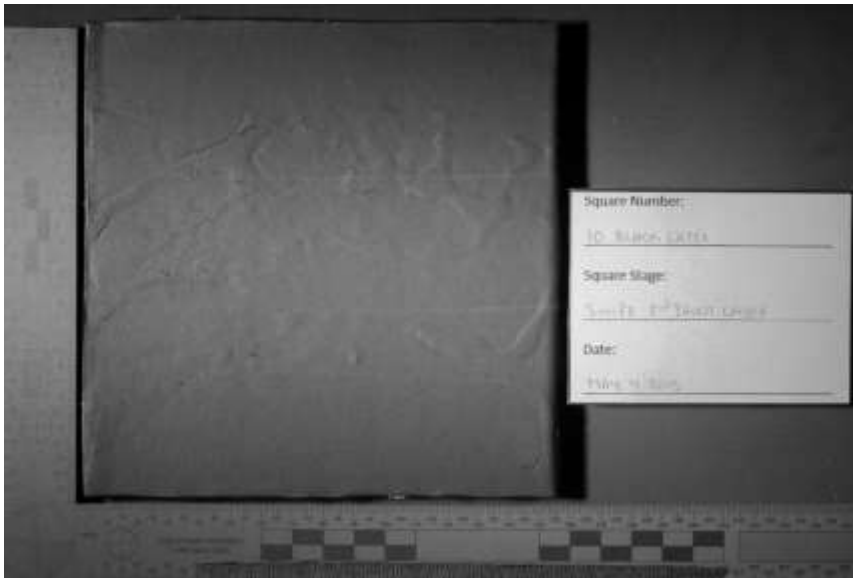


HDR



Single

Black Latex 10 – Swipe

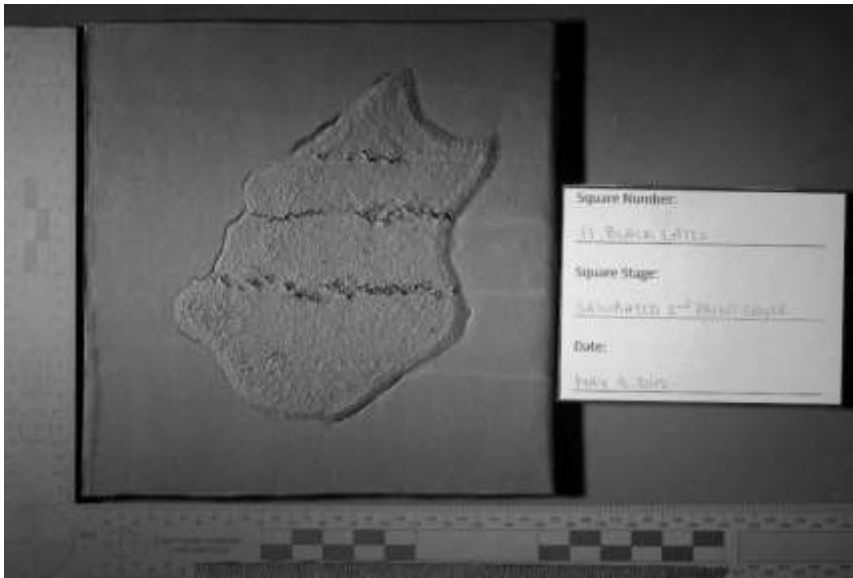


HDR



Single

Black Latex 11 – Saturated



HDR

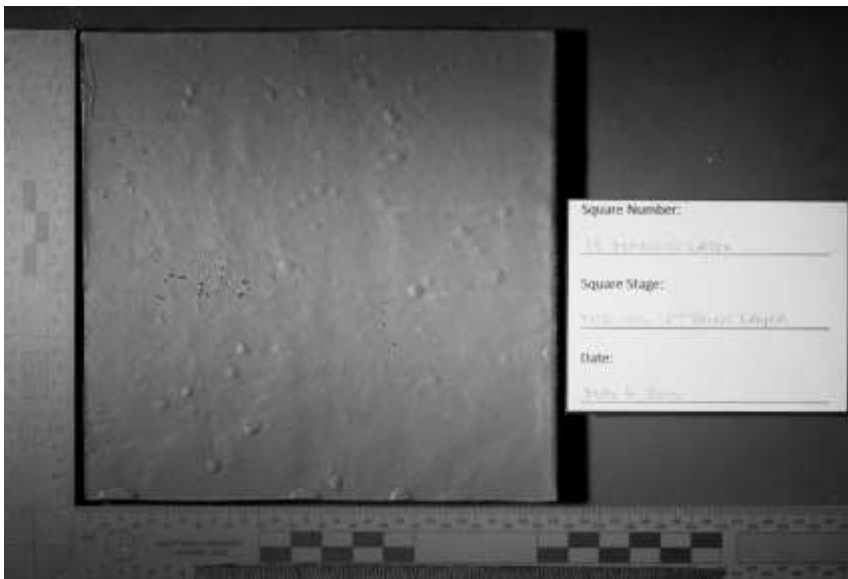


Single

Appendix 4.3.4.4. Maroon Latex Second layer of paint stage
Maroon Latex 13 – Medium Velocity

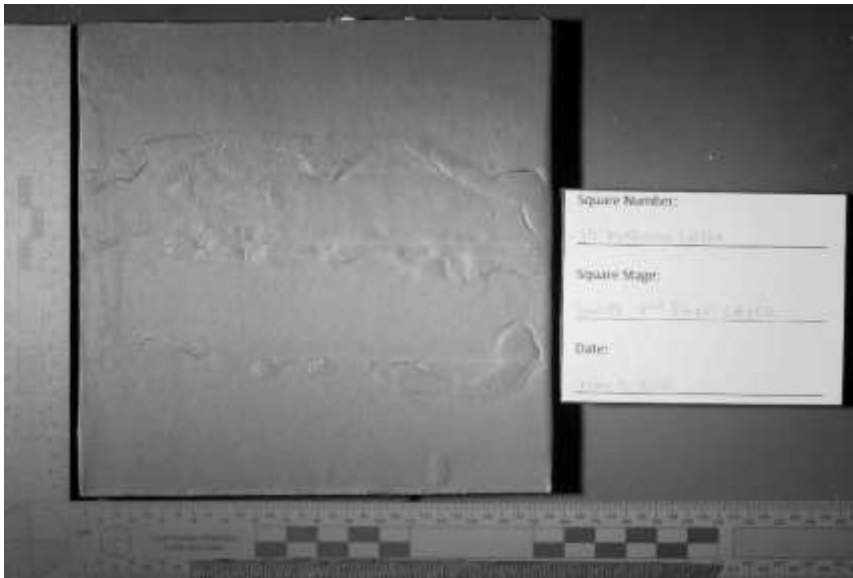


HDR

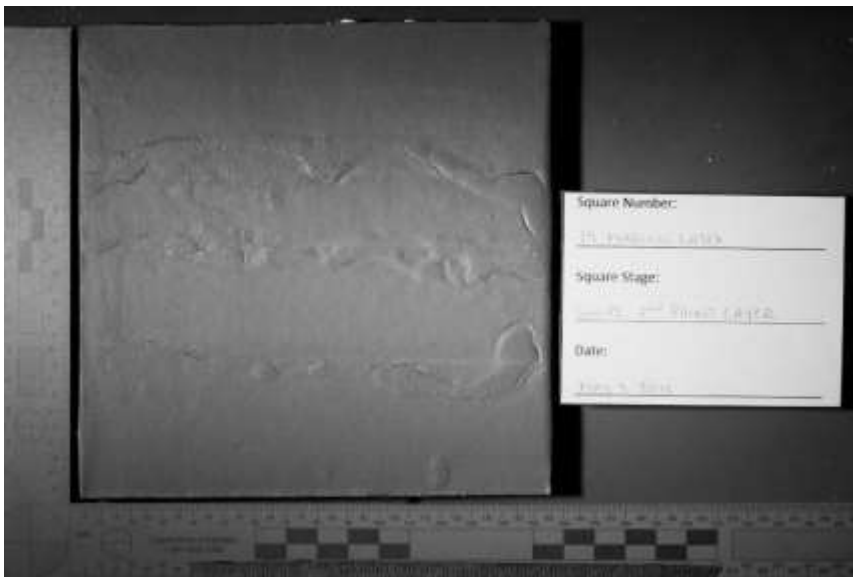


Single

Maroon Latex 14 – Swipe



HDR

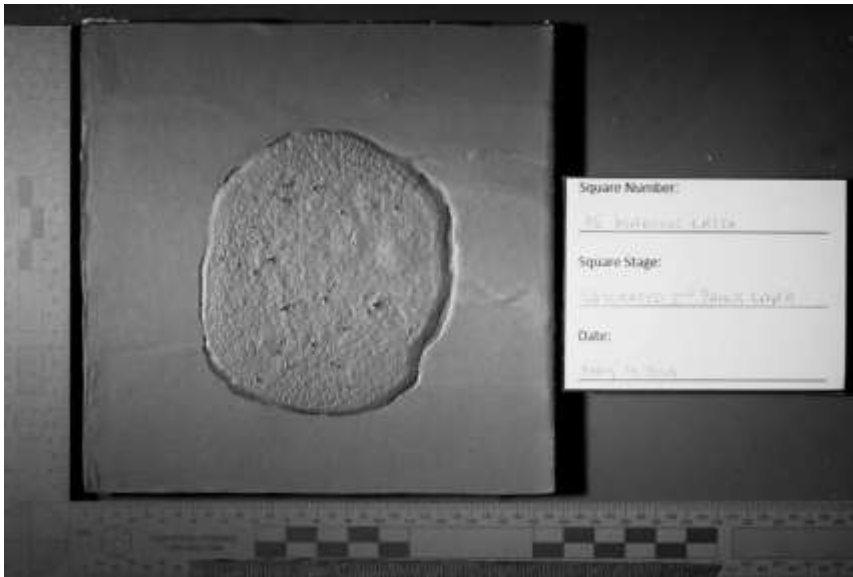


Single

Maroon Latex 15 – Saturated



HDR

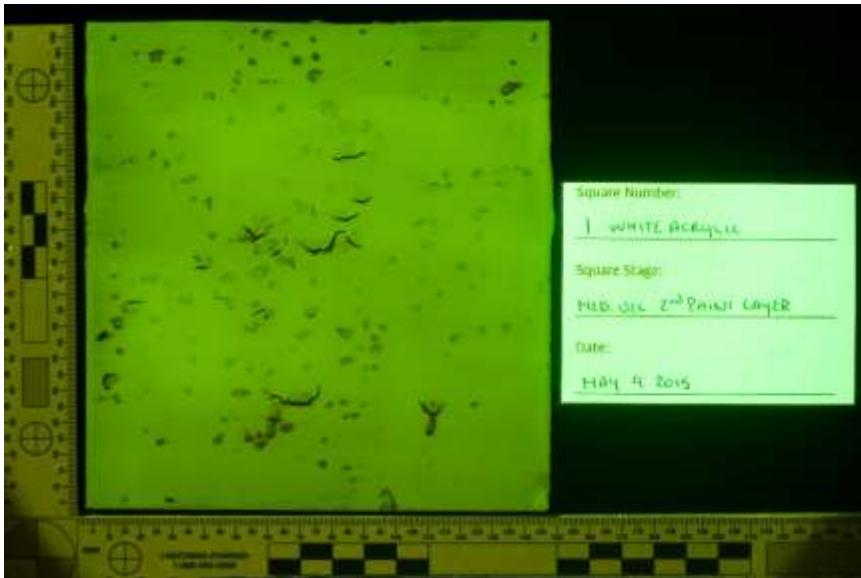


Single

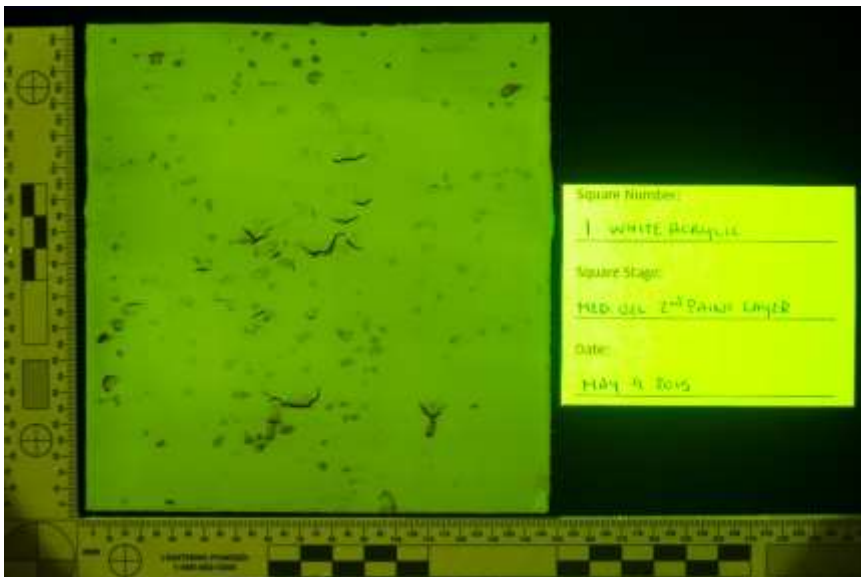
Appendix 4.3.5. Fluorescence Photography

Appendix 4.3.5.1. White Acrylic – Yellow 415nm, 445nm, 455nm; Orange 415nm, 445nm, 455nm, 475nm, 495nm; Red 415nm, 445nm, 455nm, 475nm, 575nm Second layer of paint stage

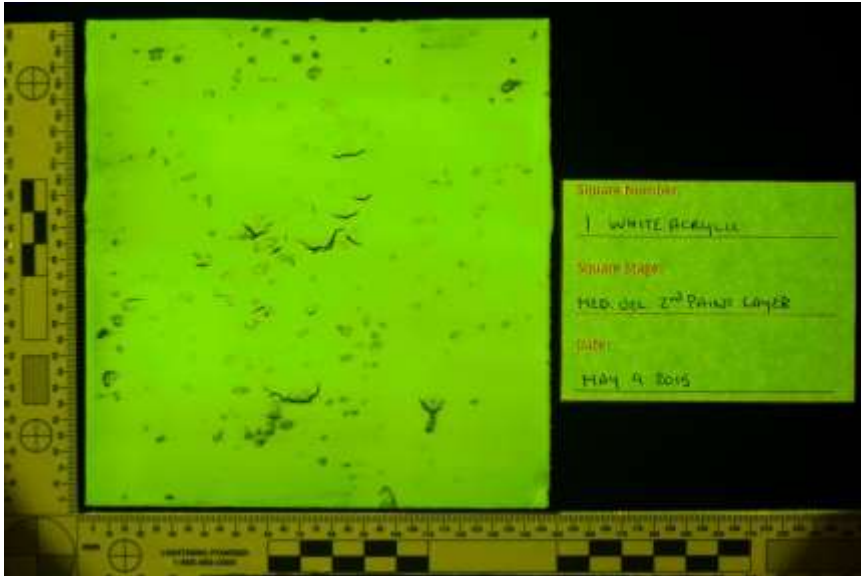
White Acrylic 1 – Medium Velocity



Yellow 415nm HDR



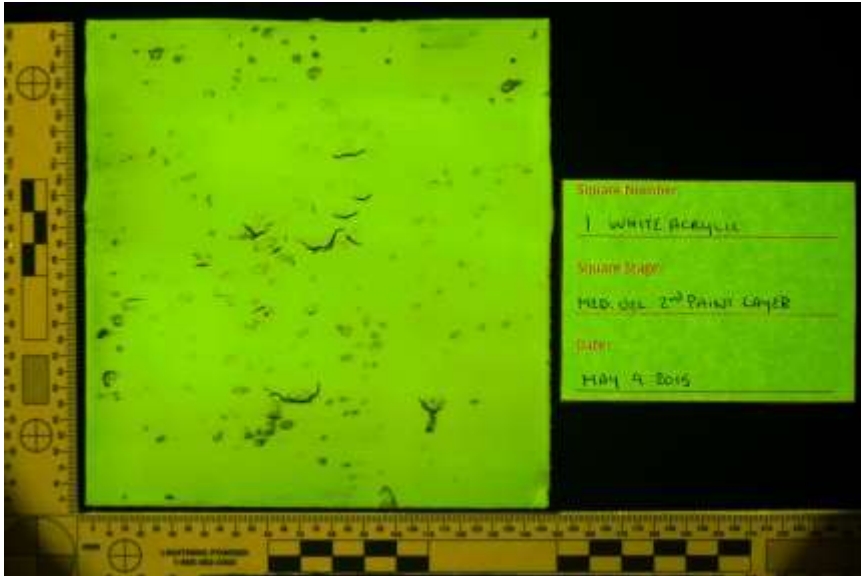
Yellow 415nm Single



Yellow 445nm HDR



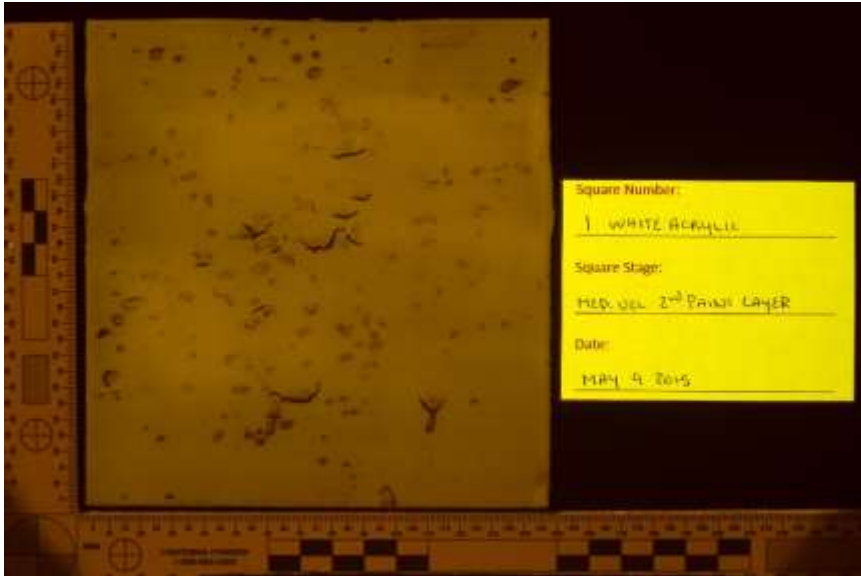
Yellow 445nm Single



Yellow 455nm HDR



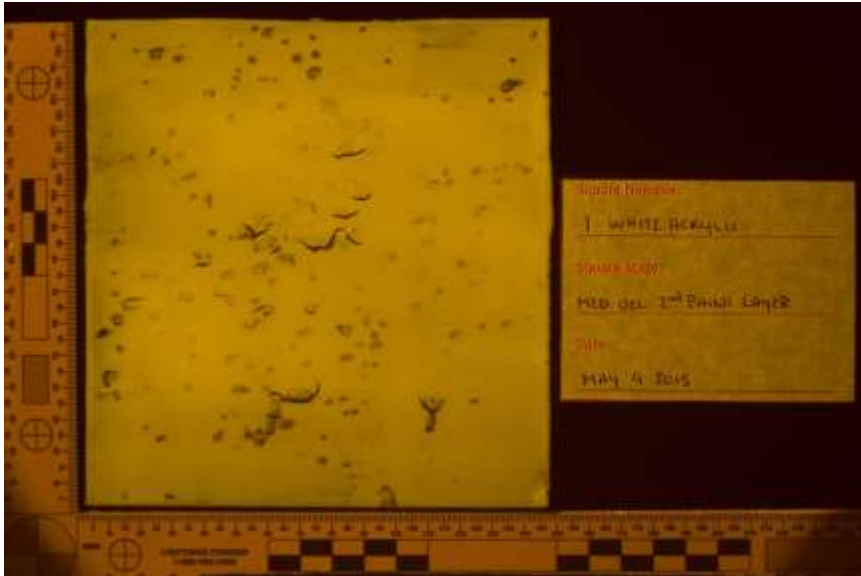
Yellow 455nm Single



Orange 415nm HDR



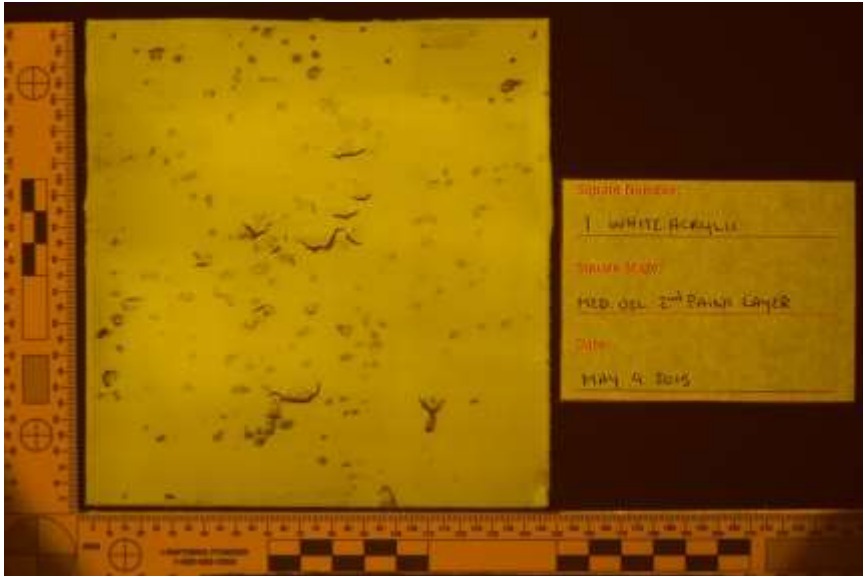
Orange 415nm Single



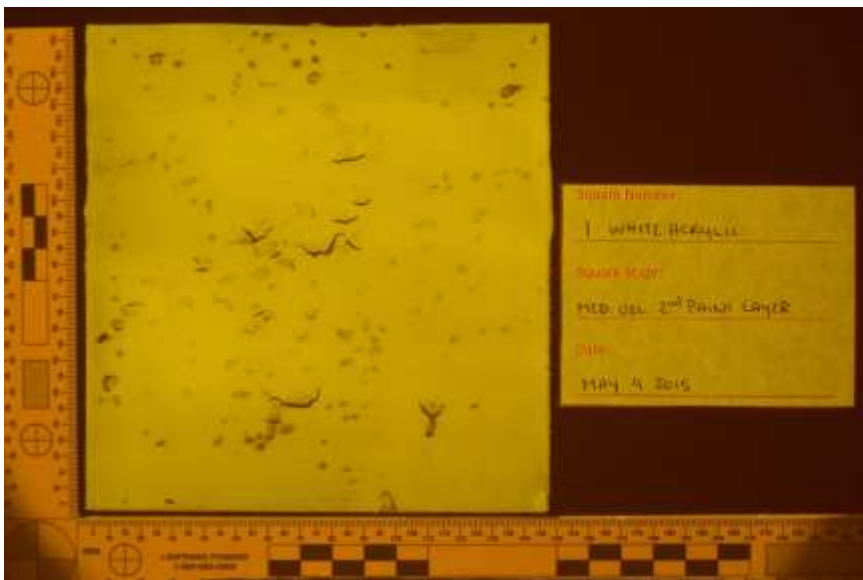
Orange 445nm HDR



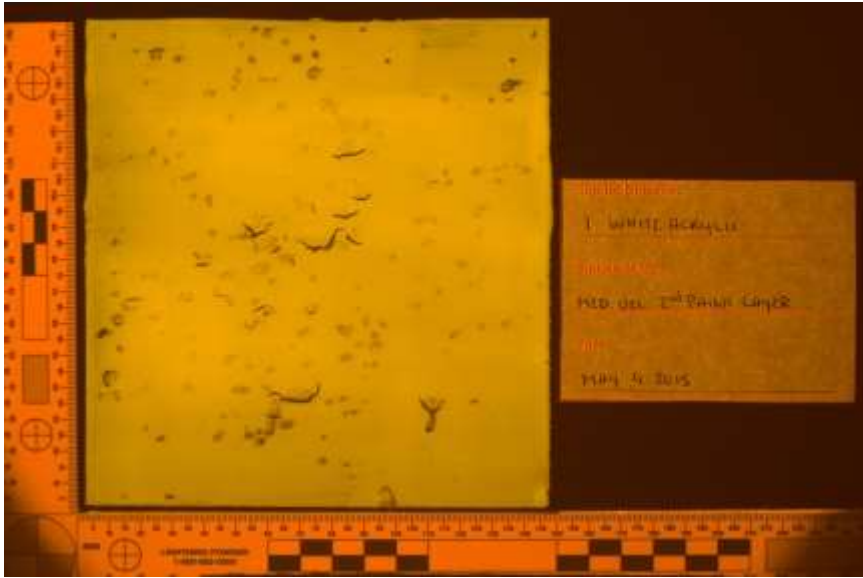
Orange 445nm Single



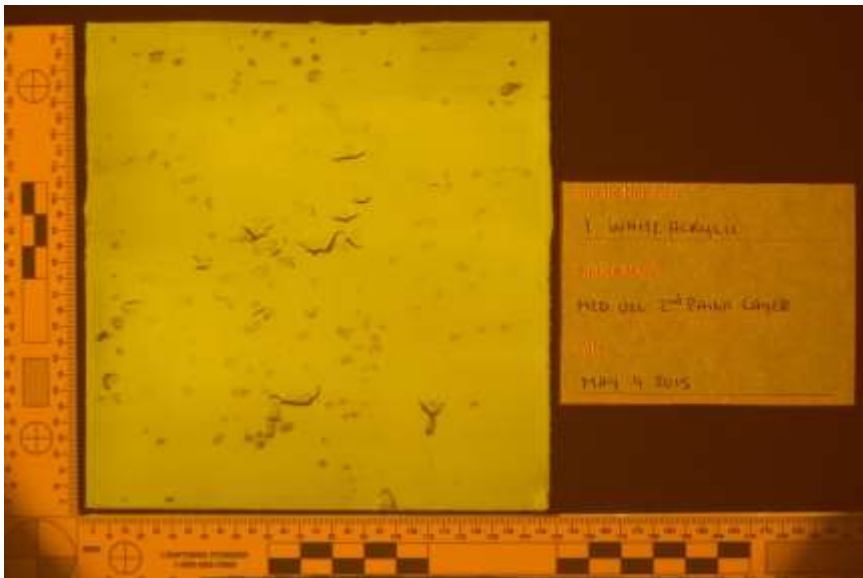
Orange 455nm HDR



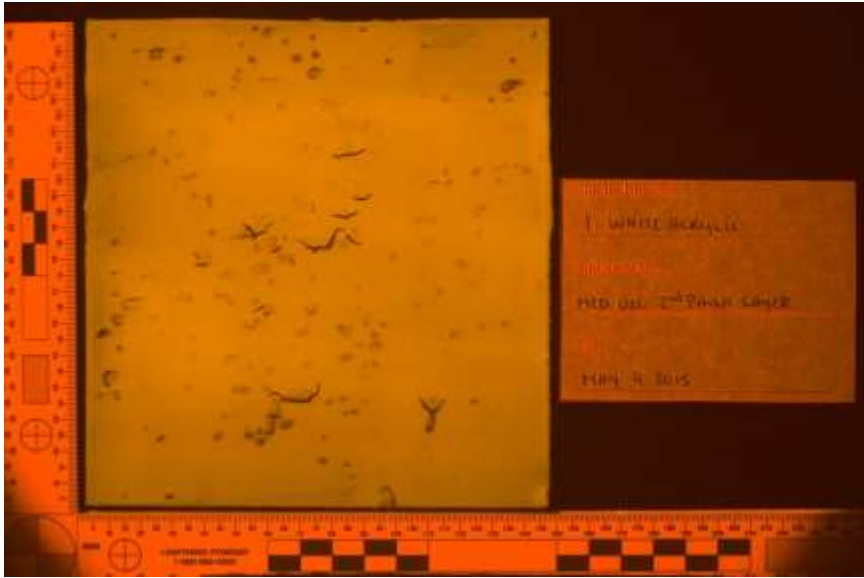
Orange 455nm Single



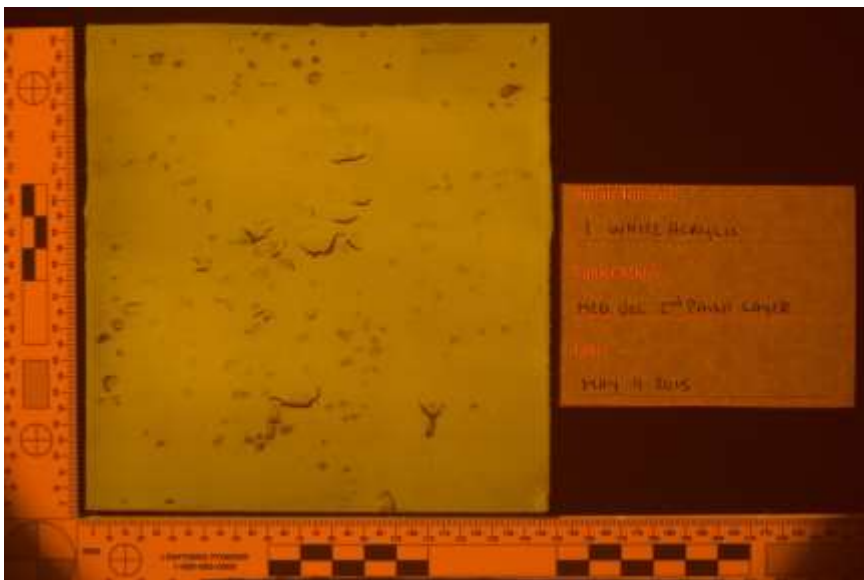
Orange 475nm HDR



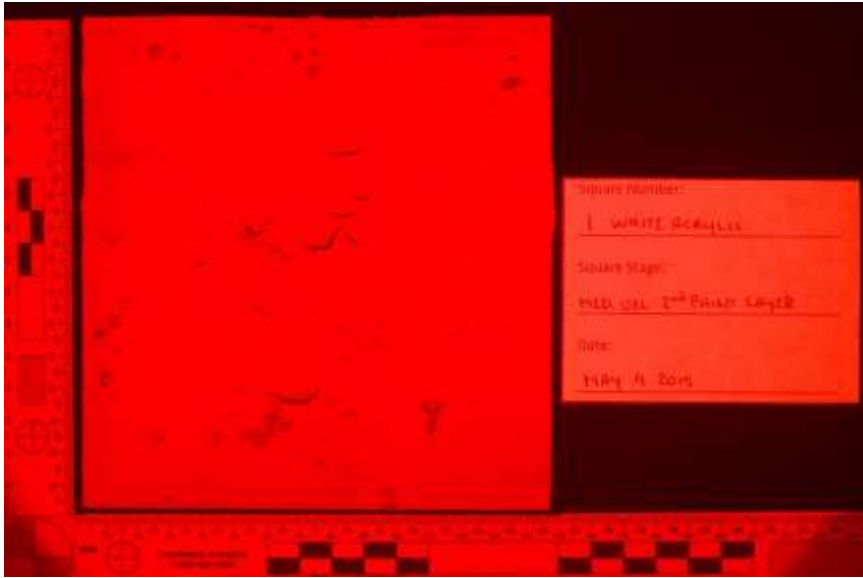
Orange 475nm Single



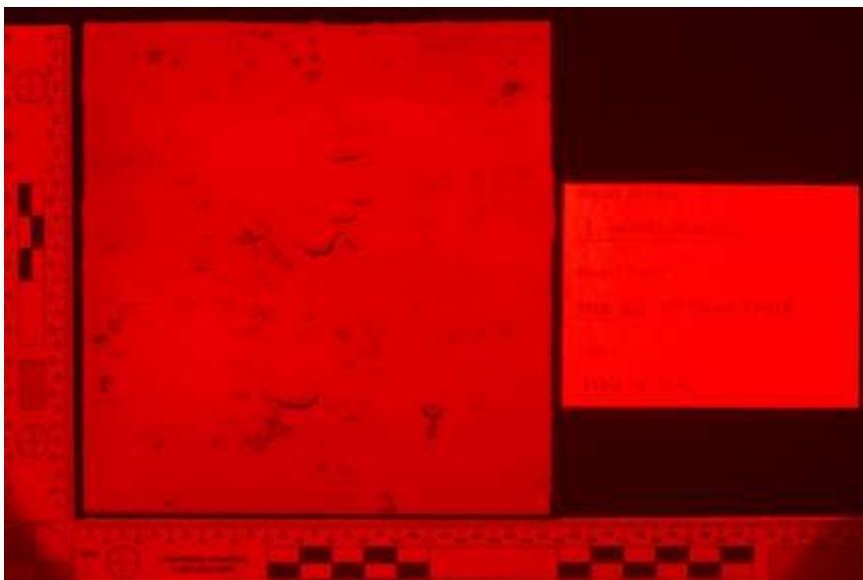
Orange 495nm HDR



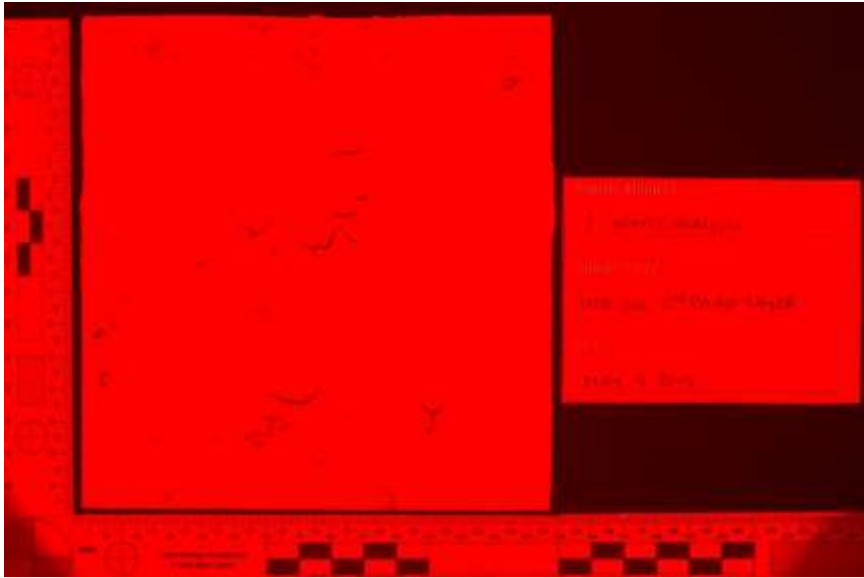
Orange 495nm Single



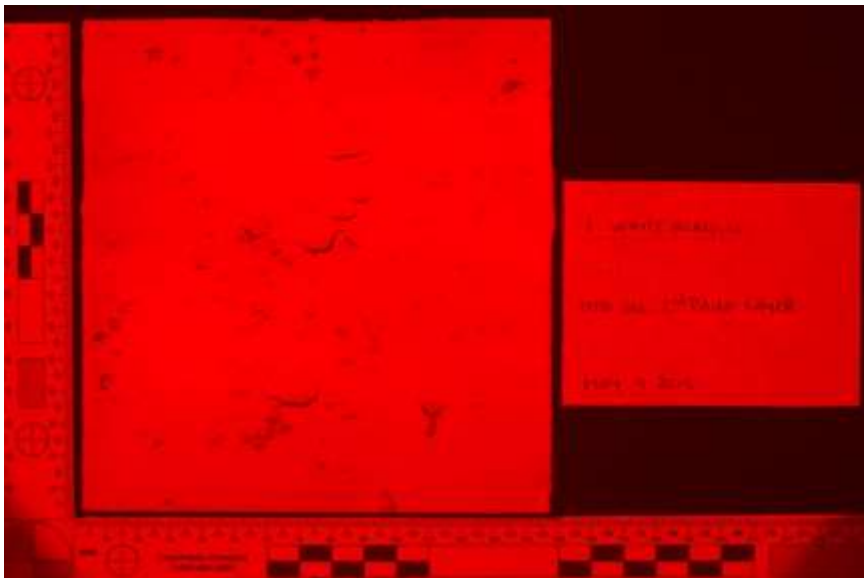
Red 415nm HDR



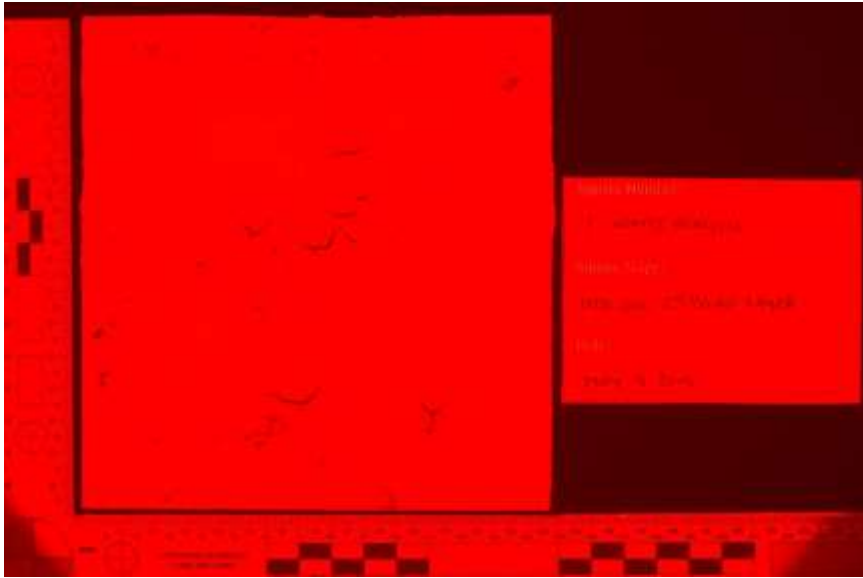
Red 415nm Single



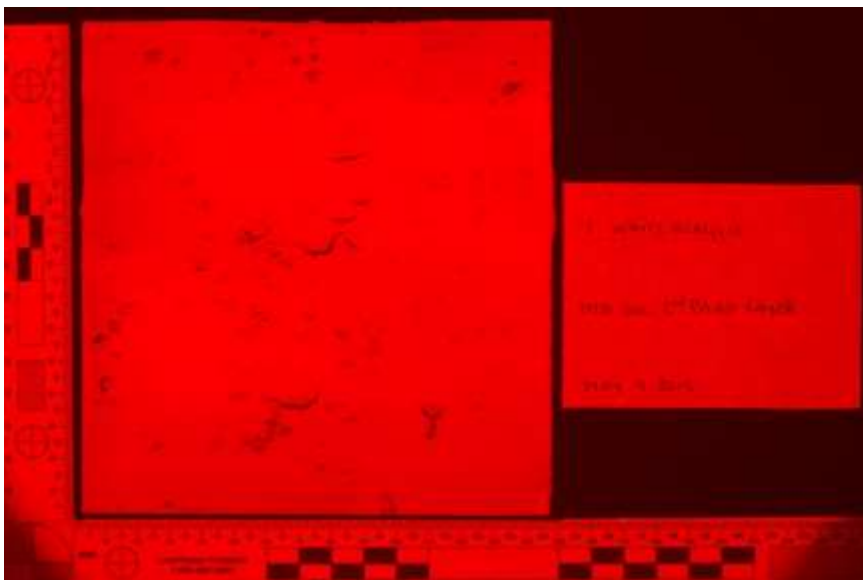
Red 445nm HDR



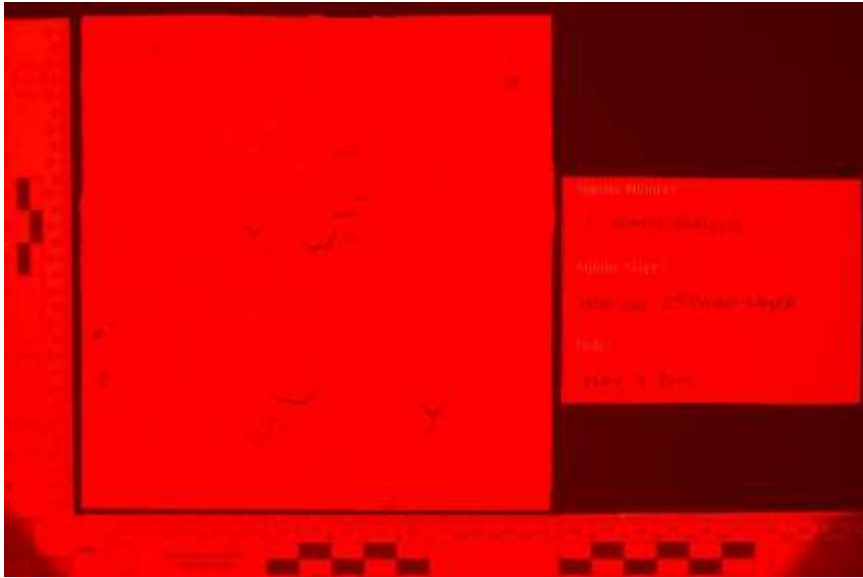
Red 445nm Single



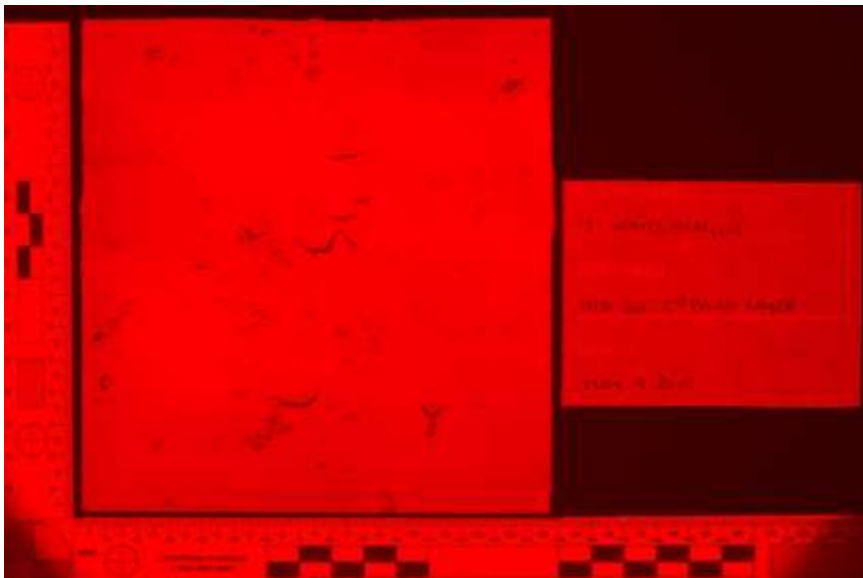
Red 455nm HDR



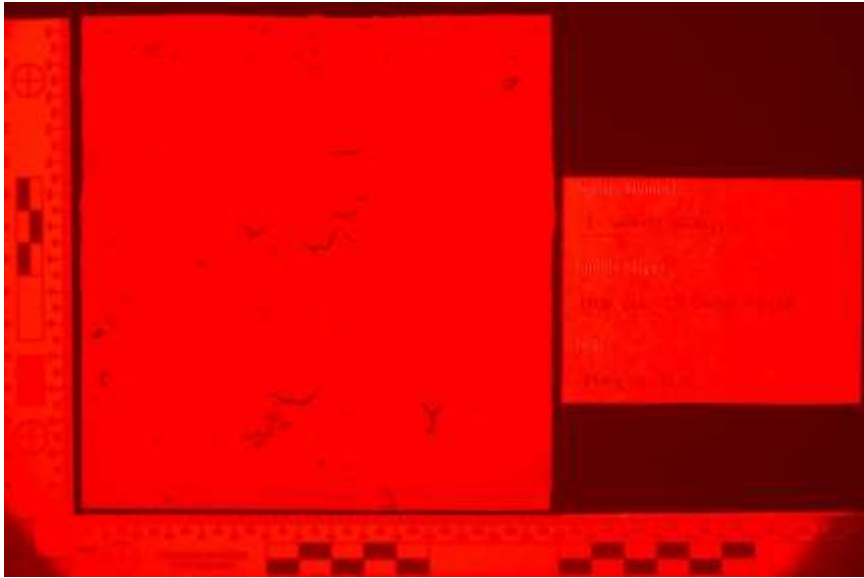
Red 455nm Single



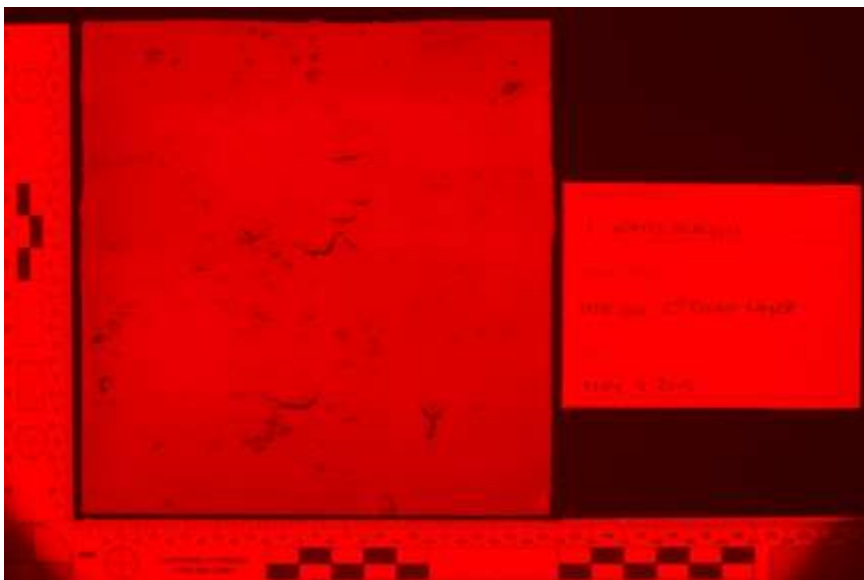
Red 475nm HDR



Red 475nm Single

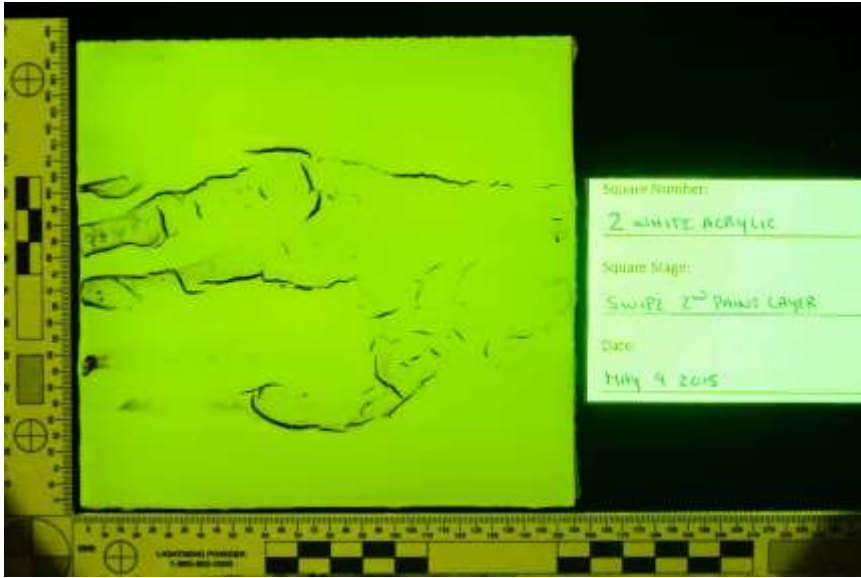


Red 575nm HDR



Red 575nm Single

White Acrylic 2 – Swipe



Yellow 415nm HDR



Yellow 415nm Single



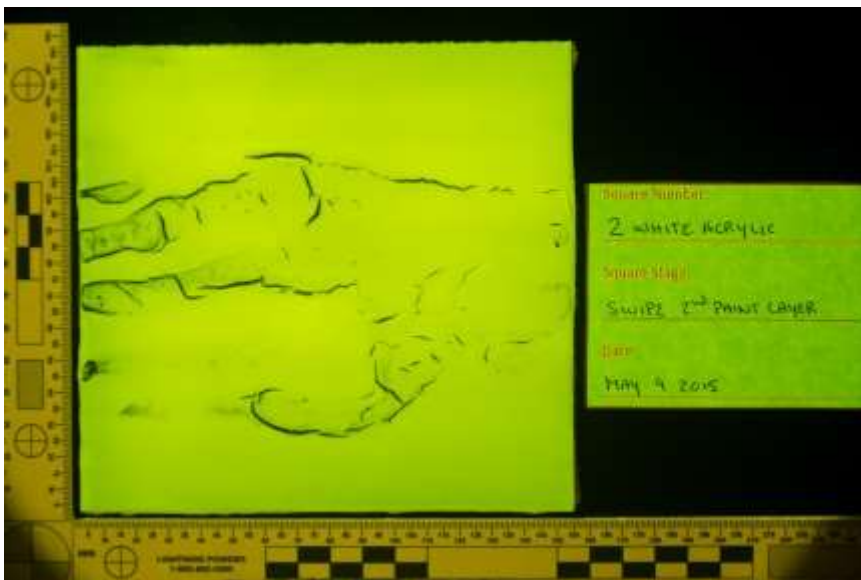
Yellow 445nm HDR



Yellow 445nm Single



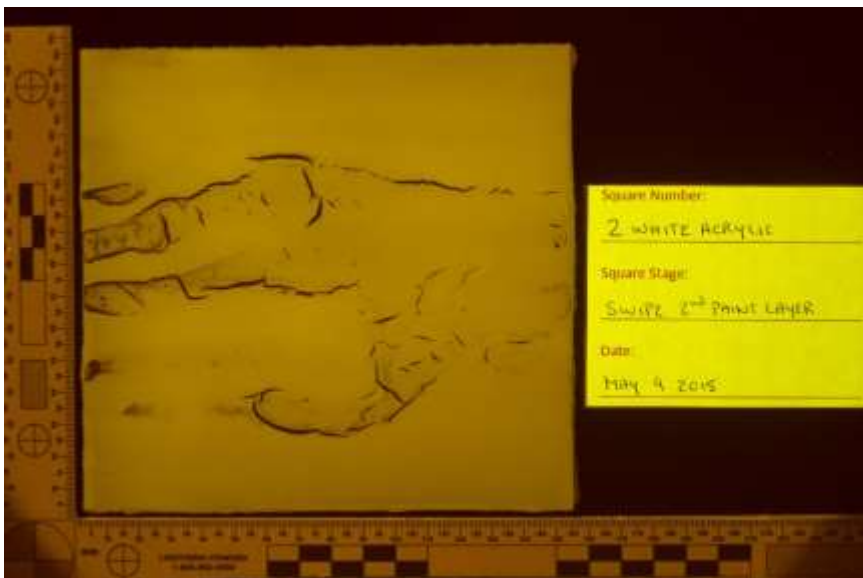
Yellow 455nm HDR



Yellow 455nm Single



Orange 415nm HDR



Orange 415nm Single



Orange 445nm HDR



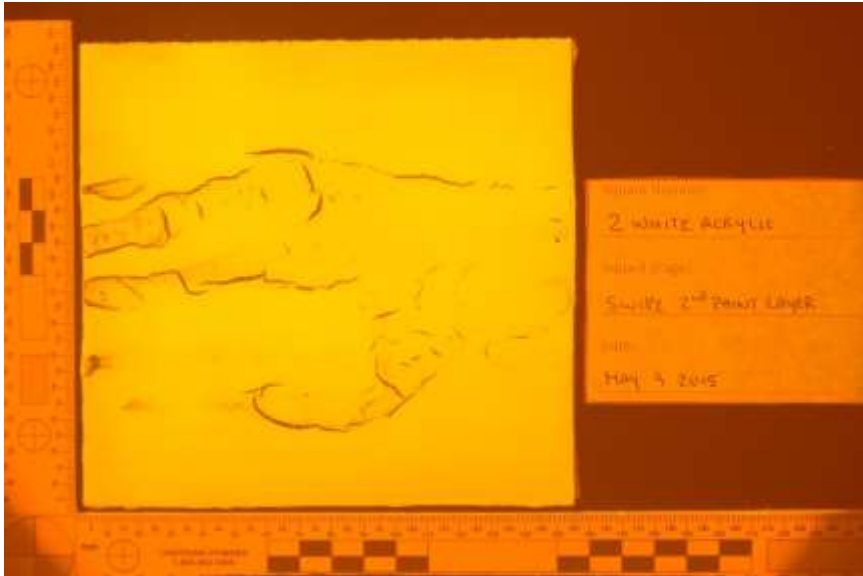
Orange 445nm Single



Orange 455nm HDR



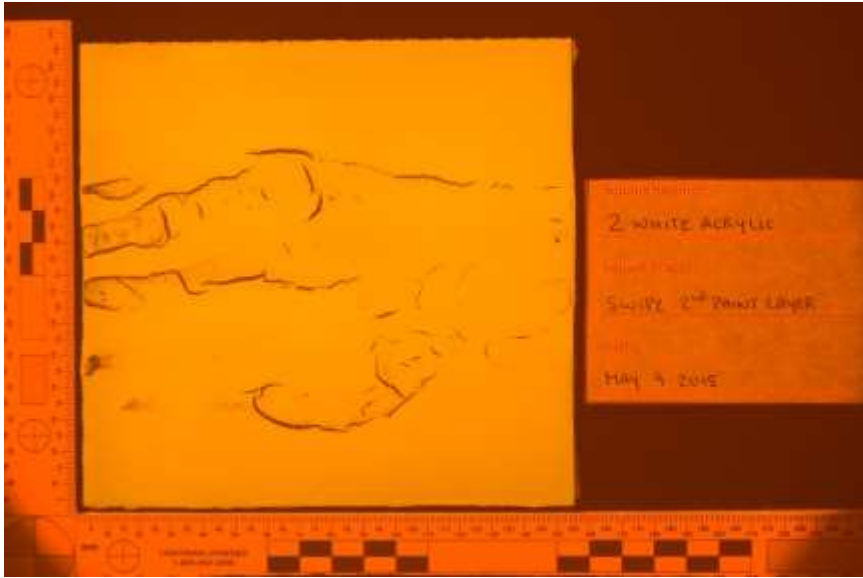
Orange 455nm Single



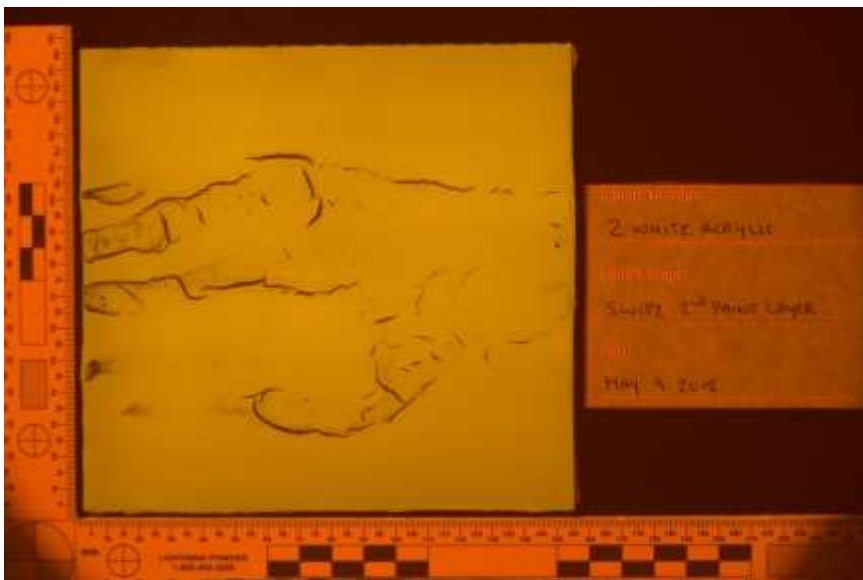
Orange 475nm HDR



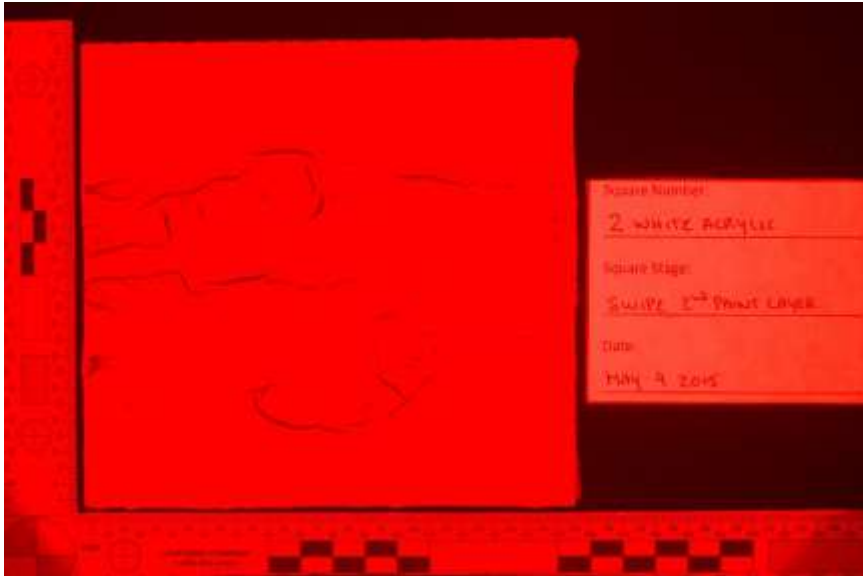
Orange 475nm Single



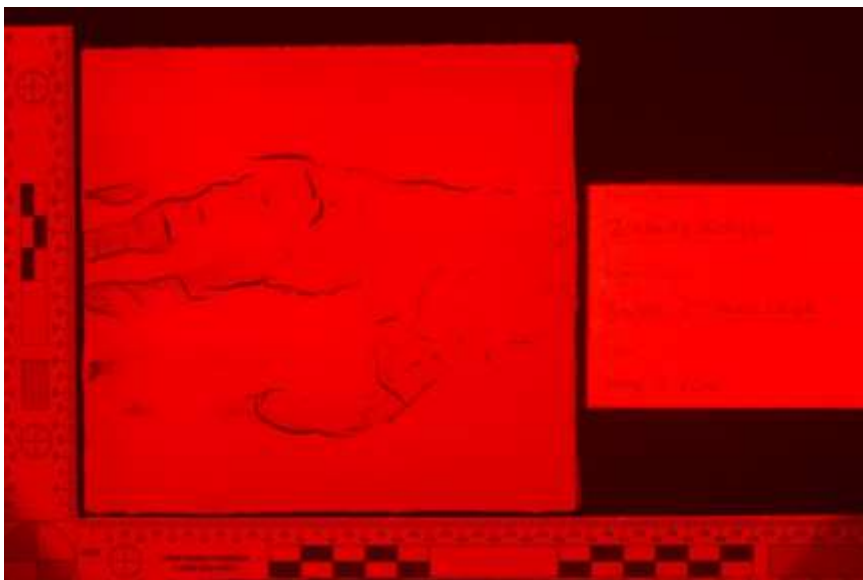
Orange 495nm HDR



Orange 495nm Single



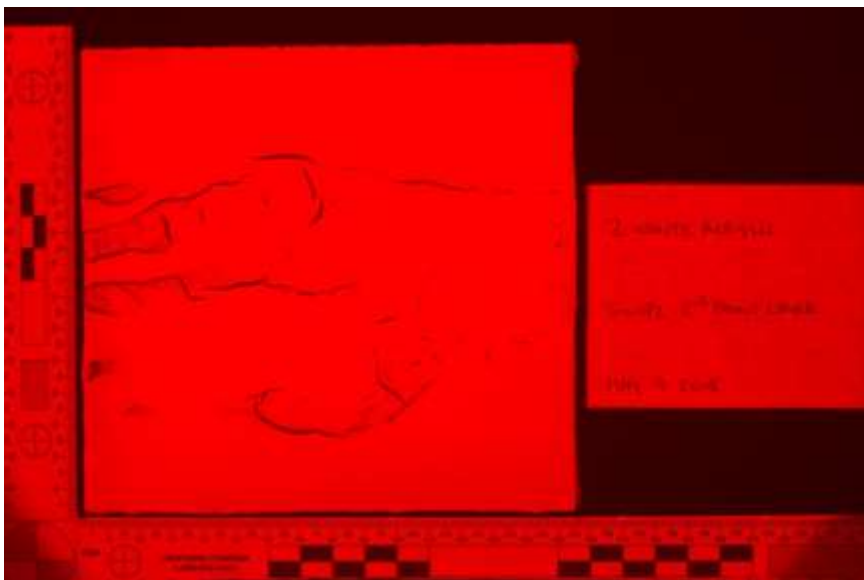
Red 415nm HDR



Red 415nm Single



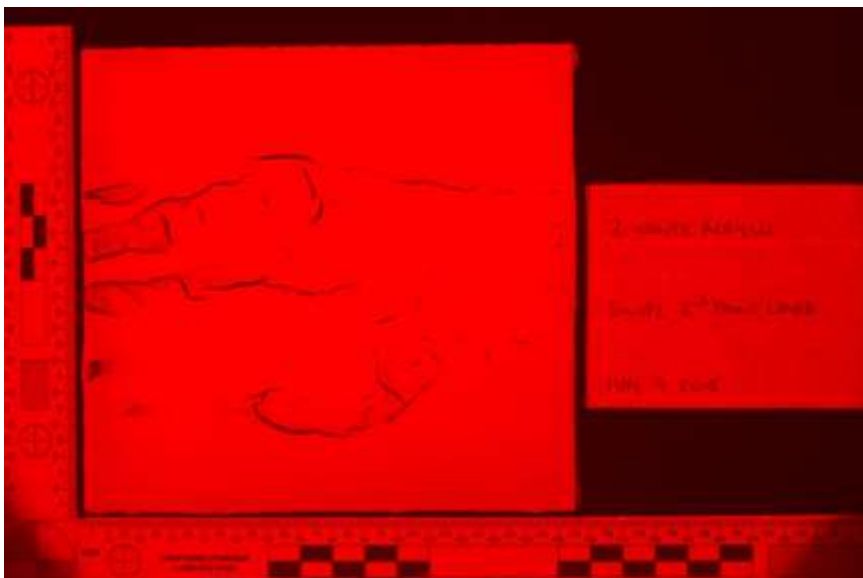
Red 445nm HDR



Red 445nm Single



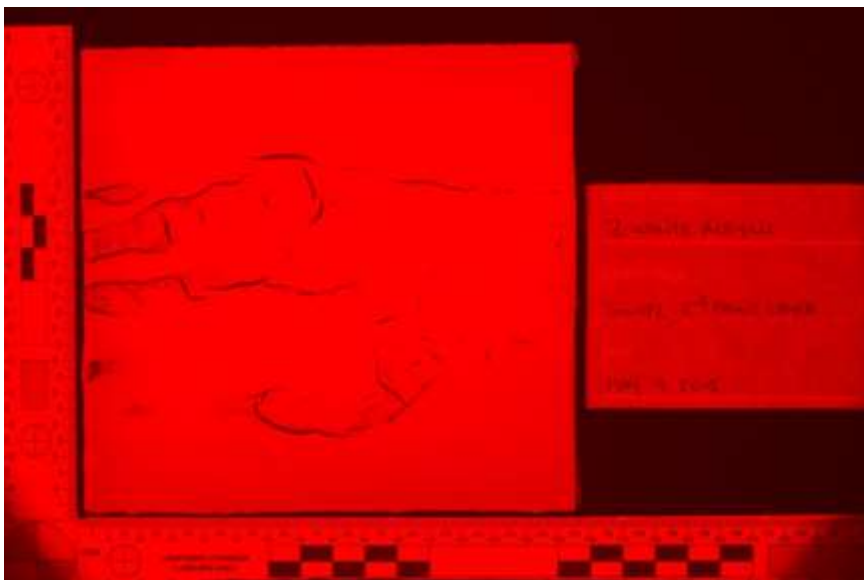
Red 455nm HDR



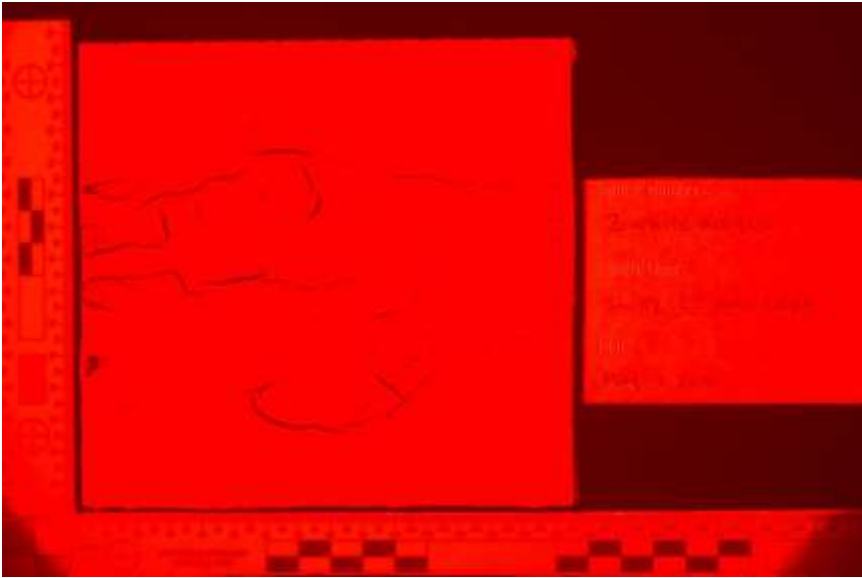
Red 455nm Single



Red 475nm HDR



Red 475nm Single



Red 575nm HDR



Red 575nm Single

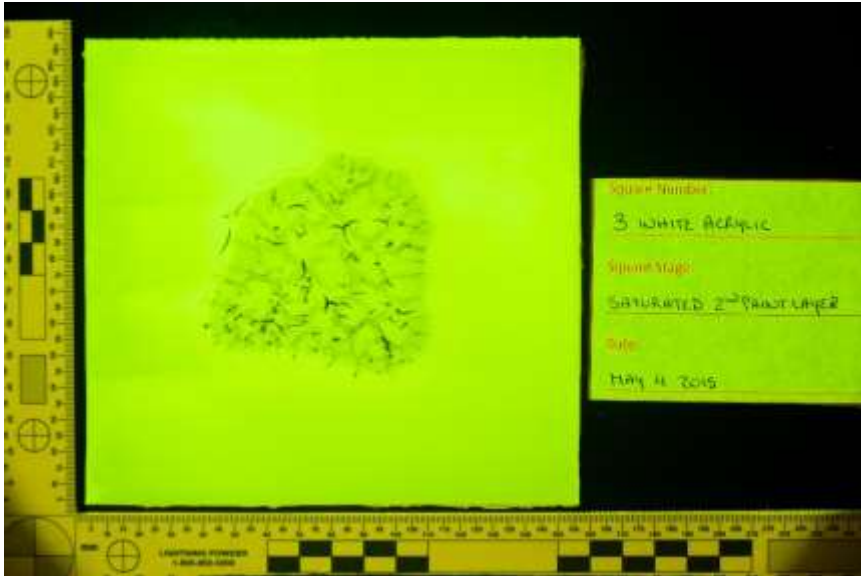
White Acrylic 3 – Saturated



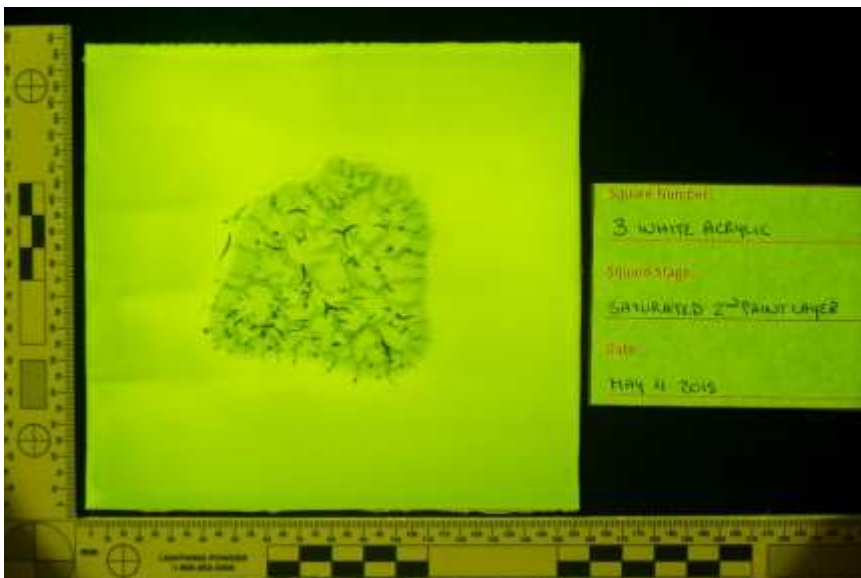
Yellow 415nm HDR



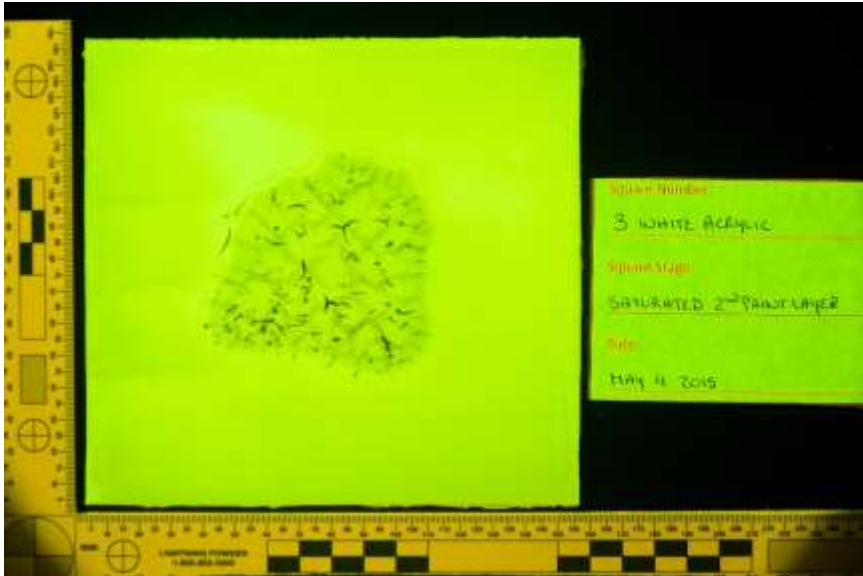
Yellow 415nm Single



Yellow 445nm HDR



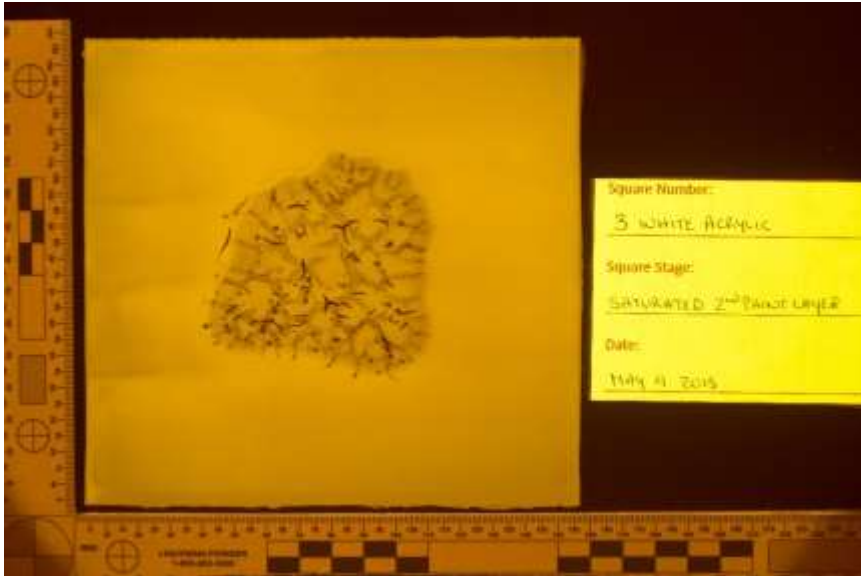
Yellow 445nm Single



Yellow 455nm HDR



Yellow 455nm Single



Orange 415nm HDR



Orange 415nm Single



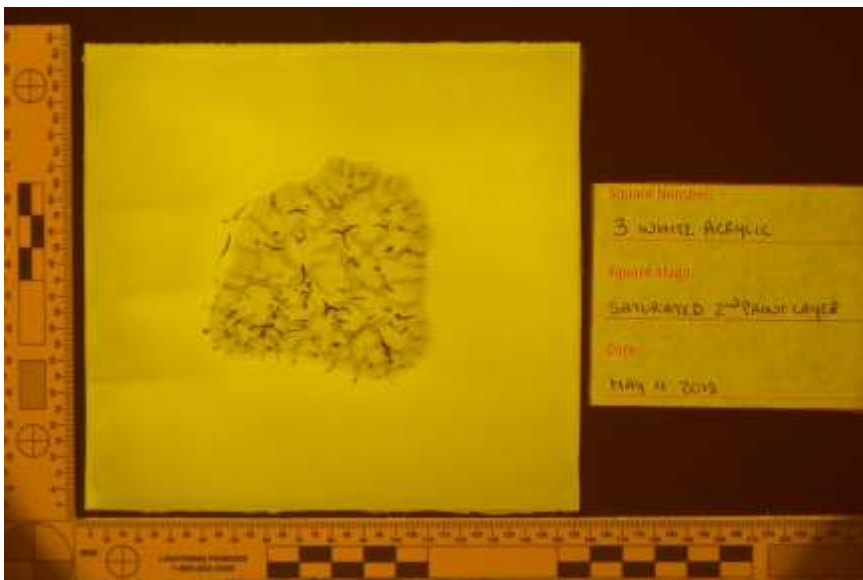
Orange 445nm HDR



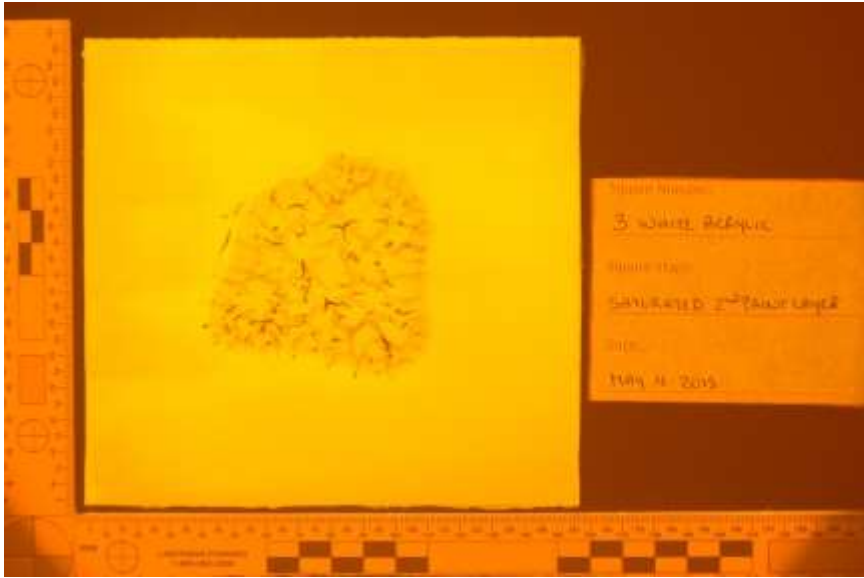
Orange 445nm Single



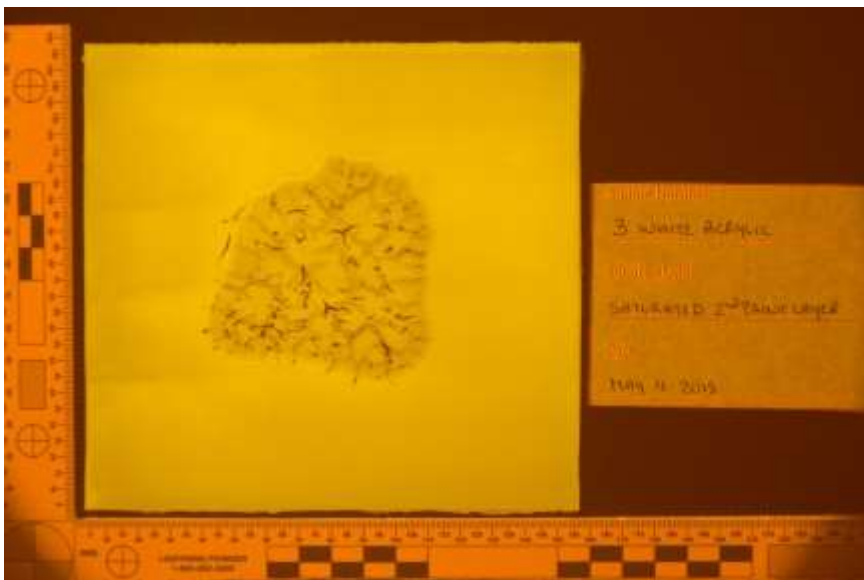
Orange 455nm HDR



Orange 455nm Single



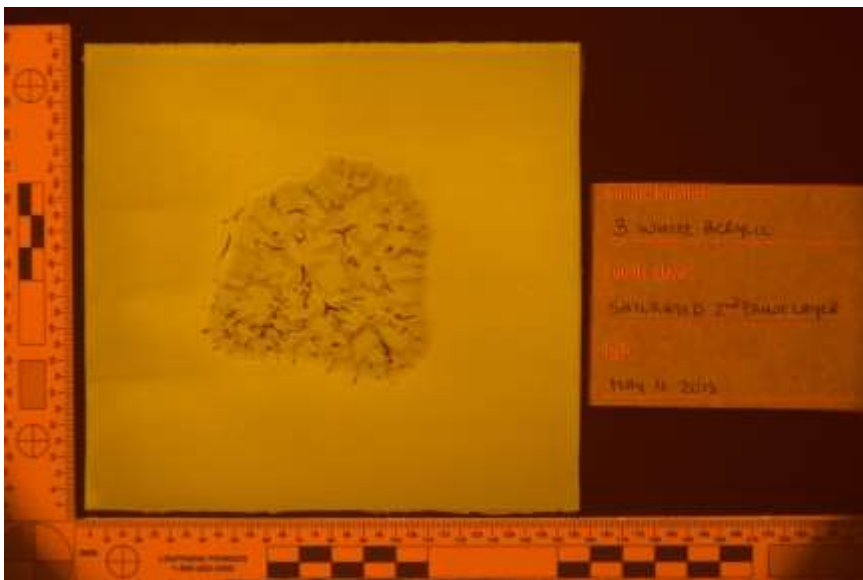
Orange 475nm HDR



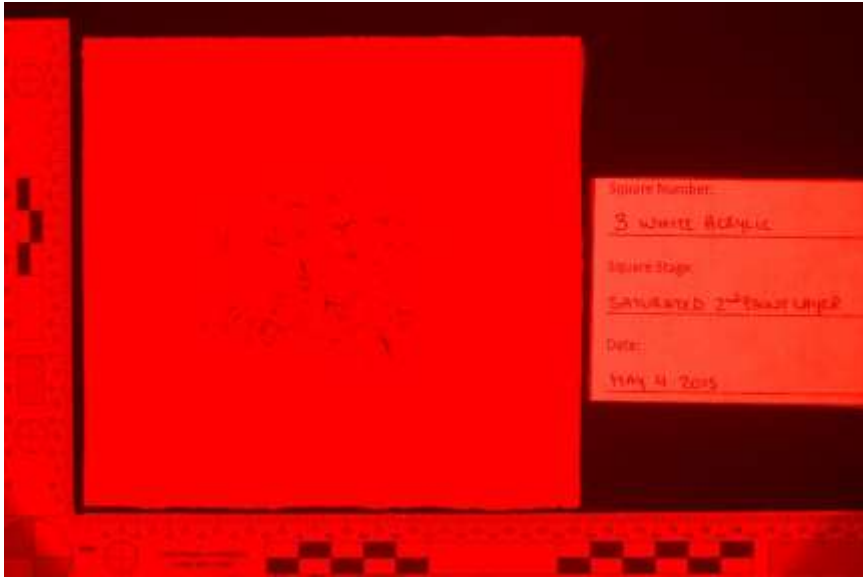
Orange 475nm Single



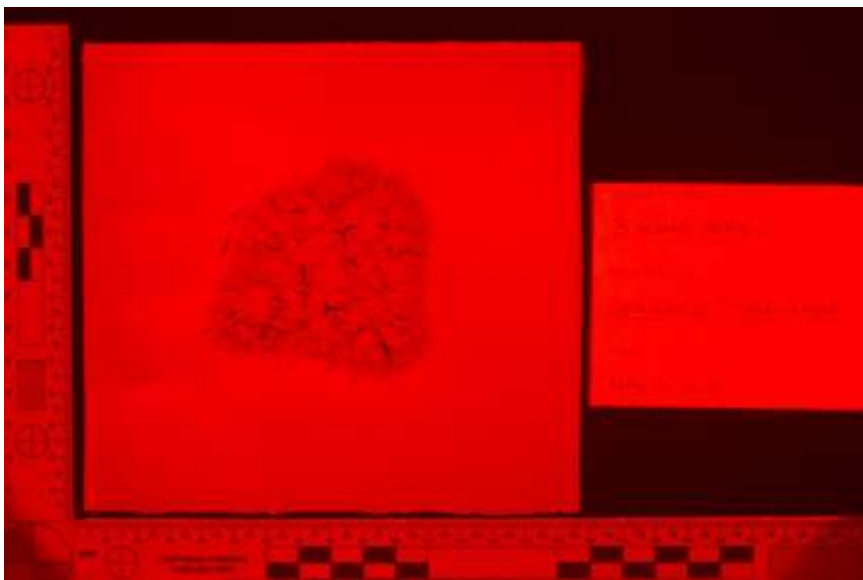
Orange 495nm HDR



Orange 495nm Single



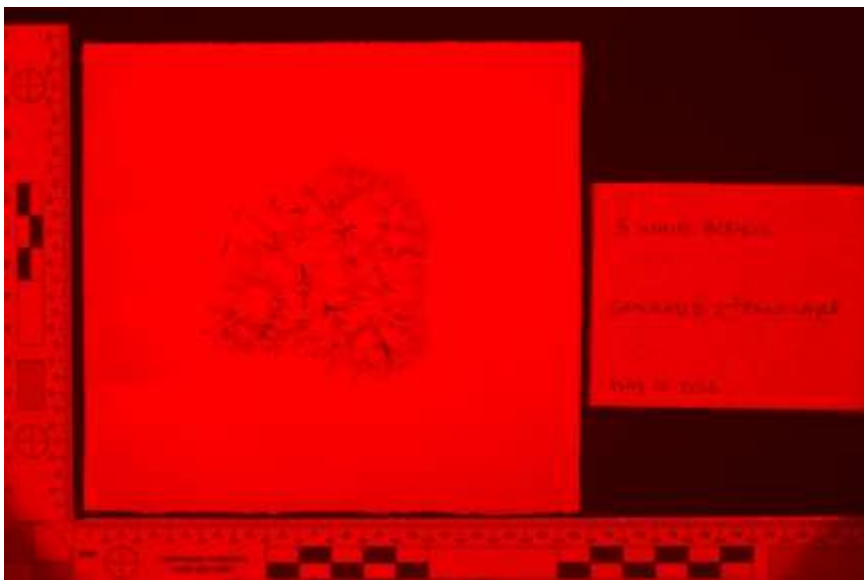
Red 415nm HDR



Red 415nm Single



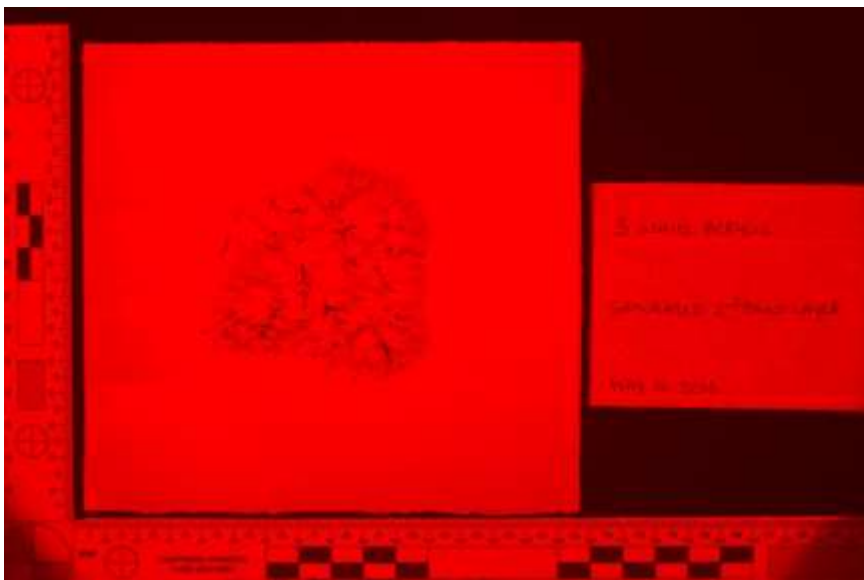
Red 445nm HDR



Red 445nm Single



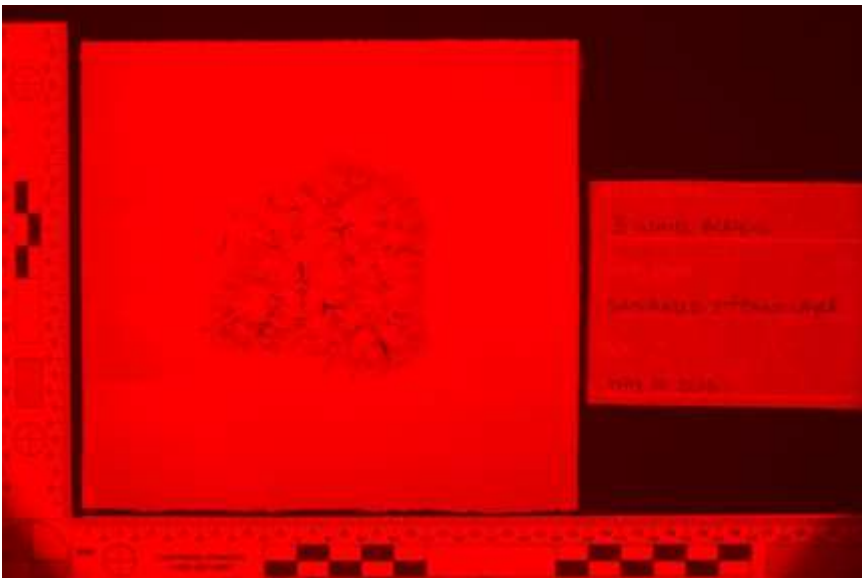
Red 455nm HDR



Red 455nm Single



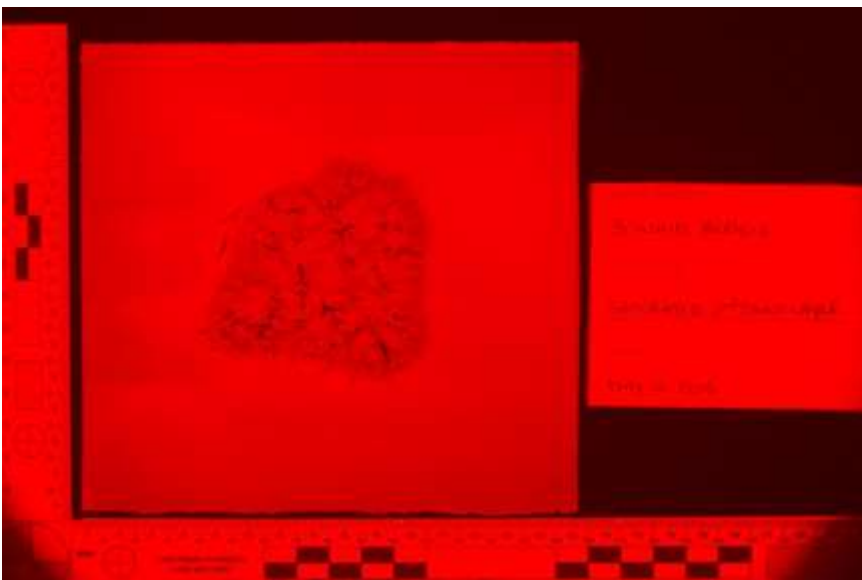
Red 475nm HDR



Red 475nm Single



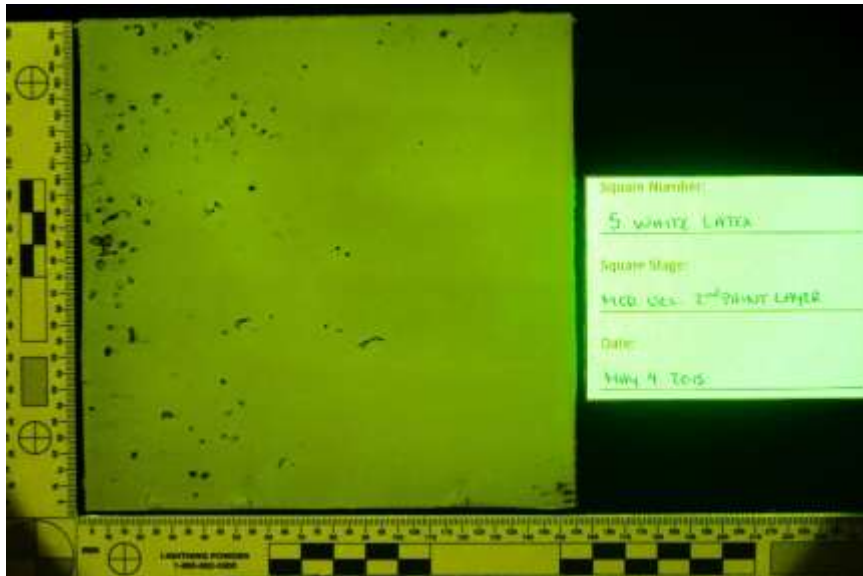
Red 575nm HDR



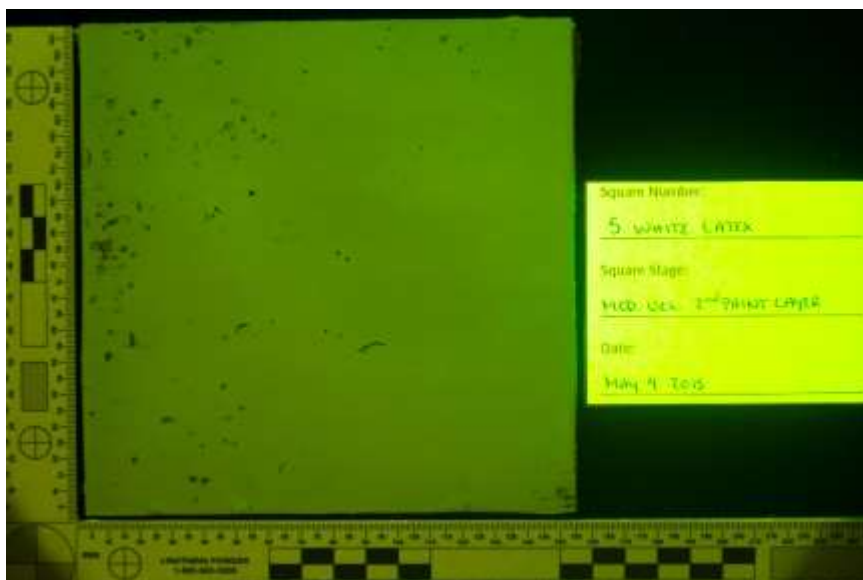
Red 575nm Single

Appendix 4.3.5.2. White Latex – Yellow 415nm, 445nm, 455nm; Orange 415nm, 445nm, 455nm, 475nm, 495nm; Red 415nm, 445nm, 455nm, 475nm, 575nm Second layer of paint stage

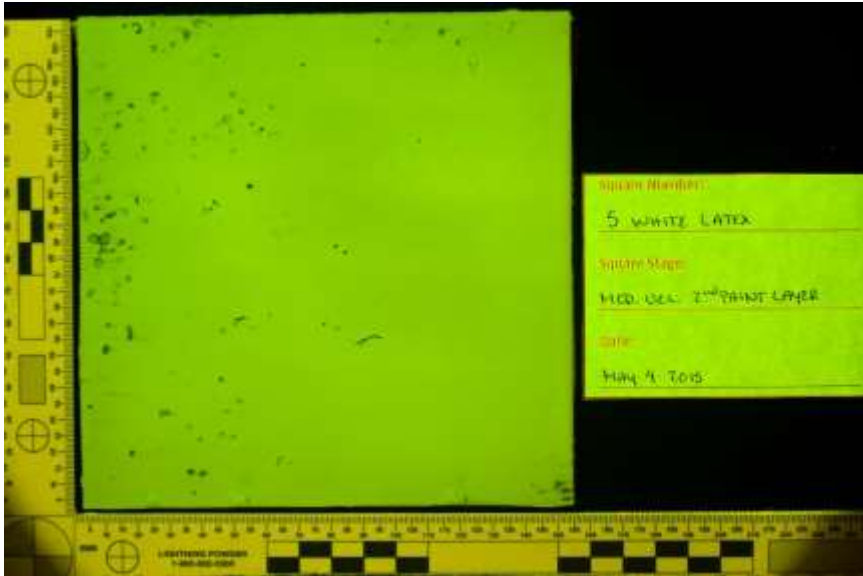
White Latex 5 – Medium Velocity



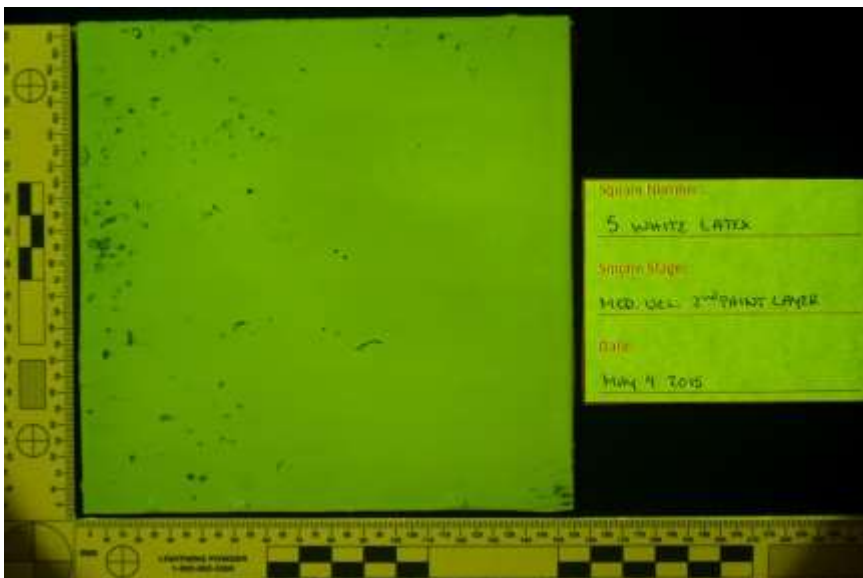
Yellow 415nm HDR



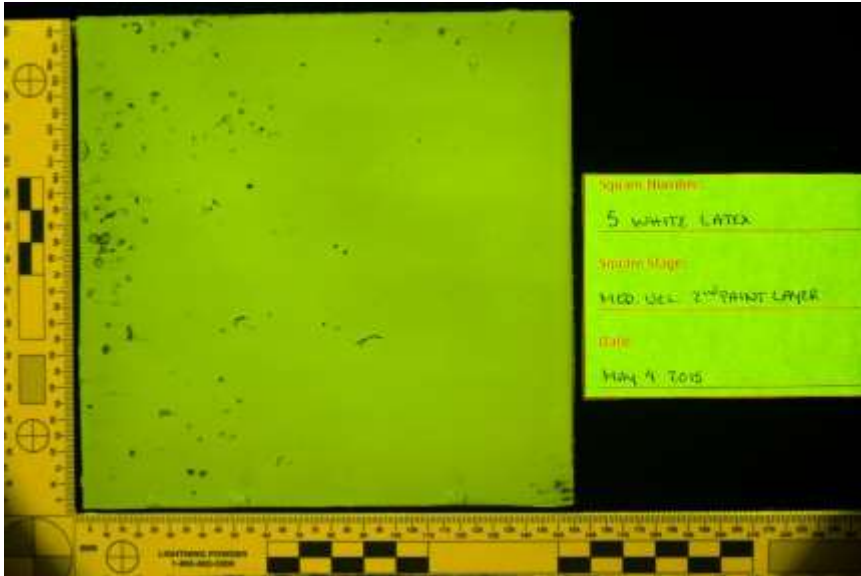
Yellow 415nm Single



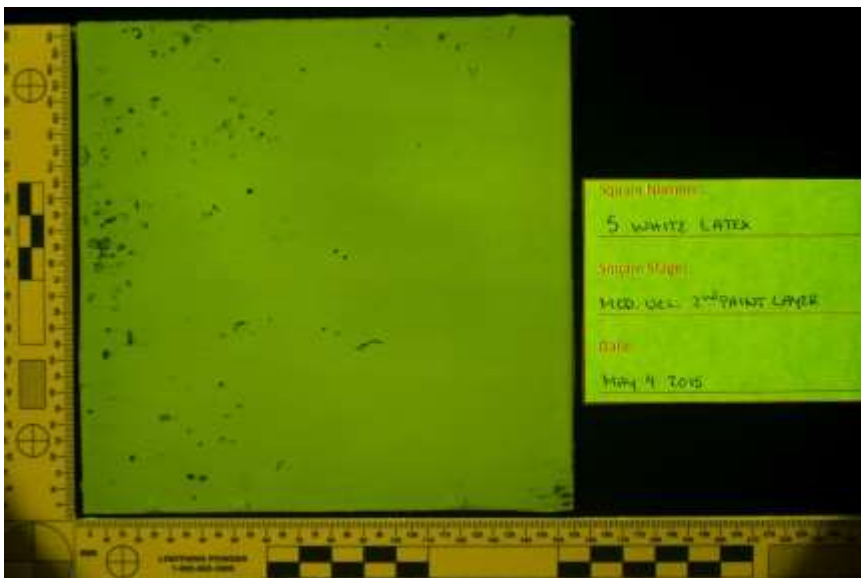
Yellow 445nm HDR



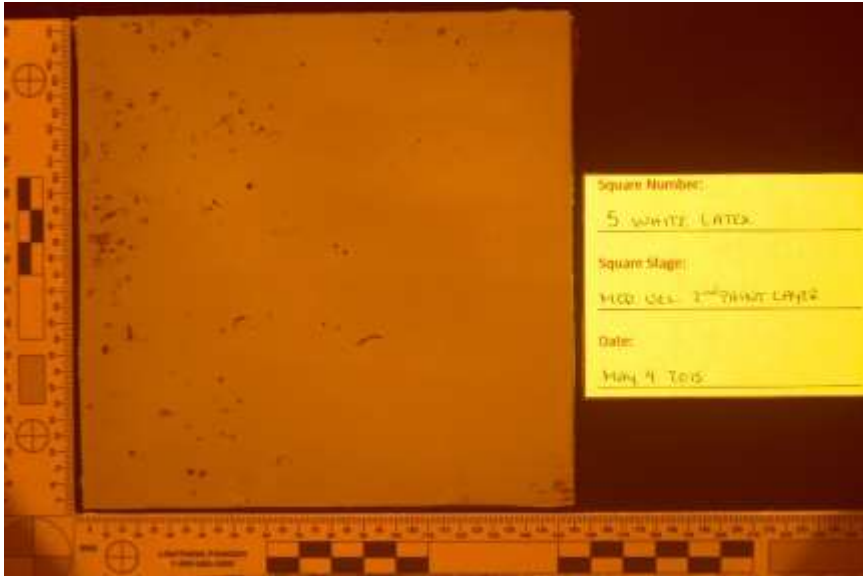
Yellow 445nm Single



Yellow 455nm HDR



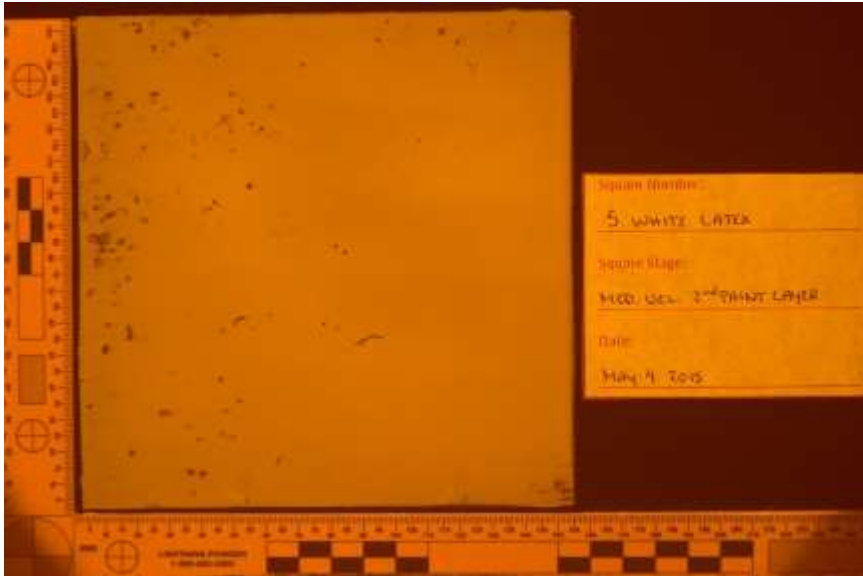
Yellow 455nm Single



Orange 415nm HDR



Orange 415nm Single



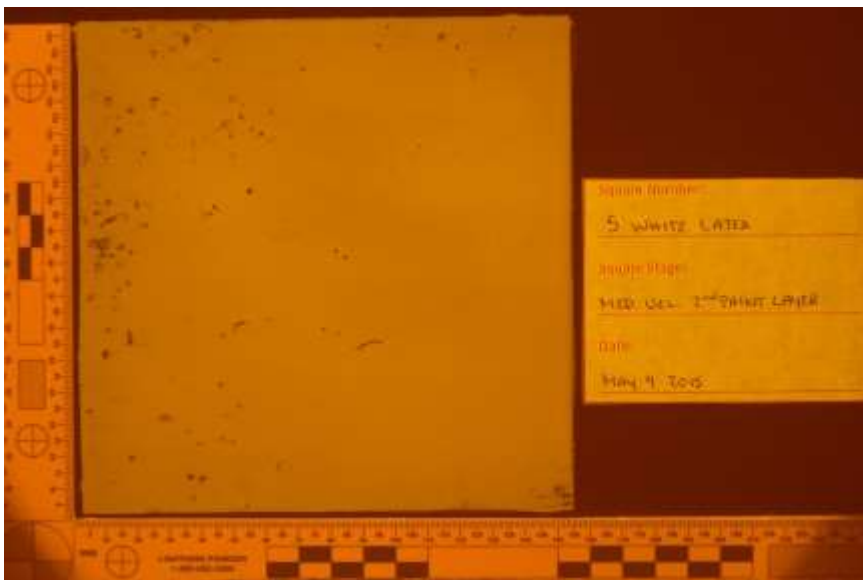
Orange 445nm HDR



Orange 445nm Single



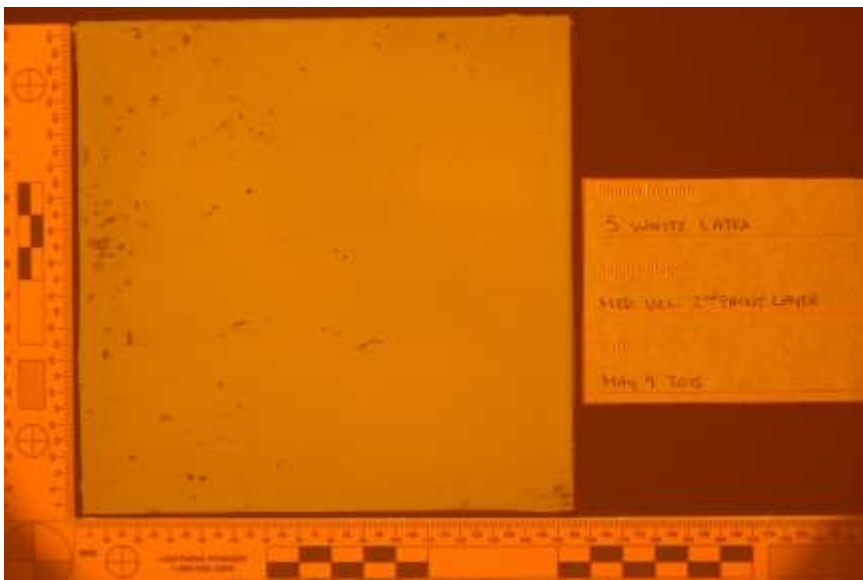
Orange 455nm HDR



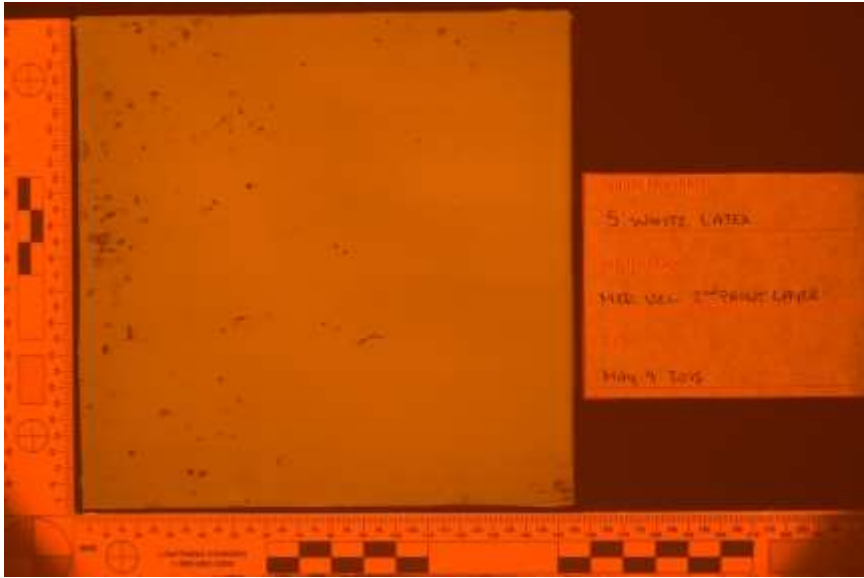
Orange 455nm Single



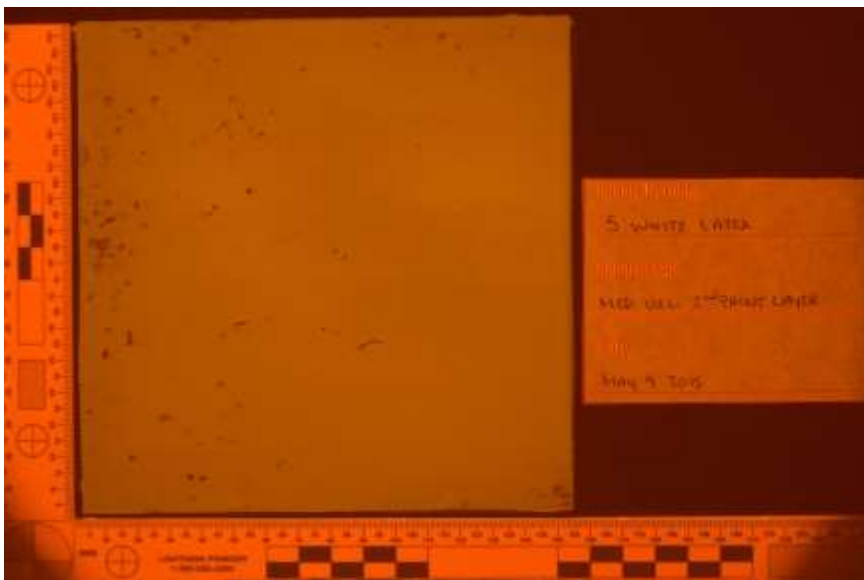
Orange 475nm HDR



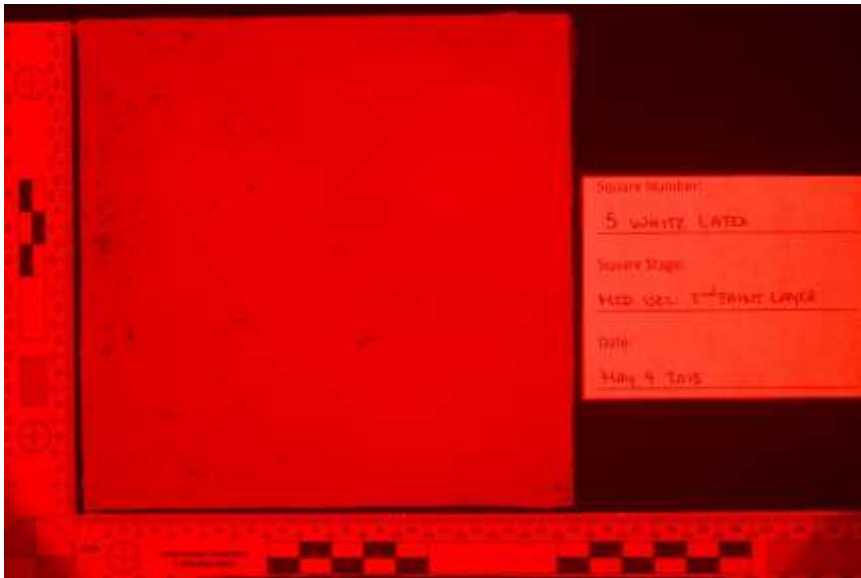
Orange 475nm Single



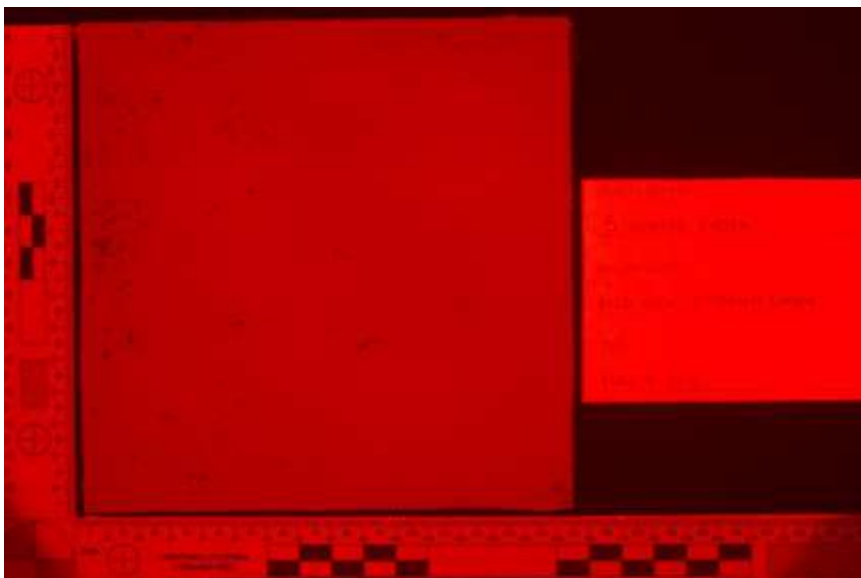
Orange 495nm HDR



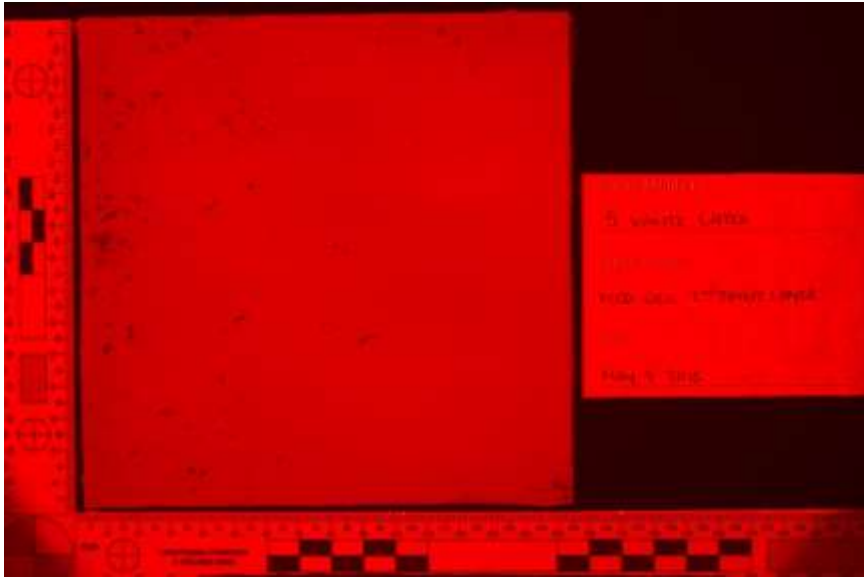
Orange 495nm Single



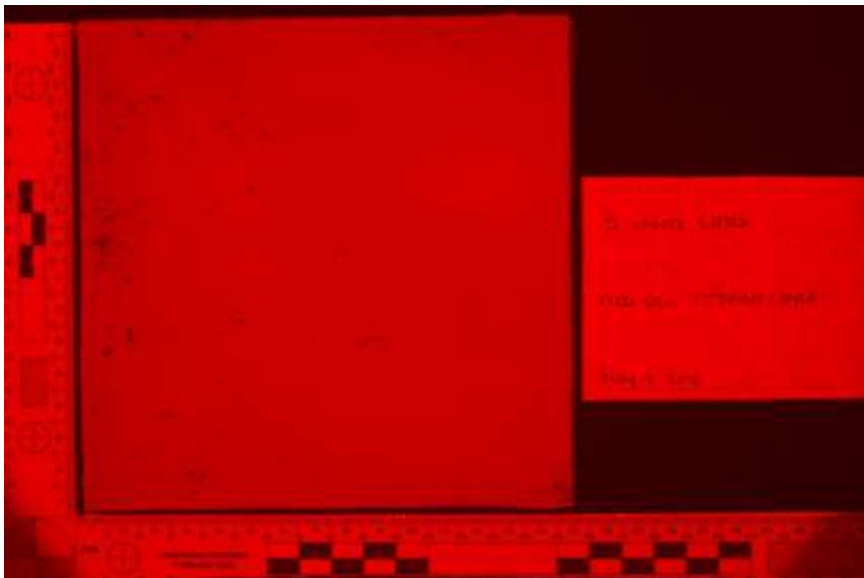
Red 415nm HDR



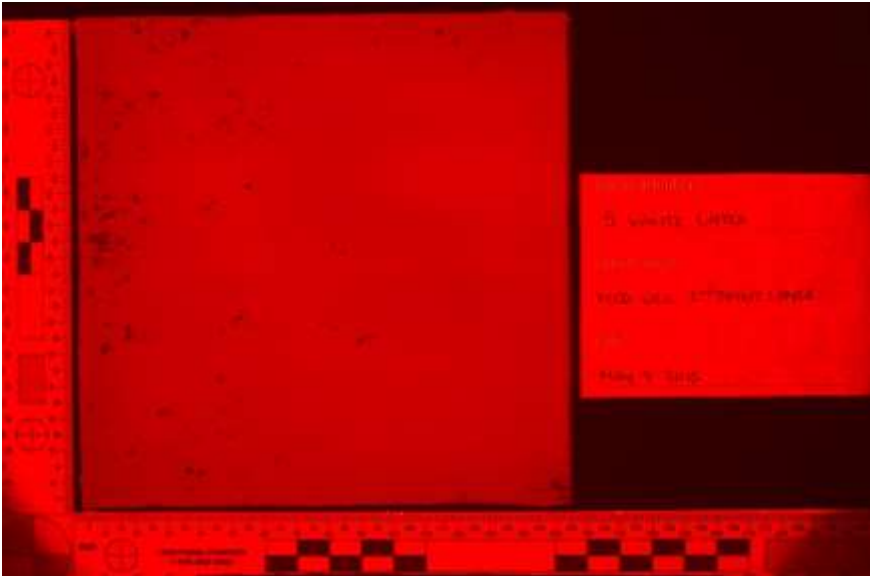
Red 415nm Single



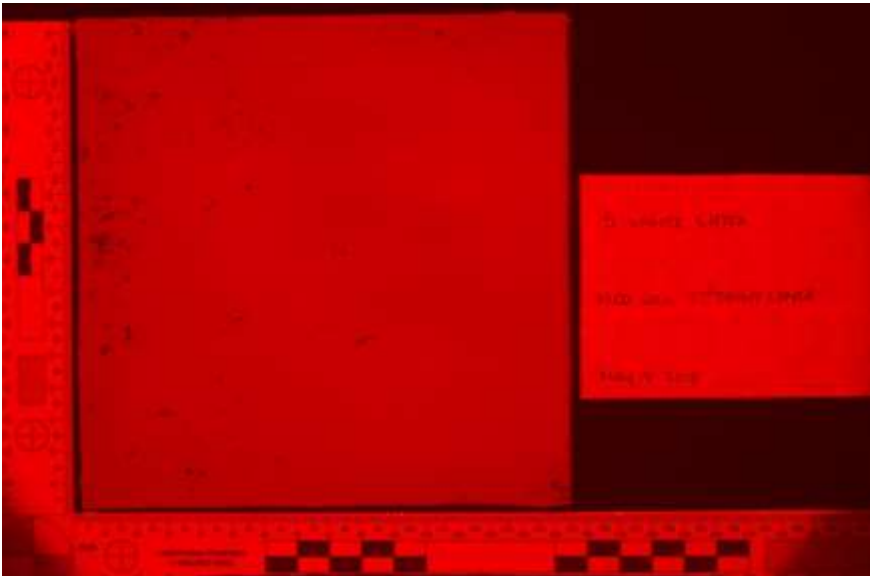
Red 445nm HDR



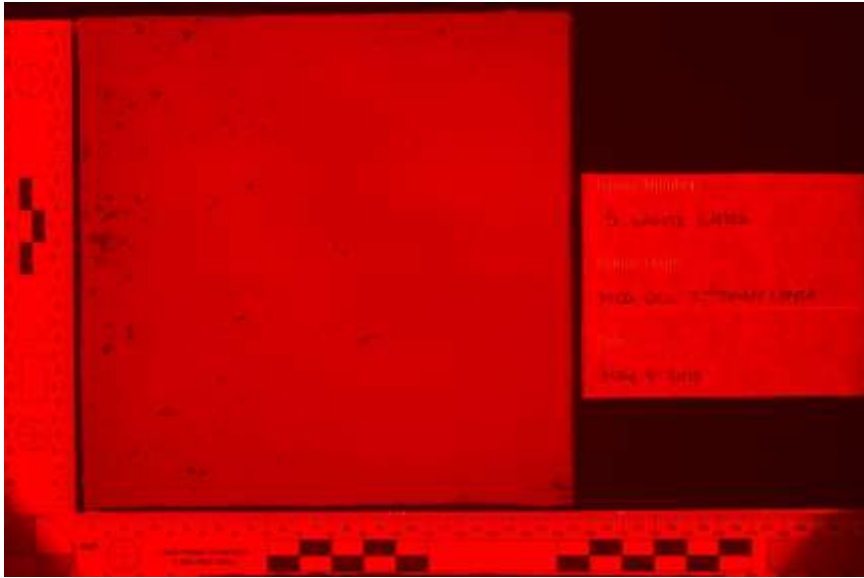
Red 445nm Single



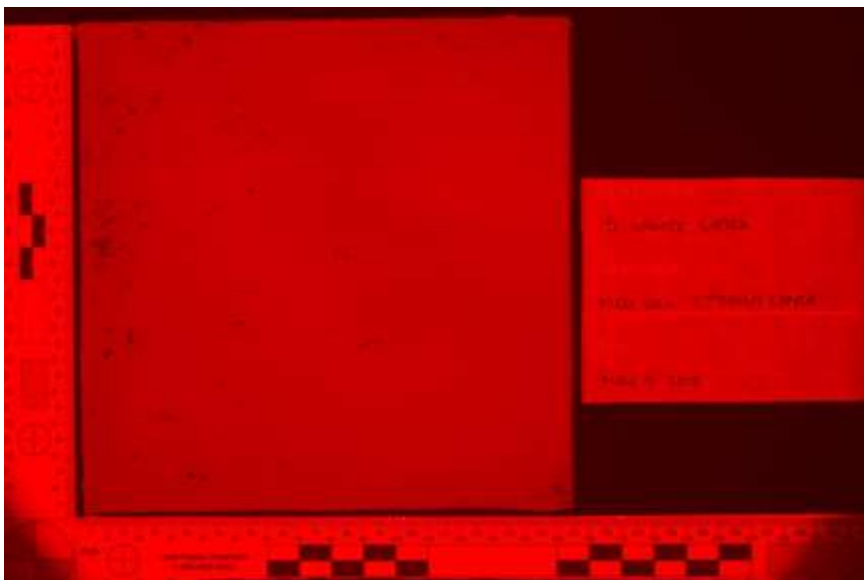
Red 455nm HDR



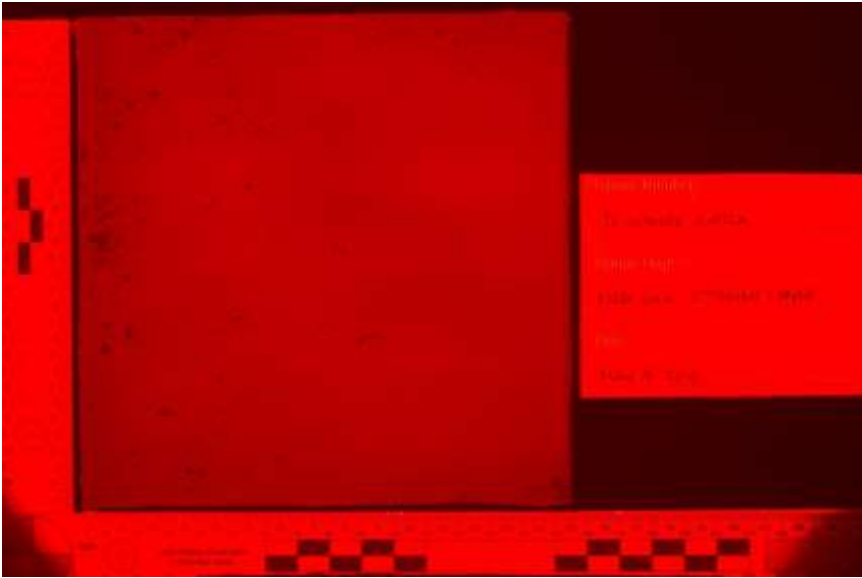
Red 455nm Single



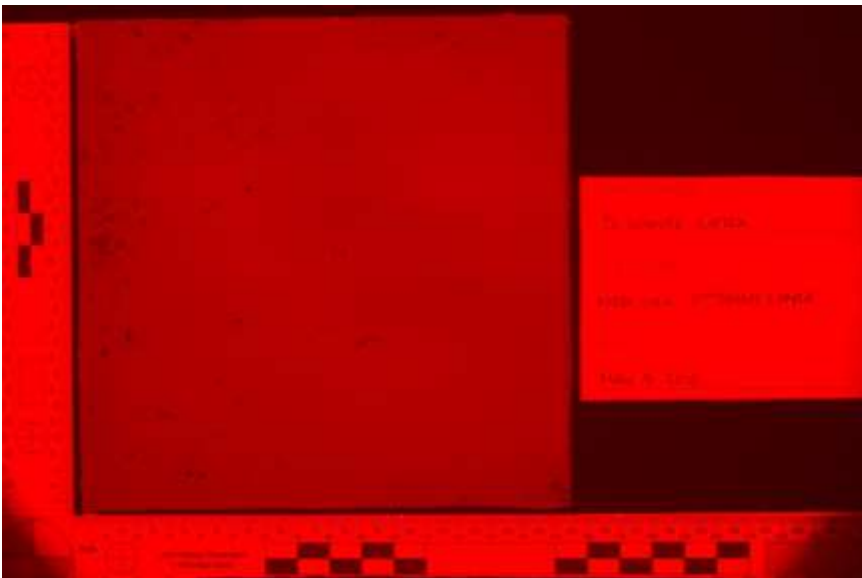
Red 475nm HDR



Red 475nm Single

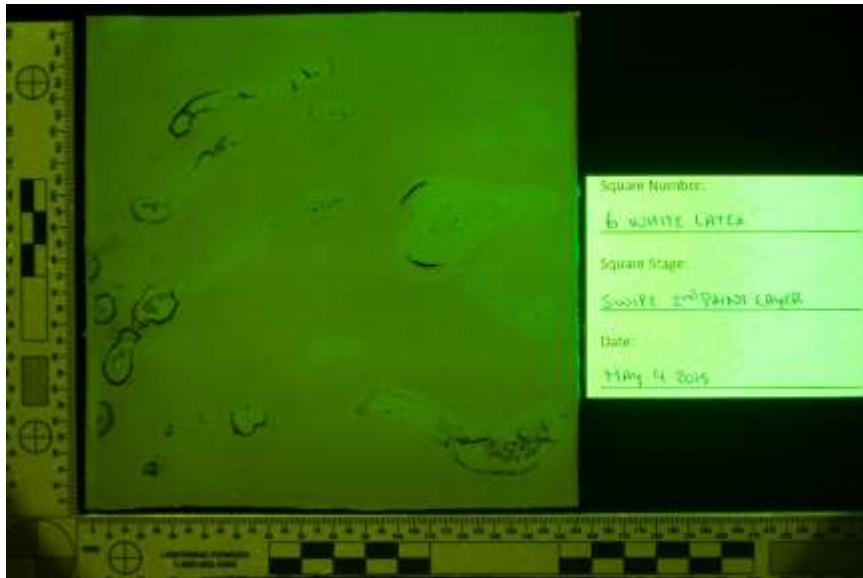


Red 575nm HDR

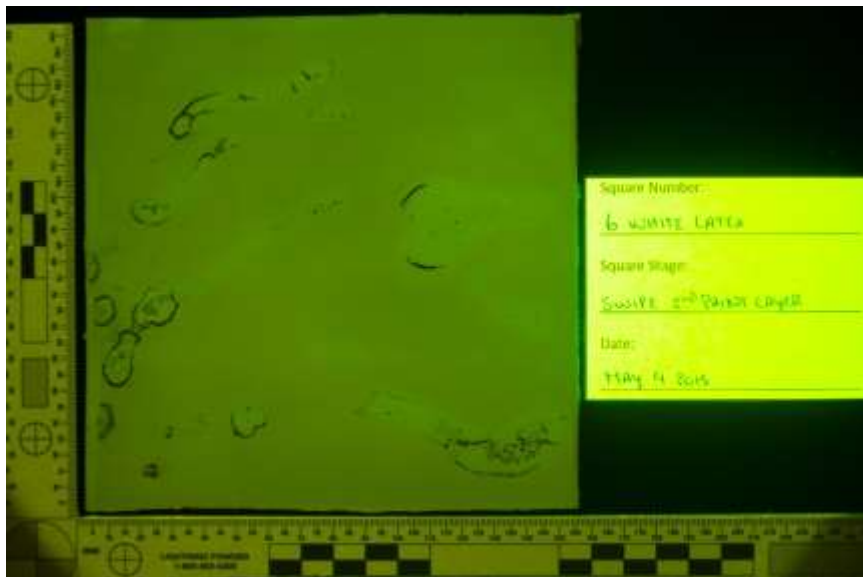


Red 575nm Single

White Latex 6 – Swipe



Yellow 415nm HDR



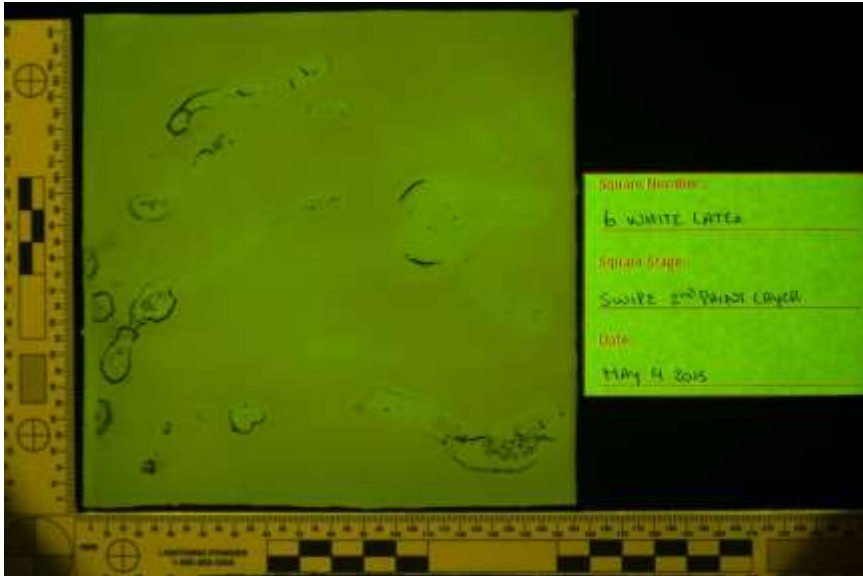
Yellow 415nm Single



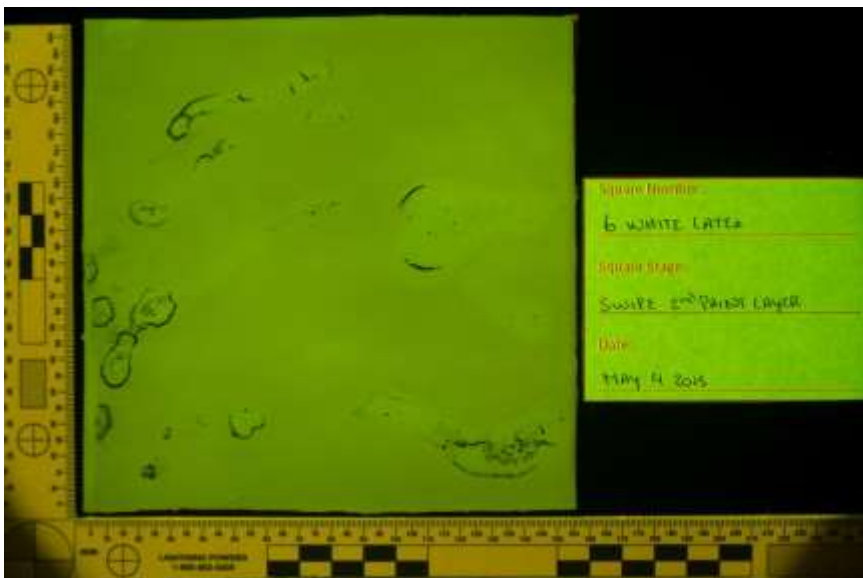
Yellow 445nm HDR



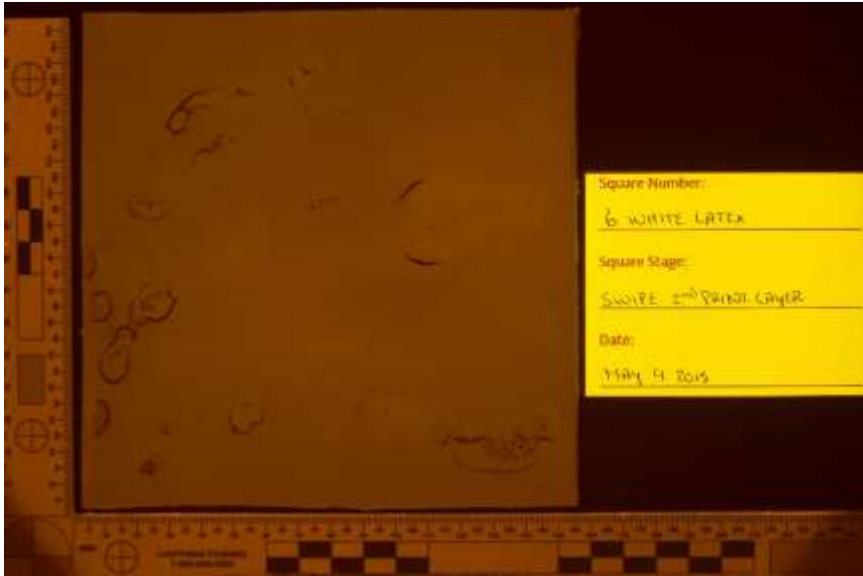
Yellow 445nm Single



Yellow 455nm HDR



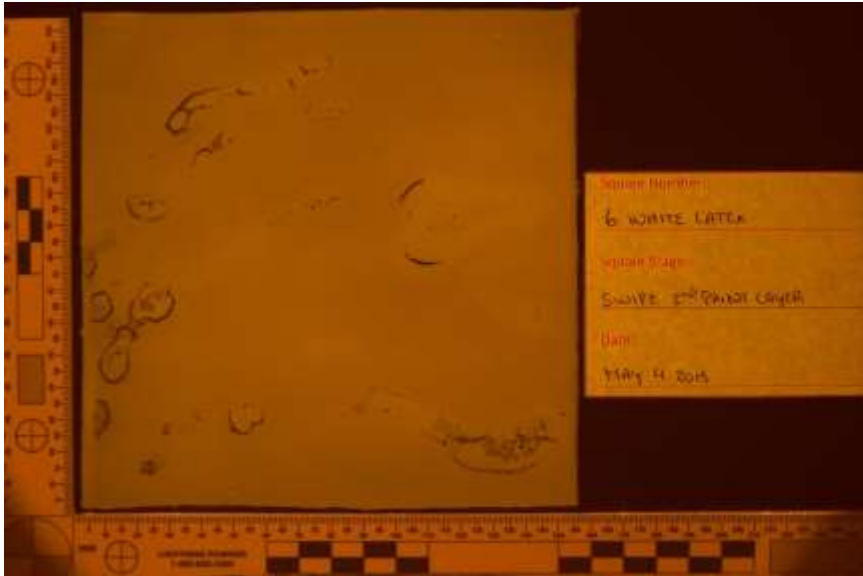
Yellow 455nm Single



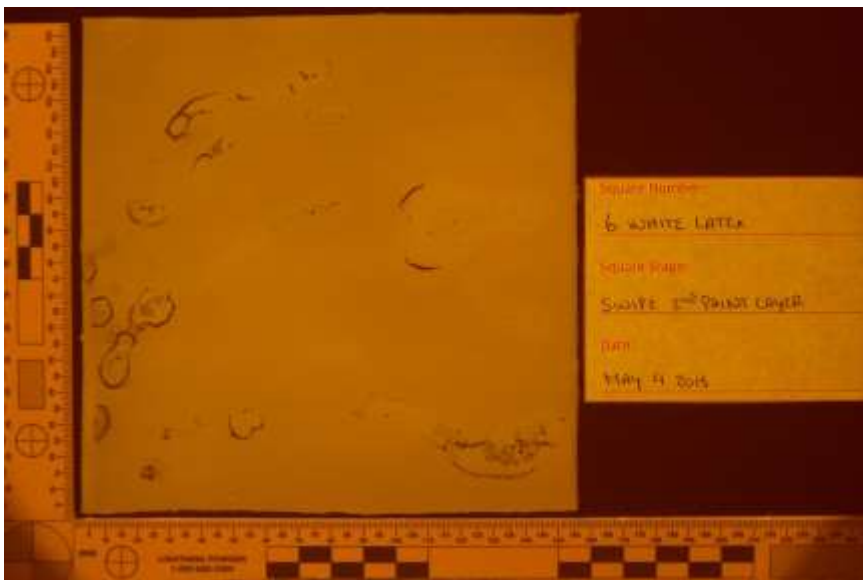
Orange 415nm HDR



Orange 415nm Single



Orange 445nm HDR



Orange 445nm Single



Orange 455nm HDR



Orange 455nm Single



Orange 475nm HDR



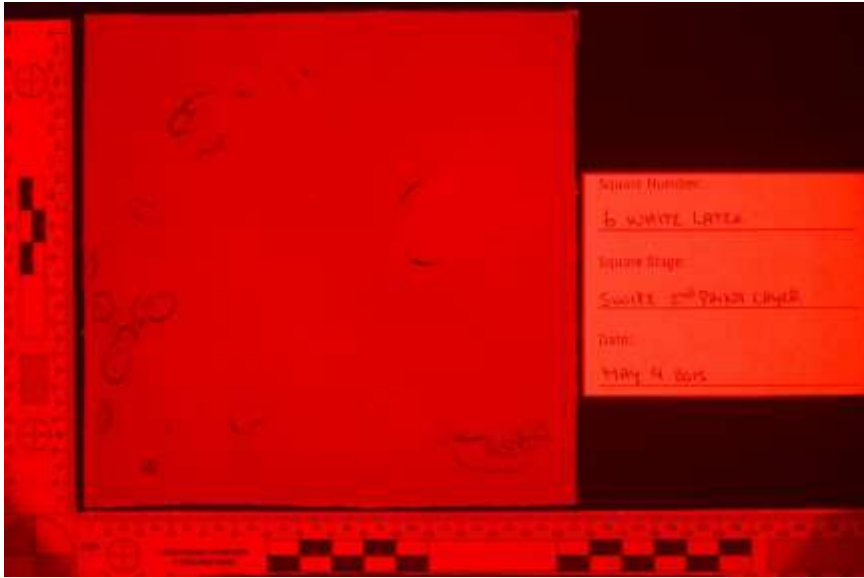
Orange 475nm Single



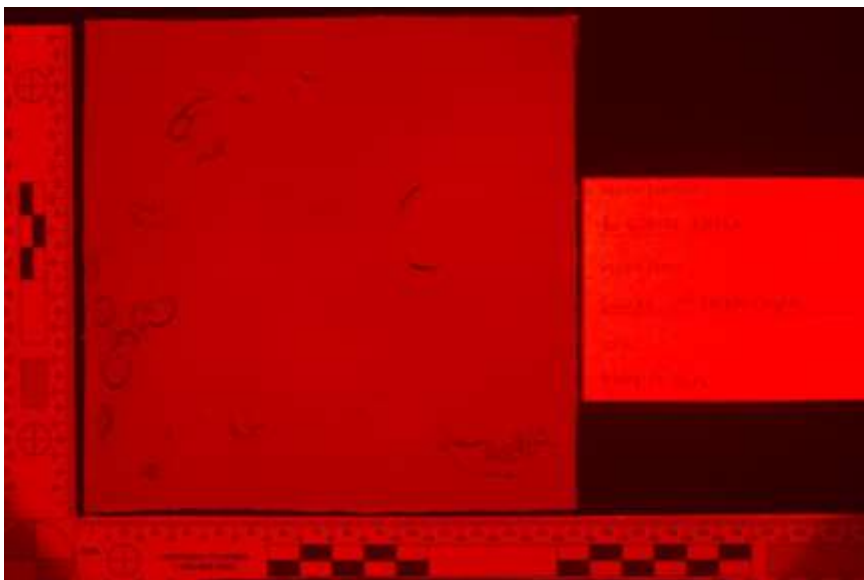
Orange 495nm HDR



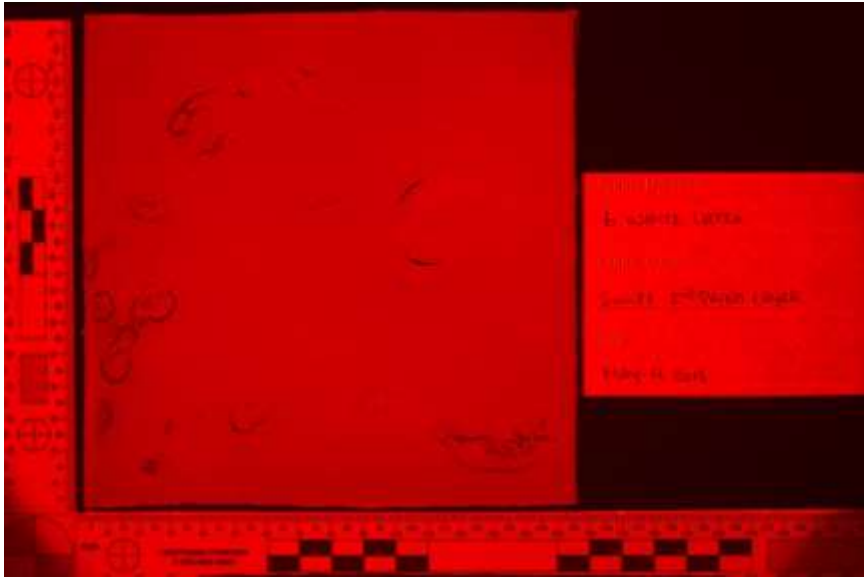
Orange 495nm Single



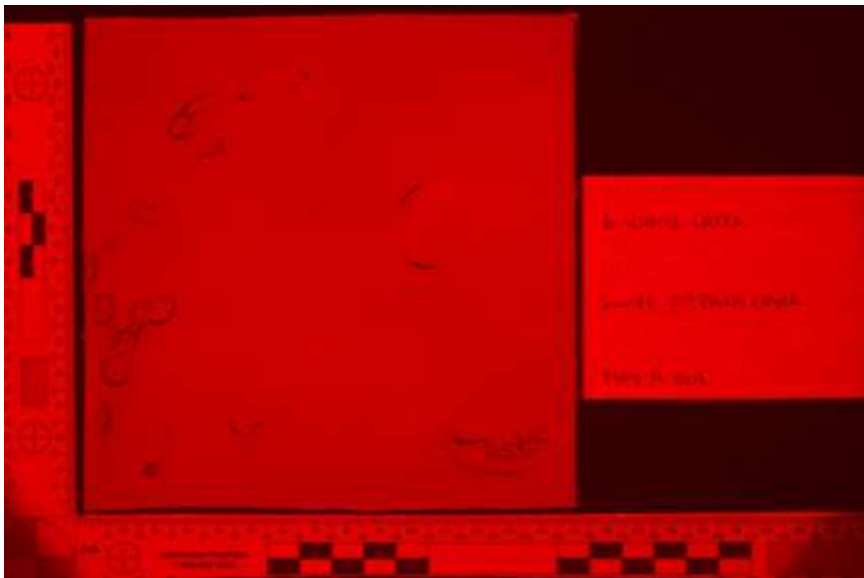
Red 415nm HDR



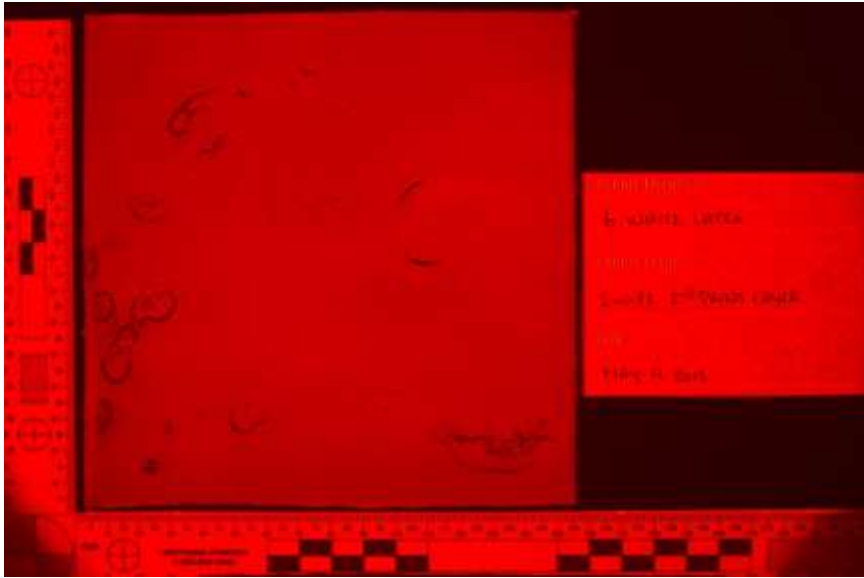
Red 415nm Single



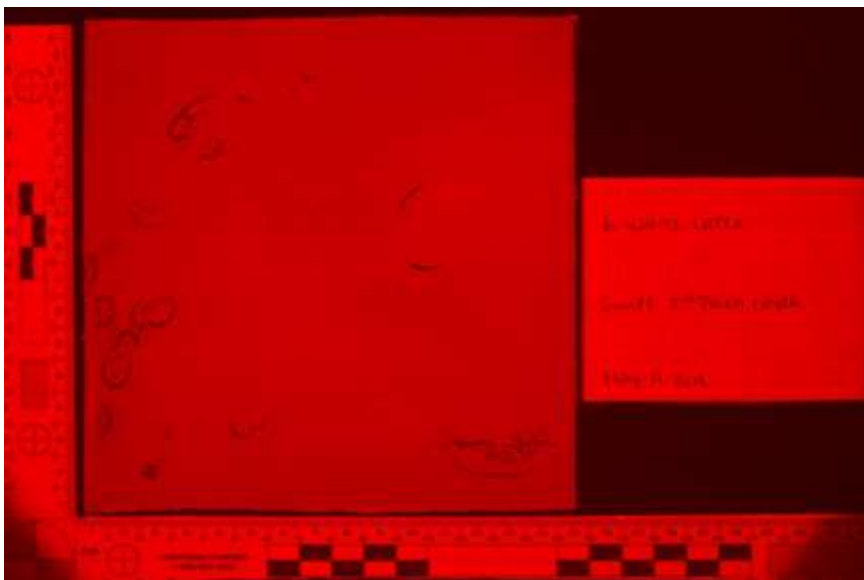
Red 445nm HDR



Red 445nm Single



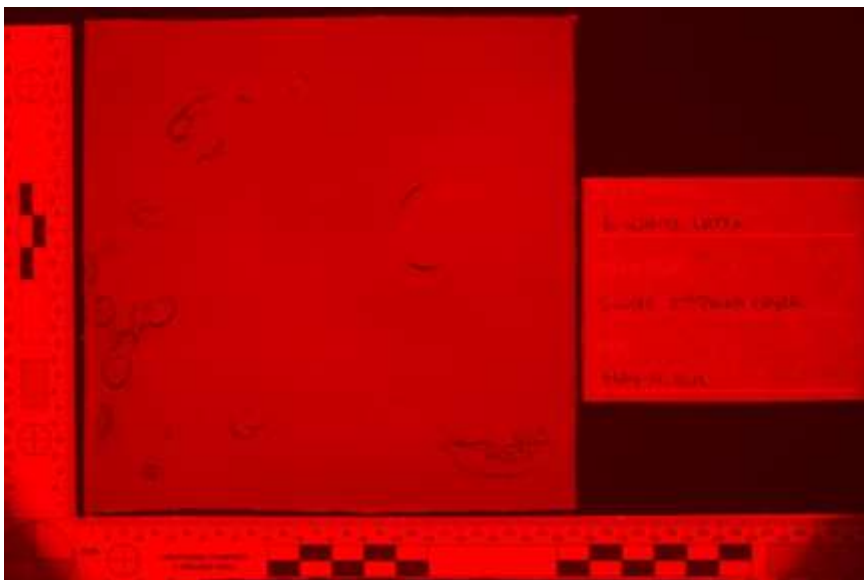
Red 455nm HDR



Red 455nm Single



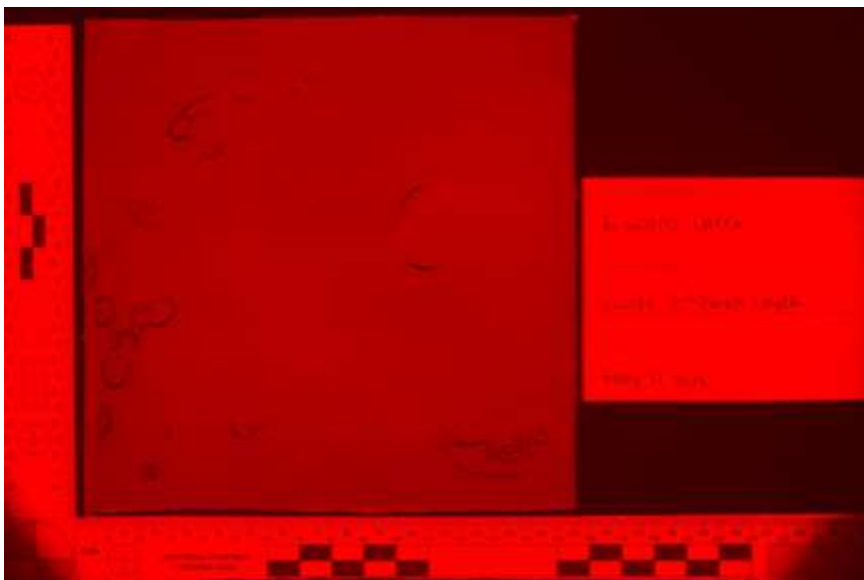
Red 475nm HDR



Red 475nm Single

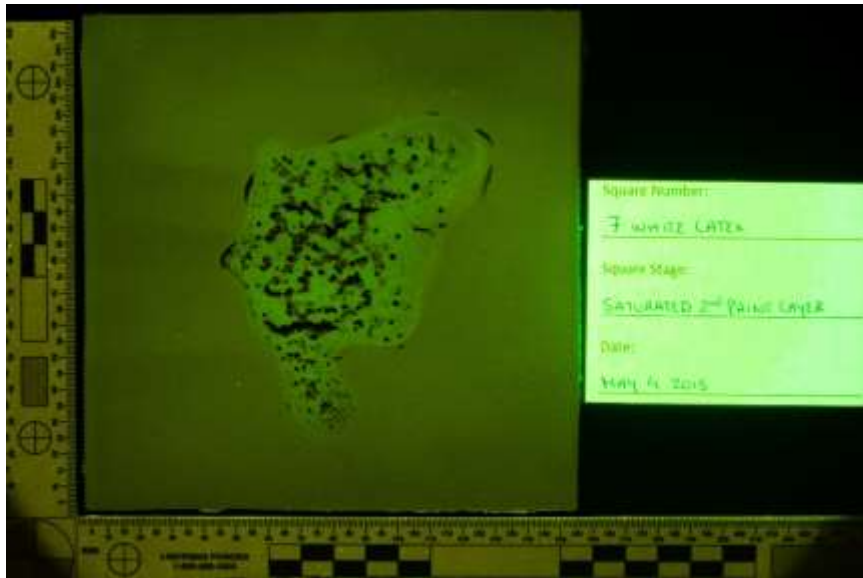


Red 575nm HDR



Red 575nm Single

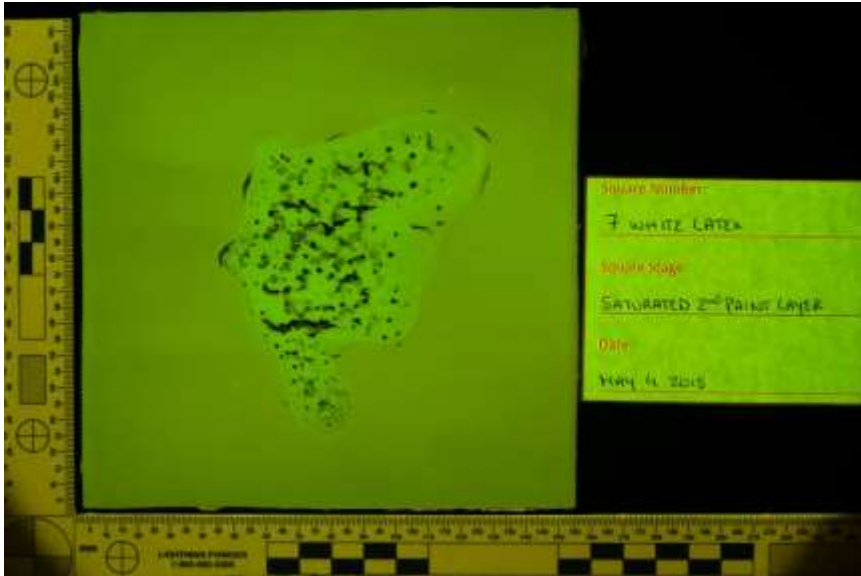
White Latex 7 – Saturated



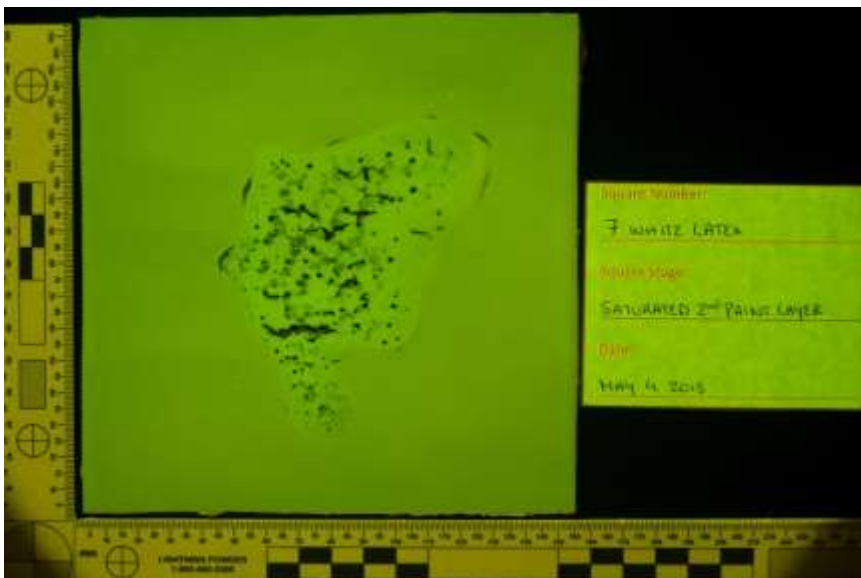
Yellow 415nm HDR



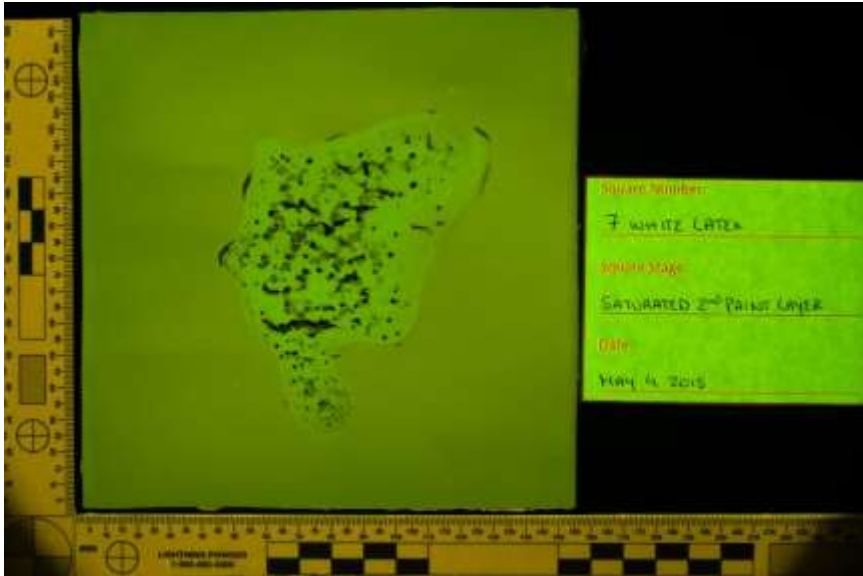
Yellow 415nm Single



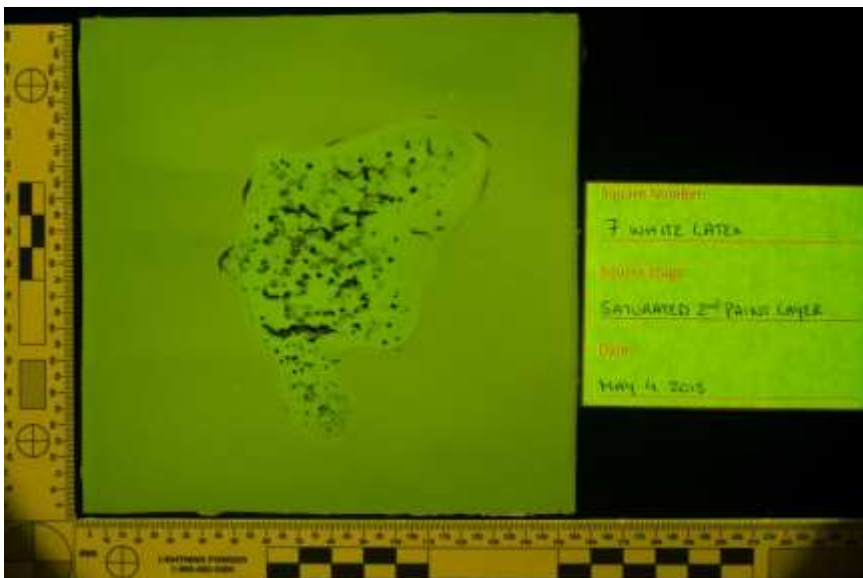
Yellow 445nm HDR



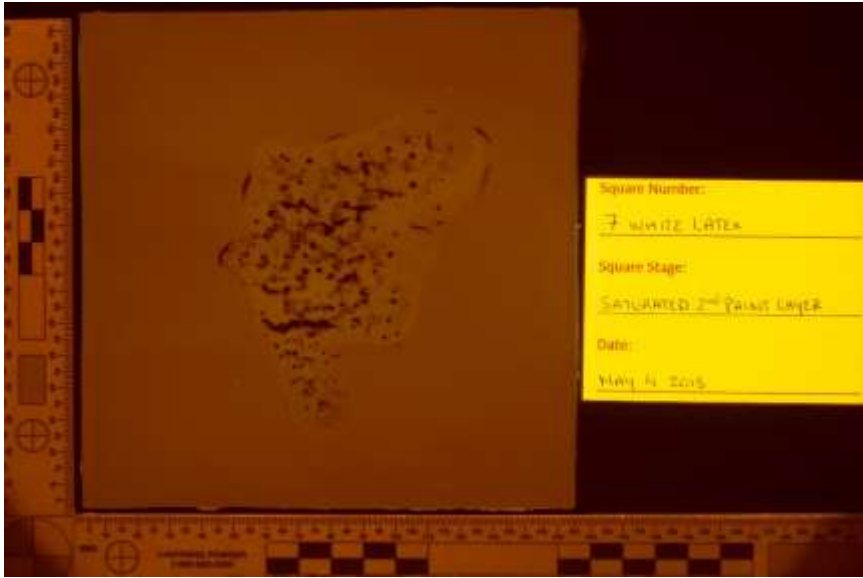
Yellow 445nm Single



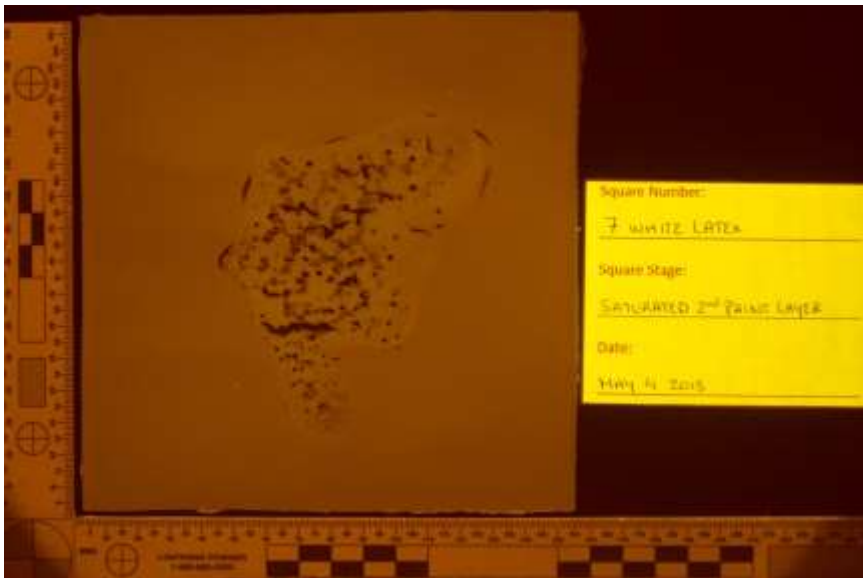
Yellow 455nm HDR



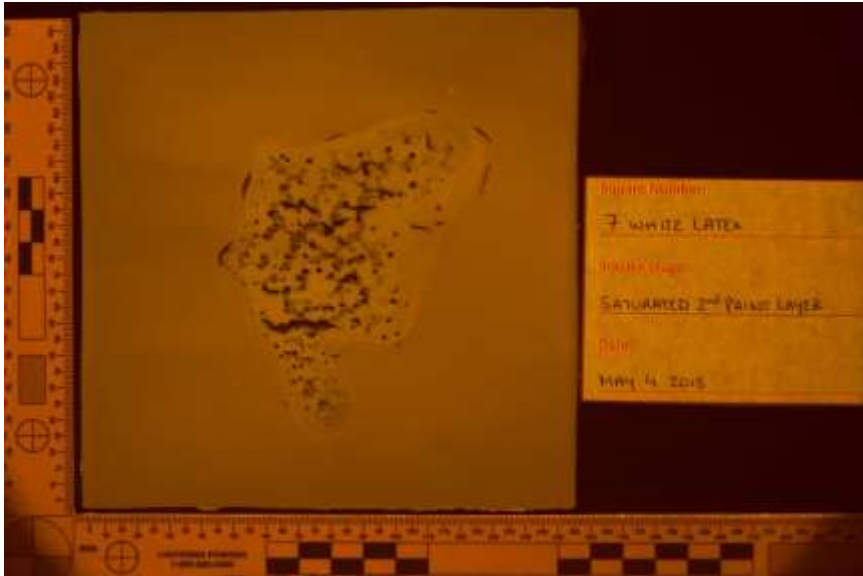
Yellow 455nm Single



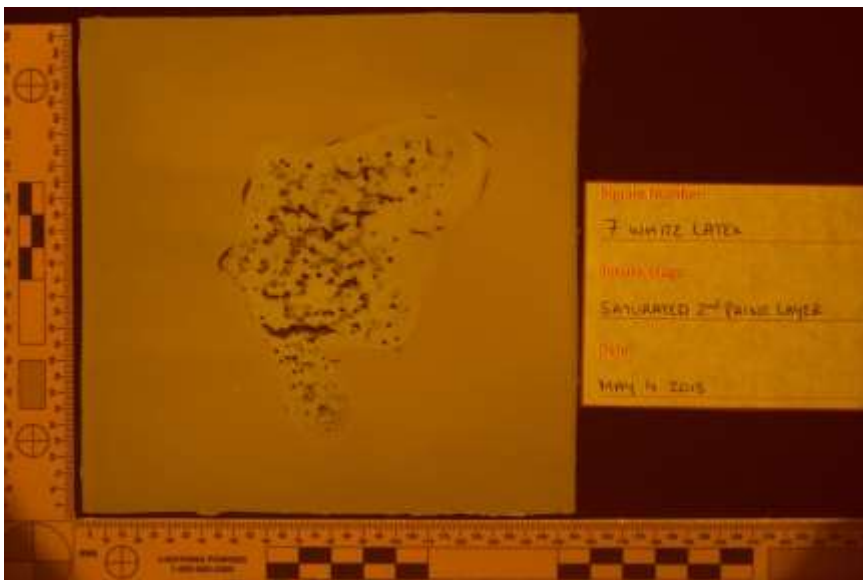
Orange 415nm HDR



Orange 415nm Single



Orange 445nm HDR



Orange 445nm Single



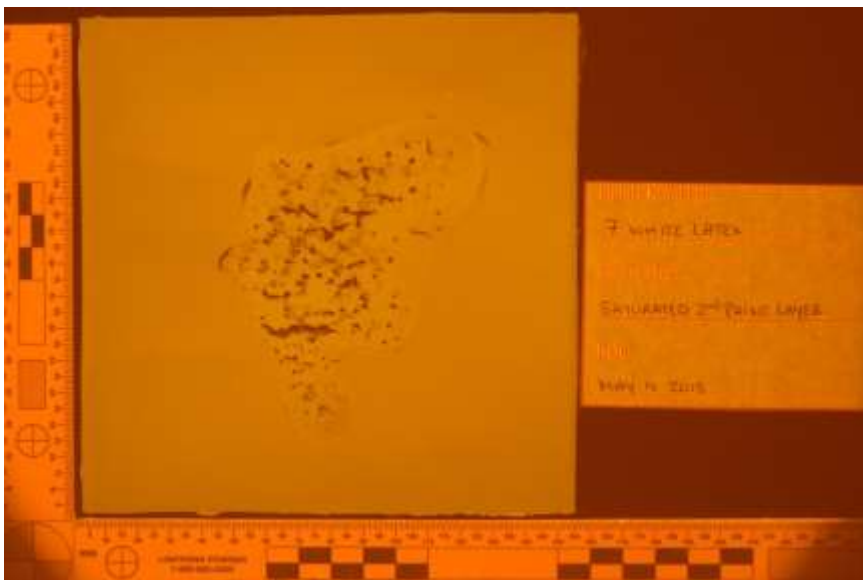
Orange 455nm HDR



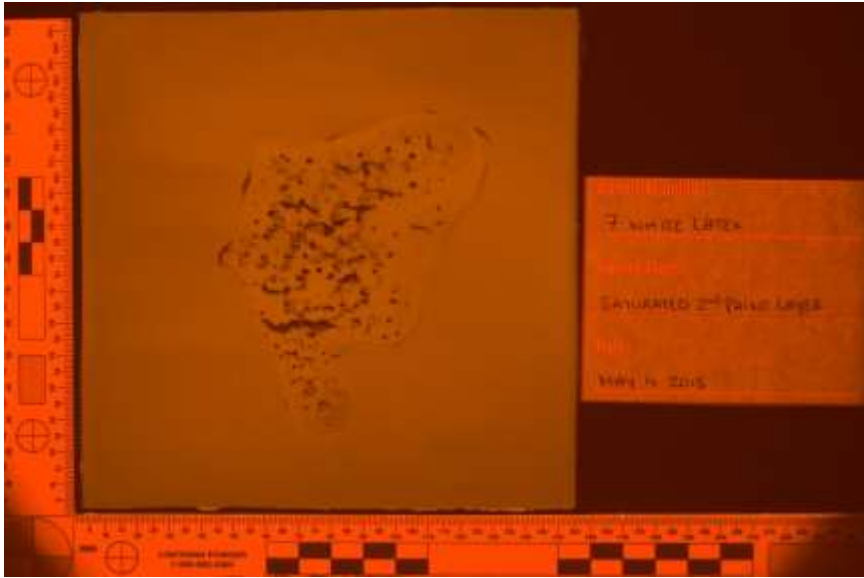
Orange 455nm Single



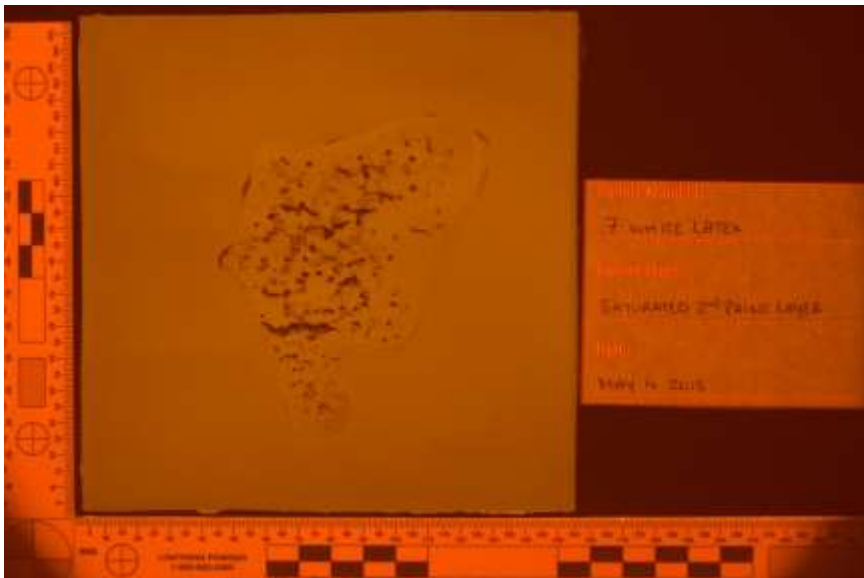
Orange 475nm HDR



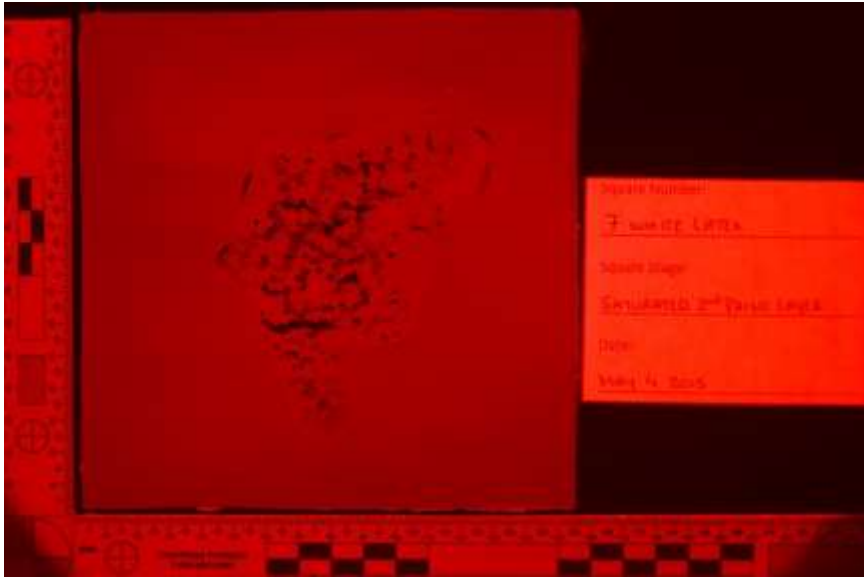
Orange 475nm Single



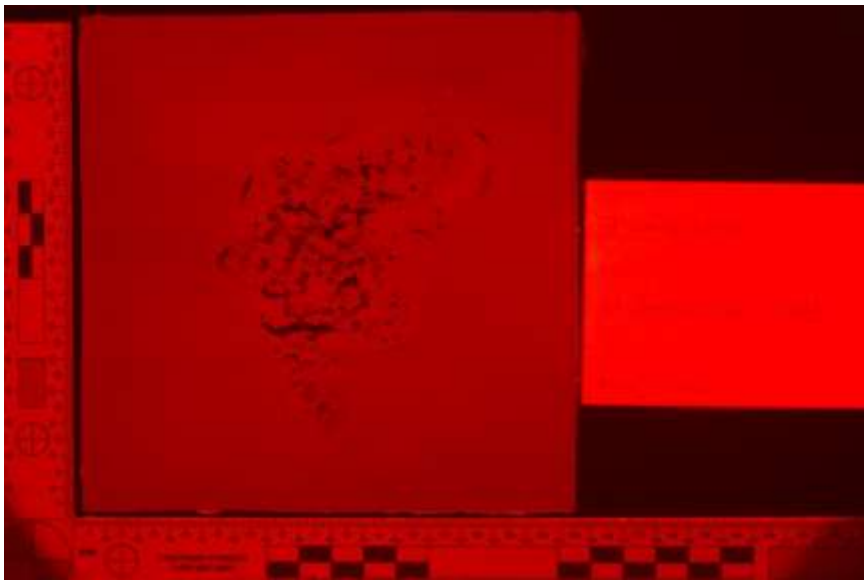
Orange 495nm HDR



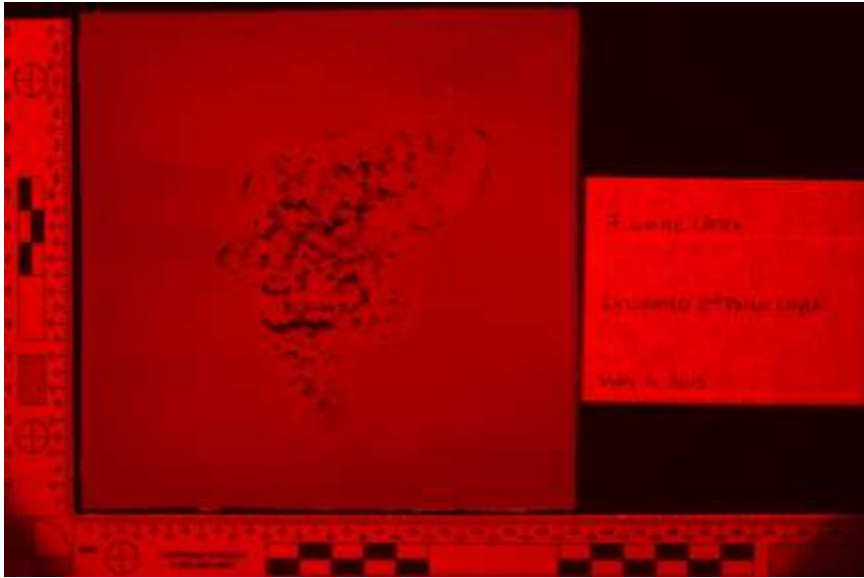
Orange 495nm Single



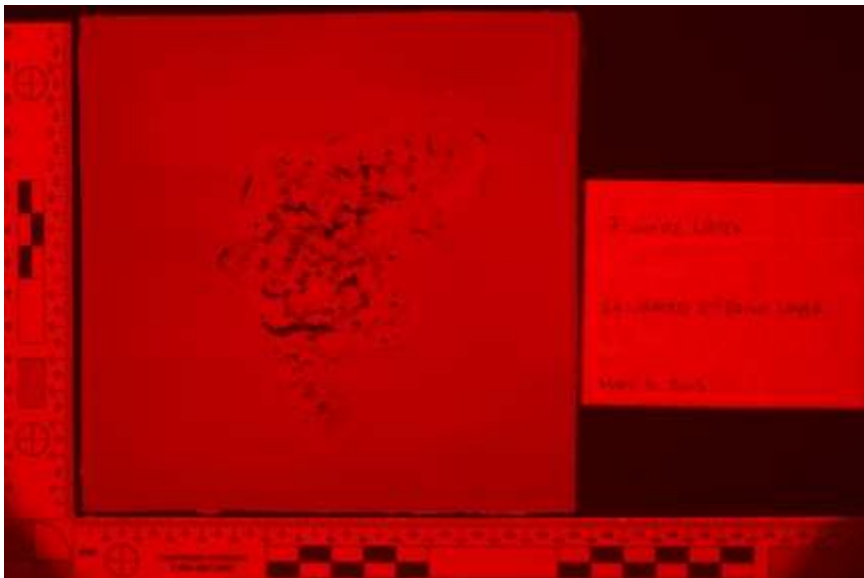
Red 415nm HDR



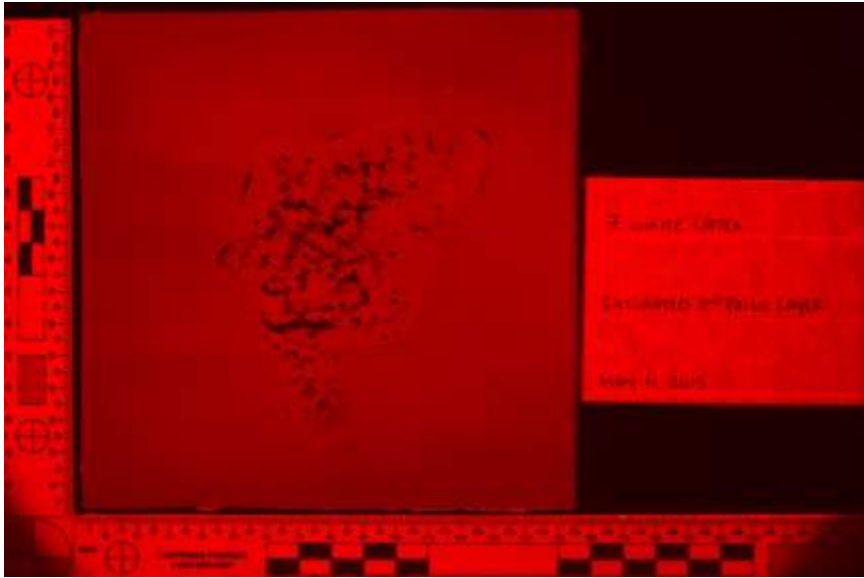
Red 415nm Single



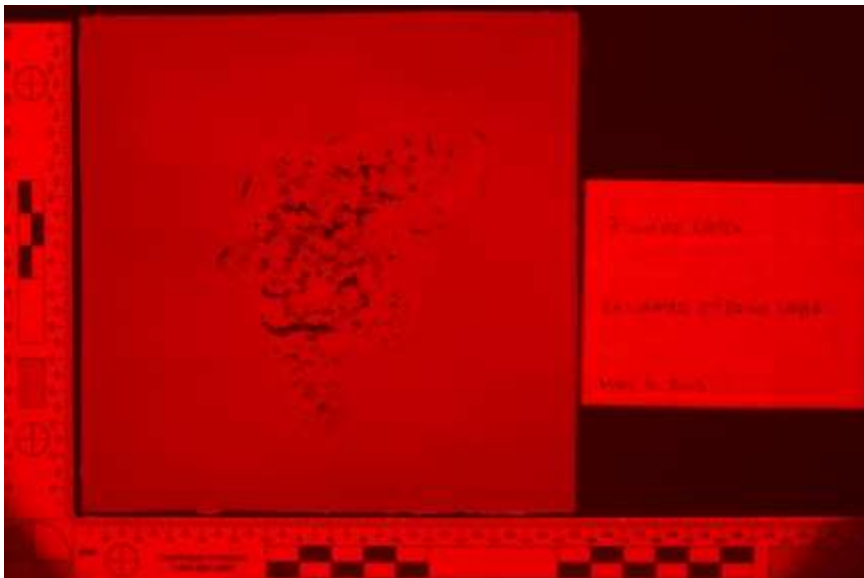
Red 445nm HDR



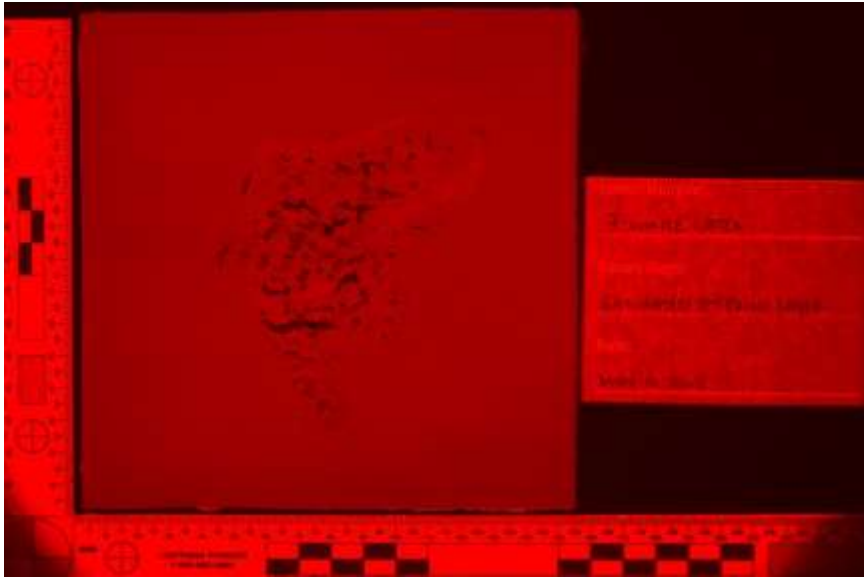
Red 445nm Single



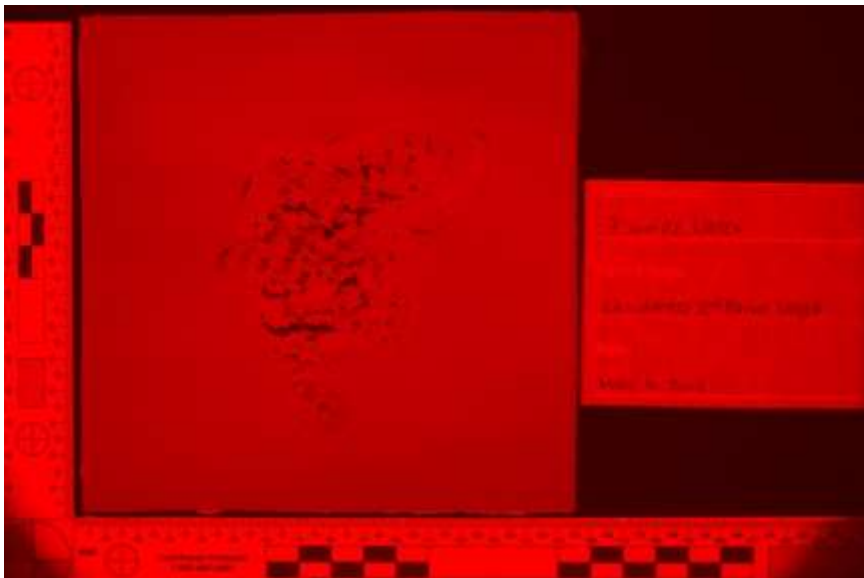
Red 455nm HDR



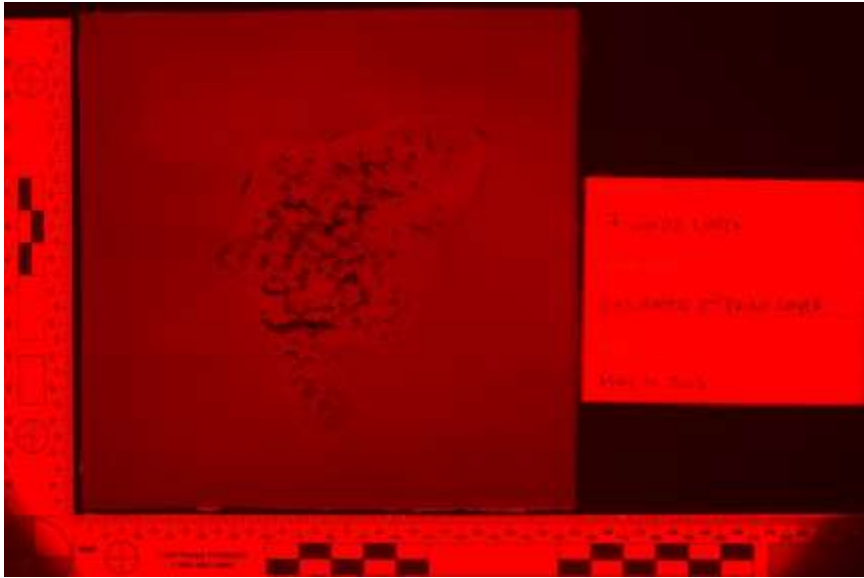
Red 455nm Single



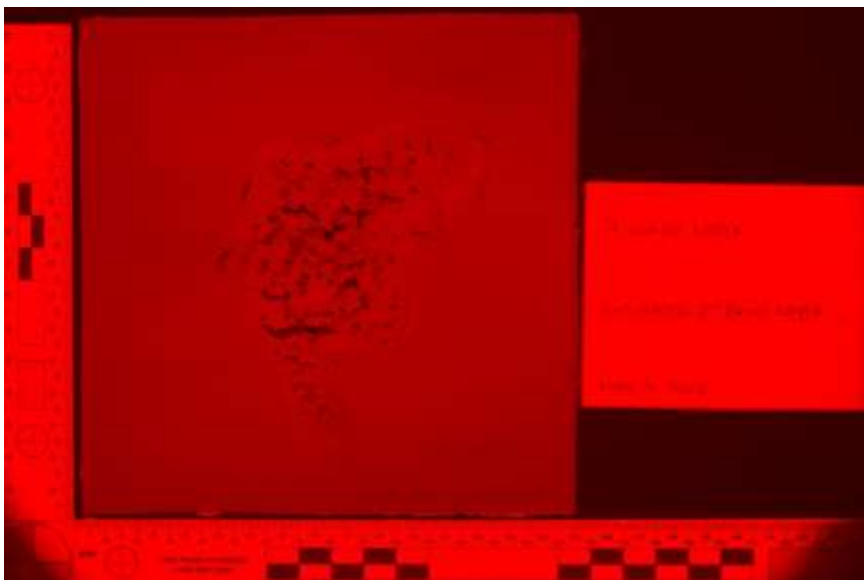
Red 475nm HDR



Red 475nm Single

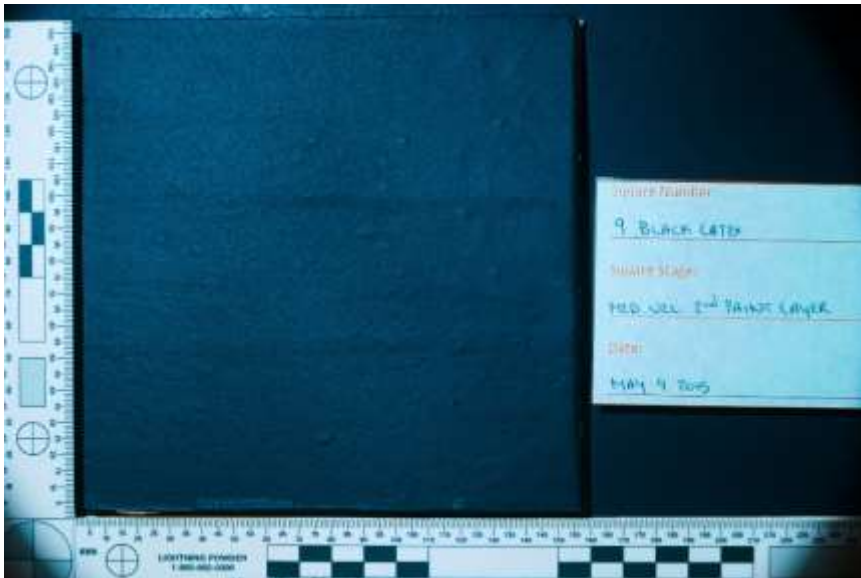


Red 575nm HDR

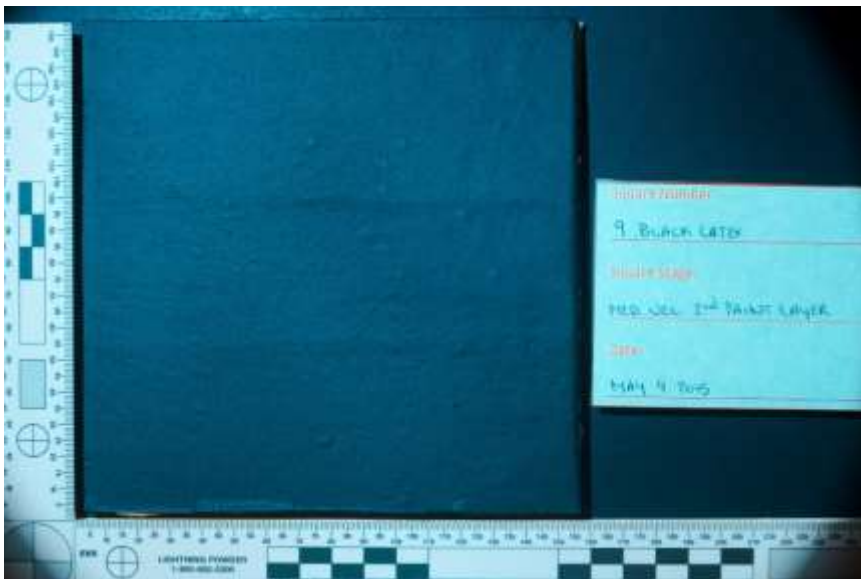


Red 575nm Single

Appendix 4.3.5.3. Black Latex – Yellow 475nm Second layer of paint stage
Black Latex 9 – Medium Velocity

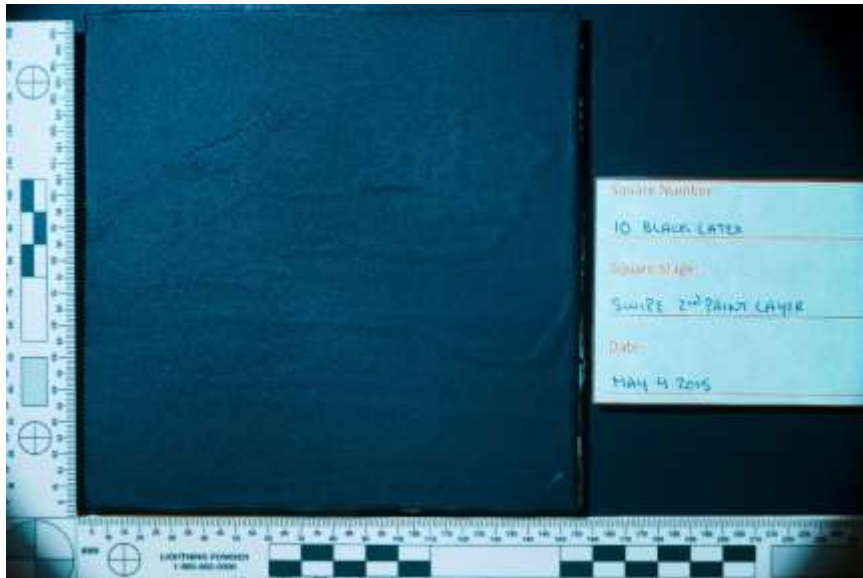


Yellow 475nm HDR

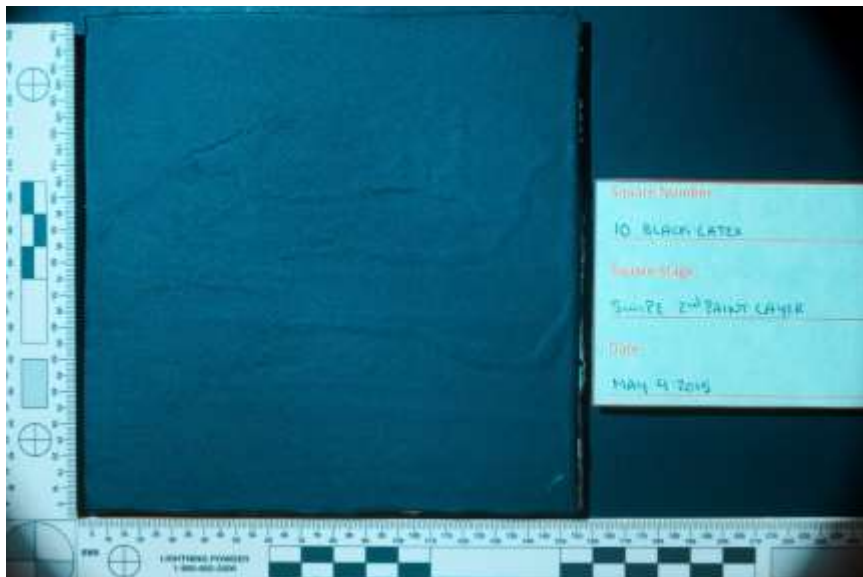


Yellow 475nm Single

Black Latex 10 – Swipe

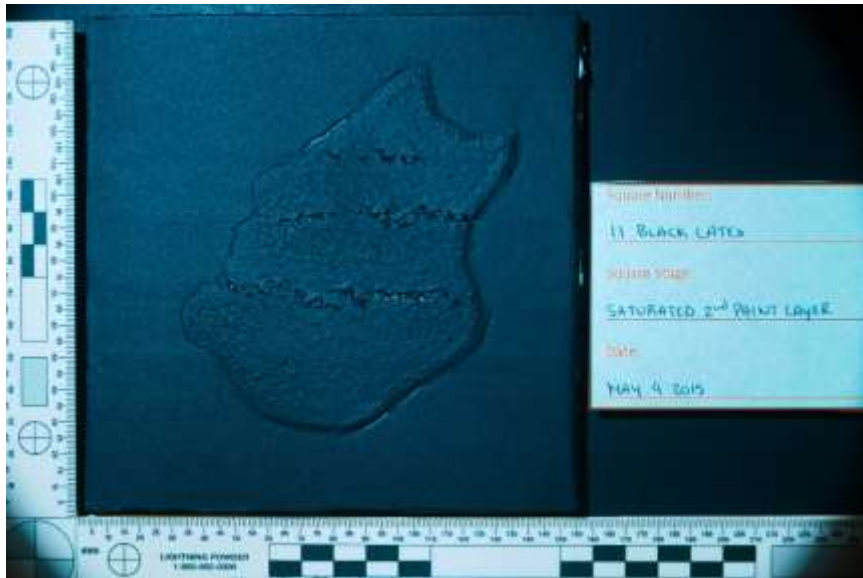


Yellow 475nm HDR

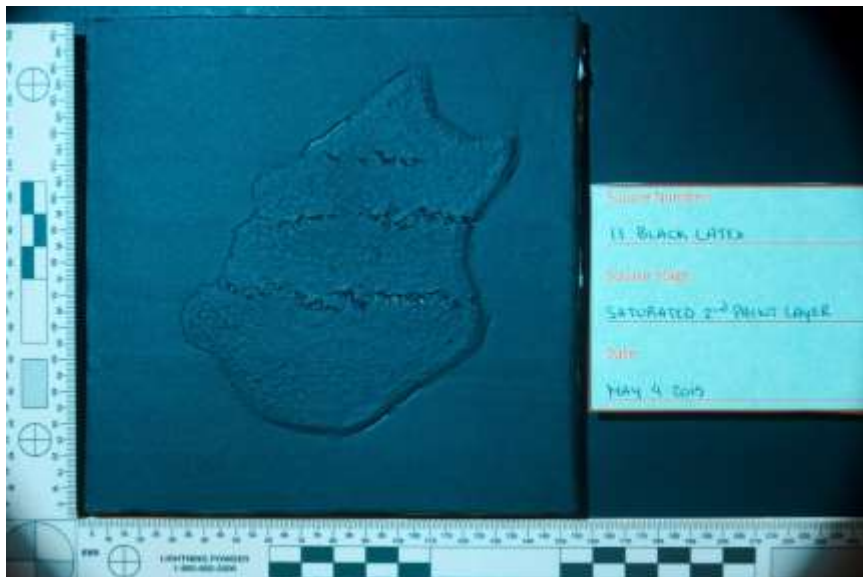


Yellow 475nm Single

Black Latex 11 – Saturated

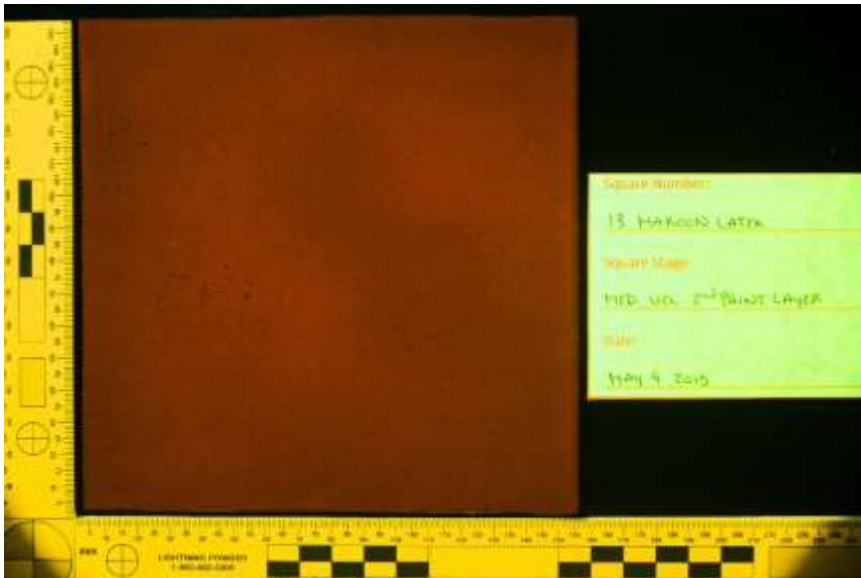


Yellow 475nm HDR

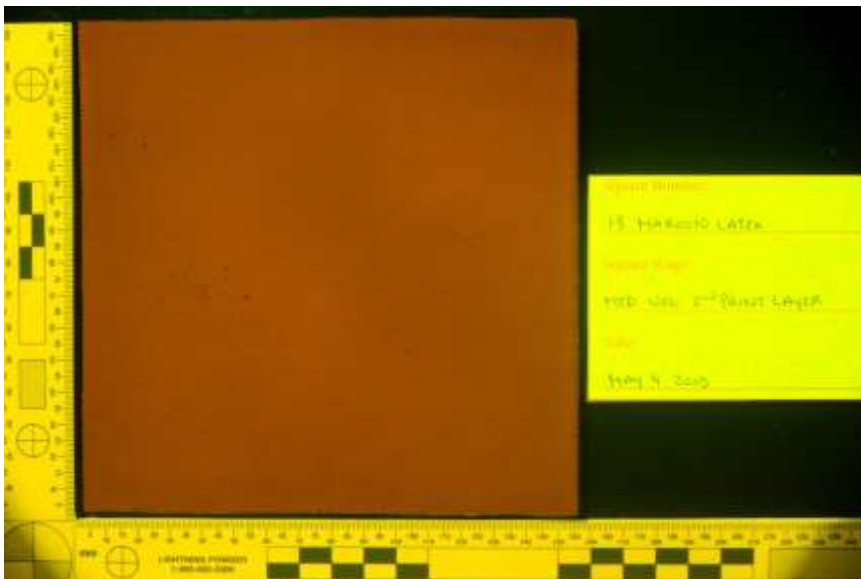


Yellow 475nm Single

Appendix 4.3.5.4. Maroon Latex – Yellow 455nm Second layer of paint stage
Maroon Latex 13 – Medium Velocity



Yellow 455nm HDR

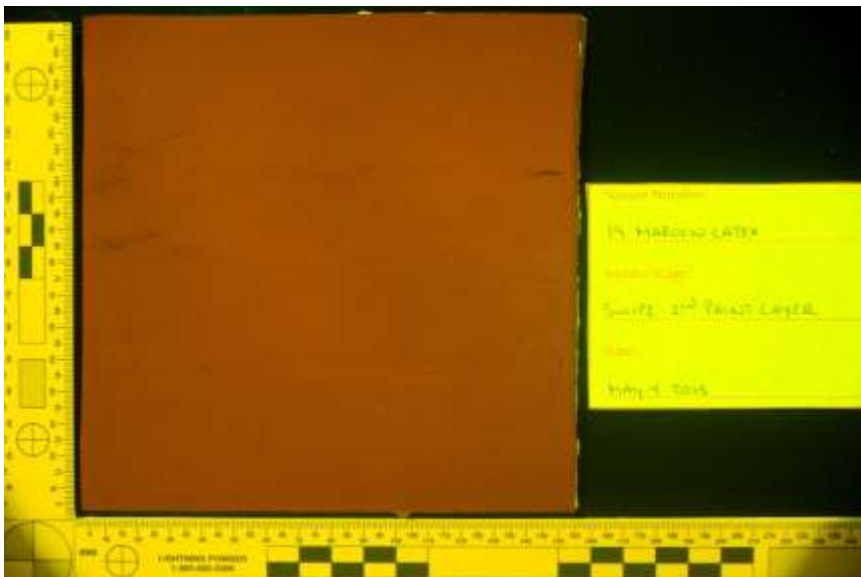


Yellow 455nm Single

Maroon Latex 14 – Swipe

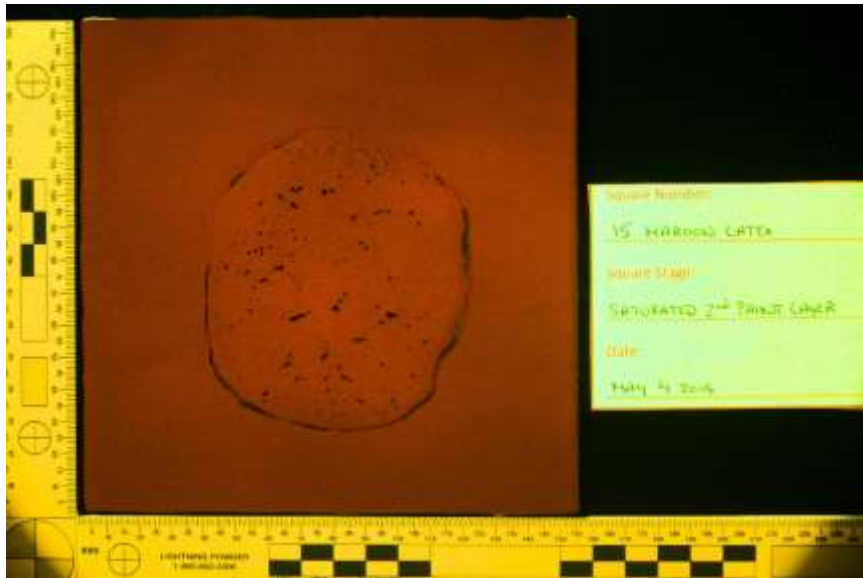


Yellow 455nm HDR

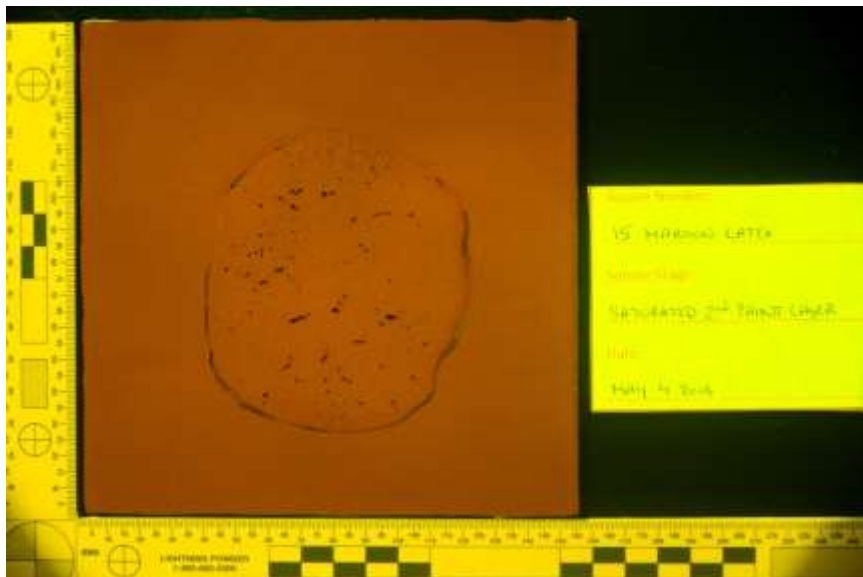


Yellow 455nm Single

Maroon Latex 15 – Saturated



Yellow 455nm HDR



Yellow 455nm Single

Luminol Testing Stage

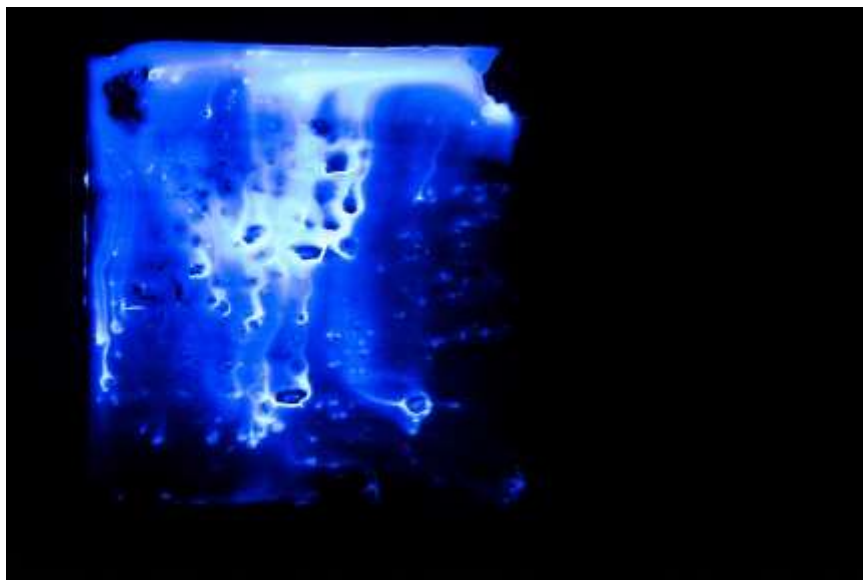
Appendix 4.4.1. Standard Photography

Appendix 4.4.1.1. White Acrylic Second layer of paint stage

White Acrylic 1 – Medium Velocity

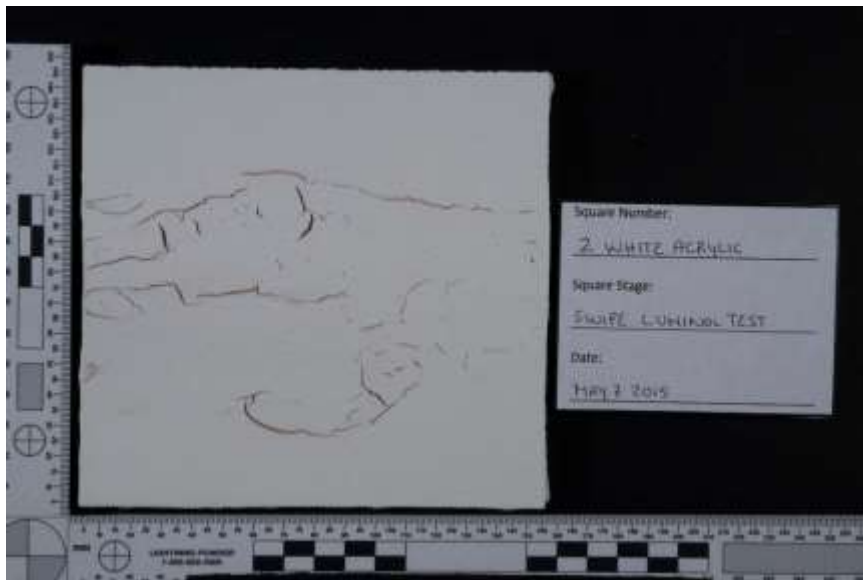


Standard



Luminol

White Acrylic 2 – Swipe

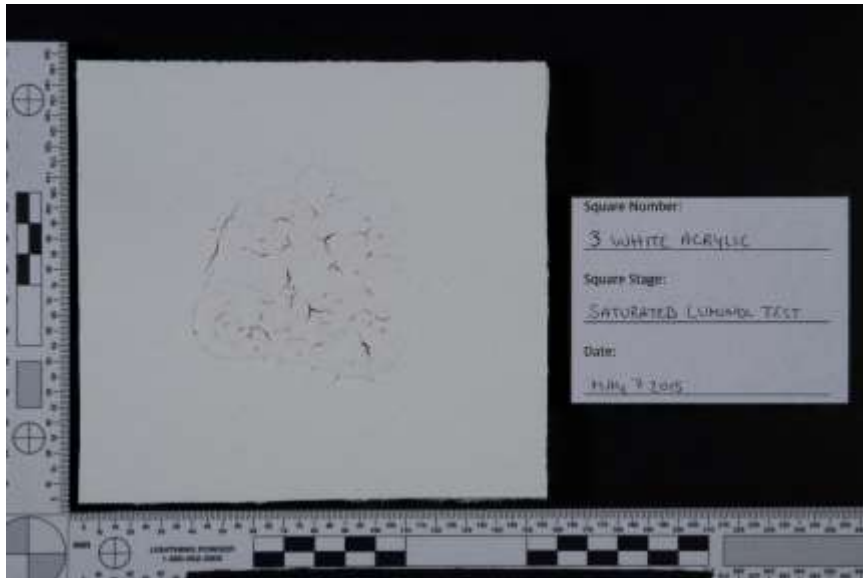


Standard



Luminol

White Acrylic 3 – Saturated

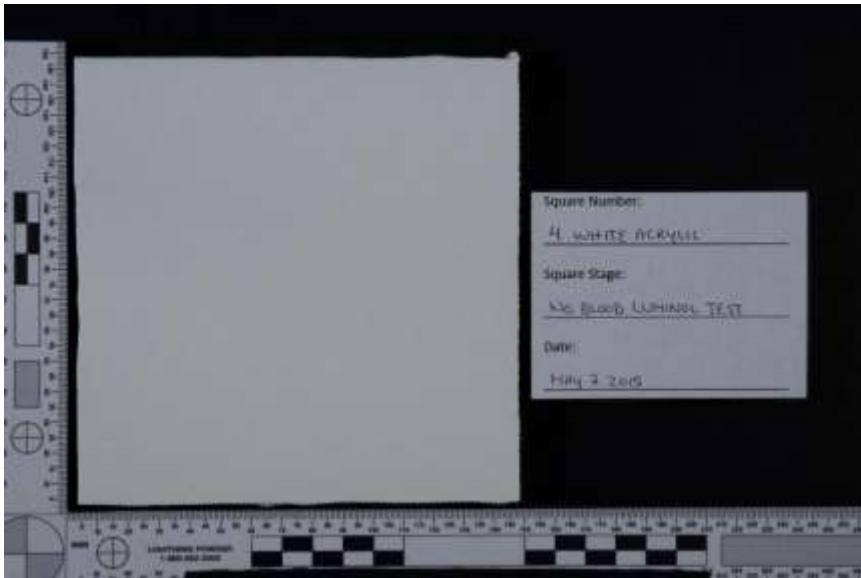


Standard



Luminol

White Acrylic 4 – Control No Bloodstain

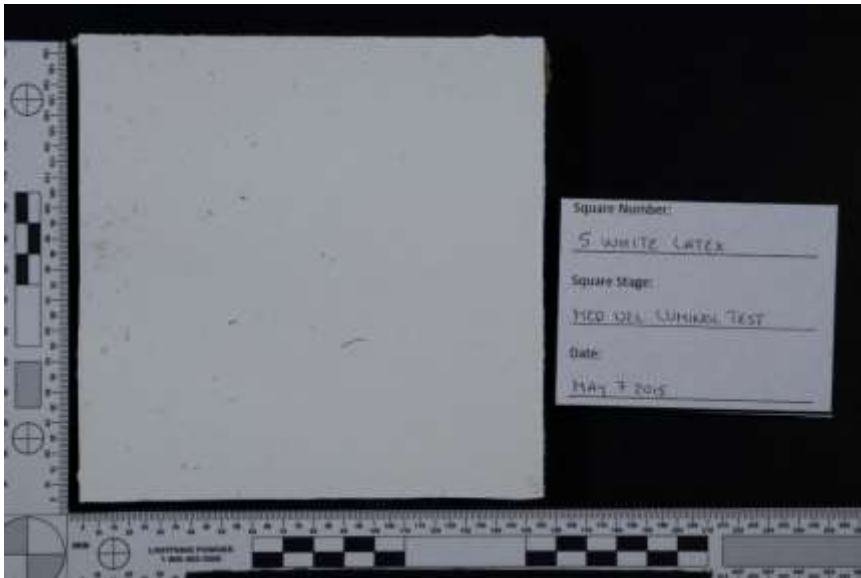


Standard

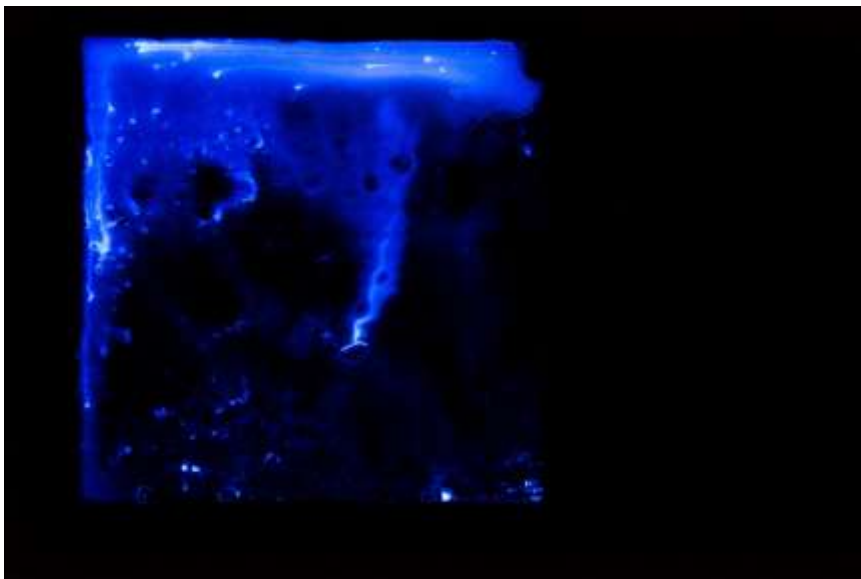


Luminol

Appendix 4.4.1.2. White Latex Second layer of paint stage
White Latex 5 – Medium Velocity

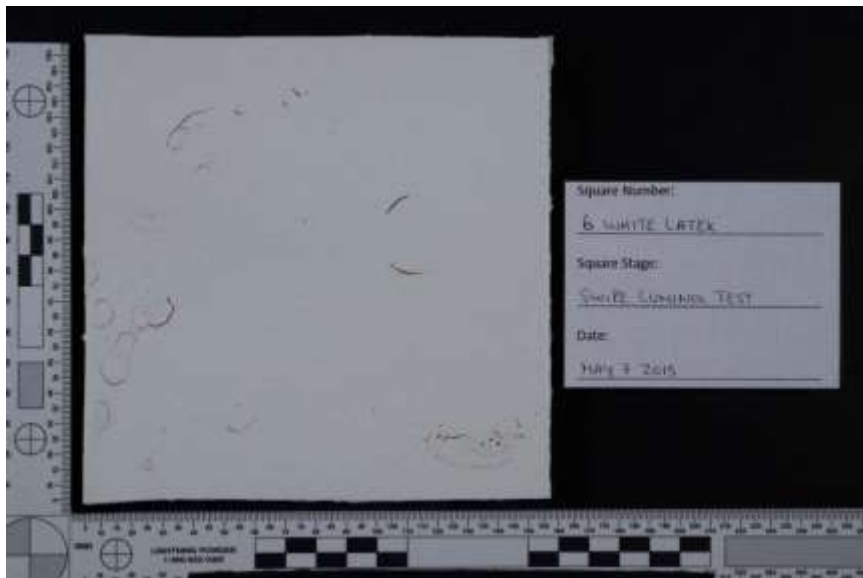


Standard

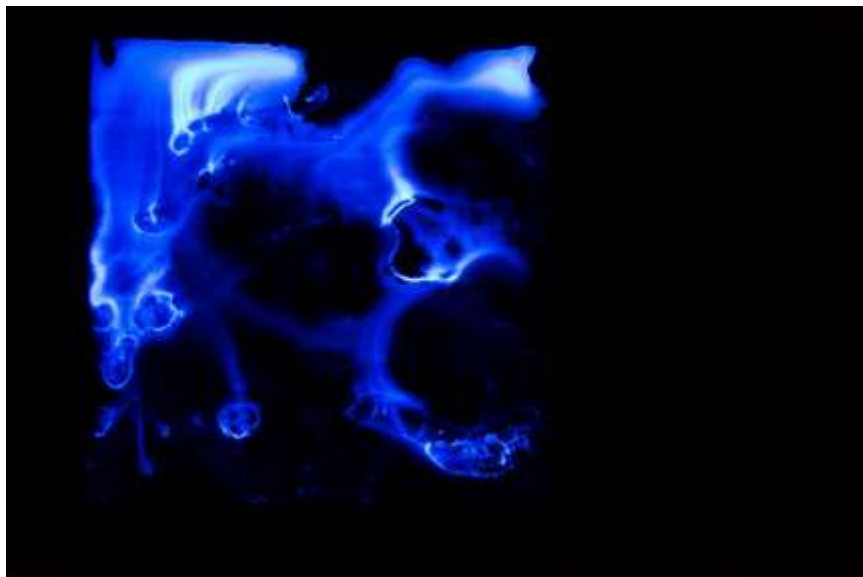


Luminol

White Latex 6 – Swipe



Standard



Luminol

White Latex 7 – Saturated

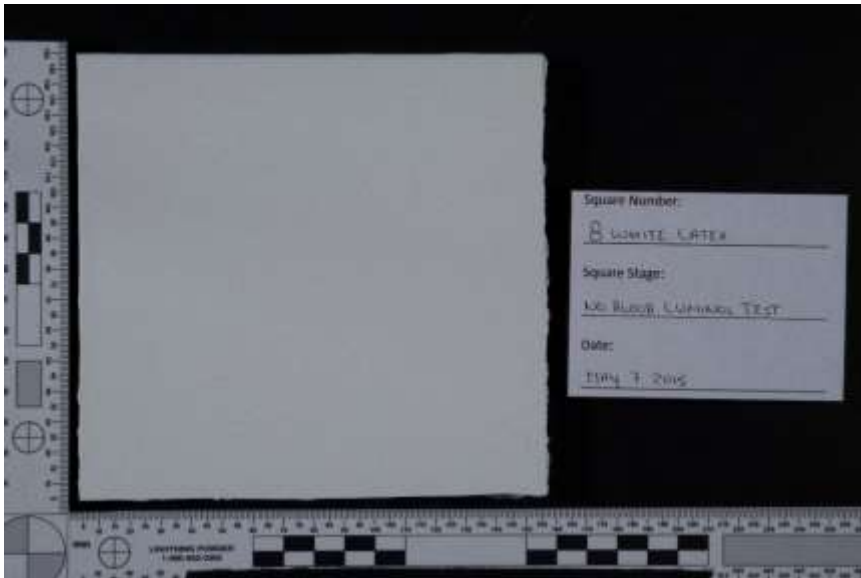


Standard



Luminol

White Latex 8 – Control No Bloodstain



Standard



Luminol

Appendix 4.4.1.3. Black Latex Second layer of paint stage
Black Latex 9 – Medium Velocity



Standard



Luminol

Black Latex 10 – Swipe



Standard



Luminol

Black Latex 11 – Saturated



Standard



Luminol

Black Latex 12 – Control No Bloodstain



Standard



Luminol

Appendix 4.4.1.4. Maroon Latex Second layer of paint stage
Maroon Latex 13 – Medium Velocity



Standard



Luminol

Maroon Latex 14 – Swipe



Standard

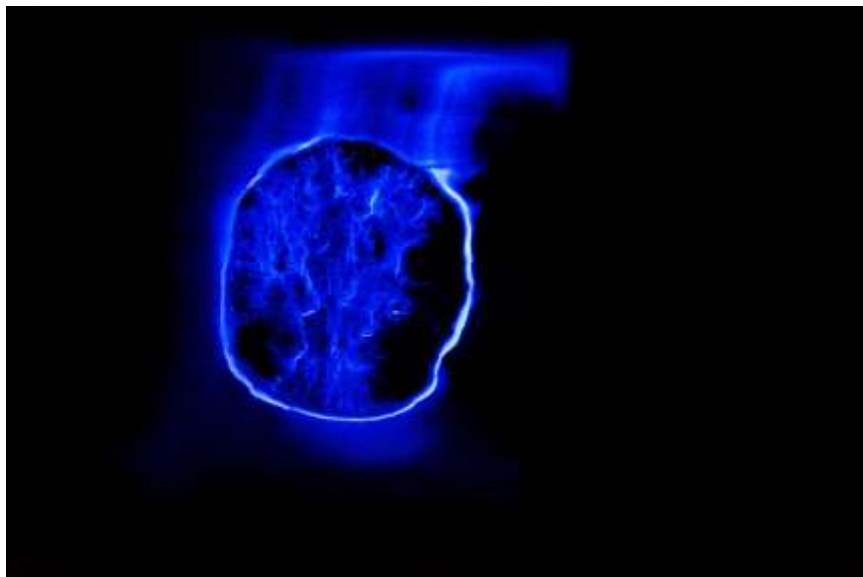


Luminol

Maroon Latex 15 – Saturated



Standard



Luminol

Maroon Latex 16 – Control No Bloodstain



Standard



Luminol